MCEER

MULTIDISCIPLINARY CENTER FOR EARTHQUAKE ENGINEERING RESEARCH

A National Center of Excellence in Advanced Technology Applications

Development and Evaluation of Simplified Procedures for Analysis and Design of Buildings with Passive Energy Dissipation Systems

by

Oscar M. Ramirez, Michael C. Constantinou,
Charles A. Kircher, Andrew S. Whittaker,
Martin W. Johnson and Juan D. Gomez
University at Buffalo, State University of New York
Department of Civil, Structural and Environmental Engineering
Ketter Hall
Buffalo, NY 14260

NOTICE

Report Doumentation Page 50272-101	1. Report No. MCEER-00-0010	2.	3. Recipient's Accession No.

4. Title and Subtitle

Development and Evaluation of Simplified Procedures for Analysis and Design of Buildings with Passive Energy Dissipation Systems

5. Report Date

12/8/00

6.

7. Authors

O.M.Ramirez, M.C.Constantinou, C.A.Kircher, A.S.Whittaker, M.W.Johnson and J.D.Gomez

8. Perfoming Organization Report No.

10. Project / Task / Work Unit No

00-2042

9. Performing Organization Name and Address

Department of Civil, Structural and Environmental Engineering
University at Buffalo, State University of New York
Buffalo, NY 14260

11.Contract (C) or Grant (G) No.

(C)

(G) EEC-9701471

12. Sponsoring Organization Name and Address

Multidisciplinary Center for Earthquake Engineering Research
State University of New York at Buffalo
Red Jacket Quadrangle
Buffalo, NY 14261

13. Type of Report / Period Covered

Technical Report

14.

15. Supplementary Notes

16. Abstract (limit 200 Words)

This report presents the development and evaluation of simplified methods of analysis and design for buildings with passive energy dissipation systems. The work described in this report was conducted under the auspices of the Buildings Seismic Safety Council Technical Subcommittee 12, Base Isolation and Energy Dissipation, for the year 2000 update of the NEHRP Recommended Provisions for Seismic Regulations for New Buildings and Other Structures. The work presented in this report includes: (1) Development of extended damping coefficients for modification of response spectra for damping in excess of 5 percent of critical; (2) Development of relationships between elastic and inelastic displacement of yielding systems with energy dissipating devices; (3) A study of displacement ductility demand in yielding structures with viscous damping systems; (4) Development of equivalent lateral force and modal analysis procedures for buildings with damping systems; (5) Validation studies of the developed analysis procedures using 3- and 6-story structures with linear viscous, nonlinear viscous, solid viscoelastic and yielding damping systems.

17. Document Analysis a. Descriptors

Earthquake Engineering. Passive energy dissipation systems. NEHRP Recommended Provisions for Seismic Regulations for New Buildings, 2000 edition. Nonlinear static analysis. FEMA-273. FEMA-274. Energy dissipation devices. Displacement ductility demand. Viscous damping systems. Equivalent lateral force methods. Modal analysis.

b. Identifiers/Open-Ended Terms

c. COSATI Field/Group

18. Availability Statement

Release Unlimited.

19. Security Class (This Report)

Unclassified

20. Security Class (This Page)

Unclassified

21. No. of Pages
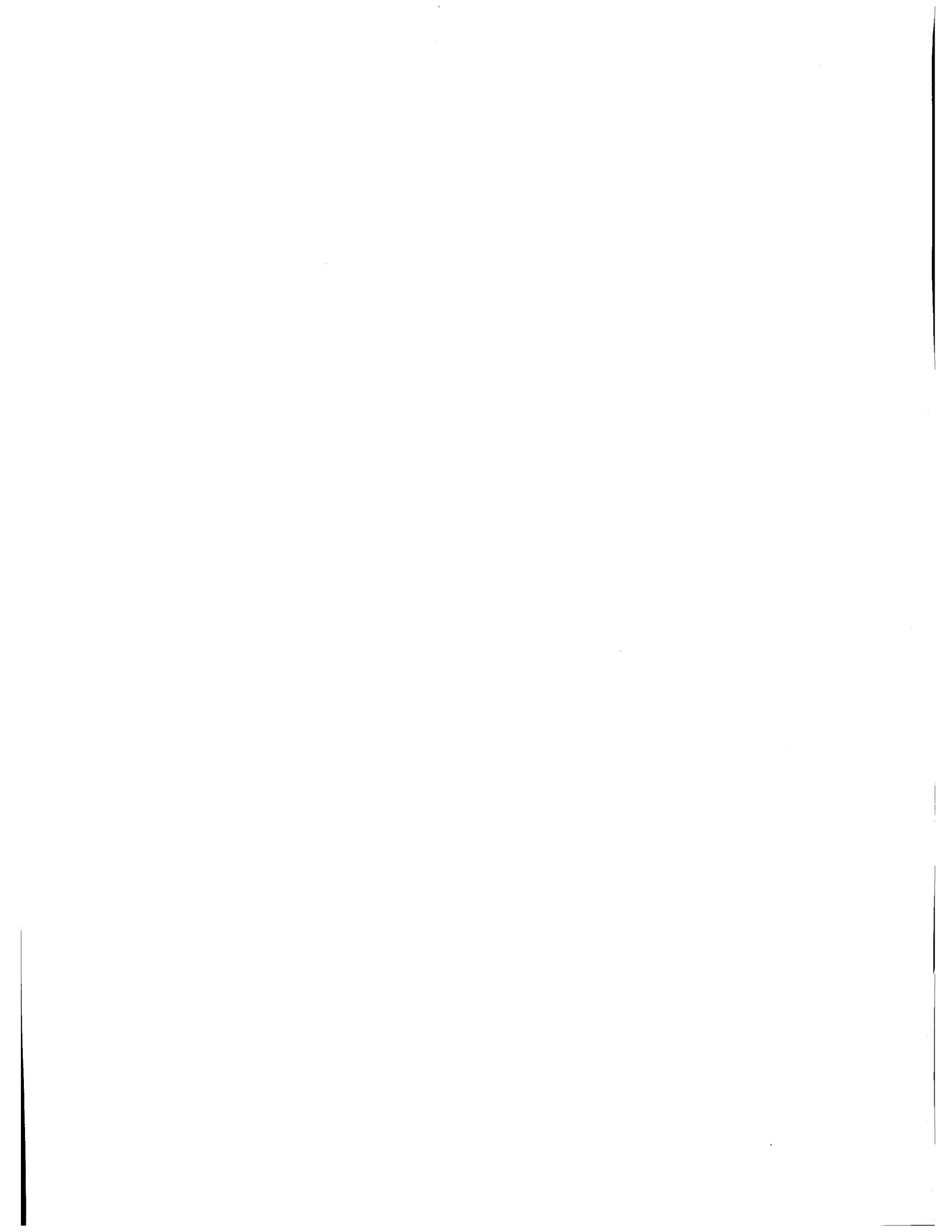
510

22. Price

Development and Evaluation of Simplified
Procedures for Analysis and Design
of Buildings with
Passive Energy Dissipation Systems

by

Oscar M. Ramirez[1], Michael C. Constantinou[2], Charles A. Kircher[3],
Andrew S. Whittaker[4], Martin W. Johnson[5] and Juan D. Gomez[6]

1   Professor, Department of Civil Engineering, Technological University of Panama; former Graduate Student, Department of Civil, Structural and Environmental Engineering, University at Buffalo, State University of New York
2   Professor and Chairman, Department of Civil, Structural and Environmental Engineering, University at Buffalo, State University of New York
3   Principal, C.A. Kircher Associates, Mountain View, California
4   Associate Professor, Department of Civil, Structural and Environmental Engineering, University at Buffalo, State University of New York
5   Group Manager, EQE International, Irvine, California
6   Graduate Student, Department of Civil, Structural and Environmental Engineering, University at Buffalo, State University of New York

MULTIDISCIPLINARY CENTER FOR EARTHQUAKE ENGINEERING RESEARCH
University at Buffalo, State University of New York
Red Jacket Quadrangle, Buffalo, NY 14261

Preface

The Multidisciplinary Center for Earthquake Engineering Research (MCEER) is a national center of excellence in advanced technology applications that is dedicated to the reduction of earthquake losses nationwide. Headquartered at the University at Buffalo, State University of New York, the Center was originally established by the National Science Foundation in 1986, as the National Center for Earthquake Engineering Research (NCEER).

Comprising a consortium of researchers from numerous disciplines and institutions throughout the United States, the Center's mission is to reduce earthquake losses through research and the application of advanced technologies that improve engineering, pre-earthquake planning and post-earthquake recovery strategies. Toward this end, the Center coordinates a nationwide program of multidisciplinary team research, education and outreach activities.

MCEER's research is conducted under the sponsorship of two major federal agencies: the National Science Foundation (NSF) and the Federal Highway Administration (FHWA), and the State of New York. Significant support is derived from the Federal Emergency Management Agency (FEMA), other state governments, academic institutions, foreign governments and private industry.

The Center's NSF-sponsored research is focused around four major thrusts, as shown in the figure below:
- quantifying building and lifeline performance in future earthquake through the estimation of expected losses;
- developing cost-effective, performance based, rehabilitation technologies for critical facilities;
- improving response and recovery through strategic planning and crisis management;
- establishing two user networks, one in experimental facilities and computing environments and the other in computational and analytical resources.
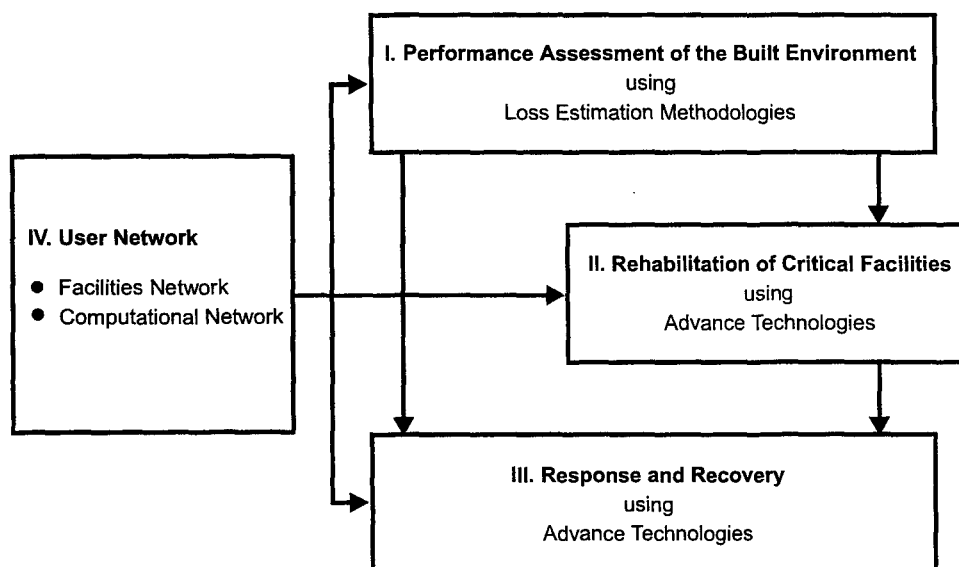
This report presents the development and evaluation of simplified methods of analysis and design for buildings with passive energy dissipation systems. The work was conducted under the auspices of the Building Seismic Safety Council, Technical Subcommittee 12, Base Isolation and Energy Dissipation, for the year 2000 update of the "NEHRP Recommended Provisions for Seismic Regulations for New Buildings and Other Structures." Topics presented in the report include development of extended damping coefficients for modification of response spectra for damping in excess of 5% of critical; development of relationships between elastic and inelastic displacement of yielding systems with energy dissipating devices; a study of displacement ductility demand in yielding structures with viscous damping systems; development of equivalent lateral force and modal analysis procedures for buildings with damping systems; and validation studies of the developed analysis procedures using 3- and 6-story structures with linear viscous, nonlinear viscous, solid viscoelastic and yielding damping systems.

ABSTRACT

This report presents the development and evaluation of simplified methods of analysis and design for buildings with passive energy dissipation systems. The work described in this report was conducted under the auspices of the Buildings Seismic Safety Council Technical Subcommittee 12, Base Isolation and Energy Dissipation, for the year 2000 update of the *NEHRP Recommended Provisions for Seismic Regulations for New Buildings and Other Structures*.

The work presented in this report includes:

(a) Development of extended damping coefficients for modification of response spectra for damping in excess of 5-percent of critical.

(b) Development of relationships between elastic and inelastic displacement of yielding systems with energy dissipating devices.

(c) A study of displacement ductility demand in yielding structures with viscous damping systems.

(d) Development of equivalent lateral force and modal analysis procedures for buildings with damping systems.

(e) Validation studies of the developed analysis procedures using 3- and 6-story structures with linear viscous, nonlinear viscous, solid viscoelastic and yielding damping systems.

ACKNOWLEDGEMENTS

TABLE OF CONTENTS

LIST OF FIGURES

SECTION 1

INTRODUCTION

1.1   Passive Energy Dissipation Systems

Conventionally designed and constructed earthquake-resistant buildings rely on significant inelastic action (energy dissipation) in selected components of the framing system in the design earthquake. For the commonly used moment-resisting frame, inelastic action should occur in the beams near the columns and in the beam-column panel zones: both zones form part of the gravity-load-resisting system. Inelastic action results in damage, which is often substantial in scope and difficult to repair. Damage to the gravity-load-resisting system can result in significant direct and indirect (business interruption) losses.

The desire to avoid damage to components of gravity-load-resisting frames in buildings following the 1989 Loma Prieta and 1994 Northridge earthquakes has spurred the development of passive energy dissipation systems. The primary objective of adding energy dissipation systems to building frames has been to focus the energy dissipation during an earthquake into disposable elements specifically designed for this purpose, and to substantially reduce (or eliminate) energy dissipation in the gravity-load-resisting frame. Because energy dissipators do not form part of the gravity frame and can be replaced after an earthquake without compromising the structural integrity of the frame.

Passive metallic yielding, viscoelastic, and viscous energy dissipators (also termed dampers in this report) are now available in the marketplace, both in the United States and overseas. Soong and Dargush (1997) and Constantinou et al. (1998) describe these passive dampers and other types of dampers under development at the time of this writing.

One impediment to the widespread use of passive energy dissipation systems has been the lack of robust and validated guidelines for the modeling, analysis, design, and testing of the dampers. The following section presents sample information on the procedures developed in the 1990s to aid in the implementation of passive energy dissipation systems.

1

1.2   Procedures for Implementation of Passive Energy Dissipators

1.2.1   General

Up to the time of this writing, five code-oriented procedures have been published related to the implementation of passive energy dissipation devices in buildings. The first procedures were published in 1992 by the Structural Engineers Association of Northern California (SEAONC). The Federal Emergency Management Agency (FEMA) included draft guidelines for the implementation of passive energy dissipation devices in new buildings in the 1994 edition of the *NEHRP Recommended Guidelines for Seismic Regulations for New Buildings* (NEHRP, 1994). Guidelines for the implementation of passive energy dissipation devices in retrofit construction were published in 1997 in the *NEHRP Guidelines for the Seismic Rehabilitation of Buildings* (FEMA, 1997). In 1999, the SEAOC Ad-Hoc Committee on Energy Dissipation published guidelines for implementing energy dissipation devices in new buildings in the SEAOC Blue Book (SEAOC, 1999) in a format consistent with that of the 1997 Uniform Building Code.

This year (2000), FEMA is to publish the 2000 edition of the *NEHRP Recommended Guidelines for Seismic Regulations for New Building*. Summary remarks on each of these documents follow.

1.2.2   1992 SEAONC Energy Dissipation Working Group

The first draft code requirements in the United States for the design and implementation of passive energy dissipation systems were prepared by the Energy Dissipation Working Group of the Base Isolation Subcommittee of SEAONC (Whittaker, et al. 1993). The philosophy adopted in this draft document was to confine inelastic activity in the structure to the energy dissipators and keep the gravity-load-resisting system elastic in the design-basis earthquake. Because the energy dissipation devices did not form part of the gravity-load-resisting system, they were considered to be replaceable following strong earthquake shaking. The SEAONC document required that the framing system *exclusive* of the energy dissipation system comply with all requirements of the 1988 Uniform Building Code, including those of base shear strength and maximum interstory drift.

The document provided general design requirements applicable to a wide range of systems, and, as such, relied on testing of system hardware to confirm the engineering parameters used in the

design, and to verify the overall adequacy of the energy dissipation system. Two types of dampers were recognized in the document: rate-independent (or displacement-dependent) dampers and rate-dependent (or velocity-dependent) dampers. Maximum responses in the energy dissipation system were computed using dynamic analysis, including response-spectrum analysis, and linear and non-linear response-history analysis. Seismic demands were described by the spectral demands of the design-basis earthquake. Design actions and deformations in the energy dissipation system were based on the design-basis earthquake analysis. All components of the energy dissipation system exclusive of the dampers were designed for forces corresponding to 120 percent of the design-basis earthquake damper displacement. Stability of the dampers had to be verified by testing for displacements and velocities corresponding to the maximum level of earthquake shaking that was expected at the building site. Whittaker et al. note that the SEAONC document "...was prepared in keeping with the most current information and the present state-of-the-practice of energy dissipation" and that because "...seismic energy dissipation is a relatively new technology and there are many design-related issues that require additional research..." that a conservative approach was taken to develop the design guidelines.

1.2.3 1994 NEHRP Recommended Provisions for Seismic Regulations for New Buildings

Whereas the 1992 SEAONC guidelines required that the lateral-force-resisting system exclusive of the dampers comply in full with the strength and interstory drift requirements of the Uniform Building Code, the 1994 *NEHRP Recommended Provisions for Seismic Regulations for New Buildings* (NEHRP, 1994) permitted the engineer to use the dampers to reduce the base shear strength of the building. The underlying assumption of these Provisions was that the damped building would suffer no more damage in a design earthquake than the corresponding conventionally framed building. The minimum design forces in the building frame could be calculated as the product of the forces associated with the framing system exclusive of the dampers and the reduction factors listed in Table 1-1 below, which were based on the work of Wu and Hanson (1989). The Provisions noted "Structural members that transmit the forces from the energy dissipation devices to the foundation [including all damper framing members] should be designed to remain elastic for 1.2 times the maximum devices forces associated with the design basis earthquake." Two types of dampers were identified in the provisions: linear viscous devices, and *other* energy dissipation devices. Linear analysis procedures were presented for

3

each type of damper. The Provisions recommended that the building design be verified by nonlinear response-history analysis.

Table 1-1 1994 NEHRP Reduction Factors for Increased Damping (NEHRP, 1994)

Fraction of Critical Damping	Reduction Factor
0.05	1.00
0.10	0.84
0.15	0.72
0.20	0.64
0.25	0.58
0.30	0.53

1.2.4 1997 NEHRP Guidelines for the Seismic Rehabilitation of Building

The 1997 *NEHRP Guidelines for the Seismic Rehabilitation of Building* (FEMA, 1997), widely known as FEMA 273, presented unified procedures for the implementation of energy dissipation devices in retrofit building construction. Consistent with the remainder of the guidelines, four analysis procedures were presented for analyzing buildings incorporating energy dissipation devices: linear static, linear dynamic, nonlinear static, and nonlinear dynamic. All four procedures were displacement (damage)-based methods rather than the traditional force-based methods such as the 1992 SEAONC and 1994 *NEHRP Recommended Provisions*. Because the products of any of these procedures were displacements and deformations, the procedures represented a paradigm shift in the practice of earthquake engineering, and have been used for performance-based earthquake engineering. FEMA 273 permitted the engineer to select performance levels and objectives, so no limits on minimum base shear strength and maximum

4

interstory drift were established in the *Guidelines*. Two types of dampers were identified in the *Guidelines*: displacement-dependent dampers; and velocity-dependent dampers.

The linear procedures of FEMA 273 could only be used if it could be demonstrated that the framing system exclusive of the dampers remained essentially elastic for the level of earthquake shaking under consideration. Further, the effective damping provided by the energy dissipation system could not exceed 30 percent of critical. The linear methods accounted for energy dissipation (damping) in the elastic frame and the dampers. FEMA 273 promoted the use of nonlinear analysis for retrofit building construction using passive energy dissipation devices. Two methods of nonlinear static analysis were presented: Method 1, also known as the Coefficient Method; and Method 2, which was a variant of the well-known Capacity Spectrum Method. These nonlinear methods accounted for energy dissipation in both the yielding frame and the dampers.

1.2.5 1999 SEAOC Recommended Lateral Force Requirements

In 1999, the Structural Engineers Association of California (SEAOC) published guidelines for implementing passive energy dissipation devices in buildings as part of the *Recommended Lateral Force Requirements and Commentary*. The guidelines follow the same format as that of the 1997 Uniform Building Code, and use the same (linear) analysis procedures as those presented in the Code for design of conventional construction, namely, equivalent lateral force, response-spectrum, and response-history analysis. Nonlinear response-history analysis is also permitted but no guidance is offered. Two types of dampers were identified in the *Requirements*: displacement-dependent dampers and velocity-dependent dampers. The framing system exclusive of the dampers has to comply with the base shear strength requirements of the Uniform Building Code regardless of the type of analysis used. Metallic-yielding (displacement-dependent) dampers can be included as part of the lateral-force-resisting system to meet these strength requirements. If either the equivalent lateral force or response-spectrum procedures is used, or if linear response-history analysis is used and the resultant demand-capacity ratios exceed 2.0, the framing system exclusive of the dampers must meet the drift requirements of the Code. If nonlinear response-history analysis is used, or if linear response-history analysis is used

and the resultant demand-capacity ratios are less than 2.0, the energy dissipation provided by the damping system may be used to satisfy the drift requirements of the Code.

1.2.6   2000 NEHRP Recommended Provisions for Seismic Regulations for New Buildings

The 2000 *NEHRP Recommended Provisions for Seismic Regulations for New Buildings and Other Structures* present completely revised procedures for implementing passive energy dissipation devices in new buildings. The December 1999 ballot version of the energy dissipation provisions (Appendix to Chapter 13) is presented in Appendix A of this report. Robust linear procedures (equivalent lateral force and response-spectrum methods) are presented for use with displacement- and velocity-dependent dampers. These procedures were developed in part by the author as part of his doctoral studies at the University at Buffalo, in close co-operation with the members of BSSC Committee TS12, who were tasked with writing new energy dissipation procedures for the *Provisions*. The studies presented in this report served to validate these procedures, which will form the national standard for implementing passive energy dissipation devices in buildings. Much additional discussion on the procedures are presented in the following chapters.

1.3   Report Organization

This report is divided into nine sections, references, and eleven appendices. Section 2 provides a description of the FEMA 273 and 274 nonlinear static analysis procedures. Procedures for modifying response spectra to account for damping in excess of 5 percent of critical are presented in Section 3. Simplified methods of analysis of yielding systems are described in Section 4. Relationships between inelastic and elastic displacement responses are presented in Section 5. A method for estimating the displacement ductility demand in yielding systems including viscous energy dissipation devices is presented in Section 6. Information from Sections 2 through 6 are integrated in Section 7 in the form of new equivalent lateral force and modal analysis procedures for implementing energy dissipation devices in new buildings. Section 8 describes the results of validation studies of the methods of Section 7 using 3- and 6-story frames. A summary, conclusions and recommendations for future work are presented in Section 9. A list of references follows Section 10. The eleven appendices provide supplemental information and detailed calculations in support of Sections 2 through 9.

SECTION 2

DESCRIPTION OF NONLINEAR STATIC ANALYSIS PROCEDURES OF FEMA 273

2.1   Introduction

The intent of performance-based seismic design is to produce structures with predictable performance levels. To achieve this, nonlinear analysis procedures are used. The most realistic of the nonlinear procedures is response-history analysis. However, this method of analysis requires a complex description of the analyzed system and the response is strongly sensitive to the models and the characteristics of the ground motion used in the analysis. Simplified nonlinear analysis methods have been developed based on the use of equivalent linear representations of the structural system.

FEMA (1997) describes two simplified nonlinear static methods of analysis: Method 1 and Method 2. Both methods are briefly described herein and subsequently some clarifications and improvements of these methods are presented.

2.2   Nonlinear Static Procedure, Method 2

2.2.1 General Description

The seismic response of yielding systems may be estimated by simplified methods of analysis in which the yielding system is replaced by an equivalent linear elastic and viscous system. Chopra and Goel (1999) recently presented a brief historical review of these methods and Iwan and Gates (1979) presented a collection of such methods and a study of their accuracy.

Method 2 of FEMA (1997) is largely based on the capacity spectrum method (Freeman et al., 1975; Freeman, 1978) but extended to include structures with damping systems. Method 2 contains a number of steps as explained below for structures with damping systems and illustrated in Figure 2-1.

(1)   A mathematical model of the structure including all the characteristics of the framing system and energy dissipation devices is developed. A relation between the base shear force and

roof displacement is established. This relationship is commonly known as the pushover curve. Although the pushover curve should be a description of the capacity of a given structure, its shape varies as a function of the pattern of lateral loads used to monotonically push the structure.

(2) A value of the roof displacement is assumed and the effective damping is determined from

$$\beta = \frac{W_D}{4\pi W_s} \qquad (2\text{-}1)$$

where W_D is the energy dissipated in a cycle of harmonic motion to the assumed displacement and W_S is the strain energy at the assumed displacement. The value of W_D includes the damping effect of the supplemental damping devices, by yielding of the framing system, and due to the structural damping inherent in the frame. For the assumed value of the roof displacement, eigenvalue analysis is performed using the secant stiffness properties of the structural elements. Using the fundamental mode properties, the pushover curve is converted to the spectral capacity curve, that is, a plot of spectral acceleration versus spectral displacement. The spectral acceleration (S_a) for the first mode representation of the structure is given by

$$S_a = \frac{V}{\overline{W}_1}g \qquad (2\text{-}2)$$

where V is the base shear, and $\overline{W}_1$ is the first modal weight given by

$$\overline{W}_1 = \frac{\sum\limits_{i}^{N}(w_i\phi_{i1})^2}{\sum\limits_{i=1}^{N}w_i\phi_{i1}^2} \qquad (2\text{-}3)$$

and where ϕ_{i1} is the first mode shape vector, w_i is the reactive weight of the ith degree of freedom, and N is the number of degrees of freedom.

8

In a similar way, the spectral displacement (S_d) for the first mode representation of the structure is given by

$$S_d = \frac{\delta_r}{\phi_{r1}\Gamma_1}$$ (2-4)

where δ_r is the roof displacement, Γ_1 is the first mode modal participation factor, and ϕ_{r1} is the ordinate of the first mode shape at the roof.

(3) The capacity curve computed in step 2 is superimposed on the design demand curve, which is a plot of spectral acceleration versus spectral displacement after modification for the effective damping. The displacement demand is determined from the intersection point of the capacity curve and the design demand curve.

(4) The assumed and computed values of the displacement are compared and the process is repeated until satisfactory convergence is achieved.

(5) The contribution of higher modes to the total response is calculated by utilizing modal analysis procedures and assuming elastic behavior with properties based on the secant stiffnesses at the displacement calculated in step (4). For this calculation, Equations (2-1) to (2-4) are used but with $\overline{W}_1$ is replaced by $\overline{W}_m$, ϕ_{i1} is replaced by ϕ_{im}, ϕ_{r1} is replaced by ϕ_{rm} and Γ_1 is replaced by Γ_m, where the subscript m denotes the mth mode of vibration. It should be noted that in this calculation, iteration is not required due to the assumption of elastic behavior. The total response is finally calculated trough the use of an appropriate combination rule.

2.2.2 Pushover Curve

The pushover curve constitutes an important major step in the simplified method of analysis. In a practical sense it represents the capacity of the structure to resist lateral loads. The pushover curve is constructed by "pushing" a mathematical model of the structure by monotonically increasing lateral loads of constant proportions. As the magnitude of the load increases, progressive yielding of the model occurs, which is accompanied by a change in the dynamic properties of the structure. Recognizing that the structural capacity and, therefore, its

9

degradation pattern is not independent of the demand, it can be concluded that the ordinates of pushover curve are a function of the assumed pattern of lateral loads.

The pattern of loads should be consistent with the expected distribution of inertia forces in the yielding structure. Some studies have suggested that the most appropriate distribution is one in which the loads change as the structure is displaced. This approach is termed *adaptive load pattern*. Researchers have proposed the use of a lateral pattern consistent with the deflected shape of the structure (Fajfar and Fischinger, 1988), the use of load patterns based on mode shapes derived from secant stiffnesses (Eberhard and Sozen, 1993), and the use of patterns in which the lateral forces are related to story resistances at each increment of loading (Reinhorn et al., 1995; Bracci et al., 1997).

The simplified analysis procedure described in FEMA (1997) requires the use of at least two different patterns of lateral loads in order to produce bounds on the response. The first one, termed a *uniform pattern*, is based on the lateral forces being proportional to the total mass at each level. The second pattern, termed a *modal pattern*, is nearly proportional to the first modal shape. Furthermore, FEMA (1997) suggests that the load pattern be computed by combination of modal responses using response-spectrum analysis and considering as many modes as necessary to capture 90% of the total mass.

2.2.3 Design Demand Curve

The seismic hazard is typically represented by the 5%-damped pseudo-acceleration response spectrum, that is a plot of spectral acceleration (acceleration at the time of maximum displacement) of a single-degree-of-freedom elastic system with 5% equivalent viscous damping versus the structural period. The pseudo-acceleration S_a and the spectral displacement S_d (maximum drift) of the single-degree-of-freedom system are related through

$$S_d = \frac{T^2}{4\pi^2} S_a \tag{2-5}$$

where T is the period. A plot of spectral acceleration versus the spectral displacement is termed the design demand curve. In this figure, points of equal period are located along lines radiating

from the origin as shown in Figure 2-2. Plots for different levels of damping are also presented in the figure.

The design demand curves for levels of damping higher than 5% are constructed by dividing the 5%-damped curve by the damping coefficient B. Values of the damping coefficient have been presented in FEMA, 1997. As shown in Table 2-1, FEMA utilizes two factors, one for the constant acceleration region of the response spectrum (B_s) and the other for the constant velocity region of the spectrum (B_1). Interestingly, the values in the constant acceleration region are larger than those in the constant velocity region, which contradicts the fact that there is little or not reduction of displacement with increasing damping in very stiff structures. Also, the values of the damping coefficient are terminated at the damping ratio of 0.5 in an apparent exercise of conservatism due to lack of data for larger levels of damping.

New values of the damping coefficient, which correctly account for reduction of the damping coefficient with reducing period and extend to critically damped systems have been established in Section 3. The case of critically and over-critically damped systems may actually arise in the higher modes of structures with viscous damping devices. Presented in Figure 2-3, the values of this study may be seen as large for damping ratio larger than 0.5 by comparison to the values in FEMA (1997). However, the damping coefficient values of this study are realistic and their use is important in correctly assessing the benefits of energy dissipation systems. The values established in this study have been utilized, after some minor simplification, in the 2000 NEHRP Recommended Provisions for Seismic Regulations for New Buildings and Other Structures, Appendix to Chapter 13, Structures with Damping Systems (NEHRP, 2000). The values of the damping coefficient in NEHRP (2000) are presented in Table 2-1 and graphically compared to the FEMA (1997) and the values of this study in Figure 2-3. As an example, Figure 2-4 presents response spectra established by using damping coefficients developed in this study. The 5%-damped spectrum is that described in NEHRP (2000) for parameters $S_{DS} = 1.0$, $S_{D1} = 0.6$ and $T_s = 0.6$ sec.

2.2.4 Calculation of Velocity Dependent Forces

Velocity dependent forces are calculated in Method 2 by utilizing pseudo-velocities as estimates of maximum velocities. This simple approach introduces errors since it is known that pseudo-

11

velocity generally under-estimates the maximum velocity for long-period structures and it generally over-estimates the maximum velocity for short-period structures. Moreover, the degree of error depends on the amount of effective damping. Sadek et al. (1999) proposed the use of correction factors to multiply the pseudo-velocity in order to obtain a better estimate of maximum velocity. The Sadek approach has been investigated in this study and found promising. Results are presented in Section 4, where it is shown that correction factors established by the approach of Sadek et al. (1999) produce good estimates of drift velocities.

2.2.5 Calculation of Maximum Actions

The seismic design forces are calculated at three stages: (a) maximum drift, (b) maximum velocity, and (c) maximum acceleration. Stages (b) and (c) are important only for structures with velocity dependent damping systems because maximum actions in buildings incorporating displacement dependent damping systems will occur at the time of maximum displacement.

The design forces at the stage of maximum acceleration are calculated as a linear combination of the forces calculated at the stages of maximum drift and maximum velocity after multiplication by combination factors CF_1 and CF_2, respectively. These factors have been developed on the basis of the assumption of linear-elastic and linear-viscous behavior (Tsopelas et al., 1997; Constantinou et al., 1998).

It is now recognized that the combination factors in FEMA (1997) are incorrect for yielding structures and for structures with nonlinear viscous damping systems. Section 4 herein presents the corrected combination factors, which have been implemented in NEHRP (2000).

2.3 Nonlinear Static Procedure, Method 1

Method 1 was developed as a simple one-step analysis method in which the roof (or target) displacement of structures exhibiting bilinear behavior is prescribed by an equation of the form

$$\delta_r = C_0 \cdot C_1 \cdot C_2 \cdot C_3 \cdot S_a \cdot \frac{T_e^2}{4\pi^2} \qquad (2\text{-}6)$$

where T_e is the elastic period of the structure, S_a is the spectral acceleration for period T_e, C_o is a coefficient relating roof displacement to spectral displacement, C_I is a coefficient relating maximum inelastic displacements to displacements calculated assuming linear elastic response, and C_2 and C_3 are coefficients to represent the effects of stiffness and strength degradation, and dynamic P-Δ effects, respectively.

As originally conceived, Method 1 can bypass steps (2) to (5) of Method 2 and can obtain the design forces and member deformations by only performing pushover analysis until the target roof displacement is reached. However, the application of Method 1 is complicated when velocity-dependent damping systems are utilized. Specifically:

(a) The effect of added damping must be considered in the evaluation of the spectral acceleration. This requires that step (2) of Method 2 is performed, however excluding the contribution from yielding of the building frame. For linear viscous and viscoelastic damping systems, this represents a simple calculation. For nonlinear viscous damping systems, an iterative procedure similar to that of Method 2 must be performed.

(b) The effects of higher modes need to be considered. These effects are important in the calculation of velocity-dependent forces.

(c) Coefficient C_I, as described in FEMA (1997), does not account for the effect of added viscous damping on the ratio of inelastic displacements to displacement calculated assuming elastic response. It will be shown in Section 5 that added viscous damping affects coefficient C_I. New expressions prescribing coefficient C_I are derived and presented in Section 5.

2.4 Calculation of Effective Damping

Equation (2-1) describes a general approach for calculating the effective damping of a structural system. The calculation requires that information on the properties and configuration of the damping system, and information on the properties of the structural frame (period, mode shape, reactive floor weights) are available. The details of calculation differ depending on the nature of the damping system. Details are presented in Section 4 where simplified methods of analysis of single-degree-of-freedom systems are evaluated and in Section 7.4 where the calculation of the effective damping in multiple-degree-of-freedom-systems is presented.

13

TABLE 2-1 Values of Damping Coefficient B

Effective Damping β	FEMA 273		This Study (Section 3)		NEHRP 2000
	B_s [1]	B_1 [2]	B_s [3]	B_1 [4]	B [5]
<0.02	0.8	0.8	0.80	0.80	0.8
0.05	1.0	1.0	1.00	1.00	1.0
0.10	1.3	1.2	1.20	1.20	1.2
0.20	1.8	1.5	1.50	1.50	1.5
0.30	2.3	1.7	1.70	1.70	1.8
0.40	2.7	1.9	1.90	1.90	2.1
0.50	3.0	2.0	2.20	2.20	2.4
0.60	3.0	2.0	2.30	2.60	2.7
0.70	3.0	2.0	2.35	2.90	3.0
0.80	3.0	2.0	2.40	3.30	3.3
0.90	3.0	2.0	2.45	3.70	3.6
1.00	3.0	2.0	2.50	4.00	4.0

1   Valid for $T \leq T_s B_s / B_1$

2   Valid for $T \geq T_s B_s / B_1$

3   Valid at $T = T_s / 5$. For $T_s / 5 < T < T_s$, B is determined by linear interpolation between values B_s and B_1. For $T < T_s / 5$, B is determined by linear interpolation between values of 1.0 (valid at T=0.0) and B_s (valid at $T = T_s / 5$).

4   Valid for $T \geq T_s$

5   Valid for $T \geq T_s$. Also B = 1.0 for T = 0.0. Values of B for $T_s < T < T_s / 5$ may be obtained by linear interpolation.

T = period, T_s = period at which the constant acceleration and constant velocity regions of the response spectrum intersect.

STEP 1 PUSHOVER ANALYSIS

δ_3 F_3

δ_2 F_2

δ_1 F_1 δ_1

$V = \Sigma F_i$

V

Assumed
Displacement
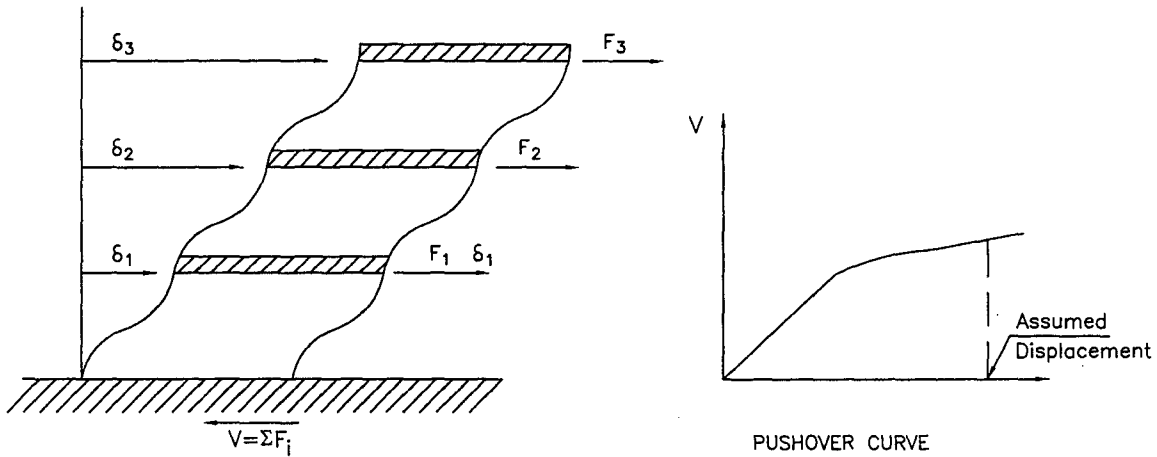
PUSHOVER CURVE

STEP 2   PERFORM EINGENVALUE ANALYSIS USING EFFECTIVE MEMBER
STIFFNESSES AT ASSUMED DISPLACEMENT
CONVERT PUSHOVER CURVE TO SPECTRAL CAPACITY CURVE

V

$$S_a = \frac{V}{\overline{W}_1} \cdot g$$

$$S_d = \frac{\delta_3}{\Gamma_1}$$

$_3 \delta$

S_a

S_d
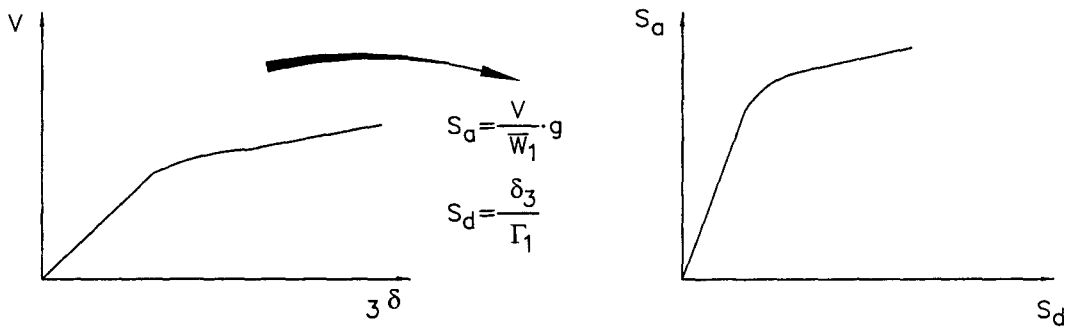
STEP 3   ESTABLISH DESIGN DEMAND SPECTRUM USING
EFFECTIVE DAMPING IN FUNDAMENTAL MODE
OVERLIE SPECTRAL CAPACITY CURVE ON DESIGN DEMAND
SPECTRUM AND CALCULATE RESPONSE

S_a

A

Spectral
Capacity
Curve

Design
Demand
Curve

$$V = \frac{A \cdot \overline{W}_1}{g}$$

$$\delta_3 = \Gamma_1 \cdot D$$

D S_d
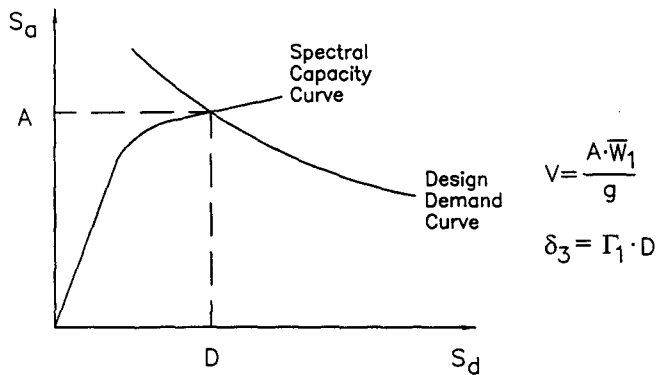
STEP 4 IF CALCULATED $\delta_3 \neq$ ASSUMED DISPLACEMENT, REPEAT STEPS 2 TO 5
STEP 5 OBTAIN HIGHER MODE RESPONSE

FIGURE 2-1 Illustration of Nonlinear Static Procedure, Method 2

15
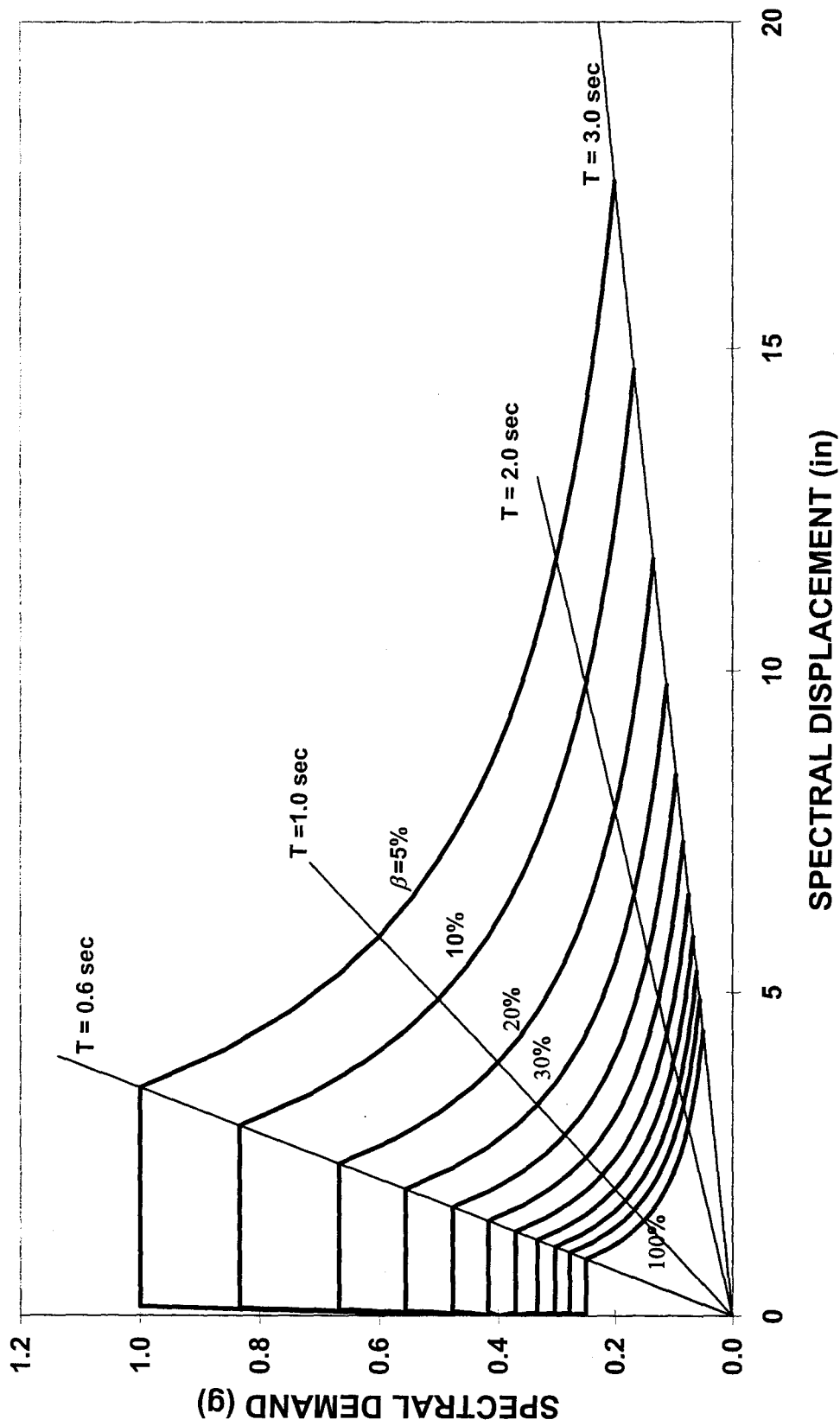
FIGURE 2-2 Example of Design Demand Curves

16
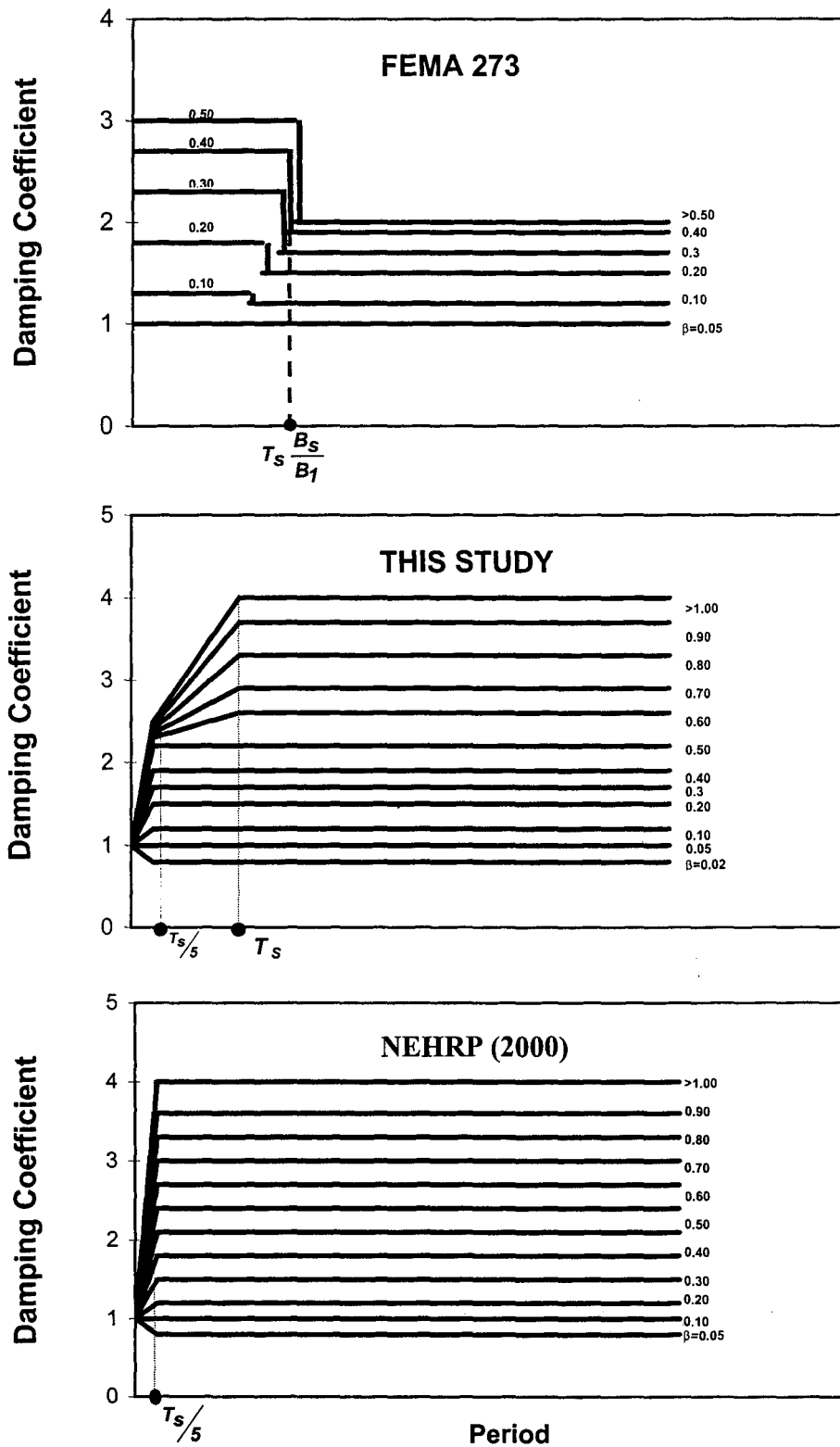
FIGURE 2-3 Damping Coefficient B as Function of Period and Damping
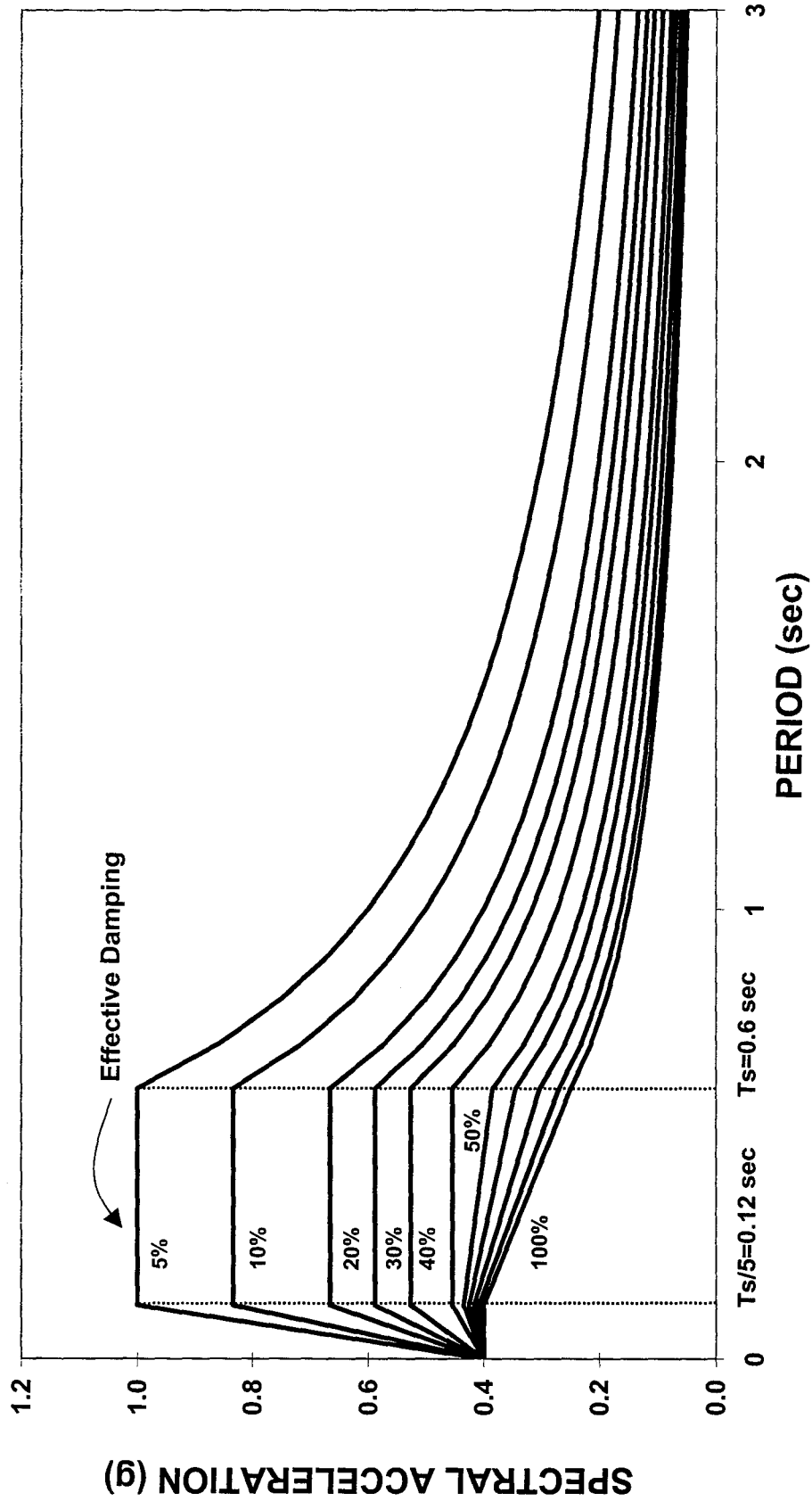
FIGURE 2-4 Acceleration Response Spectra for Various Levels of Effective Damping Established with the use of the Damping Coefficient Developed in this Study (conservative values in Table 3-3). 5%-Damped Spectrum Representative of NEHRP (2000) Design Spectrum with $S_{DS} = 1.0$, $S_{D1} = 0.6$ and $T_s = 0.6$ sec.

18

SECTION 3

MODIFICATION OF RESPONSE SPECTRUM FOR HIGHER DAMPING

3.1 Introduction

The 5%-damped elastic response spectrum represents the usual seismic loading specification. Spectra for higher damping need to be constructed for the application of simplified methods of analysis of structures with damping systems. Elastic spectra constructed for higher viscous damping are useful in the analysis of linear elastic structures with linear viscous damping systems. Moreover, they are used in the simplified analysis of yielding structures since simplified methods of analysis are based on the premise that yielding structures with damping systems may be analyzed by using equivalent linear and viscous representations. The validity and accuracy of such representations is the subject of the study reported in Section 4.

The typical approach of constructing an elastic spectrum for damping greater than 5-percent is to divide the 5%-damped spectral acceleration by a damping coefficient B:

$$S_a(T,\beta) = \frac{S_a(T,5\%)}{B} \tag{3-1}$$

where $S_a(T, \beta)$ is the spectral acceleration at period T for damping ratio β. Note that the spectral acceleration is the acceleration at maximum displacement (it does not contain any contribution from the viscous force) and is therefore related directly to the spectral displacement through equation (2-5). The damping coefficient is a function of the damping ratio and may be a function of the period.

The derivation of damping coefficients or their inverse (which may be extracted from spectrum amplification factors) may be traced back nearly 30 years (e.g., see Newmark and Hall, 1982 and several of their references). Table 3-1 has been prepared to compare values of the damping coefficient from various sources. The values attributed to Newmark and Hall (1982) have been derived from the spectrum amplification factors, that is, factors used to multiply the peak ground motion to obtain the response spectrum. These factors likely originated from data on response spectra of earthquakes which occurred prior to 1973. It should also be noted that Newmark and

19

Rosenblueth (1971) and Newmark and Hall (1969) reported amplification factors, which have not been utilized herein. The data of Newmark and Hall (1982) are limited to damping ratio of 0.20. However, the equations presented by Newmark and Hall (1982) for the amplification factor in the constant velocity region of the spectrum were utilized herein to obtain values of the damping coefficient for damping ratios up to 1.0. These values are reported in Table 3-1. Specifically, Newmark and Hall (1982) proposed for the constant velocity region of the spectrum:

$$A_\beta = 2.31 - 0.41 ln(100\beta) \tag{3-2}$$

where A_β = amplification factor for damping ratio β. Since the damping coefficient B is equal to

$$B = \frac{A_{0.05}}{A_\beta} \tag{3-3}$$

it follows that in the constant velocity region

$$B = \frac{1.65}{2.31 - 0.41 ln(100\beta)} \tag{3-4}$$

The values for the damping coefficient of Newmark and Hall (1982) in the constant velocity region of the spectrum are basically the same as those of NEHRP (2000). This is surprising since the NEHRP (2000) values were based on the study reported herein, which used different earthquake records and a different analysis procedure than that of Newmark and Hall (1982). Nevertheless, this fact may enhance our confidence in the damping coefficient values in NEHRP (2000).

The values of the damping coefficient that appeared in the 1994 NEHRP (NEHRP, 1994) were based on a study of Wu and Hanson (1989). Later, the FEMA 273 Guidelines (FEMA, 1997) were developed in which the damping coefficients were based on the work of Newmark and Hall (1982) but were extended to higher values of the damping ratio. The extension to higher values of the damping ratio was necessary since simplified methods of analysis introduced in FEMA 273 could result in high effective damping due to the combined effects of yielding of the

building frame and added viscous damping. There are two drawbacks to the damping coefficients of FEMA 273:

(a) The values for the constant acceleration region of the spectrum (region of low periods) are higher than those valid in the constant velocity region. This contradicts the fact that there is little or no reduction of displacement with increasing damping in very stiff structures. It also leads to the erroneous impression that damping systems are most effective when used on stiff structures.

(b) The effect of damping in reducing displacement is ignored when the damping ratio exceeds 50% of critical leading to conservative estimates of displacement in highly damped buildings, which may be the case for frames having good hysteretic behavior, enhanced with viscous damping systems and undergoing significant inelastic action.

The study reported in this section resulted in values of the damping coefficient in the constant velocity region which are larger than those in FEMA 273 (see column of results labeled best fit in Table 3-1). For this reason, conservative values of the damping coefficient are proposed in this study. The proposed values of the damping coefficient have been utilized, after some simplification, in the NEHRP Recommended Provisions (NEHRP, 2000).

3.2 Procedure to Establish Values of the Damping Coefficient

Using (3-1), values of coefficient B may be obtained as

$$B = \frac{S_a(T, 5\%)}{S_a(T, \beta)} \tag{3-5}$$

Equation (3-5) may be used to obtain values of coefficient B for a range of values of period T and for selected earthquake motions. The results for the selected earthquake motions may then be statistically processed to obtain average or median values.

The procedure followed herein is based on the use of scaled earthquakes which on the average represent well a specific design response spectrum. The scaling process of these earthquakes has been presented in Tsopelas et al. (1997). Herein it is sufficient to mention that the scaling

process preserves the frequency content of the records and ensures an equal contribution of these records to the average response spectrum.

The selected 20 horizontal components of 10 earthquake motions are presented in Table 3-2 together with their scale factors. Each of these earthquakes was selected to have a magnitude larger than 6.5, epicentral distance between 10 and 20 km, and site conditions characterized by site class C to D in accordance with NEHRP (2000). That is, the selected records did not include motions recorded on soft soil sites and motions with near-fault characteristics. The applicable design response spectrum had parameters $S_{DS} = 1.0$, $S_{D1} = 0.6$ and $T_S = 0.6$ sec. Figure 3-1 presents the average response spectrum of the 20 scaled motions and compares that to the target NEHRP design response spectrum. The average of the 20 scaled motions represents well the target spectrum. Figure 3-1 presents also the maximum and minimum spectral acceleration values of the 20 scaled motions. These spectra demonstrate the variability in the characteristics of the scaled motions. This variability is implicit in the definition of seismic hazard.

The 20 scaled motions have been used in the construction of elastic response spectra for higher damping. Average spectra (average of spectral acceleration values of the 20 scaled motions) are presented in Figure 3-2 for damping ratio in the range of 2 to 100-percent. The damping coefficient for a particular period was determined as the ratio of the 5%-damped design spectral acceleration to the average spectral acceleration for higher damping, as described by (3-5). Representative plots of the damping coefficient are shown in Figure 3-3. On the basis of such plots, it is reasonable to propose a trilinear relation for the damping coefficient as shown in Figure 3-4. In this relation, the damping coefficient is constant in the constant velocity region of the spectrum and it gradually reduces towards unity at zero. The proposed model requires three parameters for each damping value, B_s, B_1 and T_s, as shown in Figure 3-4.

Figure 3-5 presents graphs of the calculated damping coefficient for damping ratio in the range of 2 to 100-percent together with graphs of the coefficient produced by the calibrated trilinear model. The parameters of the model are presented in Table 3-3 and described as been based on best fit. The values of parameter B_1 based on the best fit of the calculated damping coefficient are generally higher than the values of the same parameter in the FEMA 273 Guidelines (FEMA,

1997). Accordingly, conservative values of parameters B_S and B_1 have been established to be consistent with the FEMA (1997) values. These values are listed in Table 3-3.

The proposed conservative trilinear model for the damping is utilized for all calculations described in this report. The data in Table 3-3 were made available at the time of writing of the 2000 NEHRP Recommended Provisions, and were used to establish the simpler two-parameter model for the damping coefficient that is presented in NEHRP (2000) and listed in Table 3-1.

3.3 Conclusions

This section established new values for the damping coefficient which is used in the calculation of spectral acceleration values for damping higher than 5-percent. The presented damping coefficient values are valid for viscous damping ratio in the range of 2 to 100-percent of critical. The derivation of these values was based on the analysis of response of structural systems to selected ground motions which did not include records on soft soil sites and records with near-fault characteristics. The presented values have been utilized, after some simplification, in the NEHRP (2000) Recommended Provisions.

TABLE 3-1 Damping Coefficient from Various Sources

Damping Ratio	Newmark & Hall (1982) (median values)		1994 NEHRP (all periods)	FEMA 273 (1997)		This Study* (best fit)	(conservative values)	2000 NEHRP (all periods > $T_s/5$)
	Accel. Region	Velocity Region		Accel. Region	Velocity Region	Velocity Region	Velocity Region	
0.02	0.78	0.81		0.8	0.8	0.80	0.80	0.8
0.05	1.00	1.00	1.00	1.0	1.0	1.00	1.00	1.0
0.10	1.29	1.21	1.19	1.3	1.2	1.25	1.20	1.2
0.20	1.81	1.53	1.56	1.8	1.5	1.75	1.50	1.5
0.30		1.80	1.89	2.3	1.7	2.10	1.70	1.8
0.40		2.07		2.7	1.9	2.45	1.90	2.1
0.50		2.34		3.0	2.0	2.90	2.20	2.4
0.60		2.61		3.0	2.0	3.30	2.60	2.7
0.70		2.90		3.0	2.0	3.60	2.90	3.0
0.80		3.21		3.0	2.0	4.00	3.30	3.3
0.90		3.55		3.0	2.0	4.30	3.70	3.6
1.00		3.91		3.0	2.0	4.65	4.00	4.0

* For acceleration domain, B is less than the value in table.

T_s = Period at which the constant velocity and constant acceleration regions of spectrum intersect.

Table 3-2 Motions used in Analysis and Scale Factors

Year	Earthquake	Station	Components	Scale Factor
1949	Washington	325 (USGS)	N04W, N86E	2.74
1954	Eureka	022 (USGS)	N11W, N79E	1.74
1971	San Fernando	241 (USGS)	N00W, S90W	1.96
1971	San Fernando	458 (USGS)	S00W, S90W	2.22
1989	Loma Prieta	Gilroy 2 (CDMG)	90,0	1.46
1989	Loma Prieta	Hollister (CDMG)	90,0	1.07
1992	Landers	Yermo (CDMG)	360,270	1.28
1992	Landers	Joshua (CDMG)	90,0	1.48
1994	Northdridge	Moorpark (CDMG)	180,90	2:61
1994	Northdridge	Century (CDMG)	90,360	2.27

TABLE 3-3 Values of Parameters B_S and B_1 in Proposed Model of Damping Coefficient

Damping Ratio	Values Based on Best Fit (as shown in Fig. 3-5)		Conservative Values (Consistent with FEMA 273)	
	B_S	B_1	B_S	B_1
0.02	0.80	0.80	0.80	0.80
0.05	1.00	1.00	1.00	1.00
0.10	1.25	1.25	1.20	1.20
0.20	1.75	1.75	1.50	1.50
0.30	2.10	2.10	1.70	1.70
0.40	2.20	2.45	1.90	1.90
0.50	2.30	2.90	2.20	2.20
0.60	2.40	3.30	2.30	2.60
0.70	2.50	3.60	2.35	2.90
0.80	2.60	4.00	2.40	3.30
0.90	2.70	4.30	2.45	3.70
1.00	2.75	4.65	2.50	4.00
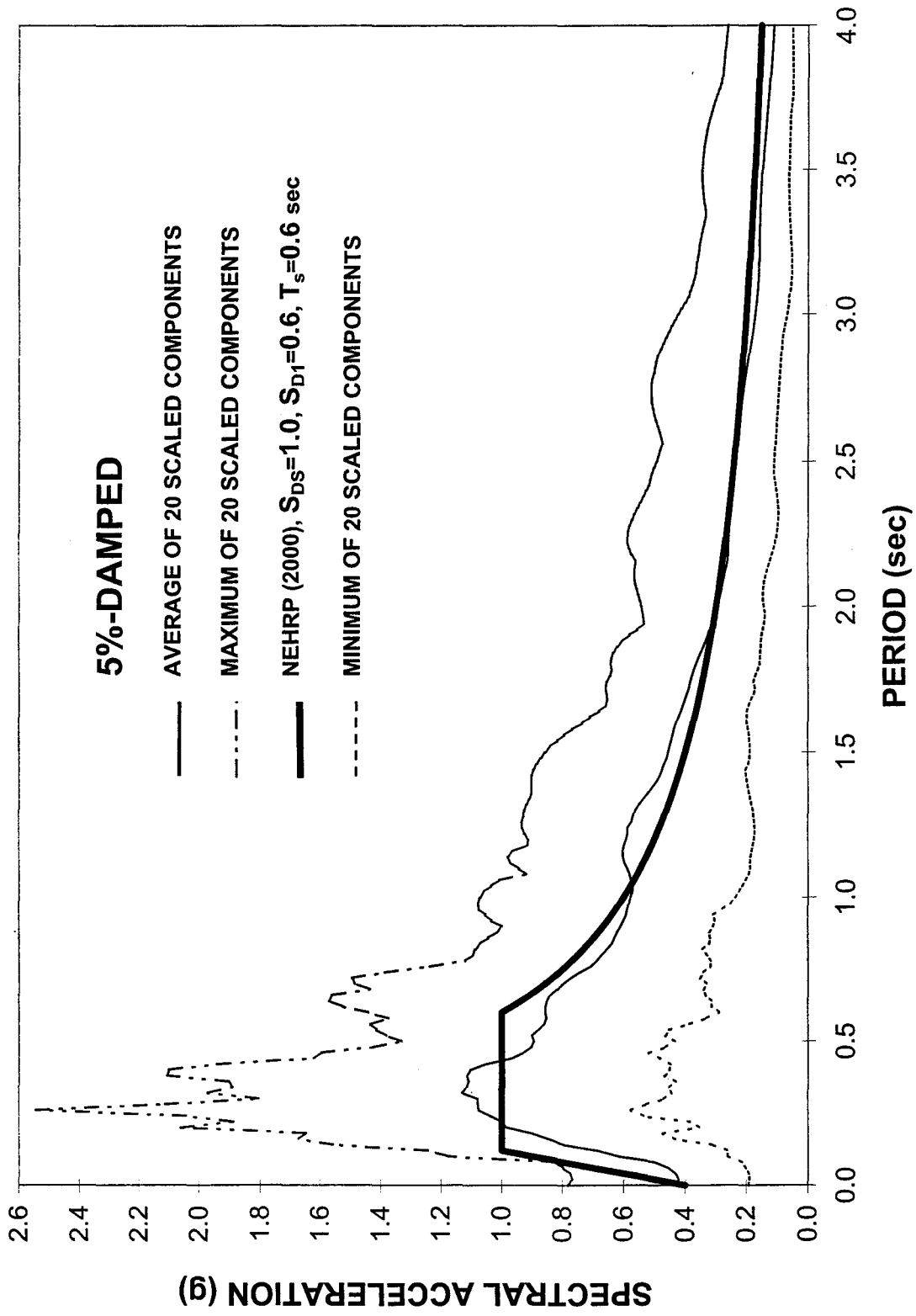
FIGURE 3-1 Maximum, Average and Minimum Spectral Acceleration Values of Scaled Motions

27
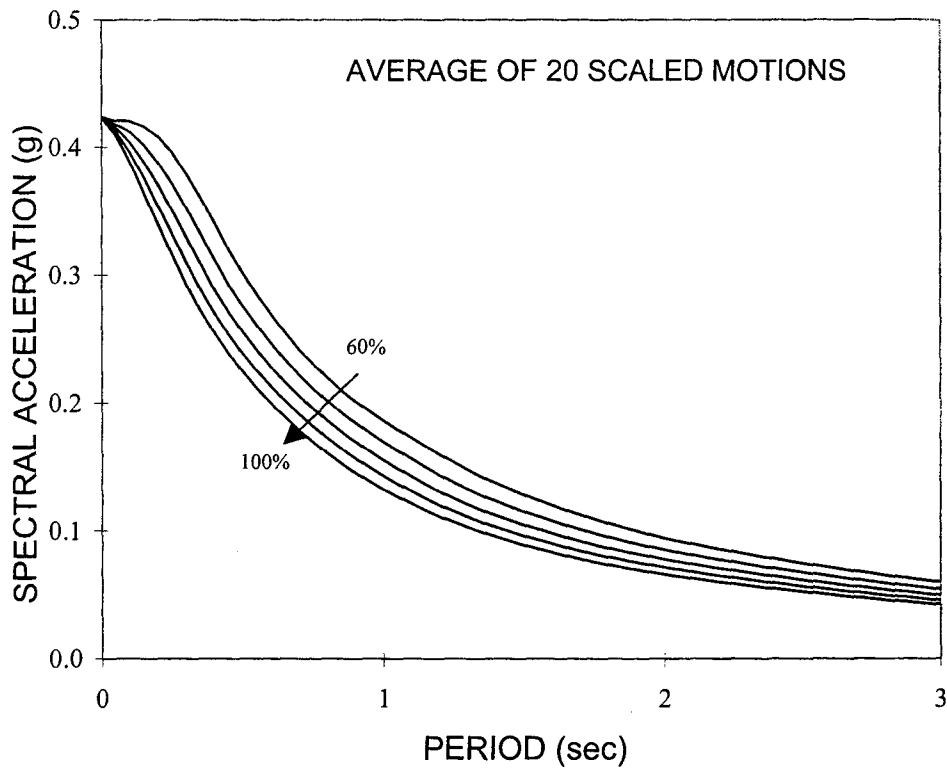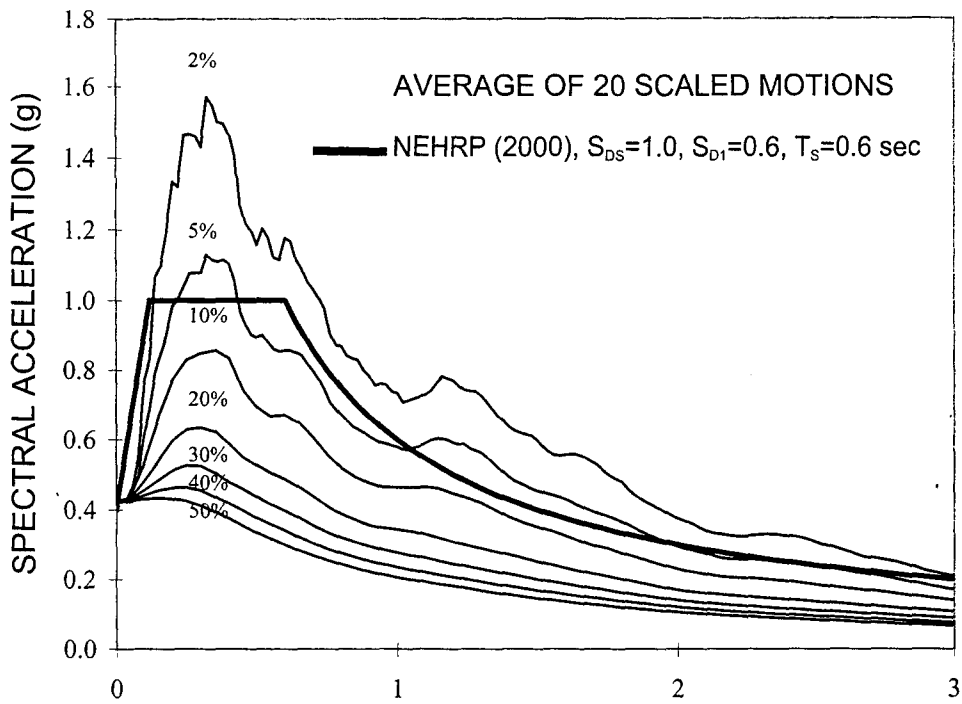
FIGURE 3-2 Average Spectra of Acceleration for Damping in the Range of 2 to
100-Percent of Critical
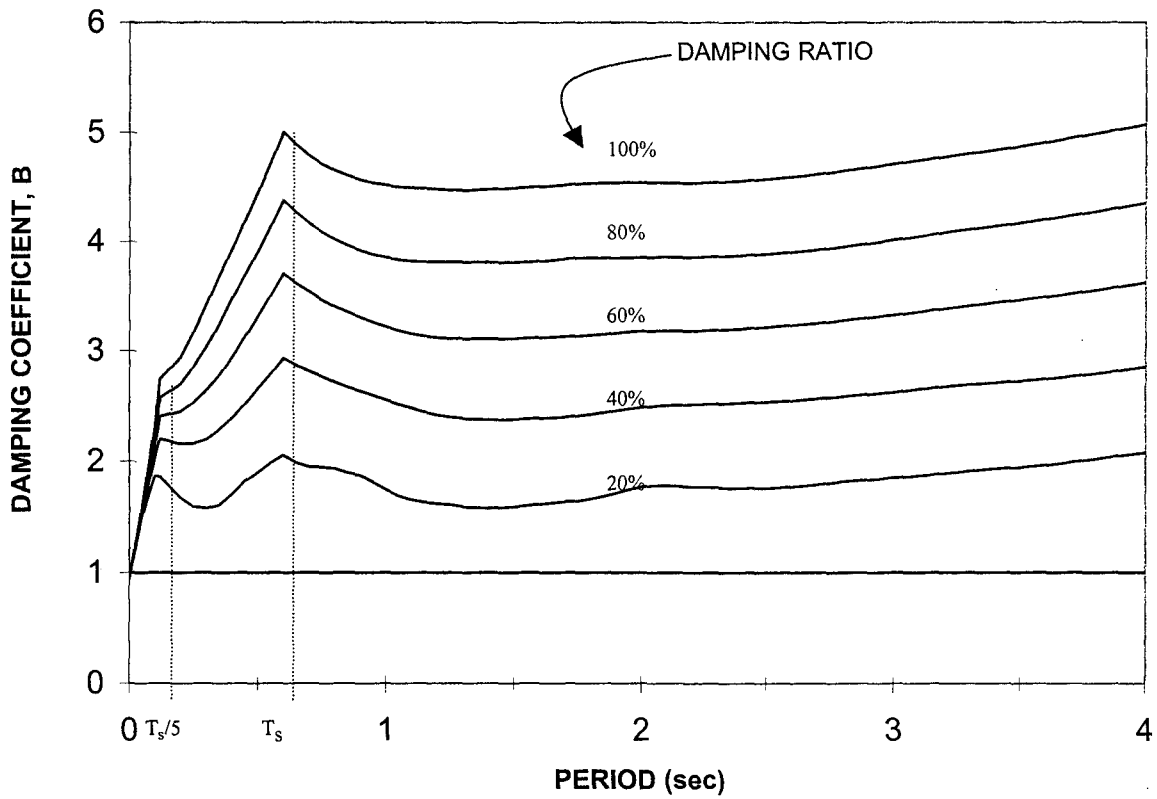
FIGURE 3-3 Calculated Damping Coefficient as Function of Period
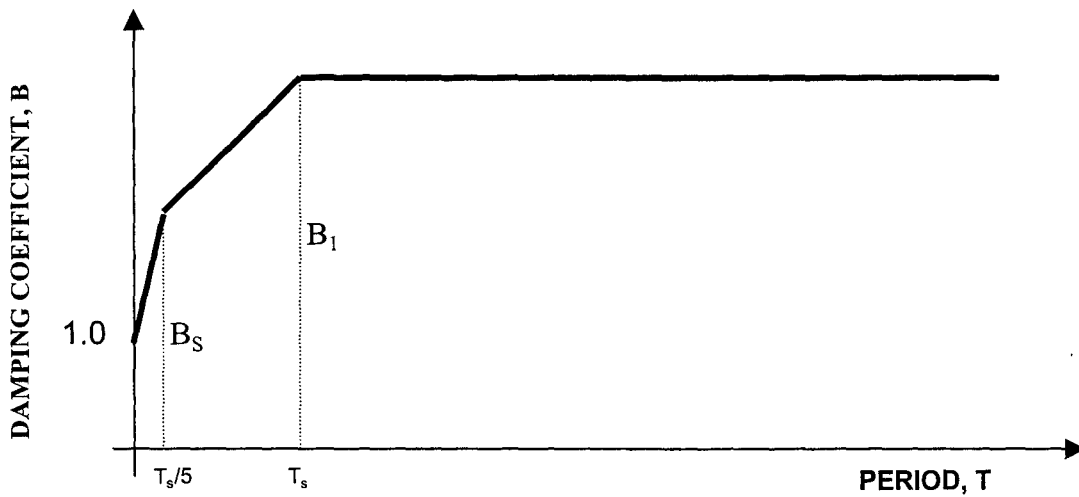
FIGURE 3-4 Proposed Relation of Damping Coefficient vs Period
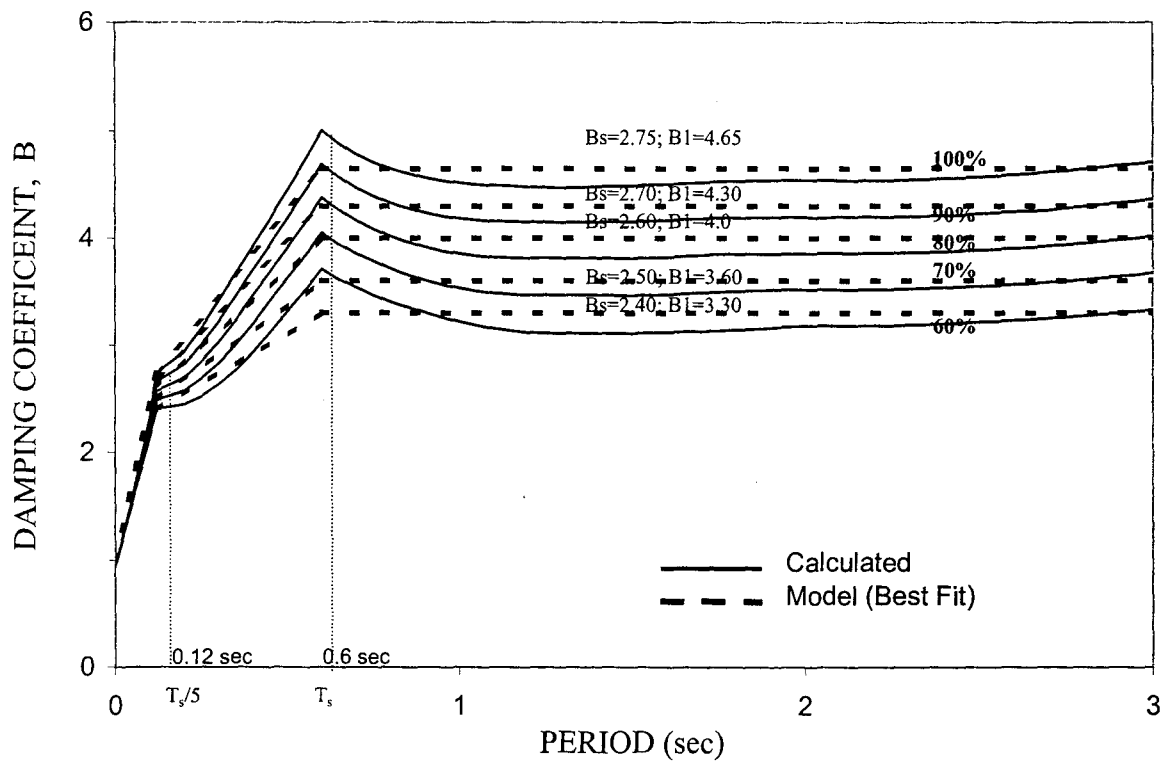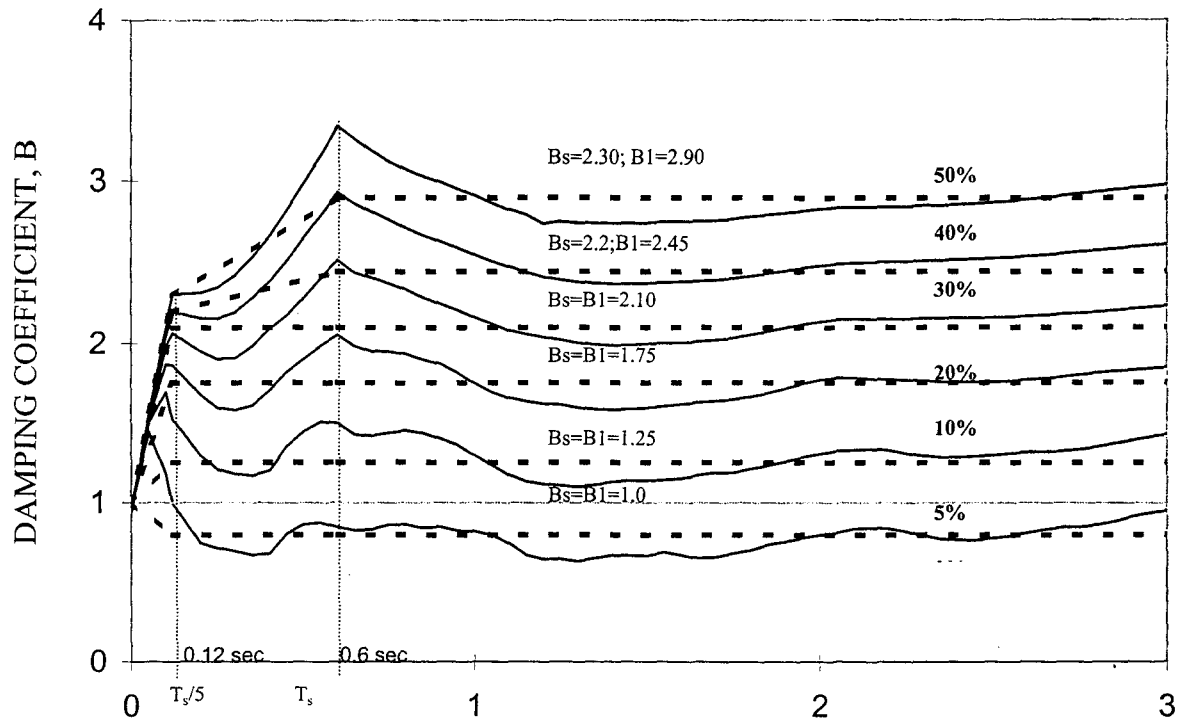
FIGURE 3-5   Comparison of Calculated Damping Coefficient to Proposed Model (Best Fit)

SECTION 4

EVALUATION OF SIMPLIFIED METHODS OF ANALYSIS OF YIELDING SINGLE-DEGREE-OF-FREEDOM SYSTEMS WITH ENERGY DISSIPATION DEVICES

4.1 Introduction

Simplified methods of analysis of structures with energy dissipation systems are based on several approximations. An important approximation is the representation of the yielding structure by an equivalent linear elastic, viscously damped single-degree-of-freedom system. The capability of such an approximation to produce realistic estimates of the peak dynamic response has been the subject of many studies (e.g, Iwan and Gates, 1979a and 1979b; Tsopelas et al., 1997; Chopra and Goel, 1999). These studies concentrated on yielding structures without damping systems and assessed the accuracy of various approximate methods in estimating the peak displacement response. Exception has been the study of Tsopelas et al.(1997) which included structures with linear viscous damping systems.

The study reported in this section extends the work of Tsopelas et al.(1997) to include nonlinear viscous and hysteretic damping systems and assesses the accuracy of Method 2 of FEMA (1997) in predicting the peak displacement, velocity and acceleration responses of single-degree-of-freedom systems. Note that by concentrating on single-degree-of-freedom systems, the application of Method 2 did not require to perform pushover analysis and to account for the contribution of higher modes to the dynamic response. These two steps may also be sources of significant errors. The contribution of these steps of the analysis to the total error is investigated in Section 8 where multi-story buildings with damping systems are analyzed.

Method 2 of FEMA (1997) requires, for single-degree-of-freedom systems, estimation of the peak displacement, calculation of the effective (secant) stiffness or equivalently the effective period, and the effective damping at the peak displacement, calculation of the peak displacement as the intersection of the capacity and demand curves, and iteration until convergence. Details of the calculation of the effective stiffness and effective damping are presented in Section 4.3 for

31

structures with damping systems consisting of linear viscous, nonlinear viscous and yielding damping devices. Further details are presented in Section 7 where the calculation of the effective properties is derived for multi-degree-of-freedom systems. Moreover, this section presents methodologies for improved prediction of the maximum velocity and presents the derivation of revised load combination factors (factors CF_1 and CF_2 in FEMA 1997) for calculating the maximum acceleration in viscously damped structures. The revised load combination factors account for inelastic action in the structural system and nonlinear viscous behavior.

Among the studies of evaluation of simplified methods of analysis the one of Chopra and Goel (1999) presented a bleak view of these simplified methods of analysis despite evidence to the contrary presented in the earlier study of Tsopelas et al. (1997). Herein the approach of Tsopelas et al. (1997) is utilized to extend the evaluation study to nonlinear viscous and hysteretic damping systems, and to assess the accuracy of improved methodologies for predicting peak velocities and peak accelerations. The results of this study are extensively presented in Gomez (2000), whereas herein only results in condensed form are presented.

4.2 Non-Linear Time History Analysis

4.2.1 General Description

Non-linear time history analysis of single-degree-of-freedom inelastic systems with damping devices were performed by numerically integrating the equation of motion:

$$m\ddot{u}(t) + F_D(t) + \frac{4\pi\beta_i m\dot{u}(t)}{T_{eff}} + F_F(t) = -ma_g(t) \tag{4-1}$$

where m is the mass, $\dot{u}$ is the relative velocity, $\ddot{u}$ is the relative acceleration, a_g is the ground acceleration, T_{eff} is the effective (or secant) period, β_i is the inherent damping ratio, F_D is the force from damping devices, and F_F is the force from inelastic structural system.

Equation (4-1) is basically identical to the one utilized by Tsopelas et al.(1997) except that the forms of the damping force F_D and structural system force F_F are different. Key to this equation is the description of inherent damping, which is described as linear viscous with

32

damping ratio equal to β_i. This ratio is defined with respect to the effective (or secant) stiffness K_{eff} of the structure (equal to the peak restoring force divided by the peak displacement). The effective (or secant) period in (4-1) is given by:

$$T_{eff} = 2\pi \sqrt{\frac{m}{K_{eff}}} \qquad (4\text{-}2)$$

All analyses were performed with β_i equal to 0.05. Equation (4-1) was numerically integrated using an adaptive predictor-corrector integration scheme and a linear interpolation scheme for the ground acceleration input (Tsopelas at al., 1997).

4.2.2 Description of Structural System Behavior

Two types of structural system behavior were considered. The first was smooth perfect bilinear hysteretic behavior (without deterioration of any kind or P-Δ effects) as depicted in Figure 4-1 and described by (Tsopelas et al., 1997) using:

$$F_F = \alpha \frac{F_y}{D_y} u + (1-\alpha) F_y Z_F \qquad (4\text{-}3)$$

$$D_y \dot{Z}_F + 0.5 |\dot{u}| Z_F |Z_F|^{\eta-1} + 0.5 \dot{u} |Z_F|^{\eta} - \dot{u} = 0 \qquad (4\text{-}4)$$

where $|.|$ stands for the absolute value, Z_F is a dimensionless variable and η is a dimensionless parameter. In this study, η was set equal to 5.0.

The perfect bilinear hysteretic system represents the best possible behavior of a yielding system. The opposite to this (but still without deterioration of either strength or stiffness) is a system that lacks the ability to dissipate energy. Such a system was analyzed by modeling it as a bilinear elastic system having the force-displacement relation depicted in Figure 4-1. This relation is mathematically described by

33

$$F_F = \begin{cases} K_1 u, \ |u| < D_1 \\[2ex] \dfrac{(K_2 - K_1)(u - D_1)^2}{2(D_2 - D_1)} \mathrm{sgn}(u) + K_1 u, \ D_1 \leq |u| \leq D_2 \\[2ex] \dfrac{(K_1 - K_2)(D_1 + D_2)}{2} + \mathrm{sgn}(u) + K_2 u, \ |u| \geq D_2 \end{cases} \qquad (4\text{-}5)$$

Note that this mathematical relation is smooth with transition points (from linear to nonlinear behavior) at displacements D_1 and D_2, which were selected to be at $0.7D_y$ and $1.3D_y$, respectively. The smoothness of the force-displacement relation, as expressed by the fact that the derivative of F_F with respect to u is continuous, facilitates numerical integration.

4.2.3 Description of Viscous Damping System

Viscous damping systems were modeled as having either linear or non-linear behavior. That is, for linear viscous behavior

$$F_D = C\dot{u} \qquad (4\text{-}6)$$

and

$$F_D = C_N \, |\dot{u}|^a \ sgn(\dot{u}) \qquad (4\text{-}7)$$

for non-linear viscous behavior. In (4-6) and (4-7) C and C_N are coefficients, $\dot{u}$ is the relative velocity and a is the damping exponent which was set equal to 0.5 in this study.

4.2.4 Description of Yielding Damping System

Yielding damping systems were modeled with smooth elasto-plastic behavior described by

$$F_D = F_d Z_D \qquad (4\text{-}8)$$

$$D_{yd}\dot{Z}_D + 0.5\,|\dot{u}|\,Z_D\,|Z_D|^{\eta-1} + 0.5\dot{u}\,|Z_D|^{\eta} - \dot{u} = 0 \qquad (4\text{-}9)$$

where Z_D is a dimensionless variable, η is equal to 5, and F_{yD} and D_{yD} are the yield force and yield displacement of the damping system, respectively.

4.2.5 Ground Motions used in the Time History Analysis

The 20 scaled horizontal components of the ten earthquakes listed in Table 3-2 were used in this study. The selection and scaling of these motions is presented in Tsopelas et al. (1997).

4.3 Analyzed Systems

The formulations of the systems analyzed in this report were described in Section 4.2. Figure 4-2 illustrates the force-displacement relations of the analyzed systems and identifies the parameters in the description of these systems. Each of these systems is characterized by the force-displacement relation of the structural frame exclusive of the damping devices (shown on the left column of Figure 4-2). Note that A_y represents the acceleration at yield of the single-degree-of-freedom system. It is convenient to describe the behavior of the structural frame in terms of the following parameters:

(a)   Elastic period, T_e:

$$T_e = 2\pi \left(\frac{D_y}{A_y} \right)^{1/2}$$

(4-10)

(b)   Post-yielding to elastic stiffness ratio: α

(c)   Ductility-based portion of the R-factor

$$R_\mu = \frac{S_{ae}}{A_y}$$

(4-11)

where S_{ae} is the spectral acceleration at period T_e and damping ratio of 5% (elastic conditions).

Each system analyzed in this study had inherent viscous damping of 5-percent as described in Section 4.2.1.

4.3.1 Bilinear Hysteretic System with Linear Viscous Damping Devices

The bilinear hysteretic system with linear viscous damping devices was originally analyzed by Tsopelas et al. (1997). Additional analyses were performed in this study for a wider range of values of period T_e and for calculating velocities which were omitted in the earlier study. This system is described by the parameters presented in Section 4.3 and the added viscous damping ratio, β_V, under elastic conditions:

$$\beta_V = \frac{CT_e}{4\pi m} \tag{4-12}$$

The parameters used in the analysis of this system are presented in Table 4-1.

4.3.2 Bilinear Hysteretic System with Nonlinear Viscous Damping Devices

The bilinear hysteretic system with nonlinear viscous damping devices is characterized by the parameters presented in Section 4.3 and two additional parameters describing the nonlinear viscous damping devices: exponent a and coefficient C_N (see Section 4.2.3 and equation 4-7). It is inconvenient to use parameter C_N and a dimensionless parameter with a physical significance similar to that of the damping ratio for linear viscous damping systems (eq. 4-12) was used instead. This parameter is defined as the effective damping ratio under elastic conditions

$$\beta_V = \frac{C_N \lambda}{2\pi m} D^{a-1} \left(\frac{2\pi}{T_e} \right)^{a-2} \tag{4-13}$$

$$\lambda = 4 \cdot 2^a \frac{\Gamma^2 (1 + a/2)}{\Gamma(2 + a)} \tag{4-14}$$

where D is the maximum displacement (drift) and Γ is the gamma function. Equation (4-13) is based on the effective damping ratio being

$$\beta = \frac{W_D}{4\pi W_s} \tag{4-15}$$

where W_D is the energy dissipated per cycle at period T_e and displacement D, and W_s is the strain energy at amplitude D. An expression for W_D has been derived in Constantinou et al. (1998) and utilized in FEMA (1997):

$$W_D = \lambda C_N D^{1+a} \left(\frac{2\pi}{T_e}\right)^a \tag{4-16}$$

Values of parameter λ are presented in Table 4-2. It may be seen that for linear viscous devices for which a equals 1.0, λ equals 3.142 (=π) and (4-13) reduces to (4-12).

The effective damping in (4-13) depends on the amplitude of displacement D as a result of the nonlinear behavior of the viscous devices. In general, iteration is needed to obtain the value of the effective damping given the properties of the structural frame and damping devices, and the characteristics of the excitation. However, herein the value of β_V is selected (say 0.15) and used for the calculation of the corresponding value of C_N. Given the period T_e and total damping under elastic conditions $(\beta_V + \beta_i)$, displacement D is calculated and then used in (4-13) and (4-14) to calculate C_N for the application of the simplified method of analysis and the time history analysis. The values of the parameters used for the studies described in this report are presented in Table 4-1.

4.3.3 Bilinear Elastic System with Linear Viscous Damping Devices

The bilinear elastic system with linear viscous damping devices is characterized by the elastic period T_e (eq. 4-12), the ductility-based R-factor R_μ (eq. 4-11), the viscous damping ratio β_V (eq. 4-10), the stiffness ratio α (=0.05) and the inherent damping ratio β_i (=0.05). The values of the parameters used for the studies described in this report are presented in Table 4-3.

4.3.4 Bilinear Hysteretic System with Yielding Damping Devices

The bilinear hysteretic system with yielding damping devices is characterized by the elastic period, T_e, in the absence of the yielding damping devices (eq. 4-10), the ductility-based portion

of the R-factor R_μ (eq. 4-11), the stiffness ratio α (=0.05), the inherent damping ratio β_i (=0.05) and the following two additional parameters:

(1) Ratio of the elastic stiffness of the structure inclusive of the damping devices to the elastic stiffness of the structure exclusive of the damping devices (see Fig. 4-3)

$$\frac{K_t}{K_f} = \frac{\dfrac{F_d}{D_{yd}} + \dfrac{F_y}{D_y}}{\dfrac{F_y}{D_y}} = 1 + \frac{F_d D_y}{F_y D_{yd}} \tag{4-17}$$

where F_y and D_y are the yield strength and yield displacement of the structural frame exclusive of the damping system, respectively, K_f is the elastic stiffness of the structural fame exclusive of the damping system (= F_y/D_y), F_d and D_{yd} are the yield strength and yield displacement of the damping system, respectively, and K_t is the elastic stiffness of the frame inclusive of the damping system.

(2) Ratio of the strength of the damping devices F_d to the strength of the structural frame F_y, F_d / F_y.

The values of the parameters used in this study are presented in Table 4-4.

4.4 Application of Simplified Method of Analysis for Bilinear Hysteretic System with Linear Viscous Damping Devices

Given values of the parameters T_e, R_μ, α, β_i, and β_V (see Section 4.3 and Table 4-1) and the response spectrum, the behavior of the system is completely defined. In the simplified method of analysis, the peak displacement D is assumed (and presumed larger than D_y) and the effective period, T_{eff}, and effective damping, β_{eff}, are calculated:

$$T_{eff} = 2\pi \left(\frac{D}{A}\right)^{1/2} \tag{4-18}$$

$$\beta_{eff} = \beta_i + \beta_V \frac{T_{eff}}{T_e} + \frac{2q_H\left(A_y D - A D_y\right)}{\pi A D} \qquad (4\text{-}19)$$

where

$$D_y = \frac{S_{ae} T_e^2}{4\pi^2 R_\mu} \qquad (4\text{-}20)$$

Note that (4-19) is based on (4-15) and includes the inherent damping, the component due to inelastic action (presumed perfectly hysteretic) and the viscous component. Moreover quantity A is defined in Figure 4-2 and represents the acceleration at maximum displacement:

$$A = A_y + \alpha \frac{A_y}{D_y}\left(D - D_y\right) \qquad (4\text{-}21)$$

It should be noted that the component of the effective damping in (4-19) due to yielding of the structural frame includes the hysteretic loop adjustment factor q_H which is utilized to reduce the area under the perfect bilinear hysteretic loop to better represent the behavior of the real structural systems. However, the systems studied in this report have perfect bilinear hysteresis behavior a value of q_H equal to 1.0 has been used.

4.5 Application of Simplified Method of Analysis for Bilinear Hysteretic System with Nonlinear Viscous Damping Devices

The behavior of this system is defined by parameters T_e, R_μ, α, β_i, β_V and a (see Section 4.3 and Table 4-1) and the response spectrum. The peak displacement D is assumed and the effective period is calculated using (4-18), (4-20) and (4-21). The effective damping is calculated using (4-15):

$$\beta_{eff} = \beta_i + \beta_V \left(\frac{T_{eff}}{T_e}\right)^{2-a} + \frac{2q_H\left(A_y D - A D_y\right)}{\pi A D} \qquad (4\text{-}22)$$

Note that for a equal to 1.0 (linear viscous damping devices), (4-22) reduces to (4-19).

4.6 Application of Simplified Method of Analysis for Bilinear Elastic System with Linear Viscous Damping Devices

This system exhibits all the characteristics of the bilinear hysteretic system with linear viscous damping devices except for the damping contribution due to inelastic action in the structure. Accordingly, (4-18), (4-20) and (4-21) hold but the effective damping is given by

$$\beta_{eff} = \beta_i + \beta_V \frac{T_{eff}}{T_e} \tag{4-23}$$

4.7 Application of Simplified Method of Analysis for Bilinear Hysteretic System with Yielding Damping Devices

The behavior of this system is described by parameters T_e, R_μ, α, β_i, K_t / K_f and F_d / F_y (see Section 4.3 and Table 4-4). The yield displacement of the structural frame, D_y, is determined from (4-20) and the yield displacement of the yielding damping devices (see Figure 4-2) is determined from:

$$D_{yd} = \frac{D_y}{\left(\dfrac{K_t}{K_f} - 1\right)} \frac{F_d}{F_y} \tag{4-24}$$

It is assumed hereafter that $F_d \le F_y$ and that $D_{yd} \le D_y$ which are both reasonable assumptions for the implementation of yielding damping systems in flexible building frames. The combined structural frame and yielding damping device lateral force-displacement relation is tri-linear as depicted in Figure 4-3. Consider now that the peak displacement D is larger than D_y, as shown in Figure 4-3. The effective period is then given by

$$T_{eff} = 2\pi \left(\frac{D}{A + A_d}\right)^{1/2} \tag{4-25}$$

where A is given by (4-21). The effective damping is given by

$$\beta_{eff} = \beta_i \left(\frac{A}{A + A_d} \right)^{1/2} + \frac{2q_H \left(A_y D - A D_y \right) + 2A_d \left(D - D_{yd} \right)}{\pi \left(A + A_d \right) D} \qquad (4\text{-}26)$$

Note that in this formulation, the inherent damping of the combined system is reduced due to the increase in stiffness under elastic conditions. It is presumed in this case that the damping system does not dissipate any energy for displacements less than D_{yd} so that T_{eff} in (4-1) is calculated on the basis of the assumption that $A_d = 0$. It is also presumed that the yielding damping system has perfect bilinear hysteretic behavior.

4.8 Calculation of Maximum Velocity and Acceleration in Systems with Viscous Damping Devices

The simplified analysis method described in Sections 4.4 to 4.7 is iterative since it is based on an assumed value of displacement D, calculation of the effective period and effective damping, calculation of the displacement using the response spectrum after modification for increased damping, and comparison of the calculated and assumed values of displacement. A limit on the calculated displacement, not being less than the displacement calculated for elastic conditions, is then enforced. The results of this analysis are values of the maximum displacement D and the acceleration A (or $A + A_d$) at maximum displacement. In addition, for systems with viscous damping devices the maximum velocity is needed for the calculation of the peak damping force. Moreover, the maximum acceleration, which is larger than A and occurs at some displacement less than D, must be calculated.

The maximum velocity is taken in this method as the pseudo-velocity, that is:

$$V = \left(\frac{2\pi}{T_{eff}} \right) D \qquad (4\text{-}27)$$

The maximum acceleration can be determined by the procedure described by Tsopelas at al. (1997) and incorporated in FEMA (1997). A more general procedure for nonlinear viscous damping devices and yielding structures is presented below.

41

The procedure for a linear elastic structure with a nonlinear viscous damping device is described first. It is assumed that the structure of stiffness K and mass m undergoes harmonic vibration at its natural frequency ω_n and amplitude D:

$$u = D\cos\omega_n t \tag{4-28}$$

with velocity

$$\dot{u} = -D\omega_n \sin\omega_n t \tag{4-29}$$

The combined restoring and damping force is given by

$$F = ku + C_N |\dot{u}|^a \operatorname{sgn}(\dot{u}) \tag{4-30}$$

Equation (4-30) may be written in the form

$$\frac{F}{m\omega_n^2 D} = -\frac{2\pi}{\lambda}\beta_V \sin^a \omega_n t + \cos\omega_n t \tag{4-31}$$

in which λ is given by (4-14), β_V is given by (4-13), and

$$\omega_n = \left(\frac{k}{m}\right)^{1/2} = \frac{2\pi}{T_e} \tag{4-32}$$

Equation (4-31) was derived using (4-28) and (4-29). The velocity is negative during the considered cycle of motion as shown in Figure 4-4.

The maximum value of F (and acceleration) occurs at a time t^* when the derivative of the right hand side of (4-31) with respect to time is zero. This results in the following

$$\frac{\sin^{2-a}\omega_n t^*}{\cos\omega_n t^*} = -\frac{2\pi a\beta_V}{\lambda} \tag{4-33}$$

This equation cannot be exactly solved for time t^* except for the case of linear viscous device ($a=1$). However, an approximate solution can be derived assuming that (see Fig. 4-4)

42

$$\omega_n t^* = \pi - \delta \qquad (4\text{-}34)$$

in which δ is a small phase lag as shown in Figure 4-4. This assumption is good when a is small (e.g., $\delta = 0$ when $a = 0$) and the phase lag can be calculated as

$$\delta = \left(\frac{2\pi a \beta_V}{\lambda}\right)^{\frac{1}{2-a}} \qquad (4\text{-}35)$$

For linear viscous damping devices, the phase lag δ may be calculated exactly as

$$\delta = \tan^{-1}\left(2\beta_V\right) \qquad (4\text{-}36)$$

Note that (4-35) provides a good approximation even in the case of linear viscous damping devices. For such a case, $a = 1$ and $\lambda = \pi$ so that (4-35) yields $\delta = 2\beta_V$. By comparison to (4-36), use of (4-35) results in an error of about 3% for $\beta_V = 0.15$ and an error of about 7% for $\beta_V = 0.25$.

The maximum acceleration is determined by substituting (4-34) and (4-35) into (4-31):

$$A_{max} = A\left(CF_1 + \frac{2\pi\beta_V}{\lambda}CF_2\right) \qquad (4\text{-}37)$$

where

$$CF_1 = \cos\delta \qquad (4\text{-}38)$$

and

$$CF_2 = \left(\sin\delta\right)^a \qquad (4\text{-}39)$$

Parameters CF_1 and CF_2 are load combination factors used to calculate the response at the time of maximum acceleration by combining the effects at the instants of maximum drift and maximum velocity.

43

Equation (4-38) describes the contribution of the restoring force to the maximum acceleration. It is valid for elastic behavior, that is, for $D < D_y$. As inelastic action occurs, the value of CF_1 increases and eventually obtains the maximum value of unity. This is recognized when considering that the maximum acceleration occurs when $u = \cos\delta \cdot D$ as seen in Figure 4-4. Moreover, the effective viscous damping ratio increases with inelastic action. Accordingly, it can be shown that

$$A_{max} = A\left(CF_1 + \frac{2\pi\beta_{veff}}{\lambda}CF_2\right) \tag{4-40}$$

where

$$\begin{array}{lll}
\text{If } D < D_y, & & CF_1 = \cos\delta \\
\text{If } D > D_y & \text{and } \cos\delta \cdot \mu < 1, & CF_1 = \cos\delta \cdot \mu \\
\text{If } D > D_y & \text{and } \cos\delta \cdot \mu \geq 1, & CF_1 = 1.0
\end{array} \tag{4-41}$$

$$\beta_{veff} = \beta_i + \beta_V\left(\frac{T_{eff}}{T_e}\right)^{2-a} \tag{4-42}$$

$$\mu = \frac{D}{D_y} \tag{4-43}$$

and CF_2 is still given by (4-39). Parameter δ is computed from (4-35) with β_V replaced by β_{veff}. Equations (4-39) and (4-41) have been used to calculate the values of the force coefficients that are tabulated in NEHRP (2000).

4.9 Results of Simplified Method of Analysis and Comparison to Results of Nonlinear Time History Analysis

The response of each analyzed system was determined using the simplified method of analysis described in Sections 4.4 to 4.8. The response spectrum with parameters $S_{DS} = 1.0$, $S_{D1} = 0.6$ and $T_s = 0.6\,\text{sec}$ was utilized together with the "conservative" values of the damping coefficient of Table 3-3. The spectra for these parameters and for damping ratio up to 100% are shown in

Figure 2-4. Figures 4-5 to 4-13 present a comparison of the results of time history analysis (average of 20 values) and the results of the simplified method of analysis. The graphs compare the calculated peak displacement, peak velocity and peak acceleration (including the viscous component) by plotting the results of the time history analysis on the vertical axis against the results of the simplified method of analysis on the horizontal axis. Points located below the diagonal "45-degree" line indicate conservatism in the prediction of the simplified method of analysis.

These figures clearly demonstrate that:

(a)   The simplified methods of analysis produce exact or conservative estimates of the peak displacement and peak acceleration.

(b)   The simplified method of analysis underpredicts the peak velocities for structures with a large effective period (say $T_{eff} > 1.5$ sec) but overpredicts the peak velocity for structures with a moderate-to-short effective period (say $T_{eff} < 1.0$ sec). The differences are as large as 50% for large effective period and as much as 100% for short effective period.

The results are consistent with the use of pseudo-velocity as a predictor of the maximum relative velocity (Chopra, 1995; Constantinou et al., 1998). The greatest errors occurred for framing systems with low ratio of post-elastic stiffness to elastic stiffness (α) and large ductility-based portion of the R-factor (R_μ). It will be demonstrated later herein that structures with damping systems designed on the basis of NEHRP (2000) typically exhibit nearly elastic behavior for the design basis earthquake. Under such conditions, the error in predicting the relative velocity by using the pseudo-velocity is relatively small and acceptable for design purposes.

4.10   Correction Factors for Velocity

It is worthy of investigating the likelihood that a simple method is developed for obtaining better estimates of the relative velocity. Sadek et al. (1999) and Pekcan et al. (1999) proposed that the relative velocity is determined as the product of pseudo-velocity and a correction factor. The correction factor was determined in these studies as the ratio of the exact relative velocity of single-degree-of-freedom to the pseudo-velocity, which was calculated as the exact displacement

45

times the natural frequency of the system. The two studies primarily differed in the selection of the earthquake records used with (a) Sadek et al. utilizing 72 horizontal components of Californian earthquakes including some with near-fault characteristics, and (b) Pekcan et al. utilizing 36 horizontal components of Californian, Japanese and other earthquakes, of which most had near-fault characteristics with peak ground velocities in the range of 1 to 1.8 m/s. Moreover, Pekcan et al. (1999) scaled the earthquake motions to have a peak ground velocity of 1 m/sec, which is somehow similar to the scaling employed by Tsopelas et al. (1997) and in our study. This scaling results in a more balanced contribution of the various earthquake components to the average response.

Values of the correction factor from the study of Sadek et al. (1999) are presented in Table 4-5. The study of Pekcan et al. (1999) utilized least square regression analysis to establish equations for the correction factor. The following equation describes the correction factor CFV for period, T, values in the range of $T_s/5$ to 3 sec. and damping ratio, β, values in the range of 5 to 40-percent, where T_s is the period value at the intersection of the constant acceleration and constant velocity regions of the response spectrum:

$$CFV = \left(\frac{T}{T_s}\right)^{0.455\beta+0.132} \tag{4-44}$$

The availability of a significant number of response-history analysis results for a wide range of parameters for yielding systems in this study facilitated the calculation of improved velocity correction factors. Utilizing results on the exact relative velocity and the pseudo-velocity from the study reported in Section 4.9, revised velocity correction factors were derived and are presented in Table 4-6. Note that these correction factors differ from those of Sadek et al. and Pekcan et al. In the following: (a) the earthquake motions used in either derivation do not contain any with near-fault characteristics, (b) the analyzed systems are nonlinear, (c) the pseudo-velocity is calculated as the product of the peak displacement and the effective frequency, both of which were calculated by approximate means (use of 5-percent damped spectrum, damping coefficient B and the effective period and damping), and (d) the factors extend to values of effective period of 4.0 sec and effective damping of 100-percent.

46

The utility of the correction factors in Tables 4-5 and 4-6, and of equation (4-44) has been investigated by recalculating the velocity in all cases of the present study as the product of pseudo-velocity and the correction factor and interpreting the period in (4-44) and in Table 4-5 as the effective period and the viscous damping ratio in (4-44) and in Table 4-5 as the effective damping. Results are presented in Figures 4-14 to 4-18 where they are compared to results of the time history analysis. Each of these figures contains four graphs in which the vertical axis represents the average value of the results of nonlinear time history analysis on the velocity and the horizontal axis represents the velocity calculated by simplified methods and without and with the use of correction factors. It is apparent that the correction factors reduce the scatter in the data and produce either very conservative results (factors of Sadek et al., 1999) or results of acceptable accuracy (factors of Pekcan et al., 1999 and revised factors of Table 4-6).

4.11 Conclusions

The simplified method of analysis, as described herein including the correction for velocity prediction of either Pekcan et al. (1999) in (4-44) or the revised ones in Table 4-6, produces estimates of the peak displacement, peak velocity and peak acceleration (including the viscous component) which are either conservative or in good agreement with the average of results of nonlinear time history analysis. The simplified method of analysis is not error-free. However, it is simple to apply, it systematically converges and produces results of sufficient accuracy for design purposes.

It should be noted that the presented results were based on the use of damping coefficients (Table 3-3, "conservative" values), which were derived from analyses using earthquake motions that did not include records on very soft soil and records with near-field characteristics. Therefore, the results may not apply in these cases.

TABLE 4-1 Values of Parameters in Study of Bilinear Hysteretic System with Viscous Damping Devices

Elastic Period T_e (second)	0.3, 0.5, 0.7, 1.0, 1.5, 2.0
Ductility-based Portion of R-factor, R_μ	2, 3.33, 5
Post-Elastic to Elastic Stiffness Ratio, α	0.05,0.10,0.25,0.50,1.0 (elastic)
Inherent Damping Ratio, β_I	0.05
Added Viscous Damping Ratio Under Elastic Conditions, β_v	Linear Viscous 0, 0.15, 0.25
	Nonlinear Viscous (a=0.5) 0.15, 0.25

TABLE 4-2 Values of Parameter λ

Exponent a	Parameter λ
0.00	4.000
0.25	3.723
0.50	3.496
0.75	3.305
1.00	3.142 (= π)
1.25	3.000
1.50	2.876
1.75	2.765
2.00	2.667

**TABLE 4-3 Values of Parameters in Study of Bilinear Elastic System
with Linear Viscous Damping Devices**

Elastic Period T_e (second)	0.3, 0.5, 0.7, 1.0, 1.5, 2.0
Ductility-based Portion of R-factor, R_μ	2, 3.33, 5
Post-Elastic to Elastic Stiffness Ratio, α	0.05
Inherent Damping Ratio, β_i	0.05
Added Viscous Damping Ratio under Elastic Conditions, β_v	0, 0.15, 0.25

**TABLE 4-4 Values of Parameters in Study of Bilinear Hysteretic System
with Yielding Damping Devices**

Elastic Period T_e (second)	0.5, 0.7, 1.0, 1.5, 2.0
Ductility-based Portion of R-factor, R_μ	2, 3.33, 5
Post-Elastic to Elastic Stiffness Ratio, α	0.05
Inherent Damping Ratio, β_i	0.05
Stiffness Ratio K_t/K_f	2, 6, 10
Strength Ratio F_d/F_y	0.1, 0.2, 0.3, 0.4, 0.5

Table 4-5 Correction Factor for Velocity (from Sadek et al., 1999)

Period (sec)	Viscous Damping Ratio								
	0.02	0.05	0.10	0.15	0.20	0.30	0.40	0.50	0.60
0.1	0.70	0.63	0.57	0.53	0.51	0.47	0.45	0.43	0.41
0.3	0.96	0.94	0.91	0.88	0.86	0.82	0.79	0.78	0.77
0.5	0.99	0.99	0.99	0.99	0.99	1.00	1.00	1.00	1.00
1.0	1.06	1.08	1.11	1.13	1.15	1.22	1.28	1.32	1.36
1.5	1.13	1.20	1.27	1.31	1.36	1.46	1.54	1.61	1.65
2.0	1.20	1.28	1.39	1.47	1.53	1.63	1.73	1.82	1.90
2.5	1.23	1.33	1.47	1.55	1.64	1.78	1.89	1.99	2.09
3.0	1.39	1.47	1.56	1.64	1.72	1.88	2.02	2.10	2.26
3.5	1.51	1.60	1.70	1.79	1.87	2.01	2.16	2.29	2.42
4.0	1.61	1.74	1.88	2.00	2.09	2.23	2.36	2.50	2.62

Period is interpreted as the effective period and viscous damping ratio is interpreted as the effective damping

TABLE 4-6 Revised Correction Factors

Effective Period (sec)	Effective Damping Ratio									
	0.10	0.20	0.30	0.40	0.50	0.60	0.70	0.80	0.90	1.00
0.3	0.72	0.70	0.69	0.67	0.63	0.60	0.58	0.58	0.54	0.49
0.5	0.75	0.73	0.73	0.70	0.69	0.67	0.65	0.64	0.62	0.61
1.0	0.82	0.83	0.86	0.86	0.88	0.89	0.90	0.92	0.93	0.95
1.5	0.95	0.98	1.00	1.04	1.05	1.09	1.12	1.14	1.17	1.20
2.0	1.08	1.12	1.16	1.19	1.23	1.27	1.30	1.34	1.38	1.41
2.5	1.05	1.11	1.17	1.24	1.30	1.36	1.42	1.48	1.54	1.59
3.0	1.00	1.08	1.17	1.25	1.33	1.42	1.50	1.58	1.67	1.75
3.5	1.09	1.15	1.22	1.30	1.37	1.45	1.52	1.60	1.67	1.75
4.0	0.95	1.05	1.15	1.24	1.38	1.49	1.60	1.70	1.81	1.81
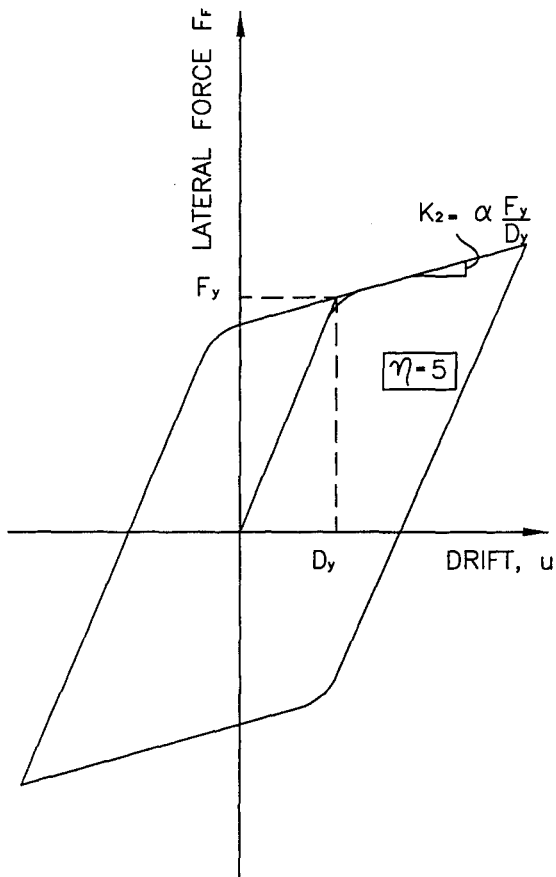
SMOOTH PERFECT BILINEAR
HYSTERETIC SYSTEM
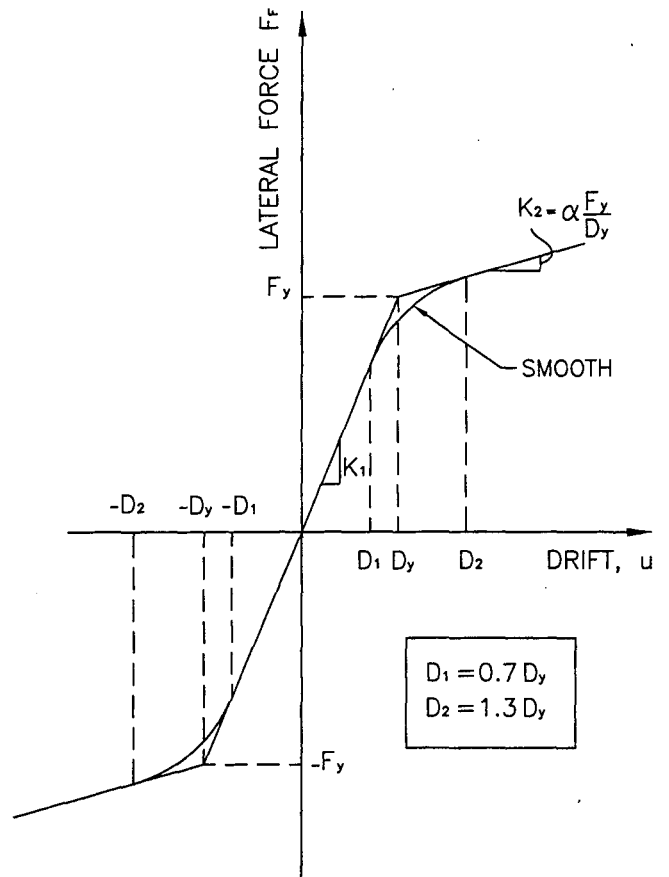
BILINEAR ELASTIC SYSTEM

FIGURE 4-1 Structural System Behavior Considered in this Study

BILINEAR HYSTERETIC SYSTEM WITH VISCOUS DAMPING DEVICES

BILINEAR ELASTIC SYSTEM WITH LINEAR VISCOUS DAMPING DEVICES

BILINEAR HYSTERETIC SYSTEM WITH YIELDING DAMPING DEVICES
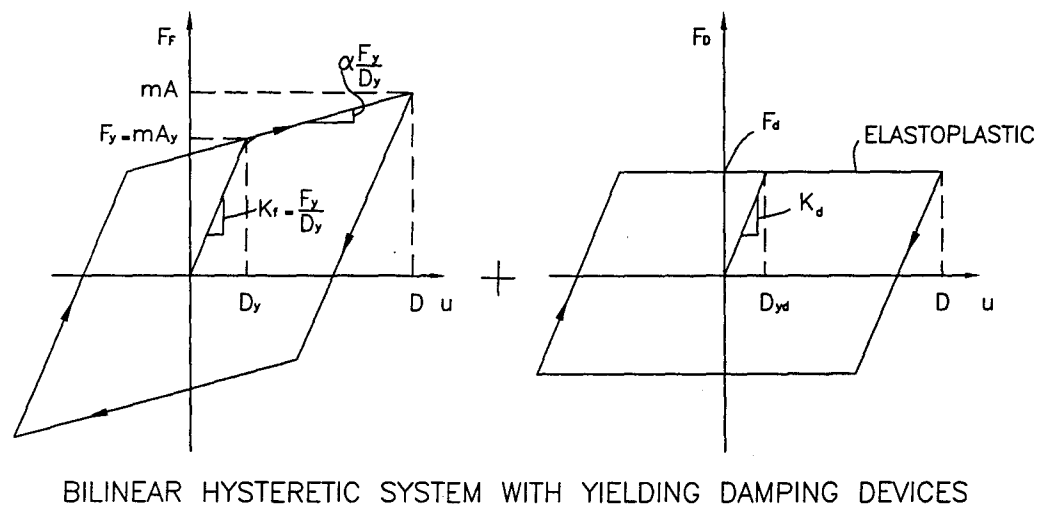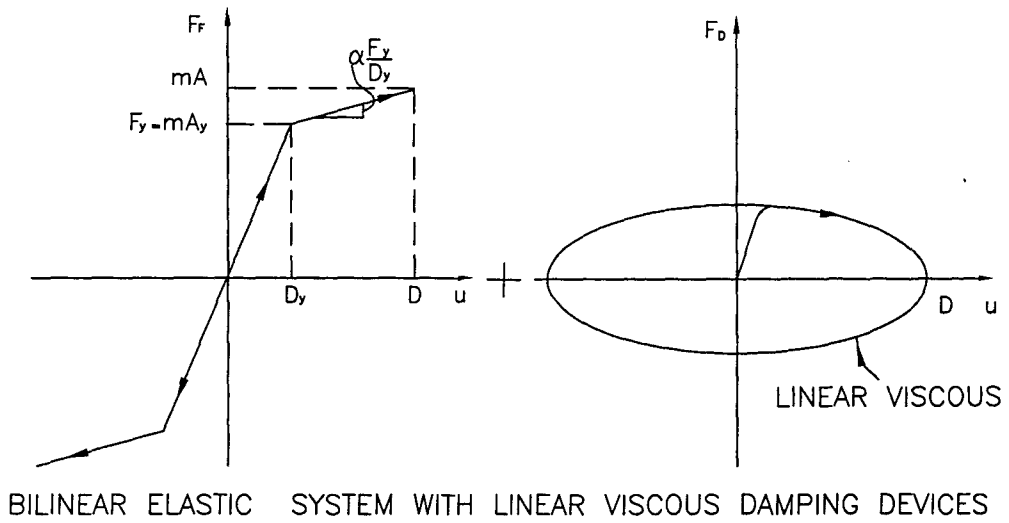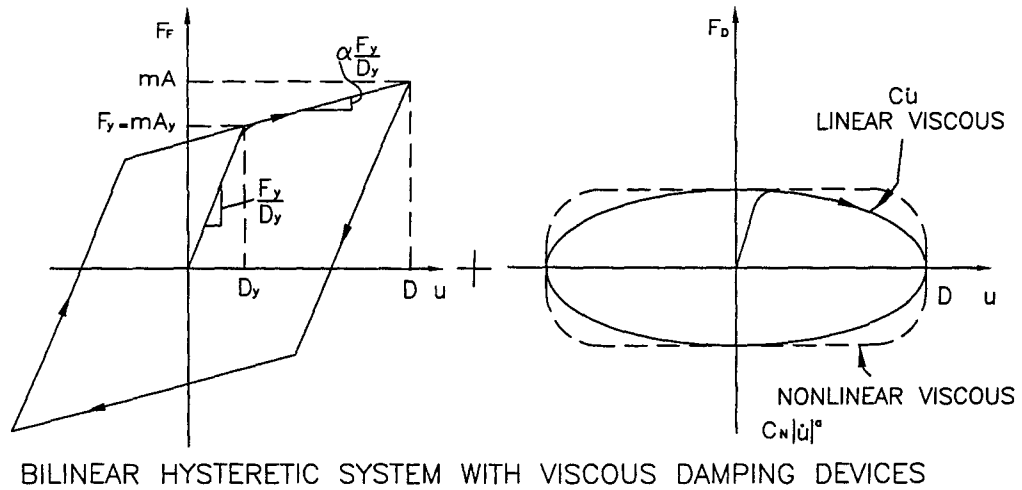
FIGURE 4-2 Illustration of Behavior of Analyzed Systems

52
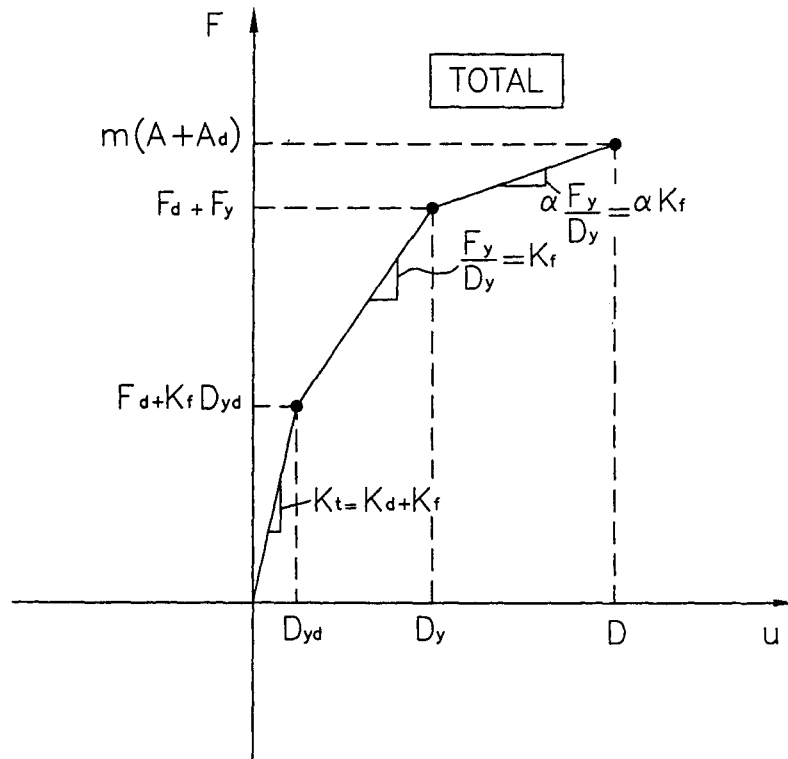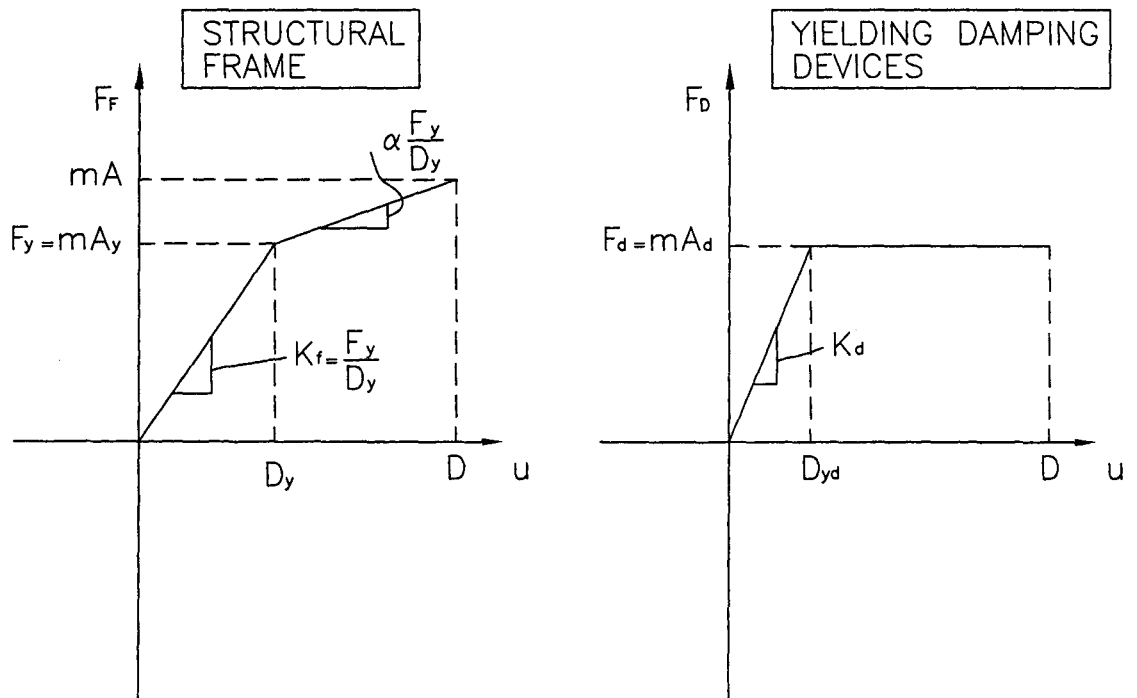
FIGURE 4-3 Behavior of Bilinear Hysteretic System with Yielding Damping Devices

53
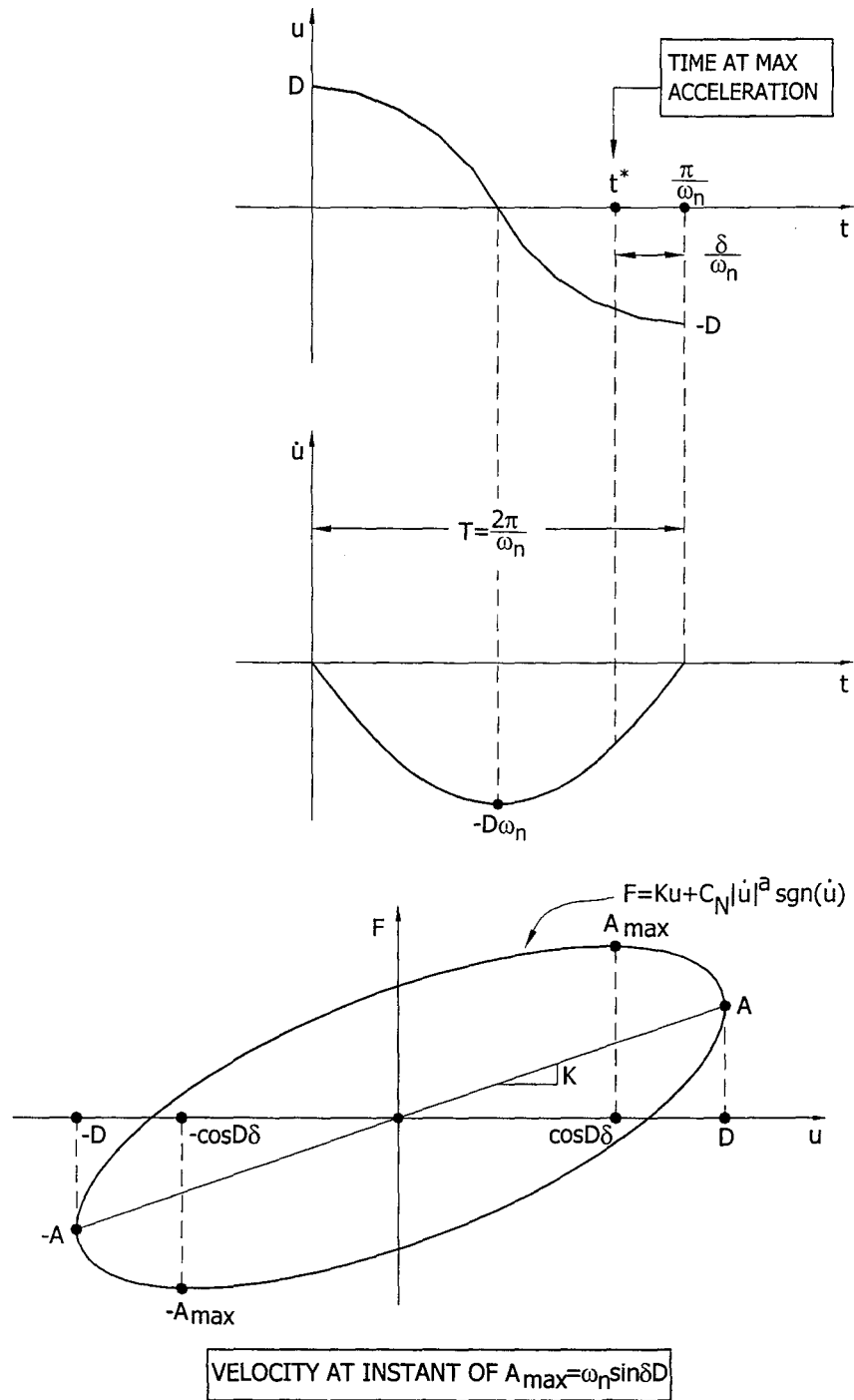
FIGURE 4-4   Harmonic Motion of Structure with Nonlinear Viscous Damping
Device and Force-Displacement Relation

Perfect Bilinear Hysteretic System (α=0.05, 0.15, 0.25, 0.5, 1.0, β_i=0.05)
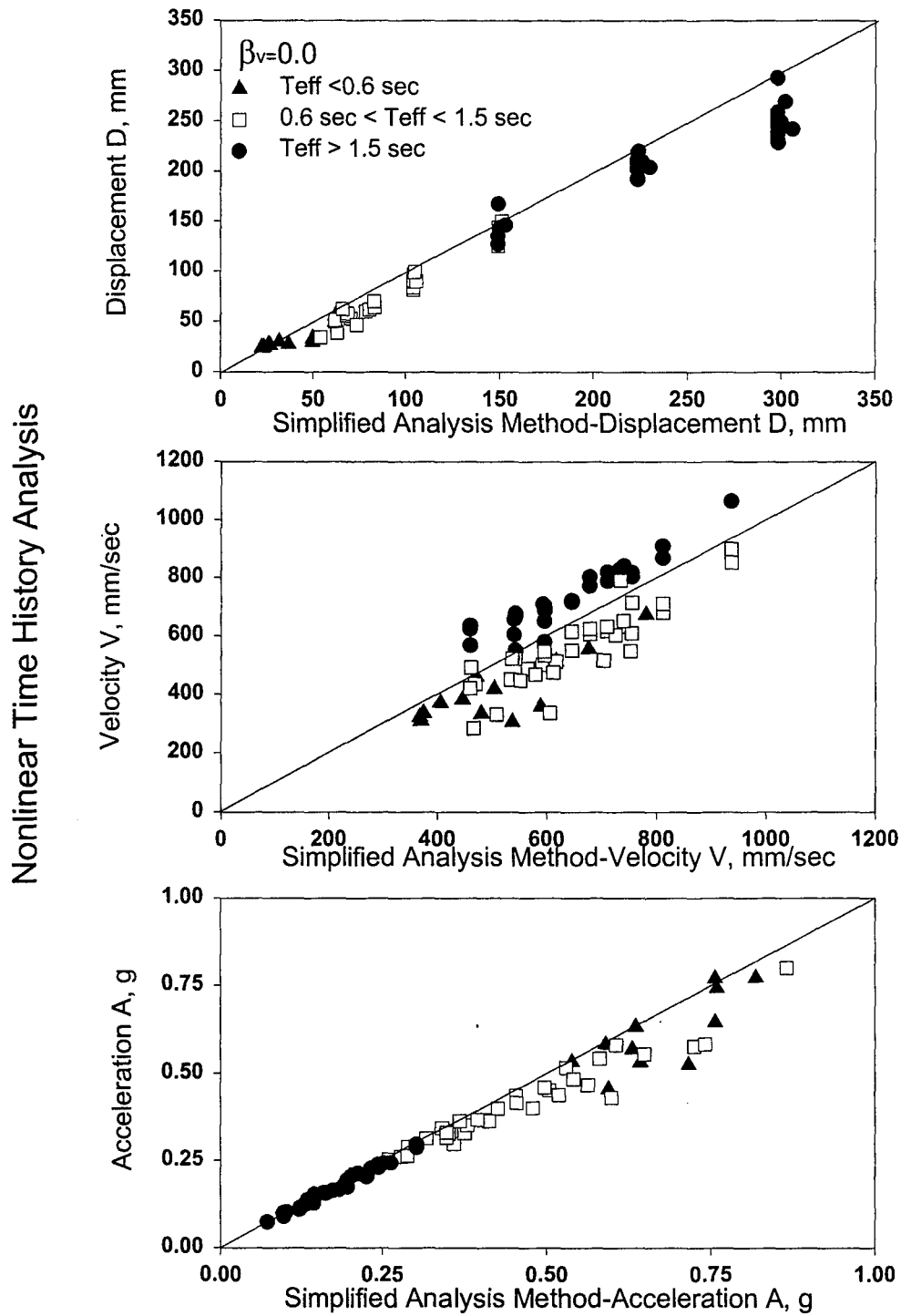
FIGURE 4-5 Comparison of Time History Analysis Results (Average of 20 values)
to Results of Simplified Method of Analysis for Bilinear Hysteretic System without
Damping Devices

Perfect Bilinear Hysteretic System (α=0.05, 0.15, 0.25, 0.5, 1.0, β_i=0.05) With Linear Viscous Damping Devices
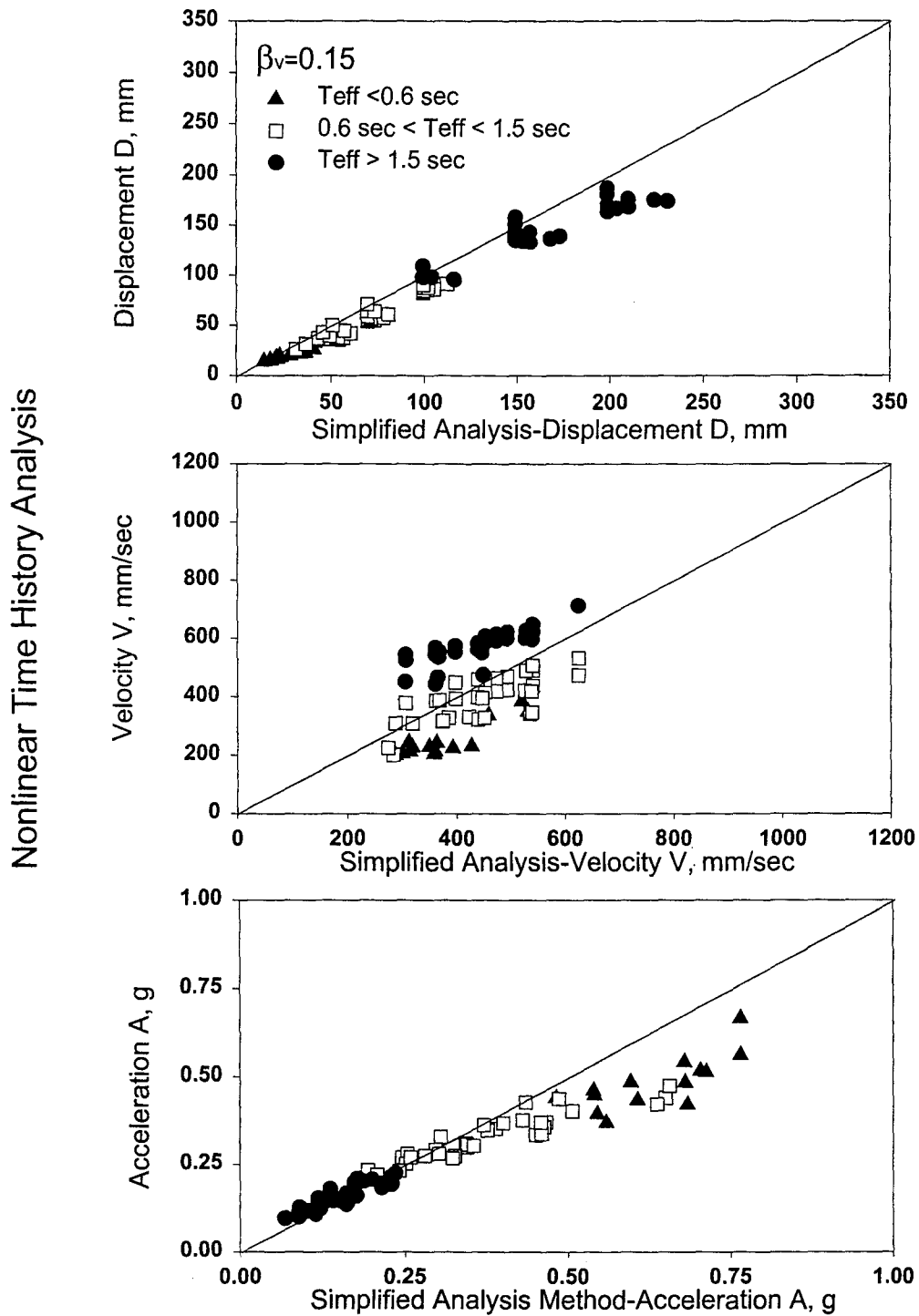
FIGURE 4-6 Comparison of Time History Analysis Results (Average of 20 values) to Results of Simplified Method of Analysis for Bilinear Hysteretic System with Linear Viscous Damping Devices, β_V = 0.15

Perfect Bilinear Hysteretic System (α=0.05, 0.15, 0.25, 0.5, 1.0, β_i=0.05) With Linear Viscous Damping Devices
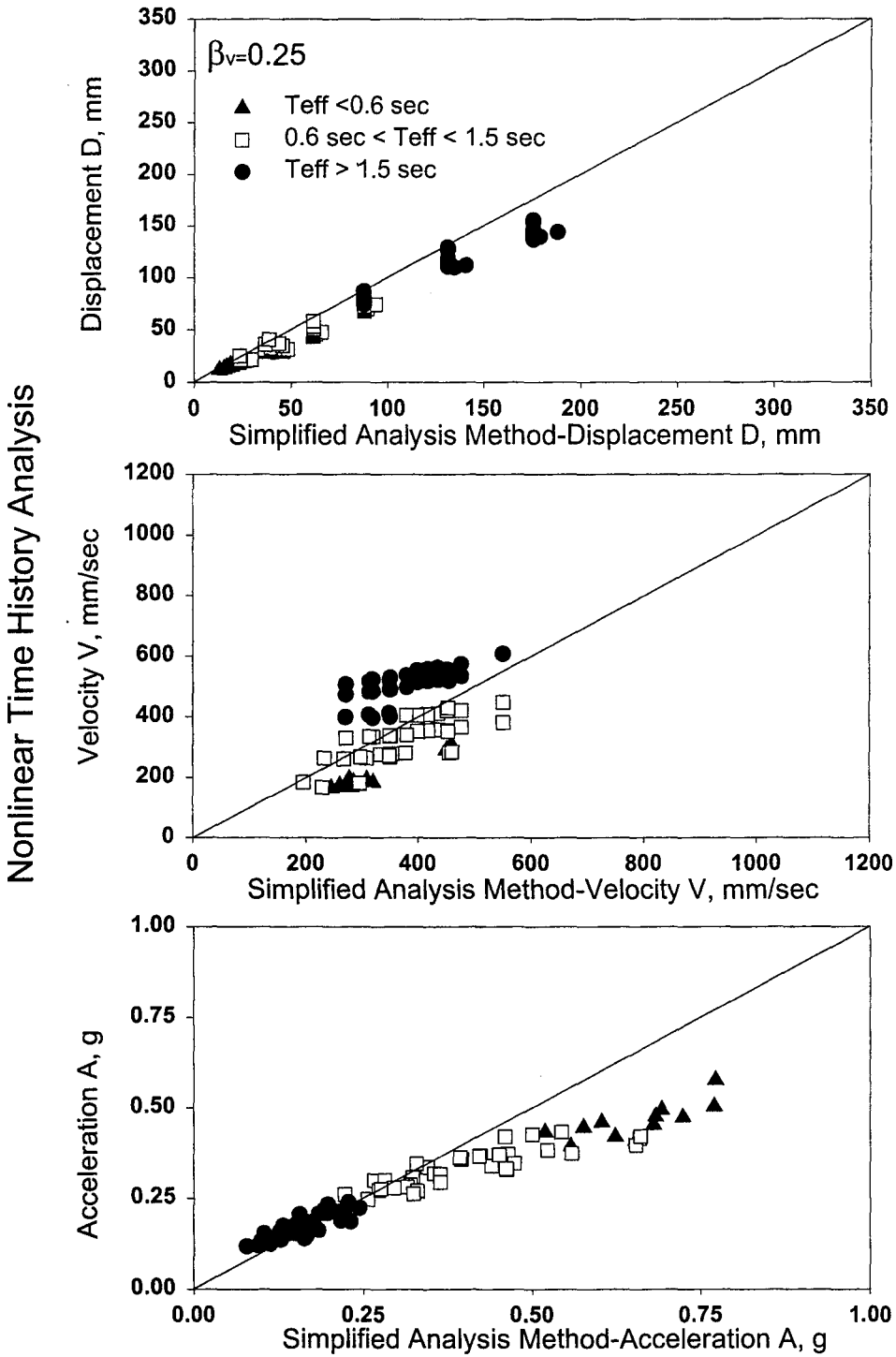
FIGURE 4-7 Comparison of Time History Analysis Results (Average of 20 values) to Results of Simplified Method of Analysis for Bilinear Hysteretic System with Linear Viscous Damping Devices, $\beta_V = 0.25$

Perfect Bilinear Hysteretic System (α=0.05, 0.15, 0.25, 0.5, 1.0, β_i=0.05)
With Non-Linear Viscous Damping Devices (a=0.5)
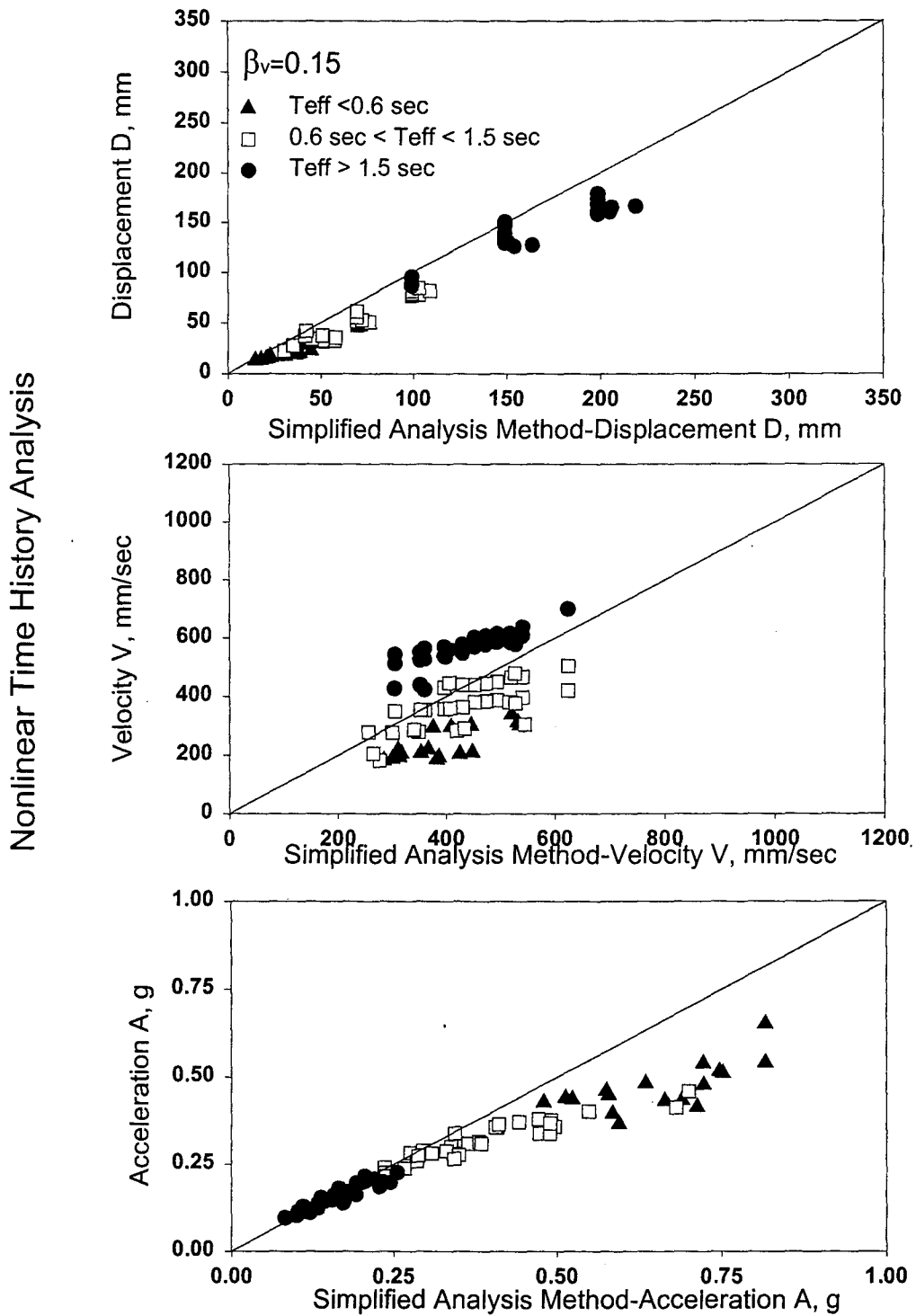
FIGURE 4-8 Comparison of Time History Analysis Results (Average of 20 values)
to Results of Simplified Method of Analysis for Bilinear Hysteretic System with
Non-Linear Viscous Damping Devices, β_V = 0.15

58

Perfect Bilinear Hysteretic System With (α=0.05, 0.15, 0.25, 0.5, 1.0, βi=0.05)
Non-Linear Viscous Damping Devices (a=0.5)
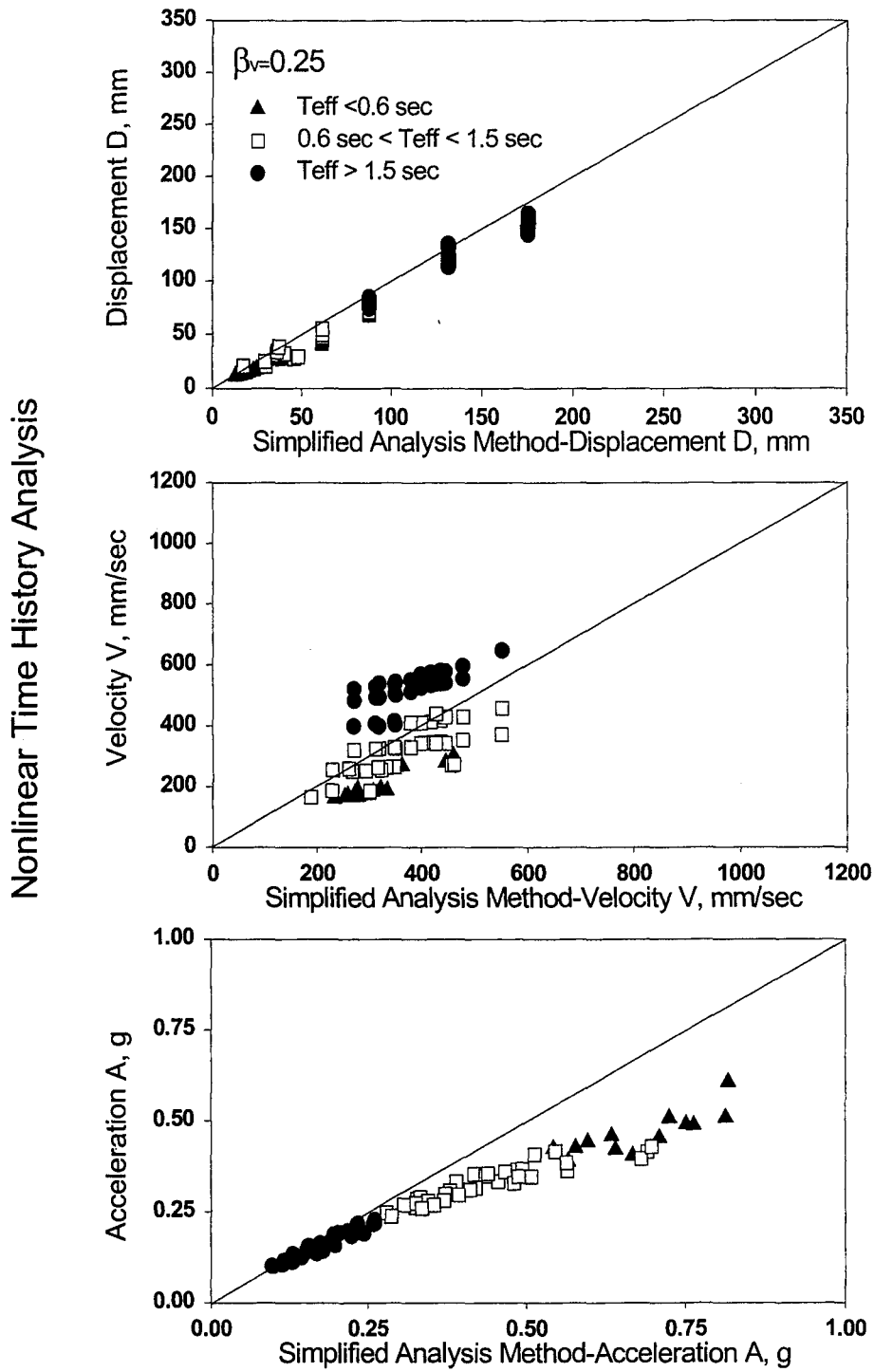
FIGURE 4-9 Comparison of Time History Analysis Results (Average of 20 values)
to Results of Simplified Method of Analysis for Bilinear Hysteretic System with
Non-Linear Viscous Damping Devices, $\beta_V = 0.25$

59

Bilinear Elastic System (α=0.05, βi=0.05)
Without Damping Devices
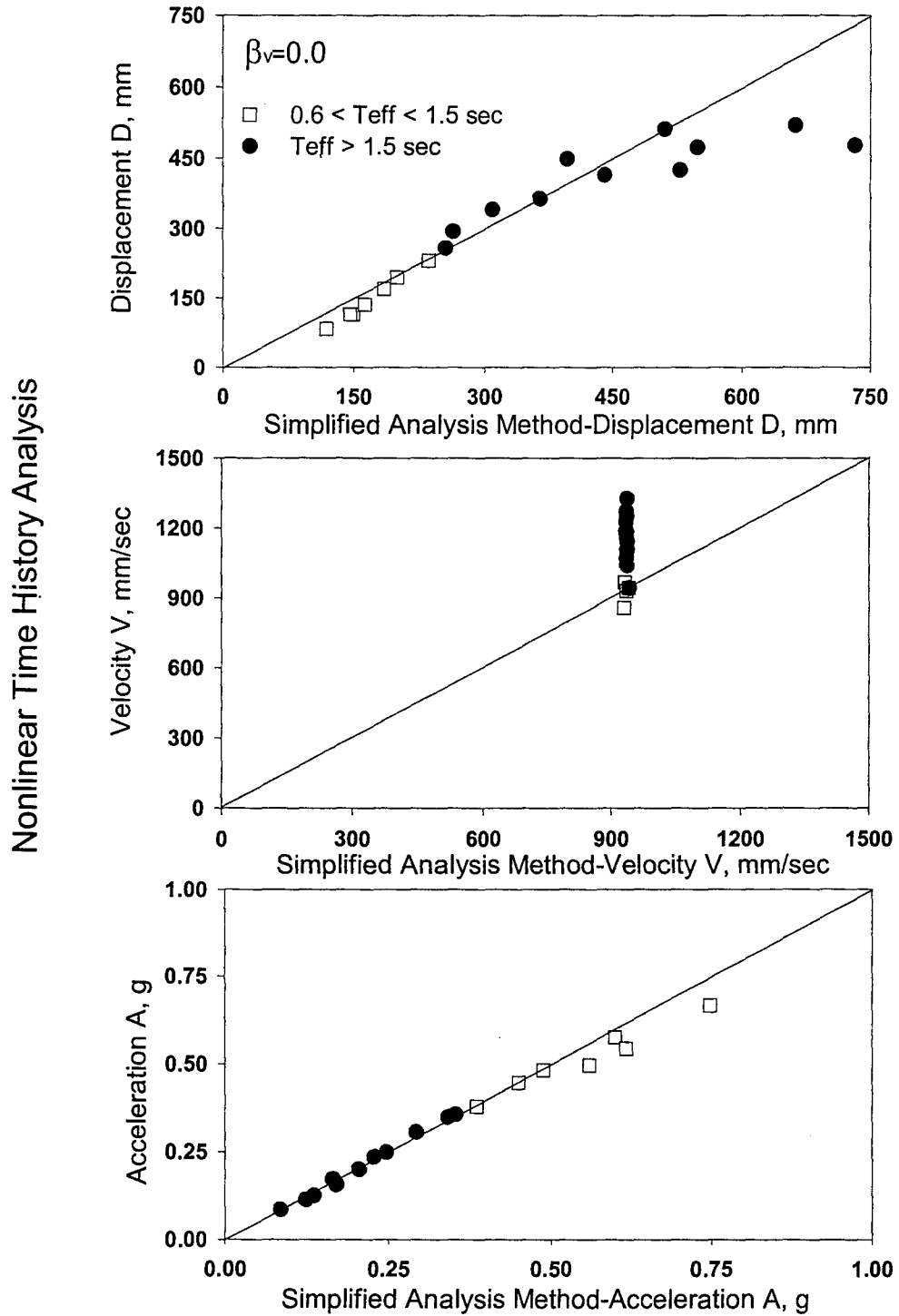
FIGURE 4-10 Comparison of Time History Analysis Results (Average of 20 values)
to Results of Simplified Method of Analysis for Bilinear Elastic System without
Damping Devices
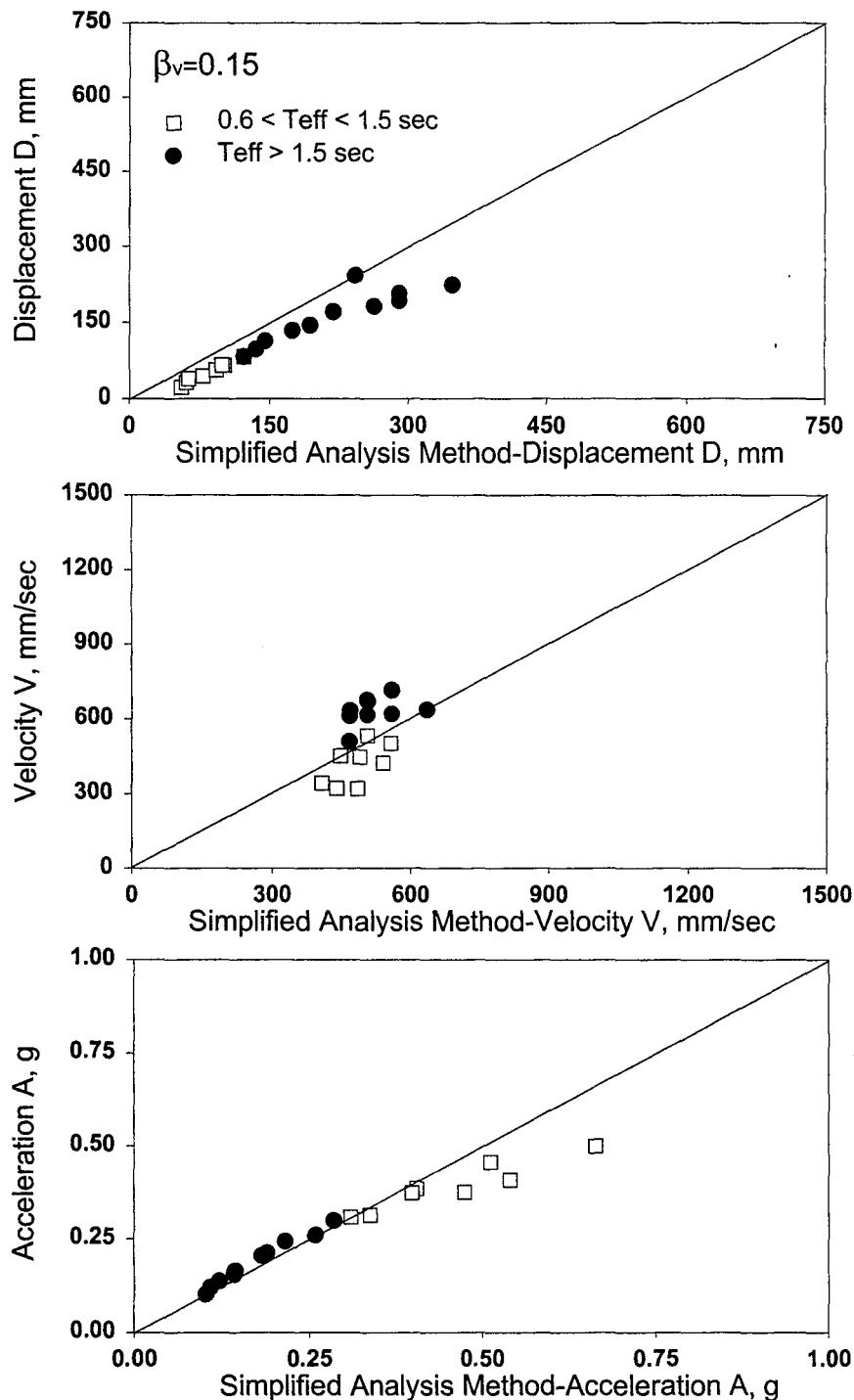
FIGURE 4-11 Comparison of Time History Analysis Results (Average of 20 values) to Results of Simplified Method of Analysis for Bilinear Elastic System with Linear Viscous Damping Devices, $\beta_V = 0.15$
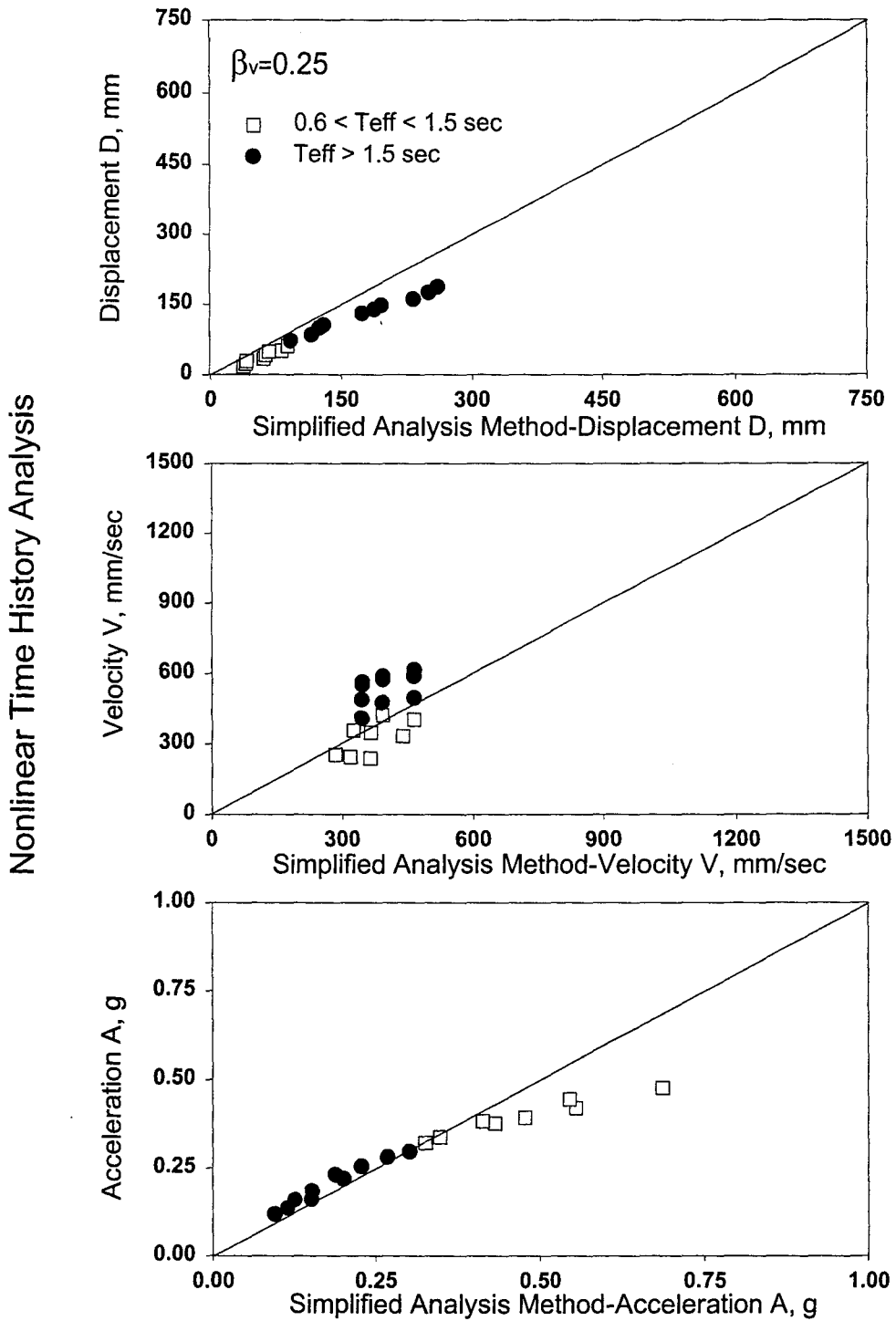
FIGURE 4-12 Comparison of Time History Analysis Results (Average of 20 values) to Results of Simplified Method of Analysis for Bilinear Elastic System with Linear Viscous Damping Devices, $\beta_V = 0.25$

Bilinear Hysteretic System (α=0.05, β_i=0.05)
With Yielding Damping Devices

FIGURE 4-13 Comparison of Time History Analysis Results (Average of 20 values)
to Results of Simplified Method of Analysis for Bilinear Hysteretic System with
Yielding Damping Devices

63

Perfect Bilinear Hysteretic System (α=0.05, 0.15, 0.25, 1.0, β_i=0.05) With Linear Viscous Damping Devices, β_v=0.15

Simplified Analysis Method-Velocity, mm/sec

FIGURE 4-14 Comparison of Velocity Predictions without and with Correction Factors for Bilinear Hysteretic System with Linear Viscous Damping Devices, β_v=0.15

Perfect Bilinear Hysteretic System (α=0.05,0.15, 0.25, 1.0, β_i=0.05)
With Linear Viscous Damping Devices, βv=0.25

FIGURE 4-15 Comparison of Velocity Predictions
without and with Correction Factors for Bilinear Hysteretic
System with Linear Viscous Damping Devices, β_v=0.25

Perfect Bilinear Hysteretic System With (α=0.05,0.15, 0.25, 1.0, β_i=0.05) Non-Linear Viscous Damping Devices (a=0.5), βv=0.15

FIGURE 4-16 Comparison of Velocity Predictions without and with Correction Factors for Bilinear Hysteretic System with Non-Linear Viscous Damping Devices, βv=0.15

Perfect Bilinear Hysteretic System With (α=0.05,0.15, 0.25, 1.0, βi=0.05) Non-Linear Viscous Damping Devices (a=0.5), βv=0.25

FIGURE 4-17 Comparison of Velocity Predictions without and with Correction Factors for Bilinear Hysteretic System with Non-Linear Viscous Damping Devices, βv=0.25

Bilinear Elastic System (α=0.05, βi=0.05)
With Linear Viscous Damping Devices, βv=0.0, 0.15, 0.25
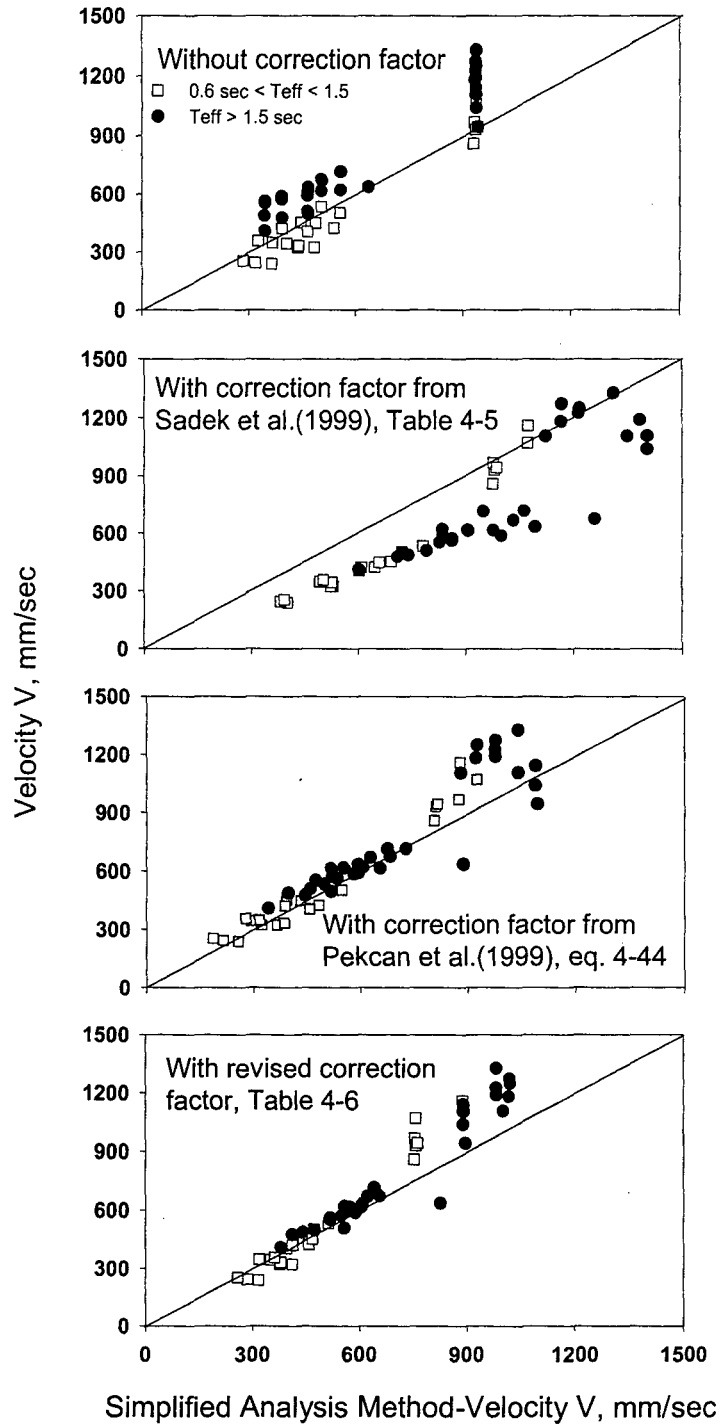
FIGURE 4-18 Comparison of Velocity Predictions
without and with Correction Factors for Bilinear Elastic
System with Linear Viscous Damping Devices

68

SECTION 5

RATIO OF INELASTIC DISPLACEMENT TO DISPLACEMENT CALCULATED ASSUMING ELASTIC BEHAVIOR

5.1 Introduction

The ratio of maximum inelastic displacement to maximum displacement calculated under elastic conditions was introduced in FEMA (1997) as coefficient C_1 to facilitate the calculation of the displacements in yielding structures.

Several studies considered the problem of deriving simple expressions for the coefficient C_1. Typically, these studies proposed expressions that relate the coefficient C_1 to structural parameters such as the elastic period, parameters related to the seismic excitation such as the value of period at the intersection of the constant velocity and constant acceleration regions of the design response spectrum, and parameters related to the response such as the ratio of elastic strength demand to yield strength. These studies did not consider the response of structures with added viscous damping.

The large nonlinear time history analysis dataset for yielding structures with damping systems permitted a re-evaluation of the C_1 coefficient. The results presented in Section 4 were used to establish damping-dependent expressions for this coefficient.

5.2 Coefficient C_1 and Review of Past Studies

Figure 5-1 illustrates the idealized behavior of a single-degree-of-freedom structure in terms of its base shear-drift relation. Under elastic conditions, the seismic demand consists of the peak force F_e and peak displacement D_{el}. Under inelastic conditions the peak displacement is D_{in}. By definition

$$C_1 = \frac{D_{in}}{D_{el}} = \frac{\mu \cdot D_y}{D_{el}} = \frac{\mu}{R_\mu} \tag{5-1}$$

where

$$\mu = \frac{D_{in}}{D_y} \qquad (5\text{-}2)$$

is the displacement ductility ratio and

$$R_\mu = \frac{F_e}{F_y} = \frac{D_e}{D_y} \qquad (5\text{-}3)$$

is the ratio of the elastic strength demand to the yield strength. R_μ is the ductility-based portion of the R-factor. For the study below, the elastic period is T_e (based on stiffness K_e), the ratio of post-elastic stiffness to elastic stiffness is equal to α, D_y is the yield displacement and F_y is the yield strength.

Miranda and Bertero (1994) presented an evaluation of studies on the ductility-based portion of the R-factor. The data of Miranda and Bertero were used to establish values for coefficient C_1 in FEMA 273. Some of the studies evaluated in Miranda and Bertero (1994) are reviewed below together with a review of other studies.

5.2.1 Study of Mander et al. (1984)

Mander et al. (1984) proposed the following relation

$$C_1 = \begin{cases} \frac{1}{R_\mu}\left[1 + \left(R_\mu - 1\right)\left(\frac{T_0}{T}\right)\right] \geq 1 \\ \\ 1 \quad for \ T_e \geq T_0 \end{cases} \qquad (5\text{-}4)$$

where T_o is the period that separates long-period from medium-period structures. Mander et al. (1984) proposed a values of $T_o = 1$ sec.

More recently, Chang and Mander (1994) re-visited the 1984 work of Mander and modified equation (5-4) by replacing the term (T_o/T_e) with the term $(T_o/T_e)^\eta$ where η is an exponent dependent on R_μ with values in the range of 1.2 to about 1.35. Moreover, T_o has been interpreted

as the period at which the maximum spectral velocity response occurs. For a typical design spectrum such as the 5%-damped spectrum depicted in Figure 3-1, and utilizing the pseudo-velocity as a measure of the maximum velocity, period T_o coincides with period T_s, that is, the period at which the constant acceleration and constant velocity regions of the design spectrum intersect. Interestingly, (5-4) is used in FEMA (1997) with T_o being the aforementioned period T_s.

5.2.2 Study of Riddell et al. (1989)

Riddell et al. (1989) established a relationship between the ductility-based portion of the R-factor, ductility and period. Such relations are useful in selecting appropriate response modification factors that are dependent on the period of the structure. Riddell et al. (1989) proposed the relation

$$
R_\mu =
\begin{cases}
1 + (\mu - 1)\dfrac{T_e}{T_0} & , \quad T_e < T_0 \\[4mm]
\mu & , \quad T_e \geq T_0
\end{cases}
\tag{5-5}
$$

where T_o ranges between 0.1 and 0.4 sec. Use of (5-1) and (5-5) results in equation (5-4).

5.2.3 Study of Nassar and Krawinkler (1991)

Nassar and Krawinkler (1991) developed a relation similar to that of Riddell et al. (1989). Their relationship was based on the results of analysis of systems with a wider range of structural parameters and different seismic excitations. The relationship is

$$
R_\mu = [1 + (\mu - 1)c]^{1/c}
\tag{5-6}
$$

where c is a parameter dependent on the elastic period and the post-elastic to elastic stiffness ratio (α). Inverting (5-6) and using (5-1) results in an expression for C_1, namely:

$$
C_1 = \frac{1}{R_\mu}\left(1 + \frac{R_\mu^c - 1}{c}\right)
\tag{5-7}
$$

that has the same basic form as (5-4).

5.2.4 Study of Vidic et al. (1992)

Vidic et al. (1992) arrived at a relation identical to that of Riddell et al. (1989) but with parameter T_o being dependent on the ductility ratio μ and the characteristics of the seismic excitation.

5.2.5 Study of Miranda (1993)

Miranda (1993) proposed the relation of (5-8) using results of analyses with a large number (124) of recorded ground motion:

$$R_\mu = 1 + \frac{\mu - 1}{\varPhi} \geq 1 \qquad (5-8)$$

where $\varPhi$ is a parameter dependent on μ, T_e and the predominant period of the ground motion.

5.2.6 Summary

It is evident that many investigators developed similar relations, relating either the coefficient C_1 to the ductility-based portion of the R-factor and the elastic period or the ductility-based portion of the R-factor to the ductility ratio and the elastic period. The latter relation was studied as early as 1973 by Newmark and Hall (1973) and then later by Riddell and Newmark (1979) who considered, in addition to other parameters, the effect of viscous damping. Unfortunately, the proposed relations are too complex to be inverted so that expressions for the coefficient C_1 can be obtained.

Of interest in the analysis of structures with viscous damping systems is a calibrated relation between coefficient C_1 and the post-elastic to elastic stiffness ratio, α (range ≤ 0.5), the elastic period, T_e, the viscous damping ratio under elastic conditions, β_v (range of 0.05 to 0.30) and the period T_s, which characterizes the design response spectrum. Such a relation does not exist in the literature and was established in this study using the results of the nonlinear time history analysis presented in Section 4.

5.3 Procedure for Development of Coefficient C_I and Results

The bilinear hysteretic simple structural system with linear viscous devices described in Section 4 was prepared with the following parameters:

(a)   Elastic period T_e from 0.2 to 3.0 sec, and in steps of 0.1 sec.

(b)   Post-elastic to elastic stiffness ratio α equal to 0.05, 0.15, 0.25, 0.50 and 1.0 ($\alpha = 1$ represents elastic behavior).

(c)   Ductility-based portion of the R-factor, R_μ equal to 2.0, 3.33 and 5.0.

(d)   Linear viscous damping ratio under elastic conditions β_v equal to 0.0, 0.15, and 0.25, plus inherent viscous damping of 0.05 for a total viscous damping ratio under elastic conditions of β_v equal to 0.05, 0.20, and 0.30.

Parameter R_μ (see eq. 5-3) can also be described by

$$R_\mu = \frac{mS_a\left(T_e, \beta = 0.05\right)}{F_y B} \tag{5-9}$$

where m is the mass, S_a is the spectral acceleration for damping of 5-percent and B is the damping coefficient for the total damping ratio.   The damping coefficient presented in Section 3 and described as the "conservative" trilinear model has been utilized in the calculation of the yield strength of the analyzed systems.   The seismic excitation consisted of the 20 scaled motions described in Section 3 and used in the analyses reported in Section 4.   Note that for these motions, $T_S = 0.6$ sec.

The coefficient C_I was obtained as the ratio of the average peak inelastic displacement to the average peak elastic displacement. Plots of this coefficient versus period T_e revealed the basic nature of the relation.   Moreover, since C_I should converge to unity when either R_μ or α are equal to unity, the following relation was considered:

$$C_l = 1 + \frac{(1-\alpha)(R_\mu - 1)}{R_\mu}\left(a\frac{T_s}{T_e}\right)^b \qquad (5\text{-}10)$$

in which parameters a and b were obtained by calibration of the model on the basis of the results of dynamic analysis. The simplest form of these parameters was found to be

$$a = a_0\left(2 + 0.45R_\mu\right) \qquad (5\text{-}11)$$

$$b = 3.24 - 0.10R_\mu - 4.5\beta_v \qquad (5\text{-}12)$$

where a_o is the parameter in Table 5-1.

Figures 5-2 to 5-4 compare values of coefficient C_l obtained by nonlinear time history analysis to the predictions of the model described by (5-10). Evidently, the proposed relation described by (5-10) describes well the calculated values of the coefficient and it follows the desired behavior for large values of period T_e. That is, (5-10) predicts a value of near unity for $T_e > T_s$.

5.4 Summary

In this section a new relation describing the ratio of peak inelastic displacement to the peak displacement assuming elastic behavior (coefficient C_l) has been presented. The new feature of this relation is the inclusion of the effect of added viscous damping. This relation may be used to obtain quick estimates of displacement demands in structures with damping systems without the need to use iterative analysis procedures. The results presented in Figures 5-2 to 5-4 illustrate effect of viscous damping on coefficient C_l. It may be noted that the effect of damping in the range of 5 to 30-percent is not significant.

TABLE 5-1 Values of Parameter a_0

Damping Ratio β_V	$\alpha=0.05$	$\alpha=0.15$	$\alpha=0.25$	$\alpha=0.50$
0.05	0.116	0.100	0.093	0.071
0.30	0.195	0.160	0.143	0.111

Linear Interpolation is Valid
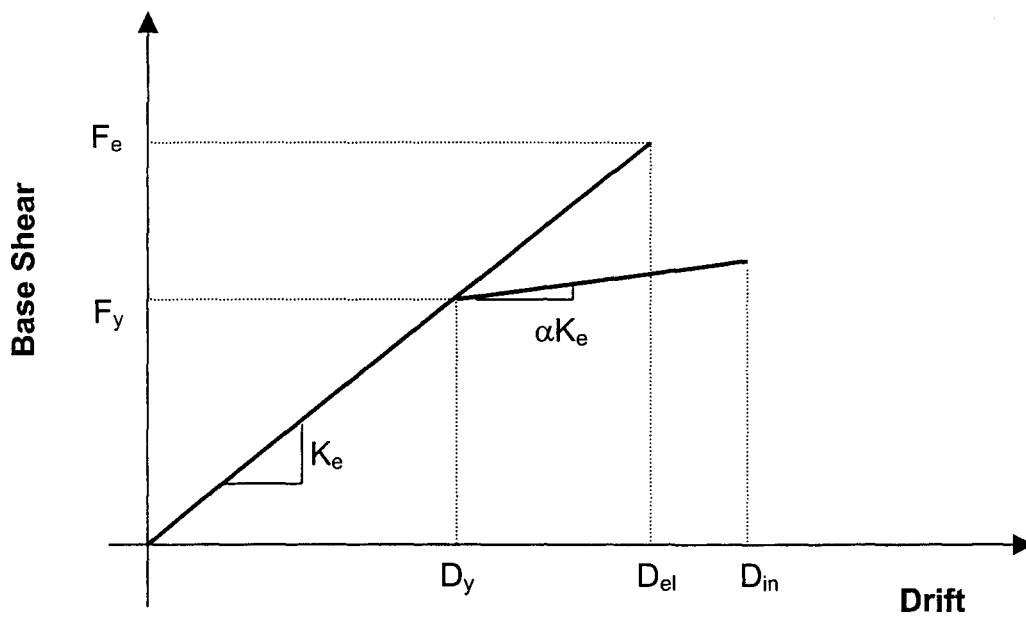
Figure 5-1 Elastic and Idealized Inelastic Behavior of Structure
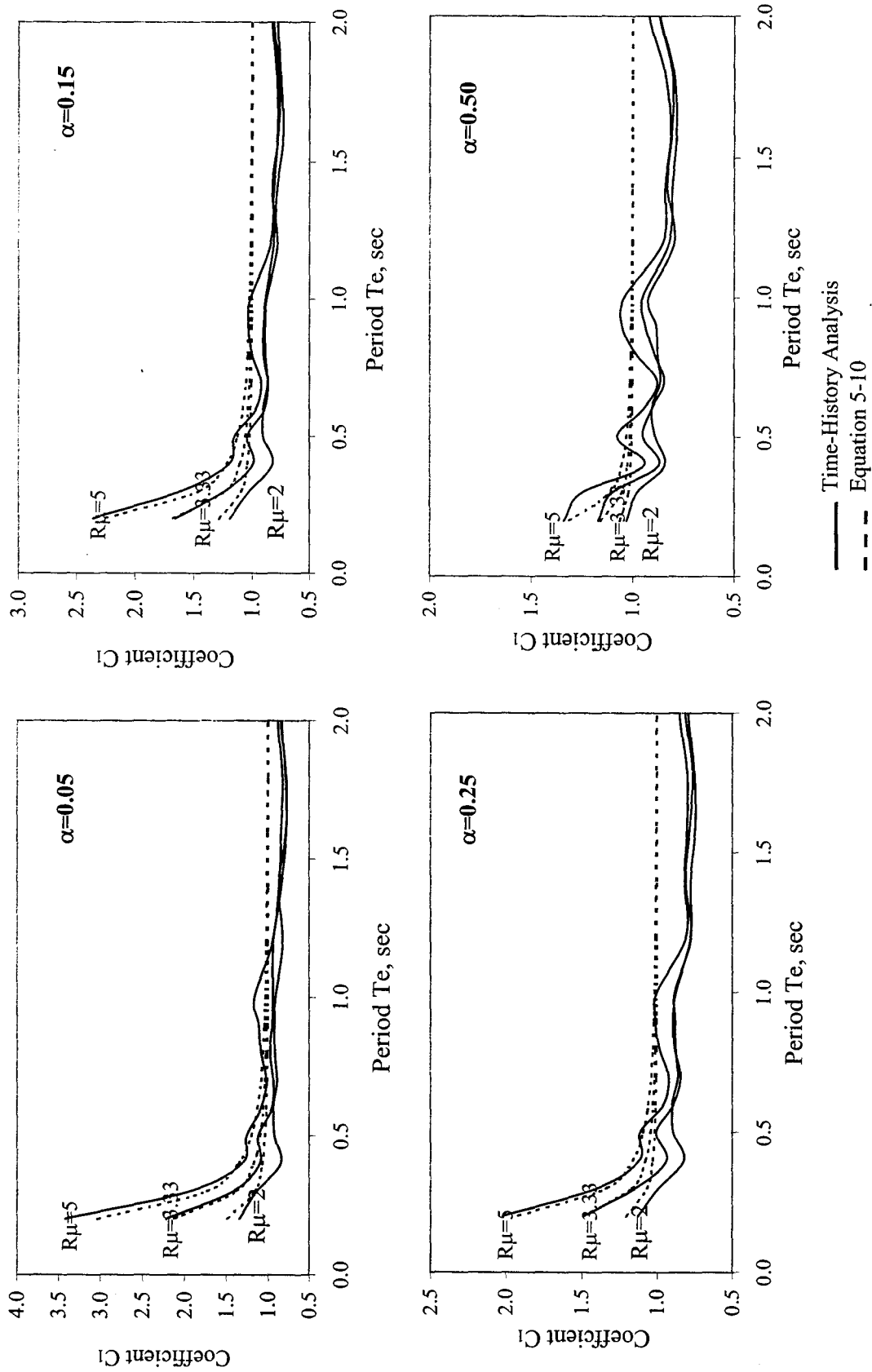
FIGURE 5-2 Comparison of Values of Coefficient C_1 Established by Nonlinear Time History Analysis to Predictions of Eq. 5-10 for Viscous Damping Ratio of 0.05
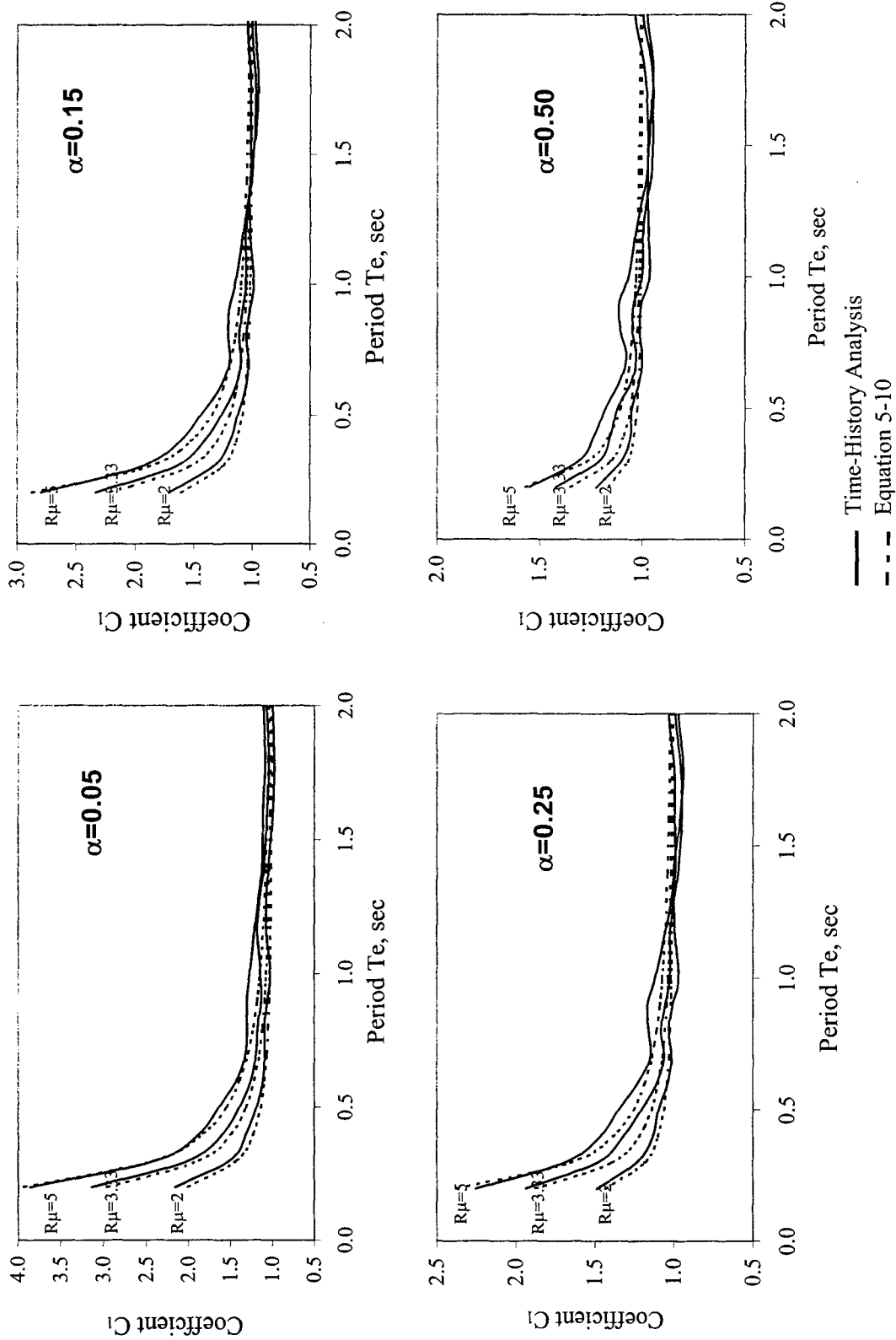
FIGURE 5-3 Comparison of Values of Coefficient C_1 Established by Nonlinear Time History Analysis to Predictions of Eq. 5-10 for Viscous Damping Ratio of 0.20
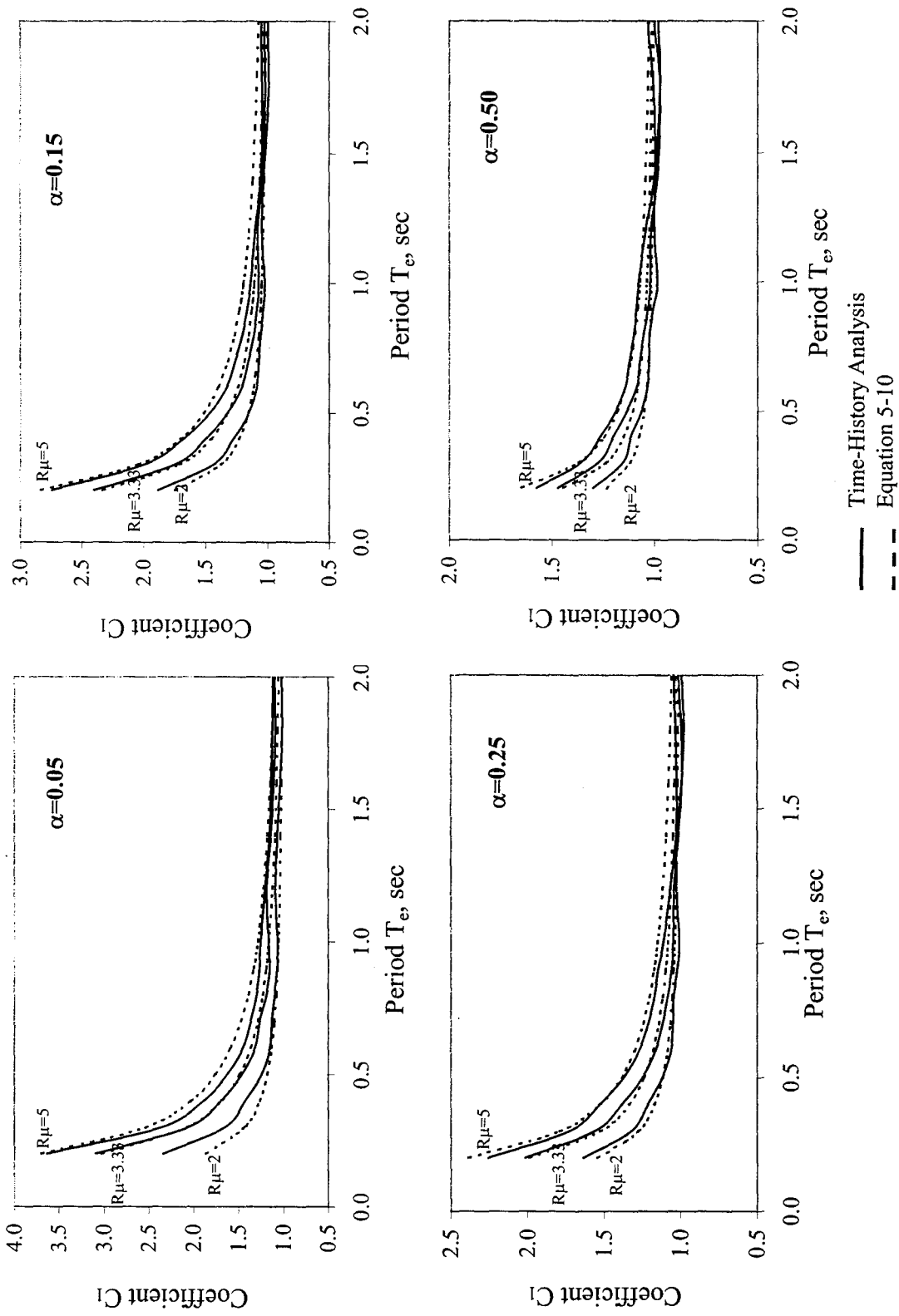
FIGURE 5-4 Comparison of Values of Coefficient C_1 Established by Nonlinear Time History Analysis to Predictions of Eq. 5-10 for Viscous Damping Ratio of 0.30

SECTION 6

DISPLACEMENT DUCTILITY DEMAND IN STRUCTURES WITH VISCOUS DAMPING SYSTEMS

6.1 Introduction

A structure without a damping system would typically be designed for code-prescribed lateral loads equal to the elastic inertia forces divided by a response modification factor (or R-factor). Such a structure will have an actual yield strength F_{yu} given by

$$F_{yu} = \frac{Elastic\,Demand}{R_\mu} \tag{6-1}$$

where R_μ is the ductility-based portion of the R-factor. In (6-1), elastic demand is the peak base shear calculated assuming that the structure is elastic with damping ratio equal to 5-percent. A structure designed on the basis of (6-1) will undergo inelastic deformations when subjected to the design earthquake.

Consider now that a structure with a viscous damping system is designed using a similar approach. The structure is designed to have an actual yield strength F_{yd} given by

$$F_{yd} = \frac{Elastic\,Demand\,(for\,5\%\,damping)}{R_\mu \cdot B} \tag{6-2}$$

where B is the damping coefficient for the viscous damping ratio of the structure under elastic conditions (say β_v). The elastic demand in (6-2) is as defined (6-1), so that the ratio elastic demand/B is the base shear of the damped structure calculated assuming that the structure is elastic with damping ratio equal to β_v. If we consider a value of $\beta_v = 0.20$ (0.05 inherent plus 0.15 added viscous damping) and a relatively flexible structure so that its elastic period T_e is larger that T_s, B is equal to 1.5 per Section 3. Accordingly for the same ductility-based portion

of the R-factor, the strength of the damped structure will be substantially less that that of the undamped structure, or for this example, $F_{yd} < 0.67\, F_{yu}$.

A question then arises as to whether the two structures will have comparable displacement ductility demands. The issue is further complicated by the fact that the damped structure has also less stiffness than the undamped structure. This section presents a systematic study that answers the displacement ductility question. This section presents results that demonstrate that the two structures indeed have comparable displacement ductility demands

6.2 Procedure for Evaluation of Displacement Ductility Demand

Bilinear hysteretic single-degree-of-freedom systems without and with linear viscous damping devices were considered. Each system without damping devices was characterized by the elastic period T_e, ductility-based portion of R-factor, R_μ, ratio of post-elastic to elastic stiffness, α, and the inherent damping ratio, $\beta_i = 0.05$. Values of $T_e = 0.2$ to 2.0 sec, $\alpha = 0.05$, 0.15, 0.25 and 0.50, and $R_\mu = 2.0$, 3.33 and 5.0 were selected.

Each system with damping devices was characterized by the same parameters β_i, α, and R_μ, a value of elastic period T_{ed} larger than T_e, and added linear viscous damping ratio $\beta_v = 0.15$ or 0.25 under elastic conditions. Accordingly, the total damping ratio under elastic conditions was either 0.20 or 0.30. The damped system had a lower yield strength than the undamped system as indicated in equations (6-1) and (6-2).

The elastic period T_{ed} of the damped system was related to the period T_e of the corresponding undamped system (damped at 5%) on the basis of the following equation:

$$\frac{T_{ed}}{T_e} = B^\eta \tag{6-3}$$

where η is a parameter dependent on the fundamental period and the shape of the beam and column sections of the structure, which was calculated as follows. The elastic period of the structure is related to the moment of inertia, I, of the beam and column sections, that is, $T \sim 1/\sqrt{I}$. The yield strength of the structure is related to the plastic moments of the beam and

columns which are proportional to the plastic section modulus and the material yield stress. Assuming that the damped and the undamped structure are made of the same material, it follows that $F_{ye}/F_{yd} = Z_e/Z_d$ where Z_e and Z_d are the plastic section moduli of the sections of the undamped and the damped structures, respectively. Consider now that both structures have elastic periods that fall within the constant acceleration domain of the design spectrum. Use of (6-1) and (6-2) results in $F_{ye}/F_{yd} = B$. Thus,

$$\frac{T_{ed}}{T_e} = \left(\frac{I_e}{I_d}\right)^{1/2} \tag{6-4}$$

$$\frac{Z_e}{Z_d} = B \tag{6-5}$$

where I_e and I_d are representative moments of inertia of the beam and columns of the undamped and the damped structures, respectively. For a rectangular $b \times h$ section, $T \sim h^3$ and $Z \sim h^2$, so that $T \sim h^3$. That is,

$$\frac{T_{ed}}{T_e} = \left(\frac{h_e}{h_d}\right)^{3/2} = \left(\frac{Z_e}{Z_d}\right)^{3/4} = B^{3/4} \tag{6-6}$$

where h_e and h_d are the heights of the sections of the undamped and the damped structures, respectively. A similar expression, but with an exponent equal to 2/3 rather than 3/4, is obtained for square sections. Similarly, for wide flange sections, equation (6-3) is valid with $\eta = 0.45$ to 0.65.

Moreover, analysis considering that both T_e and T_{ed} are within the constant velocity region of the design spectrum, results again in (6-3) but with η of the order of or larger than unity. Accordingly, analysis were performed utilizing (6-3) with $\eta = 0.5$ when $T_e < T_s$ and $\eta = 1.0$ when $T_e \geq T_s$. Note that T_s is the period at the intersection of the constant acceleration and constant velocity regions of the design spectrum.

6.3 Results

Analyses were performed using the 20 scaled motions described in Section 3. In the calculation of the period and the yield strength of the damped structure, the "conservative values" of the damping coefficient B were used (see Section 3).

Figures 6-1 and 6-2 compare the calculated average displacement ductility ratio for the undamped and the damped structures (the average is that of the 20 calculated values for each combination of parameters). The ductility demand in the two structures is nearly the same. Moreover, Figure 6-3 presents a further comparison of the displacement ductility ratio of the undamped and the 20%-damped structures with $\alpha = 0.05$. In this figure, in addition to the average, the maximum, and the minimum displacement ductility ratios of the 20 calculated values are compared. Such a representation reveals the possible scatter in the ductility demand. Interestingly, the scatter in the ductility demand in the damped structures is similar as that in the undamped structure. This further justifies the use of the design approach described by (6-3).

6.4 Conclusions

In this section a comparison of ductility demands in damped and undamped structures has been presented. The structures have been designed to have a yield strength described by (6-1) to (6-3), so that

$$\frac{F_{yd}}{F_{yu}} = \begin{cases} \dfrac{1}{B} & \text{when } T_e, T_{ed} < T_s \\[4ex] \dfrac{1}{B^2} & \text{when } T_e, T_{ed} \geq T_s \end{cases} \tag{6-7}$$

That is, the yield strength of the damped systems was between 0.35 and 0.67 times the strength of the undamped structure. The calculated average, maximum and minimum displacement ductility ratios in the two structures were nearly the same for the same R_μ and α. On the basis of these results, as well as results on inelastic spectra of structures with added viscous damping presented by Wu and Hanson (1989), NEHRP (2000) allows the design of structures with

damping systems for a seismic base shear that is the greatest of *V/B* or *0.75V*, where *V* is the minimum seismic base shear for the design of the structure without a damping system and *B* is the damping coefficient for the combined inherent and viscous damping under elastic conditions.
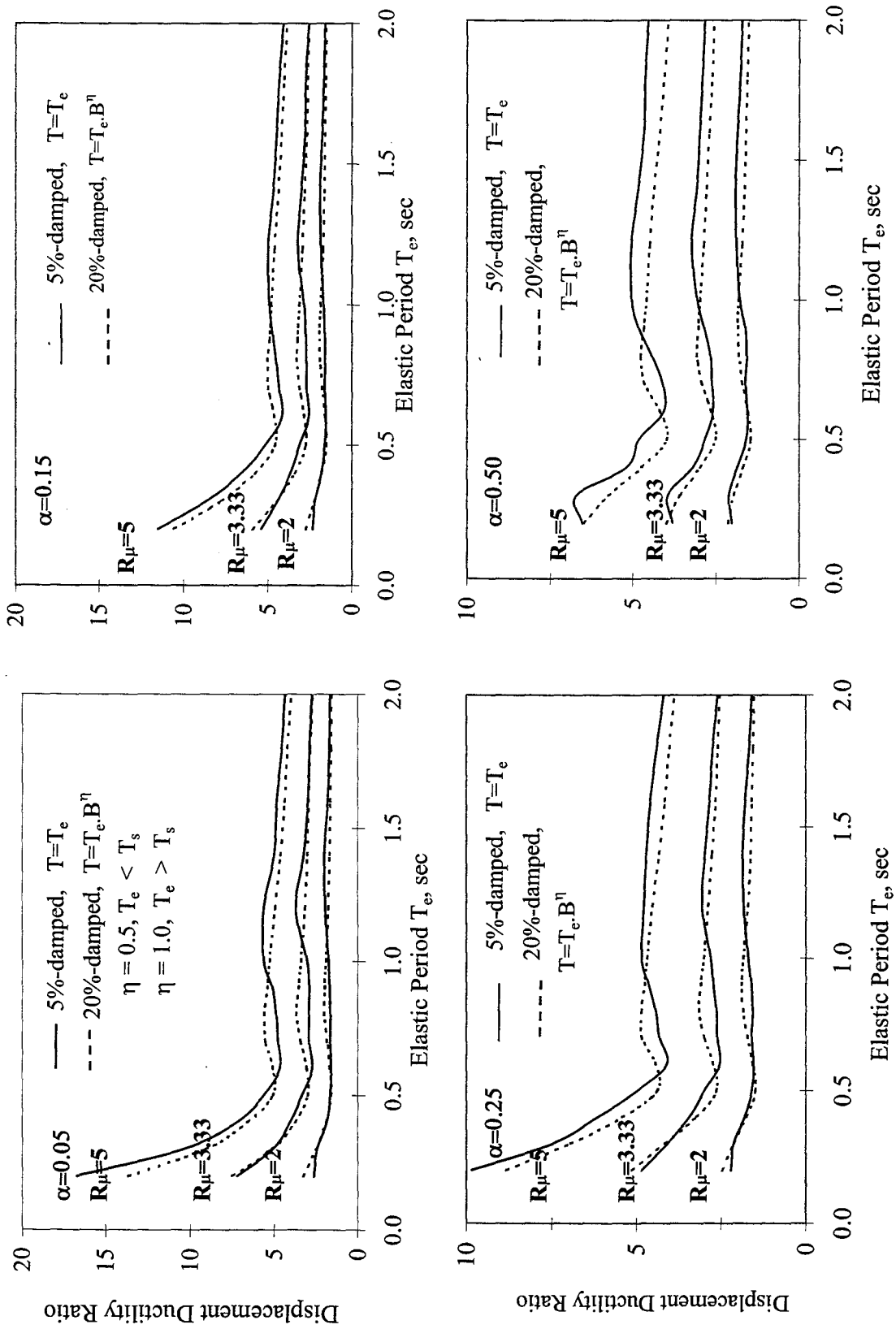
FIGURE 6-1 Comparison of Average Displacement Ductility Ratio for 5% and 20%-Damped Systems

84
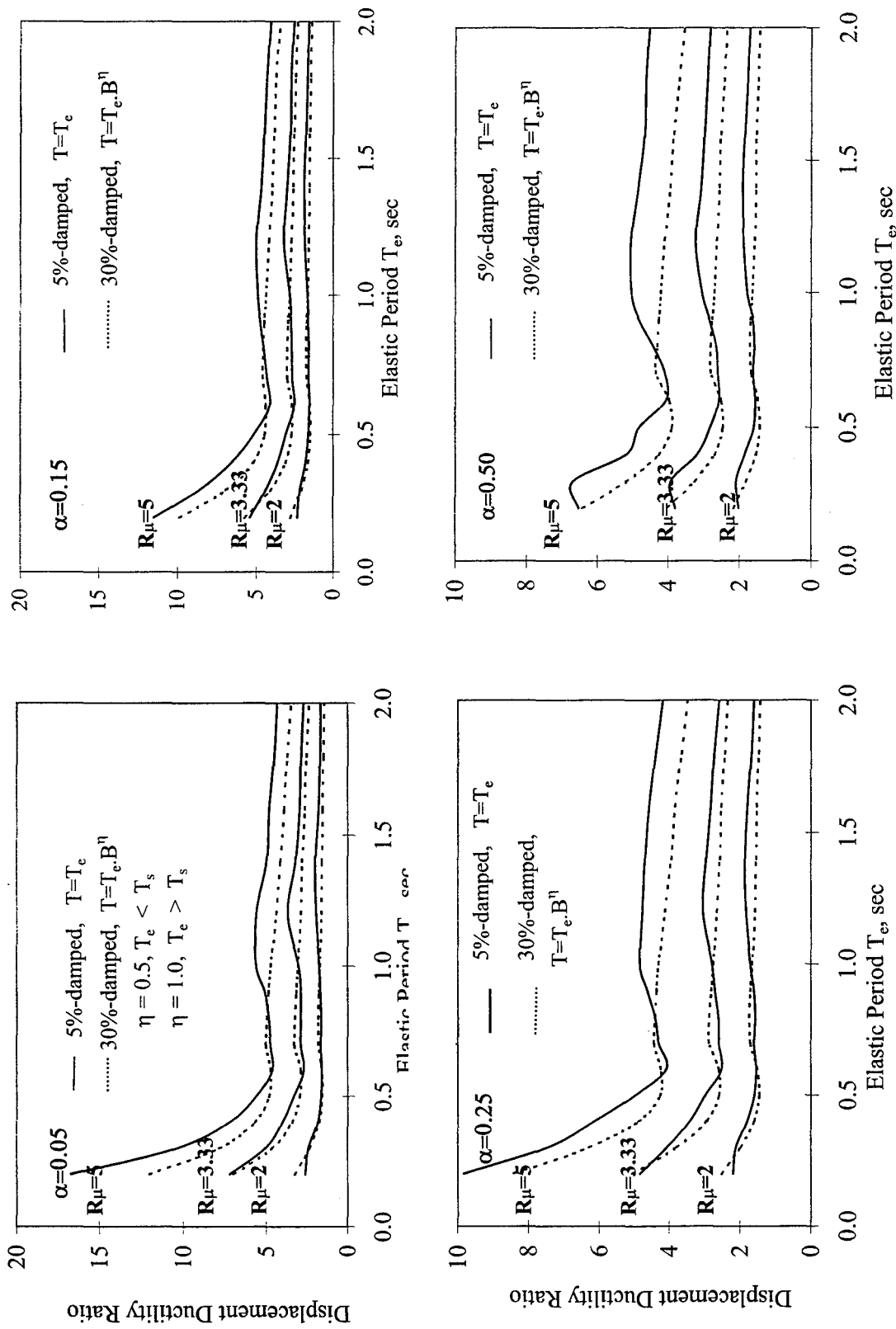
FIGURE 6-2 Comparison of Average Displacement Ductility Ratio for 5% and 30%-Damped Systems

85
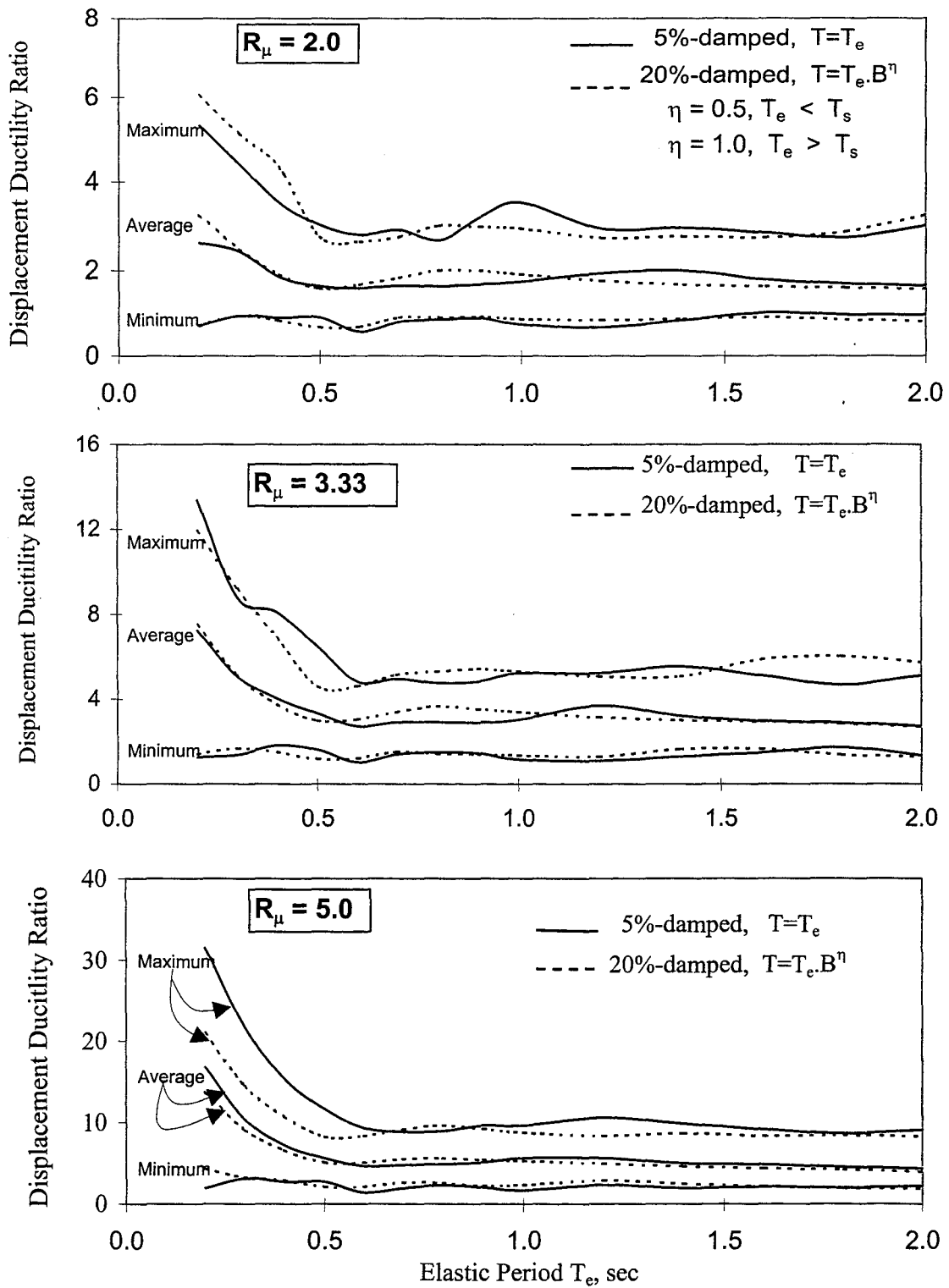
**FIGURE 6-3 Comparison of Maximum, Average and Minimum
Displacement Ductility Ratios of 5% and 20%-Damped
Systems with $\alpha = 0.05$.**

SECTION 7

DEVELOPMENT OF EQUIVALENT LATERAL FORCE AND MODAL ANALYSIS PROCEDURES FOR NEW BUILDINGS WITH DAMPING SYSTEMS

7.1 Introduction

The Nonlinear Static Procedure of FEMA 273 FEMA (1997) is the most comprehensive guideline for the evaluation of buildings with damping systems at the time of this writing. Specifically, Method 2 of FEMA (1997) is suitable for the analysis of buildings with velocity-dependent (i.e., viscous and viscoelastic) damping systems, whereas Method 1 of FEMA (1997) requires modifications along the lines of Method 2 for its application to velocity-dependent systems.

Method 2 of FEMA (1997) is somewhat cumbersome to apply because it requires to perform at least two pushover analyses, each with repeated eigenvalue analyses utilizing secant member stiffnesses. Moreover, the method is suitable for the analysis of existing buildings and does not provide guidance for preliminary sizing of members.

There is interest in the development of equivalent lateral force and modal analysis procedures for buildings with damping systems that parallel the corresponding procedures for buildings without damping systems, as in the NEHRP Recommended Provisions for Seismic Regulations for New Buildings and Other Structures (NEHRP, 1997). Such procedures could simplify the design of buildings with damping systems.

An equivalent lateral force procedure and a modal analysis procedure for damped buildings are presented in this section. They are largely based on Method 2 of FEMA (1997) but are simpler as a result of the following assumptions:

(1) The building is designed to have a proper collapse mechanism so that the distribution of drift may be reasonably estimated on the basis of either eigenvalue analysis under elastic

87

conditions or on the basis of assumptions (e.g., the drift distribution has an inverted triangular shape).

(2)   The building is analyzed in each principal direction as a model with one degree-of-freedom per floor.

(3)   The behavior of the building can be represented by an elastoplastic model.

(4)   The yield strength of the building can be estimated by either a) plastic analysis since the collapse mechanism is known, or b) using the specified minimum seismic base shear and values of the response modification (R), system overstrength (Ω_0) and deflection amplification (C_d) factors presented in NEHRP (2000).

7.2 R, R_μ, Ω_0, C_d Factors and Maximum Effective Ductility

The definitions of the response modification factor R, the ductility-based portion of R-factor R_μ (or R_d in NEHRP, 1997), the system overstrength factor Ω_0, and the deflection amplification factor C_d may be found in NEHRP (1997). A review of the values of some of these factors may be found in Uang (1991). A brief description of these parameters is presented below.

Shown in Figure 7-1 is the structural response of a one-story building. The base shear-drift relations of this building are termed capacity curves. The "actual" capacity curve shown dashed in the figure is replaced by the idealized elastoplastic capacity curve that is shown as a solid line. The elastic and inelastic responses of this building are obtained as the intersection points of the capacity curves and the demand spectra (the latter multiplied by the reactive weight W to obtain force). The yield strength of the idealized building is V_y and the elastic demand (or required elastic strength) is F_e. The inelastic displacement is D_I and is shown in Figure 7-1 to be larger than the elastic displacement D_e. The effective yield displacement is D_y, and the force and displacement at the formation of the first plastic hinge are V_s and D_s, respectively. The displacement ductility ratio (or effective ductility demand) is $\mu = D_I/D_y$. The definitions of the various factors are:

$$R_\mu = \frac{F_e}{V_y}$$ (7-1)

$$\Omega_0 = \frac{V_y}{V_s} \tag{7-2}$$

$$R = \frac{F_e}{V_s} = R_\mu \cdot \Omega_0 \tag{7-3}$$

$$C_d = \frac{D_i}{D_s} = \mu \cdot \Omega_0 \tag{7-4}$$

Note that typical structural design criteria prescribe the seismic base shear V_s (or V in 1997 NEHRP Recommended Provisions) and its distribution over the height of the building. Analysis of the building for these forces assuming elastic behavior results in the elastic drift D_s. The design drift is calculated as $C_d D_s$, which is supposed to be an estimate of the actual inelastic displacement. However, relative values of C_d and R are inconsistent, so that the design drift $C_d D_s$ is less than displacement D_i, except for structural systems for which $R/C_d = 1.0$. This fact has implications in the use of specified allowable story drift limits when the analysis procedure predicts the actual displacement (as it is the case in Method 2 and the procedure presented in this section).

The displacement ductility ratio μ may be related to factors R and Ω_o as follows. In the constant velocity region of the spectrum ($T_1 \geq T_s$), the equal displacement assumption may be used, so that $D_i = D_e$. It follows that

$$\mu = R_\mu \quad , T_1 \geq T_s \tag{7-5}$$

In the constant acceleration region of the spectrum ($T_1 < T_s$), the equal energy assumption may be used, so that

$$\mu = \frac{1}{2}\sqrt{R_\mu^2 + 1} \quad , T_1 < T_s \tag{7-6}$$

Utilizing (7-3) and introducing the importance factor I (NEHRP, 1997) the maximum effective ductility demand is

$$\mu_{max} = \frac{R}{\Omega_0 I} \quad , \; T_1 \geq T_s \tag{7-7}$$

$$\mu_{max} = \frac{1}{2} \left[\left(\frac{R}{\Omega_0 I} \right)^2 + 1 \right] \quad , \; T_1 < T_s \tag{7-8}$$

Note that in (7-7) and (7-8), T_1 is the period of the fundamental mode of vibration of the structure in the direction of interest under elastic conditions. Equations (7-7) and (7-8) are utilized in NEHRP (2000), except that T_1 is replaced by the effective period T_{eff} in (7-7) avoid a discontinuity in μ_{max} at period T_s.

7.3 Elements of Structural Dynamics

Certain results of the theory of structural dynamics are used in the development of the simplified analysis procedure. The results are derived from Clough and Penzien (1975).

Consider the earthquake response analysis of an elastic building. The building is modeled as a multi-degree-of-freedom two-dimensional system with one degree of freedom per floor. Reactive weights w_i are concentrated at the floor levels. The degrees of freedom are the horizontal displacements of each reactive weight with respect to the ground, u_i. The seismic excitation is described by the time history of the horizontal ground acceleration a_g. Neglecting damping, the equations of motion are

$$[M]\{\ddot{u}\} + [K]\{u\} = -[M]\{1\}a_g \tag{7-9}$$

where $[M]$ is the mass matrix (diagonal with elements w_i/g), $[K]$ is the stiffness matrix, $\{1\}$ is a unity vector, $\{u\}$ is a vector containing displacements u_i, and $\{\ddot{u}\}$ is a vector of accelerations, $\ddot{u}_i$.

The solution of the eigenvalue problem of (7-9) results in modal frequencies ω_m (the corresponding period, T_m is $2\pi/\omega_m$) and mode shapes $\{\phi\}_m$, where m varies between 1 and the number of degrees of freedom, N. The dynamic response of the building can be obtained by modal analysis as the superposition of modal responses by substituting in (7-9)

$$\{u\} = [\Phi]\{y\} \tag{7-10}$$

where $\{y\}$ = vector of modal displacements, $[\Phi]$ = matrix having vectors $\{\phi\}_m$ as columns. Note that in (7-10), $[\Phi]$ is defined to be dimensionless so that $\{y\}$ has dimensions of displacement. The use of the orthogonality condition results in decomposition of (7-9) into N uncoupled equations of the form

$$\ddot{y}_m + \omega_m^2 y_m = -\Gamma_m a_g \qquad (7\text{-}11)$$

where Γ_m is the modal participation factor given by

$$\Gamma_m = \frac{\displaystyle\sum_{i=1}^{N} w_i \cdot \phi_{im}}{\displaystyle\sum_{i=1}^{N} w_i \cdot \phi_{im}^2} \qquad (7\text{-}12)$$

where ϕ_{im} = element of mode shape m corresponding to degree of freedom u_i.

Equation (7-11) is used to calculate the peak values of y_m from the 5%-damped response spectrum of motion a_g (the issue of the validity of this approach for highly damped systems is discussed later on). Let the spectral displacement of motion a_g (5%-damped, frequency ω_m) be S_d and the corresponding spectral acceleration be S_a (note that $S_a = \omega_m^2 \cdot S_d$). It follows from (7-10) and (7-11) that the contribution to the displacement vector from mode m is

$$\{u\}_m = \Gamma_m \{\phi\}_m S_d = \Gamma_m \{\phi\}_m \frac{S_a}{\omega_m^2} \qquad (7\text{-}13)$$

Moreover, the peak lateral inertia forces on the building contributed by mode m are given by

$$\{F\}_m = [M]\{\phi\}_m \Gamma_m S_a \qquad (7\text{-}14)$$

and the resultant of these forces (the base shear) is given by

$$V_m = \frac{\overline{W}_m S_a}{g} \qquad (7\text{-}15)$$

91

where $\overline{W}_m$ is the mth modal weight (or effective modal load)

$$\overline{W}_m = \frac{\left(\sum_{i=1}^{N} w_i \phi_{im}\right)^2}{\sum_{i=1}^{N} w_i \phi_{im}^2} = \Gamma_m \left(\sum_{i=1}^{N} w_i \phi_{im}\right) \tag{7-16}$$

It may be shown that

$$\sum_{m=1}^{N} \overline{W}_m = \sum_{i=1}^{N} w_i = W \tag{7-17}$$

That is, the sum of the modal weights equals the total weight W of the building. Moreover, it may be shown that for any $i = 1$ to N

$$\sum_{m=1}^{N} \phi_{im} \Gamma_m = 1 \tag{7-18}$$

Hereafter the mode shapes $\{\phi\}_m$ are normalized so that ϕ_{im} is equal to 1 at the roof level. Under this condition it can be shown that

$$\sum_{m=1}^{N} \Gamma_m = 1 \tag{7-19}$$

Equations (7-17) to (7-19) allow for a theoretically consistent simple definition of a residual mode that could approximately account for the contribution of the higher modes of vibration. Specifically, the equivalent lateral force procedure described herein will utilize the contribution from the first mode and a residual mode of which the associated frequency is arbitrarily selected but the modal weight, modal participation factor and mode shape are determined on the basis of (7-17) to (7-19):

$$\overline{W}_R = W - \overline{W}_1 \tag{7-20}$$

92

$$\Gamma_R = 1 - \Gamma_I \qquad (7\text{-}21)$$

$$\{\phi\}_R = \frac{1}{\Gamma_R}\{1\} - \frac{\Gamma_I}{\Gamma_R}\{\phi\}_I \qquad (7\text{-}22)$$

It may be easily shown that the residual mode shape $\{\phi\}_R$, as defined by (7-22), satisfies the orthogonality conditions.

7.4 Viscous Damping Ratio of Elastic Building

Consider an elastic building with linear viscous damping devices. The damped system is non-classically damped and its frequencies (eigenvalues) and mode shapes (eigenvectors) are not those determined by eigenvalue analysis of the undamped system. Nevertheless, the use of the undamped frequencies and mode shapes together with energy-based calculation of the damping ratios may provide good estimates of the seismic response of damped structures. This is particularly true for buildings with complete vertical distributions of viscous damping devices (Constantinou and Symans, 1992). It may also be valid for cases of incomplete vertical distributions or cases of concentration of damping devices. A case of validity of this approach is in the approximate analysis of soil-structure interaction effects (Veletsos and Meek, 1973; Novak and El Hifnawy, 1983), whereas Constantinou and Symans (1992) demonstrated the validity of the approach in some cases of incomplete vertical distribution of damping devices.

The force-velocity relation of each linear viscous damping device is described by

$$F_{Dj} = C_j \dot{u}_{Dj} \qquad (7\text{-}23)$$

where C_j is the damper coefficient, u_{Dj} is the device relative displacement and $\dot{u}_{Dj}$ is the relative displacement between the ends of the device along the axis of the device. Moreover, the relation between the device relative displacement and the interstory drift Δ_{rj} is

$$u_{Dj} = f_j \Delta_{rj} \qquad (7\text{-}24)$$

where f_j is the displacement magnification factor. This factor equals unity for the chevron brace configuration and equals $\cos\theta_j$ for the diagonal configuration, where θ_j is the angle of inclination

93

of device j (FEMA, 1997; Constantinou et al., 1998). Figure 7-2 shows different installations of damping devices for which the displacement amplification factors can be larger than unity (Constantinou and Sigaher, 2000).

Modal damping ratios in a building can be calculated using (4-15). If it is assumed that a building undergoes harmonic vibration such that

$$\{u\} = D_{roof}\{\phi\}_m \sin\left(\frac{2\pi t}{T_m}\right) \tag{7-25}$$

where D_{roof} is the amplitude of roof displacement; T_m is the undamped m^{th} period of vibration; and $\{\phi\}_m$ is the mth undamped mode shape (normalized so that $\phi_{im} = 1$ for i corresponding to the roof displacement), the energy dissipated by the damping system per cycle of motion in mode m is

$$W_D = \frac{2\pi^2}{T_m} \sum_j C_j f_j^2 D_{roof}^2 \phi_{rj}^2 \tag{7-26}$$

where

$$\phi_{rj} = \phi_{jm} - \phi_{(j-1)m} \tag{7-27}$$

is the difference between the mth modal ordinates associated with degrees of freedom j and $(j-1)$. Note that (7-26) is based on $\Delta_{rj} = D_{roof}\phi_{rj}$. The maximum strain energy W_s is equal to the maximum kinetic energy,

$$W_s = \frac{2\pi^2}{T_m^2} \sum_i \left(\frac{w_i}{g}\right) D_{roof}^2 \phi_{im}^2 \tag{7-28}$$

and the viscous damping ratio in mode m is given by

$$\beta_{vm} = \left(\frac{T_m}{4\pi}\right) \frac{\displaystyle\sum_j C_j f_j^2 \phi_{rj}^2}{\displaystyle\sum_i \left(\frac{w_i}{g}\right)\phi_{im}^2} \tag{7-29}$$

where summation over i extends over all reactive weights and summation over j extends over all damping devices. Equation (7-29) is identical to that given in Constantinou et al. (1998) except that the displacement amplification factor f_j is used in lieu of $\cos\theta_j$.

Consider now the case of nonlinear viscous damping devices for which

$$F_{Dj} = C_{Nj} \left|\dot{u}_{Dj}\right|^{a_j} sgn(\dot{u}_{Dj}) \tag{7-30}$$

where C_{Nj} is the damper coefficient and a_j is the damper exponent. Equation (4-15) may still be used to calculate damping ratio, but the ratio will be amplitude-dependent. Assuming vibration in accordance with (7-25),

$$W_D = \sum_j \left(\frac{2\pi}{T_m}\right)^{a_j} C_{Nj} \lambda_j \left(D_{roof} f_j \phi_{rj}\right)^{1+a_j} \tag{7-31}$$

where λ_j is given by (4-14) as function of the exponent a_j (see Table 4-2). Using (7-28) which is still valid, the damping ratio for mode m equal to 1 is given by

$$\beta_{v1} = \frac{\displaystyle\sum_j (2\pi)^{a_j} \cdot T_1^{2-a_j} \cdot \lambda_j C_{Nj} f_j^{1+a_j} D_{roof}^{a_j-1} \phi_{rj}^{1+a_j}}{8\pi^3 \displaystyle\sum_i \left(\frac{w_i}{g}\right)\phi_{i1}^2} \tag{7-32}$$

Equation (7-32) reduces to (7-29) when $a_j = 1$ (linear viscous damping devices, for which $\lambda_j = \pi$).

Equations (7-29) and (7-32) are utilized for the simplified analysis of yielding damped buildings by replacing period T_1 by the effective period T_{eff}. Details are presented in the next section.

7.5 Effective Period and Effective Damping of Yielding Buildings with Damping Systems

7.5.1 Buildings with Linear Viscous Damping Systems

For a multi-degree-of-freedom building, conversion of the pushover curve to an elastoplastic spectral capacity curve (see Fig. 2-1) results in:

$$A = A_y = \frac{V_y g}{\overline{W}_1} \tag{7-33}$$

$$D_y = \frac{A_y T_1^2}{4\pi^2} = \frac{D_{yR}}{\Gamma_1} \tag{7-34}$$

where V_y is the yield strength established by pushover or plastic analysis using a pattern of lateral loads proportional to the first mode shape of the building for elastic conditions, D_y is the yield displacement in the elastoplastic spectral capacity curve, D_{yR} is the yield displacement in the elastoplastic pushover curve (the subscript R denotes roof displacement) and Γ_1 is the first mode participation factor. The effective period (in the first mode of vibration) is given by (4-18), which on the basis of (7-33) and (7-34) becomes

$$T_{eff} = T_1 \sqrt{\mu} \tag{7-35}$$

where T_1 is the first mode period for elastic conditions and μ is the displacement ductility ratio

$$\mu = \frac{D}{D_y} \tag{7-36}$$

Similarly, the effective damping is given by (4-19) but simplified to

$$\beta_{eff} = \beta_i + \beta_{v1}\sqrt{\mu} + \frac{2q_H}{\pi}\left(1 - \frac{1}{\mu}\right) \tag{7-37}$$

where β_{v1} is the damping ratio under elastic conditions given by (7-29) for m equal to 1. NEHRP (2000) utilizes (7-37) but replaces $(2/\pi)$ by $(0.64\text{-}\beta_i)$ in order to avoid overestimation of the contribution of inherent damping.

Variables T_{eff} and β_{eff} are the effective period and damping in the first mode. Higher modes of the yielded building may be conservatively assumed to possess the properties of the higher modes of the elastic building. That is, the periods are equal to T_m and the damping ratios are given by

$$\beta_m = \beta_i + \beta_{vm} \qquad (7\text{-}38)$$

where m ranges from 2 to N, and β_{vm} is given by (7-29). This is the approach followed in NEHRP (2000). Some improvement may be realized by approximately accounting for the softening of the building due to inelastic action through the use of $T_m \sqrt{\mu}$ as an estimate of the period of higher modes.

When a residual mode is used together with the first mode of vibration, the effective period of the residual mode may arbitrarily be assumed to be either T_2, $T_2 \sqrt{\mu}$ or some multiple of T_1. In NEHRP (2000), T_R is set to be equal to $0.4T_1$. The effective damping in the residual mode may be conservatively assumed to be

$$\beta_R = \beta_i + \beta_{vR} \qquad (7\text{-}39)$$

where β_{vR} is given by (7-29) with $m=R$.

7.5.2 Buildings with Nonlinear Viscous Damping Systems

Using information from Section 4.5, the effective period and effective damping of buildings with nonlinear viscous damping systems are described by equations (7-35) and (7-36), respectively, with β_{eff} equal to

$$\beta_{eff} = \beta_i + \beta_{v1}(\mu)^{1-\frac{a}{2}} + \frac{2q_H}{\pi}\left(1 - \frac{1}{\mu}\right) \qquad (7\text{-}40)$$

where β_{v1} is the damping ratio determined from (7-32) for m=1 (note that calculation of β_{v1} requires knowledge of the roof displacement, D_{roof}) and all other terms were defined previously. Equation (7-40) also assumes that all devices have the same exponent $a_j = a$.

The calculation of the damping ratio in the higher modes or the residual mode is complicated by the fact that (7-32) is not applicable to higher modes. To circumvent this difficulty, Seleemah and Constantinou (1997) resorted to a physical interpretation of the higher mode response. They viewed higher mode response as small amplitude, high frequency motion centered around the first mode response. Accordingly, one could define an effective damping constant C_{effj} for each nonlinear viscous device as illustrated in Figure 7-3. This constant is taken as the slope of the force-velocity curve of the device at the calculated device velocity in the first mode, $\dot{u}_1$:

$$C_{effj} = a_j C_{Nj} \dot{u}_1^{a_j-1} \tag{7-41}$$

Accordingly, the effective damping in the higher modes is given by

$$\beta_m = \beta_i + \beta_{vm} \quad and \quad \beta_R = \beta_i + \beta_{vR} \tag{7-42}$$

where β_{vm} and β_{vR} are calculated using (7-29) with C_{effj} in place of C_j.

7.5.3 Buildings with Viscoelastic Damping Systems

Viscoelastic damping systems exhibit stiffness and damping which are frequency-dependent (Soong and Dargush, 1997; Constantinou et al., 1998). Considering viscoelastic solid devices with bonded area A_b and total thickness h, the storage stiffness K_j and the damping constant C_j of a device are

$$K_j = \frac{G'A_b}{h} \quad , \quad C_j = \frac{G''A_b}{\omega h} \tag{7-43}$$

where G' and G'' are the storage and loss shear moduli of the viscoelastic material, respectively, and ω is the excitation frequency. Both moduli are strongly frequency-dependent but their ratio η, the loss factor, is only mildly dependent on frequency:

$$\eta = \frac{G''}{G'} \tag{7-44}$$

98

Approximately, and for the purpose of simplified analysis calculations, η may be assumed to be equal to unity. A comprehensive database of material properties for a common viscoelastic material valid for a range of temperatures, shear strain and frequency may be found in Zimmer (1999).

Evidently, simplified analysis of buildings with viscoelastic damping systems requires that: (1) the frequency of vibration in each mode is known in order to calculate the storage stiffness and damping constant of each device, and (2) the storage stiffness of each device is included in the mathematical model of the building. The additional stiffness provided by the viscoelastic damping system alters the pushover curve of the building as shown schematically in Figure 7-4. Appendix D presents an example of the analysis of a building with a viscoelastic damping system in which a simple procedure for constructing the idealized pushover curve of the damped structure is presented.

The application of the simplified analysis procedure requires iterative analysis (even under elastic conditions) since the values of storage stiffness and damping constant are frequency-dependent. A reasonable estimate of the first mode period of the damped building under elastic conditions may be obtained as follows. Let the first-mode period of the building without the damping system be T_1', and the period with the damping system be T_1. Let the first mode of vibration be $\{\phi\}_1$ and let assume that the mode remains the same after adding the damping system. This assumption would be approximately valid in damping systems with a complete vertical distribution of devices that have storage stiffness distributed approximately in proportion to the shear stiffness of the stories. It follows that

$$T_1' = 2\pi \left(\frac{\sum_i w_i \phi_i^2}{g \sum_j K_j' \phi_{rj}^2} \right)^{1/2} \tag{7-45}$$

$$T_1 = 2\pi \left(\frac{\sum_i w_i \phi_i^2}{g \sum_j \left(K_j' + K_j \cos^2 \theta_j \right) \phi_{rj}^2} \right)^{1/2} \tag{7-46}$$

where w_i, ϕ_i, ϕ_{rj} are defined in Section 7.3, K_j' is the shear stiffness of story j, K_j is the storage stiffness of devices in story j, and θ_j is the angle of inclination of devices in story j. Stiffness K_j may be written on the basis of (7-43) as

$$K_j = \frac{2\pi C_j}{\eta T_1} \tag{7-47}$$

Use of (7-45), (7-46) and (7-47) results in

$$\frac{1}{T_1^2} = \frac{1}{T_1'^2} + \frac{2}{T_1^2 \eta}\left\{\frac{T_1}{4\pi} \frac{\sum\limits_j C_j \cos^2\theta_j \phi_{rj}^2}{\sum\limits_i \left(\frac{w_i}{g}\right)\phi_i^2}\right\} \tag{7-48}$$

The quantity within the brackets in (7-48) is recognized to be damping ratio under elastic conditions, β_{v1} (see eq.7-29). Accordingly

$$T_1 = T_1'\left(1 - \frac{2\beta_{v1}}{\eta}\right)^{1/2} \tag{7-49}$$

Equation (7-49) is particularly useful in obtaining quick estimates of the period of viscoelastically damped structures (given that $\eta \approx 1$).

When the viscoelastically damped building undergoes inelastic action, the idealized spectral capacity curve is shown in Figure 7-4. The effective period is given by (4-18), which for the bilinear representation of the spectral capacity curve takes the form:

$$T_{eff} = T_1'\left(1 - \frac{2\beta_{v1}}{\eta}\right)^{1/2}\left(\frac{\mu}{1 + \alpha\mu - \alpha}\right) \tag{7-50}$$

where $\mu = D/D_y$ is the displacement ductility ratio, and α is the ratio of the post-elastic stiffness and the elastic stiffness of the viscoelastically damped building.

Similarly, the effective damping is given by (4-19), which now takes the form:

$$\beta_{eff} = \beta_i + \beta_{vI} \left(\frac{\mu}{1 + \alpha\mu - \alpha} \right)^{1/2} + \frac{2q_H}{\pi} \left(\frac{1}{1 + \alpha\mu - \alpha} - \frac{1}{\mu} \right) \qquad (7\text{-}51)$$

Typically, μ will be less than 1.5 and α will be less than 0.2, and quantity $(1 + \alpha\mu - \alpha)$ can be replaced by unity with little error. This allows the use of equations that are valid for the elastoplastic representation of the pushover curve, as done for the viscous damping systems.

It is of interest to obtain an estimate for the stiffness ratio α. On the basis of Figure 7-4 (consider that the spectral capacity curves are obtained from pushover curves that are established by pushing over with loads proportional to the first mode shape)

$$\frac{T_I}{T_I'} = \left(\frac{K_e'}{K_e} \right)^{1/2} = \left(\frac{K_e - \alpha K_e}{K_e} \right)^{1/2} \qquad (7\text{-}52)$$

Note that (7-52) was derived on the basis of the observation that the added stiffness by the damping system is αK_e. Use of (7-49) and (7-52) results in

$$\alpha = \frac{2\beta_{vI}}{\eta} \qquad (7\text{-}53)$$

NEHRP (2000) does not contain specific procedures for viscoelastic damping systems. Rather, allows for the use of procedures which are valid for linear viscous damping systems. As explained in this section, and in more detail in Appendix I, the approach of NEHRP (2000) may be used for viscoelastic damping systems provided that the effect of the damping system on the stiffness and strength of the building is accounted for.

7.5.4 Building with Yielding Damping Systems

The pushover curve of a building with a yielding damping system is approximately trilinear as shown in Figure 4-3. The idealized spectral capacity curve of the building is illustrated in Figure 7-5. In this figure, V_y is the yield strength (or base shear strength) of the building excluding the yielding damping system, and V_d is the added yield strength due to the yielding damping system. The shape of the idealized trilinear spectral capacity curve is based on the assumption that the

damping system yields prior to the yielding of the framing system (i.e., $V_d < V_y$ and $D_{yd} < D_{yf}$). Note that the strength V_d is due to the yielding damping devices in the first story, whereas the contribution of the other damping devices to the pushover and spectral capacity curves is reflected in the initial branch of the trilinear curve.

The effective period and effective damping are given by the following equations, which are valid for displacement D greater than D_{yf} (see Figure 7-5):

$$T_{eff} = 2\pi \left(\frac{D}{A_y + A_d} \right)^{1/2} \tag{7-54}$$

$$\beta_{eff} = \beta_i \left(\frac{1}{1 + A_d/A_y} \right)^{1/2} + \frac{2q_H \left(1 - \frac{1}{\mu_f} \right) + 2 \left(\frac{A_d}{A_y} \right) \left(1 - \frac{1}{\mu_d} \right)}{\pi \left(1 + A_d/A_y \right)} \tag{7-55}$$

where μ_f and μ_d are the displacement ductility ratio for the frame and the damping system, respectively, which are defined as follows::

$$\mu_f = \frac{D}{D_{yf}} \quad , \quad \mu_d = \frac{D}{D_{yd}} \tag{7-56}$$

Use of (7-54) and (7-55) requires the construction of a trilinear representation of the pushover curve of the building inclusive of the yielding damping system. For well-behaved framing systems, plastic analysis can be used to construct the pushover curve, as described in Appendix D.

It is convenient to define an elastoplastic representation of the spectral capacity curve as shown in Figure 7-5. Accordingly,

$$T_{eff} = T_1 \sqrt{\mu} \tag{7-57}$$

$$\beta_{eff} = \beta_i + \frac{2q_H}{\pi} \left(1 - \frac{1}{\mu} \right) \tag{7-58}$$

$$\mu = \frac{D}{D_y} \qquad (7\text{-}59)$$

where T_I is the initial effective period calculated using the initial slope of the elastoplastic spectral capacity curve:

$$T_I = 2\pi \left(\frac{D_o}{b(A_y + A_d)} \right)^{1/2} \qquad (7\text{-}60)$$

where b is a parameter so that the elastoplastic curve best represents the trilinear curve, D_0 is the spectral displacement at the intersection of the trilinear and the elastoplastic representation of the pushover curve and other terms have been defined previously.

Moreover, the yield displacement is given by

$$D_y = \frac{g \cdot (A_y + A_d) \cdot T_I^2}{4\pi^2} \qquad (7\text{-}61)$$

Parameter b may be taken equal to 0.6 in consistency with a similar approach followed in FEMA (1997) or it may be obtained by use of the "equal energy" approach.

7.6 Quality Factor, q_H

By definition, the quality factor q_H (called the hysteresis loop adjustment factor in NEHRP, 2000) is equal to the actual area of the hysteresis loop (consider this to be the base shear-roof displacement loop converted to spectral capacity form) divided by the area of the assumed elastoplastic representation of the loop. The actual area of the hysteresis loop is not known but can be assumed on the basis of the "quality" of the structural system. Presumably a steel special moment frame designed and constructed using of current seismic provisions would have very good hysteretic characteristics, so that q_H should be close to unity. However, an older non-ductile building would be assigned a smaller value of q_H, say 0.2 as is recommended in FEMA (1997).

Another approach to selecting values for the quality factor is by utilizing this factor to calibrate the simplified analysis procedure to predict the seismic base shear prescribed by the equivalent lateral force procedure for buildings without damping systems (NEHRP, 1997). Consider that the ground motion is described by the design response spectrum with parameters S_{DS}, S_{D1} and T_s per NEHRP (1997). Consider now a building without a damping system having a period T_1 under elastic conditions, effective period T_{eff} and effective damping β_{eff} under inelastic conditions when subjected to the design ground motion. Assume that both T_1 and T_{eff} are larger than T_s (period lies in the constant velocity region of the spectrum) and that the residual mode has period T_R that is less than T_s and damping ratio is equal to 0.05. Moreover, assume that the building exhibits elastoplastic behavior. The base shear can be calculated using (7-15) and using the SRSS combination rule:

$$V = \left\{ \left(\frac{\overline{W}_1 S_{D1}}{T_{eff} B} \right)^2 + \left(\overline{W}_R S_{DS} \right)^2 \right\}^{1/2} \tag{7-62}$$

where $\overline{W}_1$ and $\overline{W}_R$ are given by (7-16) and (7-20), respectively, and B is the damping coefficient related to the damping ratio β_{eff}. The latter is given by

$$\beta_{eff} = \frac{2q_H}{\pi} \left(1 - \frac{1}{\mu} \right) \tag{7-63}$$

where μ is the displacement ductility ratio. The effective period is given by (7-35).

Equation (7-62) predicts the base shear strength of the building, V_y. The base shear strength may be predicted by multiplying the seismic base shear prescribed in NEHRP (1997) by the system overstrength factor Ω_o:

$$V_y = \frac{S_{D1} W}{T_1 R} \Omega_0 \tag{7-64}$$

in which the importance factor has been ignored. Equating (7-62) and (7-64), using (7-35) and recognizing that $\mu = R_\mu = R/\Omega_0$ since T_1 and $T_{eff} > T_s$, results in the following equation for B:

$$B = \left\{ \left(\frac{W}{\overline{W}_I}\right)^2 \left(\frac{\Omega_0}{R}\right) - \left(\frac{\overline{W}_R}{\overline{W}_I}\right)^2 \left(\frac{S_{DS}}{S_{DI}}\right)^2 \left(\frac{R}{\Omega_0}\right) T_I^2 \right\}^{-\frac{1}{2}} \qquad (7\text{-}65)$$

The damping coefficient B may be related to the effective damping by empirical equations of the kind of (3-4). However, the following simple equation approximates very well the relation between B and β_{eff} in NEHRP (2000) and is used herein:

$$B = 0.73 + 3.27\, \beta_{eff} \qquad (7\text{-}66)$$

Substitution of (7-66) and (7-63) with $\mu = R_\mu = R/\Omega_0$ in (7-65) and recognizing that $S_{DI}/S_{DS} = T_s$, results in the following equation for q_H :

$$q_H = \frac{\left\{ \left(\frac{W}{\overline{W}_I}\right)^2 \left(\frac{\Omega_0}{R}\right) - \left(\frac{\overline{W}_R}{\overline{W}_I}\right)^2 \left(\frac{T_I}{T_s}\right)^2 \left(\frac{R}{\Omega_0}\right) \right\}^{-\frac{1}{2}} - 0.73}{2.08\left(1 - \frac{\Omega_0}{R}\right)} \qquad (7\text{-}67)$$

Equation (7-67) reveals a complex relation between q_H the ductility-based portion of the R-factor, $R_\mu = R/\Omega_0$, period ratio T_I/T_s and some general dynamic characteristics of the structure. As an approximation, $W/\overline{W}_I \approx 1.33$ and $\overline{W}_R/\overline{W}_I \approx 0.33$ (see Constantinou, 1998), so that q_H is primarily related to T_I/T_s and R/Ω_o. Moreover, (7-67) sometimes predicts either complex values or values larger than unity. For such cases q_H should be set equal to unity. Accordingly,

$$q_H \approx \frac{\left\{ 1.77\left(\frac{\Omega_0}{R}\right) - 0.11\left(\frac{T_I}{T_s}\right)^2 \left(\frac{R}{\Omega_0}\right) \right\}^{-\frac{1}{2}} - 0.73}{2.08\left(1 - \frac{\Omega_0}{R}\right)} \le 1.0 \;\; for\, T_I \ge T_s \qquad (7\text{-}68)$$

Equation (7-68) predicts values of q_H which increase with increasing values of (R/Ω_o), which is proper. However, the dependency of q_H on the period ratio T_I/T_s is complicated by the fact that large values of this ratio result in complex values of the damping coefficient B. The problem

may be traced to (7-62), in which the contribution of the residual mode $\overline{W}_R S_{DS}$ is larger than the base shear strength given by (7-64). That is, the simplified method of analysis overpredicts the base shear force.

An equation similar to (7-68) may be derived for T_1, T_{eff} and T_R less than T_s. In this case the displacement ductility ratio is given by (7-6) so that

$$q_H \approx \frac{\left\{1.77\left(\dfrac{\Omega_0}{R}\right)-0.11\right\}^{-\frac{1}{2}}-0.73}{2.08\left\{1-2\left(1+\dfrac{R^2}{\Omega_0^2}\right)^{-\frac{1}{2}}\right\}} \leq 1.0 \ \text{for} \ T_1 < T_s \qquad (7-69)$$

Equations (7-68) and (7-69) have been used to prepare Table 7-1, in which $(R/\Omega_0 I)$ has been used instead of (R/Ω_0). It is apparent that a simple rule to describe the dependency of q_H on various parameters is not easy to develop. NEHRP (2000) utilizes a simple, highly approximate but conservative rule that relates q_H to T_1/T_s as follows.

$$0.5 \leq q_H = 0.67\frac{T_s}{T_1} \leq 1.0 \qquad (7-70)$$

The relation correctly predicts the trend towards $q_H = 1.0$ in the constant acceleration domain of the spectrum but is conservative for flexible structures.

7.7 Minimum Allowable Base Shear

The application of a simplified method of analysis requires that a minimum allowable base shear be specified. On the basis of the results presented in Section 6 of this report which were incorporated into NEHRP (2000), the minimum allowable base shear V_{min} for the design of the seismic-force-resisting system is

$$V_{min} = \frac{V}{B} \geq 0.75V \qquad (7-71)$$

where V is the seismic base shear specified for a building without a damping system, and B is the damping coefficient for the damping ratio β_1 of the elastic building in the fundamental mode (the damping ratio β_1 includes the inherent damping and the added damping).

The limit $0.75V$ typically dictates the minimum strength for buildings with viscous or viscoelastic damping systems since $\beta_1 \geq 0.15$ and $B \geq 1.35$, and therefore $1/B \leq 0.74$. In buildings with yielding or hysteretic damping systems, the limit V/B may dictate design depending on the strength and yield displacement characteristics of the frame (exclusive of the damping system) and of the damping devices. One may then question the usefulness of a hysteretic damping system since the goal of drift reduction may be achieved by merely increasing the sections of the seismic-force-resisting system, an approach that is typically followed today. The addition of a hysteretic damping system will reduce displacements and increase building strength while limiting significant inelastic action to the damping system, which does not form part of gravity framing system. In the event of a major earthquake, only the dampers should be damaged (due to inelastic action). These dampers could be easily replaced after the earthquake with little or no impact on the gravity framing.

Equation (7-71) provides the seismic base shear, that is, the resultant of lateral forces acting on the building when the first plastic hinge forms. When the design of the seismic-force-resisting system is based on plastic analysis principles, the required base shear strength V_y is needed. On the basis of Section 7.2 (see Fig. 7-1), $V_y = V_{min}\Omega_0$. However, this equation would be valid if factors R and C_d were correctly specified to be equal (see Section 7.2). Until such inconsistency in the values of R and C_d is eliminated NEHRP (2000) presents equations which imply that

$$V_y = V_{min}\Omega_0 \frac{C_d}{R} \tag{7-72}$$

Equation (7-72) is used in the examples presented in Section 8 to arrive at the required base shear strength of the building. Plastic analysis principles are then used to size the seismic-force-resisting system to have base shear strength V_y and an acceptable collapse mechanism.

107

7.8 NEHRP (2000), Appendix to Chapter 13, Structures with Damping Systems

Appendix A contains the Appendix to Chapter 13 of NEHRP (2000) for the analysis and design of buildings with damping systems. This version of the Appendix was approved by the Provisions Update Committee in late 1999.

Appendix A describes two simplified analysis procedures: equivalent lateral force analysis procedure (ELF) and response spectrum-analysis-procedure (RSA). These procedures are largely based on the presentations of Sections 4 and 7 except as described below:

(1) The calculated base shear in NEHRP (2000) is the base shear at the formation of the first plastic hinge, whereas equation (7-15) describes the base shear strength for the yielding building. Note that the design base shear is equal to the base shear strength divided by the system overstrength factor Ω_o. However, NEHRP (2000) divides by factor $\Omega_0\, C_d/R$ (see equations A13.4.3.4-1 and A13.4.3.4-2) to arrive at a conservative estimate of the base shear. This conservatism will be removed when C_d is specified equal to R.

(2) NEHRP (2000) utilizes equations for the effective fundamental mode period and the effective damping which, strictly speaking, are valid for buildings with elastoplastic behavior and linear viscous damping systems. Valid equations for nonlinear viscous damping systems are presented in Section 7.5.2, viscoelastic damping systems in Section 7.5.3, and yielding damping systems in Section 7.5.4 and Appendix D.

(3) NEHRP (2000) presents equations to calculate the roof displacement (e.g., equation A13.4.4.3-1) and accordingly defines the effective ductility as the ratio of the maximum roof displacement to the roof displacement at the effective yield of the seismic-force-resisting-system. Herein, the effective ductility demand (or displacement ductility ratio) is defined as the ratio of the maximum displacement to the effective yield displacement in the first mode spectral representation of the building. The two effective ductility demands are equal.

(4) NEHRP (2000) replaces $(2/\pi)$ of equation (7-37) with $(0.64-\beta i)$ in equation A13.3.2.2-1 allow for the direct addition of inherent damping ratio β_i in equation A13.3.2-2.

(5) NEHRP (2000) utilizes pseudo-velocity to calculate the maximum velocity. Accordingly, velocities in the fundamental mode tend to be underestimated, whereas velocities in the higher modes tend to be overestimated (see Section 4.9 and Table 4-6). Examples presented in Section 8 indicate that after combination of the modal drift velocities, the error in the resultant drift velocity is significantly reduced. Analyses using the correction factors of Table 4-6 show only minor improvements in the prediction of velocity-dependent forces.

(6) NEHRP (2000) utilizes the load combination factors CF_1 and CF_2 presented herein and described in (4-35), (4-39), (4-41) and (4-42) but defines them as force coefficients C_{mFD} and C_{mFV}, respectively, and presents them in tabular form.

(7) NEHRP (2000) specifies maximum effective ductility demands (equations A13.3.5-1 and A13.3.5-2) that are consistent with (7-7) and (7-8) but uses $(R/\Omega_0 I)$ instead of (R/Ω_0), where I is the occupancy importance factor. That is, the ductility-based portion of the R-factor and the maximum ductility demand are reduced for important structures.

(8) NEHRP (2000) contains criteria for assessing the safety of the building, which include allowable story drift limits (Section A13.7.2). These limits are set equal to (R/C_d) times the allowable story drift for buildings without damping systems. The reason for this difference is that the values for R and C_d are not equal. Accordingly, the procedures described in NEHRP (2000) for buildings with damping systems predict the actual displacement response of the building, whereas the corresponding procedures for buildings without damping systems predict a smaller displacement since C_d is typically less than R. Accordingly, the specified drift limits for buildings are (C_d/R) times less than what the limits should be had the displacement prediction been correct. The NEHRP (2000) corrects for this discrepancy by increasing the drift limits by factor (R/C_d).

7.9 Conclusions

The theoretical basis of the equivalent lateral force and the response spectrum analysis procedures of NEHRP (2000) has been presented. Moreover, procedures for calculating the effective damping and effective period, and the higher mode damping ratios for buildings with

nonlinear viscous damping systems, viscoelastic damping systems and yielding damping systems have been developed. These procedures are not presented in NEHRP (2000) but are needed for the application of the NEHRP (2000) analysis methods.

TABLE 7-1 Values of Quality Factor q_H predicted by Equations (7-68) and (7-69)

$R/\Omega_o I$ \\ T_l/T_s	< 1	1	1.2	1.5	1.7	2.0	> 2.0
4/3	1.0	0.35	0.41	0.51	0.61	0.82	1.0
2	1.0	0.47	0.57	0.8	1.0	1.0	1.0
8/3	1.0	0.70	1.0	1.0	1.0	1.0	1.0
3	1.0	0.88	1.0	1.0	1.0	1.0	1.0
≥ 4	1.0	1.0	1.0	1.0	1.0	1.0	1.0
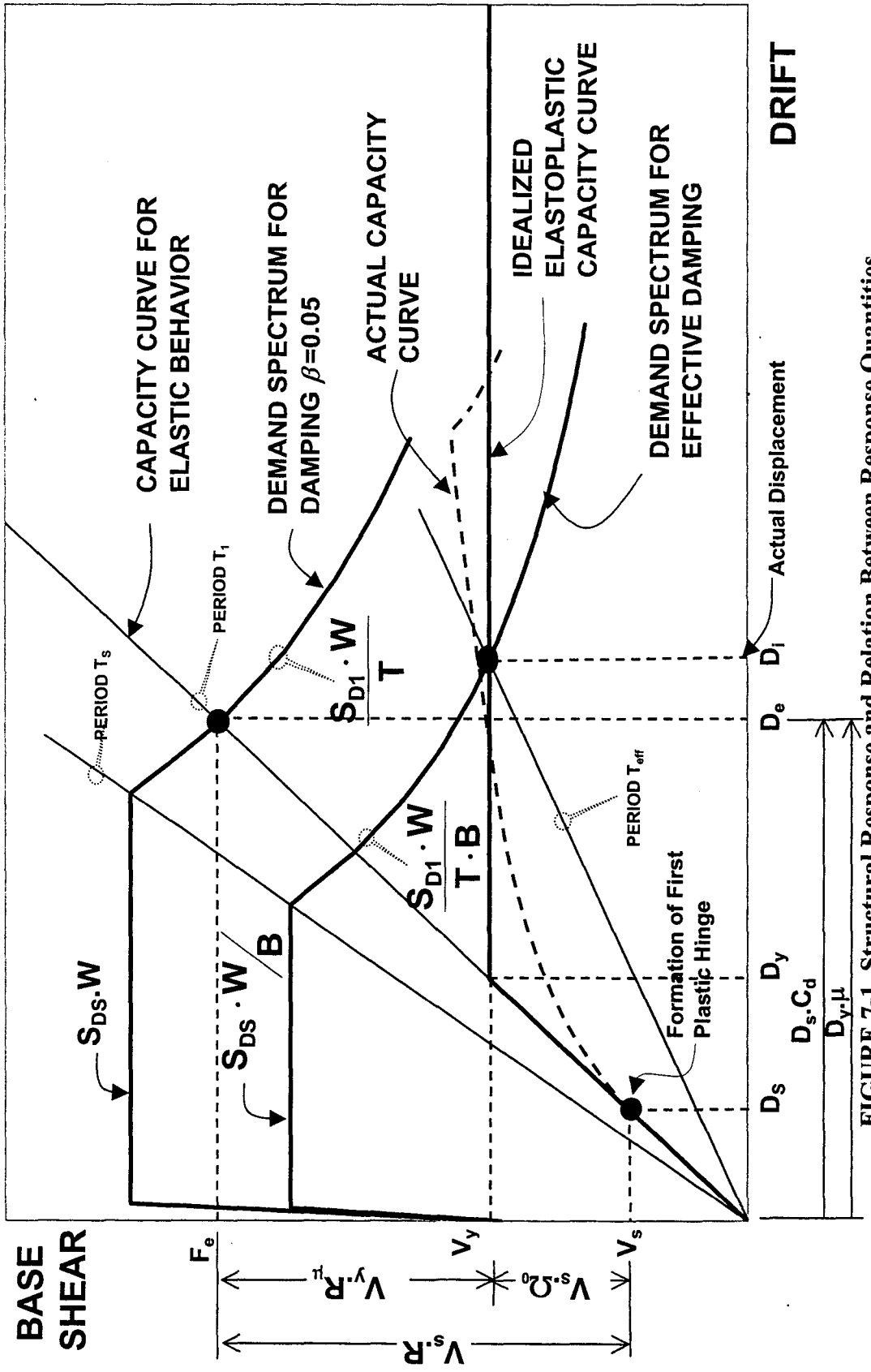
FIGURE 7-1 Structural Response and Relation Between Response Quantities

CONFIGURATION	DISPLACEMENT AMPLIFICATION FACTOR
Diagonal DAMPING DEVICE θ	$f = cos\,\theta$
Chevron	$f = 1.00$
Lower Toggle θ_2 θ_1 90°	$f = \dfrac{sin\,\theta_2}{cos(\theta_1 + \theta_2)}$
Upper Toggle 90° θ_2 θ_1	$f = \dfrac{sin\,\theta_2}{cos(\theta_1 + \theta_2)} + sin\,\theta_1$
Reverse Toggle θ_1 90° θ_2 $\alpha\ell$ ℓ	$f = \dfrac{\alpha\,cos\,\theta_1}{cos(\theta_1 + \theta_2)} - cos\,\theta_2$
Scissor-Jack θ_3 ψ	$f = \dfrac{cos\,\psi}{tan\,\theta_3}$

FIGURE 7-2 Displacement Amplification Factors for Various Damping System Configurations

113
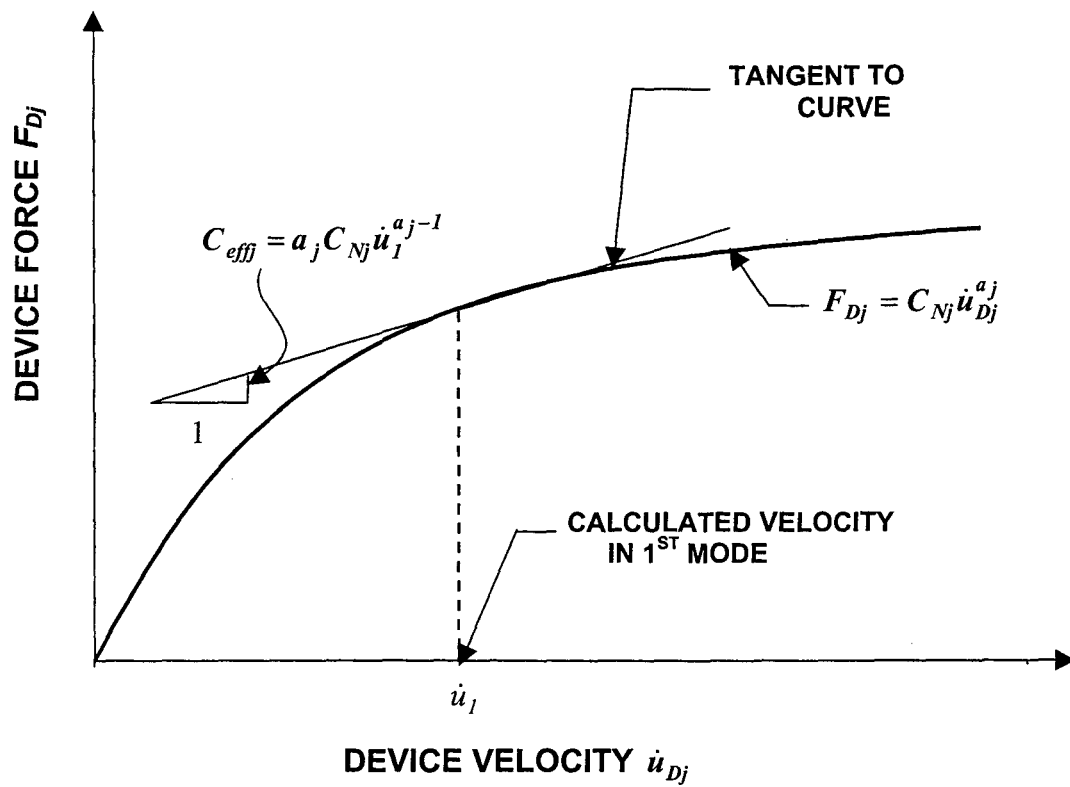
FIGURE 7-3 Effective Damping Constant of Nonlinear Viscous Damping Device for Higher Mode Response Calculation
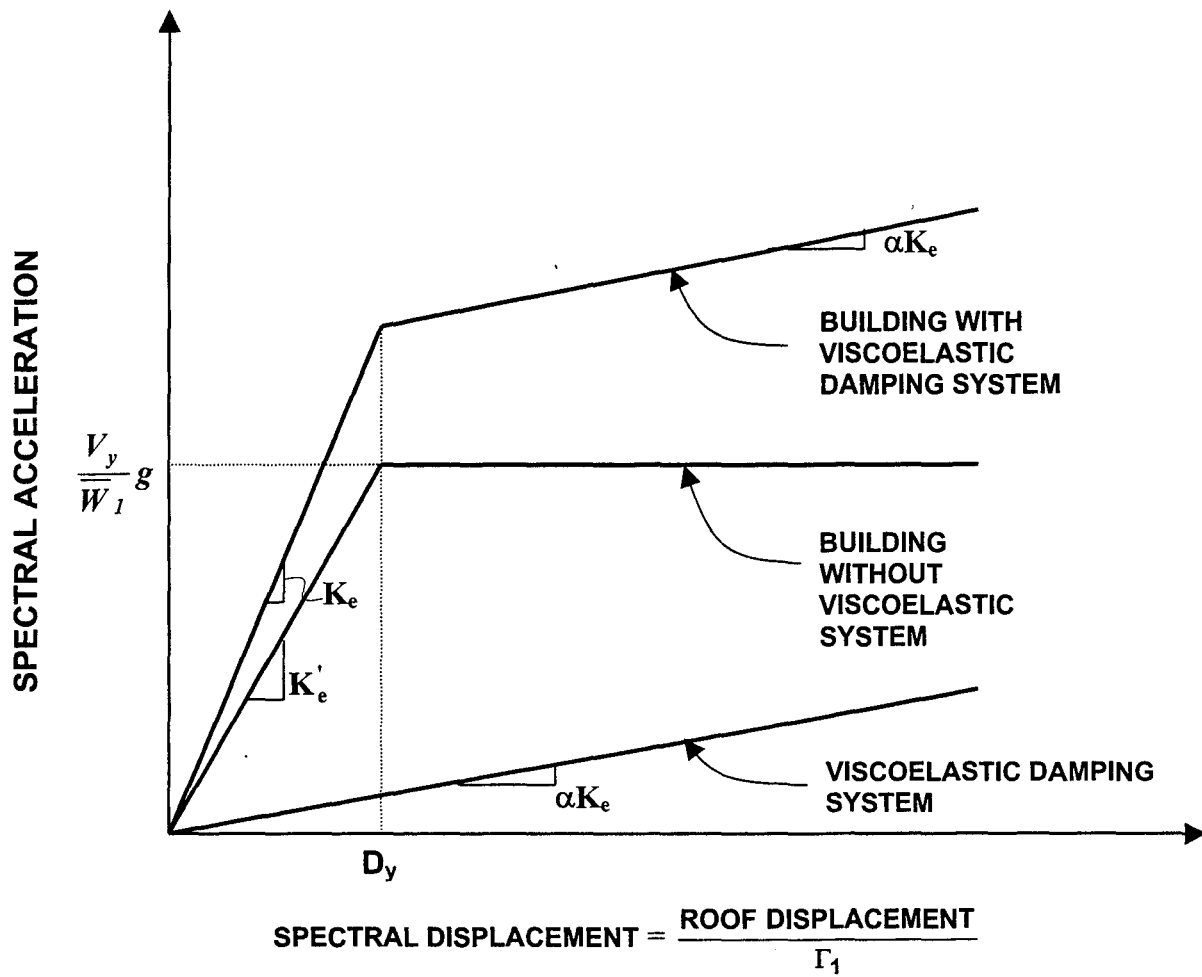
FIGURE 7-4 Idealized Spectral Capacity Curves of Building
Without and With a Viscoelastic Damping System
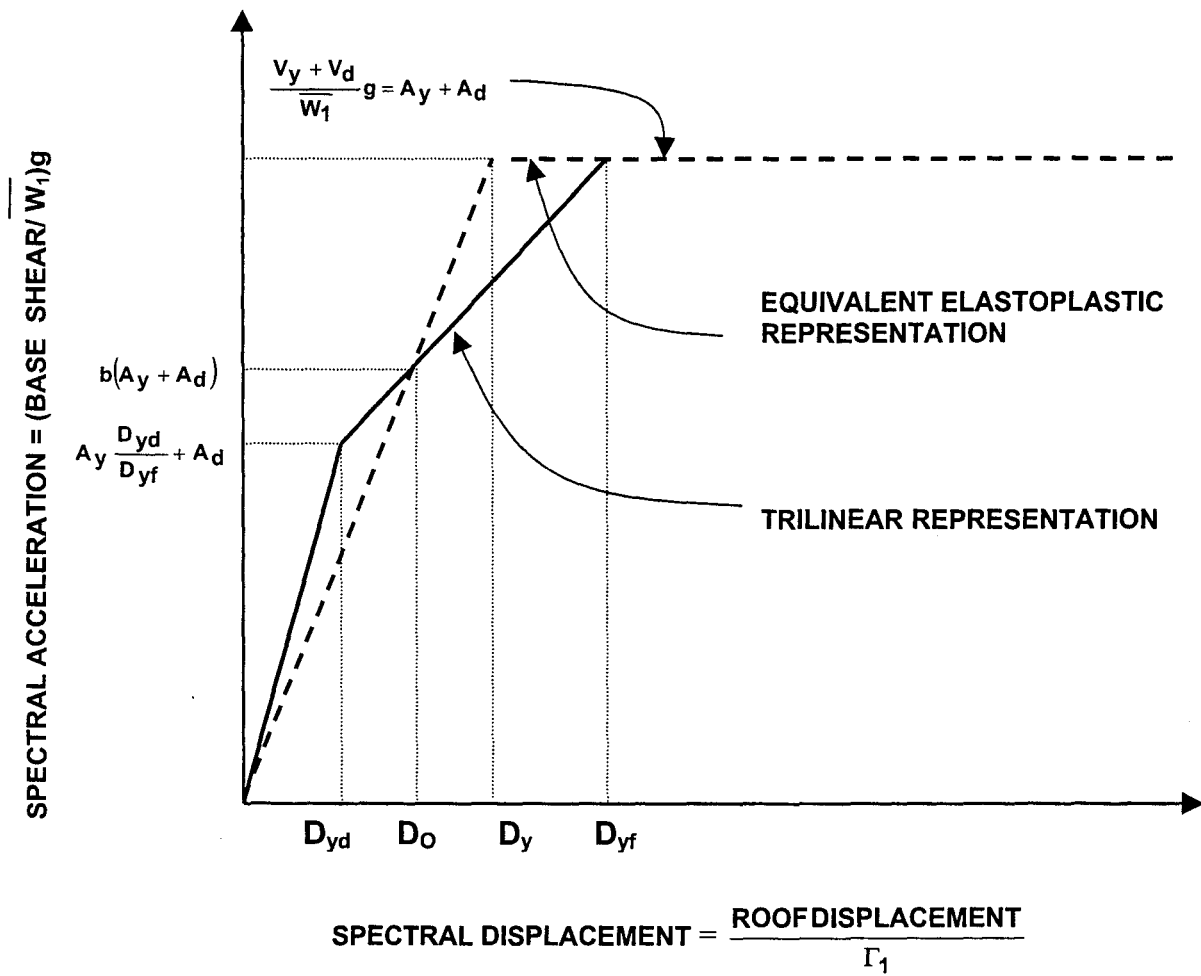
FIGURE 7-5 Idealized Trilinear and Equivalent Elastoplastic
Spectral Capacity Curves of Building with a Yielding Damping

SECTION 8

EVALUATION OF METHODS OF ANALYSIS AND DESIGN OF BUILDINGS WITH DAMPING SYSTEMS

8.1 Introduction

This section presents examples of design and analysis of buildings with damping systems. The analyses were performed using the NEHRP (2000) equivalent lateral force and response-spectrum methods and the FEMA (1997) Method 2, except as modified below:

(1) In the application of NEHRP (2000) and FEMA (1997) Method 2, the load combination factors CF_1 and CF_2 described by (4-35), (4-39), (4-41) and (4-42) were used instead either of the corresponding factors in FEMA (1997) and the force coefficients C_{mFD} and C_{mFV} listed in NEHRP (2000). This modification is of minor significance in the application of the NEHRP (2000) methods of analysis and it was done for convenience because it is easier to utilize equations rather than tables when the analysis is performed in a spreadsheet. However, the modification is of some significance for the calculation of the maximum acceleration using Method 2 of FEMA (1997).

(2) In the application of the NEHRP (2000) methods of analysis, the procedures described in Section 7 for the calculation of the effective damping, the effective period and the added strength and stiffness were followed. The procedures described in NEHRP (2000) are valid for linear viscous damping systems and for viscoelastic and yielding damping systems provided that the strength and stiffness added by the damping system are included in the mathematical model but only approximate for nonlinear viscous damping systems.

(3) The velocity correction factors presented in Section 4.9 were used in selected examples to demonstrate the significance of the correction procedure for multi-degree-of-freedom systems.

(4) The pushover analysis required by Method 2 of FEMA (1997) was performed using the recommended modal and uniform distributions of lateral load, and additional distributions based on the first mode and the adaptive patterns.

The examples presented below involve three- and six-story special steel moment frame buildings with linear viscous, nonlinear viscous, viscoelastic and yielding damping systems installed in diagonal or chevron brace configurations. Each of these frames was designed based on the procedures of NEHRP (2000) for a base shear V in the range of $0.6V_{min}$ to V_{min} and subsequently analyzed using the NEHRP (2000) and the FEMA (1997), Method 2 procedures. In all analyses, the seismic excitation was described by the response spectrum of NEHRP (1997) and FEMA (1997) with parameters $S_{DS} = 1.0$, $S_{D1} = 0.6$ and $T_s = 0.6$ sec. Each example building was also analyzed using nonlinear response history analysis using the twenty scaled motions presented in Section 3.2. The nonlinear response-history analysis data were used to study the usefulness and accuracy of the approximate methods of analysis.

8.2 Design of 3-Story and 6-Story Reference Frames

The reference frames were special steel moment frames in 3-story and 6-story buildings without damping systems. These frames were designed to meet the minimum base shear and drift limits of NEHRP (1997), Section 5.3. Later in this section, these frames are compared with the corresponding frames with damping systems to judge the benefits and drawbacks offered by the damping systems.

Appendix B presents a description of the geometry, the design parameters and loads for the example building. Figure B-1 shows the plan view and elevation of the building. The lateral force-resisting system is composed of two special steel moment frames in each direction. For such frames, NEHRP (1997) assigns $R = 8$, $C_d = 5.5$, and $\Omega_o = 3$. Also presented in Appendix B is the design of the 3-story and 6-story reference frames that satisfy the NEHRP drift limit $\Delta_a = 0.02\ h_{sx}$, where h_{sx} is the story height. Torsional effects are not included in this study. The final designs are shown in Figures B-2 and B-3, for the 3-story and the 6-story reference frames, respectively.

The weight of the 3-story reference frame W_o is approximately 215 kN (48.4 kips), and the fundamental period of vibration T_o is 1.07 sec (determined from eigenvalue analysis using IDARC2D Version 5.0, Valles et al., 1996). The minimum required base shear strength of this frame $V_{y,min}$, that is, the design base shear V according to NEHRP (1997) times the factor $C_d.\Omega_o/R$, is 1626 kN (366 kips). The actual base shear strength V_{yo} ranges between 2223 kN (500 kips) and 2775 kN (624 kips), depending on the distribution of lateral load (established using the plastic analysis approach of Appendix C, and confirmed by pushover analysis using program SAP-2000NL). That is, an overstrength ratio between 1.37 and 1.70 is obtained as a result of the drift limit criteria. The weight of the 6-story reference frame W_o is approximately 504 kN (113 kips) and has a fundamental period T_o= 1.90 sec. The minimum required strength $V_{y,min}$ is 2108 kN (474 kips), and the actual strength V_{yo} ranges between 2748 kN (618 kips) and 3646 kN (820 kips) depending on the distribution of lateral load, which represents an overstrength ratio between 1.30 and 1.73.

8.3 Design of 3-Story and 6-Story Frames with Damping Systems

Frames with damping systems may be designed in accordance with NEHRP (2000) for a seismic base shear of not less than $0.75V$, where V is the seismic base shear for the frame without a damping system. Equivalently, frames with damping systems may be designed to have a base shear strength exclusive of the damping system not less than $0.75V_y$, where V_y is the base shear strength of the frame without a damping system designed for seismic base shear V in accordance with NEHRP (1997).

Frames were designed for the building shown in Figure 8-1, with heights of three and of six stories. These frames have base shear strength in the range of 60 to 100% of V_y. Subsequently, damping systems are added to these frames and proportioned in accordance to NEHRP (2000) to meet the drift criteria. Six frames were designed: five 3-story frames with approximate base shear strengths of 60, 75, 80, 90, and 100% of V_y, and one 6-story frame with base shear strength of 75% of V_y. These frames are classified as 3S-60, 3S-75, 3S-80, 3S-90, 3S-100 and 6S-75, respectively, in which the first number denotes the number of stories and the second number denotes the percentage ratio of the actual base shear strength of the damped frame exclusive of the damping system, V_{ya}, to the base shear strength of the frame without the damping system

designed for seismic base shear V in accordance with NEHRP (1997), V_y. In each case, the base shear strength of the frame was calculated by using the plastic analysis method described in Appendix C.

Table 8-1 presents a summary of the characteristics of the six frames. Information is presented in terms of strength ratios (V_{ya}/V_y and V_{ya}/V_{yo}), weight ratio (weight of damped frame to weight of reference frame, W/W_o), lateral drift ratio of the frame without the damping system (actual maximum drift to allowed drift, Δ_{max}/Δ_a), and the period ratio (fundamental period of the damped frame to period of the reference frame, T/T_o). The maximum story drift Δ_{max} was obtained by the procedures described in NEHRP, 1997. The data of Table 8-1 show that the base shear strengths of the frames with damping systems, V_{ya}, are substantially lower than the strengths of the reference frames that were designed to meet the NEHRP drift criteria. Ratios of V_{ya}/V_{yo} ranged between 0.44 for frame 3S-60 and 0.73 for frame 3S-100.

The frames exclusive of the damping systems do not meet the drift criteria of 1997 NEHRP (less than or equal to 0.02 h_{sx}). Damping systems were designed for these frames to reduce drifts to acceptable levels. For example, frame 3S-75 with a linear viscous damping system that provides an added damping ratio of 0.10 in the first mode under elastic conditions meets the drift criteria of NEHRP (2000). The benefits offered by the damping system include (a) substantial reduction of the required strength of the frame, (b) lower floor and smaller foundations on average.

A total of nine examples utilizing the six frames of Table 8-1 were analyzed. The frames with the damping systems in these examples are illustrated in Figures 8-1 to 8-9 and are briefly described below:

(1) Example No.1: frame 3S-60 with linear viscous damping system to provide 10% viscous damping ratio when assuming elastic frame behavior (Fig. 8-1). Detailed calculations are presented in Appendix E.

(2) Example No.2: frame 3S-75 with linear viscous damping system to provide 10% viscous damping ratio when assuming elastic frame behavior (Fig. 8-2). Detailed calculations are presented in Appendices E and I.

(3) Example No.3: frame 3S-90 with linear viscous damping system to provide 10% viscous damping ratio when assuming elastic frame behavior (Fig. 8-3). Detailed calculations are presented in Appendix E.

(4) Example No.4: frame 3S-100 with linear viscous damping system to provide 20% viscous damping ratio when assuming elastic frame behavior (Fig. 8-4). Detailed calculations are not presented for this example.

(5) Example No.5: frame 6S-75 with linear viscous damping system to provide 10% viscous damping ratio when assuming elastic frame behavior (Fig. 8-5). Detailed calculations are presented in Appendix E.

(6) Example No.6: frame 3S-80 with nonlinear viscous damping system to provide 10% viscous damping ratio when assuming elastic frame behavior in the design basis earthquake (DBE) (Fig. 8-6). Detailed calculations are presented in Appendix F.

(7) Example No.7: frame 3S-80 with nonlinear viscous damping system to provide 20% viscous damping ratio when assuming elastic frame behavior in the maximum considered earthquake (MCE) (Fig. 8-7). Detailed calculations are presented in Appendix F.

(8) Example No.8: frame 3S-75 with viscoelastic solid damping system to provide 8.5% viscous damping ratio when assuming elastic frame behavior (Fig. 8-8). Detailed calculations are presented in Appendix G.

(9) Example No.9: frame 3S-75 with metallic yielding damping system (Fig. 8-9). Detailed calculations are presented in Appendix H.

Appendices E trough H present detailed calculations for the NEHRP (2000) simplified methods of analysis. Appendix I presents detailed calculations for the FEMA (1997) Method 2 (as modified herein) Example No.2 (3S-75 with linear viscous damping system).

8.4 Nonlinear Time History Analysis

Nonlinear time-history analysis was performed using Version 5.0 of program IDARC2D (Valles et al., 1996). Apart from the known capabilities of this program for the analysis of yielding systems, versions 4.0 and 5.0 of this program have enhanced capabilities for pushover analysis and elements for modeling the behavior of damping systems. These elements include a hysteretic element for modeling metallic yielding, friction, linear and nonlinear viscous, and Kelvin and Maxwell elements.

Viscous damping devices were directly modeled in program IDARC2D, Version 5.0 in their diagonal configurations, including the effect of the flexibility of the bracing to which these devices were attached. However, complexities arose in modeling viscoelastic and metallic yielding devices. Specifically:

(1) The behavior of viscoelastic solid damping devices could not be directly modeled by the three-parameter model. This model is one of a spring of stiffness K_1 and of a Maxwell element with a spring of stiffness K_2 and a dashpot of constant C_2 in parallel as shown in Figure D-5. However, the program did not accept two elements connected to the same nodes. The problem was circumvented as shown in Figure 8-10. The utilized model captured correctly the behavior of the damping device in the horizontal direction but did not correctly account for the transfer of load from the devices to the frame. The latter was judged to be of significance only for the assessment of the safety of the frame. Moreover, the utilized model did not allow for the direct calculation of the peak force in the damping devices. Rather, force histories in each of the two branches of the element had to be exported to a spreadsheet and then added.

(2) The chevron brace configuration could not be modeled in IDARC2D because the program produced erroneous results. Accordingly, the metallic yielding damping system was modeled as shown in Figure 8-11, which produced the correct lateral behavior but did not correctly account for the transfer of load from the devices to the frame. Again, this was judged to be of significance only for the safety assessment of the frame.

The frames of examples No.1 to 9 were analyzed as follows:

122

(1)   Examples No.1, 2, 3, 5, 6, 8 and 9 were analyzed for the design basis earthquake (DBE) and the maximum considered earthquake (MCE). The DBE consisted of the 20 scaled motions described in Section 3 and presented in Table 3-2. The MCE consisted of the DBE acceleration histories multiplied in amplitude by 1.5. Peak response quantities were obtained for each motion and values are presented for minimum, maximum, average, and average plus one standard deviation (1σ) responses.

(2)   Examples No.2 and No.4 were analyzed with selected near-fault ground motions to assess the validity of the NEHRP (2000) methods of analysis. The motions were the Sylmar 90 degree, and Newhall 360 degree motions from the 1994 Northridge earthquake, Pacoima Dam S16E motion from the 1971 San Fernando earthquake. These motions have strong near-fault characteristics with peak ground velocities of 0.77 m/s, 0.95 m/s and 1.1 m/s, respectively. The peak ground accelerations of these records were 0.6g, 0.59g and 1.17g, respectively. Examples No.2 and No.4 are used, together with the reference 3-story frame (illustrated in Fig. B-3), to study the extent of inelastic action and damage in frames with and without damping systems.

(3)   Example No.7 was analyzed only for MCE shaking since the design of the damping system was based on providing an effective damping ratio of 20% in this earthquake when elastic frame behavior is assumed.

8.5 Comparison of Results of Simplified Methods of Analysis to Results of Nonlinear Time History Analysis

Comparisons of results of the simplified methods of analysis to the results of nonlinear time-history analysis are presented in Tables 8-2 to 8-19. These tables present results obtained using the following procedures:

(1) NEHRP(2000) Equivalent Lateral Force (ELF) and Response Spectrum Analysis (RSA) procedures. Each of these methods was applied per Section 8.1 and again with the modification of the higher mode periods calculated as $T_m \sqrt{\mu}$, where μ is the ductility demand calculated from the analysis of the first mode response.

(2) Method 2 of FEMA (1997) as described in Section 8.1 using four different lateral force patterns. Of these patterns, two are described in FEMA (1997). The other two are one proportional to the first mode, and the second is an adaptive pattern where the lateral loads are adjusted during the pushover analysis on the basis of the calculated resistance of the various structural elements. It has been argued that the adaptive pattern of loads best captures the behavior of the yielding structure (Valles et al., 1996).

The presented results include:

(1) Peak interstory drifts.

(2) Peak interstory velocities.

(3) Peak damper forces.

(4) Story shear forces at the instance of maximum displacement (when velocities are zero).

(5) Maximum story shears (including the viscous component).

(6) Maximum floor accelerations.

The IDARC2D input files for the pushover and nonlinear time-history analysis are presented in Appendix K.

A study of the results in Tables 8-2 to 8-19 reveals the following:

(1) The use of period $T_m \sqrt{\mu}$ instead of T_m for higher modes with NEHRP (2000) methods of analysis produces slightly improved predictions of response compared with the average of the nonlinear time-history analysis. The improvement is primarily seen in the prediction of the shear force. For example, Table 8-3 presents results of the response spectrum analysis method for the story shear forces at maximum displacement as 869, 917 and 1453 kN when using period T_m. The prediction when using period $T_m \sqrt{\mu}$ is 627, 894 and 1215 kN. The average values of shear force in the nonlinear time-history analysis are 547, 985 and 1212 kN for the three stories.

(2) The simplified procedures predict conservative estimates of story drift which consistently fall between average and the average plus 1σ results of the nonlinear time-history analysis.

(3) The correction of pseudo-velocity by use of the factors of Table 4-6 improves the predictions of interstory velocity and damper force (see Tables 8-2 and 8-3). Although the improvement in the prediction is not significant, it appears that the correction is simple enough to implement so that its use is warranted. This is demonstrated in Tables 8-2 and 8-3 where values in parenthesis were obtained by use of the revised velocity correction factors of Table 4-6.

(4) The use of the adaptive load pattern in the application of Method 2 of FEMA(1997) did not produce any significant improvement in the prediction of the peak response over the use of the maximum among the responses predicted by use of the modal and uniform load patterns. Actually the use of the adaptive pattern resulted in a systematic underprediction of the maximum base shear (including the viscous component). This is best seen in Table 8-17 in which key design parameters are summarized.

(5) The prediction of key design parameters such as the peak damper force and the maximum base shear force differs considerably among the various simplified methods of analysis. Table 8-17 presents a summary of these predictions for the MCE. However, despite these differences, the prediction is generally within 30% of the average of the nonlinear time history analysis. Such accuracy is most acceptable for simplified methods of analysis.

(6) The Equivalent Lateral Force method of NEHRP (2000) tends to overpredict the damper forces and frame member actions in the lower stories. This overprediction is primarily caused by the contribution of the residual mode to the total response. The residual mode shape (see eq. 7-22) has a substantial component associated with the displacements of the lower floors of the building (e.g., see values for one of the analyzed 3-story buildings in Table E-7 and for the analyzed 6-story building in Table E-10 of Appendix E). As seen in tables E-7 and E-10, the residual mode resembles second mode of vibration but has substantially larger modal displacements in the lower floors and larger modal weight. While this results in an overprediction of the response in the upper part of the building.

125

(7) The simplified methods of analysis of NEHRP (2000) produce systematically conservative results on the story drift and results of acceptable accuracy on the damper forces and story shear forces (within 30%) in near-fault ground motions. As seen in Tables 8-18 and 8-19, there is no substantial improvement of the prediction of the simplified methods of analysis when the actual damped spectra of the near-fault motions are used. This provides some evidence that the damping coefficients in NEHRP (2000) apply to near-fault motions. However, the utilized near-fault motions and the analyzed structures are too few to provide definitive evidence on the validity of the simplified methods of analysis for near-fault motions.

8.6   Implications of Errors in the Calculation of Base Shear Strength

The base shear strength of the structure for a pattern of lateral loads proportional to the first mode is needed for the correct calculation of the contribution to the response by the first mode of vibration. Errors in the calculation of the base shear strength have effects which were investigated by analyzing the structures of examples No.1 and No.3 with incorrectly assumed base shear strength as follows:

(1) Example No.1 with an assumed base shear strength of 1310 kN rather than the correct strength of 991 kN. The correct strength was calculated by the procedures of Appendix C and is presented in Appendix E, Table E-5.

(2) Example No.3 with an assumed base shear strength of 991 kN rather than the correct strength of 1465 kN (see Appendix E, Table E-5).

Results for the first mode contribution are presented in Table 8-20. Evidently, the displacement prediction is unaffected due to the fact that is controlled by the elastic displacement lower limit. Moreover, overprediction of strength results in underprediction of the ductility demand, but this will unlikely be of any significance since the ductility demand is typically well below the limit (NEHRP, 2000, Section A13.3.5 and Section 7.2 herein). It also results in overprediction of story shear forces, which is conservative. However, underprediction of strength results in underprediction of story shear forces, and generally member actions, and overprediction of the ductility demand.

126

8.7 Effect of Viscous Damping Forces on Pushover Curve

It has been presumed in the analysis herein that the pushover curves of frames with viscous damping systems are identical to those exclusive of the damping system. This is an approximation, which likely introduces errors in the prediction of response by the simplified methods of analysis. For example, Figures 8-12 and 8-13 present calculated base shear force-first story drift loops for examples No.1 and No.2 using one of the 20 scaled motions adapted the nonlinear time-history analysis. The loops of the shear force exclusive of the damping component (dashed line in Figs. 8-12 and 8-13) do not show the expected bilinear hysteretic shape. Rather, they show a shape that closely resembles the loops for the total shear. This demonstrates that the pushover curve is affected by the viscous damping forces, likely by inducing rotations of the column ends. This phenomenon, which cannot be accounted for by the current methods of pushover analysis, affects the maximum value of member actions, which can be substantially underestimated.

8.8   Comparison of Pattern and Extend Damage in Frames without and with Damping Systems

The NEHRP (2000) procedures allow the strength of a building to be reduced below that of conventional construction if damping systems are added to the frame. For example, compare the frame of Figure B-3 (without damping devices) to the frame of Figure 8-2 (with linear viscous damping system). The two frames meet the drift and safety criteria of NEHRP (1997) and NEHRP (2000), respectively. As seen in Table 8-1, the frame with the damping system (3S-75) has a base shear strength (for a pattern of lateral loads proportional to the first mode) that is 55% of that of the frame without the damping system (referred to as the reference frame).

The pattern of plastic hinge formation and some key response quantities were investigated in (a) the reference 3-story frame (Fig. B-3), (b) the 3-story 3S-75 frame with linear viscous damping system (Example No.2, Fig. 8-2), and (c) the 3-story 3S-100 frame with linear viscous damping system (Example No.4, Fig. 8-4). It should be noted that case (b) is that of the damped frame that just meets the NEHRP (2000) drift and safety criteria, whereas case (c) is a stronger and highly damped frame. This frame is more representative of a design for substantial improvement of performance. The frames were analyzed using the scaled Northridge Century, component 360

127

degrees of Table 3-2. This motion produced responses in the frames that were similar in value to the average responses calculated using the 20 scaled motions. Analysis were performed for the DBE (the scaled Northridge record) and then again for the MCE (same motion multiplied by factor 1.5). The three frames were then analyzed using the three near-fault motions: Sylmar 90 degrees, Newhall 360 degrees, and Pacoima Dam S16E.

Figures 8-14 through 8-19 present the results of these analyses. Each graph in these figures identifies the seismic excitation, presents key responses quantities such as interstory drift ratios, peak roof displacements, base shear forces (including the damping component and peak plastic hinge rotations, and the location and sequence of formation of plastic hinges. Concentrating first on the performance of the frames in the DBE and the MCE, it is observed that:

(1)   Frame 3S-75 (Figure 8-15) with the damping system (that just meets the drift criteria of NEHRP) exhibits less drift, less plastic hinge rotation and substantially less base shear force than the reference frame without a damping system.

(2)   Frame 3S-100 (Figure 8-16) with the highly damped system performs better in both the DBE and the MCE than the lightly damped 3S-75 frame. However the performance in terms of drift ratios and the maximum plastic hinge rotation is only marginally better in the MCE.

(3)   The maximum DBE drift ratio of 0.028 (see Fig. 8-14) exceeds the limit of 0.02. This frame was designed using the equivalent lateral force method of NEHRP (1997), in which drift is calculated as the elastic displacement for the "reduced" lateral forces multiplied by the factor C_d. The actual drift is R/C_d times larger, that is, $0.02 \times R/C_d = 0.02 \times 8/5.5 = 0.029$.

For the near-fault earthquake motions, we observe that the lightly damped 3S-75 performs substantially better than the reference frame in the Pacoima motion, performs marginally better than the reference frame in the Newhall motion and performs worst in the Sylmar motion. The highly damped 3S-100 frame outperforms the other two frames in terms of maximum displacements and the plastic hinge rotations.

Buildings designed with damping systems to meet the minimum criteria of NEHRP (2000) perform comparably to or better than buildings designed without damping systems to meet the

128

minimum criteria of NEHRP (1997). Moreover, buildings with viscous damping systems offer the advantage of lower base shear force than conventional buildings without damping systems.

8.9 Conclusions

The simplified methods of analysis of NEHRP (2000) and Method 2 of FEMA (1997), as modified herein, provide systematically conservative predictions of drift, and predictions of acceptable accuracy for damper forces and member actions. These force predictions may differ by as much as $\pm 30\%$ from the average forces calculated by dynamic analysis. Interestingly, the simplified methods produced results of acceptable accuracy in near-fault seismic excitations. However, the utilized near-fault motions and analyzed structures were too few to provide conclusive evidence. Further studies with near-fault motions are warranted.

Buildings with damping systems designed to meet the minimum drift and strength criteria of NEHRP(2000) perform comparably to or better than conventional buildings without damping systems.

TABLE 8-1 Characteristics of Example Frames Exclusive of the Damping System

Frame	Number of Stories	Strength Ratio		Weight Ratio	Drift Ratio[*]	Period Ratio
		V_{ya}/V_y	V_{ya}/V_{yo}	W/W_o	Δ_{max}/Δ_a	T/T_o
3S-60	3	0.60	0.44	0.52	1.69	1.66
3S-75	3	0.75	0.55	0.57	1.50	1.48
3S-80	3	0.80	0.59	0.57	1.45	1.42
3S-90	3	0.90	0.66	0.70	1.27	1.29
3S-100	3	1.00	0.73	0.76	1.24	1.24
6S-75	6	0.75	0.58	0.60	1.35	2.43

Subscript "o" denotes property of the reference frame of Section 8.2.

Properties of reference frame of Section 8.2:
     3-Story: $V_{yo}=2223$ kN; $V_{y,min}= 1626$ kN; $W_o=215$ kN; $T_o=1.07$ sec
     6-Story: $V_{yo}=2748$ kN; $V_{y,min}= 2108$ kN; $W_o=504$ kN; $T_o=1.90$ sec

*   Frames exclusive of the damping system do not meet the drift criteria. Damping systems are added to meet the drift criteria.

Allowable story drift is $\Delta_a = 0.02\ h_{sx}$

$V_{yo} =$ base shear strength of reference frame
$V_{ya} =$ base shear strength of damped frame exclusive of damping system
$V_y =$ base shear strength of frame without a damping system designed for base shear V in accordance with NEHRP (1997).
$T =$ period of damped frame exclusive of damping system

130

TABLE 8-2 Comparison of Results of Simplified Methods of Analysis to Results of Nonlinear Time History Analysis. Case of Example No.1: 3-Story (0.60 V_y) with Linear Viscous Damping System. Analysis for the DBE

Response Quantity	STORY	SIMPLIFIED METHOD OF ANALYSIS								NONLINEAR TIME HISTORY ANALYSIS (IDARC 2D- Version 5.0)			
		NEHRP(2000) Higher Modes Using T_m		Higher Modes Using $T_m\sqrt{\mu}$		METHOD 2 (FEMA 274) LATERAL FORCE PATTERN							
		ELF	RSA	ELF	RSA	mode 1	Cvx	Unif	Adpt	Min.	Avg.	Avg. +1σ	Max.
Story Drift (mm.)	3	95	98	97	102	116	119	126	127	45	86	109	119
	2	119	114	120	114	109	109	102	102	47	102	131	151
	1	79	71	82	72	64	60	61	61	29	68	92	122
Interstory Velocity (mm/sec)	3	366(363)	507(440)	358(363)	526(462)	542(496)	543(503)	532(507)	538(510)	263	456	568	690
	2	457(452)	364(394)	446(452)	373(399)	438(422)	398(404)	379(378)	377(377)	233	445	558	625
	1	404(358)	289(276)	389(357)	299(285)	293(268)	260(245)	254(240)	252(240)	153	329	429	520
Damper Force (kN)	3	262(259)	362(314)	256(259)	375(330)	387(354)	387(359)	380(362)	384(364)	188	326	406	492
	2	326(323)	260(281)	319(323)	266(285)	313(301)	283(288)	270(270)	269(269)	166	317	398	446
	1	288(255)	207(197)	278(255)	213(203)	209(191)	185(175)	181(171)	180(1071)	109	235	306	371
Story Shear at Max. Disp. (kN)	3	509	640	497	590	514	518	580	491	325	481	609	734
	2	852	863	850	861	907	885	1099	899	511	894	1045	1272
	1	1305	1218	1277	1173	1160	1139	1359	1137	743	1093	1245	1316
Max. Story Shear (kN)	3	570(565)	725(704)	556(553)	688(667)	629(619)	634(626)	697(700)	615(613)	363	567	701	849
	2	937(939)	932(938)	934(937)	931(936)	985(956)	960(950)	1171(1166)	971(960)	562	987	1165	1286
	1	1336(1326)	1243(1240)	1299(1292)	1202(1198)	1182(1175)	1159(1153)	1385(1384)	1157(1153)	807	1314	1563	1795
Floor Acceleration (g)	3	.325(.359)	.409(.441)	.355(.352)	.439(.417)	.401(.391)	.405(.396)	.445(.448)	0.392(0.391)	0.232	0.382	0.472	0.577
	2	.161(.165)	.275(.288)	.163(.164)	.281(.276)	.319(.279)	.289(.256)	.296(.264)	.279(.242)	0.159	0.284	0.361	0.452
	1	.378(.371)	.296(.282)	.375(.350)	.273(.257)	.374(.337)	.302(.275)	.295(.266)	.284(.256)	0.178	0.335	0.448	0.551

Values in parenthesis indicate results obtained using the revised velocity correction factors of Table 4-6.

131

TABLE 8-3 Comparison of Results of Simplified Methods of Analysis to Results of Nonlinear Time History Analysis. Case of Example No.1: 3-Story (0.60 V_y) with Linear Viscous Damping System. Analysis for the MCE

Response Quantity	STORY	SIMPLIFIED METHOD OF ANALYSIS NEHRP(2000) Higher Modes Using T_m ELF	RSA	Higher Modes Using $T_m\sqrt{\mu}$ ELF	RSA	METHOD 2 (FEMA 274) LATERAL FORCE PATTERN mode 1	Cvx	Unif	Adpt	NONLINEAR TIME HISTORY ANALYSIS (IDARC 2D- Version 5.0) Min.	Avg.	Avg. +1σ	Max.
Story Drift (mm.)	3	145	149	149	159	199	189	203	184	67	124	164	207
	2	181	173	185	174	143	143	143	148	70	142	191	244
	1	121	108	129	111	102	119	101	107	44	107	154	210
Interstory Velocity (mm/sec)	3	496(493)	722(619)	451(480)	701(638)	739(769)	714(734)	707(727)	630(650)	395	605	741	919
	2	618(614)	460(516)	562(598)	490(532)	499(523)	476(510)	502(488)	503(497)	319	590	728	835
	1	579(508)	395(376)	501(484)	394(387)	372(384)	394(428)	367(360)	362(365)	224	484	633	808
Damper Force (kN)	3	354(351)	516(442)	32(343)	500(455)	528(548)	510(524)	505(519)	450(464)	282	431	529	656
	2	441(438)	328(368)	401(427)	350(379)	356(373)	340(364)	358(348)	359(355)	227	421	519	596
	1	413(362)	282(268)	358(345)	282(276)	266(274)	281(306)	262(257)	259(260)	160	345	451	577
Story Shear at Max. Disp. (kN)	3	644	868	574	627	529	517	582	471	347	547	683	796
	2	892	916	871	894	931	874	1104	899	725	985	1145	1503
	1	1614	1453	1453	1215	1167	1109	1354	1101	912	1212	1355	1507
Max. Story Shear (kN)	3	728(719)	991(957)	645(645)	780(755)	719(746)	694(712)	766(793)	635(655)	461	694	833	1004
	2	1021(1026)	1011(1023)	993(1005)	996(1006)	1032(1069)	969(1005)	1206(1232)	1003(10026)	839	1155	1317	1505
	1	1650(1631)	1478(1471)	1452(1446)	1257(1256)	1208(1240)	1162(1198)	1402(1425)	1153(1176)	1143	1610	1881	2176
Floor Acceleration (g)	3	.453(.458)	.579(.598)	.412(.415)	.498(.473)	.459(.494)	.443(.468)	.489(.521)	.405(.429)	0.300	0.469	0.563	0.688
	2	.205(.173)	.396(.378)	.166(.169)	.334(.307)	.328(.294)	.312(.281)	.330(.300)	.298(.270)	0.238	0.371	0.460	0.572
	1	.567(.554)	.441(.419)	.479(.451)	.333(.306)	.339(.318)	.309(.289)	.324(.299)	.311(.286)	0.268	0.478	0.628	0.763

Values in parenthesis indicate results obtained using the revised velocity correction factors of Table 4-6.

TABLE 8-4 Comparison of Results of Simplified Methods of Analysis to Results of Nonlinear Time History Analysis. Case of Example No.2: 3-Story (0.75V_y) with Linear Viscous Damping System. Analysis for the DBE

Response Quantity	STORY	SIMPLIFIED METHOD OF ANALYSIS								NONLINEAR TIME HISTORY ANALYSIS (IDARC 2D- Version 5.0)			
		NEHRP(2000)				METHOD 2 (FEMA 274) LATERAL FORCE PATTERN							
		Higher Modes Using T_m		Higher Modes Using $T_m\sqrt{\mu}$						Min.	Avg.	Avg. +1σ	Max.
		ELF	RSA	ELF	RSA	mode 1	Cvx	Unif	Adpt				
Story Drift (mm.)	3	88	89	88	91	115	96	100	99	39	82	104	114
	2	104	99	105	99	91	106	102	106	40	92	120	137
	1	70	62	72	63	54	61	62	59	25	63	85	103
Interstory Velocity (mm/sec)	3	389	488	382	515	569	471	462	465	250	447	543	610
	2	462	368	453	374	415	470	441	464	228	442	545	604
	1	410	280	395	291	280	295	288	291	133	322	409	469
Damper Force (kN)	3	311	390	307	414	453	378	369	373	199	357	434	487
	2	369	294	360	298	355	373	351	369	182	353	436	483
	1	327	223	316	231	213	236	231	231	106	257	327	375
Story Shear at Max. Disp. (kN)	3	579	690	574	676	602	525	622	525	360	556	695	840
	2	1029	1042	1040	1054	1088	1049	1294	1063	560	1055	1246	1458
	1	1489	1406	1481	1405	1361	1298	1578	1312	694	1339	1568	1699
Max. Story Shear (kN)	3	656	785	649	783	743	640	734	640	378	650	792	886
	2	1122	1119	1134	1134	1176	1147	1383	1161	605	1182	1399	1464
	1	1534	1439	1521	1441	1392	1338	1623	1347	800	1576	1896	2094
Floor Acceleration (g)	3	0.453	0.579	0.413	0.486	0.451	0.391	0.460	0.394	0.254	0.437	0.529	0.588
	2	0.205	0.396	0.219	0.327	0.325	0.294	0.328	0.294	0.170	0.325	0.406	0.504
	1	0.567	0.441	0.426	0.322	0.323	0.307	0.299	0.311	0.181	0.355	0.479	0.609

133

TABLE 8-5 Comparison of Results of Simplified Methods of Analysis to Results of Nonlinear Time History Analysis. Case of Example No.2: 3-Story (0.75V$_y$) with Linear Viscous Damping System. Analysis for the MCE

Response Quantity	STORY	SIMPLIFIED METHOD OF ANALYSIS								NONLINEAR TIME HISTORY ANALYSIS (IDARC 2D- Version 5.0)			
		NEHRP(2000)				METHOD 2 (FEMA 274) LATERAL FORCE PATTERN							
		Higher Modes Using T_m		Higher Modes Using $T_m\sqrt{\mu}$									
		ELF	RSA	ELF	RSA	mode 1	Cvx	Unif	Adpt	Min.	Avg.	Avg. +1σ	Max.
Story Drift (mm.)	3	131	133	134	142	152	150	155	153	58	118	156	179
	2	156	149	159	149	151	157	148	150	59	131	166	187
	1	106	94	112	96	106	106	98	97	37	96	133	176
Interstory Velocity (mm/sec)	3	524	685	485	722	603	602	602	608	374	597	725	875
	2	622	461	576	482	546	564	548	564	341	587	719	771
	1	586	376	520	395	385	389	374	379	199	464	596	717
Damper Force (kN)	3	419	547	387	578	480	480	480	485	299	477	579	699
	2	497	368	458	387	436	449	436	449	272	469	575	616
	1	468	300	414	316	307	311	298	302	159	370	476	573
Story Shear at Max. Disp. (kN)	3	709	907	654	751	529	525	631	534	476	639	784	978
	2	1073	1103	1058	1085	1049	1036	1289	1058	831	1183	1340	1592
	1	1787	1628	1659	1481	1303	1285	1583	1312	1040	1487	1720	2254
Max. Story Shear (kN)	3	818	1042	751	925	698	694	796	707	564	777	915	1088
	2	1213	1208	1196	1196	1107	1098	1356	1192	907	1379	1580	1684
	1	1845	1663	1690	1525	1352	1334	1636	1374	1198	1917	2242	2519
Floor Acceleration (g)	3	0.453	0.579	0.498	0.566	0.418	0.414	0.490	0.423	0.380	0.525	0.618	0.740
	2	0.205	0.396	0.232	0.394	0.316	0.316	0.356	0.322	0.255	0.417	0.514	0.613
	1	0.567	0.441	0.609	0.422	0.325	0.329	0.341	0.348	0.272	0.506	0.664	0.811

TABLE 8-6 Comparison of Results of Simplified Methods of Analysis to Results of Nonlinear Time History Analysis. Case of Example No.3: 3-Story ($0.90V_y$) with Linear Viscous Damping System. Analysis for the DBE

Response Quantity	STORY	SIMPLIFIED METHOD OF ANALYSIS								NONLINEAR TIME HISTORY ANALYSIS (IDARC 2D- Version 5.0)			
		NEHRP(2000)				METHOD 2 (FEMA 274) LATERAL FORCE PATTERN							
		Higher Modes Using T_m		Higher Modes Using $T_m\sqrt{\mu}$						Min.	Avg.	Avg. +1σ	Max.
		ELF	RSA	ELF	RSA	mode 1	Cvx	Unif	Adpt				
Story Drift (mm.)	3	81	81	82	83	90	88	98	92	42	79	99	110
	2	90	86	91	86	89	91	89	90	43	81	104	116
	1	59	52	61	52	51	51	46	50	23	51	66	79
Interstory Velocity (mm/sec)	3	409	479	416	497	497	491	501	477	276	439	531	577
	2	455	372	463	374	447	455	448	439	263	414	500	598
	1	395	267	408	274	279	281	273	275	143	287	352	380
Damper Force (kN)	3	361	424	369	440	440	436	445	422	244	388	470	510
	2	402	329	409	329	396	400	396	387	233	366	442	529
	1	350	236	360	240	249	249	240	245	126	254	311	336
Story Shear at Max. Disp. (kN)	3	674	773	667	760	645	636	783	587	445	687	830	983
	2	1237	1253	1236	1249	1272	1258	1574	1161	805	1233	1441	1636
	1	1730	1649	1712	1636	1561	1547	1899	1427	818	1604	1903	2219
Max. Story Shear (kN)	3	766	876	760	871	774	765	916	716	474	747	889	1027
	2	1337	1339	1338	1338	1369	1361	1681	1263	836	1396	1629	1680
	1	1781	1685	1765	1672	1601	1587	1934	1467	883	1892	2284	2503
Floor Acceleration (g)	3	0.430	0.493	0.475	0.540	0.475	0.470	0.578	0.439	0.320	0.493	0.583	0.666
	2	0.235	0.332	0.259	0.362	0.340	0.339	0.387	0.318	0.172	0.381	0.477	0.582
	1	0.399	0.310	0.444	0.334	0.326	0.327	0.353	0.323	0.200	0.387	0.520	0.691

TABLE 8-7 Comparison of Results of Simplified Methods of Analysis to Results of Nonlinear Time History Analysis. Case of Example No.3: 3-Story (0.90V_y) with Linear Viscous Damping System. Analysis for the MCE

Response Quantity	STORY	SIMPLIFIED METHOD OF ANALYSIS								NONLINEAR TIME HISTORY ANALYSIS			
		NEHRP(2000)				METHOD 2 (FEMA 274)				(IDARC 2D- Version 5.0)			
		Higher Modes Using T_m		Higher Modes Using $T_m\sqrt{\mu}$		LATERAL FORCE PATTERN							
		ELF	RSA	ELF	RSA	mode 1	Cvx	Unif	Adpt	Min.	Avg.	Avg. +1σ	Max.
Story Drift (mm.)	3	121	122	124	131	146	141	155	156	63	114	146	164
	2	135	129	139	130	132	137	129	133	66	118	152	171
	1	88	78	96	81	77	76	75	71	35	79	107	129
Interstory Velocity (mm/sec)	3	545	662	537	769	673	664	668	671	411	604	722	849
	2	607	462	598	479	615	636	604	637	369	564	678	736
	1	564	355	550	399	399	403	394	407	214	415	525	612
Damper Force (kN)	3	482	585	476	680	596	587	591	591	364	534	638	751
	2	537	408	529	422	542	565	534	565	326	498	600	651
	1	499	314	485	351	351	356	347	360	189	367	464	541
Story Shear at Max. Disp. (kN)	3	795	977	751	916	667	663	791	618	467	723	895	1156
	2	1261	1295	1254	1285	1303	1294	1583	1214	1116	1361	1499	1605
	1	2015	1855	1916	1792	1614	1614	1930	1525	1120	1786	2005	2268
Max. Story Shear (kN)	3	924	1124	885	1112	871	863	996	840	664	899	1061	1251
	2	1409	1413	1401	1405	1356	1356	1645	1387	1211	1625	1831	2040
	1	2082	1894	1965	1832	1654	1650	1970	1578	1321	2314	2701	3087
Floor Acceleration (g)	3	0.508	0.624	0.564	0.681	0.520	0.516	0.615	0.497	0.441	0.600	0.700	0.826
	2.	0.244	0.429	0.275	0.463	0.396	0.397	0.435	0.383	0.299	0.551	0.730	0.936
	1	0.591	0.455	0.644	0.481	0.455	0.467	0.461	0.490	0.299	0.551	0.730	0.936

TABLE 8-8 Comparison of Results of Simplified Methods of Analysis to Results of Nonlinear Time History Analysis. Case of Example No.5: 6-Story (0.75V$_y$) with Linear Viscous Damping System. Analysis for the DBE

Response Quantity	STORY	SIMPLIFIED METHOD OF ANALYSIS								NONLINEAR TIME HISTORY ANALYSIS (IDARC 2D- Version 5.0)			
		NEHRP(2000)				METHOD 2 (FEMA 274) LATERAL FORCE PATTERN							
		Higher Modes Using T_m		Higher Modes Using $T_m\sqrt{\mu}$									
		ELF	RSA	ELF	RSA	mode 1	Cvx	Unif	Adpt	Min.	Avg.	Avg. +1σ	Max.
Story Drift (mm.)	6	53	64	56	68	69	75	61	68	26	41	50	61
	5	79	84	77	83	88	90	79	90	38	65	84	106
	4	85	85	84	84	96	97	92	99	41	75	101	127
	3	86	85	84	83	91	88	95	92	39	73	100	131
	2	71	71	75	75	67	63	78	67	31	59	80	107
	1	68	41	70	42	34	33	39	32	18	34	44	56
Interstory Velocity (mm/sec)	6	132	348	136	344	343	369	303	327	99	190	234	265
	5	196	299	189	285	303	312	267	295	131	243	294	316
	4	212	248	205	249	268	275	245	263	142	255	315	355
	3	214	222	205	224	242	245	232	237	138	272	341	423
	2	177	198	182	204	211	203	219	207	126	259	337	433
	1	345	147	322	154	129	129	133	126	83	183	250	339
Damper Force (kN)	6	205	540	209	534	534	574	471	507	153	295	364	411
	5	304	464	293	445	471	485	414	458	204	377	456	490
	4	404	471	391	471	507	525	467	498	270	485	598	675
	3	408	422	391	427	458	467	440	449	262	516	649	804
	2	454	508	467	525	538	520	560	529	323	662	863	1109
	1	883	375	823	396	329	329	342	325	212	469	640	869
Story Shear at Max. Disp. (kN)	6	397	558	387	516	427	427	449	391	205	278	325	369
	5	940	956	920	912	871	840	1005	805	489	677	776	831
	4	1240	1218	1227	1205	1183	1129	1432	1098	751	976	1107	1232
	3	1392	1436	1396	1432	1427	1356	1752	1321	863	1211	1376	1463
	2	1653	1648	1636	1623	1596	1521	1956	1481	960	1442	1636	1699
	1	2294	1813	2201	1774	1685	1614	2045	1561	1032	1689	1967	2112

137

TABLE 8-8 Continued

Response	STORY	NEHRP(2000) Higher Modes Using T_m ELF	NEHRP(2000) Higher Modes Using T_m RSA	NEHRP(2000) Higher Modes Using $T_m \sqrt{\mu}$ ELF	NEHRP(2000) Higher Modes Using $T_m \sqrt{\mu}$ RSA	METHOD 2 (FEMA 274) LATERAL FORCE PATTERN mode 1	Cvx	Unif	Adpt	NONLINEAR TIME HISTORY ANALYSIS (IDARC 2D- Version 5.0) Min.	Avg.	Avg. +1σ	Max.
Max. Story Shear (kN)	6	427	735	418	703	636	658	618	596	222	334	390	408
	5	966	1069	938	1023	1000	978	1112	934	536	756	862	888
	4	1320	1337	1303	1325	1325	1272	1556	1241	751	1056	1198	1352
	3	1499	1542	1498	1538	1547	1476	1867	1445	867	1268	1429	1495
	2	1662	1768	1663	1752	1730	1645	2094	1610	987	1579	1813	1868
	1	2368	1861	2254	1832	1730	1650	2099	1601	1102	1948	2293	2416
Floor Acceleration (g)	6	0.272	0.469	0.267	0.447	0.348	0.350	0.360	0.327	0.149	0.225	0.265	0.279
	5	0.188	0.264	0.182	0.254	0.256	0.254	0.279	0.240	0.122	0.176	0.205	0.231
	4	0.137	0.263	0.136	0.249	0.247	0.250	0.255	0.234	0.100	0.189	0.235	0.279
	3	0.130	0.247	0.121	0.228	0.243	0.247	0.236	0.237	0.117	0.232	0.298	0.351
	2	0.193	0.255	0.173	0.241	0.246	0.249	0.236	0.240	0.155	0.298	0.392	0.491
	1	0.491	0.196	0.456	0.193	0.271	0.266	0.259	0.279	0.176	0.365	0.494	0.643

TABLE 8-9 Comparison of Results of Simplified Methods of Analysis to Results of Nonlinear Time History Analysis. Case of Example No.5: 6-Story (0.75V_y) with Linear Viscous Damping System. Analysis for the MCE

Response Quantity	STORY	SIMPLIFIED METHOD OF ANALYSIS								NONLINEAR TIME HISTORY ANALYSIS (IDARC 2D- Version 5.0)			
		NEHRP(2000)				METHOD 2 (FEMA 274)							
		Higher Modes Using T_m		Higher Modes Using $T_m\sqrt{\mu}$		LATERAL FORCE PATTERN							
		ELF	RSA	ELF	RSA	mode 1	Cvx	Unif	Adpt	Min.	Avg.	Avg. +1σ	Max.
Strory Drift (mm.)	6	84	99	84	107	75	71	59	72	36	53	65	77
	5	116	124	116	128	110	105	92	110	59	88	112	138
	4	126	126	126	127	130	127	117	133	67	106	141	173
	3	126	124	126	127	142	143	137	145	62	107	146	184
	2	112	112	112	113	129	131	141	129	47	90	124	161
	1	102	63	110	64	66	70	104	65	26	56	81	110
Interstory Velocity (mm/sec)	6	180	501	168	478	432	427	350	423	133	249	302	325
	5	250	412	233	382	374	378	312	369	188	319	383	410
	4	271	333	253	328	342	350	290	340	197	346	425	480
	3	271	290	253	297	316	331	280	308	203	380	480	584
	2	240	275	224	265	290	310	268	282	172	374	490	617
	1	511	216	419	212	206	216	267	202	124	278	372	497
Damper Force (kN)	6	279	778	258	743	671	663	542	658	206	386	469	505
	5	387	639	360	591	582	587	485	574	292	495	594	636
	4	515	634	480	622	649	667	551	645	374	657	808	911
	3	515	550	480	565	600	631	534	587	385	722	911	1109
	2	615	704	574	680	743	791	685	725	441	957	1253	1580
	1	1308	552	1072	542	525	551	685	516	319	711	953	1271
Story Shear at Max. Disp. (kN)	6	503	767	445	565	645	658	591	627	222	318	378	467
	5	1121	1153	1014	943	1005	1009	1058	956	636	790	895	1018
	4	1361	1318	1285	1223	1254	1205	1414	1178	960	1102	1200	1321
	3	1396	1493	1392	1445	1454	1365	1707	1356	1112	1349	1476	1534
	2	1778	1778	1699	1636	1663	1583	1939	1552	1303	1645	1790	1814
	1	2920	2067	2548	1814	1876	1814	2139	1770	1472	1932	2100	2254

139

TABLE 8-9 Continued

Response Quantity	STORY	SIMPLIFIED METHOD OF ANALYSIS								NONLINEAR TIME HISTORY ANALYSIS (IDARC 2D- Version 5.0)			
		NEHRP(2000)				METHOD 2 (FEMA 274) LATERAL FORCE PATTERN							
		Higher Modes Using T_m		Higher Modes Using $T_m \sqrt{\mu}$									
		ELF	RSA	ELF	RSA	mode 1	Cvx	Unif	Adpt	Min.	Avg.	Avg. +1σ	Max.
Max. Story Shear (kN)	6	536	1028	467	864	880	885	774	863	294	399	457	492
	5	1124	1314	1007	1117	1161	1156	1174	1112	701	897	1007	1092
	4	1455	1492	1370	1405	1441	1392	1570	1369	967	1236	1366	1481
	3	1549	1644	1537	1605	1627	1547	1867	1534	1116	1489	1641	1733
	2	1731	1960	1699	1829	1876	1805	2152	1770	1357	1937	2137	2281
	1	3027	2131	2539	1905	1961	1908	2312	1854	1655	2592	3002	3455
Floor Acceleration (g)	6	0.342	0.656	0.298	0.551	0.532	0.535	0.493	0.523	0.194	0.272	0.315	0.325
	5	0.205	0.337	0.189	0.314	0.334	0.326	0.309	0.326	0.156	0.213	0.249	0.299
	4	0.141	0.353	0.140	0.301	0.364	0.356	0.319	0.360	0.141	0.247	0.306	0.372
	3	0.165	0.353	0.130	0.287	0.341	0.343	0.285	0.337	0.175	0.321	0.409	0.481
	2	0.283	0.376	0.201	0.299	0.376	0.377	0.299	0.372	0.220	0.434	0.569	0.715
	1	0.738	0.299	0.590	0.264	0.328	0.325	0.295	0.328	0.265	0.544	0.736	0.965

TABLE 8-10 Comparison of Results of Simplified Methods of Analysis to Results of Nonlinear Time History Analysis. Case of Example No.6: 3-Story (0.80 V_y) with Nonlinear Viscous Damping System Designed for 10% Damping Ratio in the DBE. Analysis for the DBE

Response Quantity	STORY	SIMPLIFIED METHOD OF ANALYSIS								NONLINEAR TIME HISTORY ANALYSIS (IDARC 2D- Version 5.0)			
		NEHRP(2000)				METHOD 2 (FEMA 274)							
		Higher Modes Using T_m		Higher Modes Using $T_m\sqrt{\mu}$		LATERAL FORCE PATTERN							
		ELF	RSA	ELF	RSA	mode 1	Cvx	Unif	Adpt	Min.	Avg.	Avg. +1σ	Max.
Story Drift (mm.)	3	87	88	88	92	101	99	108	103	39	80	104	119
	2	103	96	104	96	101	107	103	103	40	86	114	131
	1	72	61	75	62	61	63	60	63	22	58	79	99
Interstory Velocity (mm/sec)	3	440	558	434	598	578	569	577	564	254	484	600	664
	2	520	382	512	388	515	522	520	512	232	441	546	595
	1	488	310	478	327	341	341	343	341	141	311	398	449
Damper Force (kN)	3	268	300	265	311	307	302	307	302	216	299	333	350
	2	291	261	288	261	289	293	289	289	207	285	317	331
	1	286	225	281	230	236	236	236	231	161	240	271	288
Story Shear at Max. Disp. (kN)	3	658	802	650	790	600	596	685	569	422	671	849	1032
	2	1096	1108	1097	1110	1112	1112	1356	1076	676	1108	1311	1507
	1	1677	1556	1663	1547	1405	1401	1676	1352	689	1420	1679	1819
Max. Story Shear (kN)	3	750	887	742	880	707	707	800	680	446	738	905	1042
	2	1219	1224	1219	1226	1227	1227	1472	1192	697	1225	1446	1578
	1	1751	1628	1735	1620	1481	1476	1752	1432	779	1617	1945	2100
Floor Acceleration (g)	3	0.480	0.567	0.474	0.562	0.437	0.435	0.510	0.421	0.300	0.494	0.599	0.681
	2	0.214	0.349	0.212	0.345	0.329	0.327	0.367	0.318	0.162	0.353	0.446	0.543
	1	0.483	0.358	0.472	0.355	0.347	0.339	0.356	0.337	0.169	0.366	0.491	0.620

TABLE 8-11 Comparison of Results of Simplified Methods of Analysis to Results of Nonlinear Time History Analysis. Case of Example No.6: 3-Story (0.80 V$_y$) with Nonlinear Viscous Damping System Designed for 10% Damping Ratio in the DBE. Analysis for the MCE

Response Quantity	STORY	SIMPLIFIED METHOD OF ANALYSIS								NONLINEAR TIME HISTORY ANALYSIS			
		NEHRP(2000)				METHOD 2 (FEMA 274)				(IDARC 2D- Version 5.0)			
		Higher Modes Using T_m		Higher Modes Using $T_m\sqrt{\mu}$		LATERAL FORCE PATTERN				Min.	Avg.	Avg. +1σ	Max.
		ELF	RSA	ELF	RSA	mode 1	Cvx	Unif	Adpt				
Story Drift (mm.)	3	136	138	142	155	171	172	176	173	61	124	162	183
	2	161	150	167	151	160	168	156	161	62	131	173	199
	1	112	95	125	100	112	119	107	112	31	94	134	173
Interstory Velocity (mm/sec)	3	622	814	588	919	800	788	795	779	406	686	856	1064
	2	734	493	693	531	684	680	672	664	354	614	752	840
	1	727	436	673	486	484	485	472	469	205	468	603	720
Damper Force (kN)	3	315	366	307	395	365	360	360	360	273	356	397	443
	2	342	293	333	300	329	329	329	325	255	336	372	394
	1	358	264	339	279	280	280	276	276	194	294	334	364
Story Shear at Max. Disp. (kN)	3	843	1097	794	939	622	560	698	578	440	719	930	1223
	2	1144	1171	1131	1158	1125	1094	1347	1040	943	1218	1341	1432
	1	2106	1867	1993	1702	1423	1378	1681	1316	894	1547	1771	1912
Max. Story Shear (kN)	3	932	1179	883	1043	751	734	836	707	614	909	1093	1328
	2	1283	1297	1270	1287	1258	1223	1476	1169	990	1446	1629	1827
	1	2173	1932	2048	1776	1516	1476	1774	1410	1187	1937	2239	2445
Floor Acceleration (g)	3	0.595	0.753	0.563	0.666	0.461	0.448	0.526	0.432	0.416	0.608	0.724	0.879
	2	0.223	0.477	0.220	0.428	0.356	0.345	0.389	0.335	0.249	0.462	0.580	0.688
	1	0.738	0.546	0.668	0.472	0.383	0.364	0.385	0.362	0.272	0.529	0.690	0.838

TABLE 8-12 Comparison of Results of Simplified Methods of Analysis to Results of Nonlinear Time History Analysis. Case of Example No.7: 3-Story (0.80 V_y) with Nonlinear Viscous Damping System Designed for 20% Damping Ratio in the MCE. Analysis for the MCE

Response Quantity	STORY	SIMPLIFIED METHOD OF ANALYSIS								NONLINEAR TIME HISTORY ANALYSIS (IDARC 2D- Version 5.0)			
		NEHRP(2000)				METHOD 2 (FEMA 274)							
		Higher Modes Using T_m		Higher Modes Using $T_m\sqrt{\mu}$		LATERAL FORCE PATTERN							
		ELF	RSA	ELF	RSA	mode 1	Cvx	Unif	Adpt	Min.	Avg.	Avg. +1σ	Max.
Story Drift (mm.)	3	106	108	108	116	123	123	127	123	42	75	97	115
	2	125	118	127	118	128	135	121	125	53	100	132	148
	1	87	74	91	77	75	70	79	78	36	79	109	132
Interstory Velocity (mm/sec)	3	508	660	483	728	638	636	611	600	235	453	566	655
	2	599	435	570	448	590	631	525	540	298	520	635	745
	1	572	363	531	392	385	395	361	363	214	412	535	623
Damper Force (kN)	3	634	723	620	766	711	711	694	689	462	641	717	770
	2	688	613	674	618	685	707	645	654	520	686	759	822
	1	687	536	655	555	551	560	534	534	440	611	697	752
Story Shear at Max. Disp. (kN)	3	717	913	683	860	605	596	671	560	382	613	833	1298
	2	1113	1139	1105	1129	1134	1120	1329	1063	1014	1350	1561	1845
	1	1815	1672	1738	1618	1432	1436	1645	1334	1343	1732	1907	2165
Max. Story Shear (kN)	3	999	1189	967	1170	956	947	1027	912	510	784	934	1087
	2	1474	1470	1465	1465	1485	1485	1667	1405	1133	1570	1778	2007
	1	2048	1881	1960	1837	1672	1663	1894	1578	1466	2172	2487	2646
Floor Acceleration (g)	3	0.638	0.759	0.617	0.747	0.526	0.520	0.600	0.492	0.351	0.545	0.642	0.734
	2	0.220	0.425	0.218	0.413	0.403	0.404	0.432	0.375	0.281	0.449	0.543	0.660
	1	0.619	0.450	0.561	0.423	0.440	0.481	0.394	0.990	0.233	0.506	0.662	0.833

TABLE 8-13 Comparison of Results of Simplified Methods of Analysis to Results of Nonlinear Time History Analysis. Case of Example No.8: 3-Story (0.75 V_y) with Viscoelastic Damping System. Analysis for the DBE

Response Quantity	STORY	SIMPLIFIED METHOD OF ANALYSIS								NONLINEAR TIME HISTORY ANALYSIS (IDARC 2D- Version 5.0)			
		NEHRP(2000)				METHOD 2 (FEMA 274) LATERAL FORCE PATTERN							
		Higher Modes Using T_m		Higher Modes Using $T_m\sqrt{\mu}$									
		ELF	RSA	ELF	RSA	mode 1	Cvx	Unif	Adpt	Min.	Avg.	Avg. +1σ	Max.
Story Drift (mm.)	3	76	77	77	78	79	80	78	79	41	94	123	139
	2	100	95	100	95	100	100	98	95	42	94	122	143
	1	72	65	73	65	61	60	65	69	25	59	79	105
Interstory Velocity (mm/sec)	3	374	454	371	472	522	516	505	508	275	493	611	725
	2	486	393	482	396	452	437	416	401	241	440	539	574
	1	427	304	421	309	316	308	316	324	132	308	395	495
Damper Force (kN)	3	392	457	394	481	494	494	489	498	240	466	592	718
	2	517	434	519	426	471	462	449	436	215	432	538	575
	1	433	324	293	290	316	311	329	342	120	296	385	462
Story Shear at Max. Disp. (kN)	3	691	810	682	798	774	756	849	1214	156	866	1128	1316
	2	1358	1355	1353	1350	1329	1281	1601	1565	707	1267	1522	1752
	1	1831	1763	1813	1752	1703	1650	2019	1703	751	1407	1705	2045
Max. Story Shear (kN)	3	755	882	890	1000	894	876	965	836	532	963	1173	1367
	2	1441	1425	1598	1582	1427	1392	1703	1316	753	1405	1672	1769
	1	1880	1804	1827	1813	1765	1707	2085	1636	922	1642	1977	2231
Floor Acceleration (g)	3	0.480	0.561	0.476	0.558	0.569	0.559	0.617	0.533	0.356	0.644	0.785	0.915
	2	0.263	0.343	0.262	0.338	0.379	0.372	0.408	0.349	0.186	0.342	0.448	0.560
	1	0.416	0.314	0.332	0.278	0.334	0.333	0.323	0.307	0.202	0.378	0.512	0.648

TABLE 8-14 Comparison of Results of Simplified Methods of Analysis to Results of Nonlinear Time History Analysis. Case of Example No.8: 3-Story (0.75 V_y) with Viscoelastic Damping System. Analysis for the MCE

Response Quantity	S T O R	SIMPLIFIED METHOD OF ANALYSIS								NONLINEAR TIME HISTORY ANALYSIS (IDARC 2D- Version 5.0)			
		NEHRP(2000)				METHOD 2 (FEMA 274) LATERAL FORCE PATTERN							
		Higher Modes Using T_m		Higher Modes Using $T_m\sqrt{\mu}$		mode 1	Cvx	Unif	Adpt	Min.	Avg.	Avg. +1σ	Max.
		ELF	RSA	ELF	RSA								
Story Drift (mm.)	3	115	116	117	125	145	146	144	142	62	132	177	210
	2	149	143	152	143	137	136	137	137	63	130	169	196
	1	107	97	113	100	86	84	87	89	37	90	123	158
Interstory Velocity (mm/sec)	3	501	632	475	727	828	844	811	793	411	678	838	1048
	2	650	489	617	514	506	492	492	492	357	580	711	801
	1	600	397	556	436	426	424	420	418	198	445	576	738
Damper Force (kN)	3	551	654	553	794	831	831	827	823	285	625	724	627
	2	727	592	732	587	560	547	556	565	343	550	669	711
	1	622	449	390	403	436	427	440	445	178	430	564	675
Story Shear at Max. Disp. (kN)	3	888	1092	850	1021	863	885	903	809	711	1066	1266	1392
	2	1640	1633	1629	1628	1156	1129	1356	1120	1036	1479	1680	1787
	1	2313	2191	2238	2145	1632	1650	1827	1552	1098	1548	1735	1916
Max. Story Shear (kN)	3	977	1193	935	1153	1565	1587	1605	1507	782	1224	1433	1645
	2	1759	1730	1746	1717	1676	1636	1876	1645	1129	1655	1888	2035
	1	2379	2244	2153	2142	1965	1970	2170	1903	1381	2007	2326	2664
Floor Acceleration (g)	3	0.623	0.761	0.682	0.597	0.736	1.013	1.024	0.961	0.535	0.812	0.880	0.945
	2	0.316	0.458	0.277	0.315	0.437	0.594	0.596	0.569	0.279	0.452	0.575	0.699
	1	0.617	0.463	0.420	0.432	0.368	0.563	0.546	0.537	0.303	0.547	0.728	0.937

145

TABLE 8-15 Comparison of Results of Simplified Methods of Analysis to Results of Nonlinear Time History Analysis. Case of Example No.9: 3-Story (0.75 V_y) with Metallic Yielding Damping System. Analysis for the DBE

Response Quantity	STORY	SIMPLIFIED METHOD OF ANALYSIS							NONLINEAR TIME HISTORY ANALYSIS			
		NEHRP(2000)				METHOD 2 (FEMA 274)			(IDARC 2D- Version 5.0)			
		Higher Modes Using T_m		Higher Modes Using $T_m\sqrt{\mu}$		LATERAL FORCE PATTERN						
		ELF	RSA	ELF	RSA	mode 1	Cvx	Unif	Min.	Avg.	Avg. +1σ	Max.
Story Drift (mm.)	3	100	107	104	117	116	116	110	55	106	129	155
	2	119	113	124	113	111	114	108	48	95	123	147
	1	83	72	91	75	83	80	85	41	68	91	121
Max. Story Shear (kN)	3	852	1037	840	1040	854	854	916	735	1111	1330	1408
	2	1340	1350	1342	1355	1410	1387	1627	1125	1638	1922	2235
	1	2151	1942	2126	1946	1814	1796	2076	1722	2030	2214	2422
Floor Acceleration (g)	3	0.544	0.662	0.536	0.664	0.546	0.546	0.585	0.472	0.705	0.841	0.886
	2	0.256	0.443	0.256	0.443	0.404	0.409	0.426	0.400	0.602	0.779	0.991
	1	0.657	0.474	0.637	0.474	0.415	0.434	0.402	0.370	0.677	0.915	1.302

TABLE 8-16 Comparison of Results of Simplified Methods of Analysis to Results of Nonlinear Time History Analysis. Case of Example No.9: 3-Story (0.75 V_y) with Metallic Yielding Damping System. Analysis for the MCE

Response	Quantity	S T O R Y	SIMPLIFIED METHOD OF ANALYSIS							NONLINEAR TIME HISTORY ANALYSIS (IDARC 2D- Version 5.0)			
			NEHRP(2000)				METHOD 2 (FEMA 274)						
			Higher Modes Using T_m		Higher Modes Using $T_m \sqrt{\mu}$		LATERAL FORCE PATTERN			Min.	Avg.	Avg. $+1\sigma$	Max.
			ELF	RSA	ELF	RSA	mode 1	Cvx	Unif				
Story Drift (mm.)		3	150	160	165	197	201	198	194	75	157	200	235
		2	178	169	196	170	165	172	166	78	142	190	228
		1	124	109	154	120	136	137	136	47	104	146	195
Max. Story Shear (kN)		3	1103	1418	1102	1229	956	960	1014	957	1318	1546	1647
		2	1412	1432	1410	1432	1472	1445	1681	1510	1845	2101	2434
		1	2727	2342	2725	2149	1899	1872	2152	1939	2217	2418	2738
Floor Acceleration (g)		3	0.703	0.905	0.704	0.784	0.610	0.612	0.647	0.607	0.836	0.982	1.052
		2	0.271	0.606	0.272	0.551	0.472	0.477	0.490	0.469	0.742	0.932	1.164
		1	0.980	0.703	0.980	0.630	0.526	0.541	0.514	0.530	0.849	1.109	1.556

147

TABLE 8-17 Summary of Key Results Produced by Various Methods of Analysis

Quantity	3-STORY No.2, 0.75Vy, Linear Viscous, MCE				6-STORY No.5, 0.75Vy, Linear Viscous, MCE				3-STORY No.6, 0.8Vy, Nonlinear Viscous, MCE				3-STORY No.8, 0.75Vy, Viscoelastic, MCE				3-STORY No.9, 0.75Vy, Metallic Devices, MCE			
	ELF	RSA	FEMA (1997)	NTHA	ELF	RSA	FEMA (1997)	NTHA	ELF	RSA	FEMA (1997)	NTHA	ELF	RSA	FEMA (1997)	NTHA	ELF	RSA	FEMA (1997)	NTHA
Drift (mm)	156	149	157 (153)	131	116 126 112	124 126 112	105 143 141	88 107 90	161	150	176 (173)	131	149	143	146 (142)	132	178	169	198	157
Damper Force (kN)	498	547	480 (485)	477	387 516 1307	778 636 703	663 667 791	495 722 957	358	366	360 (360)	356	727	654	831 (823)	625	NA	NA	NA	NA
Max. Base Shear (kN)	1739	1267	1583 (1374)	1487	3028	2130	2312 (1854)	2592	2173	1932	1774 (1410)	1937	2379	2244	2170 (1903)	2007	2725	2340	2152	2217

FEMA(1997): maximum response among the two calculated for the modal and uniform load patterns.

Value in parenthesis is peak response calculated using the adaptive load pattern.

TABLE 8-18 Comparison of Results of Simplified Methods of Analysis to Results of Nonlinear Time History Analysis. Case of Example No.2: 3-Story (0.75V$_y$) with Linear Viscous Damping System Designed for 10% Damping Ratio. Analysis for Near-Fault Ground Motions

Response Quantity	STORY	SYLMAR 90°					NEWHALL 360°					PACOIMA DAM S16E				
		Using B		NTHA	Using Actual Spectra		Using B		NTHA	Using Actual Spectra		Using B		NTHA	Using Actual Spectra	
		ELF	RSA		ELF	RSA	ELF	RSA		ELF	RSA	ELF	RSA		ELF	RSA
Story Drift (mm.)	3	145	147	107	103	105	155	152	108	142	142	172	179	125	174	176
	2	172	168	118	122	116	184	171	124	169	159	204	203	151	207	204
	1	111	105	72	83	73	130	107	86	117	100	127	127	119	132	126
Damper Force (kN)	3	383	504	484	349	461	566	608	567	507	605	421	672	457	439	535
	2	454	364	380	415	311	672	443	497	602	423	500	519	517	521	469
	1	393	285	277	381	253	661	344	332	571	337	350	389	413	418	329
Max. Story Shear (kN)	3	715	943	802	701	900	1015	1102	926	903	1097	642	1184	681	723	930
	2	1173	1152	1305	1142	1127	1301	1241	1538	1245	1193	1175	1328	1361	1193	1240
	1	1617	1558	1664	1612	1521	2239	1715	1911	2008	1695	1441	1807	1879	1610	1573

Using B: Simplified analysis procedures were applied using the actual 5%-damped spectrum of each earthquake motion, and the damping coefficient B from NEHRP (2000)

Using Actual Spectra: Simplified procedures were applied using the actual damped spectrum of each earthquake

149

TABLE 8-19 Comparison of Results of Simplified Methods of Analysis to Results of Nonlinear Time History Analysis. Case of Example No.4: 3-Story (1.0V$_y$) with Linear Viscous Damping System Designed for 20% Damping Ratio. Analysis for Near-Fault Ground Motions

Response Quantity	STORY	SYLMAR 90° Using B ELF	Using B RSA	NTHA	Using Actual Spectra ELF	Using Actual Spectra RSA	NEWHALL 360° Using B ELF	Using B RSA	NTHA	Using Actual Spectra ELF	Using Actual Spectra RSA	PACOIMA DAM S16E Using B ELF	Using B RSA	NTHA	Using Actual Spectra ELF	Using Actual Spectra RSA
Story Drift (mm.)	3	70	70	66	70	70	125	124	89	105	106	129	135	87	112	112
	2	85	82	85	84	82	150	148	111	126	123	155	153	115	134	132
	1	55	49	53	53	49	93	88	74	80	74	94	93	81	82	79
Damper Force (kN)	3	707	760	705	658	791	1036	1076	943	943	1072	960	1596	862	858	1000
	2	854	698	771	791	707	1245	1103	1221	1134	978	1152	1080	1165	1032	978
	1	707	471	538	609	485	956	703	812	894	663	840	876	880	756	640
Max. Story Shear (kN)	3	987	1053	669	937	1089	1196	1298	831	1137	1308	1145	1960	807	1070	1254
	2	1697	1648	1692	1676	1659	1934	1875	2075	1855	1802	1920	1920	1925	1829	1858
	1	2035	1890	2345	1949	1914	2259	2076	2918	2203	2061	2164	2164	2674	2070	2051

Using B: Simplified analysis procedures were applied using the actual 5%-damped spectrum of each earthquake motion, and the damping coefficient B from NEHRP (2000)

Using Actual Spectra: Simplified procedures were applied using the actual damped spectrum of each earthquake

150

TABLE 8-20 Results of Analysis of Example No.1 and No.3 Using Assumed and Actual Base Shear Strengths for the DBE

Quantity	Units	Example No.1		Example No.3	
		Using Assumed Strength V_y=1310 kN	Using Actual Strength V_y=991 kN	Using Assumed Strength V_y=991 kN	Using Actual Strength V_y=1468 kN
1. Elastic Response					
Damping Ratio, β_{Ve}		0.100	0.100	0.100	0.100
Total Damping Ratio, β_{V+I}		0.150	0.150	0.150	0.150
Damping Coefficient, B_m		1.350	1.350	1.350	1.350
Elastic Displacement, D_{em}	mm	274	274	214	214
2. Roof Displacement and Base Shear					
Assumed Ductility, μ		1.10	1.43	1.85	1.23
Effective Period, T_{1D}	sec	1.87	2.13	1.88	1.53
Eff. Viscous Damping Ratio, β_V		0.10	0.10	0.10	0.10
Hysteretic Damping, β_H		0.027	0.089	0.136	0.055
Effective Damping, β_I		0.182	0.258	0.322	0.217
Damping Coefficient, B_I		1.446	1.675	1.866	1.551
Displacement, D_{1D}	mm	267	263	212	207
Corrected Displacement, D_{1D}	mm	273	273	214	214
Seismic Coefficient, C_s		0.108	0.082	0.084	0.123
Seismic Base Shear, V_1	kN	636	480	487	711
Yield Displacement, D_y	mm	244	184	116	169
Computed Ductility, μ		1.12	1.48	1.84	1.27
3. Response at Stage of Maximum Displacement					
Lateral Floor Displacement, δ_{il}	mm	273 182 69	273 182 69	214 137 51	214 137 51
Story Drift, Δ_{jl}	mm	91 113 69	91 113 69	77 86 51	77 86 51
Design Lateral Forces, F_{il}	kN	235 290 110	178 220 83	183 217 80	271 320 119
Floor Acceleration, A_{il}	g	0.309 0.206 0.078	0.234 0.156 0.059	0.241 0.154 0.057	0.357 0.228 0.085
Actual Story Shear Forces, V_{jl}	kN	485 1084 1310	367 820 991	378 826 991	559 1220 1465
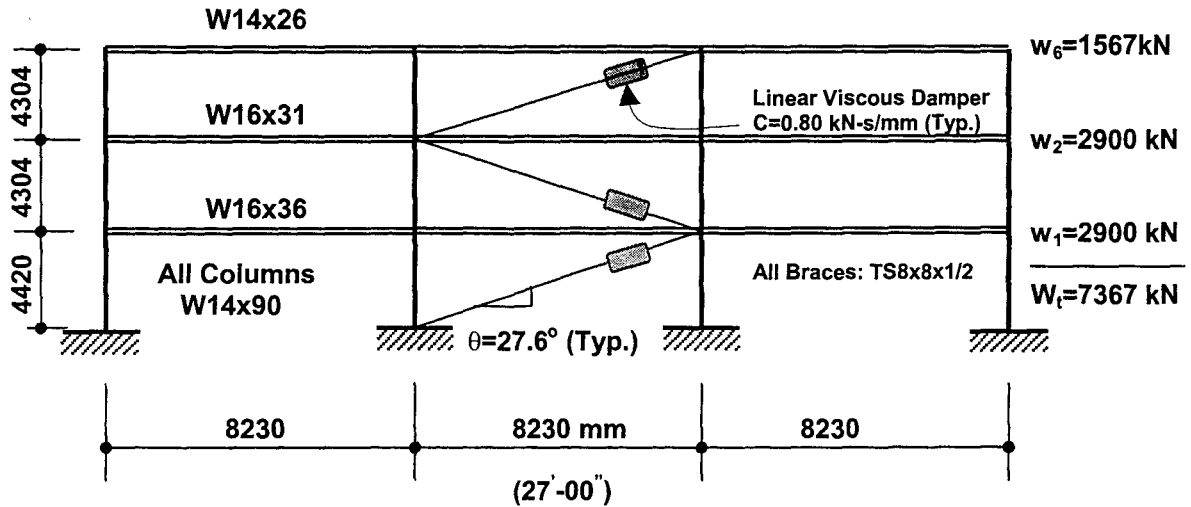
FIGURE 8-1 Example No.1: Frame 3S-60 with Linear Viscous Damping System to Provide 10% Viscous Damping Ratio when Assuming Elastic Frame Behavior
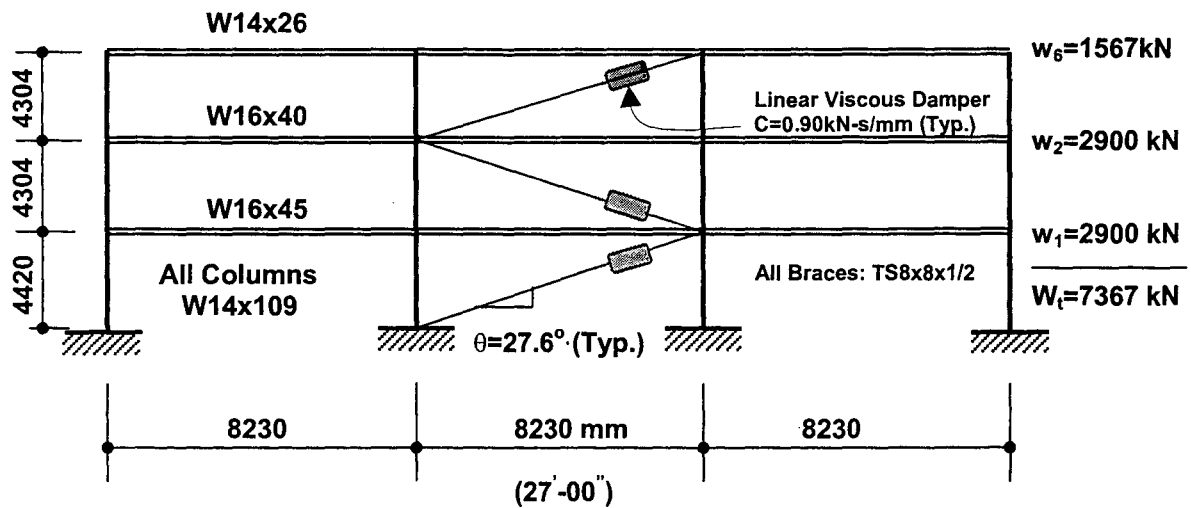
FIGURE 8-2 Example No.2: Frame 3S-75 with Linear Viscous Damping System to Provide 10% Viscous Damping Ratio when Assuming Elastic Frame Behavior
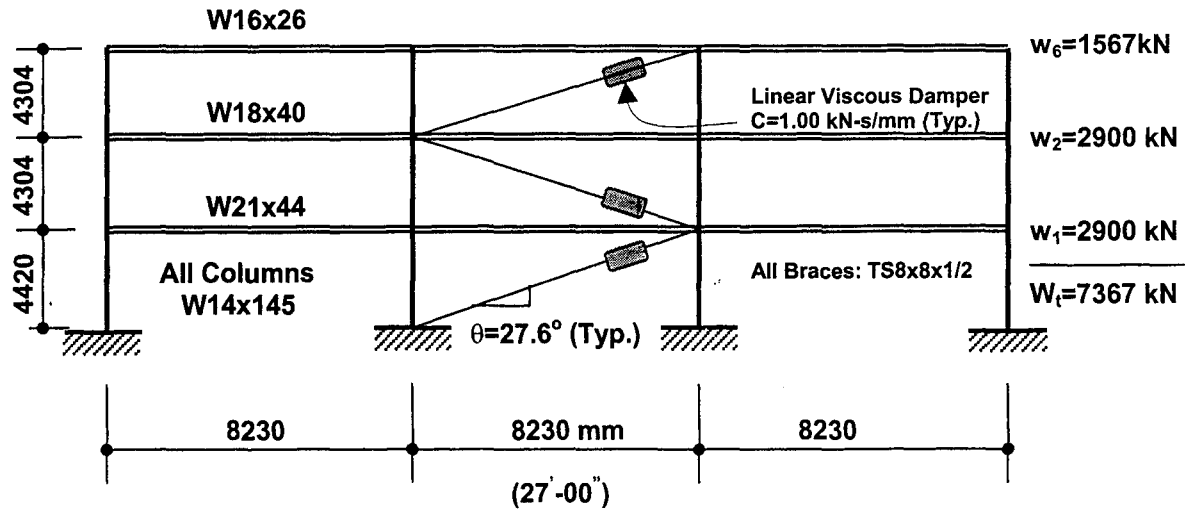
FIGURE 8-3 Example No.3: Frame 3S-90 with Linear Viscous Damping System to Provide 10% Viscous Damping when Assuming Elastic Frame Behavior
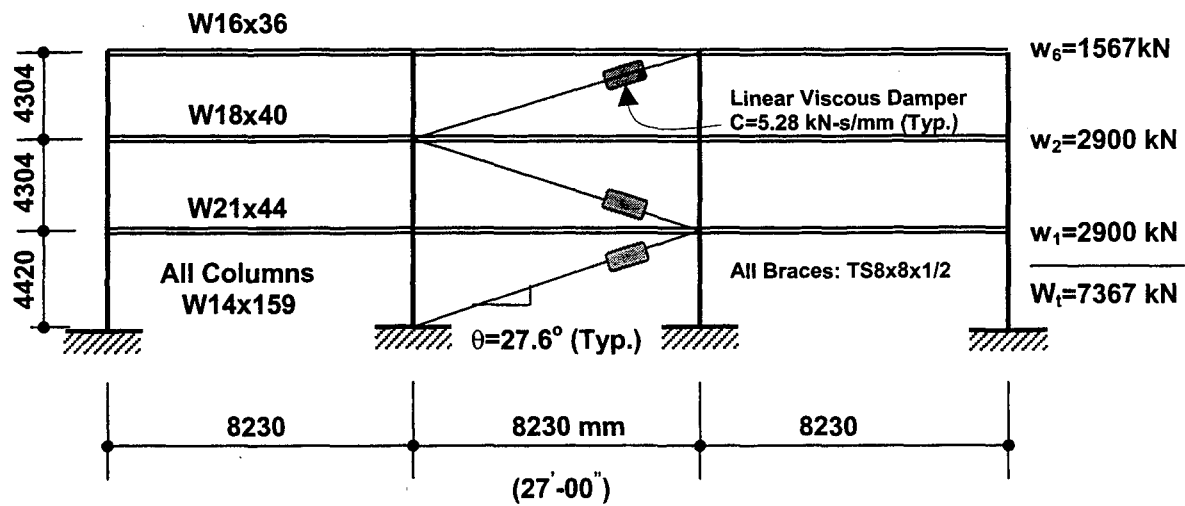
FIGURE 8-4 Example No.4: Frame 3S-100 with Linear Viscous Damping System to Provide 20% Viscous Damping Ratio when Assuming Elastic Frame Behavior

153
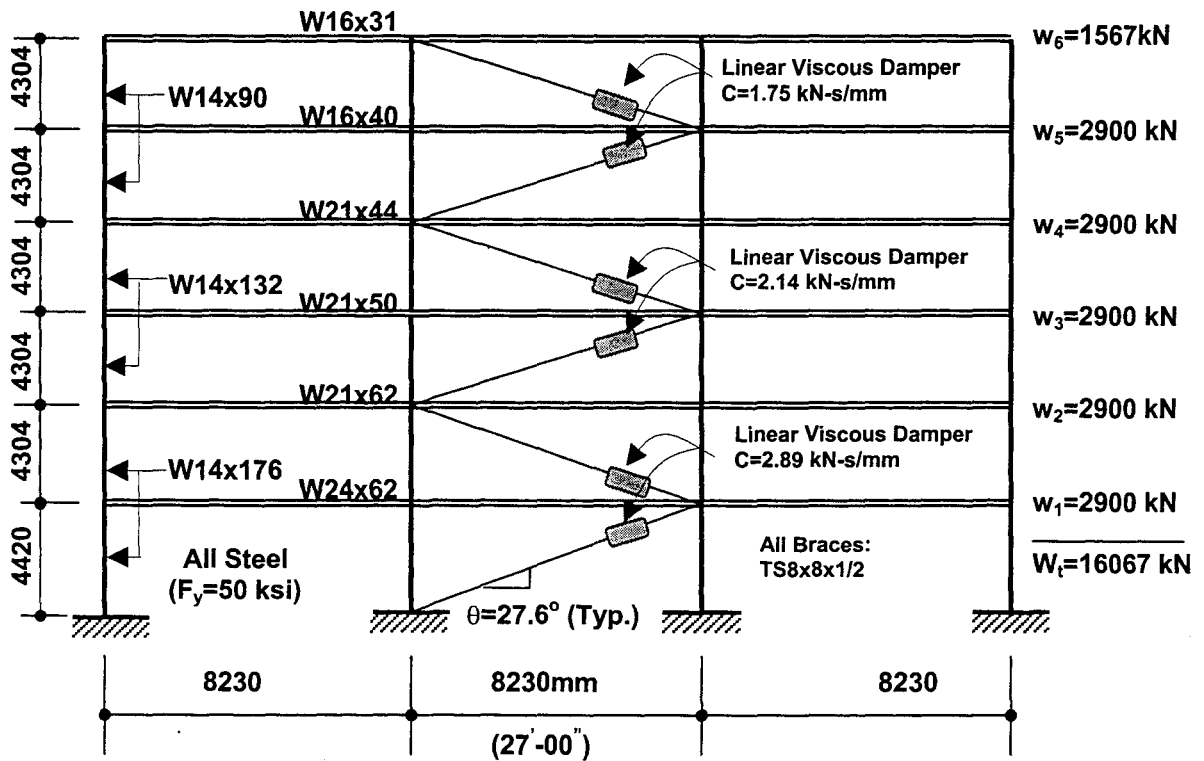
FIGURE 8-5 Example No.5: Frame 6S-75 with Linear Viscous Dampers to Provide 10% Viscous Damping Ratio when Assuming Elastic Frame Behavior
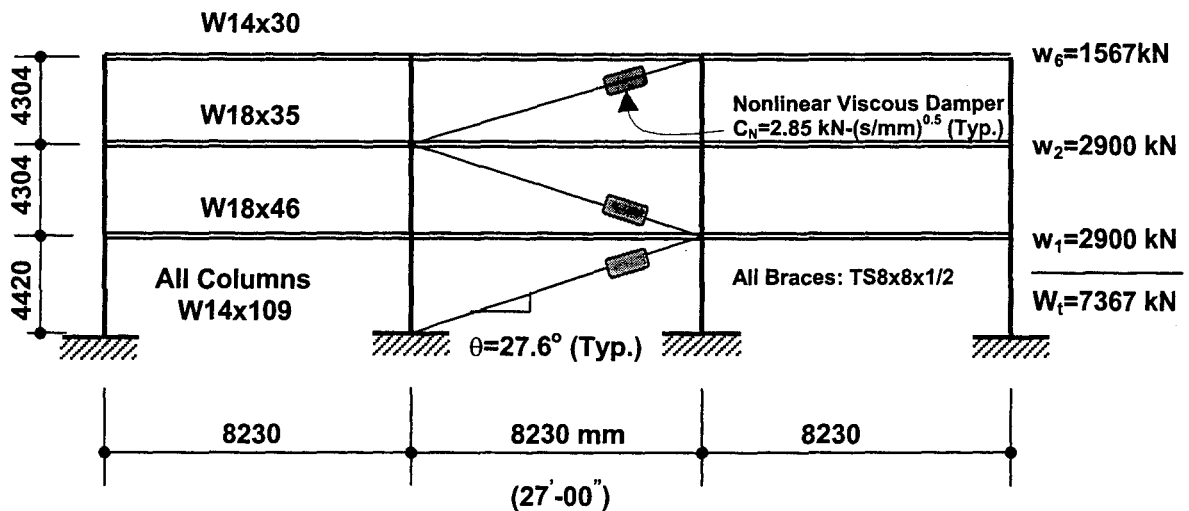
FIGURE 8-6 Example No.6: Frame 3S-80 with Nonlinear Viscous Damping System to Provide 10% Viscous Damping Ratio when Assuming Elastic Frame Behavior in the DBE

154
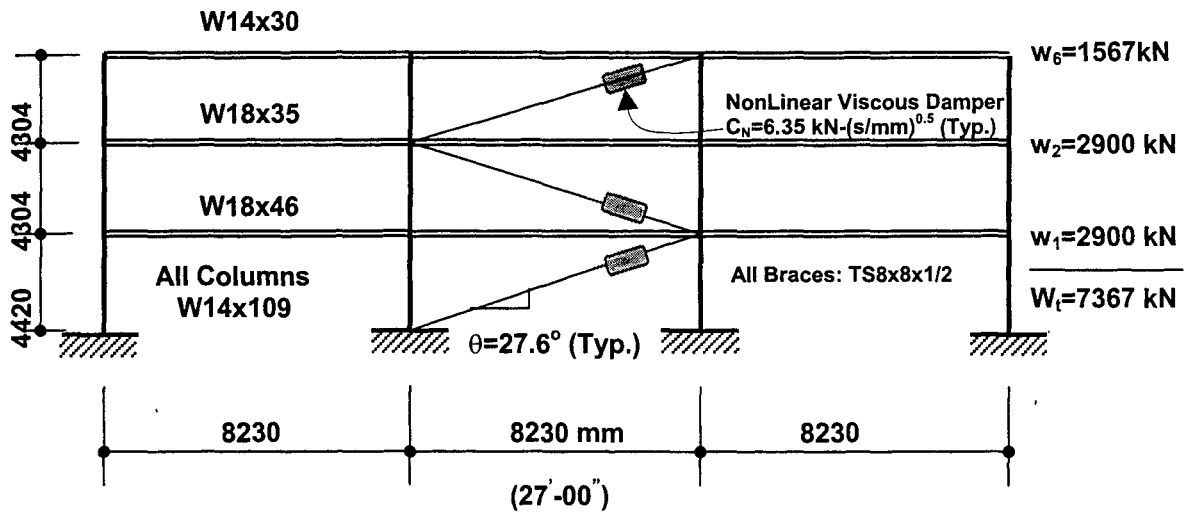
FIGURE 8-7 Example No.7: Frame 3S-80 with Nonlinear Viscous Damping System to Provide 20% Viscous Damping Ratio when Assuming Elastic Frame Behavior in the MCE
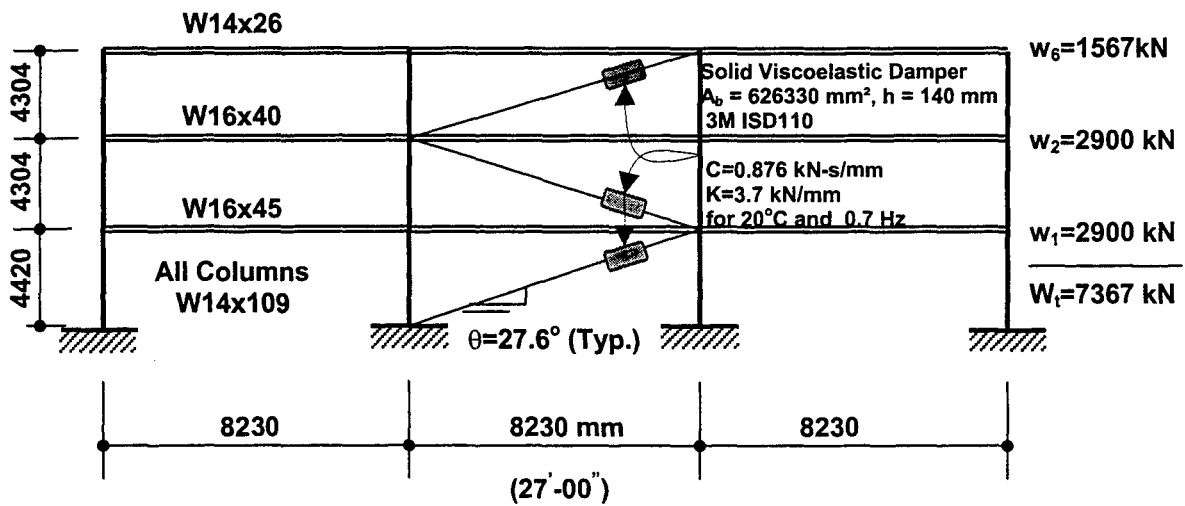
FIGURE 8-8 Example No.8: Frame 3S-75 with Viscoelastic Solid Damping System to Provide 8.5% Viscous Damping Ratio when Assuming Elastic Frame Behavior

155
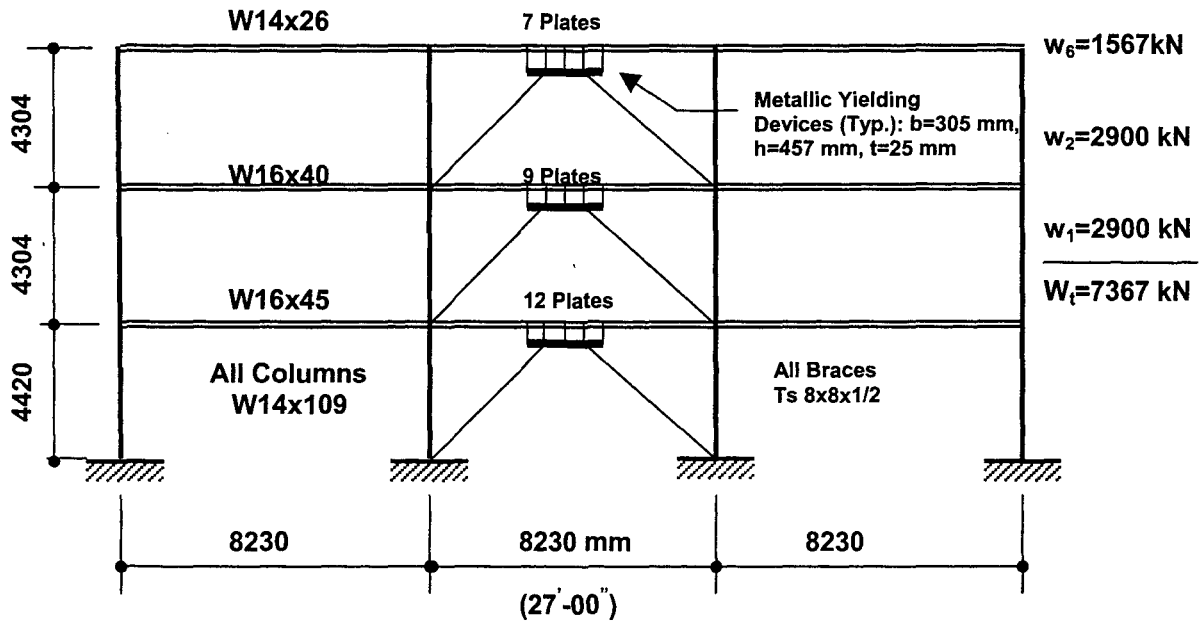
FIGURE 8-9 Example No.9: Frame 3S-75 with Metallic Yielding Damping System

156
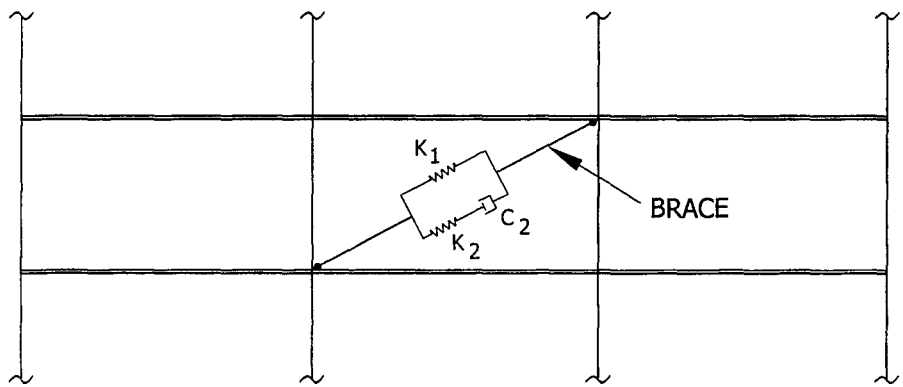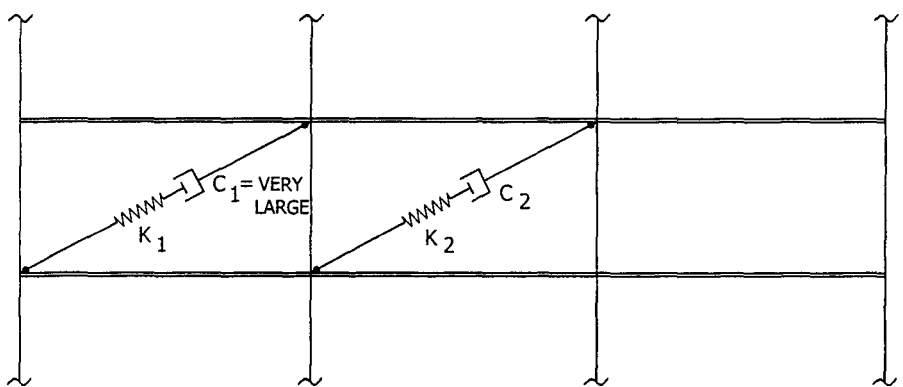
DESIRED MODEL

UTILIZED MODEL

FIGURE 8-10 Modeling of Viscoelastic Solid Damping Device in Program IDARC2D

METALLIC YIELDING DEVICE
ELASTOPLASTIC
STIFF. K_d, STRENGTH V_d

CHEVRON BRACE,
HOR. STIFF. = K_b

DESIRED MODEL

θ

UTILIZED MODEL

ELASTOPLASTIC ELEMENT
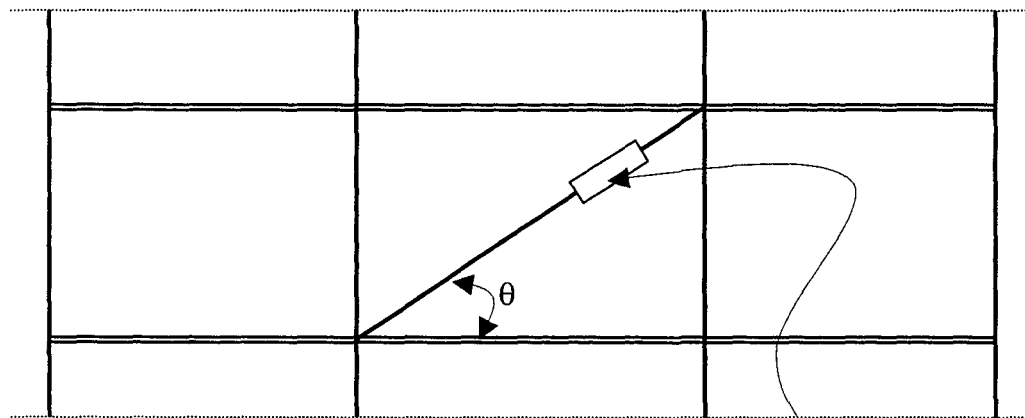
$$\text{STIFF.} = \frac{K_d \cdot K_b}{K_d + K_b \cos^2 \theta}$$

$$\text{STRENGTH} = V_d / \cos \theta$$

**FIGURE 8-11 Modeling of Metallic Yielding Damping Device in Program
IDARC2D**

158
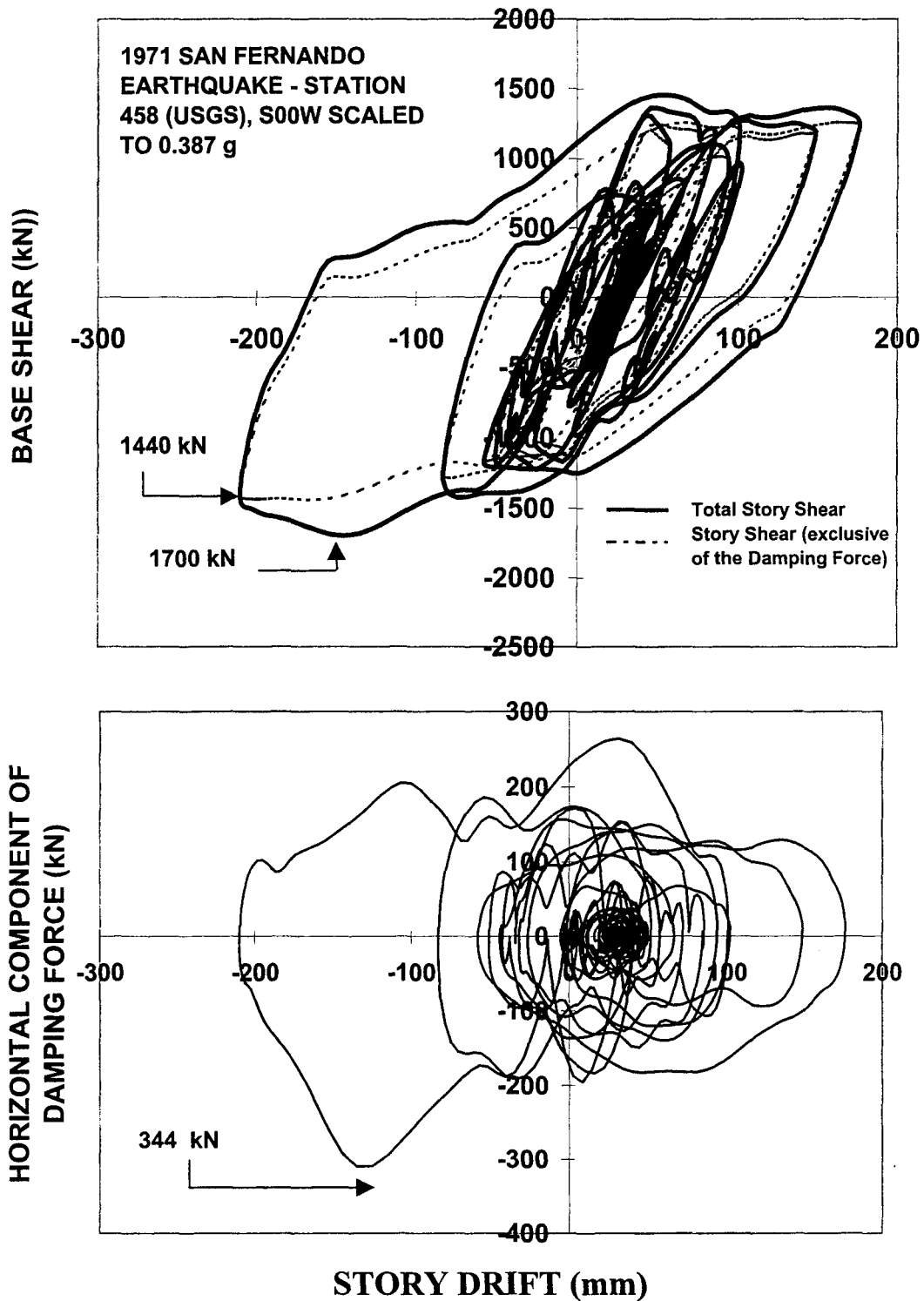
FIGURE 8-12 Base Shear-First Story Drift Loops of Frame of Example No.1:
3-Story (0.60V_y) with Linear Viscous Damping System in Scaled San Fernando,
Station 458, Component S00W Earthquake (see Table 3-2)

159
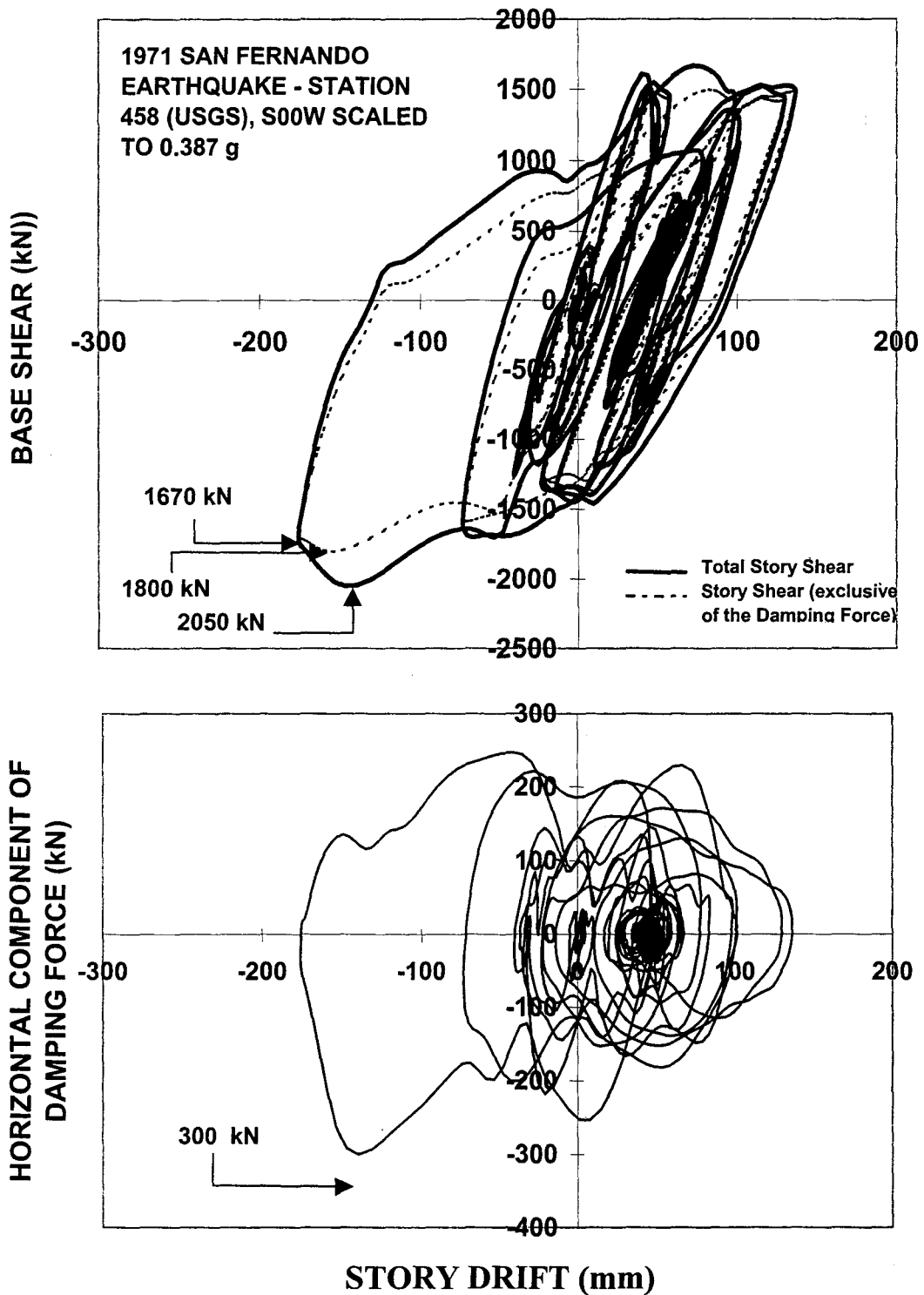
FIGURE 8-13 Base Shear-First Story Drift Loops of Frame of Example No.2: 3
Story (0.75Vy) with Linear Viscous Damping System in Scaled San Fernando,
Station 458, Component S00W Earthquake (see Table 3-2)

160

DBE
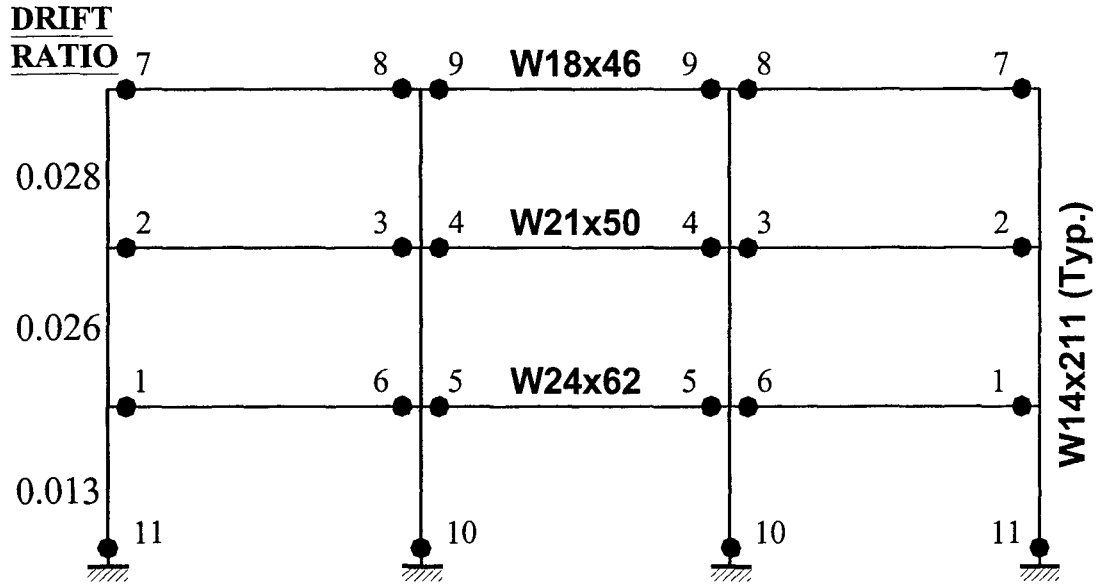
D_{roof}= 277 mm, Peak θ_p= 0.0121 rad, V_{max}= 3206 kN

MCE
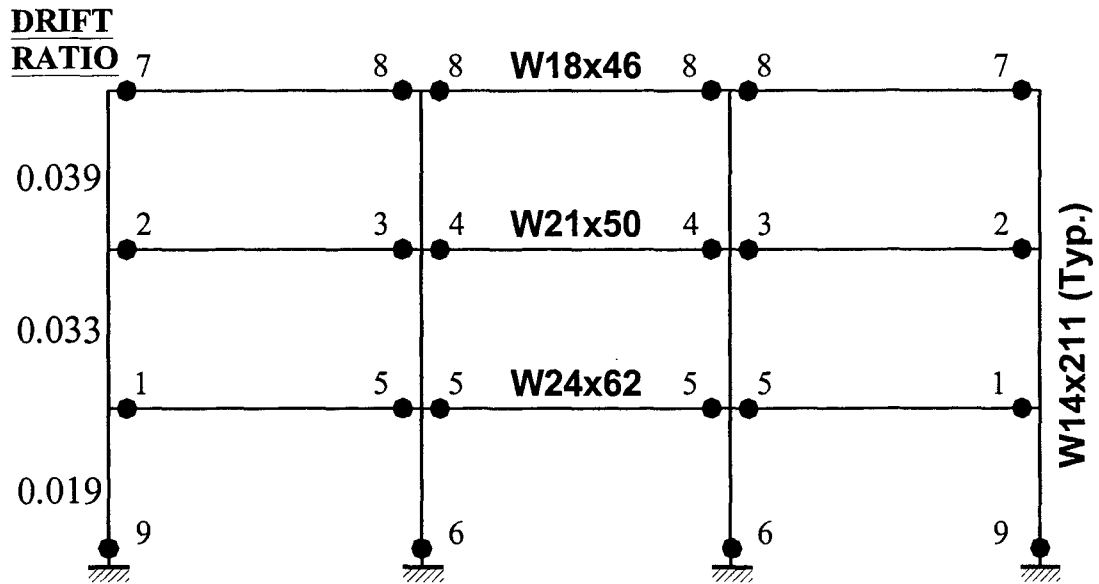
D_{roof}= 378 mm, Peak θ_p= 0.0191 rad, V_{max}= 3335 kN

FIGURE 8-14 Plastic Hinge Formation and Key Response Quantities of Frame without Damping System in DBE and MCE
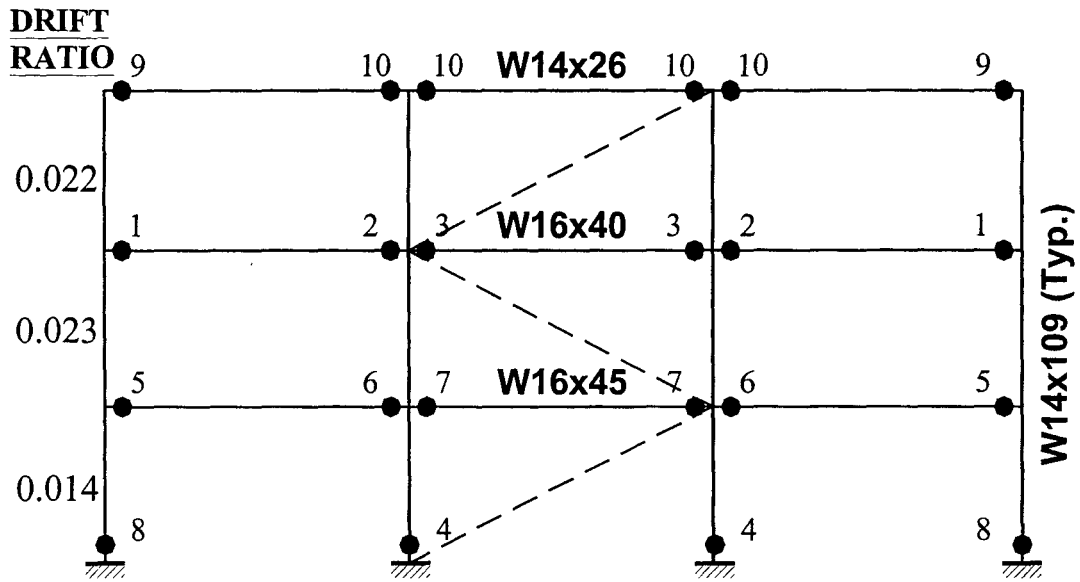
161
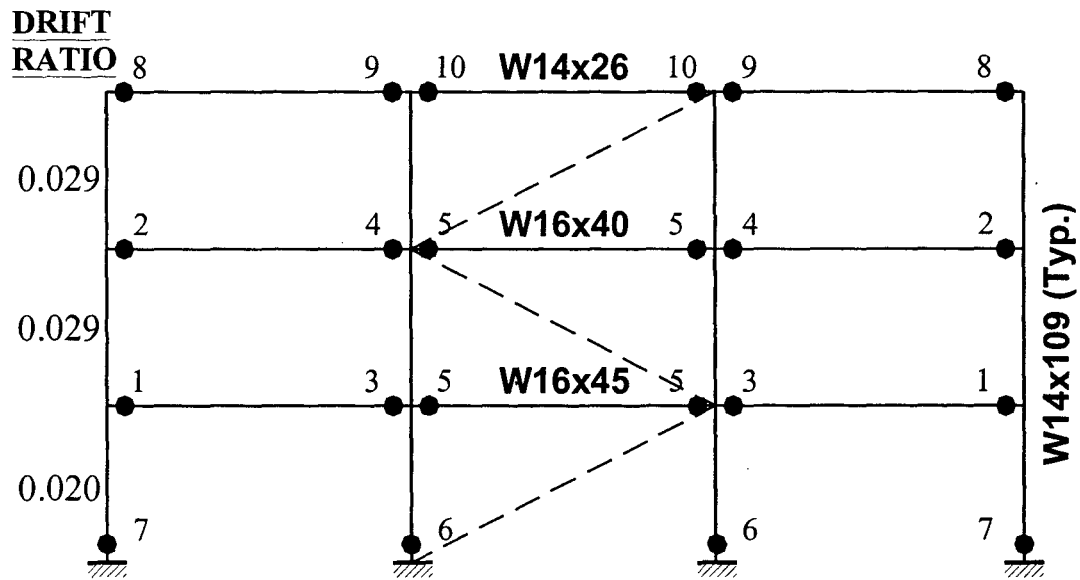
FIGURE 8-15 Plastic Hinge Formation and Key Response Quantities of Frame 3S-
75 with Linear Viscous Damping System (damping ratio of 10%) in
DBE and MCE

162

DBE

DRIFT
RATIO

W16x36

W18x40

W21x44

W14x159 (Typ.)
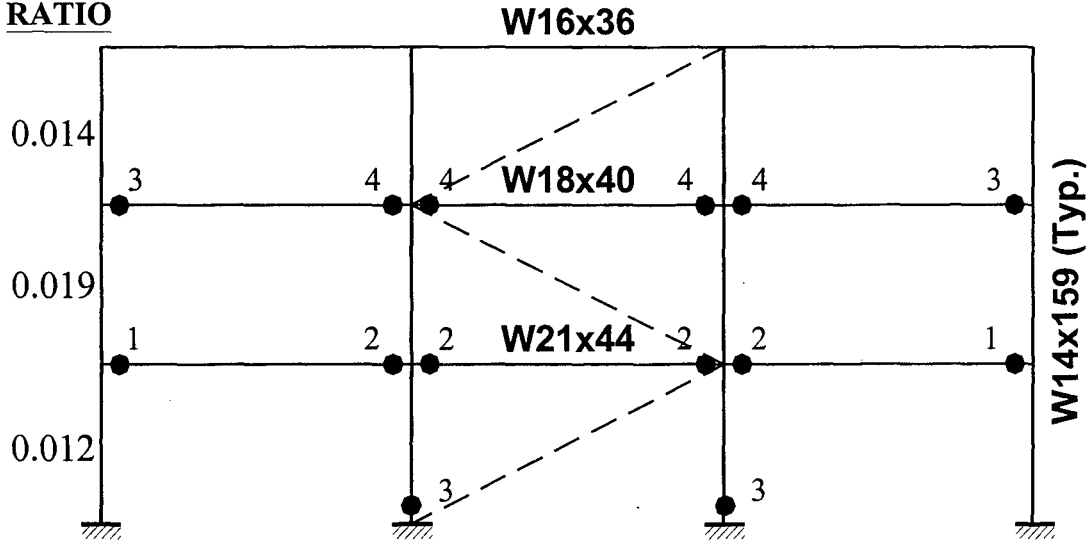
D_{roof}= 183 mm, Peak θ_p= 0.0078 rad, V_{max}= 2272 kN

MCE

DRIFT
RATIO

W16x36

W18x40

W21x44

W14x159 (Typ.)
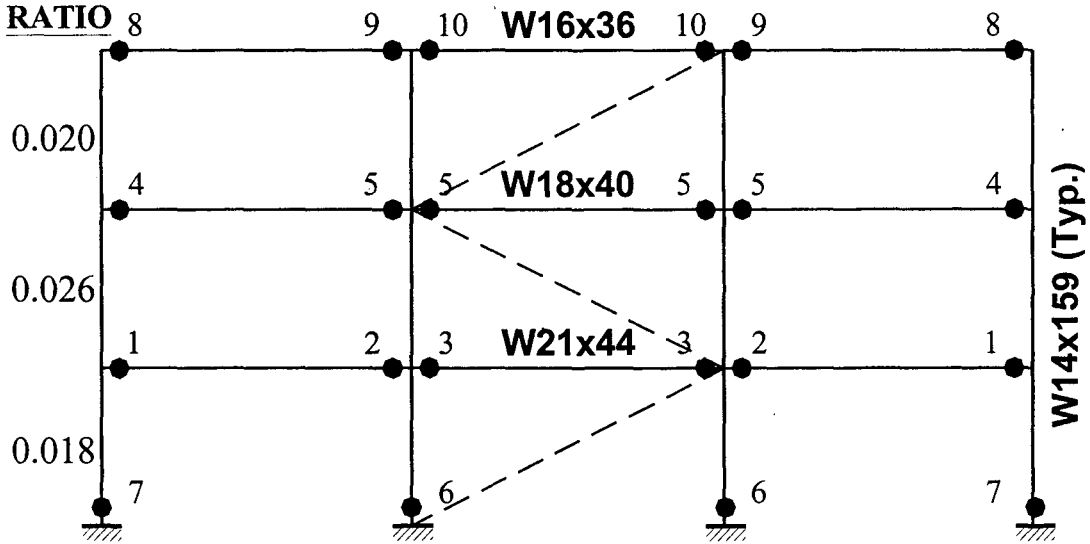
D_{roof}= 261 mm, Peak θ_p= 0.0153 rad, V_{max}= 2660 kN

FIGURE 8-16 Plastic Hinge Formation and Key Response Quantities of Frame 3S-100 with Linear Viscous Damping System (damping ratio of 20%) in DBE and MCE

163

SYLMAR 90°

DRIFT RATIO

0.016

0.020

0.012

W18x46

W21x50

W24x62

W14x211 (Typ.)

D_{roof}= 268 mm, Peak θ_p = 0.0100 rad, V_{max}= 3008 kN

NEWHALL 360°

DRIFT RATIO

0.041

0.030

0.015

W18x46

W21x50

W24x62

W14x211 (Typ.)

D_{roof}= 343 mm, Peak θ_p = 0.0123 rad, V_{max}= 3318 kN

PACOIMA S16E

DRIFT RATIO

0.042

0.042

0.029

W18x46

W21x50

W24x62

W14x211 (Typ.)

D_{roof}= 486 mm, Peak θ_p = 0.0330 rad, V_{max}= 3633 kN
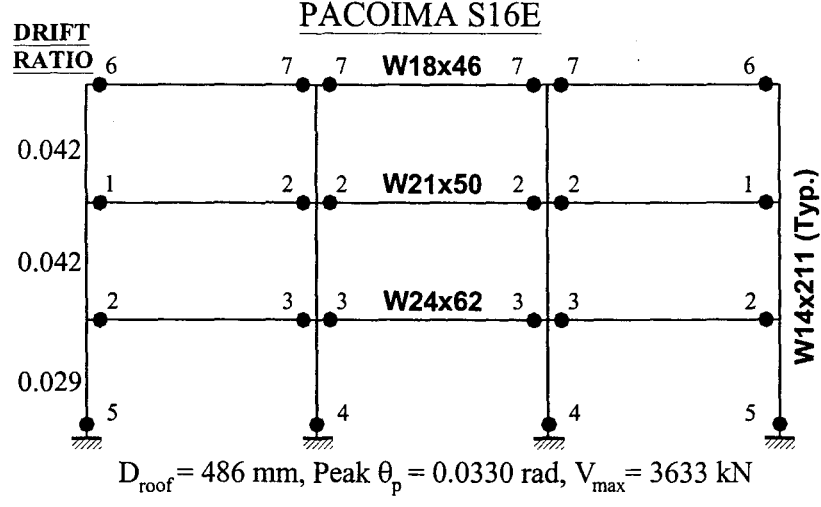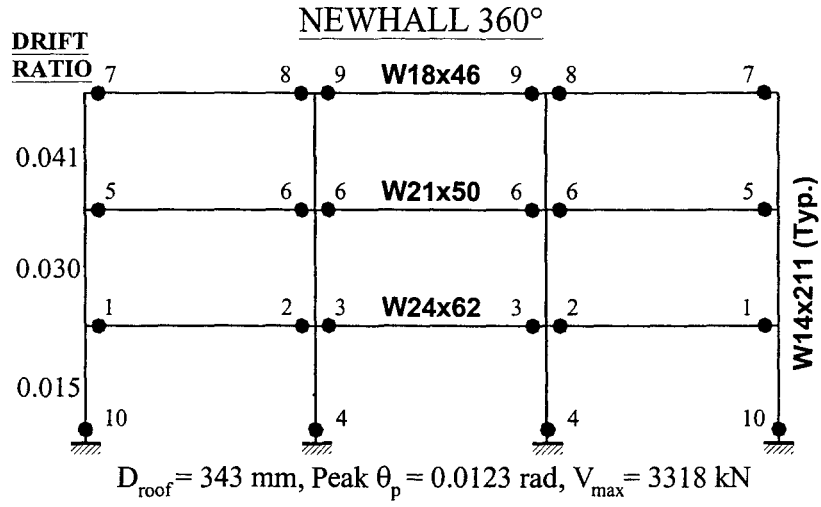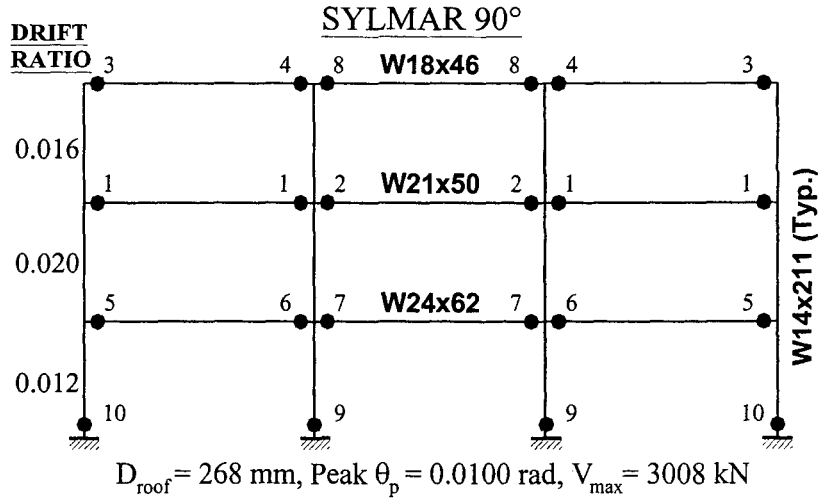
FIGURE 8-17 Plastic Hinge Formation and Key Response Quantities of Frame without Damping System in Near-Fault Seismic Excitation

164
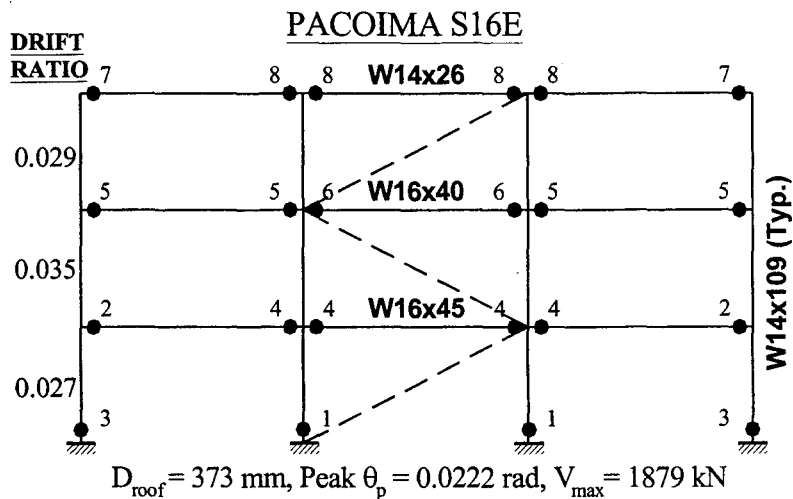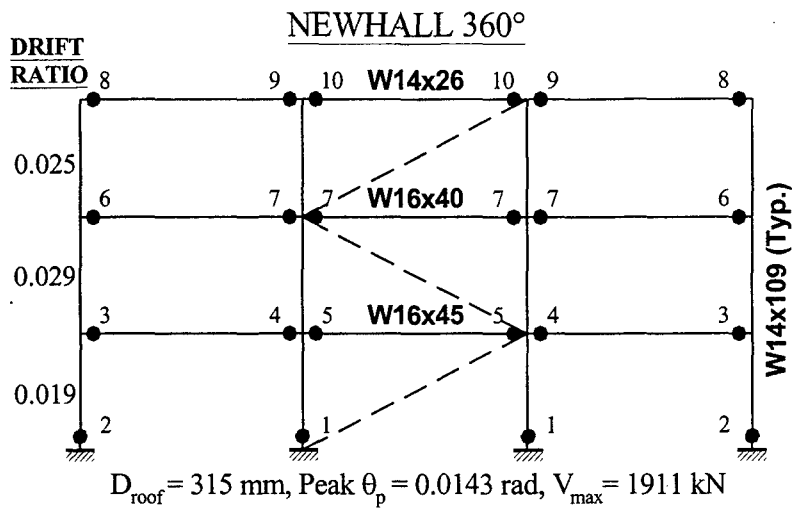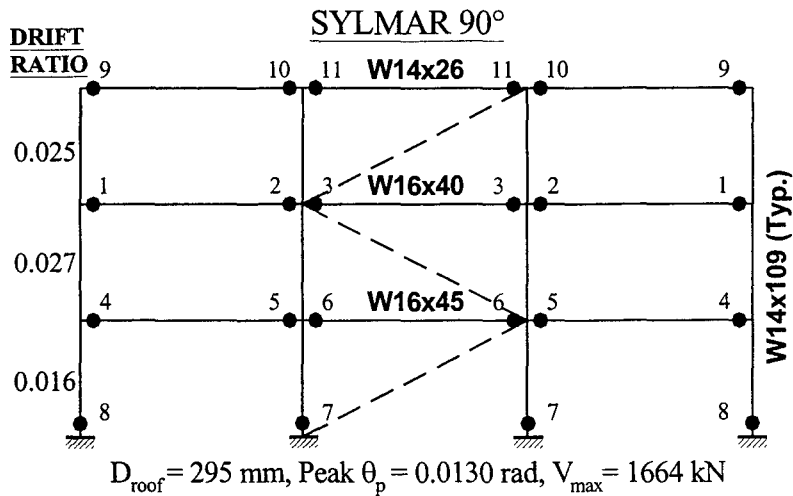
FIGURE 8-18 Plastic Hinge Formation and Key Response Quantities of Frame 3S-75 with Linear Viscous Damping System (damping ratio of 10%) in Near-Fault Seismic Excitation

165

SYLMAR 90°

W16x36

0.015

5   5   6 **W18x40** 6   5   5

0.020

1   2   3 **W21x44** 3   2   1

0.012

4   4

W14x159 (Typ.)

$D_{roof} = 201$ mm, Peak $\theta_p = 0.0072$ rad, $V_{max} = 2388$ kN

NEWHALL 360°

**DRIFT
RATIO** 8   9   10 **W16x36** 10   9   8

0.020

5   5   6 **W18x40** 6   5   5

0.026

1   2   3 **W21x44** 3   2   1

0.017

7   4   4   7

W14x159 (Typ.)

$D_{roof} = 258$ mm, Peak $\theta_p = 0.0124$ rad, $V_{max} = 2966$ kN

PACOIMA S16E

**DRIFT
RATIO** 8   9   10 **W16x36** 10   9   8

0.020

5   6   6 **W18x40** 6   6   5

0.027

1   2   3 **W21x44** 3   2   1

0.018

7   4   4   7

W14x159 (Typ.)

$D_{roof} = 282$ mm, Peak $\theta_p = 0.0168$ rad, $V_{max} = 2673$ kN

FIGURE 8-19 Plastic Hinge Formation and Key Response Quantities of Frame 3S-100 with Linear Viscous Damping System (damping ratio of 20%) in Near-Fault Seismic Excitation

166

SECTION 9

SUMMARY, CONCLUSIONS AND RECOMMENDATIONS

9.1 Summary

This report presented the development and evaluation of simplified procedures of analysis and design for structures with passive energy dissipation systems. This study concentrated on the evaluation of the inelastic response of buildings with passive metallic-yielding, viscoelastic, and viscous (linear and nonlinear) energy dissipation systems. This report served to validate robust linear procedures (equivalent-lateral-force and response-spectrum methods) for the analysis and design of new buildings with passive energy dissipation systems that are included in the *2000 NEHRP Recommended Provisions for Seismic Regulations for New Buildings, Appendix to Chapter 13* (NEHRP 2000).

The first task of this study concentrated on the modification of response spectra for levels of damping exceeding 5 percent of critical. Based on the analysis of response of structural systems to selected ground motions, which did not include records on soft soil sites or records with near-fault characteristics, new values of the damping coefficient B were. These new values of the damping coefficient are valid for viscous damping in the range of 2 to 100 percent of critical and were utilized for the evaluation of simplified methods of analysis of yielding single-degree-of-freedom systems with energy dissipation devices. The results of this study were in good agreement with the results of nonlinear time history analysis.

A calibrated relation for the ratio of maximum inelastic displacement to maximum elastic displacement, C_I, was established. The coefficient C_I was expressed as a function of the post-elastic to elastic stiffness, α (range ≤ 0.5), the elastic period, T_e, the viscous damping ratio under elastic conditions, β_v (range of 0.05 to 0.30), the ductility portion of the R-factor, R_μ, and the period T_s, which characterizes the corner point in the design response spectrum.

A systematic study of the ductility demands on damped and undamped structures was presented to determine whether the addition of viscous damping to a building would result in comparable displacement ductility demands. Damped and undamped bilinear hysteretic single-degree-of-freedom systems structures were considered. Undamped structures were characterized by the

167

elastic period, T_e; the ductility-based portion of R-factor, R_μ; the ratio of the post-elastic to elastic stiffness, α; and the inherent damping ratio, $\beta_i = 0.05$. Values of $T_e = 0.2$ to 2.0 sec, $\alpha = 0.05$, 0.15, 0.25 and 0.50, and $R_\mu = 2.0$, 3.33 and 5.0 were considered. Damped structures were characterized by the same parameters β_i, α, and R_μ, a value of elastic period T_{ed} larger than T_e, and added linear viscous damping ratio $\beta_v = 0.15$ and 0.25 under elastic conditions. The calculated average, maximum and minimum displacement ductility ratios in the damped and undamped structures were nearly the same for the same values of R_μ and α.

The core of this research project focuses on the development and evaluation of simplified procedures for the analysis of buildings with damping systems. The theoretical basis of the equivalent lateral force and the response spectrum analysis procedures of NEHRP (2000) was presented. A modification of Method 2 of FEMA (1997) was also presented. Procedures for calculating the effective damping and effective period, and the higher mode damping ratios for buildings with nonlinear viscous damping systems, viscoelastic damping systems and yielding damping systems were developed. The application of these procedures was illustrated through the analysis of 3- and 6-story steel special moment frames with passive energy dissipation devices (viscous, viscoelastic, and metallic yielding devices). Some examples were analyzed utilizing the actual damped spectra of three preselected near-fault motions. Results provided by the simplified procedures were validated by comparison to the results of nonlinear time history analysis carried out using IDARC2D.

In addition, approximate methods for the evaluation of the pushover curve of multiple-degree-of-freedom structures with viscous, viscoelastic, and metallic yielding devices were presented in this study. Important considerations in the design of metallic yielding and viscoelastic solid damping devices were identified, and sample calculations for the analysis of structures with passive damping systems were presented.

9.2 Conclusions

Key conclusions of this study are:

(1)   The proposed values of the damping coefficient B for the modification of response spectra for levels of damping greater than 5 percent of critical provided results that were in good

agreement with the results of nonlinear time history analysis of single-degree-of-freedom systems.

(2) The proposed equation for the coefficient C_1 predicts reasonably well the ratio of maximum inelastic displacement to maximum displacement under elastic conditions of systems with a wide range of values of post-elastic to elastic stiffness ratio, α, viscous damping ratio under elastic conditions, β_v; the ductility portion of the R-factor, R_μ; and the elastic period T_e.

(3) The calculated average, maximum and minimum displacement ductility ratios in damped and undamped structures were nearly the same for the same values of R_μ and α. On the basis of these results, and those presented by Wu and Hanson (1989), NEHRP (2000), permits the design of structures with damping systems for a seismic base shear that is smaller than that required for undamped (conventional) structures.

(4) Simplified methods of analysis of yielding single-degree-of-freedom systems with energy dissipation devices, including the correction for velocity prediction, produced estimates of peak displacement, peak velocity, and peak acceleration (including the viscous component), which were in good agreement with the average of results of nonlinear time history analysis. The simplified method of analysis is not error-free. However, it is simple to apply, it systematically converges, and produces results of sufficient accuracy for design purposes.

(5) The application of the simplified methods of analysis of NEHRP (2000) and Method 2 of FEMA 274(1997), as modified in this study, to steel special moment frames with damping systems, provided systematically conservative predictions of drift, and predictions of acceptable accuracy for damper forces and member actions. These force predictions may differ by as much as ± 30% from the average forces calculated by dynamic analysis.

(6) The simplified methods produced results of acceptable accuracy for near-fault seismic excitations. However, the number of near-fault motions and analyzed structures considered were too few, and broad conclusions were not drawn. Further studies with near-fault motions are warranted.

(7) Buildings with damping systems designed to meet the minimum drift and strength criteria of NEHRP (2000) perform comparably to, or better than, conventional buildings without

damping systems. Buildings with viscous damping systems can be designed for a lower base shear force than conventional buildings without damping systems for similar performance.

(8)   The approximate methods presented for the construction of the pushover curve of buildings with or without damping systems on the basis of plastic analysis can be utilized with confidence.   The developed procedure is an alternate approach to determining the base shear strength of buildings by avoiding the use of pushover analysis.

(9)   The pushover curve of buildings with viscous damping systems is affected by the viscous damping forces, likely by inducing additional rotations of the column ends.   This phenomenon, which cannot be accounted for by the current methods of pushover analysis, can lead to underestimation of the maximum value of member actions.

(10)   The procedures developed and evaluated in this study validate the accuracy of simplified methods of analysis of buildings with passive energy dissipation systems.   These procedures provided the basis for the implementation of robust linear procedures (equivalent lateral force and response-spectrum methods) for the development of national standards for implementing passive energy dissipation systems in buildings.

9.3 Recommendations for Future Research

It is important to emphasize that the procedures presented in this study have been developed for the analysis of buildings with passive energy dissipation devices taking into account a seismic demand compatible with the 1997 NEHRP spectra for soils type C or D.   Neither near-fault characteristics nor soft soil effects have been considered.   Also, the evaluation of these procedures has been limited to a few examples of 3- and 6-story steel special moment frames. While the results of these examples show that the procedures are accurate to predict global response, it is fair to say that more studies might be necessary to bound its application.   In consequence, the following recommendations are made:

(1)   The number of examples presented in this study is limited. Application of the simplified procedures to a broader variety of structures with different conditions of height and distribution of passive energy dissipation devices is encouraged to confirm results of this study.

170

(2) Further studies of structures with damping systems with near-fault motions is recommended to seek for conclusive evidence of the validity, or the need for adjustments, of the simplified procedures.

(3) It is desirable to evaluate the applicability of these procedures to the analysis of response of buildings in soft soil sites.

SECTION 10

REFERENCES

1. Bracci, J.M., Kunnath, S.K. and Reinhorn, A.M. (1997), "Seismic Performance and Retrofit Evaluation of Reinforced Concrete Structures", Journal of Structural Engineering, ASCE, 123(1), 3-10.

2. Chang, G.A and Mander, J.B. (1994), "Seismic Energy Based Fatigue Damage Analysis of Bridge Columns: Part II – Evaluation of Seismic Demand" Technical Report NCEER-94-0013, National Center for Earthquake Engineering Research, University at Buffalo, State University of New York, Buffalo, N.Y.

3. Chopra, A.K. and Goel, R.K. (1999), "Evaluation of NSP to Estimate Seismic Deformation: SDF Systems", Journal of Structural Engineering, American Society of Civil Engineers, 126(4), 482-490.

4. Chopra, A.K. (1995), "Dynamics of Structures", Prentice Hall, Englewood Cliffs, N.J.

5. Clough, R.W and Penzien, J. (1975), "Dynamics of Structures", McGraw-Hill, New York, N.Y.

6. Coffin, L. F. Jr. (1954), "A Study of Effects of Cyclic Thermal Stresses on a Ductile Metal", Trans., American Society of Mechanical Engineers, New York, 76, 931-950.

7. Computers and Structures Inc. (1998), "SAP-2000NL V7.11: Integrated Finite Element Analysis and Design of Structures", Computers and Structures Inc., Berkeley, CA.

8. Constantinou, M.C. and Sigaher, N. (2000), "Energy Dissipation System Configurations for Improved Performance", Proceedings of the 2000 Structures Congress & Exposition, ASCE, Philadelphia, PA.

9. Constantinou, M.C. and Symans, M.D. (1992), "Experimental and Analytical Investigation of Structures with Supplemental Fluid Viscous Dampers", Technical Report NCEER-92-0032, National Center for Earthquake Engineering Research, University at Buffalo, State University of New York, Buffalo, N.Y.

10. Constantinou, M.C., Soong, T.T. and Dargush, G.F. (1998), "Passive Energy Dissipation Systems for Structural Design and Retrofit", Monograph Series No.1, Multidisciplinary Center for Earthquake Engineering Research, University at Buffalo, State University of New York at Buffalo, Buffalo, N.Y.

11. Constantinou, M.C. (1998), "An Introduction to Passive Energy Dissipation", Spring Seminar, Structural Engineers Association of Northern California (SEAONC), San Francisco, CA.

12. Eberhard, M.O. and Sozen, M.A. (1993), "Behavior-Based Method to Determine Design Shear in Earthquake-Resistant Walls", Journal of Structural Engineering, ASCE, 119: (2) 619-640.

13. Fajfar, P. and Fischinger, M. (1988), "N2 – A Method for Non-Linear Seismic Analysis of Regular Structures", Proceedings of the Ninth World Conference on Earthquake Engineering, Tokyo-Kyoto, Japan.

14. FEMA - Federal Emergency Management Agency (1997), "NEHRP Guidelines for the Seismic Rehabilitation of Buildings" and "NEHRP Commentary on the Guidelines for the Seismic Rehabilitation of Buildings", Reports No. FEMA-273 and FEMA-274, Washington, D.C.

15. Freeman, S.A., Nicoletti, J.P., and Tyrell, J.V. (1975), "Evaluation of Existing Buildings for Seismic Risk – A Case Study of Puget Sound Naval Shipyard, Bremerton, Washington", Proceedings of the First U.S. National Conference on Earthquake Engineering, Earthquake Engineering Research Institute, Oakland, California.

16. Freeman, S.A. (1978), "Prediction of Response of Concrete Buildings to Severe Earthquake Motion", Douglas McHenry International Symposium on Concrete and Concrete Structures, SP-66, American Concrete Institute, Detroit, MI, 589-605.

17. Gomez, J.D. (2000), "Evaluation of Simplified Methods of Analysis of Yielding Structures with Energy Dissipation Systems", Master of Science Thesis, Department of Civil, Structural and Environmental Engineering, University at Buffalo, State University of New York, Buffalo, N.Y.

18. Iwan, W.D. and Gates, N.C. (1979a), "The Effective Period and Damping of a Class of Hysteretic Structures", Earthquake Engineering and Structural Dynamics, 7(3), 199-211.

19. Iwan, W.D. and Gates, N.C. (1979b), "Estimating Earthquake Response of Simple Hysteretic Structures", Journal of Engineering Mechanics Division, ASCE, 105 (EM3), 391-405.

20. Kelly, J.M., Skinner, M.S. and Beucke, K.E. (1980). "Experimental Testing of an Energy Absorbing Base Isolation System", Technical Report No.UCB/EERC-80/35, Earthquake Engineering Research Center, University of California, Berkeley, CA.

21. Koh, S. K. and Stephens, R.I. (1991), "Mean Stress Effects on Low Cycle Fatigue for High Strength Steel", Fatigue Fracture of Engineering Materials and Structures, 14(4), 413-428.

22. Mander, J.B., Priestley, M.J.N. and Park, R. (1984), "Seismic Design of Bridge Piers", Department of Civil Engineering, University of Canterbury, Report 84-2, February.

23. Mander, J. B., Panthaki, F. D. and Kasalanati, A. (1994),"Low-Cycle Fatigue Behavior of Reinforcing Steel", Journal of Materials in Civil Engineering, 6 (4), 453-467.

24. Manson, S. S. (1953), "Behavior of Materials Under Conditions of Thermal Stress", Heat Transfer Symposium, Engineering Research Institute, University of Michigan, Ann Arbor, 9-75.

25. Miranda, E. and Bertero, V.V. (1994), "Evaluation of Strength Reduction Factors for Earthquake-Resistant Design", Earthquake Spectra, 10(2), 357-379.

26. Miranda, E. (1993), "Site-Dependent Strength Reduction Factors", Journal of Structural Engineering, ASCE, Vol. 119, No.12, 3503-3519.

27. Nassar, A.A. and Krawinkler, H. (1991). " Seismic demands for SDOF and MDOF Systems", Report No. 95, John Blume Earthquake Engineering Research Center, Stanford University, Stanford, California.

28. NEHRP - National Earthquake Hazard Reduction Program (1994), "NEHRP Recommended Provisions for Seismic Regulations for New Buildings and Other Structures", Federal Emergency Management Agency, Report No. FEMA 222A, Washington, D.C.

29. NEHRP - National Earthquake Hazard Reduction Program (1997), "NEHRP Recommended Provisions for Seismic Regulations for New Buildings and Other Structures", Federal Emergency Management Agency, Report No. FEMA 302, Washington, D.C.

30. NEHRP - National Earthquake Hazard Reduction Program (2000), "NEHRP Recommended Provisions for Seismic Regulations for New Buildings and Other Structures", Appendix to Chapter 13, Structures with Damping Systems, Federal Emergency Management Agency, Washington, D.C., to be published.

31. Newmark, N.M and Hall, W.J. (1969), "Seismic Design Criteria for Nuclear Reactor Facilities", Proceedings Fourth World Conference on Earthquake Engineering, Santiago, Chile, 2, B-4, 37-50.

32. Newmark, N.M. and Hall, W.J. (1973), "Seismic Design Criteria for Nuclear Reactor Facilities", Report No.46, Building Practices for Disaster Mitigation, National Bureau of Standards, U.S. Department of Commerce, pp. 209-236.

33. Newmark, N.M. and Hall, W.J. (1982), "Earthquake Spectra and Design", Earthquake Engineering Research Institute, Oakland, California.

34. Newmark, N.M and Rosenblueth, E. (1971), "Fundamentals of Earthquake Engineering", Prentice-Hall, Englewood Cliffs, N.J.

35. Novak, M. and El Hifnawy, L. (1983), "Effect of Soil-Structure Interaction on Damping of Structures". Earthquake Engineering and Structural Dynamics, 11(5), 595-621.

36. Pekhan, G., Mander J.B., and Chen S.S. (1999), "Design and Retrofit Methodology for Buildings Structures with Supplemental Energy Dissipating Systems", Technical Report MCEER-99-0021, Multidisciplinary Center for Earthquake Engineering Research, University at Buffalo, State University of New York, Buffalo, N.Y.

37. Reinhorn, A.M., Li, C., and Constantinou, M.C. (1995), "Experimental and Analytical Investigation of Seismic Retrofit of Structures with Supplemental Damping Part I: Fluid Viscous Damping Devices", Technical Report NCEER-95-0001, National Center for Earthquake Engineering Research, University at Buffalo, State University of New York, Buffalo, N.Y.

38. Riddell, R. and Newmark, N.M. (1979), "Statistical Analysis of the Response of Nonlinear Systems Subjected to Earthquakes", Structural Research Series No.468, Department of Civil Engineering, University of Illinois, Urbana.

39. Riddell, R., Hidalgo, P., and Cruz, E. (1989), "Response Modification Factors for Earthquake Resistant design of Short Period Structures, Earthquake Spectra, 5(3), 571-590.

40. Sadek, F., Mohraz, B. and Riley, M.A. (1999), "Linear Static and Dynamic Procedures for Structures with Velocity-Dependent Supplemental Dampers," Building and Fire Research Laboratory, National Institute of Standards and Technology, Gaithersburg, MD.

41. SEAOC- Structural Engineers Association of California (1999), "Recommended Lateral Force Requirements and Commentary", Sacramento, CA.

42. Seleemah, A.A., and Constantinou, M.C. (1997), "Investigation of Seismic Response of Buildings with Linear and Nonlinear Fluid Viscous Dampers", Technical Report NCEER-97-004, National Center for Earthquake Engineering Research, University at Buffalo, State University of New York, Buffalo, N.Y.

43. Soong, T.T. and Dargush, G.F. (1997), "Passive Energy Dissipation Systems in Structural Engineering", John Wiley & Sons Ltd., London (UK) and New York (USA).

44. Tsai, K.C., Cheng, H.W., Hong, C.P. and Su, Y.F. (1993), "Design of Steel Triangular Plate Energy Absorbers for Seismic-Resistant Construction", Earthquake Spectra, 9(3), 505-528.

45. Tsopelas, P., Constantinou, M.C., Kircher, C.A. and Whittaker, A.S. (1997), "Evaluation of Simplified Methods of Analysis for Yielding Structures". Technical Report No. NCEER 97-0012, National Center for Earthquake Engineering Research, University at Buffalo, State University of New York, Buffalo, N.Y.

46. Tyler, R.G. (1978a), "A Tenacious Base Isolation System Using Round Steel Bars", Bulleting of the New Zealand National Society for Earthquake Engineering, 11(4), 273-281.

47. Tyler, R.G. (1978b), "Tapered Steel Energy Dissipators for Earthquake Resistant Structures". Bulletin of the New Zealand National Society for Earthquake Engineering 11(4), 282-294.

48. Uang, C. and Bertero, V.V. (1990), "Evaluation of Seismic Energy in Structures", Earthquake Engineering and Structural Dynamics, 19(1), 77-90.

49. Valles, R.E., Reinhorn, A.M., Kunnath, S.K., Li, C. and Madan, A. (1996), "IDARC2D Version 4.0: A Computer Program for the Inelastic Damage Analysis of Buildings", Technical Report NCEER-96-0010, National Center for Earthquake Engineering Research, University at Buffalo, State University of New York, Buffalo, N.Y. Information on Version 5.0 of IDARC2D can be found at http://civil.eng.buffalo.edu/idarc2d50/.

50. Veletsos, A.S. and Meek, J.W. (1974), "Dynamic Behavior of Building-Foundation Systems", Earthquake Engineering and Structural Dynamics, 3(2), 121-138.

51. Vidic, T., Fajfar, P. and Fischinger, M. (1992), "A procedure for Determining Consistent Inelastic Design Spectra", Proc. Workshop on Nonlinear Seismic Analysis of RC Structures, Bled, Slovenia.

52. Watanabe A., Hitomi, Y., Saeki, E., Wada, A., and Fujimoto, M. (1988), "Properties of Brace Encased in Buckling-Restraining Concrete and Steel Tube", Proceedings of Ninth World Conference on Earthquake Engineering, Tokyo-Kyoto, Japan, Paper No.6-7-4, Vol. IV, pp. 719-724.

53. Whittaker, A. S., Aiken, I., Bergman, D., Clark, P., Kelly, J. and Scholl, R. (1993), "Code Requirements for the Design and Implementation of Passive Energy Dissipation Systems". *Proceedings*, ATC-17-1, Seminar on Seismic Isolation, Passive Energy Dissipation, and Active Control, Applied Technology Council, Redwood City, California.

54. Wu, J., and Hanson, R.D. (1989), "Study of Inelastic Spectra with High Damping", Journal of Structural Engineering, ASCE, 115(6), 1412-1431.

55. Zimmer, M. (1999) "Characterization of Viscoelastic Materials for use in Seismic Energy Dissipation Systems", Master of Science Thesis, Department of Civil, Structural and Environmental Engineering, University at Buffalo, State University of New York, Buffalo, N.Y.

APPENDIX A

NEHRP 2000 – APPENDIX TO CHAPTER 13: STRUCTURES WITH DAMPING SYSTEMS

SCOPE: 1997 *Provisions* Appendix to Chapter 13 and *Provisions* and *Commentary* Chapter 2

PROPOSAL FOR CHANGE:

Revise the 1997 *Provisions* Appendix to Chapter 13 as follows:

Appendix to Chapter 13

~~PASSIVE ENERGY DISSIPATION SYSTEMS~~

STRUCTURES WITH DAMPING SYSTEMS

~~Passive energy dissipation systems may be used as part of the lateral-force-resisting system of a structure when special detailing is used to provide results equivalent to those obtained by use of conventional structural systems. The design criteria for structures using passive energy dissipation systems shall be consistent with the minimum requirements of an equivalent conventional structure based on these Provisions.~~

~~The design of structures using passive energy dissipation systems shall be based on rational methods of analysis, incorporating the most appropriate analysis methods, including nonlinear time-history dynamic analysis. The stiffness and damping properties of damping devices shall be accurately modeled in the analysis and shall be based on tested and independently verified data from testing of such devices. Such testing shall have subjected the devices to loads, displacements, and other imposed conditions that are consistent with design conditions.~~

~~A design review of the passive energy dissipation system and related test programs shall be performed by an independent team of registered design professionals in the appropriate disciplines and others experienced in seismic analysis methods and the theory and application of energy dissipation systems. The scope of this design review shall be consistent with that required by these Provisions for the isolation system of seismically isolated structures.~~

A13.1 GENERAL: Every *structure* with a damping system and every portion thereof shall be designed and constructed in accordance with the requirements of this appendix and the applicable requirements of Chapter 1.

> **Exception:** Motion and accelerations of seismically isolated *structures* which contain *damping devices* across the plane of isolation shall be determined in accordance with the provisions of Chapter 13. Testing and strength requirements of *damping devices* and other elements of the *damping system* shall be determined in accordance with the applicable provisions of this Appendix.

A13.2 CRITERIA SELECTION:

A13.2.1 Basis for Design: The procedure and limitations for the design of *structures* with a *damping system* shall be determined considering zoning, site characteristics, vertical acceleration, cracked section properties of concrete and masonry members, *Seismic Use Group*, configuration, structural system, and height in accordance with Sec. 5.2, except as noted below.

A13.2.2 Seismic Use Group: All portions of the *structure* shall be assigned a *Seismic Use Group* in accordance with the requirements of Sec. 1.3.

A13.2.3 Seismic Design Category: Each *structure* shall be assigned to *a Seismic Design Category* based on the *Seismic Use Group* and the design spectral response acceleration in accordance with Sec. 4.2.

> **Exception:** *Seismic Design Category A structures* with a *damping system* shall be designed using the design spectral response acceleration determined in accordance with Sec. 4.1.2.5 and the analysis methods and design provisions required for *Seismic Design Category B structures*.

A13.2.4 Configuration Requirements: *Structure* design shall consider the combination of forces that occur in the basic *seismic-force-resisting system* and the *damping system*, as defined in the following sections.

A13.2.4.1 Seismic-Force-Resisting System: *Structures* that contain a *damping system* are required to have a basic *seismic-force-resisting system* that, in each lateral direction, shall conform to one of the types indicated in Table 5.2.2.

The design of the *seismic-force-resisting system* in each direction shall comply with the requirements of Section A13.7.1 and the following:

1. The materials, detailing, construction and inspection of the *seismic-force-resisting system* shall meet all applicable requirements defined by the *Seismic Design Category*.

2. The lateral stiffness of the *seismic-force-resisting system* used to determine elastic periods and displacements shall include the modeling requirements of Sections 5.3.7 and 5.4.2.

3. The seismic base shear used for design of the *seismic-force-resisting system* shall not be less than V_{min}, where V_{min} is determined as the greater of the following values:

$$V_{min} = \frac{V}{B_{V+1}} \qquad (A13.2.4.1\text{-}1)$$

$$V_{min} = 0.75V \qquad (A13.2.4.1\text{-}2)$$

where:

V = total design shear at the *base* of the *structure* in the direction of interest, as determined using the procedure of Sec. 5.3, including Sec.5.3.3 (kip or kN), and

B_{V+I} = numerical coefficient as set forth in Table A13.3.1 for effective damping equal to the sum of viscous damping in the fundamental mode of vibration of the *structure* in the direction of interest, β_{Vm} ($m = 1$), plus inherent damping, β_I, and period of *structure* equal to T_I.

Exception: Seismic base shear used for design of the *seismic-force-resisting system* shall not be taken as less than $1.0V$, if either of the following conditions apply:

1. In the direction of interest, the *damping system* has less than two *damping devices* on each floor level, configured to resist torsion.

2. The *seismic-force-resisting system* has a vertical irregularity of Type 1b (Table 5.2.3.3) or a plan irregularity of Type 1b (Table 5.2.3.2).

4. Minimum strength requirements for *elements* of the *seismic-force-resisting-system* that are also *elements* of the *damping system* or are otherwise required to resist forces from damping devices shall meet the additional requirements of Section A13.7.3.

A13.2.4.2 Damping System: Elements of the *damping system* shall be designed to remain elastic for design loads including unreduced seismic forces of *damping devices* as required in Section A13.7.3, unless it is shown by analysis or test that inelastic response of *elements* would not adversely affect *damping system* function and inelastic response is limited in accordance with the requirements of Section A13.7.3.4.

A13.2.5 Seismic Criteria:

A13.2.5.1 Design Spectra: Spectra of the *design earthquake* and the *maximum considered earthquake* developed in accordance with Sec. 13.4.4.1 shall be used for the design and analysis of all *structures* with a *damping system*. Site-specific design spectra shall be developed and used for design of *structures* with a *damping system* if any one of the following conditions apply:

1. The *structure* is located on a Class F site or

2. The *structure* is located at a site with S_1 greater than 0.60g.

A13.2.5.2 Time Histories: Ground-motion time histories of the *design earthquake* and the *maximum considered earthquake* developed in accordance with Sec. 13.4.4.2 shall be used for design and analysis of all *structures* with a *damping system* if either of the following conditions apply:

1. The *structure* is located at a site with S_I greater than 0.60g.

2. The *damping system* is explicitly modeled and analyzed using the time history analysis method.

A13.2.6 Selection of Analysis Procedure:

A13.2.6.1 General: A structural analysis shall be made for all *structures* with a *damping system* in accordance with the requirements of this section. The structural analysis shall use linear procedures, nonlinear procedures, or a combination of linear and nonlinear procedures as described below.

The *seismic-force-resisting system* shall be designed using the procedures of either Section A13.2.6.2 or Section A13.2.6.3.

The *damping system* may be designed using the procedures of either Section A13.2.6.2 or A13.2.6.3, subject to the limitations set forth in these sections. *Damping systems* not meeting these limitations shall be designed using the nonlinear analysis methods as required in Section A13.6.

A13.2.6.2 Equivalent Lateral Force Analysis Procedure: *Structures* with a *damping system* designed using the equivalent lateral force analysis procedure of Sec. A13.4 shall be subject to the following limitations:

1. In the direction of interest, the *damping system* has at least two *damping devices* in each story, configured to resist torsion.

2. The total effective damping of the fundamental mode, β_{mD} ($m = 1$), of the *structure* in the direction of interest is not greater than 35 percent of critical.

3. The *seismic-force-resisting system* does not have a vertical irregularity of Type 1a, 1b, 2, or 3 (Table 5.2.3.3) or a plan irregularity of Type 1a or 1b (Table 5.2.3.2).

4. Floor diaphragms are rigid (Section 5.2.31).

5. The height of the *structure* above the *base* does not exceed 100 feet (30 meters).

6. Peak dynamic response of the *structure* and elements of the *damping system* are confirmed by nonlinear time history analysis, when required by Sec. A13.2.6.4.3.

A13.2.6.3 Response Spectrum Analysis: *Structures* with a *damping system* meeting the limitations of Section A13.2.6.2 may be designed using the response spectrum analysis procedure of Sec. A13.5 and *structures* not meeting the limitations of Section A13.2.6.2 shall be designed using the response spectrum analysis procedure of Sec. A13.5, subject to the following limitations:

1. In the direction of interest, the *damping system* has at least two *damping devices* in each story, configured to resist torsion,

2. The total effective damping of the fundamental mode, β_{mD} ($m = 1$), of the *structure* in the direction of interest is not greater than 35 percent of critical, and

3. Peak dynamic response of the *structure* and *elements* of the *damping system* are confirmed by nonlinear time history analysis, when required by Sec. A13.2.6.4.3.

A13.2.6.4 Nonlinear Analysis:

A13.2.6.4.1 General: Nonlinear analysis procedures of A13.6 are permitted for design of all *structures* with *damping systems* and shall be used for design of *structures* with *damping systems* not meeting linear analysis criteria of Sec. A13.2.6.3.

Nonlinear time history analysis shall be used to confirm peak dynamic response of the *structure* and elements of the *damping system* if the *structure* is located at a site with S_1 greater than 0.60g.

The nonlinear force-deflection characteristics of elements of the *seismic-force-resisting system* shall be modeled as required by Section 5.7.1 and 5.8.1. The nonlinear force-deflection characteristics of *damping devices* shall be modeled, as required, to explicitly account for device dependence on frequency, amplitude and duration of seismic loading.

A13.2.6.4.2 Nonlinear Static Analysis: *Structures* with a *damping system* designed using the nonlinear static analysis procedure of Sec. A13.6 shall be subject to the following limitations:

1. Peak dynamic response of the *structure* and elements of the *damping system* is confirmed by nonlinear time history analysis, when required by Sec. A13.2.6.4.3.

A13.2.6.4.3 Nonlinear Time History Analysis: *Structures* with a *damping system* may be designed using the nonlinear time history analysis procedure of Sec. A13.6 without limitation.

Nonlinear time history analysis shall be used to confirm peak dynamic response of the *structure* and *elements* of the *damping system* for *structures* with a *damping system* if the following conditions applies:

1. The *structure* is located at site with S_1 greater than 0.60g.

A13.3 DAMPED RESPONSE MODIFICATION:

A13.3.1 General: As required in Sections A13.4 and A13.5, response of the *structure* shall be modified for the effects of the *damping system* using coefficients prescribed in Table A13.3.1.

Table A13.3.1 Damping Coefficient, B_{V+I}, B_{1D}, B_R, B_{1M}, B_{mD} or B_{mM}

Effective Damping, β	Period of the *Structure* $\geq T_s/5$
≤ 2%	0.8
5%	1.0
10%	1.2
20%	1.5
30%	1.8
40%	2.1
50%	2.4
60%	2.7
70%	3.0
80%	3.3
90%	3.6
≥ 100%	4.0

[1]The damping coefficient is equal to 1.0 at *a period* of the *structure* equal to 0 second for all values of effective damping. Interpolation may be used for intermediate values of effective damping at periods of the *structure* between 0 second and $T_s/5$ seconds.

A13.3.2 Effective Damping: The effective damping at the *design displacement*, β_{mD}, and at the *maximum displacement*, β_{mM}, of the mth mode of vibration of the *structure* in the direction under consideration shall be calculated as follows:

$$\beta_{mD} = \beta_I + \beta_{Vm}\sqrt{\mu_D} + \beta_{HD} \tag{A13.3.2-1}$$

$$\beta_{mM} = \beta_I + \beta_{Vm}\sqrt{\mu_M} + \beta_{HM} \qquad \text{(A13.3.2-2)}$$

where:

β_{HD} = component of effective damping of the *structure* in the direction of interest due to post-yield hysteretic behavior of the *seismic-force-resisting system* and elements of the *damping system* at effective ductility demand, μ_D,

β_{HM} = component of effective damping of the *structure* in the direction of interest due to post-yield hysteretic behavior of the *seismic-force-resisting system* and elements of the *damping system* at effective ductility demand, μ_M,

β_I = component of effective damping of the *structure* due to the inherent dissipation of energy by elements of the *structure,* at or just below the effective yield displacement of the *seismic-force-resisting system*,

β_{Vm} = component of effective damping of the mth mode of vibration of the *structure* in the direction of interest due to viscous dissipation of energy by the *damping system*, at or just below the effective yield displacement of the *seismic-force-resisting system*,

μ_D = effective ductility demand on the *seismic-force-resisting system* in the direction of interest due to the *design earthquake*, and

μ_M = effective ductility demand on the *seismic-force-resisting system* in the direction of interest due to the *maximum considered earthquake*.

Unless analysis or test data supports other values, the effective ductility demand of higher modes of vibration in the direction of interest shall be taken as 1.0.

A13.3.2.1 Inherent Damping: Inherent damping, β_I, shall be based on the material type, configuration and behavior of the *structure* and nonstructural components responding dynamically at or just below yield of the *seismic-force-resisting system*. Unless analysis or test data supports other values, inherent damping shall be taken as not greater than 5% of critical for all modes of vibration.

A13.3.2.2 Hysteretic Damping: Hysteretic damping of the *seismic-force-resisting system* and elements of the *damping system* shall be based either on test or analysis, or in accordance with the following equations:

$$\beta_{HD} = q_H \left(0.64 - \beta_I\right)\left(1 - \frac{1}{\mu_D}\right) \qquad \text{(A13.3.2.2-1)}$$

$$\beta_{HM} = q_H \left(0.64 - \beta_I\right)\left(1 - \frac{1}{\mu_M}\right) \qquad \text{(A13.3.2.2-2)}$$

where:

q_H = hysteresis loop adjustment factor, as defined in Sec. A13.3.3,

μ_D = effective ductility demand on the *seismic-force-resisting system* in the direction of interest due to the *design earthquake*, as defined in Sec. A.13.3.4, and

μ_M = effective ductility demand on the *seismic-force-resisting system* in the direction of interest due to the *maximum considered earthquake*, as defined in Sec. A13.3.4.

Unless analysis or test data supports other values, the hysteretic damping of higher modes of vibration in the direction of interest shall be taken as zero.

A13.3.2.3 Viscous Damping: Viscous damping of the mth mode of vibration of the *structure*, β_{Vm}, shall be calculated as follows:

$$\beta_{Vm} = \frac{\sum_j W_{mj}}{4\pi W_m}$$

(A13.3.2.3-1)

$$W_m = \frac{1}{2}\sum_i F_{im}\delta_{im}$$

(A13.3.2.3-2)

where:

W_{mj} = work done by j^{th} damping device in one complete cycle of dynamic response corresponding to the mth mode of vibration of the *structure* in the direction of interest at modal displacements, δ_{im},

W_m = maximum strain energy in the mth mode of vibration of the *structure* in the direction of interest at modal displacements, δ_{im},

F_{im} = m^{th} mode inertial force at Level i (or mass point),

δ_{im} = deflection of Level i (or mass point) in the mth mode of vibration at the center of rigidity of the *structure* in the direction under consideration.

Viscous modal damping of *displacement-dependent damping devices* shall be based on a response amplitude equal to the effective yield displacement of the *structure*.

The calculation of the work done by individual *damping devices* shall consider orientation and participation of each device with respect to the mode of vibration of interest. The work done by individual *damping devices* shall be reduced as required to account for the flexibility of *elements*, including pins, bolts, gusset plates, brace extensions, and other components that connect *damping devices* to other *elements* of the *structure*.

A13.3.3 Hysteresis Loop Adjustment Factor: Hysteretic damping of the *seismic-force-resisting* system and elements of the *damping system* shall consider pinching and other effects that reduce the area of the hysteresis loop during repeated cycles of earthquake demand. Unless

analysis or test data support other values, the fraction of full hysteretic loop area of the *seismic-force-resisting system* used for design shall be taken as equal to the factor, q_H, as defined below:

$$q_H = 0.67 \frac{T_S}{T_I} \qquad \text{(A13.3.3-1)}$$

where:

T_s = period, in seconds, defined by the ratio, S_{DI}/S_{DS}

T_I = period, in seconds of the fundamental mode of vibration of the *structure* in the direction of the interest

The value of q_H shall not be taken as greater than 1.0, and need not be taken as less than 0.5.

A13.3.4 Effective Ductility Demand: The effective ductility demand of *seismic-force-resisting system* due to the *design earthquake*, μ_D, and due to the *maximum considered earthquake*, μ_M, shall be calculated as the ratio of the fundamental mode displacement, D_{ID} or D_{IM}, to effective yield displacement, D_Y:

$$\mu_D = \frac{D_{ID}}{D_Y} \geq 1.0 \qquad \text{(A13.3.4-1)}$$

$$\mu_M = \frac{D_{IM}}{D_Y} \geq 1.0 \qquad \text{(A13.3.4-2)}$$

$$D_Y = \left(\frac{g}{4\pi^2}\right)\left(\frac{\Omega_o C_d}{R}\right)\Gamma_I C_{SI} T_I^2 \qquad \text{(A13.3.4-3)}$$

where:

D_{ID} = fundamental mode *design displacement* at the center of rigidity of the roof level of the *structure* in the direction under consideration, Sec. A13.4.4.3 (in. or mm),

D_{IM} = fundamental mode *maximum displacement* at the center of rigidity of the roof level of *structure* in the direction under consideration, Sec. A13.4.4.6 (in. or mm),

D_Y = displacement at the center of rigidity of the roof level of the *structure* at the effective yield point of the *seismic-force-resisting system*, Sec. A13.3.4 (in. or mm),

R = response modification factor from Table 5.2.2,

C_d = deflection amplification factor from Table 5.2.2,

Ω_o = system overstrength factor from Table 5.2.2,

Γ_I =   participation factor of the fundamental mode of vibration of the *structure* in the direction of interest, Sec. A13.4.3.3 or Sec. A13.5.3.3 ($m = 1$),

C_{SI} =   *seismic response coefficient* (dimensionless) of the fundamental mode of vibration of the *structure* in the direction of interest, Sec. A13.4.3.4 or Sec. A13.5.3.4 ($m = 1$), and

T_I =   period, in seconds, of the fundamental mode of vibration of the *structure* in the direction of interest.

Design earthquake ductility demand, μ_D, shall not exceed the maximum value of effective ductility demand, μ_{max}, given in section A13.3.5.

A13.3.5 Maximum Effective Ductility Demand: For determination of the hysteresis loop adjustment factor, hysteretic damping and other parameters, ductility demand used for design of the *structure* shall not exceed the maximum value of effective ductility demand, μ_{max}, as defined below:

For $T_I < T_S$:

$$\mu_{max} = \frac{1}{2}\left(\left(\frac{R}{\Omega_o I}\right)^2 + 1\right)$$

(A13.3.5-1)

For $T_{ID} \geq T_S$:

$$\mu_{max} = \frac{R}{\Omega_o I}$$

(A13.3.5-2)

where:

I =   the occupancy importance factor determined in accordance with Sec. 1.4.

T_{ID} =   effective period, in seconds, of the fundamental mode of vibration of the *structure* at the *design displacement* in the direction under consideration.

For periods: $T_I \leq T_S \leq T_{ID}$, interpolation shall be used to determine μ_{max}.

A13.4 EQUIVALENT LATERAL FORCE ANALYSIS PROCEDURE:

A13.4.1 General: This section provides required minimum standards for equivalent lateral force analysis of *structures* with a *damping system*. For purposes of analysis, the *structure* is considered to be fixed at the *base*. See Sec. A13.2.6 for limitations on the use of this procedure.

Seismic base shear and lateral forces at floors used for design of the *seismic-force-resisting system* shall be based on the procedures of Section A13.4.3. Seismic forces, displacements and velocities used for design of the *damping system* shall be based on the procedures of Section A13.4.4.

The load combinations and acceptance criteria of Section A13.7 shall be used to check design responses of *seismic-force-resisting* and *damping systems*, respectively.

A13.4.2 Modeling Requirements: *Elements* of the *seismic-force-resisting system* shall be modeled in a manner consistent with the requirements of Section 5.3.

Elements of the *damping system* shall be modeled as required to determine design forces transferred from *damping devices* to both the ground and the *seismic-force-resisting system*. The effective stiffness of *velocity-dependent damping devices* shall be modeled.

Damping devices need not be explicitly modeled provided effective damping is calculated in accordance with the procedures of Section A13.3 and used to modify response as required in Sections A13.4.3 and A13.4.4.

The stiffness and damping properties of the *damping devices* used in the models shall be based on or verified by testing of the *damping devices* as specified in Sec. A13.10.

A13.4.3 Seismic-Force-Resisting-System Design Response:

A13.4.3.1 Seismic Base Shear: The seismic *base shear*, V, of the *seismic-force-resisting system* in a given direction shall be determined as the combination of the two modal components, V_I and V_R, in accordance with the following equation:

$$V = \sqrt{V_I^2 + V_R^2} \geq V_{min} \qquad (A13.4.3.1\text{-}1)$$

where:

V_I = design value of the seismic *base shear* of the fundamental mode in a given direction of response (kip or kN),

V_R = design value of the seismic *base shear* of the residual mode in a given direction (kip or kN), and

V_{min} = minimum allowable value of *base shear* permitted for design of the *seismic-force-resisting-system* of the *structure* in direction of the interest (kip or kN).

A13.4.3.2 Fundamental Mode Base Shear: Fundamental mode *base shear*, V_I, shall be determined in accordance with the following equation:

$$V_I = C_{SI}\overline{W_I} \qquad (A13.4.3.2\text{-}1)$$

where:

$\overline{W_I}$ = the effective fundamental mode *gravity load* including portions of the *live load* as defined by Eq. 5.4.5-2 for $m = 1$ (kip or kN).

A13.4.3.3 Fundamental Mode Properties: Fundamental mode shape, ϕ_{iI}, and participation factor, Γ_I, shall be determined by either dynamic analysis of elastic structural properties and deformational characteristics of the resisting elements or in accordance with the following equations:

$$\phi_{iI} = \frac{h_i}{h_r} \qquad (A13.4.3.3\text{-}1)$$

$$\Gamma_I = \frac{\overline{W_I}}{\sum_{i=1}^{n} w_i \phi_{iI}}$$

(A13.4.3.3-2)

where:

h_i = the height of the *structure* above the *base* to Level i (ft or m),

h_r = the height of the *structure* above the *base* to the roof level (ft or m),

w_i = the portion of the total *gravity load*, W, located or assigned to Level i.

The fundamental period, T_I, shall be determined either by dynamic analysis of elastic structural properties and deformational characteristics of the resisting *elements*, or in accordance with the following equation:

$$T_I = 2\pi \sqrt{\frac{\sum_{i=1}^{n} w_i \delta_i^2}{g \sum_{i=1}^{n} f_i \delta_i}}$$

(A13.4.3.3-3)

where:

f_i = lateral force at Level i of the *structure* distributed in accordance with Formula 5.3.4-2, and

δ_i = elastic deflection at Level i of the *structure* due to applied lateral forces f_i.

A13.4.3.4 Fundamental Mode Seismic Response Coefficient: The fundamental mode seismic response coefficient, C_{SI}, shall be determined in accordance with the following equations:

For $T_{ID} < T_S$:

$$C_{SI} = \left(\frac{R}{C_d}\right) \frac{S_{DS}}{\Omega_o B_{ID}}$$

(A13.4.3.4-1)

For $T_{ID} \geq T_S$:

$$C_{SI} = \left(\frac{R}{C_d}\right) \frac{S_{DI}}{T_{ID}(\Omega_o B_{ID})}$$

(A13.4.3.4-2)

where:

S_{DS} = the design spectral response acceleration in the short period range as determined from Sec. 4.1.2.5,

S_{D1} = the design spectral response acceleration at a period of 1 second as determined from Sec. 4.1.2.5,

B_{1D} = numerical coefficient as set forth in Table A13.3.1 for effective damping equal to β_{mD} ($m = 1$) and period of the *structure* equal to T_{1D},

A13.4.3.5 Effective Fundamental Mode Period Determination: The effective fundamental mode period at the *design earthquake*, T_{1D}, and at the *maximum considered earthquake*, T_{1M}, shall be based either on explicit consideration of the post-yield force deflection characteristics of the *structure* or in accordance with the following equations:

$$T_{1D} = T_1 \sqrt{\mu_D} \tag{A13.4.3.5-1}$$

$$T_{1M} = T_1 \sqrt{\mu_M} \tag{A13.4.3.5-2}$$

where:

T_{1M} = effective period, in seconds, of the fundamental mode of vibration of the *structure* at the *maximum displacement* in the direction under consideration.

A13.4.3.6 Residual Mode Base Shear: Residual mode *base shear*, V_R, shall be determined in accordance with the following equation:

$$V_R = C_{SR} \overline{W_R} \tag{A13.4.3.6-1}$$

where:

C_{SR} = the residual mode *seismic response coefficient* as determined in Sec. A13.4.3.8, and

$\overline{W_R}$ = the effective residual mode *gravity load* of the *structure* determined in accordance with Eq. A13.4.3.7-3 (kip or kN).

A13.4.3.7 Residual Mode Properties: Residual mode shape, ϕ_{iR}, participation factor, Γ_R, effective gravity load of the *structure*, $\overline{W_R}$, and effective period, T_R, shall be determined in accordance with the following equations:

$$\phi_{iR} = \frac{1 - \Gamma_1 \phi_{i1}}{1 - \Gamma_1} \tag{A13.4.3.7-1}$$

$$\Gamma_R = 1 - \Gamma_1 \tag{A13.4.3.7-2}$$

$$\overline{W_R} = W - \overline{W_1} \tag{A13.4.3.7-3}$$

$$T_R = 0.4T_1 \qquad\qquad\qquad \text{(A13.4.3.7-4)}$$

A13.4.3.8 Residual Mode Seismic Response Coefficient: The residual mode seismic response coefficient, C_{SR}, shall be determined in accordance with the following equation:

$$C_{SR} = \left(\frac{R}{C_d}\right)\frac{S_{DS}}{\Omega_o B_R} \qquad\qquad \text{(A13.4.3.8-1)}$$

where:

B_R =   Numerical coefficient as set forth in Table A13.3.1 for effective damping equal to β_R, and period of the *structure* equal to T_R.

A13.4.3.9 Design Lateral Force: Design lateral force in *elements* of the *seismic-force-resisting system* at Level *i* due to fundamental mode response, F_{i1}, and residual mode response, F_{iR}, of the *structure* in the direction of interest shall be determined in accordance with the following equations:

$$F_{i1} = w_i\phi_{i1}\frac{\Gamma_1}{\overline{W_1}}V_1 \qquad\qquad \text{(A13.4.3.9-1)}$$

$$F_{iR} = w_i\phi_{iR}\frac{\Gamma_R}{\overline{W_R}}V_R \qquad\qquad \text{(A13.4.3.9-2)}$$

Design forces in *elements* of the *seismic-force-resisting system* shall be determined as the square-root-sum-of-squares of the forces due to fundamental and residual modes.

A13.4.4 Damping System Design Response:

A13.4.4.1 General: Design forces in *damping devices* and other elements of the *damping system* shall be determined on the basis of the floor deflection, story drift and story velocity response parameters described in the following sections.

Displacements and velocities used to determine maximum forces in *damping devices* at each story shall account for the angle of orientation from horizontal and consider the effects of increased response due to torsion required for design of the *seismic-force-resisting system*.

Floor deflections at Level *i*, δ_{iD} and δ_{iM}, design story drifts, Δ_D and Δ_M, and design story velocities, ∇_D and ∇_M, shall be calculated for both the *design earthquake* and the *maximum considered earthquake*, respectively, in accordance with the following sections.

A13.4.4.2 Design Earthquake Floor Deflection: Fundamental and residual mode deflections due to the *design earthquake*, δ_{i1D} and δ_{iRD} (in. or mm), at the center of rigidity of Level *i* of the *structure* in the direction of interest shall be determined in accordance with the following equations:

$$\delta_{i1D} = D_{1D}\phi_{i1} \qquad\qquad \text{(A13.4.4.2-1)}$$

$$\delta_{iRD} = D_{RD}\phi_{iR} \qquad \text{(A13.4.4.2-2)}$$

where:

D_{RD} = Residual mode *design displacement* at the center of rigidity of the roof level of the *structure* in the direction under consideration, Sec. A13.4.4.3 (in or mm).

The total *design earthquake* deflection at each floor of the *structure* in the direction of interest shall be calculated as the square-root-sum-of-squares of fundamental and residual mode floor deflections.

A13.4.4.3 Design Earthquake Roof Displacement: Fundamental and residual mode displacements due to the *design earthquake*, D_{ID} and D_{IR} (in.or mm) at the center of rigidity of the roof level of the *structure* in the direction of interest shall be determined in accordance with the following equations:

$$D_{ID} = \left(\frac{g}{4\pi^2}\right)\Gamma_I \frac{S_{DI}T_{ID}}{B_{ID}} \le \left(\frac{g}{4\pi^2}\right)\Gamma_1 \frac{S_{DS}T_{ID}^2}{B_{ID}} \qquad \text{(A13.4.4.3-1)}$$

$$D_{RD} = \left(\frac{g}{4\pi^2}\right)\Gamma_R \frac{S_{DI}T_R}{B_R} \le \left(\frac{g}{4\pi^2}\right)\Gamma_R \frac{S_{DS}T_R^2}{B_R} \qquad \text{(A13.4.4.3-2)}$$

A13.4.4.4 Design Earthquake Story Drift: *Design earthquake* story drift, Δ_D, of the *structure* in the direction of interest shall be calculated in accordance with the following equation:

$$\Delta_D = \sqrt{\Delta_{ID}^2 + \Delta_{RD}^2} \qquad \text{(A13.4.4.4-1)}$$

where:

Δ_{ID} = *design earthquake* story drift due to the fundamental mode of vibration of the *structure* in the direction of interest (in. or mm), and

Δ_{RD} = *design earthquake* story drift due to the residual mode of vibration of the *structure* in the direction of interest (in. or mm).

Modal *design earthquake* story drifts, Δ_{ID} and Δ_{IR}, shall be determined in accordance with Sec. 5.3.7.1 using the floor deflections of Sec. A13.4.4.2.

A13.4.4.5 Design Earthquake Story Velocity: *Design earthquake* story velocity, V_D, of the *structure* in the direction of interest shall be calculated in accordance with the following equations:

$$V_D = \sqrt{V_{ID}^2 + V_{RD}^2} \qquad \text{(A13.4.4.5-1)}$$

$$V_{ID} = 2\pi \frac{\Delta_{ID}}{T_{ID}} \qquad \text{(A13.4.4.5-2)}$$

$$V_{RD} = 2\pi \frac{\Delta_{RD}}{T_R}$$
(A13.4.4.5-3)

where:

∇_{ID} = *design earthquake* story velocity due to the fundamental mode of vibration of the *structure* in the direction of interest (in/sec or mm/sec), and

∇_{RD} = *design earthquake* story velocity due to the residual mode of vibration of the *structure* in the direction of interest (in/sec or mm/sec).

A13.4.4.6 Maximum Earthquake Response: Total and modal *maximum earthquake* floor deflections at Level *i*, design story drift values and design story velocity values shall be based on the formulas of Sections A13.4.2, A13.4.4 and A13.4.5, respectively, except *design earthquake* roof displacements shall be replaced by *maximum earthquake* roof displacements. *Maximum earthquake* roof displacements shall be calculated in accordance with the following equations:

$$D_{IM} = \left(\frac{g}{4\pi^2}\right)\Gamma_1 \frac{S_{M1}T_{IM}}{B_{IM}} \leq \left(\frac{g}{4\pi^2}\right)\Gamma_1 \frac{S_{MS}T_{IM}^2}{B_{IM}}$$
(A13.4.4.6-1)

$$D_{RM} = \left(\frac{g}{4\pi^2}\right)\Gamma_R \frac{S_{M1}T_R}{B_R} \leq \left(\frac{g}{4\pi^2}\right)\Gamma_R \frac{S_{MS}T_R^2}{B_R}$$
(A13.4.4.6-2)

where:

S_{M1} = the *maximum considered earthquake*, 5 percent damped, spectral response acceleration at a period of 1 second adjusted for *site class* effects as defined in Sec.4.1.2.

S_{MS} = the *maximum considered earthquake*, 5 percent damped, spectral response acceleration at short periods adjusted for *site class* effects as defined in Sec. 4.1.2.

B_{IM} = Numerical coefficient as set forth in Table A13.3.1 for effective damping equal to β_{mM} (m = 1) and period of *structure* equal to T_{IM}.

A13.5 RESPONSE SPECTRUM ANALYSIS PROCEDURE

A13.5.1 General: This section provides required standards for response spectrum analysis of *structures* with a *damping system*. See Sec. A13.2.6 for limitations on the use of this procedure.

Seismic *base shear* and lateral forces at floors used for design of the *seismic-force-resisting system* shall be based on the procedures of Sec. A13.3.2. Seismic forces, displacements and velocities used for design of the *damping system* shall be based on the procedures of Section A13.3.

The load combinations and acceptance criteria of Sec. A13.7 shall be used to check design responses of *seismic-force-resisting system* and the *damping system*.

A13.5.2 Modeling and Analysis Requirements:

A13.5.2.1 General: A mathematical model of the *seismic-force-resisting system* and *damping system* shall be constructed that represents the spatial distribution of mass, stiffness and damping throughout the *structure*. The model and analysis shall conform to the requirements of Sec. 5.4.2, Sec. 5.4.3, and Sec.5.4.4 for the *seismic-force-resisting system* and to the requirements of Sec. A13.5.2.2 for the *damping system*. The stiffness and damping properties of the *damping devices* used in the models shall be based on or verified by testing of the *damping devices* as specified in Sec. A13.10.

A13.5.2.2 Damping System: The elastic stiffness of elements of the *damping system* other than *damping devices* shall be explicitly modeled. Stiffness of *damping devices* shall be modeled depending on *damping device* type:

1. *Displacement-Dependent Damping Devices:* Displacement-dependent *damping devices* shall be modeled with an effective stiffness that represents *damping device* force at the response displacement of interest (e.g., design story drift). Alternatively, the stiffness of hysteretic and friction *damping devices* may be excluded from response spectrum analysis provided design forces in *displacement-dependent damping devices*, Q_{DSD}, are applied to the model as external loads (Sec. A13.7.3.2).

2. *Velocity-Dependent Damping Devices:* Velocity-dependent *damping devices* that have a stiffness component (e.g., visco-elastic damping devices) shall be modeled with an effective stiffness corresponding to the amplitude and frequency of interest.

A13.5.3 Seismic-Force-Resisting-System Design Response:

A13.5.3.1 Seismic Base Shear: The seismic *base shear*, V, of the *structure* in a given direction shall be determined as the combination of modal components, V_m, subject to the limits of the following equation:

$$V \geq V_{min} \qquad (A13.5.3.1-1)$$

The seismic *base shear*, V, of the *structure* shall be determined by the square root sum of the squares or complete quadratic combination of modal *base shear* components, V_m.

A13.5.3.2 Modal Base Shear: Modal *base shear* of the mth mode of vibration, V_m, of the *structure* in the direction of interest shall be determined in accordance with the following equation:

$$V_m = C_{Sm} \overline{W_m} \qquad (A13.5.3.2-1)$$

where:

C_{Sm} = *seismic response coefficient* (dimensionless) of the mth mode of vibration of the *structure* in the direction of interest, Sec. A13.5.3.4 ($m = 1$) or Sec. A13.5.3.6 ($m > 1$), and

$\overline{W_m}$ = the effective gravity load of the mth mode of vibration of the *structure* determined in accordance with Eq. 5.4.5-2 (kip or kN).

A13.5.3.3 Modal Participation Factor: The modal participation factor of the mth mode of vibration, Γ_m, of the *structure* in the direction of interest shall be determined in accordance with the following equation:

$$\Gamma_m = \frac{\overline{W}_m}{\sum_{i=1}^{n} w_i \phi_{im}}$$

(A13.5.3.3-1)

where:

ϕ_{im} = displacement amplitude at the ith level of the *structure* for the fixed base condition in the mth mode of vibration in the direction of interest, normalized to unity at the roof level.

A13.5.3.4 Fundamental Mode Seismic Response Coefficient: The fundamental mode ($m = 1$) *seismic response coefficient*, C_{S1}, in the direction of interest shall be determined in accordance with the following equations:

For $T_{1D} < T_S$:

$$C_{S1} = \left(\frac{R}{C_d}\right) \frac{S_{DS}}{\Omega_o B_{1D}}$$

(A13.5.3.4-1)

For $T_{1D} \geq T_S$:

$$C_{S1} = \left(\frac{R}{C_d}\right) \frac{S_{D1}}{T_{1D}\left(\Omega_o B_{1D}\right)}$$

(A13.5.3.4-2)

A13.5.3.5 Effective Fundamental Mode Period Determination: The effective fundamental mode ($m = 1$) period at the *design earthquake*, T_{1D}, and at the *maximum considered earthquake*, T_{1M}, shall be based either on explicit consideration of the post-yield nonlinear force deflection characteristics of the *structure* or determined in accordance with the following equations:

$$T_{1D} = T_1 \sqrt{\mu_D}$$

(A13.4.3.5-1)

$$T_{1M} = T_1 \sqrt{\mu_M}$$

(A13.4.3.5-2)

A13.5.3.6 Higher Mode Seismic Response Coefficient: Higher mode ($m > 1$) seismic response coefficient, C_{Sm}, of the mth mode of vibration ($m > 1$) of the *structure* in the direction of interest shall be determined in accordance with the following equations:

For $T_m < T_S$:

$$C_{Sm} = \left(\frac{R}{C_d}\right) \frac{S_{DS}}{\Omega_o B_{mD}}$$

(A13.5.3.6-1)

For $T_m \geq T_S$:
$$C_{Sm} = \left(\frac{R}{C_d}\right) \frac{S_{D1}}{T_m(\Omega_o B_{mD})}$$

(A13.5.3.6-2)

where:

T_m = period, in seconds, of the mth mode of vibration of the *structure* in the direction under consideration,

B_{mD} = numerical coefficient as set forth in Table A13.3.1 for effective damping equal to β_{mD} and period of the *structure* equal to T_m.

A13.5.3.7 Design Lateral Force: Design lateral force at Level i due to m^{th} mode of vibration, F_{im}, of the *structure* in the direction of interest shall be determined in accordance with the following equation:

$$F_{im} = w_i \phi_{im} \frac{\Gamma_m}{\overline{W}_m} V_m$$

(A13.5.3.7-1)

Design forces in elements of the *seismic-force-resisting system* shall be determined by the square root sum of squares or complete quadratic combination of modal design forces.

A13.5.4 Damping System Design Response:

A13.5.4.1 General: Design forces in *damping devices* and other elements of the *damping system* shall be determined on the basis of the floor deflection, story drift and story velocity response parameters described in the following sections.

Displacements and velocities used to determine maximum forces in *damping devices* at each story shall account for the angle of orientation from horizontal and consider the effects of increased response due to torsion required for design of the *seismic-force-resisting system*.

Floor deflections at Level i, δ_{iD} and δ_{iM}, design story drifts, Δ_D and Δ_M, and design story velocities, ∇_D and ∇_M, shall be calculated for both the *design earthquake* and the *maximum considered earthquake*, respectively, in accordance with the following sections.

A13.5.4.2 Design Earthquake Floor Deflection: The deflection of *structure* due to the *design earthquake* at Level i in the mth mode of vibration, δ_{imD} (in. or mm), of the *structure* in the direction of interest shall be determined in accordance with the following equation:

$$\delta_{imD} = D_{mD} \phi_{im}$$

(A13.5.4.2-1)

The total *design earthquake* deflection at each floor of the *structure* shall be calculated by the square root sum of squares or complete quadratic combination of modal *design earthquake* deflections.

A13.5.4.3 Design Earthquake Roof Displacement: Fundamental ($m = 1$) and higher mode ($m > 1$) roof displacements due to the *design earthquake*, D_{1D} and D_{mD} (in. or mm), of the *structure* in the direction of interest shall be determined in accordance with the following equations:

For $m = 1$:
$$D_{ID} = \left(\frac{g}{4\pi^2}\right)\Gamma_1\frac{S_{DI}T_{ID}}{B_{ID}} \leq \left(\frac{g}{4\pi^2}\right)\Gamma_1\frac{S_{DS}T^2_{ID}}{B_{ID}} \qquad \text{(A13.5.4.3-1)}$$

For $m > 1$:
$$D_{mD} = \left(\frac{g}{4\pi^2}\right)\Gamma_m\frac{S_{DI}T_m}{B_{mD}} \leq \left(\frac{g}{4\pi^2}\right)\Gamma_m\frac{S_{DS}T^2_m}{B_{mD}} \qquad \text{(A13.5.4.3-2)}$$

A13.5.4.4 Design Earthquake Story Drift: *Design earthquake* story drift of the fundamental mode, Δ_{ID}, and higher modes, Δ_{mD} ($m > 1$), of the *structure* in the direction of interest shall be calculated in accordance with Section 5.3.7.1 using modal roof displacements of Section A13.5.4.3.

Total *design earthquake* story drift, Δ_D (in. or mm), shall be determined by the square root of the sum of squares or complete quadratic combination of modal *design earthquake* drifts.

A13.5.4.5 Design Earthquake Story Velocity: *Design earthquake* story velocity of the fundamental mode, ∇_{ID}, and higher modes, ∇_{mD} ($m > 1$), of the *structure* in the direction of interest shall be calculated in accordance with the following equations:

For $m = 1$:
$$\nabla_{ID} = 2\pi\frac{\Delta_{ID}}{T_{ID}} \qquad \text{(A13.5.4.5-1)}$$

For $m > 1$:
$$\nabla_{mD} = 2\pi\frac{\Delta_{mD}}{T_m} \qquad \text{(A13.5.4.5-1)}$$

Total *design earthquake* story velocity, ∇_D (in/sec or mm/sec), shall be determined by the square root of the sum of squares or complete quadratic combination of modal *design earthquake* velocities.

A13.5.4.6 Maximum Earthquake Response: Total modal floor deflection at Level i, design story drift values and design story velocity values shall be based on the formulas of Sections A13.5.4.2, A13.5.4.4 and A13.5.4.5, respectively, except *design earthquake* roof displacement shall be replaced by *maximum earthquake* roof displacement. *Maximum earthquake* roof displacement of the *structure* in the direction of interest shall be calculated in accordance with the following equations:

For $m = 1$:
$$D_{IM} = \left(\frac{g}{4\pi^2}\right)\Gamma_1\frac{S_{MI}T_{IM}}{B_{IM}} \leq \left(\frac{g}{4\pi^2}\right)\Gamma_1\frac{S_{MS}T^2_{IM}}{B_{IM}} \qquad \text{(A13.5.4.6-1)}$$

For $m > 1$:
$$D_{mM} = \left(\frac{g}{4\pi^2}\right)\Gamma_m\frac{S_{MI}T_m}{B_{mM}} \leq \left(\frac{g}{4\pi^2}\right)\Gamma_m\frac{S_{MS}T^2_m}{B_{mM}} \qquad \text{(A13.5.4.6-2)}$$

where:

B_{mM} = numerical coefficient as set forth in Table A13.3.1 for effective damping equal to β_{mM} and period of the *structure* equal to T_m.

A13.6 NONLINEAR ANALYSIS PROCEDURES

A13.6.1 General: The nonlinear procedures provided in Section A13.6 supplement the nonlinear procedures of Sections 5.7 and 5.8 to accommodate the use of *damping systems*. The stiffness and damping properties of the *damping devices* used in the models shall be based on or verified by testing of the *damping devices* as specified in Sec. A13.10.

A13.6.2. Nonlinear Static Analysis: The nonlinear modeling described in Section 5.7.1 and the lateral loads described in Section 5.7.2 shall be applied to the *seismic-force-resisting system*. The resulting force-displacement curve shall be used in lieu of the assumed effective yield displacement, D_Y, of Equation A13.3.4-3 to calculate the effective ductility demand due to the *design earthquake*, μ_D, and due to the *maximum considered earthquake*, μ_M, in Equations A13.3.4-1 and A13.3.4-2. The value of (R/C_d) shall be taken as 1.0 in Equations A13.4.3.4-1, A13.4.3.4-2 and A13.4.3.8-1 for the Equivalent Lateral Force Analysis Procedure, and in Equations A13.5.3.4-1, A13.5.3.4-2, A13.5.3.6-1, and A13.5.3.6-2 of the Response Spectrum Analysis Procedure.

A13.6.3 Nonlinear Response History Analysis: A nonlinear response history (time history) analysis shall utilize a mathematical model of the *structure* and the *damping system* as provided in Section 5.8 and this section. The model shall directly account for the nonlinear hysteretic behavior of *elements* of the *structure* and the *damping devices* to determine its response, through methods of numerical integration, to suites of ground motions compatible with the design response spectrum for the site.

The analysis shall be performed in accordance with Section 5.8 together with the requirements of this section.

A13.6.3.1 Damping Device Modeling: Mathematical models of *displacement-dependent damping devices* shall include the hysteretic behavior of the devices consistent with test data and accounting for all significant changes in strength, stiffness, and hysteretic loop shape. Mathematical models of *velocity-dependent damping devices* shall include the velocity coefficient consistent with test data. If this coefficient changes with time and/or temperature, such behavior shall be modeled explicitly. The elements of *damping devices* connecting damper units to the *structure* shall be included in the model.

> **Exception:** If the properties of the *damping devices* are expected to change during the duration of the time history analysis, the dynamic response may be enveloped by the upper and lower limits of device properties. All these limit cases for variable device properties must satisfy the same conditions as if the time dependent behavior of the devices were explicitly modeled.

A13.6.3.2 Response Parameters: In addition to the response parameters given in Section 5.8.3, the *design earthquake* and *maximum considered earthquake* displacements, velocities, and forces of the *damping devices* shall be determined.

A13.7 SEISMIC LOAD CONDITIONS AND ACCEPTANCE CRITERIA:

A13.7.1 General: Design forces and displacements determined in accordance with the equivalent lateral force analysis procedures of Section A13.4 or the response spectrum analysis procedure of Section 13.5 shall be checked using the strength design criteria of these *Provisions* and the seismic loading conditions of the following sections.

A13.7.2 Seismic-Force-Resisting System: The *seismic-force-resisting system* shall meet the design provisions of Sec. 5.2.2 using seismic *base shear* and design forces determined in accordance with Section A13.4.3 or Sec A13.5.3.

The design earthquake story drift, Δ_D, as determined in either Sec. A13.4.4.4 or A13.5.4.4 shall not exceed (R/C_d) times the allowable story drift, as obtained from Table 5.2.8, considering the effects of torsion as required in Section 5.2.8.

A13.7.3 Damping System: The *damping system* shall meet the provisions of Section 5.2.2 for seismic design forces determined in accordance with Sec. A13.7.3.1 and the seismic loading conditions of Section A13.7.3.2 and Section A13.5.4.

A13.7.3.1 Modal Damping System Design Forces: Modal *damping system* design forces shall be calculated on the basis of the type of *damping devices,* and the modal design story displacements and modal design story velocities determined in accordance with either Section A13.4.4 or Section A13.5.4.

> **Exception:** Modal design story displacements and velocities determined in accordance with either Section A13.4.4 or Section A13.5.4 shall be increased as required to envelop total design story displacements and velocities determined in accordance with Section A13.6, when Section A13.2.6.4.3 requires peak response to be confirmed by time history analysis.

> 1.   *Displacement-Dependent Damping Devices:* Design seismic force in *displacement-dependent damping devices* shall be based on the maximum force in the device at displacements up to and including the *design earthquake* story drift, Δ_D.

> 2.   *Velocity-Dependent Damping Devices:* Design seismic force in each mode of vibration of *velocity-dependent damping devices* shall be based on the maximum force in the device at velocities up to and including the *design earthquake* story velocity of the mode of interest.

Displacements and velocities used to determine design forces in *damping devices* at each story shall account for the angle of orientation from horizontal and consider the effects of increased floor response due to torsional motions.

A13.7.3.2 Seismic Load Conditions and Combination of Modal Responses: Seismic design force, Q_E, in each element of the *damping system* due to horizontal earthquake load shall be taken as the maximum force of the following three loading conditions:

1. Stage of Maximum Displacement: Seismic design force at the stage of maximum displacement shall be calculated in accordance with the following equation:

$$Q_E = \Omega_o \sqrt{\sum_m \left(Q_{mSFRS}\right)^2} \pm Q_{DSD} \qquad \text{(A13.7.3.2-1)}$$

where:

Q_{mSFRS} = Force in an element of the *damping system* equal to the design seismic force of the mth mode of vibration of the *seismic-force-resisting system* in the direction of interest.

Q_{DSD} = Force in an element of the *damping system* required to resist design seismic forces of *displacement-dependent damping devices*.

Seismic forces in elements of the *damping system*, Q_{DSD}, shall be calculated by imposing design forces of *displacement-dependent damping devices* on the *damping system* as pseudo-static forces. Design seismic forces of *displacement-dependent damping devices* shall be applied in both positive and negative directions at peak displacement of the *structure*.

2. Stage of Maximum Velocity: Seismic design force at the stage of maximum velocity shall be calculated in accordance with the following equation:

$$Q_E = \sqrt{\sum_m \left(Q_{mDSV}\right)^2} \qquad \text{(A13.7.3.2-2)}$$

where:

Q_{mDSV} = Force in an element of the *damping system* required to resist design seismic forces of *velocity-dependent damping devices* due to the mth mode of vibration of *structure* in the direction of interest.

Modal seismic design forces in elements of the *damping system*, Q_{mDSV}, shall be calculated by imposing modal design forces of *velocity-dependent devices* on the non-deformed *damping system* as pseudo-static forces. Modal seismic design forces shall be applied in directions consistent with the deformed shape of the mode of interest. Horizontal restraint forces shall be applied at each floor Level *i* of the non-deformed *damping system* concurrent with the design forces in *velocity-dependent damping devices* such that the horizontal displacement at each level of the *structure* is zero. At each floor Level *i*, restraint forces shall be proportional to and applied at the location of each mass point.

3. Stage of Maximum Acceleration: Seismic design force at the stage of maximum acceleration shall be calculated in accordance with the following equation:

$$Q_E = \sqrt{\sum_m \left(C_{mFD}\Omega_o Q_{mSFRS} + C_{mFV}Q_{mDSV}\right)^2} \pm Q_{DSD} \qquad \text{(A13.7.3.2-3)}$$

The force coefficients, C_{mFD} and C_{mFV}, shall be determined from Tables A13.7.3.2.1 and A13.7.3.2.2, respectively, using values of effective damping determined in accordance with the following requirements:

a.   For fundamental-mode response ($m = 1$) in the direction of interest, the coefficients, C_{1FD} and C_{1FV}, shall be based on the velocity power term, α, that relates device force to *damping device* velocity. The effective fundamental-mode damping, shall be taken as equal to the total effective damping of the fundamental mode less the hysteretic component of damping (e.g., $\beta_{1D} - \beta_{HD}$) at the response level of interest (i.e., $\mu = \mu_D$ or $\mu = \mu_M$).

b.   For higher-mode ($m > 1$) or residual-mode response in the direction of interest, the coefficients, C_{mFD} and C_{mFV}, shall be based on a value of α equal to 1.0. The effective modal damping shall be taken as equal to the total effective damping of the mode of interest (e.g., β_{mD}). For determination of the coefficient C_{mFD}, the ductility demand shall be taken as equal to that of the fundamental mode (e.g., $\mu = \mu_D$).

Table A13.7.3.2.1 Force Coefficient, C_{mFD}[a, b]

| Effective Damping | $\mu \leq 1.0$ | | | | $C_{mFD} = 1.0$[c] |
	$\alpha \leq 0.25$	$\alpha = 0.5$	$\alpha = 0.75$	$\alpha \geq 1.0$	
≤ 0.05	1.00	1.00	1.00	1.00	$\mu \geq 1.0$
0.1	1.00	1.00	1.00	1.00	$\mu \geq 1.0$
0.2	1.00	0.95	0.94	0.93	$\mu \geq 1.1$
0.3	1.00	0.92	0.88	0.86	$\mu \geq 1.2$
0.4	1.00	0.88	0.81	0.78	$\mu \geq 1.3$
0.5	1.00	0.84	0.73	0.71	$\mu \geq 1.4$
0.6	1.00	0.79	0.64	0.64	$\mu \geq 1.6$
0.7	1.00	0.75	0.55	0.58	$\mu \geq 1.7$
0.8	1.00	0.70	0.50	0.53	$\mu \geq 1.9$
0.9	1.00	0.66	0.50	0.50	$\mu \geq 2.1$
≥ 1.0	1.00	0.62	0.50	0.50	$\mu \geq 2.2$

[a] Unless analysis or test data support other values, the force coefficient C_{mFD} for visco-elastic systems shall be taken as 1.0.

[b] Interpolation shall be used for intermediate values of effective damping, α, and μ.

[c] C_{mFD} shall be taken as equal to 1.0 for values of μ greater than or equal to the values shown.

Table A13.7.3.2.2 Force Coefficient, C_{mFV}[a, b]

Effective Damping	$\alpha \leq 0.25$	$\alpha = 0.5$	$\alpha = 0.75$	$\alpha \geq 1.0$
≤ 0.05	1.00	0.35	0.20	0.10
0.1	1.00	0.44	0.31	0.20
0.2	1.00	0.56	0.46	0.37
0.3	1.00	0.64	0.58	0.51
0.4	1.00	0.70	0.69	0.62
0.5	1.00	0.75	0.77	0.71
0.6	1.00	0.80	0.84	0.77

0.7	1.00	0.83	0.90	0.81
0.8	1.00	0.90	0.94	0.90
0.9	1.00	1.00	1.00	1.00
≥ 1.0	1.00	1.00	1.00	1.00

^a Unless analysis or test data support other values, the force coefficient C_{mFD} for visco-elastic systems shall be taken as 1.0.

^b Interpolation shall be used for intermediate values of effective damping, α, and μ.

A13.7.3.3 Combination of Load Effects: The effects on the *damping system* and its *components* due to *gravity loads* and *seismic forces* shall be combined in accordance with Section 5.2.7 using the effect of horizontal seismic forces, Q_E, determined in accordance with Section A13.7.3.2.

> **Exception:** The reliability factor, ρ, shall be taken as equal to 1.0 in all cases and the special load combinations of Section 5.2.7.1 need not apply to the design of the *damping system*.

A13.7.3.4 Inelastic Response Limits: Elements of the *damping system* may exceed strength limits for design loads provided it is shown by analysis or test that:

1. Inelastic response does not adversely affect *damping system* function.

2. Element forces calculated in accordance with Sec. A13.7.3.2, using a value of Ω_o, taken as equal to 1.0, do not exceed the strength required to meet the load combinations of Sec. 5.2.7.

A13.8 DETAILED SYSTEM REQUIREMENTS:

A. 13.8.1 Damping Device Design: The design, construction and installation of *damping devices* shall be based on maximum earthquake response and the following load conditions:

1. Low-cycle, large displacement degradation due to seismic loads;

2. High-cycle, small-displacement degradation due to wind, thermal or other cyclic loads;

3. Forces or displacements due to *gravity loads*;

4. Adhesion of device parts due to corrosion or abrasion, biodegradation, moisture or chemical exposure; and

5. Exposure to environmental conditions, including but not limited to temperature, humidity, moisture, radiation (e.g., ultraviolet light) and reactive or corrosive substances (e.g., salt water).

Damping devices subject to failure by low-cycle fatigue shall resist wind forces without slip, movement, or inelastic cycling.

The design of *damping device* shall incorporate the range of thermal conditions, device wear, manufacturing tolerances, and other effects that cause device properties to vary during the lifetime of the device.

A13.8.2 Multi-Axis Movement: Connection points of *damping devices* shall provide sufficient articulation to accommodate simultaneous longitudinal, lateral, and vertical displacements of the *damping system*.

A13.8.3 Inspection and Periodic Testing: Means of access for inspection and removal of all *damping devices* shall be provided.

The *registered design professional* responsible for design of the *structure* shall establish an appropriate inspection and testing schedule for each type of *damping device* to ensure that the devices respond in a dependable manner throughout device design life. The degree of inspection and testing shall reflect the established in-service history of the *damping devices*, and the likelihood of change in properties over the design life of devices.

A13.8.4 Manufacturing Quality Control: The *registered design professional* responsible for design of the *structure* shall establish a quality control plan for the manufacture of *damping devices*. As a minimum, this plan shall include the testing requirements of Section A13.10.3.

A13.9 DESIGN REVIEW:

A13.9.1 General: Review of the design of the *damping system* and related test programs shall be performed by an independent engineering panel including persons licensed in the appropriate disciplines and experienced in seismic analysis including the theory and application of energy dissipation methods.

A13.9.2 Review Scope: The design review shall include the following:
1. Review of the earthquake ground motions used for design.
2. Review of design parameters of *damping devices*, including device test requirements, device manufacturing quality control and assurance, and scheduled maintenance and inspection requirements.
3. Review of nonlinear analysis methods incorporating the requirements of Sec. 5.8.4.
4. Review of the preliminary design of the *seismic-force-resisting system* and the *damping system*.
5. Review of the final design of the *seismic-force-resisting system* and the *damping system* and all supporting analyses.

A13.10 Required Tests of Damping Devices

A13.10.1   General: The force-velocity-displacement and damping properties used for the design of the *damping system* shall be based on the prototype tests of a selected number of *damping devices*, as specified in Sec. A13.10.2.1.

The fabrication and quality control procedures used for all prototype and production *damping devices* shall be identical.

A13.10.2   Prototype Tests.

A13.10.2.1   General: The following tests shall be performed separately on two full-size *damping devices* of each type and size used in the design, in the order listed below.

Representative sizes of each type of device may be used for prototype testing, provided both of the following conditions are met:

(1)   Fabrication and quality control procedures are identical for each type and size of devices used in the *structure*.

(2)   Prototype testing of representative sizes is accepted by the *registered design professional* responsible for design of the *structure*.

Test specimens shall not be used for construction, unless they are accepted by the *registered design professional* responsible for design of the *structure* and meet the requirements of Sec. A13.10.2 and Sec. A13.10.3.

A13.10.2.2   Data Recording: The force-deflection relationship for each cycle of each test shall be recorded.

A13.10.2.3   Sequence and Cycles of Testing: For the following test sequences, each *damping device* shall be subjected to gravity load effects and thermal environments representative of the installed condition. For seismic testing, the displacement in the devices calculated for the *maximum considered earthquake*, termed herein as the maximum earthquake device displacement, shall be used.

1.   Each *damping device* shall be subjected to the number of cycles expected in the design windstorm, but not less than 2000 continuous fully reversed cycles of wind load. Wind load shall be at amplitudes expected in the design wind storm, and applied at a frequency equal to the inverse of the fundamental period of the building $(f_1 = 1/T_1)$.

>   **Exception:** *Damping devices* need not be subjected to these tests if they are not subject to wind-induced forces or displacements, or if the design wind force is less than the device yield or slip force.

2.   Each *damping device* shall be loaded with 5 fully reversed, sinusoidal cycles at the maximum earthquake device displacement at a frequency equal to $1/T_{1M}$ as calculated in Section A13.4.3.5. Where the *damping device* characteristics vary with operating temperature, these tests shall be conducted at a minimum of 3 temperatures (minimum, ambient, and maximum) that bracket the range of operating temperatures.

>   **Exception:** *Damping devices* may be tested by alternative methods provided each of the following conditions is met:
>
>   a.   Alternative methods of testing are equivalent to the cyclic testing requirements of this section.
>
>   b.   Alternative methods capture the dependence of the *damping device* response on ambient temperature, frequency of loading, and temperature rise during testing.
>
>   c.   Alternative methods are accepted by the *registered design professional* responsible for the design of the *structure*.

3.   If the force-deformation properties of the *damping device* at any displacement less than or equal the maximum earthquake device displacement change by more than 15 percent for

changes in testing frequency from $1/T_{IM}$ to $2.5/T_I$, then the preceding tests shall also be performed at frequencies equal to $1/T_I$ and $2.5/T_I$.

If reduced-scale prototypes are used to qualify the rate dependent properties of *damping devices*, the reduced-scale prototypes should be of the same type and materials, and manufactured with the same processes and quality control procedures, as full-scale prototypes, and tested at a similitude-scaled frequency that represents the full-scale loading rates.

A13.10.2.4 Testing Similar Devices: *Damping devices* need not be prototype tested provided that both of the following conditions are met:

(1)   The *damping device* manufacturer substantiates the similarity of previously tested devices.

(2)   All pertinent testing and other *damping device* data are made available to, and accepted by the *registered design professional* responsible for the design of the *structure*.

A13.10.2.5 Determination of Force-Velocity-Displacement Characteristics: The force-velocity displacement characteristics of a *damping device* shall be based on the cyclic load and displacement tests of prototype devices specified above. Effective stiffness of a *damping device* shall be calculated for each cycle of deformation using equation 13.9.3-1.

A13.10.2.6 Device Adequacy: The performance of a prototype *damping device* shall be assessed as adequate if all of the conditions listed below are satisfied. The 15-percent limits specified below may be increased by the *registered design professional* responsible for the design of the *structure* provided that the increased limit has been demonstrated by analysis to not have a deleterious effect on the response of the *structure*.

A13.10.2.6.1 Displacement-Dependent Devices:

1.   For Section A13.10.2.3 Test 1, no signs of damage including leakage, yielding, or breakage.

2.   For Section A13.10.2.3 Tests 2 and 3, the maximum force and minimum force at zero displacement for a *damping device* for any one cycle does not differ by more than plus or minus 15 percent from the average maximum and minimum forces at zero displacement as calculated from all cycles in that test at a specific frequency and temperature.

3.   For Section A13.10.2.3 Tests 2 and 3, the maximum force and minimum force at maximum earthquake device displacement for a *damping device* for any one cycle does not differ by more than plus or minus 15 percent from the average maximum and minimum forces at the *maximum earthquake* device displacement as calculated from all cycles in that test at a specific frequency and temperature.

4.   For Section A13.10.2.3 Tests 2 and 3, the area of hysteresis loop (E_{loop}) of a *damping device* for any one cycle does not differ by more than plus or minus 15 percent from the average area of the hysteresis loop as calculated from all cycles in that test at a specific frequency and temperature.

5.   The average maximum and minimum forces at zero displacement and maximum earthquake displacement, and the average area of the hysteresis loop (E_{loop}), calculated for each test in the sequence of Section A13.10.2.3 Tests 2 and 3, shall not differ by more than plus or minus 15 percent from the target values specified by the *registered design professional* responsible for the design of the *structure*.

A13.10.2.6.2 Velocity-Dependent Devices:

1.   For Section A13.10.2.3 Test 1, no signs of damage including leakage, yielding, or breakage.

2.   For *velocity-dependent damping devices* with stiffness, the effective stiffness of a *damping device* in any one cycle of Tests 2 and 3 of Section A13.10.2.3 does not differ by more than plus or minus 15 percent from the average effective stiffness as calculated from all cycles in that test at a specific frequency and temperature.

3.   For Section A13.10.2.3 Tests 2 and 3, the maximum force and minimum force at zero displacement for a *damping device* for any one cycle does not differ by more than plus or minus 15 percent from the average maximum and minimum forces at zero displacement as calculated from all cycles in that test at a specific frequency and temperature.

4.   For Section A13.10.2.3 Tests 2 and 3, the area of hysteresis loop (E_{loop}) of a *damping device* for any one cycle does not differ by more than plus or minus 15 percent from the average area of the hysteresis loop as calculated from all cycles in that test at a specific frequency and temperature.

5.   The average maximum and minimum forces at zero displacement, effective stiffness (for *damping devices* with stiffness only), and average area of the hysteresis loop (E_{loop}) calculated for each test in the sequence of Section A13.10.2.3 Tests 2 and 3, shall not differ by more than plus or minus 15 percent from the target values specified by the *registered design professional* responsible for the design of the *structure*.

A13.10.3   Production Testing:

Prior to installation in a building, *damping devices* shall be tested to ensure that their force-velocity-displacement characteristics fall within the limits set by the *registered design professional* responsible for the design of the *structure*. All devices need not be tested. The scope and frequency of the production-testing program shall be determined by the *registered design professional* responsible for the design of the *structure*.

Add the following definitions to *Provisions* and *Commentary* Sec. 2.1:

Damping Device: A flexible structural *element* of the *damping system* that dissipates energy due to relative motion of each end of the device. *Damping devices* include all pins, bolts gusset plates, brace extensions and other components required to connect damping devices to the other *elements* of the *structure*. *Damping devices* may be classified as either displacement-dependent or velocity-dependent, or a combination thereof, and may be configured to act in either a linear or nonlinear manner.

Damping System: The collection of structural *elements* that includes all individual *damping devices*, all structural *elements* or bracing required to transfer forces from *damping devices* to the base of the *structure* and all structural *elements* required to transfer forces from *damping devices* to the *seismic-force-resisting system*.

Displacement-Dependent Damping Device: The force response of a *displacement-dependent damping device* is primarily a function of the relative displacement, between each end of the device. The response is substantially independent of the relative velocity between each end of the device, and/or the excitation frequency.

Velocity-Dependent Damping Device: The force-displacement relation for a *velocity-dependent damping device* is primarily a function of the relative velocity between each end of the device, and may also be a function of the relative displacement between each end of the device.

Revise the following definitions in *Provisions* and *Commentary* Sec. 2.2:

Q_E The effect of horizontal seismic forces ~~building forces~~ (kip or KN); see Sec. 5.2.6 or Sec. A13.7.2.

T The ~~fundamental~~ period (sec) of the fundamental mode of vibration of the structure in the direction of interest, ~~building~~ as determined in Sec. 5.3.3. ~~or the modal period (sec) of the building modified as appropriate to account for the effective stiffness of the energy dissipation system (Sec. A.13.xx).~~

T_m The ~~modal~~ period ~~of vibration~~ (sec) of the mth mode of vibration of the *structure in the direction of interest,* ~~building~~ as determined in Sec. 5.4.5 or Sec. A13.5.

V The total design shear at the base of the *structure* in the direction of interest, as determined using the procedure of Sec. 5.3, including Sec.5.3.3 (kip or kN).

W The total gravity load of the *structure* ~~building~~ as defined in Sec. 5.3.2 (kip or kN). For calculation of seismically isolated building *structure* period, W, is the total seismic dead load weight of the *structure* ~~building as defined in Sec. 5.5.2 and 5.5.3~~ above the isolation system (kip or kN).

$\overline{W}$ The effective gravity load of the *structure* ~~building~~ as defined in Sec. 5.5.2 and 5.5.3 (kip or kN)

$\overline{W}_m$ The effective ~~modal~~ gravity load of mth mode of vibration of the *structure* determined in accordance with Eq. 5.4.5-1 (kip or kN).

V_l The design value of the seismic base shear of the fundamental mode in a given direction, as determined in Sec. 5.4.8 or Sec. A13.4.3.2 (kip or kN).

ϕ_{im} The displacement amplitude at the ith level of the *structure* ~~building~~ for the fixed base condition ~~when vibrating in its mth mode~~ in the mth mode of vibration in the direction of interest, normalized to unity at the roof level, Sec. 5.4.5 and Sec. A13.5.

Add the following definitions to *Provisions* and *Commentary* Sec. 2.2:

B_{1D} Numerical coefficient as set forth in Table A13.3.1 for effective damping equal to β_{mD} ($m = 1$) and period of *structure* equal to T_{1D}.

B_{1M} Numerical coefficient as set forth in Table A13.3.1 for effective damping equal to β_{mM} ($m = 1$) and period of *structure* equal to T_{1M}.

B_{mD} Numerical coefficient as set forth in Table A13.3.1 for effective damping equal to β_{mD} and period of *structure* equal to T_m.

B_{mM} Numerical coefficient as set forth in Table A13.3.1 for effective damping equal to β_{mM} and period of *structure* equal to T_m.

B_R Numerical coefficient as set forth in Table A13.3.1 for effective damping equal to β_R and period of *structure* equal to T_R.

B_{V+1} Numerical coefficient as set forth in Table A13.3.1 for effective damping equal to the sum of viscous damping in the fundamental mode of vibration of the *structure* in the direction of interest, β_{Vm} ($m = 1$), plus inherent damping, β_I, and period of *structure* equal to T_I.

C_{mFD} Force coefficient as set forth in Table A13.7.3.2.1.

C_{mFV} Force coefficient as set forth in Table A13.7.3.2.2.

C_{S1} *Seismic response coefficient* (dimensionless) of the fundamental mode of vibration of the *structure* in the direction of interest, Sec. A13.4.3.4 or Sec. A13.5.3.4 ($m = 1$).

C_{Sm} *Seismic response coefficient* (dimensionless) of the mth mode of vibration of the *structure* in the direction of interest, Sec. A13.5.3.4 ($m = 1$) or Sec. A13.5.3.6 ($m > 1$).

C_{SR} *Seismic response coefficient* (dimensionless) of the residual mode of vibration of the *structure* in the direction of interest, Sec. A13.4.3.8.

D_{1D} Fundamental mode *design displacement* at the center of rigidity of the roof level of the *structure* in the direction under consideration, Sec. A13.4.4.3 (in. or mm).

D_{1M} Fundamental mode *maximum displacement* at the center of rigidity of the roof level of the *structure* in the direction under consideration, Sec. A13.4.4.6 (in. or mm).

D_{mD} *Design displacement* at the center of rigidity of the roof level of the *structure* due to the mth mode of vibration in the direction under consideration, Sec. A13.5.4.3 (in. or mm).

D_{mM} *Maximum displacement* at the center of rigidity of the roof level of the *structure* due to the mth mode of vibration in the direction under consideration, Sec. A13.5.4.6 (in. or mm).

D_{RD} Residual mode *design displacement* at the center of rigidity of the roof level of the *structure* in the direction under consideration, Sec. A13.4.4.3 (in. or mm).

D_{RM} Residual mode *maximum displacement* at the center of rigidity of the roof level of the *structure* in the direction under consideration, Sec. A13.4.4.6 (in. or mm).

D_Y Displacement at the center of rigidity of the roof level of the *structure* at the effective yield point of the *seismic-force-resisting system*, Sec. A13.3.4 (in. or mm).

f_i Lateral force at Level i of the *structure* distributed approximately in accordance with Equation 5.3.4-2, Sec. A13.4.3.3.

F_{i1} Inertial force at Level i (or mass point i) in the fundamental mode of vibration of the *structure* in the direction of interest, Sec. A13.4.3.9.

F_{im} Inertial force at Level i (or mass point i) in the mth mode of vibration of the *structure* in the direction of interest, Sec. A13.5.3.7.

F_{iR} Inertial force at Level i (or mass point i) in the residual mode of vibration of the *structure* in the direction of interest, Sec. A13.4.3.9.

h_r Height of the *structure* above the *base* to the roof level (ft or m), Sec. A13.4.3.3.

q_H Hysteresis loop adjustment factor as determined in Sec. A13.3.3.

Q_{DSD} Force in an element of the *damping system* required to resist design seismic forces of *displacement-dependent damping devices*, Sec. A13.7.3.2.

Q_{mDSV} Force in an element of the *damping system* required to resist design seismic forces of *velocity-dependent damping devices* due to the mth mode of vibration of *structure* in the direction of interest, Sec. A13.7.3.2.

Q_{mSFRS} Force in an element of the *damping system* equal to the design seismic force of the mth mode of vibration of the *seismic force resisting system* in the direction of interest, A13.7.3.2.

T_1 Period, in seconds, of the fundamental mode of vibration of the *structure* in the direction of interest, Sec. A13.4.3.3.

T_{1D} Effective period, in seconds, of the fundamental mode of vibration of the *structure* at the *design displacement* in the direction under consideration, as prescribed by Sec. A13.4.3.5 or Sec. A13.5.3.5.

T_{1M} Effective period, in seconds, of the fundamental mode of vibration of the *structure* at the *maximum displacement* in the direction under consideration, as prescribed by Sec. A13.4.3.5 or Sec. A13.5.3.5.

T_m Period, in seconds, of the mth mode of vibration of the *structure* in the direction under consideration, Sec. A13.5.3.6.

T_R Period, in seconds, of the residual mode of vibration of the *structure* in the direction under consideration, Sec. A13.4.3.7.

211

V_m Design value of the seismic *base shear* of the mth mode of vibration of the *structure* in the direction of interest, Sec. 5.4.5 or Sec. A13.5.3.2 (kip or kN).

V_{min} Minimum allowable value of *base shear* permitted for design of the *seismic-force-resisting system* of the *structure* in the direction of interest, Sec. A13.2.4.1 (kip or kN).

V_R Design value of the seismic *base shear* of the residual mode of vibration of the *structure* in a given direction, as determined in Sec. A13.4.3.6 (kip or kN).

$\overline{W}_I$ Effective fundamental mode *gravity load* of the *structure* including portions of the live load determined in accordance with Eq. 5.4.5-2 for $m = 1$ (kip or kN).

$\overline{W}_R$ Effective residual mode *gravity load* of the *structure* determined in accordance with Eq. A13.4.3.7-3 (kip or kN).

α Velocity power term relating *damping device* force to *damping device* velocity.

β_{mD} Total effective damping of the mth mode of vibration of the *structure* in the direction of interest at the *design displacement*, Sec. A13.3.2.

β_{mM} Total effective damping of the mth mode of vibration of the *structure* in the direction of interest at the *maximum displacement*, Sec. A13.3.2.

β_{HD} Component of effective damping of the *structure* in the direction of interest due to post-yield hysteretic behavior of the *seismic-force-resisting system* and elements of the *damping system* at effective ductility demand, μ_D, Sec. A13.3.2.2.

β_{HM} Component of effective damping of the *structure* in the direction of interest due to post-yield hysteretic behavior of the *seismic-force-resisting system* and elements of the *damping system* at effective ductility demand, μ_M, Sec. A13.3.2.2.

β_I Component of effective damping of the *structure* due to the inherent dissipation of energy by elements of the *structure*, at or just below the effective yield displacement of the *seismic-force-resisting system*, Sec. A13.3.2.1.

β_R Total effective damping in the residual mode of vibration of the *structure* in the direction of interest, calculated in accordance with Sec. A13.3.2 ($\mu_D = 1.0$ and $\mu_M = 1.0$).

β_{Vm} Component of effective damping of the mth mode of vibration of the *structure* in the direction of interest due to viscous dissipation of energy by the *damping system*, at or just below the effective yield displacement of the *seismic-force-resisting system*, Sec. A13.3.2.3.

δ_i Elastic deflection of Level i of the *structure* due to applied lateral force, f_i, Sec. A13.4.3.3 (in. or mm).

δ_{iID} Fundamental mode *design earthquake* deflection of Level i at the center of rigidity of the *structure* in the direction under consideration, Sec. A13.4.4.2 (in. or mm).

δ_{iD} Total *design earthquake* deflection of Level i at the center of rigidity of the *structure* in the direction under consideration, Sec. A13.4.4.2 (in. or mm).

δ_{iM} Total *maximum earthquake* deflection of Level i at the center of rigidity of the *structure* in the direction under consideration, Sec. A13.4.4.2 (in. or mm).

δ_{iRD} Residual mode *design earthquake* deflection of Level i at the center of rigidity of the *structure* in the direction under consideration, Sec. A13.4.4.2 (in. or mm).

δ_{im} Deflection of Level i in the mth mode of vibration at the center of rigidity of the *structure* in the direction under consideration, Sec. A13.5(in. or mm).

Δ_{ID} *Design earthquake* story drift due to the fundamental mode of vibration of the *structure* in the direction of interest, Sec. A13.4.4.4 (in. or mm).

Δ_{D} Total *design earthquake* story drift of the *structure* in the direction of interest, Sec. A13.4.4.4 (in. or mm).

Δ_{M} Total *maximum earthquake* story drift of the *structure* in the direction of interest, Sec. A13.4.4.6 (in. or mm).

Δ_{mD} *Design earthquake* story drift due to the mth mode of vibration of the *structure* in the direction of interest, Sec. A13.4.4.4 (in. or mm).

Δ_{RD} *Design earthquake* story drift due to the residual mode of vibration of the *structure* in the direction of interest, Sec. A13.4.4.4 (in. or mm).

μ Effective ductility demand on the *seismic-force-resisting system* in the direction of interest.

μ_{D} Effective ductility demand on the *seismic-force-resisting system* in the direction of interest due to the *design earthquake*, Sec. A.13.4.

μ_{M} Effective ductility demand on the *seismic-force-resisting system* in the direction of interest due to the *maximum considered earthquake*, Sec. A13.4.

μ_{max} Maximum allowable effective ductility demand on the *seismic-force-resisting system* due to *design earthquake*, Sec. A13.3.5.

ϕ_{il} Displacement amplitude at Level i of the fundamental mode of vibration of the *structure* in the direction of interest, normalized to unity at the roof level, Sec. A13.4.3.3.

ϕ_{iR} Displacement amplitude at Level i of the residual mode of vibration of the *structure* in the direction of interest, normalized to unity at the roof level, Sec. A13.4.3.7.

Γ_{I} Participation factor of the fundamental mode of vibration of the *structure* in the direction of interest, Sec. A13.4.3.3 or Sec. A13.5.3.3 ($m = 1$).

Γ_{m} Participation factor of the mth mode of vibration of the *structure* in the direction of interest, Sec. A13.5.3.3.

Γ_R Participation factor of the residual mode of vibration of the *structure* in the direction of interest, Sec. A13.4.3.7.

∇_{lD} *Design earthquake* story velocity due to the fundamental mode of vibration of the *structure* in the direction of interest, Sec. A13.4.4.5 (in/sec or mm/sec).

∇_D Total *design earthquake* story velocity of the *structure* in the direction of interest, Sec. A13.4.4.5 (in/sec or mm/sec).

∇_M Total *maximum earthquake* story velocity of the *structure* in the direction of interest, Sec. A13.4.4.6 (in/sec or mm/sec).

∇_{mD} *Design earthquake* story velocity due to the mth mode of vibration of the *structure* in the direction of interest, Sec. A13.4.4.5 (in/sec or mm/sec).

∇_{RD} *Design earthquake* story velocity due to the residual mode of vibration of the *structure* in the direction of interest, Sec. A13.4.4.5 (in/sec or mm/sec).

APPENDIX B

DESCRIPTION OF EXAMPLE BUILDINGS WITHOUT DAMPING SYSTEMS AND DESIGN OF LATERAL FORCE RESISTING SYSTEMS PER NEHRP (1997)

B.1 Introduction

This appendix presents a description of the 3-story and the 6-story buildings that are utilized in the development of design examples for damping systems, in the application of the NEHRP (2000) and FEMA (1997) methods of analysis and in the assessment of the accuracy of these methods. Moreover, the appendix presents the design of special steel moment frames for these buildings without damping systems to meet the strength and drift criteria of NEHRP (1997). A comparison of these frames to those of the same buildings with damping systems illustrates the benefits and drawbacks offered by the damping systems.

B.2 Description of 3-Story Building

This residential building is of regular configuration, constructed of steel, 41.15 m (135′) x 41.15 m (135′) in plan, and 13.028 m (42′-9″) high. A typical floor plan and a typical elevation are shown in Figure B-1. Columns are spaced at 8.23 m (27′-0″) o.c. Wind and earthquake resistance is provided by two three-span special moment frames in each direction, located on the perimeter of the building and are indicated by heavy lines in Figure B-1. Floors are assumed to behave as rigid diaphragms, and torsional effects are not considered. Moreover, the building is assumed to be located at a site characterized by a design response spectrum with parameters S_{D1} = 0.6, S_{DS} = 1.0, T_s = 0.6 sec. per NEHRP (1997).

Design Parameters

The building is designed to meet 1997 NEHRP Recommended Provisions for Seismic Regulations for New Buildings and Other Structures.

215

Loads

Roof Dead Load:	*1.68 kN/m² (35 psf)*
Roof Live Load:	*0.96 kN/m² (20 psf)*
Floor Dead load:	*3.35 kN/m² (70 psf)*
Floor Live Load:	*1.68 kN/m² (35 psf)*
Cladding:	*1.20 kN/m² (25 psf)*

Reduced floor live load of 35 psf is assumed for all floors for convenience. Unreduced live load is 40 psf.

Material

Steel with yield strength:	$F_y = 0.345 \ kN/mm^2 \ (50 \ ksi)$

Weight of the Building

Third Floor (roof):	$w_3 = 3,134 \ kN$
Second Floor:	$w_2 = 5,800 \ kN$
First Floor:	$w_1 = 5,800 \ kN$
	$W_T = 14,734 \ kN$

Design Coefficients per Table 5.2.2, 1997 NEHRP

For Special Steel Moment Frame

Response Modification Factor:	$R = 8.0$
System Overstrength Factor:	$\Omega_0 = 3.0$
Deflection Amplification Factor:	$C_d = 5.5$

Allowable Story Drift per Table 5.2.8, 1997 NEHRP

For Seismic Group I:	$\Delta_a = 0.02h_{sx}$

Evaluation of Design Gravity Loads

Gravity loads on beams are summarized in Table B-1 using the loads described in Section B.3.1 and the tributary width to each beam of the special steel moment frame.

Table B-1 Uniform Gravity Loads on Beams of Typical Special Steel Moment Frame

Floor i	Tributary Width (m)	Floor Dead Load (kN/m)	Cladding (kN/m)	Total Dead Load (kN/m)	Live Load (kN/m)	1.2D+1.6L (kN/m)
3	4.725	7.9	2.6	10.5	4.5	19.8
2	4.725	15.8	5.2	21.0	8.0	38.0
1	4.725	15.8	5.2	21.0	8.0	38.0

B.3 Design of Typical 3-Story Special Steel Moment Frame

Seismic Base Shear V and Minimum Required Base Shear Strength V_y

Fundamental Period of the Structure, T (per Chapter 5.3.3, NEHRP, 1997)

Approximate fundamental period T_a (eq. 5.3.3.1-1):

$$T_a = C_t (h_n)^{\frac{3}{4}}$$
$$C_t = 0.035$$
$$T_a = 0.035(42.74)^{\frac{3}{4}} \qquad \therefore T_a = 0.585\, sec$$

$$T \le C_u \cdot T_a$$
$$C_u = 1.2 \quad (For\ S_{D1} > 0.4, Table\ 5.5.3)$$
$$T \le 1.2 \times 0.585 = 0.702 \qquad \therefore T = 0.70\, sec$$

Seismic Response Coefficient, C_s (eq. 5.3.2.1-2)

$$C_s = \frac{S_{D1}}{RT} = \frac{0.6}{8 \times 0.70} = 0.107$$

Seismic Base Shear, V (eq. 5.3.2)

$$V = C_s \cdot W_T$$
$$V = 0.107 x 14,734 \qquad \therefore V = 1,577\, kN\ (355\ kips)$$

The design base shear of each frame is $V = 788.5\ kN\ (177.5\ kips)$. This does not include the additional component due to torsion, which is neglected in this

217

example. Accordingly, the minimum required base shear strength of the frame V_y (see Section 7 herein) is

$$V_y = V \cdot \frac{C_d \cdot \Omega_o}{R} = 788.5 \times \frac{5.5 \times 3.0}{8} = 1,626 \, kN \, (366 \, kips)$$

Vertical Distribution of Seismic Forces

The vertical distribution of the seismic forces is described in Section 5.3.4 (NEHRP, 1997).

$$C_{Vx_i} = \frac{W_i h_i^k}{\sum\limits_{j=1}^{n} W_j h_j^k} \qquad \text{for } T = 0.70 \, sec \qquad k = 1.10$$

As required by eq. (5.2.7-1), evaluation of the seismic load E requires the calculation of the redundancy reliability factor ρ. Using eq. (5.2.4.2) with a typical floor area of 1,693 m² (18,225 ft²) and a value of $r_{max} = 0.10$, the factor ρ is calculated as

$$\rho = 2 - \frac{20}{0.10 \cdot \sqrt{18225}} = 1.26$$

The lateral seismic forces are presented in Table B-2.

Table B-2 Lateral Seismic Forces for 3-Story Frame

Floor	w_i^* (kN)	h_i (m)	$w_i h_i^k$	C_{vxi}	F_{xi} (kN)	ρF_{xi} (kN)
3	1567	13.03	5.27E+04	0.363	286	360
2	2900	8.72	6.27E+04	0.432	341	430
1	2900	4.42	2.97E+04	0.204	161	203

*: Reactive weight of each frame

$$\sum_{i=1}^{N} w_i h_i^k = 145,100$$

218

Preliminary Design of Beams

Beams are proportioned for the maximum of the bending moments obtained from gravity loads, and load combination given by $U = 1.2D + 0.5L \pm E$. The corresponding bending moments are estimated as

$$M_{uG} = \frac{q_u l^2}{12} \qquad q_u = 1.2D + 1.6L \quad \text{(for gravity loads)}$$

$$M_{u(G+E)} = (1.2q_D + 0.5q_L)\frac{L^2}{12} + \rho M_E \quad \text{(for gravity + seismic loads)}$$

Computations of the design bending moments for beams are presented in Table B-3

TABLE B-3 Calculation of Design Bending Moments of Beams

Level	1.2D +1.6L (kN/m)	1.2D+0.5L (kN/m)	M_{uG} (kN.m)	ρM_E (kN.m)	M_{G+E} (kN.m)
Roof	19.8	14.9	102.3	129.1	205.8
2	38.0	29.2	196.3	420.1	571.3
1	38.0	29.2	196.3	785.9	937.1

It may be noted that the governing design moments of the beams result from the combination of gravity and seismic loads in all floors. Accordingly the following sections are selected as follows:

Third Floor: W14x26   , $\phi M_p = 205 \ kN.m$

Second Floor: W21x50   , $\phi M_p = 560 \ kN.m$

First Floor: W24x76   , $\phi M_p = 1016 \ kN.m$

Preliminary Design of Columns

Columns are proportioned to satisfy strong column/weak beam conditions, that is the sum of the columns moment capacity must be greater than the sum of beam moment capacities at any joint. W14 sections are assumed. Plastic hinges in beams are assumed to form at a distance of $(d_c/2+d_b)$, where d_c and d_b are the depth of the column and beam sections, respectively, at any joint. It is further assumed that all columns have the same section along the entire height of the 3-story building.

Interior joints at the first floor represent the most critical location for the design of the column. A factor of 1.25 is applied to the sum of the beam moments to assure strong column/weak beam mechanism. With reference to Figure B-2:

Beam section: W24x76
$$M_{pb} = 1129 \, kN \cdot m \; (833^{'-k})$$

Location of plastic hinge:
$$L' = \frac{d_c}{2} + d_b = \frac{356}{2} + 610 = 788mm \; (2.6')$$

Beam effective length:
$$L_p = 8230 - 2 \cdot 788 = 6654mm = 6.654 \, m \; (21.8')$$

Shear at plastic hinge:
$$V_p = \frac{2M_p}{L_p} = \frac{2 \times 1129}{6.654} = 340 \, kN \; (76.5 \; kips)$$

Column total moment:
$$M_c = 2(M_{pb} + V_p L') \times 1.25$$
$$= 2(1129 + 340 \times 0.788) \times 1.25$$
$$= 3492 \, kN \cdot m \, (2576^{'-k})$$

Moment in first-story column: $M_{pc} = 0.6 M_c$

(assumed) $M_{pc} = 0.6 \times 3492 = 2095kN \cdot m \, (1545^{'-k})$

Required plastic section modulus:
$$Z_x = \frac{2095 \cdot 1000}{0.345} = 6,072,464 \, mm^3 \; (371 in^3)$$

Try W14x211:   *$Z_x = 6,390,955mm^3$ (390 in^3)*

220

The fundamental period of the proposed frame obtained by eigenvalue analysis was $T_1 = 1.12$ sec. Seismic forces evaluated on the basis of this period were used to perform elastic analysis of the frame using program SAP-2000NL. The story drift obtained in the third floor exceeded the allowable limit by 10%. The design of the frame was altered by adjusting the sections to satisfy the drift criteria. Figure B-3 shows the preliminary design of the frame. Observe that the sections have changed with respect to those established using the strength criteria.

Calculation of Story Drifts

For calculation of story drifts, the actual period of the building was utilized (see Section 5.3.7.1, NEHRP, 1997) and the lateral forces were calculated.

Period of the revised frame: $T_1 = 1.07$ sec (based in eigenvalue analysis in program SAP-2000NL)

Seismic response coefficient: $C_s = \dfrac{0.6}{8 \times 1.07} = 0.07$

Seismic base shear: $V = 0.07 \times \dfrac{14734}{2} = 516\,kN\ (116.0\,kips)$

Table B-4 shows a summary of the calculations carried out to evaluate the story drifts Δ_i of the frame. Lateral floor displacements δ_{xe} are obtained from elastic analysis of the frame performed in program SAP-2000NL. Note that for $T_1 = 1.07$ sec, the exponent k is equal to 1.285.

TABLE B-4 Calculation of Story Drifts of 3-Story Frame

Level	h_i (m)	w_i (kN)	$w_i h_i^k$	C_{vx}	F_{xi} (kN)	δ_{Xe} (mm)	$C_d \delta_{xe}$ (mm)	Δ_i (mm)	Δ/h_{sx}
3	13.03	1567	42440	0.3897	201	36	198	66	0.015
2	8.72	2900	46877	0.4305	222	24	132	82	0.019
1	4.42	2900	19578	0.1798	93	9	50	50	0.011

$$\sum w_i h_i^k = 108{,}895$$

As shown is Table B-4, the value of story drifts satisfy the NEHRP (1997) limit of $0.02h_{sx}$, therefore the preliminary design of this frame is satisfactory. The weight of the designed frame is 215 kN (48.4 kips).

B.4 Design of 6-Story Special Steel Moment Frame

Consider that the building of Figure B-1 has six stories. Assume that the number and distribution of special steel moment frames remains as shown. Furthermore, assume that the interstory height and floors weights also remain unchanged. This section presents the design of the 6-story special steel moment frame following the same approach as in the 3-story example.

Seismic Base Shear V and Minimum Required Strength V_y

Fundamental Period of Building, T (per Chapter 5.3.3, NEHRP, 1997)

Height of the structure: $h_n = 4420 + 5 \times 4304 = 25940mm$ (85.1')

Approximate period: $T_a = 0.035(85.10)^{3/4} = 0.98 \, sec$

Upper bound period: $T_I = 1.2 \times 0.98 = 1.18 \, sec$

Seismic Response Coefficient, C_s

$$C_s = \frac{0.6}{8 \times 1.18} = 0.0636$$

Seismic Base Shear

Total weight of building: $W_T = 3134 + 5 \times 5800 = 32,134kN \, (7,227 \, kips)$

Seismic weight per frame: $W = 16,067 \, kN \, (3,614 \, kips)$

Seismic base shear: $V = 0.0636 \times 16067 = 1,022 \, kN \, (230 \, kips)$

Minimum required base shear strength: $V_y = 1022 \times \dfrac{5.5 \times 3}{8} = 2,108 \, kN \, (474 \, kips)$

Vertical Distribution of Seismic Forces

Exponent k (for $T=1.18 \, sec.$): $k = 1.34$

Redundancy reliability factor: $\rho = 1.26$

Calculations of the vertical distribution of seismic forces per frame are presented in Table B-5.

TABLE B-5 Lateral Seismic Forces for 6-Story Frame

Level	w_i (kN)	h_i (m)	$w_i h_i^k$	C_{vxi}	F_{xi} (kN)	ρF_{xi} (kN)
6	1567	25.94	1.23E+05	0.2054	210	265
5	2900	21.63	1.78E+05	0.2982	305	384
4	2900	17.33	1.33E+05	0.2215	226	285
3	2900	13.03	0.94E+05	0.1511	154	194
2	2900	8.72	0.53E+05	0.0883	91	115
1	2900	4.42	0.21E+05	0.0355	36	45

$$\sum_{i=1}^{N} w_i h_i^k = 602,000$$

Preliminary Design of Beams

Beams are proportioned for the maximum of the bending moments obtained from gravity loads according to load combination $U_1 = 1.2D + 1.6L$, and combination of gravity and seismic loads according to load combination $U_2 = 1.2D + 0.5L \pm E$. The moments were calculated on the basis of the equations presented in B.5.3 herein and the selected beams sections are shown in Table B-6.

TABLE B-6 Summary of Design Moments and Selected Beam Sections

Level	M_{uG} (kN.m)	$M_{1.2D+0.5L}$ (kN.m)	ρM_E (kN.m)	$M_{u(G+E)}$ (kN.m)	Section	$\phi_b . M_p$ (kN.m)
6	102.3	76.7	95.0	171.8	*W14x26*	204.6
5	196.3	151.2	327.8	479.1	*W21x44*	485.2
4	196.3	151.2	567.8	719.0	*W21x62*	731.9
3	196.3	151.2	739.6	890.8	*W24x68*	900.0
2	196.3	151.2	850.4	1001.2	*W24x76*	1016.5
1	196.3	151.2	907.8	1059.0	*W24x84*	1138.4

223

Preliminary Design of Columns

Columns are proportioned to satisfy strong column/weak beam conditions. Columns have splices at two-story intervals. The design moment of the bottom column at a splice is assumed to take 60% of the sum of the moment capacities of beams at the interior joints, including the additional moment produced by the shear at the plastic hinges.

The effect of the axial load in reducing the moment capacity of the columns is taken into account according to $M_{pc} = Z_x (F_y-P_u/A_c)$. The ultimate axial load in columns is established using the load combination $U = 1.2D \pm E + 0.5L$ (eq. A4-5, AISC LRFD, 1995) with E given by eq. 5.2.7-1, NEHRP (1997). Gravity axial loads are established from Table B-1, and $\rho=1.26$ (eq.5.2.4.2, NEHRP, 1997). Table B-7 presents a summary of the calculations and the selected column sections.

The natural period of the proposed frame T_1 obtained by eigenvalue analysis was $T_1 = 2.16$ sec. Seismic forces evaluated on the basis of this period were used to perform elastic analysis of the frame using program SAP-2000NL. The story drifts obtained exceeded the allowable limit by up to 40%. That is, the design of the moment frame (without damping system) is governed by drift limits rather than strength criteria.

TABLE B-7 Summary of Design Moments and Selected Column Sections

Stories	Beam Section	M_{pb} (kN.m)	L' (m)	L_p (m)	V_p (kN)	ΣM_{pb} (kN.m)	$0.6M_c$ (kN.m)	Section
1-2	W24x84	1264.4	7.88	6.65	380	3910.9	2346.6	*W14x257*
3-4	W24x68	999.9	7.88	6.65	301	3092.7	1855.6	*W14x211*
5-6	W21x44	539.1	7.11	6.81	158	1628.6	977.0	*W14x109*

The design of the frame was altered by adjusting the sections to satisfy the drift criteria. Figure B-4 shows the preliminary design of the frame. Observe that the sections have been increased in size from those needed to satisfy the strength requirements.

Calculation of Story Drifts

Seismic forces are evaluated using the fundamental period obtained by eigenvalue analysis of the proposed design of the frame shown in Figure B-4:

Fundamental period: $T_1 = 1.90\,sec$

Seismic coefficient: $C_S = \dfrac{0.6}{8x1.90} = 0.0395$

Seismic base shear: $V = 0.0395 \times 16067 = 635kN\,(142.8\,kips)$

Exponent: $k = 1.70$

Table B-8 presents a summary of the calculations carried out for the 6-story frame shown in Figure B-4. Static analysis to obtain elastic displacements was performed using program SAP-2000NL. As shown in Table B-8, the drifts at all stories satisfy the limit of 0.02 h_{sx}. The frame weighs approximately 504 kN (113 kips), compared with the initial design, which did not meet the drift criteria, that weighed 370 kN (83 kips).

Table B-8 Calculation of Story Drifts of 6-Story Frame

Level	w_i (kN)	h_i (m)	$w_i h_i^k$	C_{vx}	F_{xi} (kN)	δ_{xe} (mm)	$C_d\delta_{xe}$ (mm)	Δ_i (mm)	Δ_i/h_{sx}
6	1567	25.94	3.97E+05	0.2355	150	70	385	49	0.014
5	2900	21.64	5.40E+05	0.3200	203	61	336	77	0.018
4	2900	17.33	3.70E+05	0.2195	139	47	259	77	0.018
3	2900	13.03	2.28E+05	0.1251	86	33	182	77	0.018
2	2900	8.72	1.15E+05	0.0683	43	19	105	66	0.015
1	2900	4.42	0.36E+05	0.0216	14	7	39	39	0.009

$\displaystyle\sum_{i=1}^{N} w_i h_i^k : 16.86E+05$

225
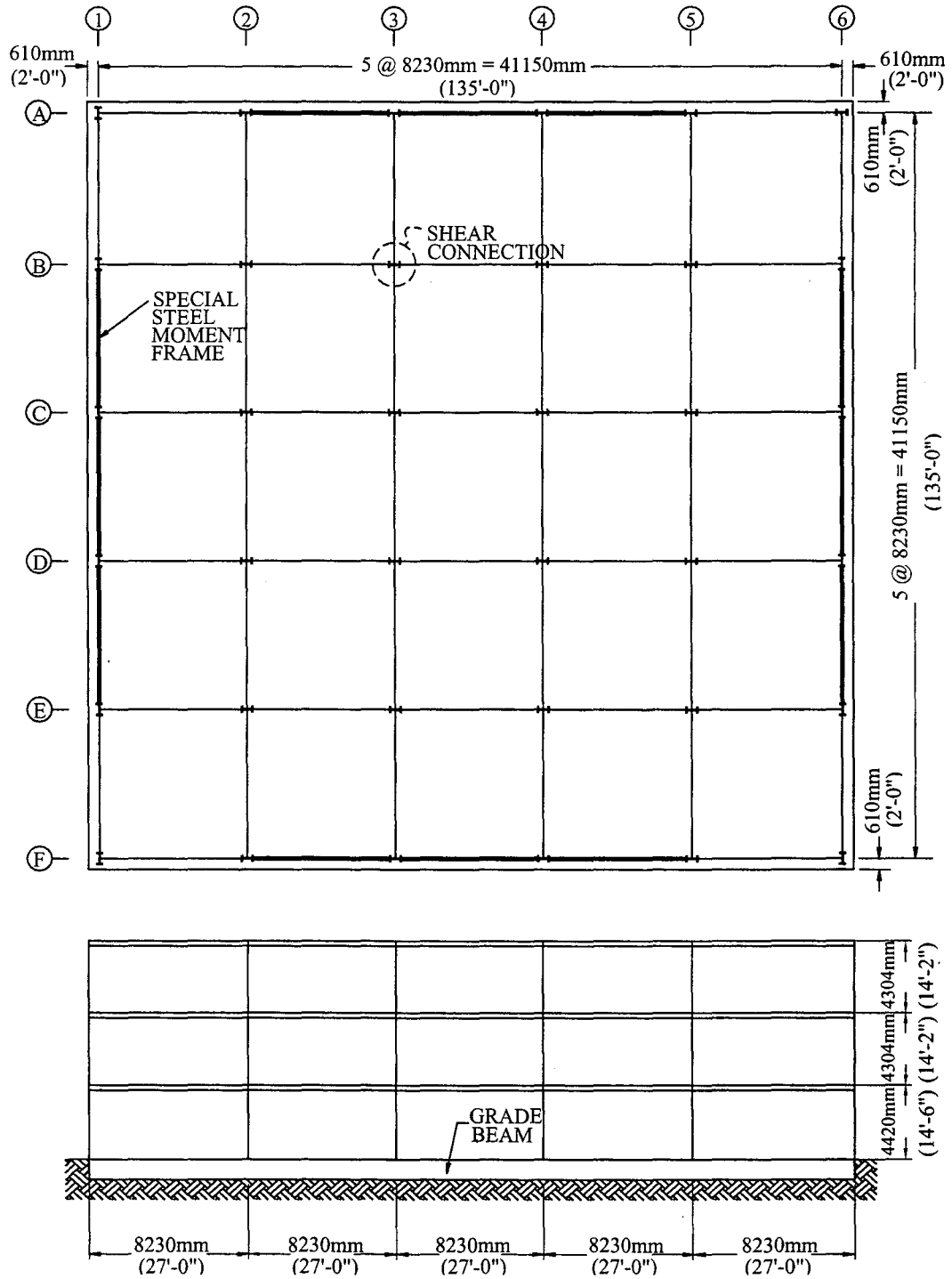
FIGURE B-1 Plan View and Elevation of Example 3-Story Building

226
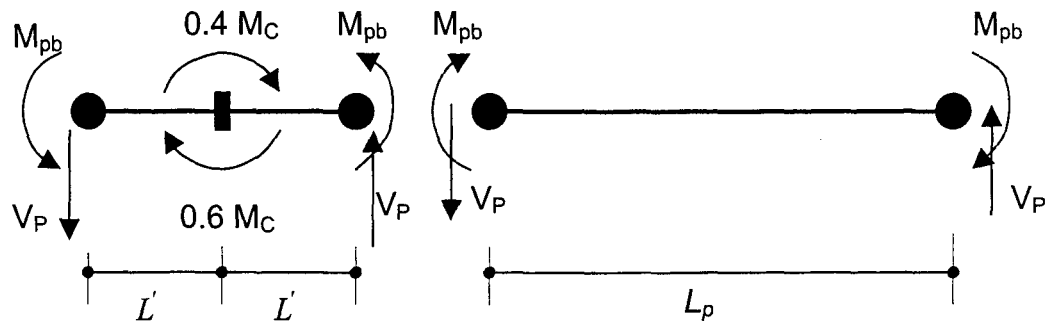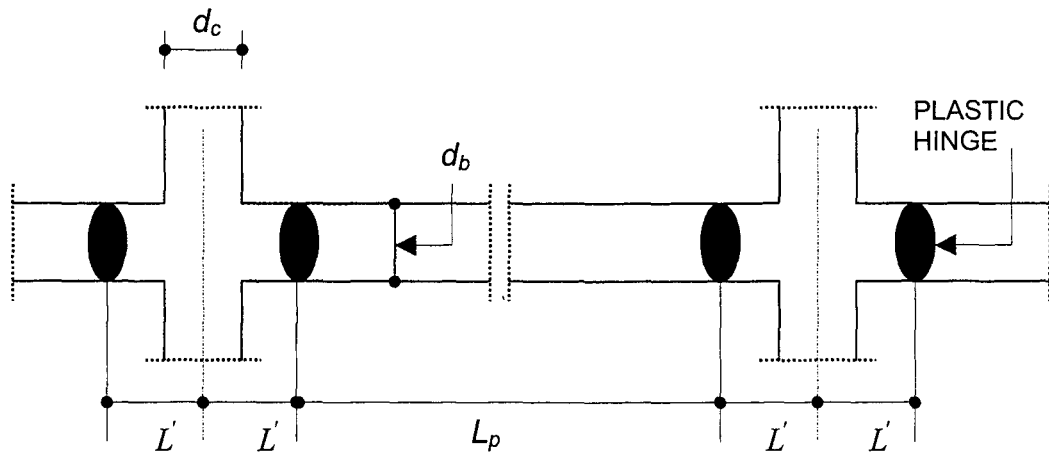
$$M_c = 2\left[M_{pb} + V_p L'\right]$$

(effect of shear forces due to gravity loads ignored)

FIGURE B-2 Geometry and Equilibrium at Interior Beam to Column Joint at First Floor
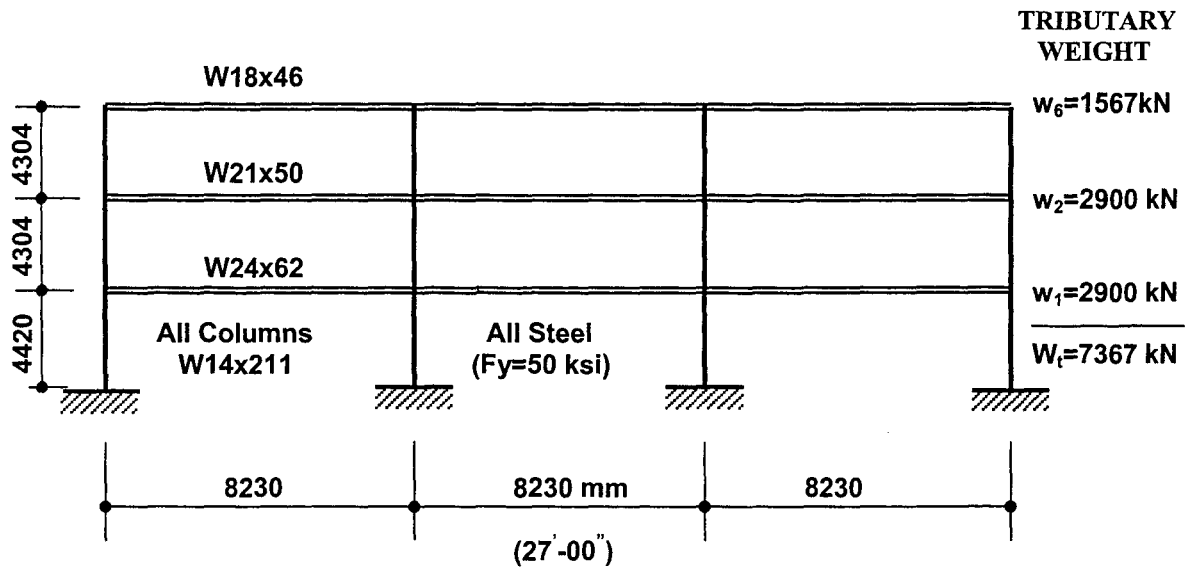
FIGURE B-3 3-Story Special Steel Moment Frame Designed to Meet
NEHRP (1997) Criteria without a Damping System
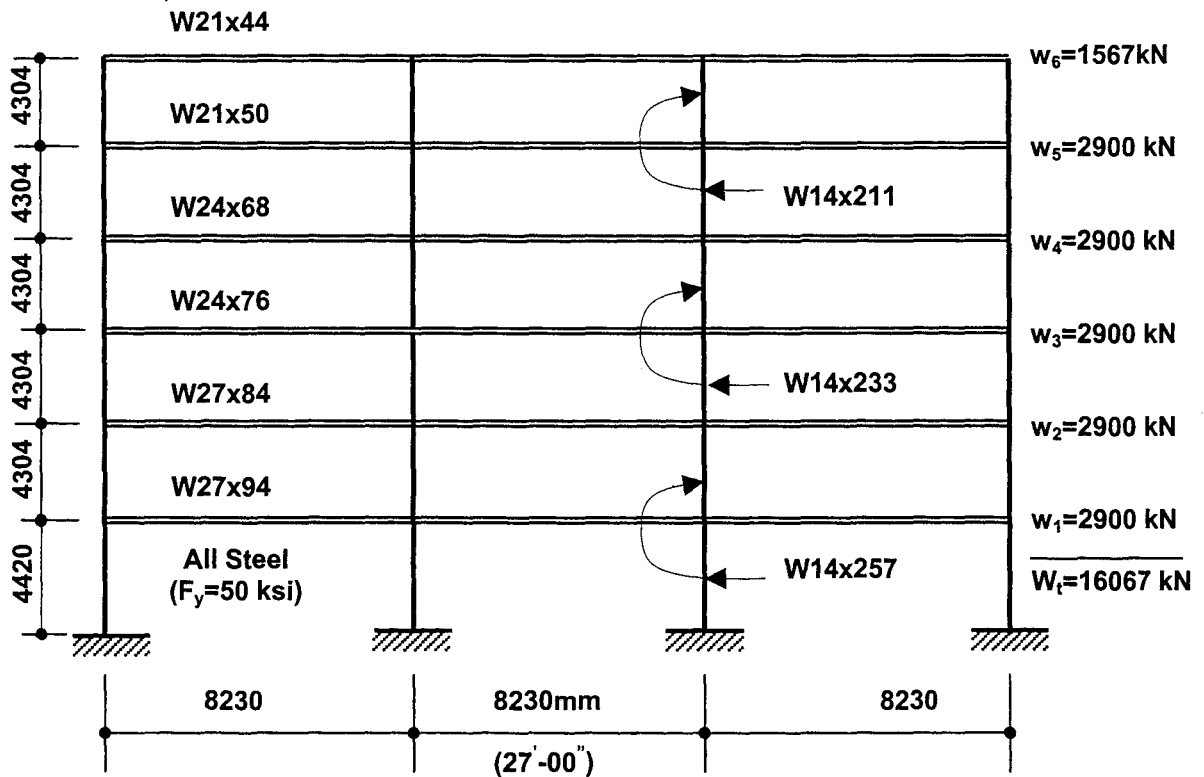
FIGURE B-4 6-Story Special Steel Moment Frame Designed to Meet
NEHRP (1997) Criteria without a Damping System

APPENDIX C

APPROXIMATE CONSTRUCTION OF PUSHOVER CURVE OF BUILDINGS WITHOUT AND WITH DAMPING SYSTEMS ON THE BASIS OF PLASTIC ANALYSIS

C.1 Introduction

This appendix presents a plastic analysis-based approach to construct the pushover curve of moment-frame buildings without viscous, viscoelastic or metallic yielding damping systems. A simple method to determine the base shear strength of these systems is developed that applies under the following assumptions: (a) a proper collapse mechanism, consisting of plastic hinges at the beam ends and column bases, develops, (b) the pattern of lateral load remains constant during pushover, (c) plastic hinges develop at both ends of beams at equal distances from the centerline of columns, and (d) the frame exhibits elastoplastic behavior. The developed procedure is intended as an alternate approach to determining the base shear strength of buildings by avoiding the use of pushover analysis. It should be noted that the pushover curve may be approximately constructed when the base shear strength is known as follows: the behavior of the structural frame, exclusive of the damping system, is assumed to be elastoplastic and the ascending branch of the elastoplastic pushover curve is determined on the basis of the elastic stiffness of the frame. When the pattern of loads is proportioned to the first mode of the frame, the stiffness is directly related to the fundamental elastic period of the frame.

C.2 Base Shear Strength of Buildings without Damping Systems

The procedure described in this section applies for moment frames without damping systems. However, the procedure applies also to frames with purely viscous damping systems since such systems do not exhibit any stiffness or strength. Rather, it is assumed that the damping forces merely reduce the displacement demand due to the increased viscous damping. However, as discussed in Section 8 the situation is more complex and pure viscous damping may alter the pushover curve.

Consider the N-story, n-bay moment frame subjected to an arbitrary distribution of lateral load as shown in Figure C-1(a). Different span length, story height, and corresponding beam and column ultimate bending capacities are assumed at any level. The base shear strength of the frame, V_y, is defined as the base shear of the frame at the collapse stage (Figure C-1(b)).

Based on the assumptions stated above, the work done by the forces applied to the structure must be equal to the energy dissipated at plastic hinge locations, that is,

$$\sum_{i=1}^{N} F_i \cdot D_i = \sum_{k=1}^{K} M_{pck} \cdot \theta + 2 \sum_{i=1}^{N} \sum_{j=1}^{n} M_{pbij} \cdot \beta_{ij} \qquad (\text{C-1})$$

where F_i = lateral load applied at level i, D_i = lateral displacement of level i, M_{pck}= plastic moment at base of first-story column at column line k, M_{pbij} = plastic moment of beam at level i and span j, β_{ij} = rotation of beam plastic hinge at level i and span j, and θ = rotation of plastic hinge at base of columns. From Figure C-1(c), β_{ij} can be calculated by

$$\beta_{ij} = \theta \cdot \left(\frac{1}{1 - 2\alpha_{ij}} \right) \qquad (\text{C-2})$$

where α_{ij} = length factor for beam hinge location at level i and span j (see Fig. C-1(c)).

Equilibrium of forces in the horizontal direction of the whole structure at the collapse stage requires that the sum of lateral forces must equal the base shear strength, V_y, that is,

$$\sum_{i=1}^{N} F_i = \sum_{i=1}^{N} \lambda_i V_y = V_y \qquad (\text{C-3})$$

where the lateral force at any level, F_i, are expressed as a fraction of the base shear strength, F_i = $\lambda_i V_y$. Parameter λ_i is a force distribution factor that depends on the lateral force pattern (first mode, modal, uniform, etc.) utilized to push over the structure (see Section 8). Substitution of (C-2) and (C-3) in (C-1) results in

$$V_y = \frac{1}{\sum\limits_{i=1}^{N}(\lambda_i \cdot h_i)} \cdot \left\{ \sum_{k=1}^{K} M_{pck} + \left[2 \sum_{i=1}^{N} \sum_{j=1}^{n} (M_{pbij} \cdot \chi_{ij}) \right] \right\} \qquad \text{(C-4)}$$

where, h_i = height of level i above the hinge at the base of the structure as shown in Figure C-1(b), and

$$\chi_{ij} = \frac{1}{1 - 2\alpha_{ij}} \qquad \text{(C-5)}$$

Equation (C-4) applies to frames of any geometry provided the collapse mechanism is as shown in Figure C-1(b). However, in practical applications it is common to have same size first-story columns, so that $M_{pck} = M_{pc}$, and same size beams, so that $M_{pbij} = M_{pbi}$ in all spans of a level. Accordingly $\chi_{ij} = \chi_i = 1/(1 - 2\alpha_i)$ and (C-4) takes the simpler form:

$$V_y = \frac{1}{\sum\limits_{i=1}^{N}(\lambda_i \cdot h_i)} \cdot \left\{ (n+1)M_{pc} + 2n \cdot \sum_{i=1}^{N}(M_{pbi} \cdot \chi_i) \right\} \qquad \text{(C-6)}$$

An idealized elastoplastic representation of the pushover curve of a building is characterized by the base shear strength, V_y, and the yield displacement, D_y, as shown in Figure C-2. These quantities vary depending on the pattern of lateral load applied to the system. Consider that the pattern of lateral load is proportional to the first mode of the frame under elastic conditions. The yield displacement can be obtained from the relation between the base shear strength V_y and the fundamental period of the building under elastic conditions, T_i:

$$D_y = \left(\frac{g}{4\pi^2}\right) \cdot \Gamma_1 \cdot \left(\frac{V_y}{\overline{W}_1}\right) \cdot T_1^2 \qquad \text{(C-7)}$$

where Γ_1 = first modal participation factor and $\overline{W}_1$ = first modal weight.

C.2.1 Example C-1

Consider the frame depicted in Figure C-3(a). Assume that plastic hinges in beams form at distance of half the depth of the column section plus one depth of the beam section ($d_c/2+d_b$), and in columns at a distance of one depth (d_c) of column section from the base of the frame. Consider also a lateral force pattern proportional to the first mode.

General Information

Number and Length of Spans: $n = 3$; $L_b = 8230$ mm

Number of Stories: $N = 3$

Material Properties: $F_y = 345$ MPa (50 ksi)

Column Properties: W14x109 ($d_c = 356$ mm; $M_{pc} = 1084$ kN-m)

Beam Properties:
| | | |
Third floor: W14x26 ($d_b = 356$ mm; $M_{pb3} = 227$ kN-m)
Second Floor: W16x40 ($d_b = 406$ mm; $M_{pb2} = 412$ kN-m)
First-Floor: W16x45 ($d_b = 406$ mm; $M_{pb1} = 465$ kN-m)

Floors Weight: $w_3 = 1,567$ kN; $w_2 = w_1 = 2,900$ kN

Story Height: $h_3 = 12,928$ mm; $h_2 = 8,624$ mm; $h_1 = 4,320$ mm

Eigenvalue Analysis: $T_1 = 1.58$ sec.; $\{\phi_1\}^T = [1.000, 0.657, 0.250]$; $\overline{W}_1 = 5871$ kN ; $\Gamma_1 = 1.399$

Evaluation of Parameters α_i, χ_i, and $M_{pbi}\cdot\chi_i$

Parameter α_i is calculated according to $\alpha_i = (d_c/2+d_b)/L_b$, and χ_i is calculated by (C-5).

Floor i	M_{pbi} (kN-m)	α_i	χ_i	$M_{pbi}\cdot\chi_i$ (kN-m)
3	227	0.065	1.149	261
2	412	0.071	1.166	480
1	465	0.071	1.166	542

$$\sum_{i=1}^{N} M_{pbi} \cdot \chi_i = 1283 \text{ kN.m}$$

232

Evaluation of Term $\left[(n+1)M_{pc} + 2n\sum_{i=1}^{N} M_{pbi} \cdot \chi_i\right]$

$$\left[(n+1)M_{pc} + 2n\sum_{i=1}^{N} M_{pbi} \cdot \chi_i\right] = (3+1)\cdot 1084 + 2\cdot 3\cdot 1283 = 12034 \ kN\cdot m$$

First-Mode Pattern Base Shear Strength and Yield Displacement

Calculation of the base shear strength using (C-6) requires evaluation of the term $\sum_{i=1}^{N} \lambda_i \cdot h_i$,

where parameter λ_i is for the first-mode lateral force pattern. This pattern is described by

$\lambda_i = \dfrac{w_i \phi_{i1}}{\sum_{m=1}^{N} w_m \phi_{m1}}$. Calculations are summarized below:

Floor i	w_i (kN)	ϕ_{i1}	h_i (mm)	$w_i \cdot \phi_{i1}$ (kN)	λ_i	$\lambda_i \cdot h_i$ (mm)
3	1567	1.000	12670	1567	0.3734	4731
2	2900	0.657	8367	1905	0.4539	3798
1	2900	0.250	4063	725	0.1727	702

$$\sum_{i=1}^{N} w_i \cdot \phi_{i1} = 4197 kN \qquad \sum_{i=1}^{N} \lambda_i \cdot h_i = 9231 \ mm$$

Note that in the calculation of h_i it was assumed that plastic hinges form at a distance of 356 mm (14") from the base of the structure. Equation (C-6) gives the base shear strength

$$V_y = \left(\frac{1}{9229}\right)\cdot(12034\cdot 1000) = 1304 \ kN$$

Moreover, the yield displacement is calculated by use of (C-7):

233

$$D_y = \left(\frac{9810}{4\pi^2}\right) x 1.4 x \left(\frac{1304}{5871}\right) x 1.58^2 = 192mm$$

Modal (C_{vx}) Pattern Base Shear Strength

Calculation of the base shear strength using (C-6) requires evaluation of the term $\sum\limits_{i=1}^{N} \lambda_i \cdot h_i$,

where parameter λ_i for the modal (C_{vx}) lateral force pattern is described by $\lambda_i = \dfrac{w_i h_i^k}{\sum\limits_{m=1}^{N} w_m h_m^k}$. In

this case of period of $T = 1.58$ sec, the exponent k (NEHRP, 1997) is equal to 1.54. Calculations are summarized below:

Floor i	w_i (kN)	h_i (mm)	h_i (mm)	$w_i \cdot h_i^k$ x10^6	λ_i	$\lambda_i \cdot h_i$ (mm)
3	1567	13028	12670	3404	0.4259	5396
2	2900	8724	8367	3397	0.4250	3556
1	2900	4420	4063	1192	0.1491	606

$$\sum_{i=1}^{N} w_i \cdot h_i^k = 7993 \qquad \sum_{i=1}^{N} \lambda_i \cdot h_i = 9558$$

The base shear strength of the frame for the modal (C_{vx}) lateral force pattern is obtained from (C-6) as

$$V_y = \left(\frac{1}{9558}\right) \cdot (12034 \cdot 1000) = 1259 kN$$

Uniform Pattern Base Shear Strength

Calculation of the base shear strength using (C-6) requires evaluation of the term $\sum_{i=1}^{N} \lambda_i \cdot h_i$.

Parameter λ_i for the uniform lateral force pattern is described by $\lambda_i = \dfrac{w_i}{\sum_{i=1}^{N} w_i}$. Calculations are summarized below:

Floor	w_i (kN)	λ_i	h_i (mm)	$\lambda_i \cdot h_i$ (mm)
3	1567	0.2127	12670	2695
2	2900	0.3936	8367	3294
1	2900	0.3936	4063	1600

$$\sum_{i=1}^{N} \lambda_i \cdot h_i^* = 7589 \text{ mm}$$

Thus, the base shear strength of the frame for the uniform lateral force pattern is obtained from (C-6) as

$$V_y = \left(\frac{1}{7589}\right) \cdot (12034 \cdot 1000) = 1586\,kN$$

Pushover Analysis

Pushover analysis of the frame was performed by using program SAP-2000 NL (version 7.11). The results of the pushover analysis are compared to the predictions of the simple analysis. Two cases are examined for this example: a) pushover analysis without gravity loads and P-Δ effects, and b) pushover analysis with gravity load equal to 14 kN/m at the top floor, and 28 kN/m at the lower floors, and with the P-Δ effects included. Additionally, it is assumed that joints are stiffened within a length equal to half the height of the depth of the column in the horizontal

235

direction, and half the depth of the beam in the vertical direction. At the base, it is assumed that the length of the stiffened portion is equal to the depth of the column section. In this analysis, hinges at beams and columns are modeled to have elastoplastic behavior without considering the effect of axial load. The lateral load is proportional to the first mode. Results are summarized in Tables C-1 and C-2, and are illustrated in Figure C-4. It may be observed the results of plastic analysis compare very well to those of the pushover analysis for all patterns of lateral loads examined.

C.2.2 Examples C-2, C-3, C-4 and C-5

Figures C-3 (b), (c), (d) and (e) show the frames analyzed in examples C-2 through C-5, respectively. Following the same procedure presented in example C-1, the base shear strength V_y of each of these examples was obtained using the plastic analysis approach for the aforementioned pattern of lateral loads. Observe that while the frames of examples C-1, C-2 and C-3 are symmetrical with equal beam sizes at all levels, constant column sections, and equal span lengths, the frame of example C-4 has different (asymmetrical) span lengths and column sizes per column line. In this case the more general expression given by (C-4) was utilized for evaluation of the base shear strength. Furthermore, the 6-story, 3-span frame of example C-5 is included to verify the accuracy of the plastic analysis approach to predict the base shear strength of systems in which the effect of axial loads might be significant. Pushover analysis was performed using program SAP-2000 NL (version 7.11) following the approach of example C-1. However, in example C-5 plastic hinges at the columns were modeled considering the P-M interaction relationship.

C.2.3 Analysis and Results of Examples C-1 through C-5

Table C-1 presents a summary of the results obtained by the plastic analysis approach and by the pushover analyses performed with program SAP-2000NL. It may be observed that the base shear strength predicted by plastic analysis compares well with that predicted by program SAP-2000NL for the case when the gravity load and P-Δ effects are not included. Moreover, plastic analysis slightly overpredicts the base shear strength obtained by SAP-2000NL for the case when gravity load and P-Δ effects are included. It is also evident that consideration of gravity load and

236

P-Δ effects reduces the capacity of the frame. Additionally, consideration of the P-M interaction relationship in the modeling of plastic hinges in columns of example C-5 (6-story frame) results in a decrease of the capacity of the frame, but still the prediction by the plastic analysis approach is acceptable for practical purposes.

The approximate method presented herein has been derived on the basis of the assumption that plastic hinges develop in all beams along the height of the building. It is possible that a particular frame reaches its capacity without developing plastic hinges at all beams. This is likely to occur when the uniform lateral load pattern is applied in tall frames, and depending on the relative beam/column stiffness and plastic capacities. For instance, example C-5 (6-story) reaches the base shear strength under uniform pattern before hinging of the top floor beams. However, the prediction of the base shear strength by the plastic analysis approach was still acceptable for practical purposes.

On the basis of the results presented in this section, it can be stated that the plastic analysis approach can be used with confidence in the prediction of the base shear strength of moment frames with (or without) viscous damping systems provided that the frames have regular geometry, and uniform distribution of strength and stiffness.

C.3 Pushover Curves of Buildings with Yielding Damping Systems

In this section plastic analysis is utilized for the approximate construction of the pushover curve of buildings with yielding damping devices. It is assumed that all the damping devices yield prior to yielding of the framing system.

Consider the frame with damping devices in chevron type configuration subjected to a prescribed pattern of lateral load as shown in Figure C-5a. As the lateral load increases, yielding of the damping devices occurs at a specific story as shown in Figure C-5(b). In this case, yielding of the devices at the second story is shown. As the lateral load increases further, all damping devices yield while the frame is still elastic as illustrated in Figure C-5(c). Eventually a plastic collapse mechanism develops as shown in Figure C-5(d).

Figure C-6 shows a pushover curve and a trilinear representation of the pushover curve of a building with a yielding damping system. The various stages of the pushover illustrated in Figure C-5 are represented by the points a, b, c, and d on the pushover curve of Figure C-6. Segments OA, AB, and BC define the trilinear representation of the pushover curve. Segment OA represents the behavior of the combined system prior to yielding of the damping devices. The stiffness of the system in this portion of the curve, K_t, is equal to the sum of the global stiffness of the frame, K_f, and of the devices, K_d. Segment AB represents the behavior of the system after yielding of the devices. The stiffness of the system in this segment is equal to the stiffness of the frame, K_f.

Consider that a frame with metallic yielding devices is pushed laterally by loads that are proportional to the first mode resulting in the displacements D_i. The displacement of floor i, D_i, can be related to the roof displacement by $D_i = \phi_{i1}.D_{roof}$. Accordingly, the interstory drift between levels j and i can be written as, $\Delta_j = D_j - D_i$, or $\Delta_j = (\phi_{j1} - \phi_{i1}).D_{roof}$, or $\Delta_j = \phi_{rj}.D_{roof}$, where ϕ_{rj} is the modal drift. When yielding of the damping devices occurs at story j, the interstory drift can be written as $\Delta_{y_j} = \phi_{rj}.D_{roof\ yj}$, from where the displacement of the roof when yielding of the devices at level j occurs can be expressed as

$$D_{roof_{yj}} = \frac{\Delta_{y_j}}{\phi_{rj}} \tag{C-8}$$

The displacement of the roof when all damping devices yield (point A in Figure C-6), D_{yd}, can be defined as the maximum value of the displacement obtained by (C-8)

$$D_{yd} = \max_j \left(\frac{\Delta_{yj}}{\phi_{rj}} \right) \tag{C-9}$$

Using the modal properties of the combined system, it can be shown that base shear of the building when all damping devices yield, $V_d + K_f.D_{yd}$ (see Fig. C-6) is given by

238

$$V_d + K_f D_{yd} = \left(\frac{4\pi^2}{gT_{1c}^2}\right) \cdot \left(\frac{D_{yd}}{\Gamma_1}\right) \cdot \overline{W}_1 \qquad\qquad \text{(C-10)}$$

where, T_{1c} = fundamental period of the combined system, Γ_1 = first modal participation factor of the combined system, and $\overline{W}_1$ = first modal weight of the combined system.

The base shear strength of the system, V, is equal to the sum of the yield strength of the frame, V_y, and the strength of the devices in the first story, V_{d1}, when yielding of both the frame and the devices occurs, that is

$$V = V_y + V_d = V_y + V_{d1} \qquad\qquad \text{(C-11)}$$

Of interest is to note that strength V_d is contributed by the yielding damping devices at the first story, whereas the contribution of the other damping devices to the pushover curve is reflected in the initial branch of the trilinear pushover curve. However, the above assumptions are true if the yielding of the damping devices does not change the plastic collapse mechanism of the frame, which may often occur.

Equations (C-9), (C-10) and (C-11) are sufficient to characterize the trilinear representation of the behavior of the combined system. Note that the yield displacement of the frame (exclusive of the devices) D_{yf} is presumed known. Moreover, definition of an equivalent elastoplastic representation of the pushover curve as shown in Figure C-7 is desirable for application of simplified analysis procedures. The effective initial stiffness, K_1, of the equivalent elastoplastic representation can be defined as the slope of the straight line that intersects the trilinear curve at a base shear equal to bV, where b is a parameter selected so that the elastoplastic curve best represent the trilinear curve. Herein a value of b equal to 0.6 is used in consistency with a similar approach followed in FEMA (1997). The value of the roof displacement at the intersection point, D_o, can be easily established on the basis of Figure C-7 and the modal properties of the frame (without damping devices) as

$$D_o = \left(\frac{g}{4\pi^2}\right) \cdot \Gamma_{1f} \cdot \left(\frac{0.6V - V_d}{W_{1f}}\right) \cdot T_{1f}^2 \qquad\qquad \text{(C-12)}$$

where, Γ_{1f} = first modal participation factor of the frame (without damping devices), T_{1f} = fundamental period of the frame (without damping devices), and $\overline{W}_{1f}$ = first modal weight (without damping devices).

The effective initial (secant) period, T_1, of the structure inclusive of the damping system in its equivalent elastoplastic representation can be expressed as

$$T_1 = 2\pi. \sqrt{\frac{D_0 / \Gamma_1}{\left(\dfrac{0.6V}{\overline{W}_1}\right) \cdot g}} \qquad (C\text{-}13)$$

Accordingly, the yield displacement of the equivalent elastoplastic representation is given by

$$D_y = \left(\frac{g}{4\pi^2}\right) \cdot \Gamma_1 \cdot T_1^2 \cdot \left(\frac{V}{\overline{W}_1}\right) \qquad (C\text{-}14)$$

Equations (C-11),(C-13) and (C-14), along with the modal properties of the combined system (under elastic conditions) can be directly used in the application of the simplified analysis procedures.

It should be noted that parameters D_y, and D_o are defined herein as the values of the roof displacement at which, respectively, yielding occurs and the base shear equals 0.6V. However, in Section 7.5.4 the same symbols are used to denote the corresponding quantities in the spectral representation of the pushover curve. That is, the two quantities differ by factor Γ_1 as illustrated in Figure 7-4.

C.3.1 Example C-6

Consider the 3-story special steel moment frame with triangular metallic yielding devices (Tsai et al., 1993) as shown in Figure C-8(a). The devices are made of steel with yield strength F_y = 248 MPa (36 ksi) and the dimensions shown in Figure C-8(b). They are supported on steel square tube TS8x8x1/2 braces in a chevron configuration. The base shear strength of the frame

240

exclusive of the damping devices and for a lateral load pattern proportional to the first mode is V_y = 1220 kN (275 kips) and the corresponding yield displacement is D_{yf} = 182 mm. The base shear strength and the yield displacement of the frame exclusive of the yielding damping devices were determined by the procedures described in Section C.2. Eigenvalue analysis of the frame exclusive of the damping devices gave: T_{lf} = 1.58 sec, $\overline{W}_{1f}$ = 5871 kN, and Γ_{1f} = 1.399. Eigenvalue analysis of the frame inclusive of the damping devices gave: T_{lc} = 1.133 sec, $\{\phi_{1c}\}^T$ = [1.000 0.708 0.296], $\{\phi_{rj}\}^T$ = [0.292 0.412 0.296], $\overline{W}_1$ = 6125 kN and Γ_1 = 1.3676. Calculations for the construction of the pushover curve of the building follow.

General Information

Number of yielding steel devices per story

First story:	$N_1 = 12$
Second Story:	$N_2 = 9$
Third Story:	$N_3 = 7$

Dimensions of yielding steel devices: $b = 305\ mm;\ h = 457\ mm;\ t = 25.4\ mm$
(see Fig. C-8)

Yield strength of the yielding steel devices: $F_y = 248\ MPa\ (36\ ksi)$

Young's Modulus: $E = 200\ kN/mm^2$

Yield Strength and Stiffness of Damping Devices

The yield strength V_d and stiffness K_d of yielding steel devices are given by (E-28) and (E-30) in Appendix E.

$$V_{di} = N_i \frac{F_y b t^2}{4h} = N_i \frac{0.248 x 305 x 25.4^2}{4 x 457} = 26.70 N_i$$

241

$$V_{d1} = 26.7x12 = 320 \ kN$$
$$V_{d2} = 26.7x9 = 240 \ kN$$
$$V_{d3} = 26.7x7 = 187 \ kN$$

$$K_{di} = N_i \frac{Ebt^3}{6h_i^3} = N_i \frac{200x305x25.4^3}{6x457^3} = 1.746 \ N_i$$

$$K_{d1} = 1.746x12 = 21.0 \ kN\!/_{mm}$$
$$\therefore \quad K_{d2} = 1.746x9 = 15.7 \ kN\!/_{mm}$$
$$K_{d3} = 1.746x7 = 12.2 \ kN\!/_{mm}$$

Yield Displacement of Damping Devices

The yield displacement of the devices is given by (E-18) as $\Delta_{yi} = \frac{3}{2} \cdot \left(\frac{F_y}{E} \cdot \frac{h^2}{t} \right)_i$. Accordingly,

$$\Delta_{yi} = \frac{3}{2} x \left(\frac{0.248}{200} x \frac{457^2}{25.4} \right)_i = 15.3 \ mm$$

It may be noted that since the devices in all stories have the same dimensions h and t and are made of the same material, the yield displacement is the same in all stories.

Evaluation of D_{yd}

According to (C-9), D_{yd} is equal to the maximum value of the ratio Δ_{yi}/ϕ_{rj}, for j=1 to the number of stories. Since the yield displacement in this case is constant, it is obvious that the maximum ratio occurs at the story for which ϕ_{rj} is minimum, that is,

$$D_{yd} = \frac{15.3}{0.292} = 52.4 \ mm$$

Evaluation of $V_d + K_f D_{yd}$

$V_d + K_f D_{yd}$ is given by (C-10)

$$V_d + K_f D_{yd} = \left(\frac{4\pi^2}{9810 x 1.133^2} \right) x \left(\frac{52.4}{1.3676} \right) x 6125 = 736.5 \, kN$$

Base Shear Strength of Frame Inclusive of Damping System, V

According to (C-11), the base shear strength V is equal to the sum of the base shear strength of the frame V_y (exclusive of the damping devices) and the yield strength of the devices in the first story V_{d1}. Accordingly,

$$V = V_y + V_{d1} = 1220 + 320 = 1540 \, kN$$

The values of D_{yd}, $V_d + K_f D_{yd}$ and V, along with the yield displacement of the frame D_{yf} are sufficient to define the trilinear representation of the pushover curve of the system.

Evaluation of Displacement D_0

Using (C-12)

$$D_0 = \left(\frac{9810}{4\pi^2} \right) x 1.399 x \left(\frac{0.6 x 1540 - 320}{5871} \right) x 1.58^2 = 89.3 \, mm$$

Effective Initial (secant) Period T_1

Using (C-13)

$$T_1 = 2\pi \sqrt{ \frac{ 90.3 \big/ 1.3676 }{ \left(\frac{0.6 x 1540}{6125} \right) x 9810 } } = 1.327 \, sec$$

Yield Displacement D_y

Using (C-14)

$$D_y = \left(\frac{9810}{4\pi^2} \right) x 1.3676 x \left(\frac{1540}{6125} \right) x 1.327^2 = 150.5 \, mm$$

243

The base shear strength V and the corresponding yield displacement D_y are sufficient to characterize the elastoplastic representation of the trilinear curve of the frame.

Pushover Curve

Pushover analysis of the structure inclusive of the damping devices was performed using program SAP-2000NL. The structure was pushed with loads proportional to the first mode. Hinges in beams and columns were modeled using elastoplastic models of behavior. Hinges in beams were assumed to form at the faces of the columns, while hinges were assumed to form in the columns at a height of 356 mm (14 in.) from the base. Joints were assumed to be stiff within a distance equal to half the depth of the beam (or column) section. A similar model was utilized to perform the pushover analysis of the frame without the damping devices.

Figure C-9 presents the pushover curves obtained by program SAP-2000NL for the frame with and without the damping devices. Also shown are the trilinear and the elastoplastic representations of the pushover curve as constructed using the approximate procedures presented in this section. Evidently, the presented simplified analysis procedure predicts very well the pushover curve of the frame with a yielding damping system.

C.4 Pushover Curve of Buildings with Viscoelastic Damping systems

Viscoelastic damping systems increase both the stiffness and the strength of a building as shown in Figure C-10. The bilinear representation of the pushover curve in this case is characterized by the yield displacement D_y, the base shear strength V_y, and the post-elastic to elastic stiffness ratio α. These parameters are related to the properties and geometry of the damping system and the base shear strength, V_{yf}, and yield displacement, D_{yf}, of the frame exclusive of the damping system. The latter may be determined by the procedures described in Section C.2.

Consider a frame with solid viscoelastic devices subjected to a prescribed pattern of lateral loads as shown in Figure C-11 (a). Each viscoelastic device is characterized by the effective stiffness, K_j, and effective damping constant, C_j. However, for the pushover analysis only the stiffness part is considered as illustrated in Figure C-11 (b). These stiffnesses represent the

244

storage stiffness of each device evaluated at the fundamental frequency of the system (Constantinou et al., 1998).

The global initial stiffness K_t of the combined system is equal to the sum of the stiffnesses of the frame (exclusive of the devices) and the stiffness provided by the devices. It can be shown that K_t can be expressed as function of the fundamental period of the frame inclusive of the damping devices, T_1, the first modal participation factor Γ_1 and the first modal weight $\overline{W}_1$ of the combined system

$$K_t = \left(\frac{2\pi}{T_1}\right)^2 \cdot \frac{\overline{W}_1}{\Gamma_1 \cdot g} \tag{C-15}$$

Period T_1 and the modal properties of the frame inclusive of the damping devices can be determined by eigenvalue analysis. However, when a complete vertical distribution of the damping devices is used, the fundamental mode shapes of the frame with and without the damping system have small differences so that the mode shape of the frame without the damping system may be used. Accordingly, (7-49) and (7-53) may be used to estimate period T_1 and parameter α.

Construction of the pushover curve requires knowledge of the yield displacement D_y. This displacement is assumed to be the one of the frame exclusive of the damping systems, which can be calculated by the procedures of section C.2. It follows that the base shear strength of the combined system is given by

$$V_y = \left(\frac{4\pi^2}{g \cdot T_1^2}\right)\left(\frac{\overline{W}_1}{\Gamma_1}\right) \cdot D_y \tag{C-16}$$

C.4.1 Example C-7

Consider the 3-story special steel moment frame with the uniform vertical distribution of viscoelastic devices shown in Figure C-12(a). Each of these viscoelastic devices has bonded area equal to $A_b = 626{,}330$ mm² (four 15.5 by 15.5 in. areas) and thickness $h = 140$ mm (5.5 in.) made of material 3M ISD110 (Zimmer, 1999) with approximate storage and loss shear moduli

$G' \approx G'' = 0.83\,MPa$ at temperature of 20° C and frequency of about 0.7 Hz. Note that stiffness K is the storage stiffness and damping constant C is the loss stiffness divided by frequency as described by equation (7-43). Note that the frequency is the frequency of the mode of interest. In this case the frequency is that of the first mode of the frame inclusive of the damping system estimated by (7-49) with $\eta = 1.0$. It should be noted that the dimensions of the viscoelastic devices appear large. The large dimensions resulted from the restriction of a shear strain amplitude in the viscoelastic material of 100% in the maximum considered earthquake (1.5 times the design basis earthquake). Such limit appears reasonable at this time but improvements in the materials and bonding processes may justify higher limits. These devices provide additional viscous damping ratio of 0.086 under elastic conditions. The damping ratio β_{V1} was calculated on the basis of (7-29) with $f_j = cos\theta_j$ and using the mode shape and period T_1 of the frame inclusive of the damping devices (including the storage stiffness of the devices). However, the same result was obtained when use was made of the mode shape of the frame exclusive of the damping system and the period based on (7-49).

The base shear strength of the frame (exclusive of the damping devices) is 1220 kN (275 kips) and the corresponding yield displacement is 182 mm. Eigenvalue analysis of the frame (exclusive of the devices) gave: $T_{1f} = 1.58$ sec, $\{\phi_{i1}\}^T = [1.000\ 0.657\ 0.250]$, $\overline{W}_{1f} = 5871$ kN, and $\Gamma_{1f} = 1.399$. Eigenvalue analysis of the frame inclusive of the damping devices gave: $T_{1c} = 1.473$ sec, $\{\phi_{i1}\}^T = [1.000\ 0.684\ 0.275]$, $\overline{W}_1 = 6013$ kN and $\Gamma_1 = 1.38$. The results of the eigenvalue analysis of the frame with the damping devices are presented for the purpose of demonstrating (a) the usefulness of (7-49) in predicting the period, and (b) that the modal properties of the frame with the damping devices are basically the same as those of the frame exclusive of the damping system.

General Information

Base shear strength of the frame (w/o devices): $V_{yf} = $ *1220 kN*

Yield displacement of the frame (w/o devices): $D_{yf} = $ *182 mm*

Damping constant of the devices $C_j = $ *0.876 kN-s/mm*

Storage stiffness of the devices : $K_j =$ 3.70 $kN\text{-}s/mm$

Calculation of Initial Stiffness, K_t

Stiffness K_t was evaluated by (C-15) using the approximate period given by (7-49) with $\eta = 1.0$ and the modal properties of the frame without damping devices:

$$T_1 \approx 1.58x\sqrt{1 - \frac{2x0.086}{1.0}} = 1.44 \ sec$$

$$K_t = \left(\frac{2\pi}{1.44}\right)^2 x \frac{5871}{1.399x9810} = 8.1 \ kN / mm$$

Also use of (C-15) with the modal properties of the frame inclusive of the damping system gives

$$K_t = \left(\frac{2\pi}{1.473}\right)^2 x \frac{6013}{1.38 \cdot 9810} = 8.1 \ kN / mm$$

Base Shear Strength of the Combined System, V_y

Using (C-16)

$$V_y = \left(\frac{4\pi^2}{9810x1.44^2}\right) x \left(\frac{5871}{1.399}\right) x182 = 1482 \ kN$$

Post-Elastic to Elastic Stiffness Ratio, α

Using (7-53)

$$\alpha = \frac{2x0.086}{1.0} = 0.172$$

Pushover Analysis

Pushover analysis of the frame with the damping devices as shown in Figure C-11(b) was performed in program SAP-2000NL. The structure was pushed over by forces proportional to the first mode using the modal properties of the combined system under elastic conditions. Hinges in

247

beams and columns were modeled as elastoplastic elements. Hinges in beams were assumed to form at the faces of the columns while hinges at the base of the structure are assumed to develop at a height of 356 mm (14 in.) above the base. Joints were assumed to be stiff within a distance equal to half the depth of the beam (or column) section.

Figure C-13(a) present the pushover curves of the frame with and without the damping system as obtained by program SAP-2000NL and compares them to the results of approximate analysis. Evidently, the approximate analysis predicts well the pushover curve. It is of interest to observe that the addition of the viscoelastic devices caused an increase of about 20% in both the strength and the stiffness of the frame.

Examples C-8 and C-9

Example C-8 is also a 3-story frame as shown in Figure C-12 (b) but much stiffer and stronger then the frame of example C-7. The damping devices provide an additional viscous damping β_{V1} equal to 0.06 under elastic conditions. The base shear strength of the frame (exclusive of the devices) is 3210 kN (722 kips) and the corresponding yield displacement is 173 mm. Eigenvalue analysis of the combined system (frame with damping devices) gave: $T_{1c} = 1.365$ sec, $\{\phi_{i1}\}^T =$ [1.000 0.792 0.413], $\overline{W}_1 = 11955$ kN and $\Gamma_1 = 1.31$. Using these modal properties:

(C-15): $$K_t = \left(\frac{2\pi}{1.365}\right)^2 x\frac{11955}{1.31x9810} = 19.7 \ kN/mm$$

(C-16): $$V_y = \left(\frac{4\pi^2}{9810x1.365^2}\right)x\left(\frac{11955}{1.31}\right)x173 = 3410 \ kN$$

(7-53): $$\alpha = \frac{2x0.06}{1.0} = 0.12$$

Figure C-13(b) compares the approximate pushover curve to that obtained by analysis using program SAP-2000NL. The comparison is very good.

Example C-9 is a 6-story frame as shown in Figure C-12(c). The viscoelastic devices provide an

additional viscous damping β_{V1} equal to 0.12 under elastic conditions. The base shear strength of the frame (exclusive of the damping devices) is 1730 kN (389 kips) and the corresponding yield displacement is 360 mm. Eigenvalue analysis of the combined system (frame with damping devices) gave: $T_{1c} = 2.367$ sec, $\{\phi_{i1}\}^T = [1.000\ \ 0.893\ \ 0.717\ \ 0.568\ \ 0.302\ \ 0.113]$, $\overline{W}_1 = 12392$ kN and $\Gamma_1 = 1.39$. Using these modal properties:

(C-15):
$$K_t = \left(\frac{2\pi}{2.363}\right)^2 x \frac{12392}{1.39x9810} = 6.4\ kN/mm$$

(C-16):
$$V_y = \left(\frac{4\pi^2}{9810x2.363^2}\right)x\left(\frac{12392}{1.39}\right)x360 = 2313\ kN$$

(7-53):
$$\alpha = \frac{2x0.12}{1.0} = 0.24$$

The pushover curve in this case is also constructed using program SAP-2000NL and utilizing the first mode lateral load distribution and the modal properties of the combined system under elastic conditions. Plastic hinges in beams were modeled using an elastoplastic model, whereas plastic hinges in the columns were modeled using the M-P interaction relationship. Gravity loads and P-Δ effects were also included in the analysis. As shown in Figure C-13(c) the approximate pushover curve compares well with the one obtained by program SAP-2000NL although it may be seen that the predicted strength is about 7% larger than the actual one.

TABLE C-1 Comparison of Base Shear Strength Calculated by Plastic Analysis and Analysis Using Program SAP-2000NL

Example	Lateral Load Pattern	Plastic Analysis V_y (kN)	SAP-2000NL Pushover V_y (kN) A	B
C-1	First Mode	1304	1312	1272
	Modal (C_{vx})	1259	1263	1227
	Uniform	1585	1592	1530
C-2	First Mode	1744	1765	1734
	Modal (C_{vx})	1718	1734	1707
	Uniform	2133	2161	2112
C-3	First Mode	2435	2450	2419
	Modal (C_{vx})	2421	2454	2423
	Uniform	2990	3015	2970
C-4	First Mode	3314	3295	3210
	Modal (C_{vx})	3130	3068	2992
	Uniform	3698	3695	3584
C-5	First Mode	1848	1881	1730
	Modal (C_{vx})	1666	1690	1574
	Uniform	2375	2410	2188

A = pushover analysis without gravity load and P-Δ effects
B = pushover analysis with gravity load and P-Δ effects

TABLE C-2 Comparison of Yield Displacement Calculated by Plastic Analysis and Analysis Using Program SAP-2000NL

Example	First Mode Properties T_I (sec)	$\overline{W}_I$ (kN)	Γ_I	Weight (kN)	Plastic Analysis V_y (kN)	D_y (mm)	SAP-2000 Pushover Analysis with P-Δ and Gravity Loads Effects V_y (kN)	D_y (mm)
C-1	1.580	5871	1.40	7368	1304	192	1272	188
C-2	1.331	5803	1.41	7367	1744	186	1734	185
C-3	1.119	5749	1.41	7367	2435	186	2419	185
C-4	1.403	11934	1.32	13339	3314	179	3210	173
C-5	2.678	12081	1.41	16067	1848	385	1730	360

Pattern of Lateral Loads Proportional to First Mode

250
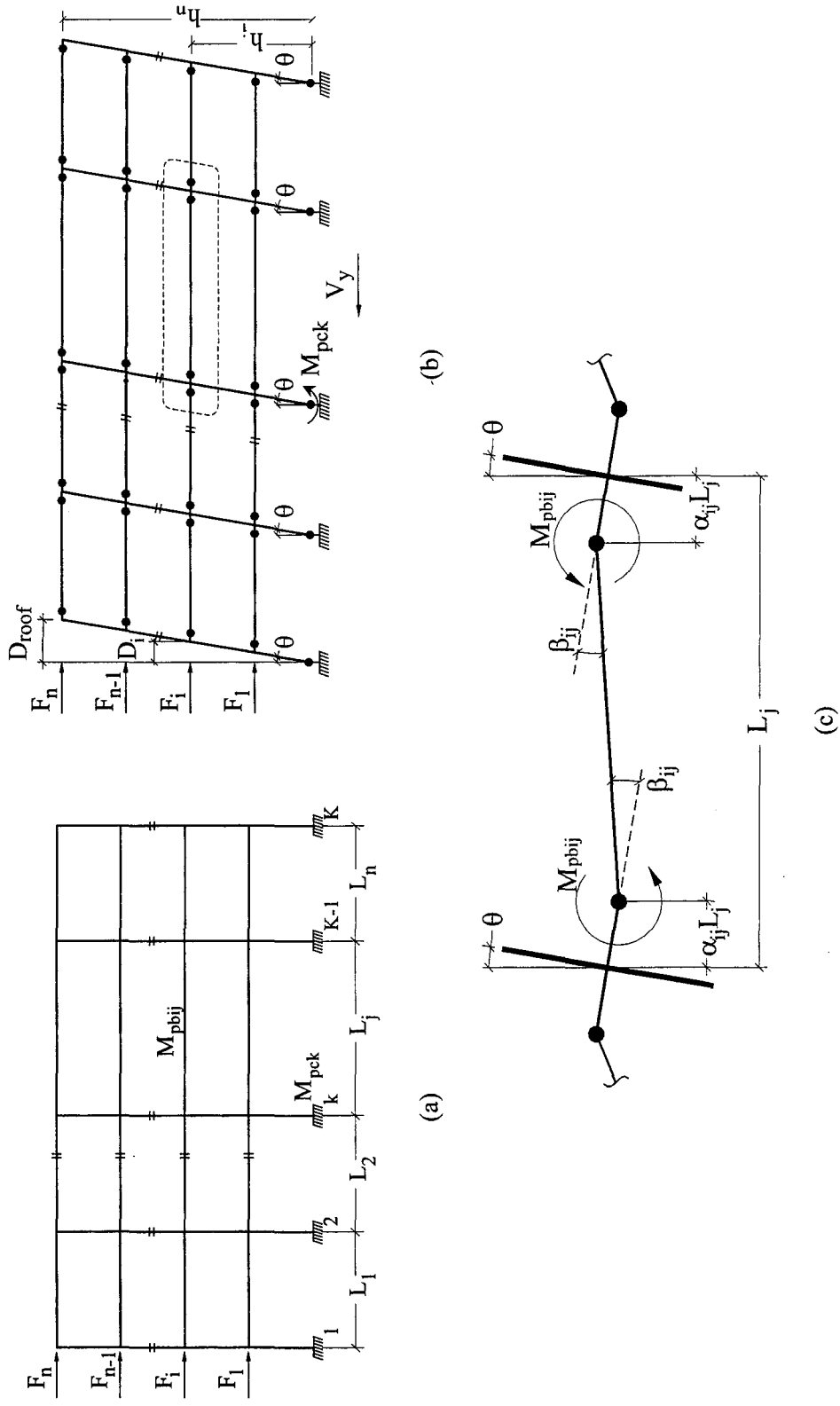
FIGURE C-1 N-Story, n-Bay Moment Frame and Assumed Collapse Mechanism
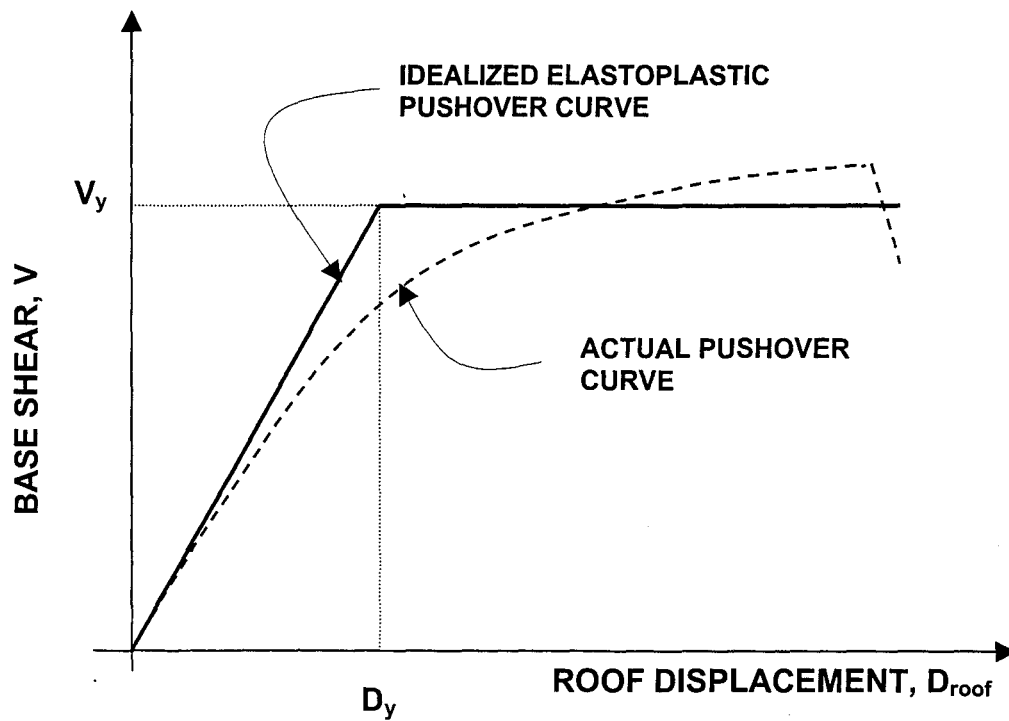
FIGURE C-2 Bilinear Representation of Pushover Curve of Building without a Damping System (or with a Viscous Damping System)
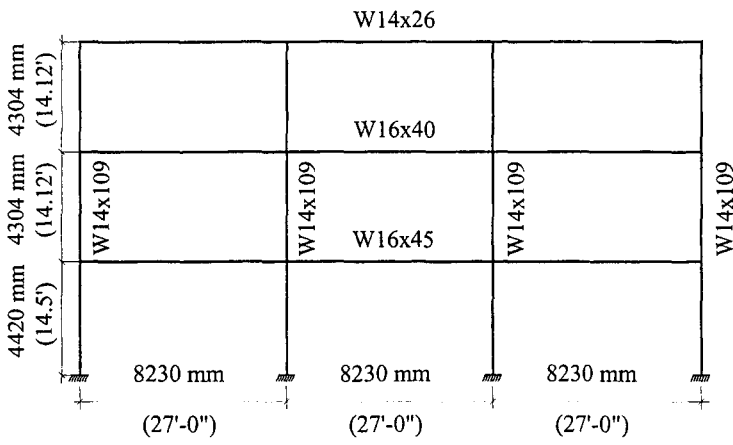
(a) Example C-1

Floor Weight

W_3=1567 kN (352.4 kips)
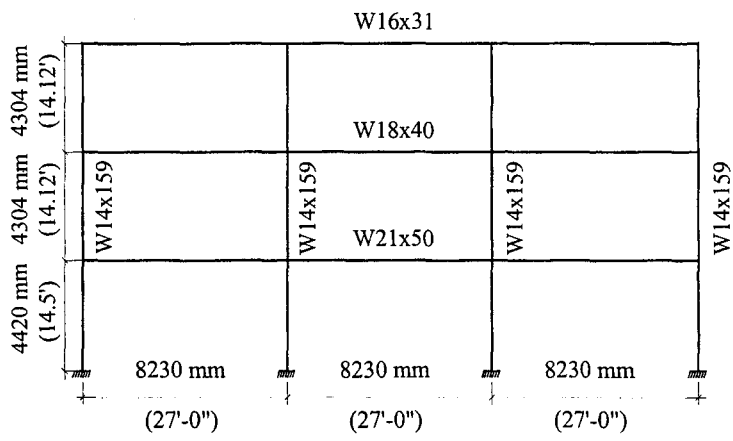
W_2=2900 kN (652.2 kips)

W_1=2900 kN (652.2 kips)

W_T=7367 kN (1656.8 kips)

(b) Example C-2
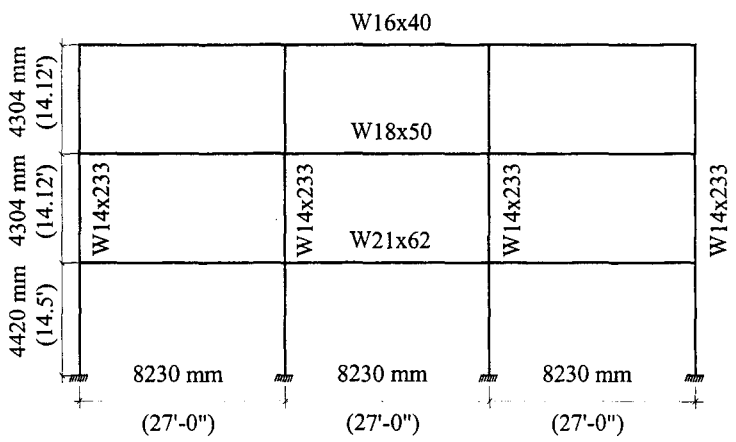
W_3=1567 kN (352.4 kips)

W_2=2900 kN (652.2 kips)

W_1=2900 kN (652.2 kips)

W_T=7367 kN (1656.8 kips)

(c) Example C-3

W_3=1567 kN (352.4 kips)

W_2=2900 kN (652.2 kips)

W_1=2900 kN (652.2 kips)

W_T=7367 kN (1656.8 kips)

FIGURE C-3 Analyzed Steel Moment Frames

253
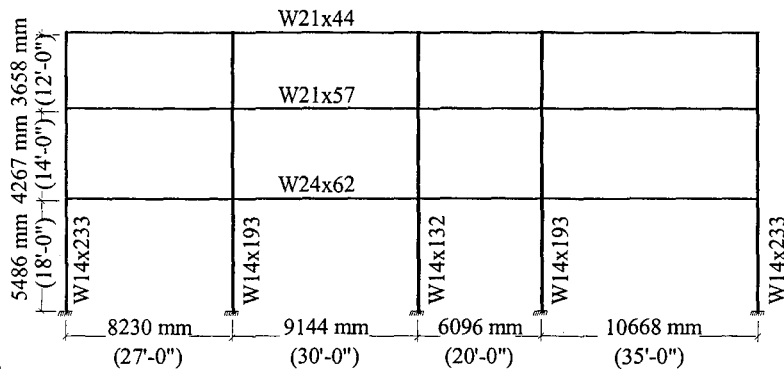
(d) Example C-4

Floor Weight	
W_3=2668 kN	(600 kips)
W_2=5336 kN	(1200 kips)
W_1=5336 kN	(1200 kips)
W_T=13340 kN	(3000 kips)

(e) Example C-5
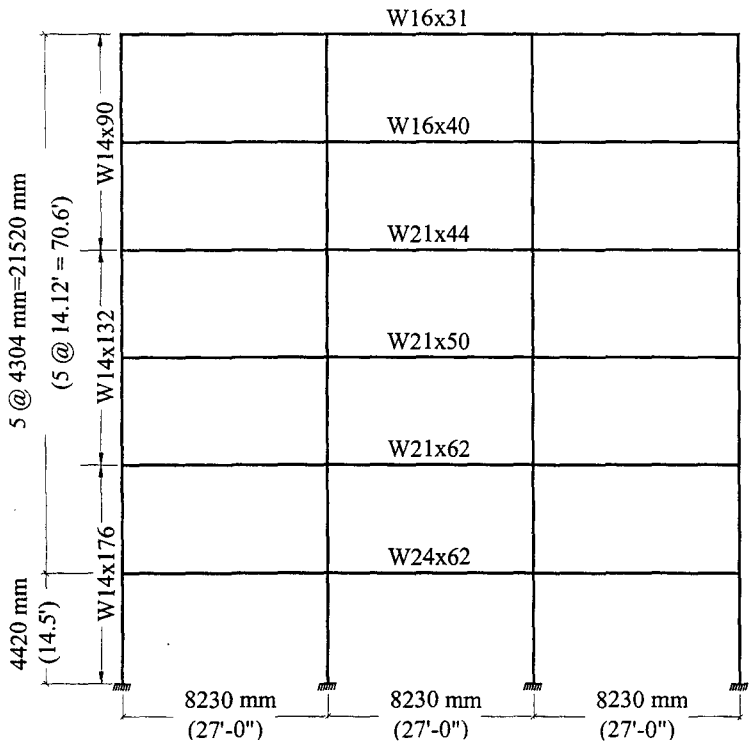
Floor Weight	
W_6=1567 kN	(352.4 kips)
W_5=2900 kN	(652.2 kips)
W_4=2900 kN	(652.2 kips)
W_3=2900 kN	(652.2 kips)
W_2=2900 kN	(652.2 kips)
W_1=2900 kN	(652.2 kips)
W_T=16067 kN	(3613.4 kips)

FIGURE C-3 continued

254
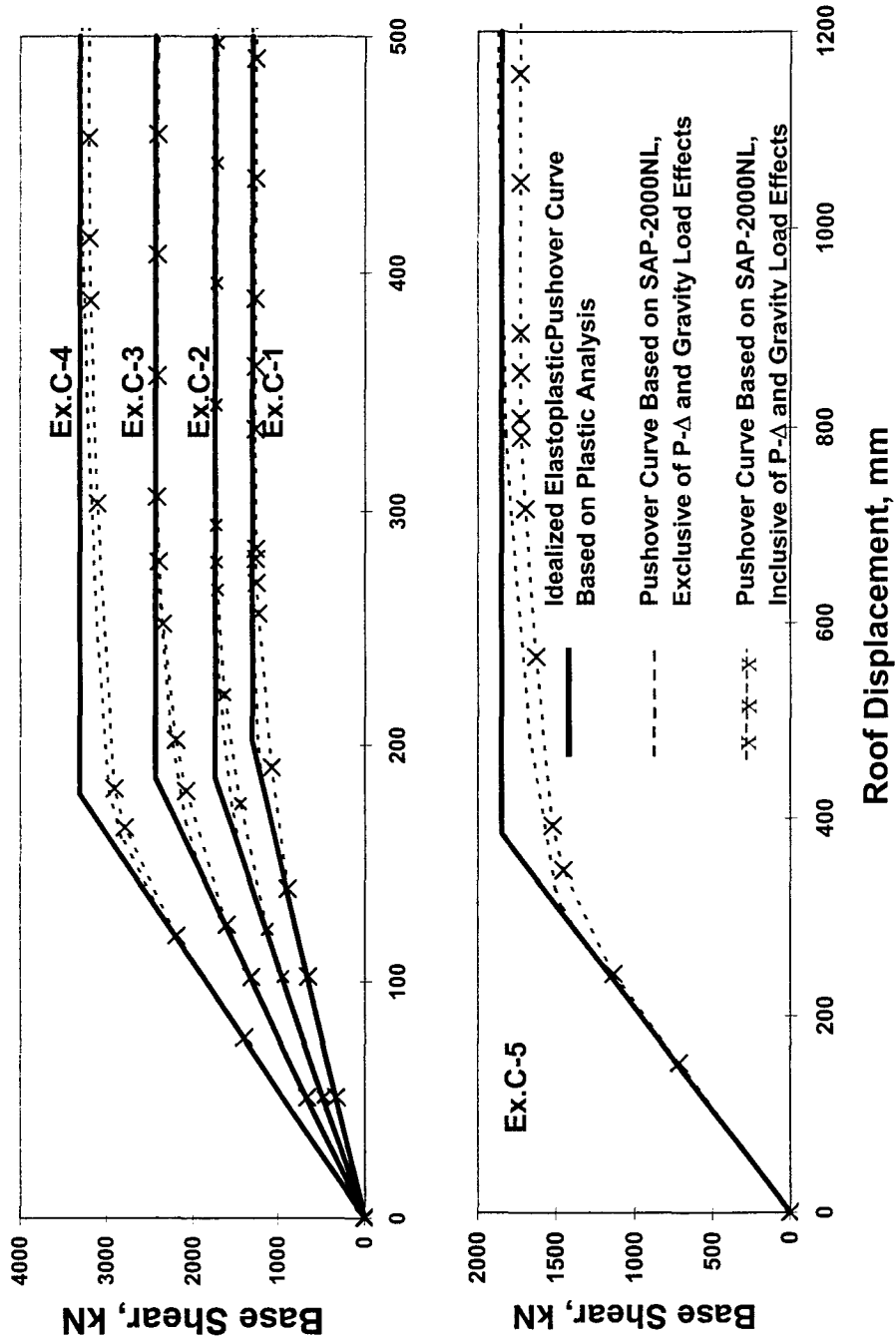
FIGURE C-4 Comparison of Idealized Elastoplastic Pushover Curves Based on Plastic Analysis and Pushover Curves Calculated Using Program SAP-2000NL

255

ELASTIC BEHAVIOR
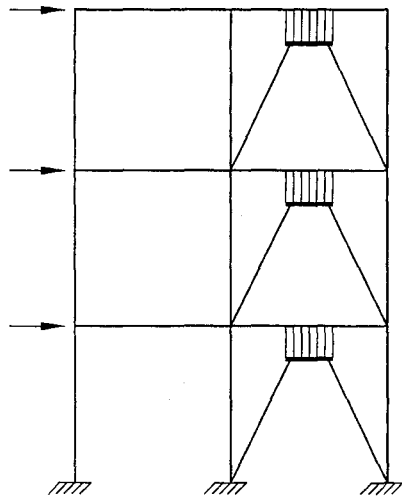
FIRST YIELDING IN DAMPING
DEVICES

(a)
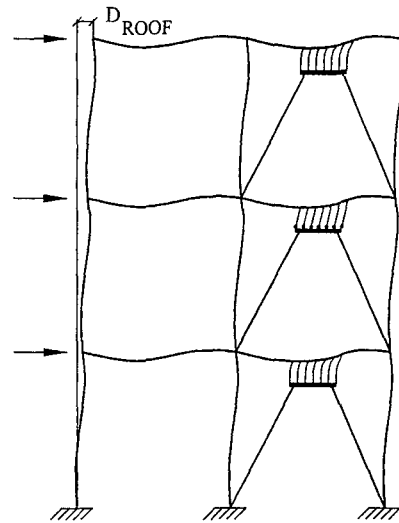
(b)

YIELDING IN ALL DAMPING DEVICES,
FRAME STILL ELASTIC

COLLAPSE MECHANISM

(c)
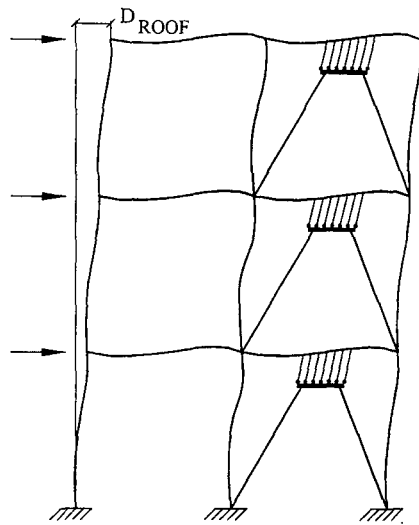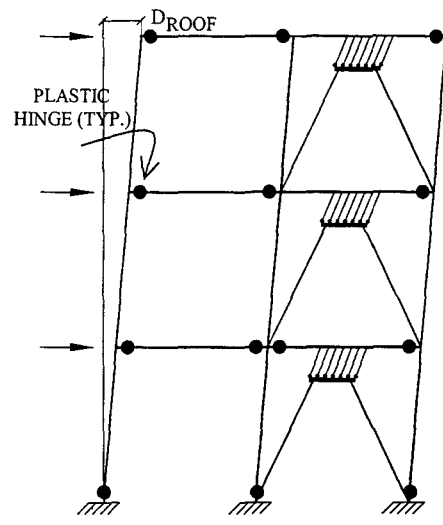
(d)

FIGURE C-5 Frame with Metallic Damping Devices
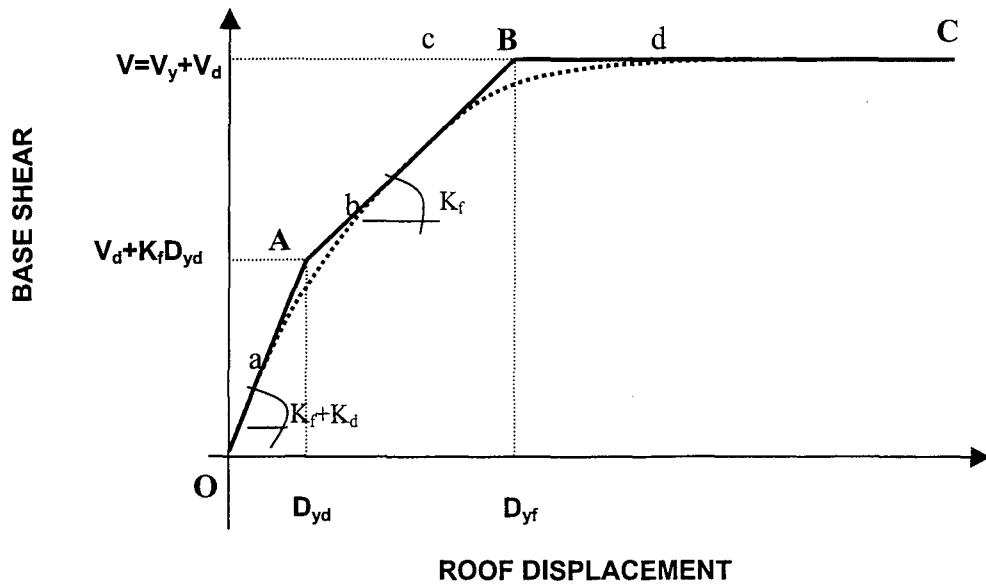
FIGURE C-6 Trilinear Representation of Pushover Curve of Building with Yielding Damping System
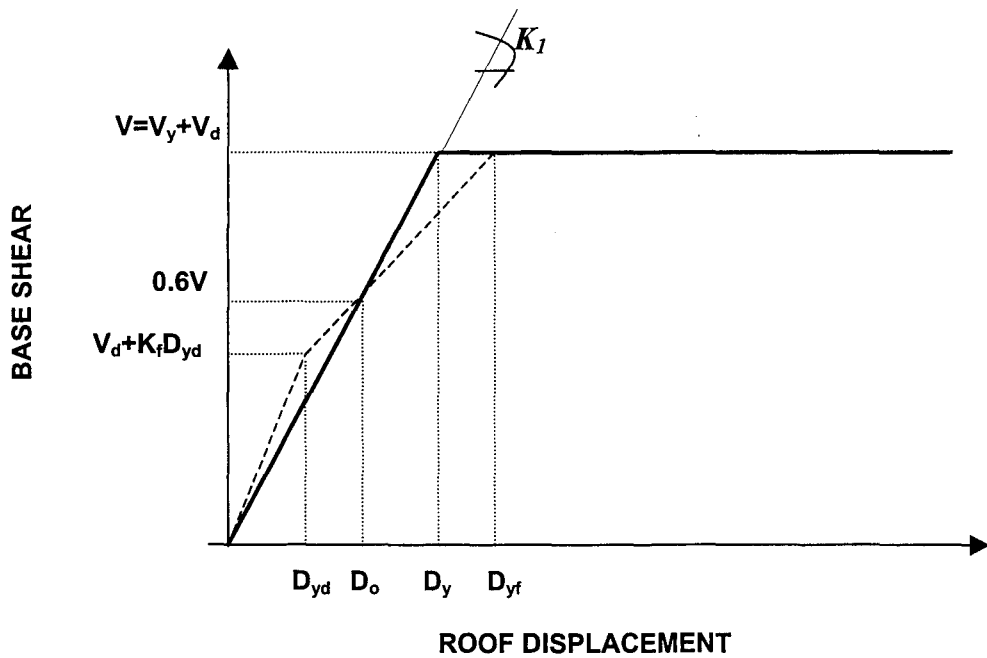
FIGURE C-7 Trilinear and Equivalent Elastoplastic Representation of Pushover Curve of Building with Yielding Damping System

257
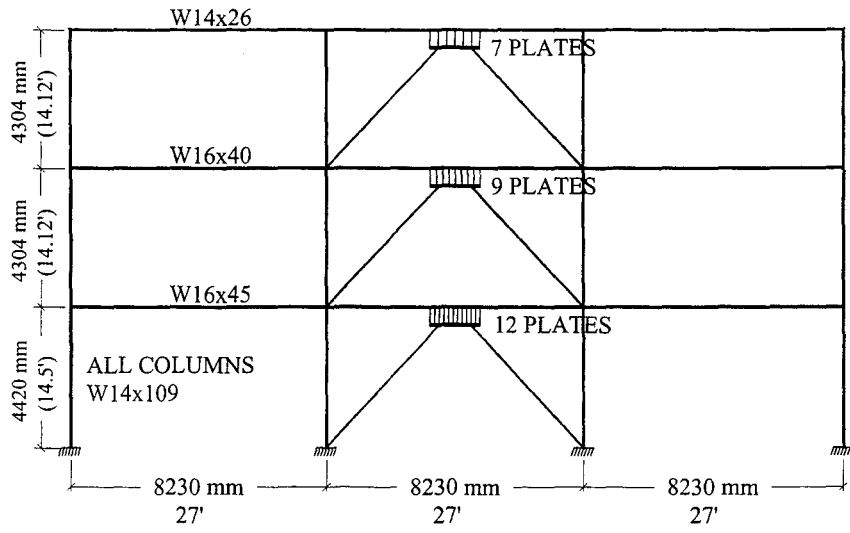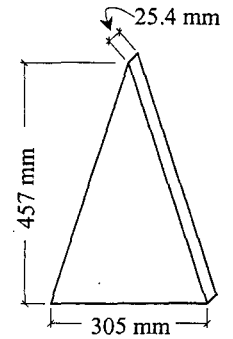
FIGURE C-8 Frame of Example C-6 with Metallic Yielding Devices
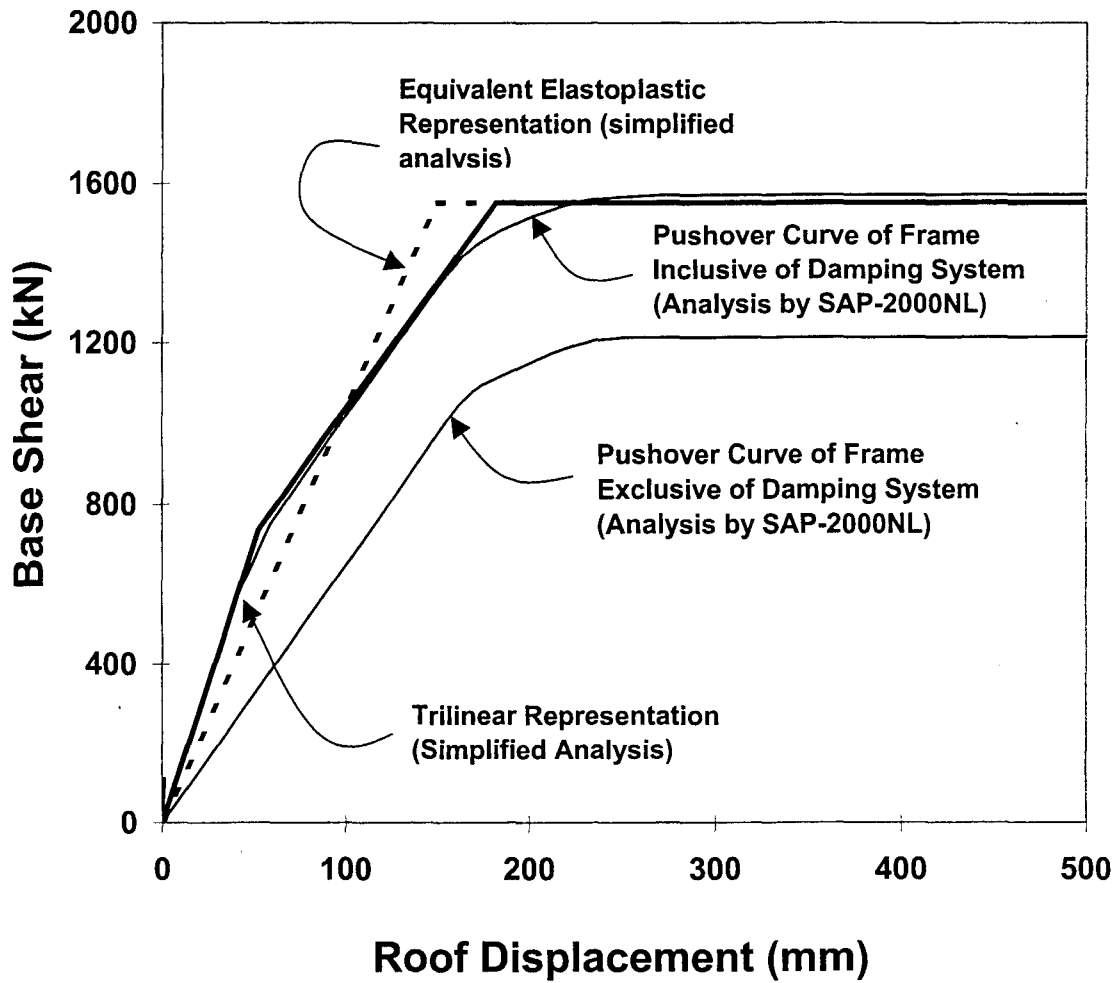
FIGURE C-9 Comparison of Pushover Curves of Frame with and without Yielding Damping System Obtained by Simplified Analysis and by Computer Analysis

259
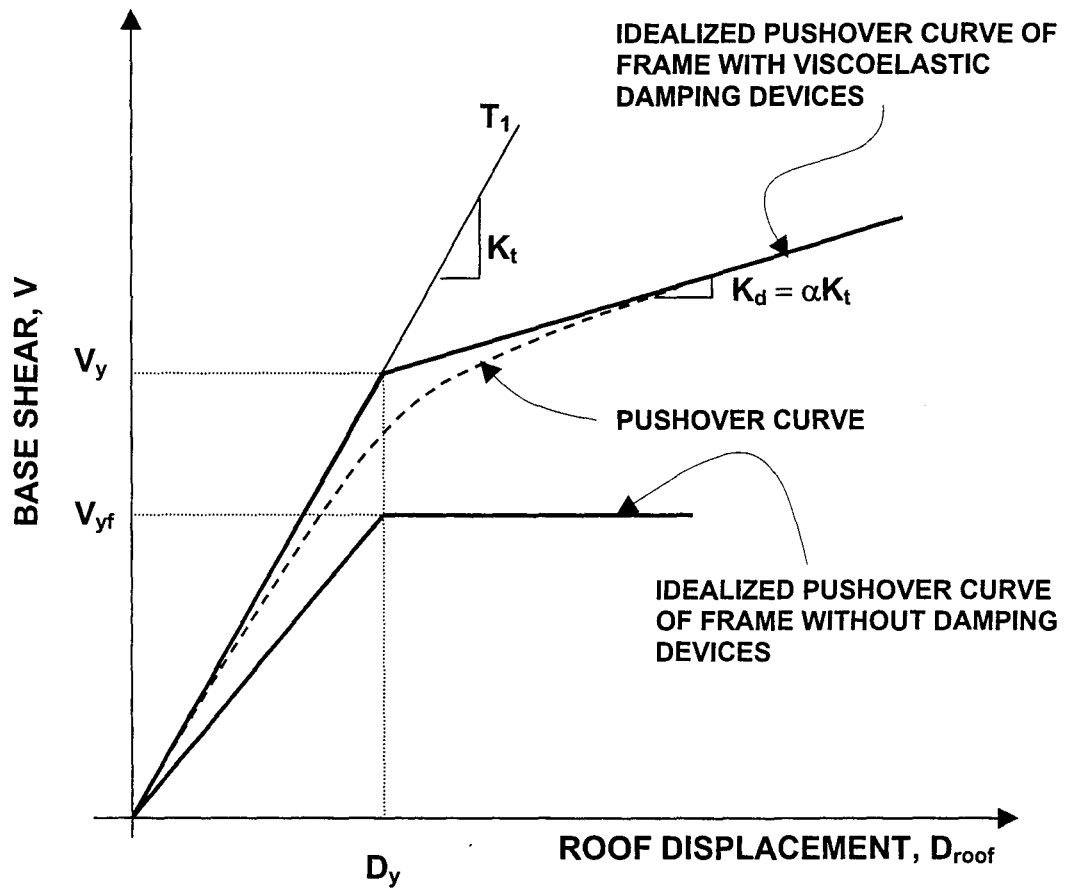
FIGURE C-10 Pushover Curves of Frame with Viscoelastic Damping Devices
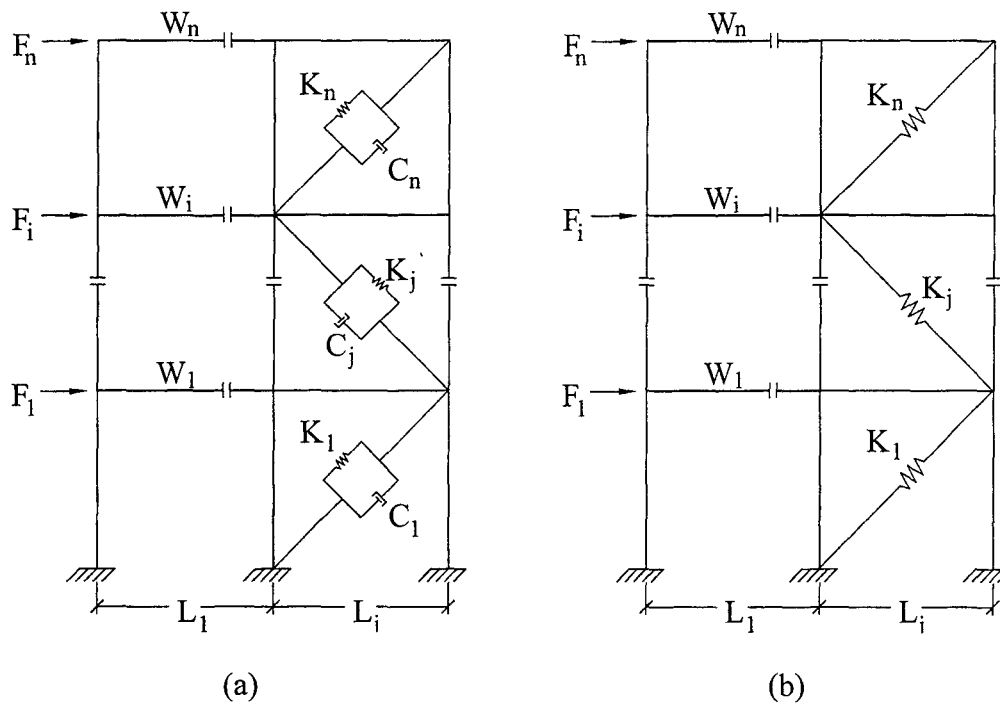
FIGURE C-11 Frame with Viscoelastic Damping System
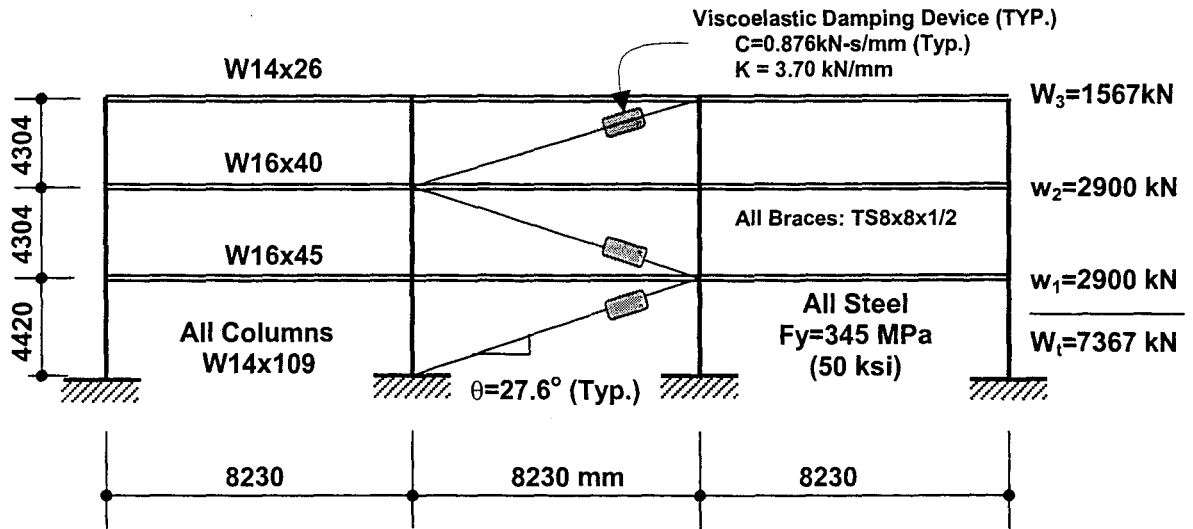
(a)
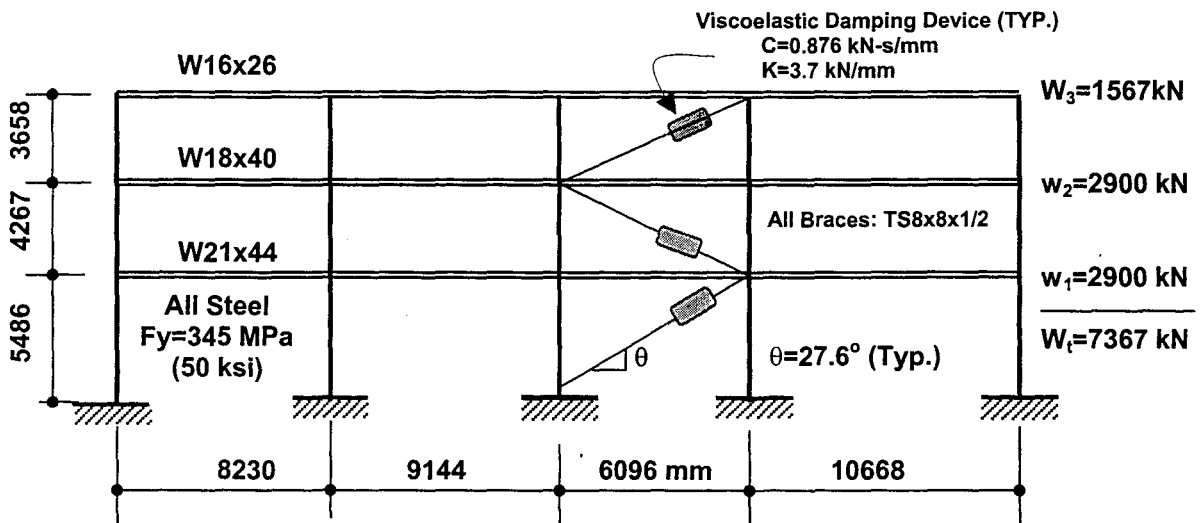
(b)

FIGURE C-12 Examples of Steel Moment Frames with Viscoelastic Solid Devices

262
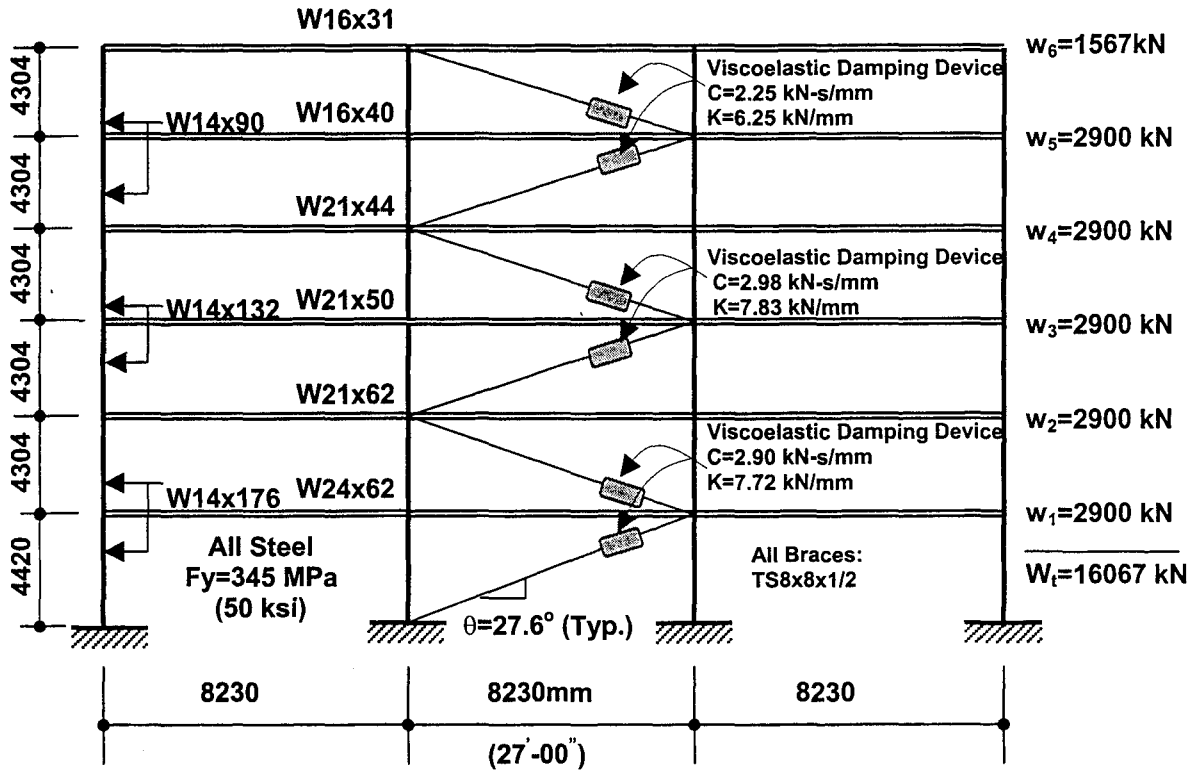
FIGURE C-12 Examples of Steel Moment Frames with Viscoelastic Solid Devices (continued)

263
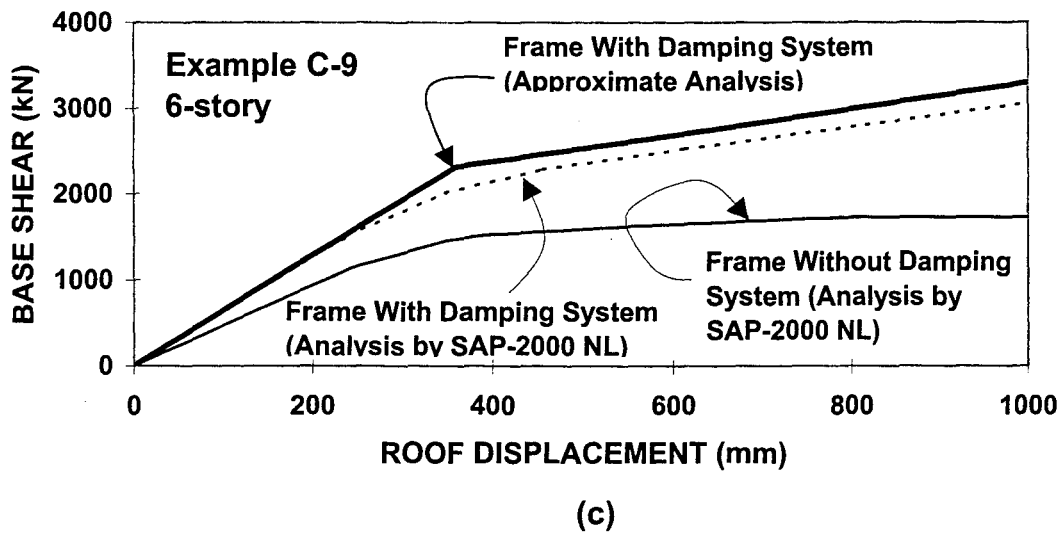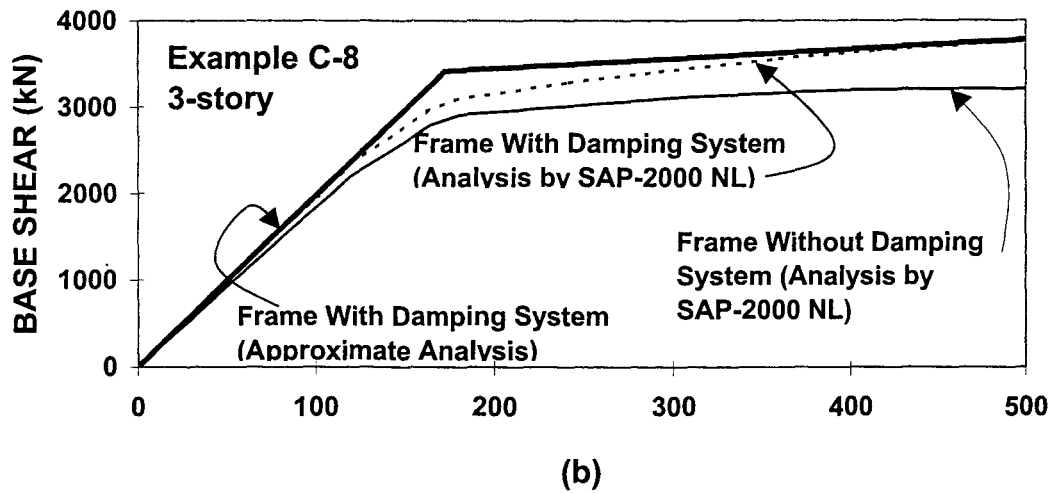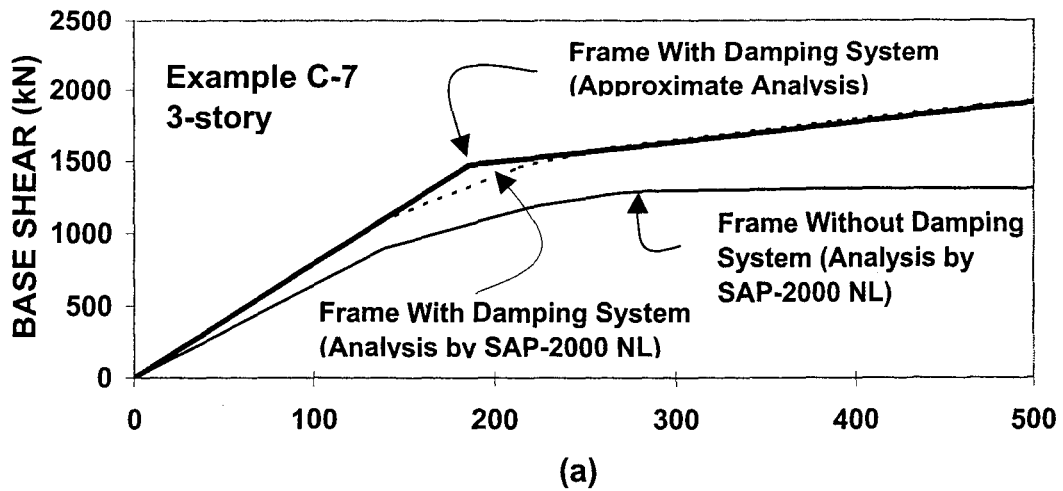
FIGURE C-13 Comparison of Pushover Curves of Buildings with Viscoelastic
Damping Systems

APPENDIX D

CONSIDERATIONS IN THE DESIGN OF

METALLIC YIELDING AND VISCOELASTIC SOLID DAMPING DEVICES

D.1 Introduction

This appendix presents some information on metallic yielding and on viscoelastic solid damping devices, which is of significance in their design. In the case of metallic yielding devices, the presentation concentrates on triangular plate devices (Tsai et al., 1993) since this type of device is utilized in the examples presented in this work. The information presented in this appendix can also be applied to other types of metallic yielding devices such as the unbonded steel braces (Watanabe et al., 1988). In the case of viscoelastic devices, information is presented on the mechanical properties of one commonly available and used material, 3M ISD110 (Soong and Dargush, 1997). Data from Zimmer (1999), who conducted an extensive experimental study to evaluate the properties of this material for a wide range of frequency, temperature, and strain are presented.

D.2 Metallic Yielding Devices

Triangular plate damping devices or T-ADAS devices (Tsai et al., 1993; Soong and Dargush, 1997; Constantinou et al., 1998) are shaped and loaded as shown in Figure D-1. The triangular shape ensures yielding over the entire height of the device.

Triangular plate elements were originally conceived as damping devices in seismic isolation systems (Tyler, 1978a;Tyler, 1978b). The original work of Tyler consisted of experiments and design procedures for a variety of yielding steel devices, including triangular and round devices. An important consideration in the design of these devices is low-cycle fatigue. The approach followed herein in the design of these devices is to specify the number of cycles that the device should be capable of sustaining in either the design-basis earthquake or maximum-considered earthquake. Various studies on low-cycle fatigue relate the maximum strain or plastic strain to the number of cycles, N_f, at failure (Manson, 1953; Coffin, 1954; Koh and Stephens, 1991;

Mander et al., 1994). In general, a relation between the amplitude of strain (half the strain range) and the number of cycles at failure, N_f, may be written in the form:

$$\varepsilon_{max} = AN_f^{-b}$$

(D-1)

Values $A = 0.08$ and $b = 0.3$ result in an equation which reasonably represents the low-cycle fatigue behavior of low strength steel devices. Note that this behavior is typically different from that of specimens of the steel used in these devices (e.g., see Tyler, 1978a).

Utilizing this relation and requiring that $N_f = 100$ in the design-basis earthquake, the allowable maximum strain in the plate is calculated to be $\varepsilon_{max} = 0.02$. Moreover, the maximum displacement ductility in the device, μ_d, calculated as the ratio of the maximum and yield displacements at the point of application of the load, D_{max} and D_y, respectively, may be shown to be for the triangular plate device

$$\mu_d = \frac{D_{max}}{D_y} = \frac{2}{3}\left(\frac{\varepsilon_{max}}{\varepsilon_y}\right)$$

(D-2)

where ε_y is the yield strain of the material. Note that for an unbonded brace (brace in uniaxial tension and compression without instability problems), $\mu_d = \varepsilon_{max} / \varepsilon_y$. Accordingly, use of A36 steel (minimum yield stress $250\ MPa = 36\ ksi$) with $\varepsilon_y = 0.00125$ results in maximum allowable strain $\varepsilon_{max} = 0.02$ and allowable ductility demand $\mu_d = 10.7$ for triangular plate devices.

To understand the implications of these limits on strain and ductility for triangular plate devices, one has to relate the yield displacement D_y and the maximum displacement D_{max} of the device to the yield strain ε_y, the maximum strain ε_{max} and the geometry of the device. It is easily derived that

$$D_y = \frac{3}{2}\left(\frac{\varepsilon_y h^2}{t}\right)$$

(D-3)

$$D_{max} = \left(\frac{\varepsilon_{max} h^2}{t}\right)$$

(D-4)

Based on NEHRP (2000), the drift limit in the design-basis earthquake is R/C_d times the allowable story drift. For a special steel moment frame, seismic group I, the drift limit is $(R/C_d)(0.02h_{sx})$ or about $(8/5.5)(0.02 \times 4000 \, mm) = 116 \, mm$. Consider a design in which triangular plate devices are designed in a chevron configuration to have a displacement of not much less than 116 mm in the design-basis earthquake. For A36 steel with $\varepsilon_{max} = 0.02$ and using (D-4) results in the requirement that $h^2/t = 5{,}800 \, mm$. Selecting $t = 25.4 \, mm$ (1 in.), $h = 384 \, mm$ (15 in.). The width, b (typically less than h) and the number of triangular plates are selected in order to achieve the desired yield strength. For this calculation, the yield strength V_d of a single triangular plate may be calculated by

$$V_d = \left(\frac{F_y b t^2}{4h} \right) \qquad \qquad \text{(D-5)}$$

where F_y = yield stress of steel.

As an example, consider a singular triangular plate device with dimensions $b = 305 \, mm$, $h = 457 \, mm$, $t = 25.4 \, mm$ with $F_y = 250 \, MPa$ (A36 steel). It has yield strength $V_d = 26.9 \, kN$ and allowed maximum displacement $D_{max} = 165 \, mm$ in the design-basis earthquake (for $N_f = 100$). For this displacement, the maximum strain in the device is $\varepsilon_{max} = 0.02$. By comparison, consider that unbonded steel braces are used rather than triangular plate devices. The braces are installed in the diagonal configuration at an angle $\theta = 28°$ with an effective length of $9{,}300 \, mm$. For a drift of $165 \, mm$ in the design-basis earthquake, the brace axial deformation is $146 \, mm$ and therefore the maximum strain is $146/9{,}300 = 0.016$. At this strain the predicted number of cycles to failure is 213, which is very good.

For the maximum-considered earthquake, the displacement is approximately 1.75 times larger, so that for the triangular plate devices $D_{max} = 289 \, mm$, $\varepsilon_{max} = 0.035$ and $N_f = 16$, which is arguably sufficient. For the unbonded steel brace device, $D_{max} = 256 \, mm$, $\varepsilon_{max} = 0.027$ and $N_f = 37$, which is very good

D.3 Viscoelastic Solid Devices

Information on viscoelastic solid devices may be found in Soong and Dargush (1997), Constantinou et al. (1998) and FEMA (1997). Herein, we present a brief description of the

behavior of these devices, mechanical data for viscoelastic material 3M ISD110 and a simple procedure for the mathematical modeling of these devices for dynamic response-history analysis.

Figure D-2 presents typical force-displacement loops of a full size device with bonded area $A_b = 92,903~mm^2$ and thickness $h = 88.9~mm$ (Zimmer, 1999). It was subjected to 10 cycles of displacement of amplitudes equal to the thickness (i.e., shear strain $\gamma = u_o / h = 1.0$). The substantial reduction of effective stiffness and energy dissipated per cycle is a result of the increase in temperature of the device from $20°~C$ to $26.9°~C$ during testing. The effect of temperature, whether ambient or due to heating, is an important consideration in the design of buildings with these devices.

Figure D-3 illustrates an idealized loop of a viscoelastic device, in which the physical significance of the storage stiffness K' and the loss stiffness K'' is presented. These properties are extracted from experimental data and transformed to values of the storage-shear modulus $G' = K' h / A_b$ and the loss shear modulus $G'' = K'' h / A_b$.

Zimmer (1999) conducted an extensive experimental study on viscoelastic material 3M ISD110 and concluded that shear strain in the range of 25 to 100% does not have significant effect on the mechanical properties of the material. Rather, temperature and frequency have important effects on the properties, which were quantified in the range of 10 to $50°~C$ and 0.1 to $3~Hz$, respectively. Figure D-4 presents data on the storage- and loss-shear moduli of this material as a function of temperature and frequency. The trends seen in this figure are identical to those identified in Soong and Dargush (1997) but the values of the moduli in Figure D-4 are lower than those reported in Soong and Dargush (1997), which were obtained from tests at low strains, with the majority of the tests conducted at a strain level of 5%.

Various models for the modeling the dynamic behavior of viscoelastic solid devices have been proposed and described in Soong and Dargush (1997) and Constantinou et al. (1998). Of these, the simplest is Kelvin model, which consists of a spring of stiffness K and a dashpot (linear viscous device) of constant C in parallel (see Figure C-11(a)). These parameters are defined as

$$K = \left(\frac{G' A_b}{h} \right)$$

(D-6)

268

$$C = \left(\frac{G'' A_b}{h\omega} \right)$$ (D-7)

where ω is the frequency of vibration, which is typically selected to be the fundamental frequency of the structure. The Kelvin model is appropriate for simplified analysis for which the frequency is assumed and subsequently confirmed. This approach was followed for the application of the simplified methods of analysis using the data of Figure D-4 and similar data in non-logarithmic scale in Zimmer (1999).

The simplest models that are capable of capturing the frequency dependence of these devices are either the Standard Linear Solid described in FEMA (1997) or the Three-Parameter Model depicted in Figure D-5, for which the predictions are identical to those of the Standard Linear Solid. The Three-Parameter Model has been utilized herein for performing dynamic response-history analysis. The parameters of this model are obtained from

$$K_1 = \left(\frac{A_b}{h} \right) G_0$$ (D-8)

$$K_2 = \left(\frac{A_b}{h} \right)(G_\infty - G_0)$$ (D-9)

$$C_1 = \left(\frac{G_\infty - G_0}{\omega_m} \right)\left(\frac{A_b}{h} \right)$$ (D-10)

in which G_0 is the storage-shear modulus at zero frequency, G_∞ is the storage-shear modulus at very large frequencies and ω_m is the frequency at which the loss-shear modulus is maximum. Values of parameters G_0, G_∞ and ω_m have been presented in Zimmer (1999) as a function of temperature. Table D-1 presents the calibrated values of these parameters used in the analyses of Appendix G. It should be noted that the effect of temperature rise due to viscous heating cannot be captured with this model. Rather, bounding analysis after analytically calculating the temperature rise needs to be performed.

269

TABLE D-1 Values of Parameters in Three-Parameter Model (Zimmer, 1999)

Temperature (°C)	G_0 (MPa)	G_∞ (MPa)	ω_m (rad/sec)
10	1.66	12.02	16.08
15	0.98	8.83	18.66
20	0.56	5.99	24.94
22	0.50	4.43	26.08
24	0.43	3.98	27.02
26	0.35	3.16	26.70
28	0.28	2.46	26.14
30	0.25	1.94	25.76
35	0.16	1.05	24.00
40	0.14	0.78	28.65
45	0.10	0.43	24.88
50	0.10	0.35	24.13
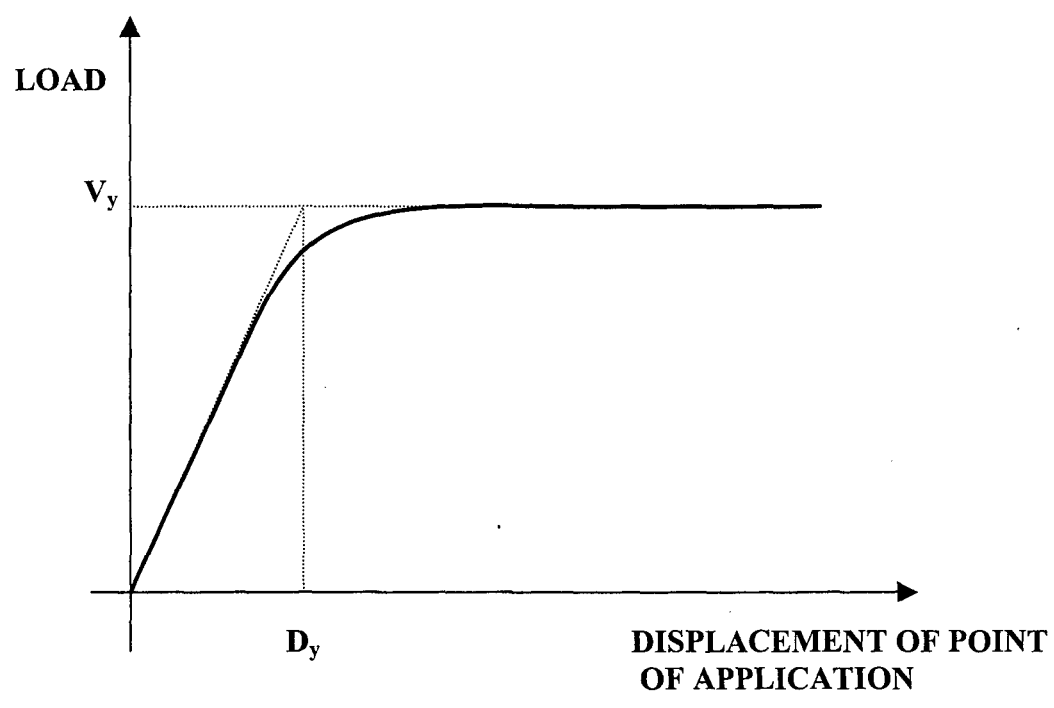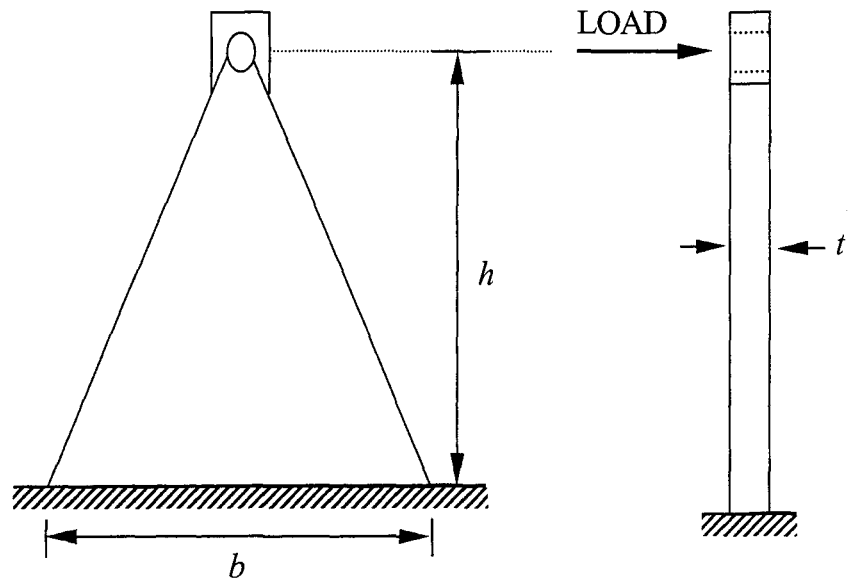
FIGURE D-1 Illustration of Triangular Plate Damping Device And Assumed Behavior
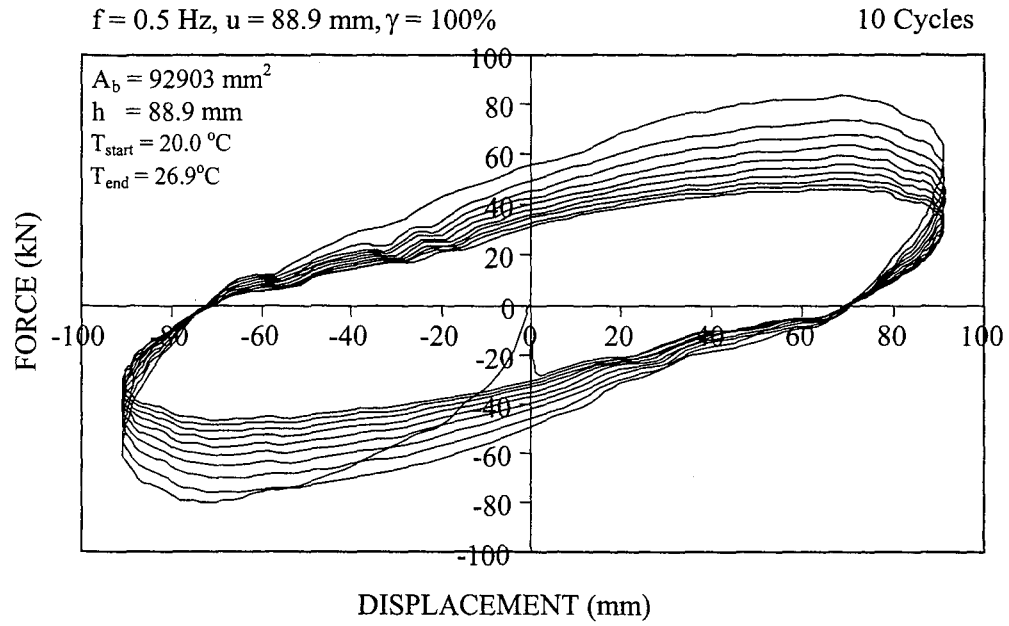
FIGURE D-2 Typical Force-Displacement Loops of Viscoelastic Solid Device
(Zimmer, 1999)
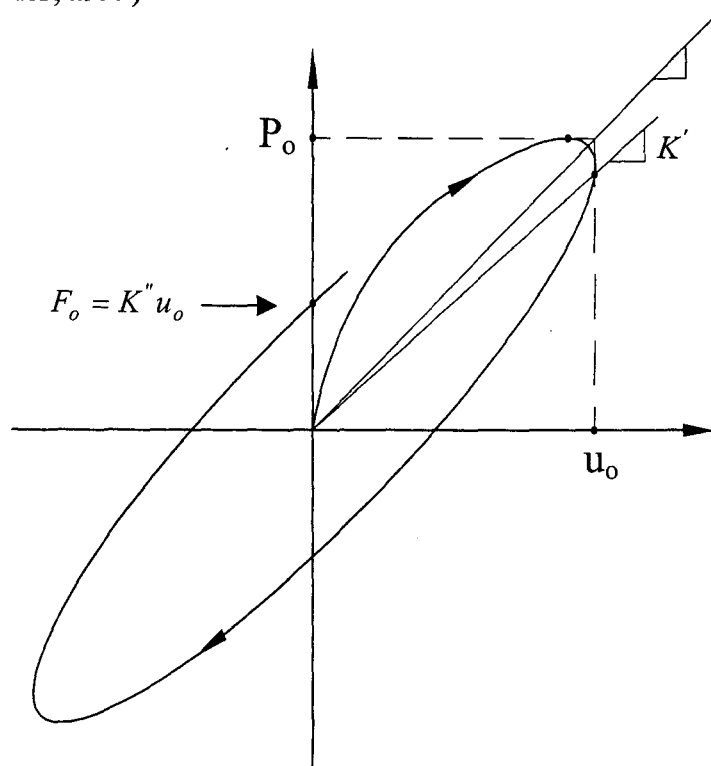
FIGURE D-3 Idealized Force-Displacement Loop of Viscoelastic Material and
Illustration of Mechanical Properties

272
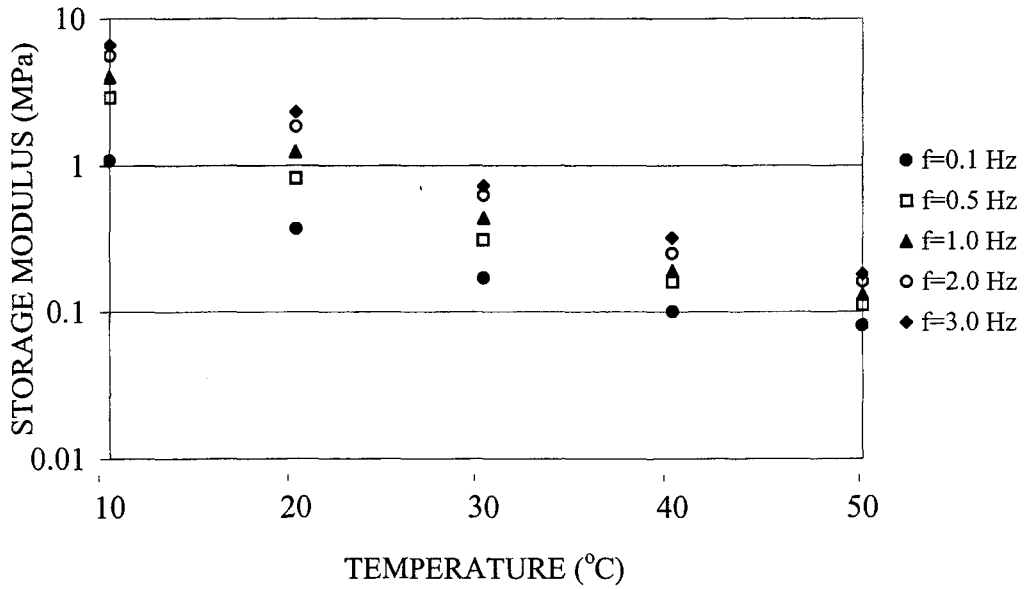
STORAGE MODULUS G'

LOSS MODULUS G"
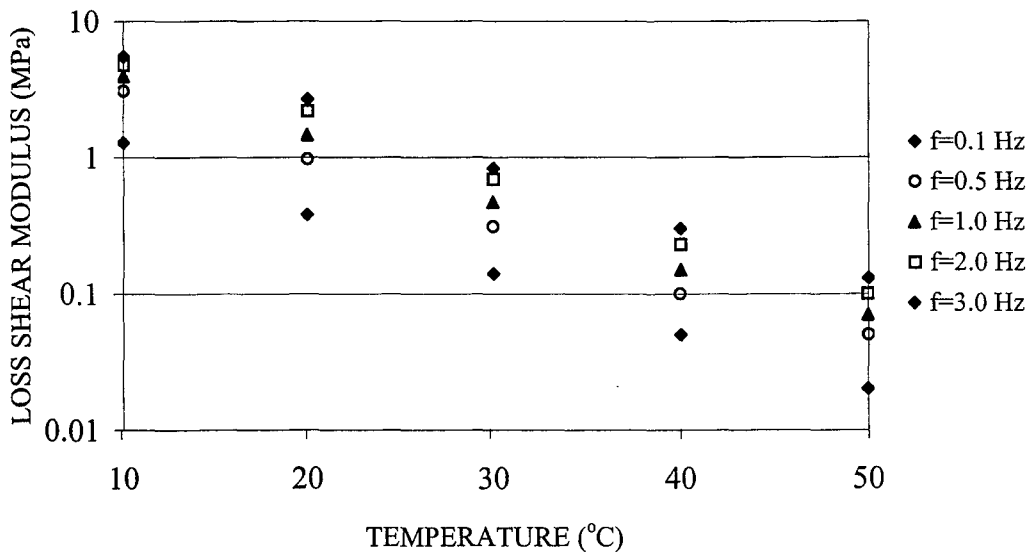
FIGURE D-4 Dependence of Storage and Loss Shear Moduli on Frequency and Temperature
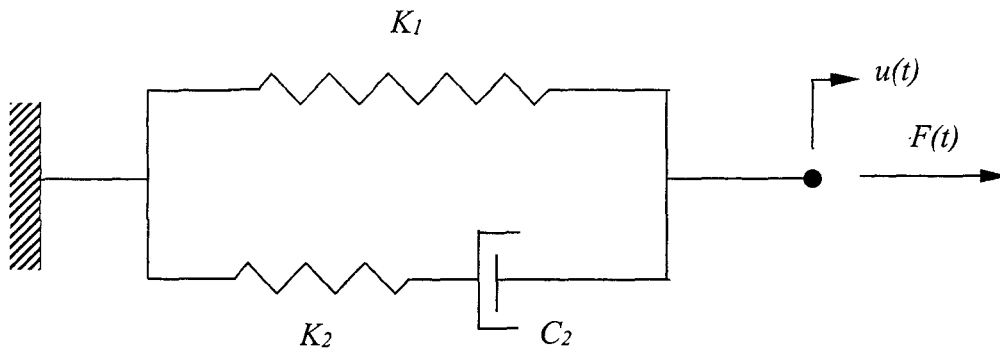
FIGURE D-5 The Three-Parameter Model

APPENDIX E

DETAILED CALCULATIONS FOR THE SIMPLIFIED ANALYSIS OF 3-STORY AND 6-STORY FRAMES WITH LINEAR VISCOUS DAMPING SYSTEM

E.1 Introduction

This appendix presents detailed calculations in the application of the equivalent lateral force (ELF) and of the response spectrum analysis (RSA) procedures of NEHRP (2000) for the analysis of buildings with linear viscous damping systems. These procedures are applied as described in Appendix A subject to the modifications described in Section 8.1.

The presentation in this appendix consists of:

(a) Detailed calculations for the 3-story special steel moment frame 3S-75 shown in Figure 8-2 and denoted as example No.2 in Section 8.

(b) Summary calculations for the 3-story special steel moment frames 3S-60 and 3S-90 shown in Figures 8-1 and 8-3 and denoted as examples No.1 and No.3 in Section 8, respectively.

(c) Summary calculations for the 6-story special steel moment frame 6S-75 shown in Figure 8-5 and denoted as example No.5 in Section 8.

E.2 Detailed Calculations for 3-Story Frame 3S-75 with Linear Viscous Damping System

Parameters

Tributary Weight

Third Floor (roof):		$w_3 = 1567\,kN$
Second Floor:		$w_2 = 2900\,kN$
First Floor:		$w_1 = 2900\,kN$

Design Coefficients per Table 5.2.2, 1997 NEHRP

For Special Steel Moment Frame

Response Modification Factor: $R = 8.0$

System Overstrength Factor: $\Omega_0 = 3.0$

Deflection Amplification Factor: $C_d = 5.5$

Importance Factor: $I = 1.0$

Description of the System

The analyzed frame is a special steel moment frame with a linear viscous damping system as shown in Figure 8-2. This frame is one of two such frames in each principal direction of a building with the plan and elevation shown in Figure B-1 in Appendix B. In the analysis of the building, torsional effects were disregarded for simplicity. The building is located at a site characterized by a design response spectrum with parameters $S_{D1} = 0.6$, $S_{DS} = 1.0$ and $T_s = 0.6$ sec per NEHRP (1997). This characterization is that of the design-basis earthquake (DBE). The maximum-considered earthquake (MCE) is characterized by a response spectrum with ordinates 1.5 larger than those of the DBE.

The damping system of the frame (as well as of each of the other four identical frames of the building in Figure B-1) consists of linear viscous damping devices installed in the diagonal configuration as shown in Figure 8-2. The damping ratio in the fundamental mode of vibration of the frame under elastic conditions is $\beta_{V1} = 0.10$ (damping provided by damping system) plus an assumed inherent damping ratio $\beta_I = 0.05$ for a total damping ratio $\beta_{V1} + \beta_I = 0.15$. The corresponding damping coefficient $B_{V+I} = 1.35$ (Table A13.3.1 and Table 3-3, column for B_I, conservative values). On the basis of NEHRP (2000) Section A13.2.4.1, the seismic base shear for the design of this frame is $V_{min} = 0.75V$, where V is determined by the procedures of NEHRP (1997), Section 5.3. The seismic base shear V was determined in Section B.3 to be 788.5 kN, so that $V_{min} = 0.75V = 0.75 \times 788.5 = 591.4$ kN.

The approach followed herein to design the frame started with the calculation of the required base shear strength of the frame V_y per (7-72), so that

$$V_y = V_{min} \cdot \frac{\Omega_o \cdot C_d}{R} = 591.4x\frac{3x5.5}{8} = 1220 \; kN$$

The frame was then designed to have a proper collapse mechanism (weak beam/strong columns) and to have a base shear strength equal to approximately 1220 kN when pushed over by lateral loads proportional to the first mode of the frame under elastic conditions. Subsequently, the frame was analyzed by the plastic analysis procedure of Appendix C.2 was calculated to be V_y = 1220 kN. The model utilized for the plastic analysis was as shown in Figure C-1 with distance $a_{ij}L_j$ equal to $d_c/2$, where d_c = column depth. That is, hinges were assumed to form at the beam to column interface. Note that the analyses in the examples of Appendix C were based on a different location of the plastic hinge. The selection of the location of the hinges at distance $d_c/2$ was based on the corresponding limitation for the location of the beam plastic hinges in Program IDARC2D-version 5.0. This program was later utilized in the dynamic response history analysis of the frame and it was desirable to have consistency between the simplified model and the model in this computer program.

Eigenvalue analysis of the frame performed in program IDARC 2D-version 5.0 gave: T_1 = 1.58 sec, $\{\phi_{i1}\}^T$= [1.000 0.657 0.250], T_2 = 0.49 sec, $\{\phi_{i2}\}^T$= [1.000 –0.560 -0.690] and T_3 = 0.24 sec, $\{\phi_{i3}\}^T$= [1.000 –1.618 –2.096].

Modal Properties of Frame

The modal weights (or effective modal gravity loads), $\overline{W}_m$, are given by (7-16), while the corresponding modal participation factors, Γ_m, are given by (7-12) or (A13.4.3.3.-2).

First Mode

$$\overline{W}_1 = \frac{(1567 \times 1.000 + 2900 \times 0.657 + 2900 \times 0.250)^2}{(1567 \times 1.000^2 + 2900 \times 0.657^2 + 2900 \times 0.250^2)} = \frac{4197.3^2}{3000.0} = 5871kN$$

$$\Gamma_1 = \frac{4197.3}{3000.0} = 1.3991$$

Second Mode

$$\overline{W}_2 = \frac{[1567 \times 1.000 + 2900 \times (-0.560) + 2900 \times (-0.690)]^2}{(1567 \times 1.000^2 + 2900 \times -0.560^2 + 2900 \times -0.690^2)} = \frac{(-2058)^2}{3857.1} = 1098 \ kN$$

$$\Gamma_2 = \frac{-2058}{3857.1} = -0.5336$$

Third Mode

$$\overline{W}_3 = \frac{[1567 \times 1.000 + 2900 \times (-1.618) + 2900 \times (2.069)]^2}{[1567 \times 1.000^2 + 2900 \times (-1.618)^2 + 2900 \times 2.069^2]} = \frac{2953.2^2}{21899.31} = 398 \ kN$$

$$\Gamma_3 = \frac{2953.2}{21899.31} = 0.1348$$

Residual Mode

Using (A13.4.3.7-1)

$$\overline{W}_R = 7367 - 5872 = 1495 \ kN$$

Using (A13.4.3.7-2)

$$\Gamma_R = 1 - 1.399 = -0.3991$$

The residual mode shape was calculated by using (A13.4.3.7-1) as

$$\phi_R = \frac{\begin{Bmatrix} 1.0 \\ 1.0 \\ 1.0 \end{Bmatrix} - 1.3991 \begin{Bmatrix} 1.000 \\ 0.657 \\ 0.250 \end{Bmatrix}}{-0.3991} = \begin{Bmatrix} 1.0000 \\ -0.2024 \\ -1.6292 \end{Bmatrix}$$

Viscous Damping Ratios under Elastic Conditions

Equation (7-29) was used to calculate the damping ratio in each mode using $C_j = 0.9 \ kN \cdot s / mm$ and $f_j = cos \theta_j$, where $\theta_j = 27.6°$ (see Figure 8-2).

278

$$\beta_{vm} = \left(\frac{T_m}{4\pi}\right) \frac{\sum\limits_{j} C_j \cos^2 \theta_j \phi_{rj}^2}{\sum\limits_{i} \left(\frac{w_i}{g}\right) \phi_{im}^2}$$

First Mode (T_1= 1.58 sec)

Modal Drift

$$\{\phi_r\}_1 = \begin{Bmatrix} 1 - 0.657 \\ 0.657 - 0.25 \\ 0.25 \end{Bmatrix} = \begin{Bmatrix} 0.343 \\ 0.407 \\ 0.250 \end{Bmatrix} \quad , \qquad \sum_i w_i \phi_{i1}^2 = 3000.0$$

$$\beta_{V1} = \left(\frac{1.58}{4\pi}\right) \frac{0.9 \times \cos^2 27.6° \times 9810 x\left(0.343^2 + 0.407^2 + 0.25^2\right)}{3000} = 0.10$$

Second Mode (T_2= 0.49 sec)

Modal Drift

$$\{\phi_r\}_2 = \begin{Bmatrix} 1 - (-0.5600) \\ -0.5600 - (-0.6900) \\ -0.6900 \end{Bmatrix} = \begin{Bmatrix} 1.560 \\ 0.130 \\ -0.690 \end{Bmatrix} \quad , \qquad \sum_i w_i \phi_{i2}^2 = 3857.1 \, kN$$

$$\beta_{V2} = \left(\frac{0.49}{4\pi}\right) \times 0.90 \times \cos^2 27.6° \times 9810 \times \frac{\left(1.560^2 + 0.130^2 + 0.690^2\right)}{3857.10} = 0.205$$

Third Mode (T_3=0.24 sec)

Modal Drift

$$\{\phi_r\}_3 = \begin{Bmatrix} 1 - (-1.6180) \\ -1.6180 - 2.0960 \\ 2.0960 \end{Bmatrix} = \begin{Bmatrix} 2.6180 \\ -3.7140 \\ 2.0960 \end{Bmatrix} \quad , \qquad \sum_i w_i \phi_{i3}^2 = 21899.31 \, kN$$

$$\beta_{V3} = \left(\frac{0.24}{4\pi}\right) \times 0.90 \times \cos^2 27.6° \times 9810 \times \frac{\left(2.618^2 + 3.714^2 + 2.096^2\right)}{21899.31} = 0.151$$

Residual Mode ($T_R = 0.4T_1 = 0.632$ sec, A13.4.3.7-4)

Modal Drift

$$\{\phi_r\}_R = \left\{ \begin{array}{c} 1-(-0.2024) \\ -0.2024-(-1.6292) \\ -1.6292 \end{array} \right\} = \left\{ \begin{array}{c} 1.2024 \\ 1.4268 \\ -1.6292 \end{array} \right\}$$

$$w_i\phi_{rj}^2 = 1567 \times 1.000^2 + 2900 \times (-0.2024)^2 + 2900 \times (-1.6292)^2 = 9383.25$$

$$\beta_{VR} = \left(\frac{0.632}{4\pi}\right) \times 0.90 \times \cos^2 27.6^\circ \times 9810 \times \frac{\left(1.2024^2 + 1.4268^2 + 1.692^2\right)}{9383.25} = 0.228$$

CALCULATION OF RESPONSE IN DESIGN BASIS EARTHQUAKE

FIRST MODE RESPONSE ($T_1 = 1.58$ sec $> T_s$)

Inelastic Roof Displacement

Assumed Effective Ductility: $\mu_D = 1.29$

Effective Period: $\qquad\qquad\qquad\qquad T_{1D} = T_1\sqrt{\mu} = 1.58\sqrt{1.29} = 1.795\ sec$ (A13.4.3.5-1)

Effective Damping Ratio

Quality Factor: $\qquad q_H = 0.67\dfrac{T_s}{T_1} = 0.67 \times \dfrac{0.60}{1.58} = 0.254 < 0.50$ (A13.3.3-1)

$$\text{use } q_H = 0.50$$

Hysteretic Damping: $\qquad \beta_{H_D} = 0.50 \times (0.64 - 0.05)\left(1 - \dfrac{1}{1.29}\right) = 0.066$ (A13.3.2.2-1)

Effective Damping: $\qquad \beta_{1_D} = 0.05 + 0.10\sqrt{1.29} + 0.066 = 0.23$ (A13.3.2-1)

Damping Coefficient: $\quad B_{1D} = 1.59$ (Table A13.3.1)

Roof Displacement, D_{1D}

For $T_{1D} > T_s$

$$D_{ID} = \left(\frac{9810}{4\pi^2}\right) \times 1.3991 \times 0.6 \times \frac{1.795}{1.59} = 235\, mm \qquad \text{(A13.4.4.3-1)}$$

Total viscous damping ratio under elastic conditions: $\beta_{V+I} = 0.10 + 0.05 = 0.15$

Damping coefficient: $B = 1.35$ (Table A13.3.1)

The roof displacement for elastic behavior of the frame is:

$$D = \left(\frac{9810}{4\pi^2}\right) \times 1.3991 \times 0.6 \times \frac{1.58}{1.35} = 244\, mm$$

Since $D_{ID} < D$, use $D_{ID} = 244mm$

Base Shear

Seismic Coefficient: $\left(\frac{8}{5.5}\right) \times \dfrac{0.6}{1.795 \times (3 \times 1.59)} = 0.102$ (A.13.4.3.4-1)

Base Shear $\qquad V_1 = 0.102 \times 5871 = 599\, kN$ (A13.4.3.1-1)

The contribution of the first mode to the base shear strength of the frame is given by (7-72)

$$V_y = V_1 \frac{\Omega_o C_d}{R} = 599 \times \frac{3 \times 5.5}{8} = 1235\, kN$$

The calculated contribution to the base shear strength of *1235 kN* is nearly identical to the actual base shear strength of *1220 kN*. Had the two were different, the assumed ductility demand would have been incorrect and the process should be repeated with a new assumed ductility demand.

Displacement at Effective Yield (Yield Displacement) D_y

$$D_y = \left(\frac{g}{4\pi^2}\right)\left(\frac{\Omega_o \cdot C_d}{R}\right)\Gamma_1 \cdot C_S \cdot T_1^2 \qquad \text{(A13.3.4-3)}$$

$$D_y = \left(\frac{9810}{4\pi^2}\right)\left(\frac{3 \times 5.5}{8}\right) \times 1.399 \times 0.102 \times 1.58^2 = 183\, mm$$

Effective Ductility Demand μ_D

$$\mu_D = \frac{D_{ID}}{D_y} \qquad\qquad\qquad\text{(A13.3.4-1)}$$

$$\mu_D = \frac{244}{183} = 1.33 \approx 1.29 \ (\textit{assumed}), \text{ no further iteration is necessary.}$$

$$\mu_{max} = \frac{R}{\Omega_o I} \qquad\qquad\qquad\text{(A13.5-2)}$$

$$\mu_{max} = \frac{8}{3 \times 1.0} = 2.667 \qquad\qquad \mu_D < \mu_{max}$$

The difference between the estimated and the assumed ductility demand is due to adjustment of the inelastic displacement to meet the condition that it is not less than the elastic displacement.

Response at Stage of Maximum Displacement

Lateral Floor Displacements, δ_{i1D}, and Story Drifts, Δ_{i1D}

$$\delta_{i1D} = D_{1D} \cdot \phi_{i1} \qquad\qquad\qquad\text{(A13.4.4.2-1)}$$

$$\delta_{i1D} = 244 \times \begin{Bmatrix} 1.0000 \\ 0.6570 \\ 0.2500 \end{Bmatrix} = \begin{Bmatrix} 244 \\ 160 \\ 61 \end{Bmatrix} mm$$

$$\Delta_{i1D} = \begin{Bmatrix} 84 \\ 99 \\ 61 \end{Bmatrix} mm$$

Design Lateral Forces, F_{i1}, Design Story Shear Forces, V_{i1}, and Floor Accelerations A_{i1}

$$F_{i1} = w_i \cdot \phi_{i1} \cdot \frac{\Gamma_i}{\overline{W}_{D1}} \cdot V_{1D} \qquad\qquad\qquad\text{(A13.4.3.9-1)}$$

$$F_{i_1} = \left\{ \begin{array}{l} 1567 \times 1.0 \times \dfrac{1.3991}{5872} \times 599 \\[2ex] 2900 \times 0.657 \times \dfrac{1.3991}{5872} \times 599 \\[2ex] 2900 \times 0.250 \times \dfrac{1.3991}{5872} \times 599 \end{array} \right\} = \left\{ \begin{array}{l} 224 \\ 272 \\ 104 \end{array} \right\} kN$$

$$A_{i_1} = \left(F_{i_1} \Big/ w_i \right) \times \left(\frac{C_d \cdot \Omega_o}{R} \right)$$

$$A_{i_1} = \left\{ \begin{array}{l} 224 \Big/ 1567 \\[1ex] 272 \Big/ 2900 \\[1ex] 104 \Big/ 2900 \end{array} \right\} \times \left(\frac{5.5 \times 3}{8} \right) = \left\{ \begin{array}{l} 0.295 \\ 0.193 \\ 0.075 \end{array} \right\} g$$

$$V_{i_1} = \left\{ \begin{array}{l} 224 \\ 496 \\ 600 \end{array} \right\} kN$$

Note that the actual story shear forces (=strength) are equal to $V_{i_1} \dfrac{\Omega_o C_d}{R}$

Response at Stage of Maximum Velocity

Story Velocity, $\nabla_{i_{1D}}$

$$\nabla_{i_{1D}} = \frac{2\pi}{T_{1D}} \cdot \Delta_{i_{1D}} \qquad\qquad\qquad\qquad (A13.4.4.5\text{-}2)$$

$$\nabla_{i_{1D}} = \frac{2\pi}{1.795} \cdot \left\{ \begin{array}{l} 84 \\ 99 \\ 61 \end{array} \right\} = \left\{ \begin{array}{l} 294 \\ 347 \\ 214 \end{array} \right\} mm / sec$$

Force in Damping Devices, $Fd_{i_{1D}}$

$$Fd_{i_{1D}} = C_i \cdot \nabla_{i_{1D}} \cdot cos\,\theta_i \qquad\qquad\qquad\qquad (7\text{-}23)$$

$$Fd_{i_{1D}} = 0.90x \begin{Bmatrix} 294 \\ 347 \\ 214 \end{Bmatrix} \times cos\,27.6 = \begin{Bmatrix} 235 \\ 277 \\ 171 \end{Bmatrix} kN$$

Horizontal Component of Damping Forces

$$V_{d_{i_{1D}}} = \begin{Bmatrix} 235 \\ 277 \\ 171 \end{Bmatrix} \times cos\,27.6 = \begin{Bmatrix} 208 \\ 245 \\ 151 \end{Bmatrix} kN$$

Seismic Design Forces

Illustrated below are the seismic design forces
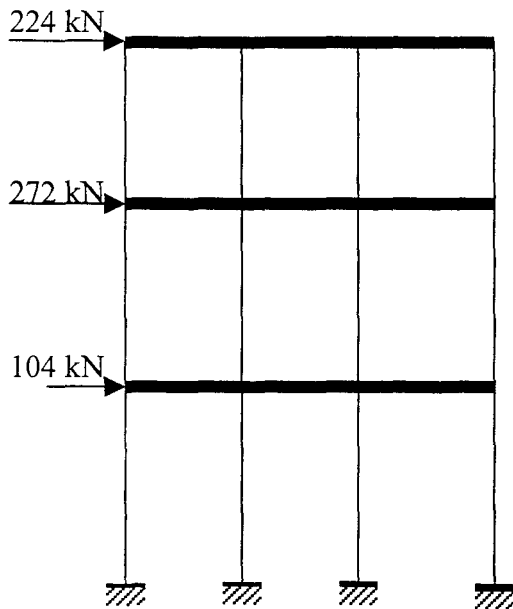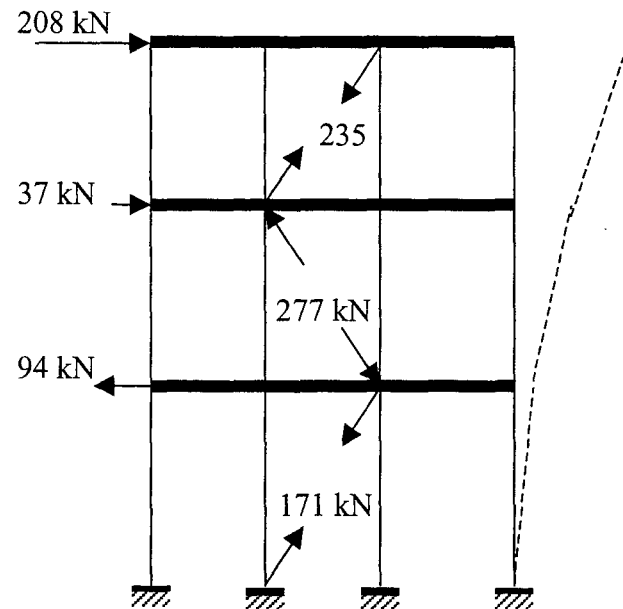
reduced forces	actual forces
Stage of Maximum Displacement	**Stage of Maximum Velocity**

Response at Stage of Maximum Acceleration

Force Coefficients

Effective viscous damping: $\beta_{eff} = \beta_i + \beta_{v1}\sqrt{\mu} = 0.05 + 0.10\sqrt{1.33} = 0.165$

284

$$CF_1 = cos\left[tan^{-1}\left(2\beta_{eff}\right)\right]$$

(4-41)

$$CF_1 = cos\left[tan^{-1}\left(2 \times 0.165\right)\right] = 0.951$$

$$CF_1 \mu = 0.95 \times 1.33 = 1.264 > 1.0 \qquad\qquad \therefore use\, CF_1 = 1.0$$

$$CF_2 = sin\left[tan^{-1}\left(2\beta_{eff}\right)\right]$$

(4-39)

$$CF_2 = sin\left[tan^{-1}\left(2 \times 0.165\right)\right] = 0.313$$

Note that coefficients CF_1 and CF_2 are identical to coefficients C_{IFD} and C_{IFV} in Tables A13.7.3.2.1 and A13.7.3.2.2 of NEHRP (2000). Using effective damping of *0.165* in these tables, $C_{IFD} = 1.0$ and $C_{IFV} = 0.311$, that is, almost exactly the values derived by use of (4-39) and (4-41).

Maximum Lateral Inertia Forces

Maximum actual lateral inertia forces per floor are calculated according to

$$F_{i1,max} = CF_1 \cdot F_{i1}\left|_{Max\,Disp} \cdot \frac{C_d\Omega_o}{R} + CF_2 \cdot F_{iD}\right|_{Max\,Velocity}$$

$$F_{i1,max} = 1.0 \times \begin{Bmatrix} 224 \\ 272 \\ 104 \end{Bmatrix} \times \left(\frac{3 \times 5.5}{8}\right) + 0.313 \times \begin{Bmatrix} 208 \\ 37 \\ -94 \end{Bmatrix} = \begin{Bmatrix} 527 \\ 573 \\ 186 \end{Bmatrix} kN$$

Maximum Acceleration

The maximum floor accelerations are calculated by

$$A_{i1,max} = F_{i2}\Big/ w_i$$

$$A_{i2} = \begin{Bmatrix} 520\big/1567 \\ -572\big/2900 \\ -243\big/2900 \end{Bmatrix} = \begin{Bmatrix} 0.332 \\ 0.197 \\ 0.084 \end{Bmatrix}$$

285

Maximum Story Shear, $V_{i1,max}$

$$V_{i1,max} = CF_1 \cdot V_{i1}\Big|_{Max\,Disp} \cdot \frac{C_d \Omega_o}{R} + CF_2 \cdot V_{i1}\Big|_{Max\,Velocity}$$

$$V_{i1,max}\Big|_{Max\,Velocity} = Fd_{i1} \cdot \cos\theta_i$$

$$V_{i1,max} = 1.000 \times \begin{Bmatrix} 224 \\ 496 \\ 600 \end{Bmatrix} \times \left(\frac{3 \times 5.5}{8}\right) + 0.313 \times \cos 27.6 \times \begin{Bmatrix} 238 \\ 282 \\ 173 \end{Bmatrix} = \begin{Bmatrix} 528 \\ 1101 \\ 1285 \end{Bmatrix} kN$$

The maximum story shear can also be calculated by using the maximum lateral forces.

SECOND MODE RESPONSE (T_2=0.49 sec < T_s)

Effective Damping Ratio: $\beta_{2D} = 0.205 + 0.05 = 0.255$ $\therefore B_{2D} = 1.665$ (Table A13.3.1)

Roof Displacement, D_{2D}

$$D_{2D} = \left(\frac{g}{4\pi^2}\right) \times \Gamma_2 \times \frac{S_{DS}T_2^2}{B_{2D}} \qquad\qquad \text{(A13.5.4.3-2)}$$

$$D_{2D} = \left(\frac{9810}{4\pi^2}\right) \times 0.5336 \times \frac{1.0 \times 0.49^2}{1.665} = 19\ mm$$

Seismic Base Shear, V_2

$$V_2 = C_{S2} \cdot \overline{W}_2 \qquad\qquad \text{(A13.5.3.2-1)}$$

$$C_{S2} = \left(\frac{R}{C_d}\right)\frac{S_{DS}}{\Omega_o B_{2D}} \qquad\qquad \text{(A13.5.3.6-1)}$$

$$C_{S2} = \left(\frac{8}{5.5}\right)\frac{1.0}{3 \times 1.665} = 0.291$$

$$V_2 = 0.291 x 1098 = 320\ kN$$

Response at Stage of Maximum Displacement

Lateral Floor Displacement and Story Drifts

$$\delta_{i2D} = D_{2D} \cdot \phi_{i2} \tag{A13.5.4.2-1}$$

$$\delta_{i2D} = 19 \times \begin{Bmatrix} 1.000 \\ -0.560 \\ -0.690 \end{Bmatrix} = \begin{Bmatrix} 19 \\ -11 \\ -13 \end{Bmatrix} mm$$

$$\Delta_{i2D} = \begin{Bmatrix} 30 \\ 2 \\ -13 \end{Bmatrix} mm$$

Design Lateral Forces, F_{i2}, Design Story Shears, V_{i2}, and Accelerations, A_{i2}

$$F_{i2} = w_i \cdot \phi_{i2} \cdot \frac{\Gamma_2}{\overline{W}_2} \cdot V_{2D} \tag{A13.5.3.7-1}$$

$$F_{i2} = \begin{Bmatrix} 1567 \times 1.0 \times \dfrac{0.5336}{1098} \times 320 \\ 2900 \times -0.560 \times \dfrac{0.5336}{1098} \times 320 \\ 2900 \times -0.690 \times \dfrac{0.5336}{1098} \times 320 \end{Bmatrix} = \begin{Bmatrix} 244 \\ -253 \\ -311 \end{Bmatrix} kN$$

$$A_{i2} = \left(F_{i2} \big/ W_i \right) \times \left(\frac{C_d \cdot \Omega_o}{R} \right)$$

$$A_{i2} = \begin{Bmatrix} 244 \big/ 1567 \\ -253 \big/ 2900 \\ -311 \big/ 2900 \end{Bmatrix} \times \left(\frac{5.5 \times 3}{8} \right) = \begin{Bmatrix} 0.321 \\ -0.180 \\ -0.221 \end{Bmatrix} g$$

$$V_{i2} = \begin{Bmatrix} 244 \\ -9 \\ -320 \end{Bmatrix} kN$$

Story Velocity ∇_{i2D}

$$\nabla_{i2D} = \frac{2\pi}{T_2} \cdot \Delta_{i2}$$

(A13.5.4.5-2)

$$\nabla_{i2D} = \frac{2\pi}{0.49} \times \begin{Bmatrix} 30 \\ 2 \\ -13 \end{Bmatrix} = \begin{Bmatrix} 385 \\ 26 \\ -167 \end{Bmatrix} mm/sec$$

Forces in Damping Devices, Fd_{i2D}

$$Fd_{i2D} = C_i \cdot \nabla_{i2} \cdot \cos\theta_i$$

(7-23)

$$F_{d_{i2D}} = 0.90 \times \begin{Bmatrix} 30 \\ 2 \\ -13 \end{Bmatrix} \times \cos 27.6^\circ = \begin{Bmatrix} 385 \\ 26 \\ -167 \end{Bmatrix} kN$$

Seismic Design Forces
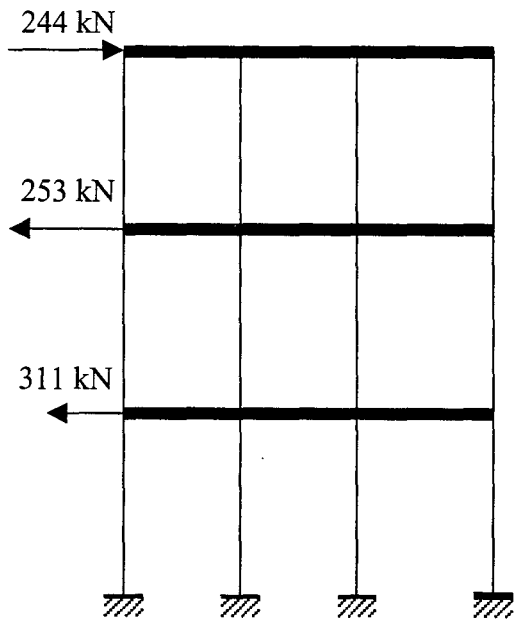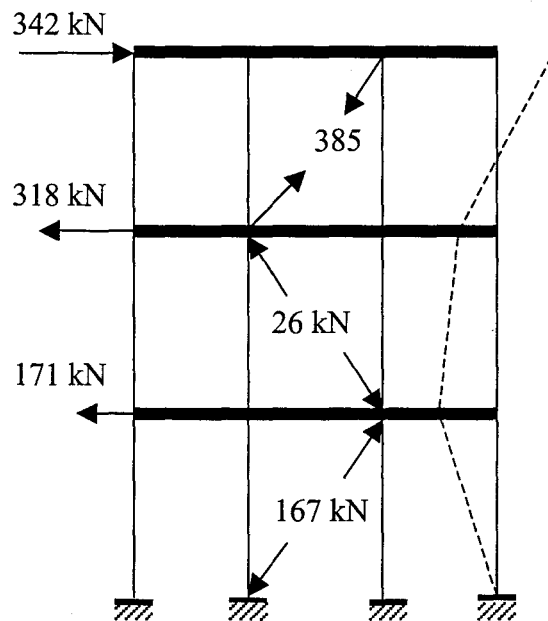
reduced forces   actual forces

Stage of Maximum Displacement   **Stage of Maximum Velocity**

288

Response at Stage of Maximum Acceleration

Force Coefficients

$$\beta_{V_2} = 0.205 + 0.05 = 0.255$$

$$CF_1 = cos\left[tan^{-1}\left(2\beta_{V_2}\right)\right] \qquad (4\text{-}41)$$

$$.\quad CF_1 = cos\left[tan^{-1}\left(2 \times 0.255\right)\right] = 0.891$$

$$CF_2 = sin\left[tan^{-1}\left(2\beta_{V_2}\right)\right] \qquad (4\text{-}39)$$

$$CF_2 = sin\left[tan^{-1}\left(2 \times 0.255\right)\right] = 0.454$$

Maximum Acceleration

$$A_{i2,max} = \left(CF_1 + 2\beta_{V_2} \times CF_2\right) \cdot A_{i_2} \qquad (4\text{-}40)$$

$$A_{i2,max} = \left(0.891 + 2 \times 0.255 \times 0.454\right) \cdot \begin{Bmatrix} 0.321 \\ -0.180 \\ -0.221 \end{Bmatrix} = \begin{Bmatrix} 0.360 \\ -0.202 \\ -0.248 \end{Bmatrix} g$$

Maximum Story Shear, $V_{i2,max}$

$$V_{i2,max} = CF_1 \cdot V_{i2}\bigg|_{Max\,Disp} \cdot \frac{C_d\Omega_o}{R} + CF_2 \cdot V_{i2}\bigg|_{Max\,Velocity}$$

$$V_{i2,max} = 0.891 \times \begin{Bmatrix} 244 \\ -9 \\ -320 \end{Bmatrix} \times \left(\frac{3 \times 5.5}{8}\right) + 0.454 \times \begin{Bmatrix} 272 \\ 19 \\ -118 \end{Bmatrix} = \begin{Bmatrix} 572 \\ -8 \\ -642 \end{Bmatrix} kN$$

THIRD MODE RESPONSE (T_3=0.24 sec < T_s)

Effective Damping Ratio: $\quad \beta_{3D} = 0.151 + 0.05 = 0.201 \qquad \therefore B_{3D} = 1.503 \qquad$ (Table A13.3.1)

Roof Displacement, D_{3D}

$$D_{3D} = \left(\frac{g}{4\pi^2}\right) \times \Gamma_3 \times \frac{S_{DS}T_3^2}{B_{3D}}$$

(A13.5.4.3-2)

$$D_{3D} = \left(\frac{9810}{4\pi^2}\right) \times 0.1348 \times \frac{1.0 \times 0.24^2}{1.503} = 1\ mm$$

Seismic Base Shear, V_3

$$V_3 = C_{S3} \cdot \overline{W}_3$$

(A13.5.3.2-1)

$$C_{S3} = \left(\frac{R}{C_d}\right) \frac{S_{DS}}{\Omega_o B_{3D}}$$

(A13.5.3.6-1)

$$C_{S3} = \left(\frac{8}{5.5}\right) \frac{1.0}{3 \times 1.503} = 0.323$$

$$V_3 = 0.323 \times 398 = 129\ kN$$

Response at Stage of Maximum Displacement

Lateral Floor Displacement and Story Drifts

$$\delta_{i3D} = D_{3D} \cdot \phi_{i3}$$

(A13.5.4.2-1)

$$\delta_{i3D} = 1.0 \times \begin{Bmatrix} 1.000 \\ -1.618 \\ 2.096 \end{Bmatrix} = \begin{Bmatrix} 1 \\ -2 \\ 2 \end{Bmatrix} mm$$

$$\Delta_{i3D} = \begin{Bmatrix} 3 \\ -4 \\ 2 \end{Bmatrix} mm$$

Design Lateral Forces, F_{i3}, Design Story Shears, V_{i3}, and Floor Accelerations, A_{i3}

$$F_{i3} = w_i \cdot \phi_{i3} \cdot \frac{\Gamma_3}{\overline{W}_3} \cdot V_{3D}$$

(A13.5.3.7-1)

$$F_{i3} = \left\{ \begin{array}{c} 1567 \times 1.0 \times \dfrac{0.1348}{398} \times 129 \\[2mm] 2900 \times -1.618 \times \dfrac{0.1348}{398} \times 129 \\[2mm] 2900 \times 2.096 \times \dfrac{0.1348}{398} \times 129 \end{array} \right\} = \left\{ \begin{array}{c} 69 \\ -205 \\ 266 \end{array} \right\} kN$$

$$A_{i3} = \left(F_{i3} \middle/ W_i \right) \times \left(\frac{C_d \cdot \Omega_o}{R} \right)$$

$$A_{i_3} = \left\{ \begin{array}{c} 69 \middle/ 1567 \\ -205 \middle/ 2900 \\ 266 \middle/ 2900 \end{array} \right\} \times \left(\frac{5.5 \times 3}{8} \right) = \left\{ \begin{array}{c} 0.091 \\ -0.146 \\ 0.189 \end{array} \right\} g$$

$$V_{i3} = \left\{ \begin{array}{c} 69 \\ -136 \\ 130 \end{array} \right\} kN$$

Response at Stage of Maximum Velocity

Story Velocity ∇_{i3D}

$$\nabla_{i3D} = \frac{2\pi}{T_3} \cdot \Delta_{i3} \tag{A13.5.4.5-2}$$

$$\nabla_{i3D} = \frac{2\pi}{0.24} \times \left\{ \begin{array}{c} 3 \\ -4 \\ 2 \end{array} \right\} = \left\{ \begin{array}{c} 79 \\ -105 \\ 52 \end{array} \right\} mm/sec$$

Forces in Damping Devices, Fd_{i3D}

$$Fd_{i3D} = C_i \cdot \nabla_{i3D} \cdot \cos\theta_i \tag{7-23}$$

$$Fd_{i3D} = 0.90 \times \left\{ \begin{array}{c} 79 \\ -105 \\ 52 \end{array} \right\} \times \cos 27.6^o = \left\{ \begin{array}{c} 63 \\ -84 \\ 42 \end{array} \right\} kN$$

291

Seismic Design Forces

reduced forces	actual forces
Stage of Maximum Displacement	**Stage of Maximum Velocity**
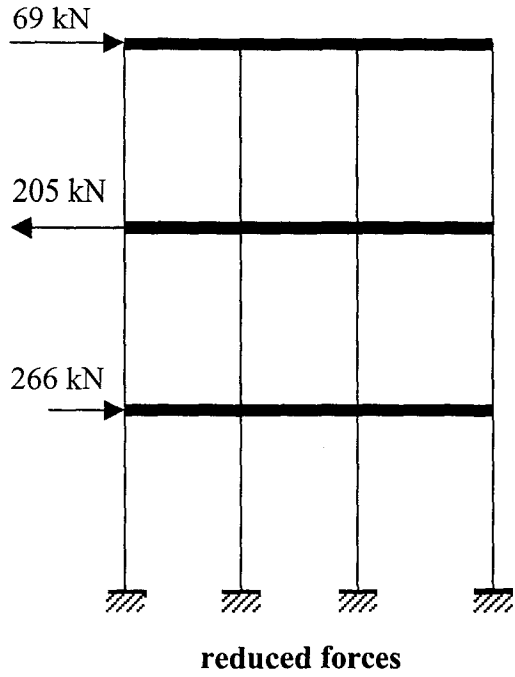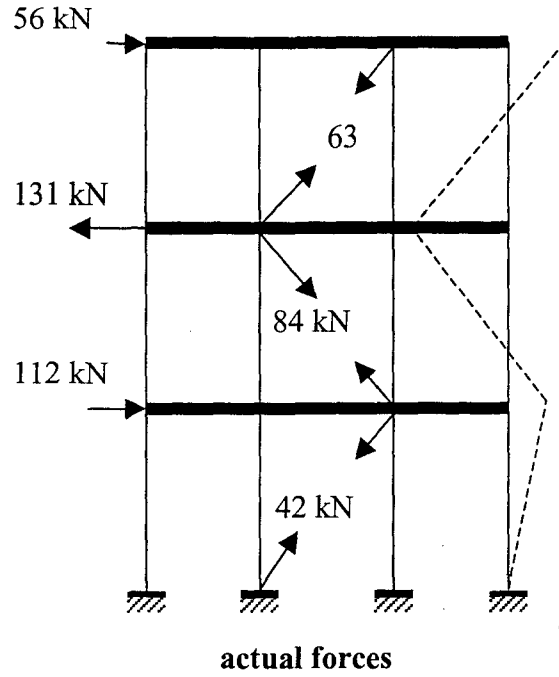
Response at Stage of Maximum Acceleration

Force Coefficients

$$\beta_{V_3} = 0.151 + 0.05 = 0.201$$

$$CF_1 = cos\left[tan^{-1}\left(2\beta_{V_3}\right)\right] \tag{4-41}$$

$$CF_1 = cos\left[tan^{-1}\left(2 \times 0.201\right)\right] = 0.928$$

$$CF_2 = sin\left[tan^{-1}\left(2\beta_{V_3}\right)\right] \tag{4-39}$$

$$CF_2 = sin\left[tan^{-1}\left(2 \times 0.201\right)\right] = 0.373$$

Maximum Acceleration

$$A_{i3,max} = \left(CF_1 + 2\beta_{V_3} \times CF_2\right) \cdot A_{i3} \tag{4-40}$$

$$A_{i3,max} = \left(0.928 + 2 \times 0.201 \times 0.373\right) \cdot \begin{Bmatrix} 0.091 \\ -0.146 \\ 0.189 \end{Bmatrix} = \begin{Bmatrix} 0.098 \\ -0.157 \\ 0.204 \end{Bmatrix} g$$

Maximum Story Shear, $V_{i3,max}$

$$V_{i3,max} = CF_1 \cdot V_{i3}\Big|_{Max\,Disp} \cdot \frac{C_d \Omega_o}{R} + CF_2 \cdot V_{i3}\Big|_{Max\,Velocity}$$

$$V_{i3,max} = 0.928 \times \begin{Bmatrix} 69 \\ -136 \\ 130 \end{Bmatrix} \times \left(\frac{3 \times 5.5}{8}\right) + 0.373 \times \begin{Bmatrix} 56 \\ -74 \\ 37 \end{Bmatrix} = \begin{Bmatrix} 153 \\ -288 \\ 263 \end{Bmatrix} kN$$

RESIDUAL MODE RESPONSE (T_R=0.632 sec > T_s)

Effective Damping Ratio: $\beta_{RD} = 0.228 + 0.05 = 0.278$ $\therefore B_{RD} = 1.734$ (Table A13.3.1)

Roof Displacement, D_{RD}

$$D_{RD} = \left(\frac{g}{4\pi^2}\right) \times \Gamma_R \times \frac{S_{D1} T_R}{B_{RD}} \qquad \text{(A13.4.4.3-2)}$$

For $T_R > T_o$

$$D_{RD} = \left(\frac{9810}{4\pi^2}\right) \times 0.3991 \times \frac{0.6 \times 0.632}{1.734} = 22\,mm$$

Seismic Base Shear, V_R

$$V_R = C_{SR} \cdot \overline{W}_R \qquad \text{(A13.4.3.6-1)}$$

$$C_{SR} = \left(\frac{R}{C_d}\right) \frac{S_{Ds}}{\Omega_o B_{RD}} \qquad \text{(A13.4.3.8-1)}$$

$$C_{SR} = \left(\frac{8}{5.5}\right) \frac{1.0}{3 \times 1.734} = 0.28$$

$$V_R = 0.28 \times 1495 = 419\,kN$$

Response at Stage of Maximum Displacement

Lateral Floor Displacement and Story Drifts

$$\delta_{iR} = D_{RD} \cdot \phi_{iR} \qquad\qquad \text{(A13.4.4.2-2)}$$

$$\delta_{iR} = 22 \times \left\{ \begin{array}{c} 1.000 \\ -0.2024 \\ -1.6292 \end{array} \right\} = \left\{ \begin{array}{c} 22 \\ -4 \\ -36 \end{array} \right\} mm$$

$$\Delta_{iR} = \left\{ \begin{array}{c} 26 \\ 32 \\ -36 \end{array} \right\} mm$$

Design Lateral Inertia Forces, F_{iR}, Design Story Shear Forces, V_{iR}, and Floor Accelerations, A_{iR}

$$F_{iR} = w_i \cdot \phi_{i2} \cdot \frac{\Gamma_3}{\overline{W}_R} \cdot V_{RD} \qquad\qquad \text{(A13.5.3.7-1)}$$

$$F_{iR} = \left\{ \begin{array}{c} 1567 \times 1.0 \times \dfrac{0.3991}{1495} \times 419 \\[2mm] 2900 \times -0.2024 \times \dfrac{0.3991}{1495} \times 419 \\[2mm] 2900 \times -1.6292 \times \dfrac{0.3991}{1495} \times 419 \end{array} \right\} = \left\{ \begin{array}{c} 175 \\ -66 \\ -528 \end{array} \right\} kN$$

$$A_{iR} = \left(F_{iR} \middle/ w_i \right) \times \left(\frac{C_d \cdot \Omega_o}{R} \right)$$

$$A_{i_R} = \left\{ \begin{array}{c} 175 \middle/ 1567 \\ -66 \middle/ 2900 \\ -528 \middle/ 2900 \end{array} \right\} \times \left(\frac{5.5 \times 3}{8} \right) = \left\{ \begin{array}{c} 0.230 \\ -0.047 \\ -0.376 \end{array} \right\} g$$

$$V_{iR} = \left\{ \begin{array}{c} 175 \\ 109 \\ -419 \end{array} \right\} kN$$

Response at Stage of Maximum Velocity

Story Velocity, $\nabla_{i_{RD}}$

$$\nabla_{i_R} = \frac{2\pi}{T_R} \cdot \Delta_{i_R} \qquad\qquad \text{(A13.5.4.5-2)}$$

$$\nabla_{i_R} = \frac{2\pi}{0.632} \times \begin{Bmatrix} 26 \\ 32 \\ -36 \end{Bmatrix} = \begin{Bmatrix} 259 \\ 318 \\ -358 \end{Bmatrix} mm/sec$$

Forces in Damping Devices, $Fd_{i_{RD}}$

$$Fd_{i_R} = C_i \cdot \nabla_{i_R} \cdot \cos\theta_i \qquad\qquad \text{(7-23)}$$

$$Fd_{i_R} = 0.90 \cdot \begin{Bmatrix} 259 \\ 318 \\ -358 \end{Bmatrix} \times \cos 27.6^o = \begin{Bmatrix} 207 \\ 254 \\ -286 \end{Bmatrix} kN$$

Seismic Design Forces
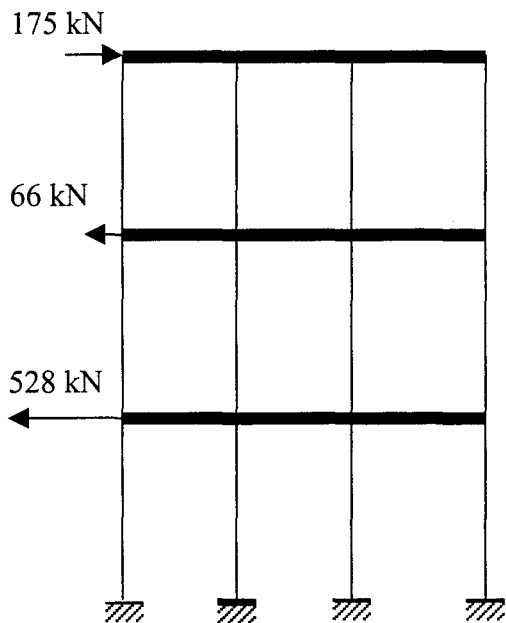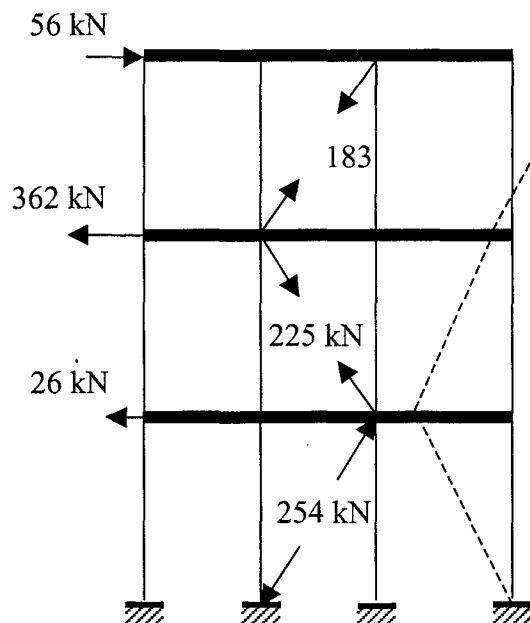
reduced forces	actual forces
Stage of Maximum Displacement	**Stage of Maximum Velocity**

295

Response at Stage of Maximum Acceleration

Force Coefficients

$$\beta_{V_R} = 0.228 + 0.05 = 0.278$$

$$CF_1 = cos\left[tan^{-1}\left(2\beta_{V_R}\right)\right] \tag{4-41}$$

$$CF_1 = cos\left[tan^{-1}\left(2 \times 0.278\right)\right] = 0.874$$

$$CF_2 = sin\left[tan^{-1}\left(2 \times 0.278\right)\right] = 0.486$$

Maximum Acceleration

$$A_{i_R,max} = \left(CF_1 + 2\beta_{V_R} \times CF_2\right) \cdot A_{i_R} \tag{4-40}$$

$$A_{i_R,max} = \left(0.874 + 2 \times 0.278 \times 0.486\right) \cdot \begin{Bmatrix} 0.230 \\ -0.047 \\ -0.376 \end{Bmatrix} = \begin{Bmatrix} 0.263 \\ -0.054 \\ -0.430 \end{Bmatrix} g$$

Maximum Story Shear, $V_{i_R,max}$

$$V_{i_R,max} = CF_1 \cdot V_{i_R}\Big|_{Max\,Disp} \cdot \frac{C_d\Omega_o}{R} + CF_2 \cdot V_{i_R}\Big|_{Max\,Velocity}$$

$$V_{i_R,max} = 0.874 \times \begin{Bmatrix} 175 \\ 109 \\ -419 \end{Bmatrix} \times \left(\frac{3 \times 5.5}{8}\right) + 0.486 \times \begin{Bmatrix} 183 \\ 225 \\ -254 \end{Bmatrix} = \begin{Bmatrix} 404 \\ 306 \\ 879 \end{Bmatrix} kN$$

Total responses resulting from modal combinations were calculated by use of the SRSS combination rule. Table E-1 presents a summary of the modal properties of the frame and Tables E-2 and E-3 present summaries of the results of the analysis for each mode and the total response calculated by both the ELF and the RSA procedures for the DBE and MCE, respectively.

296

E.3 Summary Calculations for 3-Story Frames 3S-60 and 3S-90 with Linear Viscous Damping Systems

Frame 3S-60 is shown in Figure 8-1 and is described as example No.1 in Section 8. This special moment frame does not meet the minimum seismic base shear requirement of NEHRP(2000) since it has been designed for $V_{min} = 0.6V = 0.6 \times 788.5 = 473 \ kN$, or equivalently, it has been designed to have a base shear strength equal to $V_y = V_{min}.\Omega_o.C_d/R = 473 \times 3.0 \times 5.5/8 = 976 \ kN$ for a pattern of lateral loads proportional to the first mode. Its actual base shear strength for this pattern of loads was calculated by the procedures of Appendix C.2 (beam hinges at the beam to column interface) to be $V_y = 971 \ kN$. Summary calculations for this frame are presented in Tables E-4, E-5 and E-6.

Frame 3S-90 is shown in Figure 8-3 and is described as example No.3 in Section 8. The frame has been designed for seismic base shear equal to $V_{min} = 0.90V = 0.9 \times 788.5 = 709.7 \ kN$, or equivalently it has been designed to have a base shear strength $V_y = V_{min}.\Omega_o.C_d/R = 709.7 \times 3.0 \times 5.5/8 = 1464 \ kN$ for a pattern of lateral loads proportional to the first mode. The base shear strength of the frame for this pattern of loads was calculated by the procedures of Appendix C.2 to be $V_y = 1468 \ kN$. Summary calculations for this frame are presented in Tables E-7, E-8, and E-9.

E.4 Summary Calculations for 6-Story Frame 6S-75 with Linear Viscous Damping System

Frame 6S-75 is the 6-story frame shown in Figure 8-5 and described as Example No.5 in Section 8. It has been designed for seismic base shear equal to $V_{min} = 0.75V$, where V was calculated in accordance with Section 5.3 of NEHRP (1997). That is, period $T = 1.2 \times 0.035 \times (85.1)^{0.75} = 1.18$ sec, $C_s = \dfrac{S_{D1}}{T(R/I)} = \dfrac{0.6}{1.18(8/1)} = 0.0636$, $V = C_s W = 0.0636 \times 16,067 = 1022 \ kN$, and $V_{min} = 0.75 \times 1022 = 767 \ kN$. Actually, the frame was designed to have a base shear strength for a pattern of lateral loads proportional to the first mode $V_y = V_{min}.\Omega_o.C_d/R = 767 \times 3.0 \times 5.5/8 = 1582 \ kN$. The frame was analyzed using the procedures of Appendix C.2 and its actual base shear strength was found to be $V_y = 1597 \ kN$. Summary calculations for this frame are presented in Tables E-10, E-11, and E-12.

TABLE E-1 Modal Properties of Frame 3S-75

Quantity	Mode 1	Mode 2	Mode 3	Residual Mode
T_m, sec	1.58	0.49	0.24	0.632
$\{\phi_{im}\}$	1.000 0.657 0.250	1.000 -0.560 -0.690	1.000 -1.618 2.096	1.0000 -0.2024 -1.6292
$\overline{W}_m$, kN	5871	1098	398	1496
Γ_m	1.3991	-0.5334	0.1348	-0.3991

TABLE E-2 Modal Response Calculations for Example No.2: 3-Story Frame (V_{min}=0.75V) with Linear Viscous Damping System. Analysis for the DBE

Quantity	Units	Mode 1 (m=1)	Mode 2 (m=2)	Mode 3 (m=3)	Mode R (m=R)	SRSS ELF	SRSS RSA
1. Elastic Response							
Damping Ratio, β_{Ve}		0.101	0.205	0.152	0.228		
Total Damping Ratio, β_{V+I}		0.151	0.255	0.202	0.278		
Damping Coefficient, B_m		1.352	1.666	1.505	1.735		
Elastic Displacement, D_{em}	mm	244	19	1	22		
2. Roof Displacement and Base Shear							
Assumed Ductility, μ		1.29	1	1	1		
Effective Period, T_{ID}	sec	1.80	0.49	0.24	0.63		
Eff. Viscous Damping Ratio, β_V		0.114	0.205	0.152	0.228		
Hysteretic Damping, β_H		0.066	0	0	0		
Effective Damping, β_m		0.230	0.255	0.202	0.278		
Damping Coefficient, B_m		1.590	1.666	1.505	1.735		
Displacement, D_{mD}	mm	235					
Corrected Displacement, D_{mD}	mm	244	19	1	22		
Seismic Coefficient, C_s		0.102	0.436	0.483	0.419		
Seismic Base Shear, V_m	kN	599	320	129	419	731	691
Yield Displacement, D_y	mm	183	----------	----------	----------		
Computed Ductility, μ		1.33	----------	----------	----------		
3. Response at Stage of Maximum Displacement							
Lateral Floor Displacement, δ_{ij}	mm	244	19	1	22		
		160	-11	-2	-4		
		61	-13	3	-35		
Story Drift, Δ_{jm}	mm	84	30	3	26	88	89
		99	2	-5	31	104	99
		61	-13	3	-35	70	62
Design Lateral Forces, F_{im}	kN	220	243	68	175		
		267	-252	-204	-66		
		102	-311	264	-527		
Floor Acceleration, A_{im}	g	0.293	0.480	0.134	0.345	0.453	0.579
		0.193	-0.269	-0.217	-0.070	0.205	0.396
		0.073	-0.331	0.282	-0.562	0.567	0.441
Actual Story Shear Forces, V_{jm}	kN	453	502	140	360	579	690
		1004	-18	-280	224	1029	1042
		1213	-659	265	-863	1489	1406

299

4. Response at Stage of Maximum Velocity							
Drift Velocity, ∇_{im}	mm/sec	290	382	88	259	389	488
		344	32	-125	307	462	368
		212	-169	70	-351	410	280
Force in Damping Devices, Fd_{jm}	kN	232	305	70	207	311	390
		275	25	-100	245	369	294
		169	-135	56	-280	327	223
Horizontal Damper Force, Vd_{jm}	kN	206	270	62	183		
		244	23	-88	218		
		150	-120	50	-249		

5. Response at Stage of Maximum Acceleration							
Ducitility, μ		1.33	1	1	1		
Eff. Viscous Damping Ratio, β_V		0.165	0.255	0.202	0.278		
Parameter δ		0.330	0.472	0.384	0.508		
Coefficient CF_1		0.951	0.891	0.928	0.874		
Product $CF_1 . \mu$		1.264	0.891	0.928	0.874		
Force Coefficient, CF_1 or C_{mFD}		1.000	0.891	0.928	0.874		
Force Coefficient, CF_2 or C_{mFV}		0.313	0.454	0.374	0.486		
Max.Floor Acc., $A_{im,max}$	g	0.330	0.364	0.098	0.261	0.421	0.501
		0.194	0.202	0.154	0.052	0.201	0.320
		0.082	0.248	0.200	0.430	0.438	0.329
Maximum Story Shear, $V_{jm,max}$ (actual)	kN	517	570	153	404	656	785
		1080	-6	-293	302	1122	1119
		1260	-641	264	-875	1534	1439

TABLE E-3 Modal Response Calculations for Example No.2: 3-Story Frame (V$_{min}$=0.75V) with Linear Viscous Damping System. Analysis for the MCE

Quantity	Units	Mode 1 (m=1)	Mode 2 (m=2)	Mode 3 (m=3)	Mode R (m=R)	SRSS ELF	SRSS RSA
1. Elastic Response							
Damping Ratio, β_{Ve}		0.101	0.205	0.152	0.228		
Total Damping Ratio, β_{V+I}		0.151	0.255	0.202	0.278		
Damping Coefficient, B_m		1.352	1.666	1.505	1.735		
Elastic Displacement, D_{em}	mm	365	29	2	32		
2. Roof Displacement and Base Shear							
Assumed Ductility, μ		2	1	1	1		
Effective Period, T_{1D}	sec	2.23	0.49	0.24	0.63		
Eff. Viscous Damping Ratio, β_V		0.142	0.205	0.152	0.228		
Hysteretic Damping, β_H		0.148	0	0	0		
Effective Damping, β_m		0.340	0.255	0.202	0.278		
Damping Coefficient, B_m		1.919	1.666	1.505	1.735		
Displacement, D_{mD}	mm	364					
Corrected Displacement, D_{mD}	mm	365	29	2	32		
Seismic Coefficient, C_s		0.102	0.436	0.483	0.419		
Seismic Base Shear, V_m	kN	597	479	192	627	866	790
Yield Displacement, D_y	mm	182	----------	----------	----------		
Computed Ductility, μ		2	----------	----------	----------		
3. Response at Stage of Maximum Displacement							
Lateral Floor Displacement, δ_{ij}	mm	365	29	2	32		
		240	-16	-3	-7		
		91	-20	4	-53		
Story Drift, Δ_{jm}	mm	125	45	5	39	131	133
		149	4	-7	46	156	149
		91	-20	4	-53	106	94
Design Lateral Forces, F_{im}	kN	223	365	102	262		
		271	-378	-306	-99		
		103	-466	396	-791		
Floor Acceleration, A_{im}	g	0.293	0.480	0.134	0.345	0.453	0.579
		0.193	-0.269	-0.217	-0.070	0.205	0.396
		0.073	-0.331	0.282	-0.562	0.567	0.441
Actual Story Shear Forces, V_{jm}	kN	460	752	211	540	709	907
		1019	-27	-420	337	1073	1103
		1232	-988	397	-1294	1787	1628

4. Response at Stage of Maximum Velocity							
Drift Velocity, ∇_{im}	mm/sec	352	573	132	388	524	685
		418	48	-187	461	622	461
		257	-253	105	-527	586	376
Force in Damping Devices, Fd_{jm}	kN	282	458	105	310	419	547
		334	38	-149	368	497	368
		205	-202	84	-421	468	300
Horizontal Damper Force, Vd_{jm}	kN	250	406	93	275		
		296	34	-132	326		
		182	-179	75	-373		

5. Response at Stage of Maximum Acceleration							
Ducitility, μ		2	1	1	1		
Eff. Viscous Damping Ratio, β_V		0.192	0.255	0.202	0.278		
Parameter δ		0.367	0.472	0.383	0.508		
Coefficient CF_1		0.933	0.891	0.927	0.874		
Product $CF_1 . \mu$		1.872	0.891	0.927	0.874		
Force Coefficient, CF_1 or C_{mFD}		1.000	0.891	0.927	0.874		
Force Coefficient, CF_2 or C_{mFV}		0.359	0.455	0.374	0.486		
Max.Floor Acc., $A_{im,max}$	g	0.351	0.545	0.147	0.387	0.522	0.665
		0.199	0.298	0.231	0.070	0.211	0.426
		0.088	0.328	0.288	0.609	0.615	0.445
Maximum Story Shear, $V_{jm,max}$ (actual)	kN	549	855	230	606	818	1042
		1125	-9	-439	453	1213	1208
		1297	-962	396	-1312	1845	1663

302

TABLE E-4 Modal Properties of Frame 3S-60

Quantity	Mode 1	Mode 2	Mode 3	Residual Mode
T_m, sec	1.78	0.54	0.27	0.712
$\{\phi_{im}\}$	1.000 0.667 0.252	1.000 -0.543 -0.760	1.000 -1.550 1.957	1.0000 -0.184 -1.658
$\overline{W}_m$, kN	5889	1095	383	1478
Γ_m	1.3915	-0.5308	0.1393	-0.3915

TABLE E-5 Modal Response Calculations for Example No.1: 3-Story Frame (V_{min}=0.60V) with Linear Viscous Damping System. Analysis for the DBE

Quantity	Units	Mode 1 (m=1)	Mode 2 (m=2)	Mode 3 (m=3)	Mode R (m=R)	SRSS ELF	RSA
1. Elastic Response							
Damping Ratio, β_{Ve}		0.100	0.200	0.154	0.231		
Total Damping Ratio, β_{V+I}		0.150	0.250	0.204	0.281		
Damping Coefficient, B_m		1.350	1.651	1.511	1.742		
Elastic Displacement, D_{em}	mm	273	23	2	24		
2. Roof Displacement and Base Shear							
Assumed Ductility, μ		1.43	1	1	1		
Effective Period, T_{1D}	sec	2.13	0.54	0.27	0.71		
Eff. Viscous Damping Ratio, β_V		0.120	0.200	0.154	0.231		
Hysteretic Damping, β_H		0.089	0	0	0		
Effective Damping, β_m		0.258	0.255	0.202	0.278		
Damping Coefficient, B_m		1.675	1.666	1.505	1.735		
Displacement, D_{mD}	mm	263					
Corrected Displacement, D_{mD}	mm	273	23	2	24		
Seismic Coefficient, C_S		0.082	0.294	0.321	0.278		
Seismic Base Shear, V_m	kN	480	322	123	411	633	591
Yield Displacement, D_y	mm	184	----------	----------	----------		
Computed Ductility, μ		1.48	----------	----------	----------		
3. Response at Stage of Maximum Displacement							
Lateral Floor Displacement, δ_{ij}	mm	273 / 182 / 69	23 / -13 / -16	2 / -3 / 3	24 / -4 / -40		
Story Drift, Δ_{jm}	mm	91 / 113 / 69	36 / 4 / -16	4 / -6 / 3	28 / 35 / -40	95 / 119 / 79	98 / 114 / 71
Design Lateral Forces, F_{im}	kN	178 / 220 / 83	244 / -246 / -319	70 / -201 / 254	171 / -58 / -524		
Floor Acceleration, A_{im}	g	0.234 / 0.156 / 0.059	0.322 / -0.175 / -0.227	0.092 / -0.143 / 0.180	0.225 / -0.041 / -0.373	0.325 / 0.161 / 0.378	0.409 / 0.275 / 0.296
Actual Story Shear Forces, V_{jm}	kN	367 / 820 / 991	504 / -2 / -661	145 / -271 / 253	352 / 233 / -849	509 / 852 / 1305	640 / 863 / 1218

TABLE E-5 continued

4. Response at Stage of Maximum Velocity							
Drift Velocity, ∇_{im}	mm/sec	269 335 203	418 44 -191	99 -136 76	249 310 -349	366 457 404	507 364 289
Force in Damping Devices, Fd_{jm}	kN	192 239 145	298 32 -137	71 -97 54	178 222 -249	262 326 288	362 260 207
Horizontal Damper Force, Vd_{jm}	kN	170 212 129	264 28 -121	63 -86 48	158 196 -221		

5. Response at Stage of Maximum Acceleration							
Ductility, μ		1.48	1	1	1		
Eff. Viscous Damping Ratio, β_V		0.170	0.250	0.204	0.281		
Parameter δ		0.327	0.464	0.387	0.511		
Coefficient CF_1		0.947	0.894	0.926	0.872		
Product $CF_1 . \mu$		1.411	0.894	0.926	0.872		
Force Coefficient, CF_1 or C_{mFD}		1.000	0.894	0.926	0.872		
Force Coefficient, CF_2 or C_{mFV}		0.321	0.448	0.377	0.489		
Max.Floor Acc., $A_{im,max}$	g	0.269 0.161 0.050	0.363 -0.193 -0.226	0.101 -0.152 0.185	0.245 -0.029 -0.396	0.364 0.163 0.399	0.463 0.293 0.296
Maximum Story Shear, $V_{jm,max}$ (actual)	kN	422 888 1032	569 10 -645	157 -283 252	384 299 -848	570 937 1336	725 932 1243

305

TABLE E-6 Modal Response Calculations for Example No.1: 3-Story Frame (V_min=0.60V) with Linear Viscous Damping System. Analysis for the MCE

Quantity	Units	Mode 1 (m=1)	Mode 2 (m=2)	Mode 3 (m=3)	Mode R (m=R)	SRSS ELF	SRSS RSA
1. Elastic Response							
Damping Ratio, β_{Ve}		0.100	0.200	0.154	0.231		
Total Damping Ratio, β_{V+I}		0.150	0.250	0.204	0.281		
Damping Coefficient, B_m		1.350	1.651	1.511	1.742		
Elastic Displacement, D_{em}	mm	410	35	3	36		
2. Roof Displacement and Base Shear							
Assumed Ductility, μ		2.26	1	1	1		
Effective Period, T_{1D}	sec	2.68	0.54	0.27	0.71		
Eff. Viscous Damping Ratio, β_V		0.150	0.200	0.154	0.231		
Hysteretic Damping, β_H		0.164	0	0	0		
Effective Damping, βm		0.365	0.255	0.202	0.278		
Damping Coefficient, B_m		1.995	1.666	1.505	1.735		
Displacement, D_{mD}	mm	417					
Corrected Displacement, D_{mD}	mm	417	35	3	36		
Seismic Coefficient, C_s		0.082	0.441	0.481	0.418		
Seismic Base Shear, V_m	kN	481	482	185	617	783	706
Yield Displacement, D_y	mm	184	----------	----------	----------		
Computed Ductility, μ		2.26	----------	----------	----------		
3. Response at Stage of Maximum Displacement							
Lateral Floor Displacement, δ_{ij}	mm	417 / 278 / 105	35 / -19 / -25	3 / -4 / 5	36 / -7 / -59		
Story Drift, Δ_{jm}	mm	139 / 173 / 105	54 / 6 / -25	6 / -9 / 5	42 / 53 / -59	145 / 181 / 121	149 / 173 / 108
Design Lateral Forces, F_{im}	kN	178 / 220 / 83	366 / -368 / -479	105 / -302 / 381	256 / -87 / -786		
Floor Acceleration, A_{im}	g	0.293 / 0.193 / 0.073	0.480 / -0.269 / -0.331	0.134 / -0.217 / 0.282	0.345 / -0.070 / -0.562	0.453 / 0.205 / 0.567	0.579 / 0.396 / 0.441
Actual Story Shear Forces, V_{jm}	kN	368 / 821 / 993	756 / -4 / -991	217 / -406 / 379	528 / 349 / -1273	644 / 892 / 1614	868 / 916 / 1453

TABLE E-6 continued

4. Response at Stage of Maximum Velocity

Drift Velocity, ∇_{im}	mm/sec	326	627	149	374	496	722
		407	66	-205	466	618	460
		247	-287	114	-524	579	395
Force in Damping Devices, $F d_{jm}$	kN	233	448	106	267	354	516
		290	47	-146	332	441	328
		176	-205	81	-374	413	282
Horizontal Damper Force, $V d_{jm}$	kN	206	397	94	236		
		257	42	-129	295		
		156	-181	72	-331		

5. Response at Stage of Maximum Acceleration

Ducitility, μ		2.26	1	1	1		
Eff. Viscous Damping Ratio, β_V		0.200	0.250	0.204	0.281		
Parameter δ		0.381	0.464	0.387	0.511		
Coefficient CF_1		0.928	0.894	0.926	0.872		
Product $CF_1 . \mu$		2.102	0.894	0.926	0.872		
Force Coefficient, CF_1 or C_{mFD}		1.000	0.894	0.926	0.872		
Force Coefficient, CF_2 or C_{mFV}		0.372	0.448	0.377	0.489		
Max.Floor Acc., $A_{im,max}$	g	0.284	0.545	0.151	0.368	0.465	0.632
		0.163	-0.289	-0.228	-0.044	0.169	0.403
		0.046	-0.339	0.277	-0.593	0.595	0.440
Maximum Story Shear, $V_{jm,max}$ (actual)	kN	444	853	236	576	728	991
		917	15	-425	448	1021	1011
		1051	-968	378	-1272	1650	1478

TABLE E-7 Modal Properties of Frame 3S-90

Quantity	Mode 1	Mode 2	Mode 3	Residual Mode
T_m, sec	1.38	0.43	0.21	0.552
$\{\phi_{im}\}$	1.000 0.639 0.237	1.000 -0.586 -0.697	1.000 -1.648 2.146	1.0000 -0.2405 -1.6218
$\overline{W}_m$, kN	5799	1170	398	1568
Γ_m	1.4105	-0.5426	0.1322	-0.4105

TABLE E-8 Modal Response Calculations for Example No.3: 3-Story Frame (V$_{min}$=0.90V) with Linear Viscous Damping System. Analysis for the DBE

Quantity	Units	Mode 1 (m=1)	Mode 2 (m=2)	Mode 3 (m=3)	Mode R (m=R)	SRSS ELF	SRSS RSA
1. Elastic Response							
Damping Ratio, β_{Ve}		0.101	0.199	0.146	0.219		
Total Damping Ratio, β_{V+I}		0.151	0.249	0.196	0.269		
Damping Coefficient, B_m		1.352	1.649	1.490	1.707		
Elastic Displacement, D_{em}	mm	214	15	1	18		
2. Roof Displacement and Base Shear							
Assumed Ductility, μ		1.23	1.0	1.0	1.0		
Effective Period, T_{1D}	sec	1.530	0.430	0.210	0.552		
Eff. Viscous Damping Ratio, β_V		0.112	0.199	0.146	0.219		
Hysteretic Damping, β_H		0.055	0.000	0.000	0.000		
Effective Damping, βm		0.217	0.249	0.196	0.269		
Damping Coefficient, B_m		1.551	1.649	1.490	1.707		
Displacement, D_{mD}	mm	207					
Corrected Displacement, D_{mD}	mm	214	15	1	18		
Seismic Coefficient, C_s		0.123	0.294	0.326	0.284		
Seismic Base Shear, V_m	kN	711	344	130	445	839	800
Yield Displacement, D_y	mm	169	----------	----------	----------		
Computed Ductility, μ		1.27	----------	----------	----------		
3. Response at Stage of Maximum Displacement							
Lateral Floor Displacement, δ_{ij}	mm	214	15	1	18		
		137	-9	-2	-4		
		51	-11	2	-30		
Story Drift, Δ_{jm}	mm	77	24	3	23	81	81
		86	2	-4	25	90	86
		51	-11	2	-30	59	52
Design Lateral Forces, F_{im}	kN	271	250	67	183		
		320	-271	-206	-81		
		119	-323	268	-548		
Floor Acceleration, A_{im}	g	0.357	0.329	0.089	0.240	0.430	0.493
		0.228	-0.193	-0.146	-0.058	0.235	0.332
		0.085	-0.229	0.190	-0.390	0.399	0.310
Actual Story Shear Forces, V_{jm}	kN	559	516	139	377	674	773
		1220	-44	-285	209	1237	1253
		1465	-709	267	-922	1730	1649

4. Response at Stage of Maximum Velocity							
Drift Velocity, ∇_{im}	mm/sec	318	350	77	257	409	479
		354	25	-110	286	455	372
		209	-154	62	-336	395	267
Force in Damping Devices, $F_{d\,jm}$	kN	281	310	68	227	361	424
		313	22	-98	253	402	329
		185	-136	55	-297	350	236
Horizontal Damper Force, $V_{d\,jm}$	kN	249	275	60	201		
		277	19	-86	224		
		164	-121	49	-263		
5. Response at Stage of Maximum Acceleration							
Ducitility, μ		1.27	1.00	1.00	1.00		
Eff. Viscous Damping Ratio, β_V		0.16	0.25	0.20	0.27		
Parameter δ		0.31	0.46	0.37	0.49		
Coefficient CF_1		0.95	0.89	0.93	0.88		
Product $CF_1 . \mu$		1.21	0.89	0.93	0.88		
Force Coefficient, CF_1 or C_{mFD}		1.00	0.89	0.93	0.88		
Force Coefficient, CF_2 or C_{mFV}		0.31	0.45	0.37	0.47		
Max.Floor Acc., $A_{im,max}$	g	0.406	0.373	0.097	0.273	0.489	0.559
		0.231	0.212	0.155	0.055	0.237	0.349
		0.097	0.227	0.194	0.423	0.434	0.314
Maximum Story Shear, $V_{jm,max}$ (actual)	kN	635	584	151	427	766	876
		1305	-30	-297	290	1337	1339
		1515	-688	267	-936	1781	1685

310

TABLE E-9 Modal Response Calculations for Example No.3: 3-Story Frame (V_{min}=0.90V) with Linear Viscous Damping System. Analysis for the MCE

Quantity	Units	Mode 1 (m=1)	Mode 2 (m=2)	Mode 3 (m=3)	Mode R (m=R)	SRSS ELF	SRSS RSA
1. Elastic Response							
Damping Ratio, β_{Ve}		0.101	0.199	0.146	0.219		
Total Damping Ratio, β_{V+I}		0.151	0.249	0.196	0.269		
Damping Coefficient, B_m		1.352	1.649	1.490	1.707		
Elastic Displacement, D_{em}	mm	322	23	1	27		
2. Roof Displacement and Base Shear							
Assumed Ductility, μ		1.9	1.0	1.0	1.0		
Effective Period, T_{1D}	sec	1.892	0.430	0.210	0.552		
Eff. Viscous Damping Ratio, β_V		0.138	0.199	0.146	0.219		
Hysteretic Damping, β_H		0.138	0.000	0.000	0.000		
Effective Damping, β_m		0.326	0.249	0.196	0.269		
Damping Coefficient, B_m		1.879	1.649	1.490	1.707		
Displacement, D_{mD}	mm	317					
Corrected Displacement, D_{mD}	mm	322	23	1	27		
Seismic Coefficient, C_s		0.123	0.441	0.488	0.426		
Seismic Base Shear, V_m	kN	712	516	194	668	976	900
Yield Displacement, D_y	mm	169	--------	--------	--------		
Computed Ductility, μ		1.91	--------	--------	--------		
3. Response at Stage of Maximum Displacement							
Lateral Floor Displacement, δ_{ij}	mm	322 / 206 / 76	23 / -13 / -16	1 / -2 / 3	27 / -7 / -44		
Story Drift, Δ_{jm}	mm	116 / 129 / 76	36 / 3 / -16	4 / -6 / 3	34 / 38 / -44	121 / 135 / 88	122 / 129 / 78
Design Lateral Forces, F_{im}	kN	271 / 321 / 119	375 / -407 / -484	101 / -308 / 402	274 / -122 / -822		
Floor Acceleration, A_{im}	g	0.357 / 0.228 / 0.085	0.494 / -0.289 / -0.344	0.133 / -0.219 / 0.286	0.361 / -0.087 / -0.585	0.508 / 0.244 / 0.591	0.624 / 0.429 / 0.455
Actual Story Shear Forces, V_{jm}	kN	559 / 1221 / 1467	774 / -65 / -1063	209 / -428 / 401	565 / 314 / -1383	795 / 1261 / 2015	977 / 1295 / 1855

TABLE E-9 continued

4. Response at Stage of Maximum Velocity							
Drift Velocity, ∇_{im}	mm/sec	386	525	115	385	545	662
		429	37	-165	429	607	462
		253	-231	94	-504	564	355
Force in Damping Devices, F_{djm}	kN	341	465	102	341	482	585
		380	33	-146	379	537	408
		224	-204	83	-445	499	314
Horizontal Damper Force, V_{djm}	kN	302	412	91	302		
		337	29	-130	336		
		198	-181	73	-395		
5. Response at Stage of Maximum Acceleration							
Ducitility, μ		1.91	1.00	1.00	1.00		
Eff. Viscous Damping Ratio, β_V		0.19	0.25	0.20	0.27		
Parameter δ		0.36	0.46	0.37	0.49		
Coefficient CF_1		0.94	0.89	0.93	0.88		
Product $CF_1 \cdot \mu$		1.79	0.89	0.93	0.88		
Force Coefficient, CF_1 or C_{mFD}		1.00	0.89	0.93	0.88		
Force Coefficient, CF_2 or C_{mFV}		0.35	0.45	0.37	0.47		
Max.Floor Acc., $A_{im,max}$	g	0.425	0.559	0.145	0.409	0.590	0.717
		0.232	0.318	0.232	0.082	0.246	0.457
		0.101	0.340	0.291	0.635	0.643	0.459
Maximum Story Shear, $V_{jm,max}$ (actual)	kN	666	876	227	641	924	1124
		1340	-46	-445	436	1409	1413
		1536	-1032	400	-1405	2082	1894

312

TABLE E-10 Modal Properties of Frame 6S-75

Quantity		Mode 1	Mode 2	Mode 3	Mode 4	Mode 5	Mode 6	Resid. Mode
T_m, sec		2.60	0.93	0.51	0.33	0.23	0.17	1.04
$\{\phi_{im}\}$		1.000	1.000	1.000	1.000	1.000	1.000	1.000
		0.872	0.289	-0.456	-1.148	-1.721	-2.200	0.565
		0.682	-0.411	-0.709	0.435	2.660	5.569	-0.082
		0.476	-0.698	0.175	0.872	-2.112	-10.369	-0.783
		0.268	-0.582	0.784	-0.634	-0.293	14.923	-1.490
		0.096	-0.249	0.487	-0.845	2.383	-15.385	-2.075
W_m, kN		12045	2129	917	449	296	230	4022
Γ_m		1.4163	-0.6614	0.3853	-0.1989	0.0701	-0.0115	-0.4163

313

TABLE E-11 Modal Response Calculations for Example No.5: 6-Story Frame (V$_{min}$=0.75V) with Linear Viscous Damping System. Analysis for the DBE

Quantity	Units	Mode 1 (m=1)	Mode 2 (m=2)	Mode 3 (m=3)	Mode 4 (m=4)	Mode 5 (m=5)	Mode 6 (m=6)	Mode R (m=R)	SRSS ELF	SRSS RSA
1. Elastic Response										
Damping Ratio, β_{Ve}		0.103	0.286	0.365	0.354	0.326	0.320	0.456		
Total Damping Ratio, β_{V+I}		0.153	0.336	0.415	0.404	0.376	0.370	0.506		
Damping Coefficient, B_m		1.358	1.909	2.146	2.112	2.028	2.010	2.419		
Elastic Displacement, D_{em}	mm	285.3	72.6	30.1	12.8	6.5	3.6	64.1		
2. Roof Displacement and Base Shear										
Assumed Ductility, μ		1.25	1.00	1.00	1.00	1.00	1.00	1.00		
Effective Period, T_{1D}	sec	2.91	0.93	0.51	0.33	0.23	0.17	1.04		
Eff. Viscous Damping Ratio, β_v		0.115	0.286	0.365	0.354	0.326	0.320	0.456		
Hysteretic Damping, β_H		0.059	0.000	0.000	0.000	0.000	0.000	0.000		
Effective Damping, β_m		0.224	0.336	0.415	0.404	0.376	0.370	0.506		
Damping Coefficient, B_m		1.572	1.909	2.146	2.112	2.028	2.010	2.419		
Displacement, D_{mD}	mm	390	------	------	------	------	------	------		
Corrected Displacement, D_{mD}	mm	404	48.0	11.6	2.5	0.5	0.0	26.7		
Seismic Coefficient, C_s		0.064	0.164	0.226	0.230	0.239	0.241	0.200		
Seismic Base Shear, V_m	kN	767	530	303	165	101	55	1192	1418	1001
Yield Displacement, D_y	mm	312	------	------	------	------	------	------		
Computed Ductility, μ		1.29	------	------	------	------	------	------		

314

TABLE E-11 continued

3. Response at Stage of Maximum Displacement

Quantity	Units	Mode 1 (m=1)	Mode 2 (m=2)	Mode 3 (m=3)	Mode 4 (m=4)	Mode 5 (m=5)	Mode 6 (m=6)	Mode R (m=R)	SRSS ELF	SRSS RSA
Lateral Floor Displacement, δ_{ij}	mm	404	48	12	3	0	0	27		
		352	14	-5	-3	-1	0	15		
		276	-20	-8	1	1	0	-2		
		192	-34	2	2	-1	0	-21		
		108	-28	9	-2	0	1	-40		
		39	-12	6	-2	1	-1	-55		
Story Drift, Δ_{jm}	mm	52	34	17	5	1	0	12	53	64
		77	34	3	-4	-2	0	17	79	84
		83	14	-10	-1	2	1	19	85	85
		84	-6	-7	4	-1	-1	19	86	85
		69	-16	3	1	-1	1	16	71	71
		39	-12	6	-2	1	-1	-55	68	41
Design Lateral Forces, F_{im}	kN	141	170	136	72	26	4	131		
		228	91	-115	-152	-84	-18	137		
		178	-129	-179	58	129	45	-20		
		124	-219	44	115	-103	-83	-189		
		70	-183	198	-84	-14	120	-361		
		25	-78	123	-112	116	-124	-502		
Floor Acceleration, A_{im}	g	0.186	0.224	0.180	0.094	0.035	0.006	0.172	0.253	0.356
		0.162	0.065	-0.082	-0.108	-0.059	-0.013	0.097	0.189	0.229
		0.127	-0.092	-0.127	0.041	0.092	0.032	-0.014	0.128	0.228
		0.089	-0.156	0.031	0.082	-0.073	-0.059	-0.135	0.161	0.221
		0.050	-0.130	0.141	-0.060	-0.010	0.085	-0.257	0.261	0.224
		0.018	-0.056	0.087	-0.080	0.082	-0.088	-0.357	0.358	0.179
Actual Story Shear Forces, V_{jm}	kN	291	350	281	148	54	9	270	397	558
		762	538	44	-166	-118	-27	552	940	956
		1130	271	-325	-47	148	65	511	1240	1218
		1386	-181	-234	191	-63	-107	120	1392	1436
		1531	-559	174	18	-93	140	-624	1653	1648
		1583	-720	428	-213	146	-115	-1660	2294	1813

TABLE E-11 continued

Quantity	Units	Mode 1 (m=1)	Mode 2 (m=2)	Mode 3 (m=3)	Mode 4 (m=4)	Mode 5 (m=5)	Mode 6 (m=6)	Mode R (m=R)	SRSS ELF	RSA
4. Response at Stage of Maximum Velocity										
Drift Velocity, ∇_{im}	mm/sec	112	231	208	104	34	5	70	132	348
		166	227	36	-77	-54	-12	104	196	299
		180	93	-126	-21	59	24	113	212	248
		182	-38	-87	73	-23	-38	114	214	222
		150	-108	42	10	-33	46	94	177	198
		84	-81	70	-41	30	-23	-334	345	147
Force in Damping Devices, $F_{d_{jm}}$	kN	173	358	323	162	52	8	109	205	540
		257	352	56	-119	-84	-18	162	304	464
		342	177	-240	-40	113	46	215	404	471
		345	-72	-165	139	-43	-73	217	408	422
		384	-277	109	26	-85	118	241	454	508
		215	-207	178	-105	76	-60	-856	883	375
Horizontal Damper Force, $V_{d_{jm}}$	kN	154	317	286	143	46	7	96	181	478
		228	312	50	-106	-75	-16	143	269	411
		303	157	-213	-36	100	41	190	358	418
		306	-63	-147	123	-38	-65	192	361	374
		341	-245	96	23	-75	104	214	402	450
		190	-183	158	-93	67	-53	-759	782	333

316

TABLE E-11 continued

Quantity	Units	Mode 1 (m=1)	Mode 2 (m=2)	Mode 3 (m=3)	Mode 4 (m=4)	Mode 5 (m=5)	Mode 6 (m=6)	Mode R (m=R)	SRSS ELF	SRSS RSA
5. Response at Stage of Maximum Acceleration										
Ductility, μ		1.29	1.00	1.00	1.00	1.00	1.00	1.00		
Eff. Viscous Damping Ratio, β_V		0.16	0.34	0.42	0.40	0.38	0.37	0.51		
Parameter δ		0.32	0.59	0.69	0.68	0.64	0.64	0.79		
Coefficient CF_1		0.95	0.83	0.77	0.78	0.80	0.80	0.70		
Product $CF_1 . \mu$		1.23	0.83	0.77	0.78	0.80	0.80	0.70		
Force Coefficient, CF_1 or C_{mFD}		1.00	0.83	0.77	0.78	0.80	0.80	0.70		
Force Coefficient, CF_2 or C_{mFV}		0.31	0.56	0.64	0.63	0.60	0.59	0.71		
Max.Floor Acc., $A_{im,max}$	g	0.217	0.298	0.255	0.131	0.045	0.007	0.165	0.272	0.469
		0.170	0.055	0.115	0.138	0.073	0.015	0.080	0.188	0.264
		0.135	0.106	0.156	0.047	0.110	0.037	0.021	0.137	0.263
		0.089	0.172	0.039	0.098	0.087	0.069	0.095	0.130	0.247
		0.054	0.143	0.162	0.068	0.016	0.103	0.186	0.193	0.255
		0.034	0.058	0.081	0.087	0.095	0.103	0.490	0.491	0.196
Maximum Story Shear, $V_{jm,max}$ (actual)	kN	340	468	399	205	71	11	258	427	735
		833	620	66	-195	-139	-32	489	966	1069
		1225	313	-386	-59	178	76	494	1320	1337
		1482	-186	-274	226	-74	-124	221	1499	1542
		1638	-600	195	28	-119	175	-286	1662	1768
		1642	-700	430	-224	157	-124	-1706	2368	1861

317

TABLE E-12 Modal Response Calculations for Example No.5: 6-Story Frame
(V$_{min}$=0.75V) with Linear Viscous Damping System. Analysis for the MCE

Quantity	Units	Mode 1 (m=1)	Mode 2 (m=2)	Mode 3 (m=3)	Mode 4 (m=4)	Mode 5 (m=5)	Mode 6 (m=6)	Mode R (m=R)	SRSS ELF	SRSS RSA
1. Elastic Response										
Damping Ratio, β_{Ve}		0.103	0.283	0.358	0.353	0.335	0.317	0.462		
Total Damping Ratio, β_{V+I}		0.153	0.333	0.408	0.403	0.385	0.367	0.512		
Damping Coefficient, B_m		1.358	1.909	2.146	2.112	2.028	2.010	2.419		
Elastic Displacement, D_{em}	mm	608	71.8	16.9	3.9	0.8	0.1	40.5		1001
2. Roof Displacement and Base Shear										
Assumed Ductility, μ		1.93	1.00	1.00	1.00	1.00	1.00	1.00		
Effective Period, T_{1D}	sec	3.61	0.93	0.51	0.33	0.23	0.17	1.04		
Eff. Viscous Damping Ratio, β_V		0.143	0.283	0.358	0.353	0.335	0.317	0.462		
Hysteretic Damping, β_H		0.142	0.000	0.000	0.000	0.000	0.000	0.000		
Effective Damping, β_m		0.335	0.333	0.408	0.403	0.385	0.367	0.512		
Damping Coefficient, B_m		1.905	1.909	2.146	2.112	2.028	2.010	2.419		
Displacement, D_{mD}	mm	603	------	------	------	------	------	------		
Corrected Displacement D_{mD}	mm	608	71.8	16.9	3.9	0.8	0.1	40.5		
Seismic Coefficient, C_s		0.063	0.246	0.339	0.344	0.359	0.362	0.301		
Seismic Base Shear, V_m	kN	767	530	303	165	101	55	1192	1418	
Yield Displacement, D_y	mm	312	------	------	------	------	------	------		
Computed Ductility, μ		1.95	------	------	------	------	------	------		

TABLE E-12 continued

3. Response at Stage of Maximum Displacement

Quantity	Units	Mode 1 (m=1)	Mode 2 (m=2)	Mode 3 (m=3)	Mode 4 (m=4)	Mode 5 (m=5)	Mode 6 (m=6)	Mode R (m=R)	SRSS ELF	SRSS RSA
Lateral Floor Displacement, δ_{ij}	mm	608	72	17	4	1	0	41		
		527	21	-7	-4	-1	0	22		
		414	-28	-13	1	2	0	-3		
		291	-51	2	4	-1	-1	-31		
		168	-44	14	-2	-1	1	-58		
		59	-19	9	-4	2	-1	-83		
Story Drift, Δ_{jm}	mm	82	51	24	8	2	0	18	84	99
		113	49	6	-5	-3	-1	25	116	124
		123	23	-15	-3	3	1	28	126	126
		123	-7	-12	6	0	-1	28	126	124
		109	-25	5	2	-2	1	24	112	112
		59	-19	9	-4	2	-1	-83	102	63
Design Lateral Forces, F_{im}	kN	141	254	198	110	48	11	199		
		226	138	-153	-219	-142	-39	202		
		178	-183	-274	45	183	79	-29		
		125	-331	42	205	-99	-119	-279		
		72	-287	295	-107	-69	141	-530		
		25	-122	194	-199	181	-127	-752		
Floor Acceleration, A_{im}	g	0.186	0.334	0.261	0.144	0.063	0.014	0.262	0.321	0.489
		0.161	0.098	-0.109	-0.156	-0.101	-0.027	0.143	0.216	0.287
		0.126	-0.130	-0.195	0.032	0.130	0.056	-0.021	0.128	0.303
		0.089	-0.236	0.030	0.146	-0.071	-0.085	-0.199	0.218	0.313
		0.051	-0.204	0.210	-0.076	-0.049	0.100	-0.377	0.380	0.326
		0.018	-0.087	0.138	-0.141	0.129	-0.090	-0.535	0.535	0.268
Actual Story Shear Forces, V_{jm}	kN	291	524	409	226	99	22	410	503	767
		758	809	94	-225	-194	-58	826	1121	1153
		1125	432	-471	-133	182	105	766	1361	1318
		1383	-252	-385	289	-23	-142	190	1396	1493
		1532	-843	224	70	-165	148	-902	1778	1778
		1584	-1095	625	-340	208	-114	-2453	2920	2067

319

TABLE E-12 continued

4. Response at Stage of Maximum Velocity

Quantity	Units	Mode 1 (m=1)	Mode 2 (m=2)	Mode 3 (m=3)	Mode 4 (m=4)	Mode 5 (m=5)	Mode 6 (m=6)	Mode R (m=R)	SRSS ELF	SRSS RSA
Drift Velocity, ∇_{ime}	mm/sec	142	-170	57	34	-64	51	148	205	245
		197	-126	110	-73	46	-24	-501	538	273
		214	0	0	0	0	0	0	214	214
		214	3034	2609	1368	522	97	980	1003	4268
		189	2935	608	-855	-735	-196	1361	1374	3214
		103	1664	-1941	-636	781	406	1810	1813	2779
Force in Damping Devices, Fd_{jm}	kN	220	531	457	240	91	17	172	279	778
		305	514	106	-150	-129	-34	238	387	639
		406	291	-340	-111	137	71	317	515	634
		406	-88	-273	217	-15	-93	317	515	550
		485	-434	146	87	-163	129	378	615	704
		263	-323	281	-186	118	-61	-1281	1308	552
Horizontal Damper Force, Vd_{jm}	kN	195	471	405	212	81	15	152	247	689
		271	455	94	-133	-114	-30	211	343	567
		360	258	-301	-99	121	63	281	457	562
		360	-78	-242	192	-13	-83	281	457	488
		430	-385	130	77	-145	115	335	545	624
		233	-286	249	-165	105	-54	-1136	1159	489

320

TABLE E-12 continued

Quantity	Units	Mode 1 (m=1)	Mode 2 (m=2)	Mode 3 (m=3)	Mode 4 (m=4)	Mode 5 (m=5)	Mode 6 (m=6)	Mode R (m=R)	SRSS ELF	SRSS RSA
5. Response at Stage of Maximum Acceleration										
Ducitility, μ		1.95	1.00	1.00	1.00	1.00	1.00	1.00		
Eff. Viscous Damping Ratio, β_v		0.19	0.33	0.41	0.40	0.39	0.37	0.51		
Parameter δ		0.37	0.59	0.68	0.68	0.66	0.63	0.80		
Coefficient CF_1		0.93	0.83	0.77	0.78	0.79	0.81	0.70		
Product $CF_1 \cdot \mu$		1.82	0.83	0.77	0.78	0.79	0.81	0.70		
Force Coefficient, CF_1 or C_{mFD}		1.00	0.83	0.77	0.78	0.79	0.81	0.70		
Force Coefficient, CF_2 or C_{mFV}		0.36	0.55	0.63	0.63	0.61	0.59	0.72		
Max.Floor Acc., $A_{im,max}$	g	0.231	0.445	0.366	0.197	0.082	0.017	0.252	0.342	0.656
		0.170	0.085	0.152	0.196	0.121	0.031	0.115	0.205	0.337
		0.138	0.146	0.237	0.032	0.152	0.064	0.032	0.141	0.353
		0.089	0.260	0.036	0.176	0.084	0.098	0.139	0.165	0.353
		0.060	0.228	0.244	0.084	0.066	0.121	0.277	0.283	0.376
		0.042	0.091	0.133	0.162	0.154	0.107	0.736	0.738	0.299
Maximum Story Shear, $V_{jm,max}$ (actual)	kN	362	697	573	309	128	26	395	536	1028
		856	925	133	-258	-224	-65	728	1124	1314
		1255	502	-555	-165	218	122	736	1455	1492
		1513	-252	-451	346	-26	-163	334	1549	1644
		1686	-915	256	102	-219	187	-390	1731	1960
		1668	-1070	642	-369	229	-124	-2526	3027	2131

DETAILED CALCULATIONS FOR THE SIMPLIFIED ANALYSIS OF A 3-STORY FRAME WITH NONLINEAR VISCOUS DAMPING SYSTEM

F.1 Introduction

This appendix presents detailed calculations in the application of the equivalent lateral force (ELF) and response-spectrum analysis (RSA) procedures of NEHRP(2000) for the analysis of buildings with nonlinear viscous damping systems. These procedures are applied as described in Appendix A subject to the modifications described in Section 8.1 and Section 7.5.2. The presentation in the appendix consists of:

(1) Detailed calculations for the 3-story special steel moment frame 3S-80 shown in Figure 8-6 and denoted as example No.6 in Section 8.

(2) Summary calculations for the 3-story special steel moment frame 3S-80 shown in Figure 8-7 and denoted as example No.7 in Section 8.

F.2 Detailed Calculations for 3-Story Frame 3S-80 with Nonlinear Damping System (Example No.6)

Parameters

The seismic tributary weights are: for the third floor 1567 kN, and 2900 kN for the second and first floors. The design coefficients per Table 5.2.2 of the 1997 NEHRP Recommended Provisions for special steel moment frames are: $R = 8.0$, $\Omega_o = 3.0$, $C_d = 5.5$, and $I = 1.0$.

Description of the System

The analyzed frame is a special steel moment frame with a nonlinear viscous damping system as shown in Figure 8-6. This frame is one of two such frames in each principal direction of the building with the plan and elevation shown in Figure B-1 of Appendix B. Torsional effects were disregarded in the analysis. The building is located at a site characterized by a design response spectrum with parameters $S_{D1} = 0.6$, $S_{DS} = 1.0$ and $T_s = 0.6$ sec per NEHRP (1997). This characterization is that of the design basis-earthquake (DBE). The maximum considered

earthquake (MCE) is characterized by a response spectrum with ordinates 1.5 larger than those of the DBE.

The damping system in the frame (as well as each of the other four identical frames of the building in Figure B-1) consists of nonlinear viscous damping devices with velocity exponent a = 0.5, installed in the diagonal configuration shown in Figure 8-6. The damping ratio in the fundamental mode of vibration of the frame under elastic conditions for the design basis earthquake is β_{V1}= 0.10 (damping provided by the damping system) plus an assumed inherent damping ratio β_I= 0.05 for a total damping ratio $\beta_{VI} + \beta_I = 0.15$. The corresponding damping coefficient is B_{V+I} = 1.35 (Table A13.3.1 and Table 3-3, column for B_1, conservative values). The seismic base shear strength for the design of this frame was selected to be $0.80V$, which is larger than the minimum required on the basis of NEHRP (2000) Section A13.2.4.1, $V_{min}=0.75V$, where V is determined by the procedures of NEHRP (1997), Section 5.3. The seismic base shear V has been determined in Section B.3 to be *788.5 kN*, so that $0.80V= 0.80x788.5 = 630.8\ kN$.

The approach followed to design the frame started with the calculation of the required base shear strength of the frame V_y per (7-72) with *0.80V* in place of V_{min}, such that

$$V_y = (0.80V) \cdot \frac{\Omega_o \cdot C_d}{R} = 630.8x\frac{3x5.5}{8} = 1301\,kN$$

The frame was then designed to have a base shear strength equal to approximately 1301 kN when pushed over by lateral loads proportional to the first mode of the frame under elastic conditions. Subsequently, the frame was analyzed by the plastic analysis procedure of Appendix C.2 and $V_y= 1260\ kN\ (\approx 0.78V)$. Note that pushover analysis of the frame performed with program IDARC2D-Version 5.0 gave $V_y = 1262\ kN$. The model utilized for the plastic analysis is shown in Figure C-1 with distance $a_{ij}L_j$ equal to $d_c/2$, where d_c is the column depth. Thus, hinges were assumed to form at the beam-to-column interface.

Eigenvalue analysis of the frame performed in program IDARC2D-Version 5.0 gave: T_1 = 1.52 sec, $\{\phi_{i1}\}^T$= [1.000 0.655 0.248], T_2 = 0.48 sec, $\{\phi_{i2}\}^T$= [1.000 −0.555 -0.711] and T_3 = 0.24 sec, $\{\phi_{i3}\}^T$= [1.000 −1.578 1.992]. The modal properties of the frame are summarized in Table F-1.

CALCULATION OF RESPONSE IN DESIGN BASIS EARTHQUAKE

FIRST MODE RESPONSE (T$_1$ = 1.52 sec)

Viscous Damping Ratio under Elastic Conditions

Equation (7-32) gives the damping ratio. For a = 0.5 and λ = 3.496, (7-32) becomes

$$\beta_{V1} = 0.556 \cdot \left(\frac{T}{2\pi}\right)^{2/3} \frac{\sum_j C_{N1} \cdot \left(\cos\theta_j \cdot \phi_{rj}\right)^{3/2}}{\left(D_{roof}\right)^{1/2} \cdot \sum_i \left(\frac{w_i}{g}\right)\phi_{i1}^2}$$

Observe that application of (7-32) requires estimation of the roof displacement for elastic behavior. Assume that a damping constant of C_{N1}=14.47 kN.(s/mm)$^{0.5}$ provides a viscous damping ratio of β_{V1}=0.10. The procedure to evaluate β_{V1} is as follows:

Effective viscous damping ratio (under elastic conditions): $\beta_{V+I} = 0.05 + 0.10 = 0.15$

Damping Coefficient: $B_{V+I} = 1.35$ (Table A13.3.1)

The roof displacement for elastic behavior of the frame is:

$$D = \left(\frac{9810}{4\pi^2}\right) \times 1.4 \times \frac{0.6}{1.35} \times 1.52 = 235mm$$

Viscous damping ratio (under elastic conditions)

   Modal Drift

$$\{\phi_r\}_I = \begin{Bmatrix} 1-0.655 \\ 0.655-0.248 \\ 0.248 \end{Bmatrix} = \begin{Bmatrix} 0.345 \\ 0.407 \\ 0.248 \end{Bmatrix} \quad , \quad \sum_i w_i\phi_{i1}^2 = 2989.5$$

$$\beta_{V1} = 0.556 \times \left(\frac{1.52}{2\pi}\right)^{2/3} \times 9810 \times 14.47 \times \left(\cos^{1.5} 27.6°\right) \times \frac{\left(0.345^{1.5} + 0.407^{1.5} + 0.248^{1.5}\right)}{\sqrt{235 \times 2989.5}}$$

$$\beta_{VI} = 0.10$$

Had the viscous damping ratio been different, the computations would have to be repeated for a new value of C_{NI}.

Roof Displacement

Assumed Effective Ductility: $\quad \mu_D = 1.27$

Effective Period: $\qquad T_{ID} = 1.52(1.27)^{1/2} = 1.713 \, sec$ $\qquad\qquad$ (A13.4.3.5-1)

Effective Damping Ratio

Quality factor: $\qquad q_H = 0.67 \times \dfrac{0.6}{1.52} = 0.26 < 0.50$ $\qquad\qquad$ (A13.3.3.-1)

Hysteretic Damping: $\quad \beta_{HD} = 0.50 \times (0.64 - 0.05) \times \left(1 - \dfrac{1}{1.27}\right) = 0.0627$ $\qquad$ (A13.3.2.2-1)

Effective Damping: $\quad \beta_{ID} = 0.05 + 0.10 \times (1.27)^{3/4} + 0.0627 = 0.233$ $\qquad\qquad$ (7-40)

Damping Coefficient: $B_{ID} = 1.60$ $\qquad\qquad\qquad\qquad\qquad\qquad$ (Table A13.3.1)

Roof Displacement: $\quad D_{ID} = \left(\dfrac{9810}{4\pi^2}\right) \times 1.40 \times \dfrac{0.6 \times 1.713}{1.60} = 223mm$ $\qquad$ (A13.4.4.3-1)

Corrected Displacement: $\quad$ Since $D_{ID} < D$, use $D_{Id} = 235 \, mm$

Base Shear

Seismic coefficient: $\quad C_{s1} = \left(\dfrac{8}{5.5}\right) \times \dfrac{0.6}{1.713 \times (3 \times 1.60)} = 0.106$ $\qquad\qquad$ (A13.4.3.4-2)

Base shear: $\qquad V_1 = 0.106 \times 5861 = 621xkN$ $\qquad\qquad\qquad\qquad$ (A13.4.3.2-1)

The contribution of the first mode to the base shear strength of the frame is given by (7-72)

$$V_y = V_1 \frac{\Omega_o \cdot C_d}{R} = 621 \times \frac{3 \times 5.5}{8} = 1281 kN$$

The calculated contribution to the base shear strength of 1281 is close to the actual base shear strength of 1260 kN.

Displacement at Effective Yield (Yield Displacement) Dy

$$D_y = \left(\frac{9810}{4\pi^2}\right) \times \left(\frac{3 \times 5.5}{8}\right) \times 1.40 \times 0.106 \times 1.52^2 = 176mm \qquad \text{(A13.3.4-3)}$$

Effective Ductility Demand: $\qquad \mu_D = \frac{235}{176} = 1.33 \approx 1.27 \qquad\qquad$ (A13.3.4-1)

$$\mu_{max} = \frac{8}{3x1} = 2.667 \qquad\qquad\qquad \text{(A13.5-2)}$$

$$\mu_D < \mu_{max}$$

The difference between the estimated and the assumed ductility demand is due to the correction of the roof displacement to meet the condition that it is not less than the elastic displacement.

Response at Stage of Maximum Displacement

Lateral Floor Displacement, δ_{i1D}, and Story Drifts, Δ_{j1D}

$$\delta_{i1D} = 235 \times \begin{Bmatrix} 1.000 \\ 0.655 \\ 0.248 \end{Bmatrix} = \begin{Bmatrix} 235 \\ 154 \\ 58 \end{Bmatrix} mm \qquad\qquad \text{(A13.4.4.2-1)}$$

$$\Delta_{j1D} = \begin{Bmatrix} 81 \\ 96 \\ 58 \end{Bmatrix} mm$$

Design Lateral Forces, F_{i1}, Design Story Shears, V_{j1}, and Floor Accelerations, A_{i1}

$$F_{iI} = \left\{ \begin{array}{l} 1567 \times 1.0 \times \dfrac{1.40}{5860} \times 621 \\[3mm] 2900 \times 0.655 \times \dfrac{1.40}{5860} \times 621 \\[3mm] 2900 \times 0.248 \times \dfrac{1.40}{5860} \times 621 \end{array} \right\} = \left\{ \begin{array}{c} 232 \\ 282 \\ 107 \end{array} \right\} kN \qquad \text{(A13.4.3.9-1)}$$

$$A_{iI} = \frac{F_{iI}}{w_i} \cdot \left(\frac{C_d \Omega_o}{R} \right) = \left\{ \begin{array}{c} \dfrac{232}{1567} \\[3mm] \dfrac{282}{2900} \\[3mm] \dfrac{107}{2900} \end{array} \right\} \times \left(\frac{5.5 \times 3}{8} \right) = \left\{ \begin{array}{c} 0.305 \\ 0.200 \\ 0.076 \end{array} \right\} g$$

Observe that for calculation of A_{iI}, lateral inertia forces are multiplied by factor $C_d.\Omega_o/R$ to convert them into real (unreduced) forces.

$$V_{iID} = \left\{ \begin{array}{c} 232 \\ 514 \\ 621 \end{array} \right\} (kN)$$

Response at Stage of Maximum Velocity

Story Velocity:
$$\nabla_{iID} = \frac{2\pi}{1.713} \times \left\{ \begin{array}{c} 81 \\ 96 \\ 58 \end{array} \right\} = \left\{ \begin{array}{c} 297 \\ 352 \\ 213 \end{array} \right\} \frac{mm}{sec} \qquad \text{(A13.4.4.5-2)}$$

Force in Damping Devices:
$$F_{diI} = 14.47 \times \left\{ \begin{array}{c} 297^{\frac{1}{2}} \\ 352^{\frac{1}{2}} \\ 213^{\frac{1}{2}} \end{array} \right\} \times (\cos 27.6^\circ)^{0.5} = \left\{ \begin{array}{c} 235 \\ 256 \\ 199 \end{array} \right\} kN \qquad \text{(7-30)}$$

328

Response at Stage of Maximum Acceleration

Force Coefficients

Effective viscous damping:

$$\beta_{V+1} = 0.05 + 0.10 \times (1.27)^{0.75} = 0.17$$

Parameter δ:

$$\delta = \left(\frac{2\pi \times 0.5}{3.496} \times 0.17\right)^{\frac{2}{3}} = 0.286 \, rads \qquad (4\text{-}35)$$

Force Coefficient CF_1:

$$CF_1 = cos \, \delta = cos(0.286) = 0.959 \qquad (4\text{-}41)$$

$$CF_1 \cdot \mu = 0.959 \times 1.33 = 1.279 > 1.0 \quad \therefore \quad use \, CF_1 = 1.000$$

Force Coefficient CF_2:

$$CF_2 = [sin(0.286)]^{\frac{1}{2}} = 0.531 \qquad (4\text{-}39)$$

Maximum Lateral Inertia Forces

$$F_{i1,max} = CF_1 \cdot F_{i1}\Big|_{Max\,Disp} \cdot \frac{C_d \Omega_o}{R} + CF_2 \cdot F_{iD}\Big|_{Max\,Velocity}$$

$$F_{i1,max} = 1.0 \times \begin{Bmatrix} 232 \\ 287 \\ 107 \end{Bmatrix} \times \left(\frac{3 \times 5.5}{8}\right) + 0.531 \times \begin{Bmatrix} 208 \\ 19 \\ -51 \end{Bmatrix} = \begin{Bmatrix} 589 \\ 602 \\ 194 \end{Bmatrix} kN$$

Maximum Floor Accelerations

$$A_{i1,max} = \frac{F_{i1,max}}{w_i} = \begin{Bmatrix} 589/1567 \\ 602/2900 \\ 194/2900 \end{Bmatrix} = \begin{Bmatrix} 0.378 \\ 0.206 \\ 0.067 \end{Bmatrix} g$$

Maximum Story Shear

$$V_{imax} = 1.0 \times \begin{Bmatrix} 479 \\ 1060 \\ 1281 \end{Bmatrix} + 0.531 \times \begin{Bmatrix} 208 \\ 227 \\ 176 \end{Bmatrix} = \begin{Bmatrix} 589 \\ 1181 \\ 1374 \end{Bmatrix} (kN)$$

SECOND MODE RESPONSE (T₂=0.48 sec<Tₛ)

Effective Damping Ratio

Damping Constant in Higher Modes

$$C_i = \frac{1}{2}C_{Ni}\nabla_{i1}^{-\frac{1}{2}} = \frac{1}{2} \times 14.4 \times \begin{Bmatrix} (297 \times \cos 29.6)^{-\frac{1}{2}} \\ (352 \times \cos 27.6)^{-\frac{1}{2}} \\ (213 \times \cos 27.6)^{-\frac{1}{2}} \end{Bmatrix} = \begin{Bmatrix} 0.444 \\ 0.408 \\ 0.524 \end{Bmatrix} kN \cdot s/_{mm} \qquad (7\text{-}41)$$

Viscous Damping Ratio under Elastic Conditions

$$\beta_{V2} = \left(\frac{0.48}{4\pi}\right) \times \left(\frac{\cos^2 27.6°}{1/_{9810}}\right) \times \left[\frac{0.444 \times 1.555^2 + 0.408 \times 0.156^2 + 0.524 \times (-0.711)^2}{1567 \times 1.0^2 + 2900 \times (-0.555)^2 + 2900 \times (-0.711)^2}\right] \quad (7\text{-}29)$$

$$\beta_{V2} = 0.10$$

Effective Damping Ratio: $\quad \beta_{2D} = 0.10 + 0.05 = 0.15$

Damping Coefficient: $\quad B_{2D} = 1.35$ $\hfill$ (Table A13.3.1)

Roof Displacement: $\quad D_{2D} = \left(\frac{9810}{4\pi^2}\right) \times 0.536 \times \frac{1.0}{1.35} \times 0.48^2 = 23mm \quad$ (A13.5.4.3-2)

Seismic Base Shear

Seismic coefficient: $\quad C_{s2} = \left(\frac{8}{5.5}\right) \times \frac{1.0}{3 \times 1.35} = 0.359 \hfill$ (A13.5.3.6-1)

Base shear: $\quad V_2 = 0.359 \times 1128 = 405\,kN \hfill$ (A13.5.3.2-1)

Response at Stage of Maximum Displacement

Lateral Floor Displacements, δ_{i2D}, and Story Drifts, Δ_{j2D}

$$\delta_{i2D} = 23 \times \begin{Bmatrix} 1.000 \\ -0.555 \\ -0.711 \end{Bmatrix} = \begin{Bmatrix} 23 \\ -13 \\ -16 \end{Bmatrix} mm \qquad\qquad (A13.5.4.2\text{-}1)$$

$$\Delta_{i2D} = \begin{Bmatrix} 36 \\ 3 \\ -16 \end{Bmatrix} mm$$

Design Lateral Forces, F_{i2}, Design Story Shears, V_{i2}, and Floor Accelerations, A_{i2}

$$F_{i2} = \begin{Bmatrix} 1567 \times 1.0 \times \dfrac{0.536}{1128} \times 405 \\ 2900 \times (-0.555) \times \dfrac{0.536}{1128} \times 405 \\ 2900 \times (-0.711) \times \dfrac{0.536}{1128} \times 405 \end{Bmatrix} = \begin{Bmatrix} 302 \\ -310 \\ -397 \end{Bmatrix} kN \qquad \text{(A13.5.3.7-1)}$$

$$A_{i2} = \dfrac{F_{i2}}{w_i} \cdot \left(\dfrac{C_d \cdot \Omega_o}{R} \right) = \begin{Bmatrix} \dfrac{302}{1567} \\ \dfrac{-310}{2900} \\ \dfrac{-397}{2900} \end{Bmatrix} \times \dfrac{3 \times 5.5}{8} = \begin{Bmatrix} 0.397 \\ -0.220 \\ -0.282 \end{Bmatrix} g$$

$$V_{i2} = \begin{Bmatrix} 302 \\ -8 \\ -405 \end{Bmatrix} kN$$

Response at Stage of Maximum Velocity

Story Velocity
$$\nabla_{i2D} = \left(\dfrac{2\pi}{0.48} \right) \times \begin{Bmatrix} 36 \\ 3 \\ -16 \end{Bmatrix} = \begin{Bmatrix} 471 \\ -39 \\ -209 \end{Bmatrix} \dfrac{mm}{sec} \qquad \text{(A13.5.4.5-2)}$$

Forces in Damping Devices:
$$F_{di2} = \begin{Bmatrix} 0.44 \times 471 \\ 0.408 \times (-39) \\ 0.524 \times (-209) \end{Bmatrix} \times \cos 27.6 = \begin{Bmatrix} 184 \\ 14 \\ -97 \end{Bmatrix} kN \qquad \text{(7-23)}$$

Response at Stage of Maximum Acceleration

Force Coefficients

331

$$\beta_{V2} = 0.05 + 0.10 = 0.15$$

$$CF_1 = cos[tan^{-1} (2 \times 0.15)] = 0.958 \tag{4-41}$$

$$CF_2 = sin[tan^{-1} (2 \times 0.15)] = 0.287 \tag{4-39}$$

Maximum Floor Acceleration

$$A_{i2,max} = [0.958 + 2 \times 0.15 \times 0.287] \times \begin{Bmatrix} 0.397 \\ -0.230 \\ -0.282 \end{Bmatrix} = \begin{Bmatrix} 0.415 \\ -0.230 \\ -0.294 \end{Bmatrix} g \tag{4-40}$$

Maximum Story Shear

$$V_{i2,max} = CF_1 \cdot V_{i2} \Big|_{Max\,Disp} \cdot \frac{C_d \Omega_o}{R} + CF_2 \cdot V_{i2} \Big|_{Max\,Velocity}$$

$$V_{i2\,max} = 0.958 \times \begin{Bmatrix} 623 \\ -17 \\ -835 \end{Bmatrix} + 0.287 \times \begin{Bmatrix} 163 \\ 12 \\ -86 \end{Bmatrix} = \begin{Bmatrix} 644 \\ -13 \\ -825 \end{Bmatrix} kN$$

THIRD MODE RESPONSE (T_3 = 0.24 sec < T_s)

Effective Damping Ratio

Viscous Damping Ratio under Elastic Conditions

$$\beta_{V3} = \left(\frac{0.24}{4\pi}\right) \times \frac{cos^2\,27.6 \times [0.444 \times 2.578^2 + 0.408 \times 3.57^2 + 0.524 \times 1.992^2]}{\left(\frac{1}{9800}\right) \times [1567 \times 1.0^2 + 2900 \times 1.578^2 + 2900 \times 1.992^2]} \tag{7-29}$$

$$\beta_{V3} = 0.074$$

Effective Damping Ratio: $\beta_{3D} = 0.074 + 0.05 = 0.124$

Damping Coefficient: $B_3 = 1.272$ (Table A13.3.1)

Roof Displacement: $D_{3D} = \left(\frac{9810}{4\pi^2}\right) \times 0.136 \times \frac{1.0}{1.272} \times 0.24^2 = 1.50\ mm$ (A13.5.4.3-2)

Seismic Base Shear

Seismic Coefficient: $C_{s3} = \dfrac{8}{5.5} \times \dfrac{1.0}{3 \times 1.272} = 0.381$

(A13.5.3.6-1)

Base Shear: $V_3 = 0.381 \times 378 = 144\ kN$ (A13.5.3.2-1)

Response at Stage of Maximum Displacement

Lateral Floor Displacements, δ_{i3D}, and Story Drifts, Δ_{j3D}

$$\delta_{i3D} = 1.5 \times \begin{Bmatrix} 1.0 \\ -1.578 \\ 1.992 \end{Bmatrix} = \begin{Bmatrix} 1.5 \\ -2.4 \\ 3.0 \end{Bmatrix} mm$$

(A13.5.4-2)

$$\Delta_{i3D} = \begin{Bmatrix} 3.9 \\ -5.4 \\ 3.0 \end{Bmatrix} mm$$

Design Lateral Forces, F_{i3}, Design Story Shears, V_{j3}, and Floor Accelerations, A_{i3}

$$F_{i3} = \begin{Bmatrix} 1567 \times 1.0 \times \dfrac{0.136}{378} \times 144 \\ 2900 \times (-1.578) \times \dfrac{0.136}{378} \times 144 \\ 2900 \times 1.992 \times \dfrac{0.136}{378} \times 144 \end{Bmatrix} = \begin{Bmatrix} 81 \\ -237 \\ 299 \end{Bmatrix} kN$$

(A13.5.3.7-1)

$$A_{i3} = \dfrac{F_{i3}}{w_i} \cdot \left(\dfrac{C_d \Omega_o}{R} \right) = \begin{Bmatrix} \dfrac{81}{1567} \\ \dfrac{-237}{2900} \\ \dfrac{299}{2900} \end{Bmatrix} \times \left(\dfrac{3 \times 5.5}{3} \right) = \begin{Bmatrix} 0.107 \\ -0.168 \\ 0.213 \end{Bmatrix} g$$

$$V_{i3} = \begin{Bmatrix} 81 \\ -156 \\ 143 \end{Bmatrix} kN$$

Response at Stage of Maximum Velocity

Story Velocity:

$$\nabla_{i3} = \left(\frac{2\pi}{0.24}\right) \times \begin{Bmatrix} 3.9 \\ -5.4 \\ 3.0 \end{Bmatrix} = \begin{Bmatrix} 102 \\ -141 \\ 79 \end{Bmatrix} \frac{mm}{sec} \qquad (A13.5.4.5\text{-}2)$$

Forces in Damping Devices:

$$F_{di3} = \begin{Bmatrix} 0.44 \times 102 \\ 0.408 \times (-141) \\ 0.524 \times 79 \end{Bmatrix} \times \cos 27.6 = \begin{Bmatrix} 40 \\ -51 \\ 37 \end{Bmatrix} kN \qquad (7\text{-}23)$$

Response at Stage of Maximum Acceleration

Force Coefficients

$$\beta_{V3} = 0.074 + 0.05 = 0.124$$

$$CF_1 = \cos[\tan^{-1}(2 \times 0.124)] = 0.971 \qquad (4\text{-}41)$$

$$CF_2 = \sin[\tan^{-1}(2 \times 0.124)] = 0.241$$

Maximum Floor Accelerations

$$A_{i3,max} = [0.971 + 2 \times 0.124 \times 0.241] \times \begin{Bmatrix} 0.107 \\ -0.168 \\ 0.213 \end{Bmatrix} = \begin{Bmatrix} 0.110 \\ -0.173 \\ 0.220 \end{Bmatrix} g \qquad (4\text{-}40)$$

Maximum Story Shear

$$V_{i2,max} = CF_1 \cdot V_{i2}\Big|_{Max\,Disp} \cdot \frac{C_d \Omega_o}{R} + CF_2 \cdot V_{i2}\Big|_{Max\,Velocity}$$

$$V_{i3,max} = 0.971 \times \begin{Bmatrix} 167 \\ -322 \\ 295 \end{Bmatrix} + 0.241 \times \begin{Bmatrix} 35 \\ -45 \\ 33 \end{Bmatrix} = \begin{Bmatrix} 171 \\ -324 \\ 294 \end{Bmatrix} kN$$

RESIDUAL MODE RESPONSE ($T_R = 0.4 \times 1.52 = 0.608$ sec $> T_s$)

Effective Damping Ratio

Viscous damping ratio under elastic conditions:

$$\beta_{vR} = \left(\frac{0.608}{4\pi}\right) \times \frac{\cos^2 27.6 \times [0.444 \times 1.2075^2 + 0.408 \times 1.4245^2 + 0.524 \times 1.6320^2]}{\left(\frac{1}{9810}\right) \times [1567 \times 1.0^2 + 2900 \times (-.2094)^2 + 2900 \times (-1.6320)^2]} \quad (7\text{-}29)$$

$$\beta_{vR} = 0.114$$

Effective Damping Ratio: $\quad\quad \beta_R = 0.114 + 0.05 = 0.164$

Damping Coefficient: $\quad\quad\quad B_R = 1.392$ $\quad\quad\quad\quad\quad\quad\quad\quad\quad\quad\quad\quad$ (Table A13.3.1)

Roof Displacement: $\quad\quad\quad D_{RD} = \left(\frac{9810}{4\pi^2}\right) \times 0.40 \times \frac{0.6}{1.392} \times 0.608 = 26\,mm$

Seismic coefficient: $\quad\quad\quad C_{sR} = \left(\frac{8}{5.5}\right) \times \frac{1.0}{3 \times 1.392} = 0.348$ $\quad\quad\quad$ (A13.4.3.8-1)

Base shear: $\quad\quad\quad\quad\quad\quad V_R = 0.348 \times 1507 = 524\,kN$ $\quad\quad\quad\quad\quad\quad$ (A13.4.3.6-1)

Response at Stage of Maximum Displacement

Lateral Floor Displacements, δ_{iRD}, and Story Drifts, Δ_{iRD}

$$\delta_{iRD} = 26 \times \begin{Bmatrix} 1.000 \\ -0.2075 \\ -1.6320 \end{Bmatrix} = \begin{Bmatrix} 26 \\ -5 \\ -42 \end{Bmatrix} mm \quad\quad (A13.4.4.2\text{-}2)$$

$$\Delta_{iRD} = \begin{Bmatrix} 31 \\ 37 \\ -42 \end{Bmatrix} mm$$

Design Lateral Forces, F_{iR}, Design Story Shears, V_{iR}, and Floor Accelerations, A_{iR}

$$F_{iR} = \begin{Bmatrix} 1567 \times 1.0 \times \dfrac{0.40}{1507} \times 524 \\ 2900 \times (-0.2075) \times \dfrac{0.40}{1507} \times 524 \\ 2900 \times (-1.632) \times \dfrac{0.40}{1507} \times 524 \end{Bmatrix} = \begin{Bmatrix} 218 \\ -84 \\ -658 \end{Bmatrix} kN \quad\quad (A13.4.3.9\text{-}2)$$

$$A_{iR} = \frac{F_{iR}}{w_i}\left(\frac{C_d\Omega_o}{R}\right) = \begin{Bmatrix} \dfrac{218}{1567} \\ \dfrac{-84}{2900} \\ \dfrac{-658}{2900} \end{Bmatrix} \times \left(\frac{3\times5.5}{8}\right) = \begin{Bmatrix} 0.287 \\ -0.060 \\ -0.468 \end{Bmatrix} g$$

$$V_{iR} = \begin{Bmatrix} 218 \\ 134 \\ -524 \end{Bmatrix} kN$$

Response at Stage of Maximum Velocity

Story Velocity:
$$\nabla_{iR} = \left(\frac{2\pi}{0.608}\right) \times \begin{Bmatrix} 31 \\ 37 \\ -42 \end{Bmatrix} = \begin{Bmatrix} 320 \\ 382 \\ -434 \end{Bmatrix} \frac{mm}{sec} \qquad \text{(A13.4.4.5-3)}$$

Forces in Damping Devices:
$$F_{diR} = \begin{Bmatrix} 0.44\times320 \\ 0.408\times382 \\ 0.524\times(-434) \end{Bmatrix} \cos 27.6° = \begin{Bmatrix} 125 \\ 138 \\ -202 \end{Bmatrix} kN$$

Response at Stage of Maximum Acceleration

Force Coefficients

$$\beta_{VR} = 0.114 + 0.05 = 0.164$$

$$CF_1 = \cos[\tan^{-1}(2\times0.164)] = 0.950 \qquad \text{(4-41)}$$

$$CF_2 = \sin[\tan^{-1}(2\times0.164)] = 0.312 \qquad \text{(4-39)}$$

Maximum Floor Acceleration:

$$A_{iR,max} = [0.95 + 2\times0.164\times0.312] \times \begin{Bmatrix} 0.287 \\ -0.060 \\ -0.468 \end{Bmatrix} = \begin{Bmatrix} 0.302 \\ -0.063 \\ -0.493 \end{Bmatrix} g \qquad \text{(4-40)}$$

Maximum Story Shear:

$$V_{iR,max} = CF_1 \cdot V_{i2}\Big|_{Max\,Disp} \cdot \frac{C_d\Omega_o}{R} + CF_2 \cdot V_{i2}\Big|_{Max\,Velocity}$$

336

$$V_{iR,max} = 0.95 \times \begin{Bmatrix} 450 \\ 276 \\ -1081 \end{Bmatrix} + 0.312 \times \begin{Bmatrix} 111 \\ 122 \\ -179 \end{Bmatrix} = \begin{Bmatrix} 462 \\ 300 \\ -1083 \end{Bmatrix} (kN)$$

Total responses resulting from modal combinations were calculated by use of the SRSS combination rule. Table F-1 presents a summary of the modal properties of the frame and Tables F-2 and F-3 present summaries of the results of the analysis for each mode and the total response calculated by both the ELF and RSA procedures for the DBE and the MCE, respectively.

F.3 Summary Calculations for 3-Story Frame 3S-80 with Nonlinear Viscous Damping (Example No.7)

Frame 3S-80 with nonlinear viscous damping system to provide a viscous damping ratio under elastic conditions of $\beta_{V1} = 0.20$ in the MCE is described as example No.7 in Section 8 and is shown in Figure 8-7. It may be noted that this frame is the same frame of example No.6, with higher damping. Summary calculations for this frame are presented in Table F-4 for the maximum considered earthquake.

TABLE F-1 Modal Properties of Frame 3S-80

Quantity	Mode 1	Mode 2	Mode 3	Residual Mode
T_m, sec	1.52	0.48	0.24	0.608
$\{\phi_{im}\}$	1.000 0.655 0.248	1.000 -0.555 -0.711	1.000 -1.578 1.992	1.0000 -0.2087 -1.6346
$\overline{W}_m$, kN	5861	1128	378	1506
Γ_m	1.3994	-0.5357	0.1363	-0.3994

TABLE F-2 Modal Response Calculations for Example No.6: 3-Story Frame (V$_{min}$= 0.80V) with 10% Nonlinear Viscous Damping in the DBE.
Analysis for the DBE

Quantity	Units	Mode 1 (m=1)	Mode 2 (m=2)	Mode 3 (m=3)	Mode R (m=R)	SRSS ELF	SRSS RSA
1. Elastic Response							
Damping Ratio, β_{Ve}		0.100	0.101	0.074	0.114		
Total Damping Ratio, β_{V+I}		0.150	0.151	0.124	0.164		
Damping Coefficient, B_m		1.350	1.353	1.273	1.391		
Elastic Displacement, D_{em}	mm	235	23	2	26		
2. Roof Displacement and Base Shear							
Assumed Ductility, μ		1.27	1	1	1		
Effective Period, T_{1D}	sec	1.713	0.480	0.240	0.608		
Eff. Viscous Damping Ratio, β_V		0.120	0.101	0.074	0.114		
Hysteretic Damping, β_H		0.063	0.000	0.000	0.000		
Effective Damping, βm		0.233	0.151	0.124	0.164		
Damping Coefficient, B_m		1.60	1.35	1.27	1.39		
Displacement, D_{mD}	mm	223					
Corrected Displacement, D_{mD}	mm	235	23	2	26		
Seismic Coefficient, C_s		0.106	0.358	0.381	0.349		
Seismic Base Shear, V_m	kN	621	404	144	525	813	755
Yield Displacement, D_y	mm	176	----------	----------	----------		
Computed Ductility, μ		1.33	----------	----------	----------		
3. Response at Stage of Maximum Displacement							
Lateral Floor Displacement, δ_{ij}	mm	235	23	2	26		
		154	-13	-2	-5		
		58	-16	3	-43		
Story Drift, Δ_{jm}	mm	81	35	4	31	87	88
		96	4	-5	37	103	96
		58	-16	3	-43	72	61
Design Lateral Forces, F_{im}	kN	232	301	81	218		
		282	-309	-237	-84		
		107	-396	299	-660		
Floor Acceleration, A_{im}	g	0.305	0.396	0.107	0.288	0.419	0.511
		0.200	-0.220	-0.169	-0.060	0.209	0.342
		0.076	-0.282	0.213	-0.469	0.475	0.361
Actual Story Shear Forces, V_{jm}	kN	479	621	167	451	658	802
		1060	-17	-322	278	1096	1108
		1281	-833	296	-1083	1677	1556

4. Response at Stage of Maximum Velocity							
Drift Velocity, ∇_{im}	mm/sec	297	461	103	325	440	558
		352	46	143	383	520	382
		213	211	80	439	488	310
Force in Damping Devices, Fd_{jm}	kN	235	182	41	128	268	300
		256	17	52	139	291	261
		199	98	37	205	286	225
Horizontal Damper Force, Vd_{jm}	kN	208	161	36	114		
		226	15	-46	124		
		176	-87	33	-181		
5. Response at Stage of Maximum Acceleration							
Ducitility, μ		1.33	1	1	1		
Eff. Viscous Damping Ratio, β_V		0.170	0.151	0.124	0.164		
Parameter δ		0.286	0.294	0.244	0.317		
Coefficient CF_1		0.959	0.957	0.970	0.950		
Product $CF_1 . \mu$		1.279	0.957	0.970	0.950		
Force Coefficient, CF_1 or C_{mFD}		1.000	0.957	0.970	0.950		
Force Coefficient, CF_2 or C_{mFV}		0.531	0.290	0.242	0.312		
Max.Floor Acc., $A_{im,max}$	g	0.378	0.409	0.109	0.296	0.480	0.567
		0.206	0.225	0.170	0.058	0.214	0.349
		0.067	0.280	0.213	0.479	0.483	0.358
Maximum Story Shear, $V_{jm,max}$ (actual)	kN	589	641	171	464	750	887
		1181	-12	-323	302	1219	1224
		1374	-823	295	-1086	1751	1628

TABLE F-3 Modal Response Calculations for Example No.6: 3-Story Frame (V$_{min}$= 0.80V) with 10% Nonlinear Viscous Damping in the DBE. Analysis for the MCE

Quantity	Units	Mode 1 (m=1)	Mode 2 (m=2)	Mode 3 (m=3)	Mode R (m=R)	SRSS ELF	RSA
1. Elastic Response							
Damping Ratio, β_{Ve}		0.080	0.091	0.067	0.102		
Total Damping Ratio, β_{V+I}		0.130	0.141	0.117	0.152		
Damping Coefficient, B_m		1.289	1.322	1.250	1.356		
Elastic Displacement, D_{em}	mm	369	35	2	40		
2. Roof Displacement and Base Shear							
Assumed Ductility, μ		2.02	1	1	1		
Effective Period, T_{1D}	sec	2.16	0.48	0.24	0.61		
Eff. Viscous Damping Ratio, β_V		0.14	0.09	0.07	0.10		
Hysteretic Damping, β_H		0.15	0.00	0.00	0.00		
Effective Damping, βm		0.33	0.14	0.12	0.15		
Damping Coefficient, B_m		1.90	1.32	1.25	1.36		
Displacement, D_{mD}	mm	355					
Corrected Displacement, D_{mD}	mm	369	35	2	40		
Seismic Coefficient, C_s		0.106	0.550	0.582	0.536		
Seismic Base Shear, V_m	kN	622	621	220	808	1020	906
Yield Displacement, D_y	mm	176	---------	---------	---------		
Computed Ductility, μ		2.09	---------	---------	---------		
3. Response at Stage of Maximum Displacement							
Lateral Floor Displacement, δ_{ij}	mm	369	35	2	40		
		242	-19	-4	-8		
		91	-25	5	-65		
Story Drift, Δ_{jm}	mm	127	54	6	48	136	138
		150	5	-8	57	161	150
		91	-25	5	-65	112	95
Design Lateral Forces, F_{im}	kN	233	462	124	336		
		282	-474	-363	-130		
		107	-608	458	-1016		
Floor Acceleration, A_{im}	g	0.293	0.480	0.134	0.345	0.453	0.579
		0.193	-0.269	-0.217	-0.070	0.205	0.396
		0.073	-0.331	0.282	-0.562	0.567	0.441
Actual Story Shear Forces, V_{jm}	kN	480	953	256	693	843	1097
		1062	-26	-492	425	1144	1171
		1283	-1279	453	-1670	2106	1867

340

4. Response at Stage of Maximum Velocity							
Drift Velocity, ∇_{jm}	mm/sec	370	708	158	500	622	814
		436	71	219	590	734	493
		266	324	122	676	727	436
Force in Damping Devices, $F_{d_{jm}}$	kN	261	250	56	177	315	366
		284	23	71	192	342	293
		221	135	51	282	358	264
Horizontal Damper Force, $V_{d_{jm}}$	kN	231	222	49	156		
		251	20	-63	170		
		196	-119	45	-250		

5. Response at Stage of Maximum Acceleration							
Ducitility, μ		2.09	1	1	1		
Eff. Viscous Damping Ratio, β_V		0.185	0.141	0.117	0.152		
Parameter δ		0.302	0.274	0.229	0.295		
Coefficient CF_I		0.955	0.963	0.974	0.957		
Product $CF_I . \mu$		1.998	0.963	0.974	0.957		
Force Coefficient, CF_I or C_{mFD}		1.000	0.963	0.974	0.957		
Force Coefficient, CF_2 or C_{mFV}		0.546	0.271	0.227	0.291		
Max.Floor Acc., $A_{im.max}$	g	0.387	0.624	0.166	0.452	0.595	0.753
		0.204	0.344	0.260	0.090	0.223	0.477
		0.086	0.429	0.326	0.733	0.738	0.546
Maximum Story Shear, $V_{jm,max}$ (actual)	kN	606	977	261	708	932	1179
		1199	-19	-494	456	1283	1297
		1390	-1264	451	-1670	2173	1932

TABLE F-4 Modal Response Calculations for Example No.6: 3-Story Frame ($V_{min}= 0.80V$) with 20% Nonlinear Viscous Damping in the MCE.
Analysis for the MCE

Quantity	Units	Mode 1 (m=1)	Mode 2 (m=2)	Mode 3 (m=3)	Mode R (m=R)	SRSS ELF	RSA
1. Elastic Response							
Damping Ratio, β_{Ve}		0.200	0.212	0.156	0.238		
Total Damping Ratio, β_{V+I}		0.250	0.262	0.206	0.288		
Damping Coefficient, B_m		1.651	1.686	1.517	1.766		
Elastic Displacement, D_{em}	mm	288	27	2	31		
2. Roof Displacement and Base Shear							
Assumed Ductility, μ		1.53	1	1	1		
Effective Period, T_{1D}	sec	1.88	0.48	0.24	0.61		
Eff. Viscous Damping Ratio, β_V		0.28	0.21	0.16	0.24		
Hysteretic Damping, β_H		0.10	0.00	0.00	0.00		
Effective Damping, βm		0.43	0.26	0.21	0.29		
Damping Coefficient, B_m		2.18	1.69	1.52	1.77		
Displacement, D_{mD}	mm	269					
Corrected Displacement, D_{mD}	mm	288	27	2	31		
Seismic Coefficient, C_s		0.106	0.431	0.479	0.412		
Seismic Base Shear, V_m	kN	623	487	181	620	879	811
Yield Displacement, D_y	mm	174	----------	----------	----------		
Computed Ductility, μ		1.66	----------	----------	----------		
3. Response at Stage of Maximum Displacement							
Lateral Floor Displacement, δ_{ij}	mm	288 189 71	27 -15 -19	2 -3 4	31 -6 -50		
Story Drift, Δ_{jm}	mm	99 117 71	42 4 -19	5 -7 4	37 44 -50	106 125 87	108 118 74
Design Lateral Forces, F_{im}	kN	233 283 107	362 -372 -476	102 -299 377	258 -100 -780		
Floor Acceleration, A_{im}	g	0.293 0.193 0.073	0.480 -0.269 -0.331	0.134 -0.217 0.282	0.345 -0.070 -0.562	0.453 0.205 0.567	0.579 0.396 0.441
Actual Story Shear Forces, V_{jm}	kN	481 1064 1285	747 -20 -1003	211 -405 373	532 326 -1282	717 1113 1815	913 1139 1672

4. Response at Stage of Maximum Velocity							
Drift Velocity, ∇_{jm}	mm/sec	332	555	130	384	508	660
		392	56	180	453	599	435
		239	254	101	519	572	363
Force in Damping Devices, $F_{d_{jm}}$	kN	549	459	107	317	634	723
		596	42	137	345	688	613
		465	247	98	506	687	536
Horizontal Damper Force, $V_{d_{jm}}$	kN	486	406	95	281		
		528	38	-121	305		
		412	-219	87	-448		

5. Response at Stage of Maximum Acceleration							
Ducitility, μ		1.66	1	1	1		
Eff. Viscous Damping Ratio, β_V		0.325	0.262	0.206	0.288		
Parameter δ		0.440	0.483	0.390	0.523		
Coefficient CF_1		0.905	0.886	0.925	0.866		
Product $CF_1 \cdot \mu$		1.499	0.886	0.925	0.866		
Force Coefficient, CF_1 or C_{mFD}		1.000	0.886	0.925	0.866		
Force Coefficient, CF_2 or C_{mFV}		0.653	0.464	0.381	0.500		
Max.Floor Acc., $A_{im,max}$	g	0.509	0.543	0.148	0.384	0.638	0.759
		0.210	0.293	0.225	0.066	0.220	0.425
		0.102	0.341	0.276	0.610	0.619	0.450
Maximum Story Shear, $V_{jm,max}$ (actual)	kN	798	850	231	601	999	1189
		1409	-1	-421	435	1474	1470
		1554	-990	378	-1335	2048	1881

APPENDIX G

DETAILED CALCULATIONS FOR THE SIMPLIFIED ANALYSIS OF A 3-STORY FRAME WITH VISCOELASTIC DAMPING SYSTEM

G.1 Introduction

This appendix presents detailed calculations in the application of the equivalent lateral force (ELF) and response-spectrum analysis (RSA) procedures of NEHRP (2000) for the analysis of buildings with viscoelastic damping systems. These procedures are applied as described in Appendix A subject to the modifications described in Sections 7.5.3 and 8.1 herein. The presentation in the appendix consists of detailed calculations for the 3-story special steel moment frame 3S-75 shown in Figure 8-8 and denoted as example No.8 in Section 8.

G.2 Detailed Calculations for 3-Story Frame 3S-75 with Viscoelastic Damping System

Parameters

The seismic tributary weights are: for the third floor 1567 kN, and 2900 kN for the second and first floors. The design coefficients per Table 5.2.2 of the 1997 NEHRP Recommended Provisions for special steel moment frames are: $R = 8.0$, $\Omega_o = 3.0$, $C_d = 5.5$, and $I = 1.0$.

Description of the System

The analyzed frame is the 3-story special steel moment frame with a viscoelastic damping system shown in Figure 8-8. The damping system in the frame consists of solid viscoelastic damping devices installed in the diagonal configuration, made of material 3M ISD110 (Zimmer, 1999), and designed to sustain 100% strain in the MCE. Each of these devices has a bonded area of $A_b = $ 626,330 mm² and thickness $h = 140$ mm with approximate storage- and loss-shear moduli $G' \approx G'' = 0.83\,MPa$ at a temperature of 20°C and frequency of about 0.7Hz in the first mode. The corresponding stiffness and damping constant are, respectively, $K = 3.70\ kN/mm$ and $C = 0.876\ kN.s/mm$. The damping ratio in the fundamental mode of vibration of the frame is $\beta_{V1} = 0.086$ (damping provided by the damping system) plus an assumed inherent damping ratio $\beta_I =$

0.05 for a total damping ratio of $\beta_{VI} + \beta_I = 0.136$. The corresponding damping coefficient is $B_{V+I} = 1.308$ (Table A13.3.1). Using Section A13.2.4.1 of NEHRP (2000), the seismic base shear for the design of this frame is controlled by $V_{min} = V/B_{V+I}$ (per eq. A13.2.4.1-1), where the seismic base shear V has been determined in Section B.3 to be 788.5 kN, so that $V_{min} = 788.5/1.308 = 602.8\ kN$. The required base shear strength of the frame V_y per (7-72) is $V_y = 602.8x3x5.5/8 = 1243.3\ kN$. The base shear strength of the frame (inclusive of the damping devices) is $V_y = 1482$ kN (see example C-7) which is larger than the required base shear strength. Example C-7 also gives the yield displacement of the system $D_y = 182\ mm$, the initial stiffness, $K_e = 8.10\ kN/mm$, and the post-elastic stiffness, $\alpha K_e = 1.39\ kN/mm$.

Eigenvalue analysis of the frame using program SAP-2000NL adopting springs of stiffness K to model the contribution of stiffness of the devices in each story gave: $T_1 = 1.473$ sec, $\{\phi_{i1}\}^T =$ [1.000 0.684 0.275], $T_2 = 0.475$ sec, $\{\phi_{i2}\}^T =$ [1.000 −0.498 -0.689] and $T_3 = 0.253$ sec, $\{\phi_{i3}\}^T =$ [1.000 −1.484 1.874]. Modal properties of the frame are summarized in Table G-1.

Viscous Damping Ratio under Elastic Conditions

Equation (7-29) was used to calculate the damping ratio in each mode with $f_j = cos\theta_j$, where $\theta_j = 27.6°$ (see Figure 8-2). For the first mode, the damping ratio under elastic conditions using $C = 0.876\ kN.s/mm$ was $\beta_{V1} = 0.086$. Because of the frequency dependence of these properties, properties were re-evaluated for higher modes. The procedure started by assuming that the frequency of the higher mode was equal to the frequency calculated by eigenvalue using properties calculated for a frequency equal to the first mode frequency. Using the calculated higher mode frequency, the storage and loss shear moduli, G' and G'', respectively, were obtained from Figure G-1. The storage stiffness K_j and the damping constant C_j were then calculated using (7-43). The higher mode frequency was then calculated by eigenvalue analysis of the frame with spring constant K_j in each story. This process was repeated the calculated and assumed frequencies converged. The procedure was applied in each mode to obtain the correct frequency and the damping constant of the devices. For the residual mode, the damping constant of the device was directly evaluated by using the frequency corresponding to $T_R = 0.4T_1$. Table G-

2 summarizes the calculations of the elastic period T_m, damping constant C_j and viscous damping β_{Vm} ratio under elastic conditions for each mode.

FIRST-MODE RESPONSE (T_1=1.473 sec)

Roof Displacement

Assumed Effective Ductility: $\mu_D = 1.21$

Effective Period: $\qquad\qquad T_{1D} = 1.473\sqrt{1.21} = 1.618\,sec$ $\qquad\qquad$ (A13.4.3.5-1)

Effective Damping Ratio:

Quality Factor: $\qquad q_H = 0.67 \times \dfrac{0.6}{1.618} = 0.25 < 0.50$ $\qquad\qquad$ (A13.3.3-1)

$\qquad\qquad\qquad$ use $q_H = 0.50$

Hysteretic Damping: $\qquad \beta_{HD} = (0.64 - 0.05) \times 0.5 \times \left(1 - \dfrac{1}{1.21}\right) = 0.051$ $\qquad$ (A13.3.2.2-1)

Effective Damping: $\qquad \beta_{1D} = 0.05 + 0.086\sqrt{1.21} + 0.051 = 0.196$ $\qquad$ (A13.3.2-1)

Damping Coefficient: $\quad B_{1D} = 1.488$ $\qquad\qquad\qquad\qquad\qquad$ (Table A13.3.1)

Roof Displacement: $\qquad D_{1D} = \left(\dfrac{9810}{4\pi^2}\right) \times 1.38 \times \dfrac{0.6}{1.488} \times 1.618 = 223mm$ $\qquad$ (A13.3.2-1)

Corrected Roof Displacement:

The effective viscous damping ratio is $\beta_{V+I} = 0.086 + 0.05 = 0.135$, and the corresponding damping coefficient from Table (A13.3.1) is $B_{V+I} = 1.308$. Accordingly, the displacement of the roof for elastic behavior is

$$D = \left(\frac{9810}{4\pi^2}\right) \times 1.38 \times \frac{0.6}{1.308} \times 1.473 = 232mm$$

Since $D_{1D} < D$, use $D_{1D} = 232\,mm$

Base Shear

Seismic Coefficient: $C_{s1} = \left(\dfrac{8}{5.5}\right) \times \dfrac{0.6}{1.618 \times 3 \times 1.488} = 0.121$ (A13.4.3.4-2)

Base Shear: $V_1 = 0.121 \times 6013 = 728\ kN$ (A13.4.3.2-1)

Displacement at Effective Yield (Yield Displacement)

$D_y = \left(\dfrac{9810}{4\pi^2}\right) \times \left(\dfrac{3 \times 5.5}{8}\right) \times 1.38 \times 0.121 \times 1.473^2 = 186\,mm$ (A13.3.4-3)

Effective Ductility Demand: $\mu_D = \dfrac{232}{186} = 1.25$ (A13.3.4-1)

$$\mu_D < \mu_{max} = \dfrac{8}{3 \times 1.0} = 2.67$$

It may be noted that $V_1 = 728$ kN converges to the base shear strength of the frame assuming elastoplastic behavior. The contribution of the restoring force from the devices must be added to obtain the actual base shear as shown in the sketch below
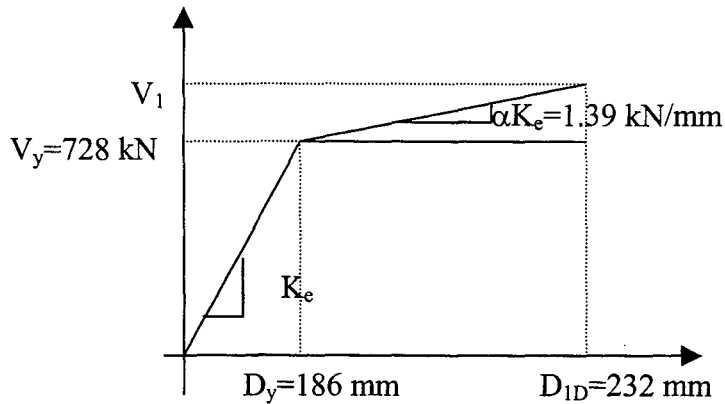
The contribution of the restoring force to the base shear is

$$V_{1R} = 1.39 \times (232 - 186) = 64\ kN$$

The actual base shear is

$$V_1 = 728 + 64 = 792\ kN$$

348

The contribution of the first mode to the base shear strength of the frame is given by (7-72)

$$V_1 = 728 \times \left(\frac{3 \times 5.5}{8} \right) + 64 = 1565 \, kN$$

Response at Stage of Maximum Displacement

Lateral floor displacements, δ_{i1D}, and story drifts, Δ_{i1D}

$$\delta_{i1D} = 232 \times \begin{Bmatrix} 1.000 \\ 0.684 \\ 0.275 \end{Bmatrix} = \begin{Bmatrix} 232 \\ 159 \\ 64 \end{Bmatrix} mm \qquad \text{(A13.4.4.2-1)}$$

$$\Delta_{i1D} = \begin{Bmatrix} 73 \\ 95 \\ 64 \end{Bmatrix} mm$$

Design Lateral Forces, F_{i1}, Design Story Shears, V_{i1}, and Floor Accelerations, A_{i1}

$$Fi_1 = \begin{Bmatrix} 1567 \times 1.000 \times \dfrac{1.38}{6013} \times 792 \\[2mm] 2900 \times 0.684 \times \dfrac{1.38}{6013} \times 792 \\[2mm] 2900 \times 0.275 \times \dfrac{1.38}{6013} \times 792 \end{Bmatrix} = \begin{Bmatrix} 285 \\ 361 \\ 145 \end{Bmatrix} kN \qquad \text{(A13.4.3.9-1)}$$

$$A_{i1} = \frac{F_{i1}}{w_i} \cdot \left(\frac{C_d \Omega_o}{R} \right) = \begin{Bmatrix} \dfrac{285}{1567} \\[2mm] \dfrac{361}{2900} \\[2mm] \dfrac{145}{2900} \end{Bmatrix} \times \left(\frac{3 \times 5.5}{8} \right) = \begin{Bmatrix} 0.375 \\ 0.257 \\ 0.103 \end{Bmatrix} g$$

$$V_{i1} = \begin{Bmatrix} 285 \\ 646 \\ 791 \end{Bmatrix} kN$$

Response at Stage of Maximum Velocity

Story Velocities, ∇_{i1D}

349

$$\nabla_{iID} = \frac{2\pi}{1.618} \begin{Bmatrix} 73 \\ 95 \\ 64 \end{Bmatrix} = \begin{Bmatrix} 284 \\ 369 \\ 249 \end{Bmatrix} mm/sec \qquad \text{(A13.5.4.5-1)}$$

Force in Damping Devices, F_{diD}

$$F_{dDi} = 0.876 \times \begin{Bmatrix} 284 \\ 369 \\ 249 \end{Bmatrix} \cos 27.6° = \begin{Bmatrix} 221 \\ 287 \\ 193 \end{Bmatrix} kN \qquad \text{(7-23)}$$

Horizontal Component of Damping Forces

$$V_{di1} = \begin{Bmatrix} 221 \\ 287 \\ 193 \end{Bmatrix} \cos 27.6° = \begin{Bmatrix} 196 \\ 254 \\ 171 \end{Bmatrix} kN$$

Lateral Force from Dampers

$$F_{di1} = \begin{Bmatrix} 196 \\ 254-196 \\ 171-254 \end{Bmatrix} = \begin{Bmatrix} 196 \\ 58 \\ -83 \end{Bmatrix} kN$$

Damper Axial Restoring Force F_{ir}

$$F_{ir} = K_{di} \cdot \Delta_i \cdot \cos\theta_i$$

$$F_{ir} = 3.70 \times \begin{Bmatrix} 73 \\ 95 \\ 64 \end{Bmatrix} \cos 27.6° = \begin{Bmatrix} 239 \\ 312 \\ 210 \end{Bmatrix} kN$$

Maximum Axial Damping Force, F_{Di1}

The response at maximum velocity is obtained as the combination of the viscous and the restoring force components of the dampers as follows:

Storage and Loss Shear Moduli: $\quad G'_{(\omega)} = G''_{(\omega)} = 0.83$ MPa $\qquad$ (Table G-2)

Loss Factor: $\qquad\qquad\qquad \eta = \dfrac{G''(w)}{G'(w)} = 1.0 \qquad\qquad$ (7-44)

350

Maximum axial damping force, F_{Di1}

$$tan^{-1}\eta = tan^{-1} (1.0) = 0.785$$
$$cos (tan^{-1}\eta) = cos (0.785) = 0.707$$
$$sin (tan^{-1}\eta) = sin (0.785) = 0.707$$

$$F_{Di1} = 0.707 \times \begin{Bmatrix} 239 \\ 312 \\ 210 \end{Bmatrix} + 0.707 \times \begin{Bmatrix} 221 \\ 287 \\ 193 \end{Bmatrix} = \begin{Bmatrix} 325 \\ 423 \\ 285 \end{Bmatrix} kN$$

Response at Stage of Maximum Acceleration

Force Coefficients

Ductility demand: $\mu_D = 1.25$

Effective viscous damping: $\beta_{eff} = 0.05 + 0.095 = 0.145$

Parameter δ: $\delta = tan^{-1} (2 \times 0.145) = 0.282$ (4-36)

Force Coefficient CF_1 :

$$CF_1 = cos (0.282) = 0.961$$

$CF_1\mu = 0.961 \times 1.25 = 1.20 > 1.000$ use $CF_1 = 1.0$ (4-41)

Force Coefficient CF_2 : $CF_2 = sin (0.282) = 0.278$ (4-39)

Maximum Lateral Inertia Forces

$$F_{i1,max} = CF_1 \cdot F_{i1}\big|_{Max.Disp} \cdot \frac{C_d \Omega_o}{R} + CF_2 \cdot Fd_i\big|_{Max.Velocity}$$

$$F_{i1,max} = 1.0 \times \begin{Bmatrix} 285 \\ 361 \\ 145 \end{Bmatrix} \times \frac{5.5 \times 3}{8} + 0.278 \times \begin{Bmatrix} 196 \\ 58 \\ -83 \end{Bmatrix} = \begin{Bmatrix} 642 \\ 761 \\ 276 \end{Bmatrix} kN$$

Maximum Acceleration, $A_{i1,max}$

$$A_{i1,max} = \frac{F_{i1,max}}{w_i} = \left\{\begin{array}{c} \dfrac{642}{1567} \\ \dfrac{761}{2900} \\ \dfrac{276}{2900} \end{array}\right\} = \left\{\begin{array}{c} 0.410 \\ 0.262 \\ 0.095 \end{array}\right\} g$$

Maximum Story Shear, $V_{i1,max}$

$$V_{i1,max} = 1.0 \times \left\{\begin{array}{c} 588 \\ 1332 \\ 1631 \end{array}\right\} + 0.278 \times \left\{\begin{array}{c} 196 \\ 254 \\ 171 \end{array}\right\} = \left\{\begin{array}{c} 643 \\ 1403 \\ 1679 \end{array}\right\} kN$$

SECOND MODE RESPONSE ($T_2 = 0.446$ sec)

Elastic Response

Viscous Damping Ratio: $\beta_{V2} = 0.176$

Effective Damping Ratio: $\beta_{2D} = 0.05 + 0.176 = 0.226$ (A13.3.2-1)

Damping Coefficient: $B_{1D} = 1.578$ (Table A13.3.1)

Roof Displacement: $D_{2D} = \left(\dfrac{9800}{4\pi^2}\right) \times 0.53 \times \dfrac{1.000}{1.578} \times 0.446^2 = 17mm$ (A13.5.4.3-2)

Base Shear

Seismic Coefficient: $C_{s2} = \left(\dfrac{8}{5.5}\right) \times \dfrac{1.0}{3 \times 1.578} = 0.307$ (A13.5.3.6-2)

Base Shear: $V_2 = 0.307 \times 956 = 293 \ kN$ (A13.5.3.2-1)

Required base shear strength: $\qquad V_2 = 293 \times \left(\dfrac{3 \times 5.5}{8} \right) = 604 \ kN$

Response at Stage of Maximum Displacement

Lateral Displacements, δ_{i2} and Story Drifts, Δ_{i2}

$$\delta_{i2} = 17 \times \left\{ \begin{array}{c} 1.000 \\ -0.458 \\ -0.6801 \end{array} \right\} = \left\{ \begin{array}{c} 17 \\ -8 \\ -12 \end{array} \right\} \ mm \qquad \text{(A13.5.4.2-1)}$$

$$\Delta_{i2} = \left\{ \begin{array}{c} 25 \\ 4 \\ -12 \end{array} \right\} \ mm$$

Lateral Inertia Forces, F_{i2}

$$F_{i2} = \left\{ \begin{array}{c} 1567 \times 1.0 \times \dfrac{0.53}{956} \times 293 \\[2mm] 2900 \times (-0.458) \times \dfrac{0.53}{956} \times 293 \\[2mm] 2900 \times (-0.6801) \times \dfrac{0.53}{956} \times 293 \end{array} \right\} = \left\{ \begin{array}{c} 254 \\ -216 \\ -320 \end{array} \right\} \ kN \qquad \text{(A13.5.3.7-1)}$$

use:

$$F_{i2} = \left\{ \begin{array}{c} 254 \\ -216 \\ -320 \end{array} \right\} \ kN$$

Floor Acceleration, A_{i2}

$$A_{i2} = \dfrac{F_{i2} \cdot \left(\dfrac{\Omega_0 C_d}{R} \right)}{w_i} = \left\{ \begin{array}{c} \dfrac{254}{1567} \\[2mm] \dfrac{-216}{2900} \\[2mm] \dfrac{-320}{2900} \end{array} \right\} \times \left(\dfrac{3 \times 5.5}{8} \right) = \left\{ \begin{array}{c} 0.334 \\ -0.154 \\ -0.228 \end{array} \right\} \ g$$

353

Story Shears, V_{i2}

$$V_{i2} = \begin{Bmatrix} 254 \\ 38 \\ -282 \end{Bmatrix} kN$$

Response at Stage of Maximum Velocity

Story Velocities, ∇_{i2D}

$$\nabla_{i2D} = \frac{2\pi}{0.446} \begin{Bmatrix} 25 \\ 4 \\ -12 \end{Bmatrix} = \begin{Bmatrix} 352 \\ 56 \\ -169 \end{Bmatrix} mm/sec \tag{A13.5.4.5-2}$$

Force in Damping Devices, Fd_{i2D}

$$Fd_{i2D} = 0.857 \times \begin{Bmatrix} 352 \\ 56 \\ -169 \end{Bmatrix} \cos 27.6° = \begin{Bmatrix} 267 \\ 43 \\ -128 \end{Bmatrix} kN \tag{7-23}$$

Hence,

$$Vd_{i2D} = \begin{Bmatrix} 237 \\ 38 \\ -113 \end{Bmatrix} kN$$

Damper Axial Restoring Force, F_{ri2}

$$F_{ri2} = K_2 \cdot \Delta_{i2} \cdot \cos\theta_i$$

$$K_2 = \frac{G'(w)\Delta_b}{h} = \frac{1.90 \times 10^{-3} \times 626330}{140} = 8.5 kN/mm$$

$$\therefore F_{Ri2} = 8.5 \times \begin{Bmatrix} 25 \\ 4 \\ -12 \end{Bmatrix} \cos 27.6° = \begin{Bmatrix} 188 \\ 30 \\ -90 \end{Bmatrix} kN$$

Maximum Axial Damping Force, F_{Di2}

Storage and Loss Shear Moduli: $G'(\omega) = 1.90$ MPa; $G''(\omega) = 2.32$ MPa   (Table G-2)

Loss Factor: $\eta = \dfrac{G''(w)}{G'(w)} = \dfrac{2.32}{1.90} = 1.22$ (7-44)

Maximum Axial Damping Force

$tan^{-1} \eta = tan^{-1} (1.22) = 0.884$

$cos (tan^{-1} \eta) = cos (0.884) = 0.634$

$sin (tan^{-1} \eta) = sin (0.884) = 0.773$

$$F_{Di2} = 0.634 \times \begin{Bmatrix} 188 \\ 30 \\ -90 \end{Bmatrix} + 0.773 \times \begin{Bmatrix} 267 \\ 43 \\ -128 \end{Bmatrix} = \begin{Bmatrix} 326 \\ 52 \\ -156 \end{Bmatrix} kN$$

Response at Stage of Maximum Acceleration

Force Coefficients

Effective viscous damping ratio: $\beta_{veff} = 0.05 + 0.176 = 0.226$

Parameter δ $\delta = tan^{-1} (2 \times 0.226) = 0.424$ (4-36)

Force coefficient CF_1: $CF_1 = cos (0.424) = 0.911$ (4-41)

Force Coefficient CF_2: $CF_2 = sin (0.424) = 0.411$ (4-39)

Maximum Acceleration

$$A_{i2} = [0.911 + 2 \times 0.226 \times 0.411] \times \begin{Bmatrix} 0.33 \\ -0.156 \\ -0.231 \end{Bmatrix} = \begin{Bmatrix} 0.362 \\ -0.171 \\ -0.253 \end{Bmatrix} g$$ (4-40)

Maximum Story Shears, $V_{i2,max}$

$V_{i2,max} = CF_1 V_{i2}|_{Max Disp.} + CF_2 V_{i2}|_{Max Velocity}$

$$= 0.911 \times \begin{Bmatrix} 518 \\ 66 \\ -604 \end{Bmatrix} + 0.411 \times \begin{Bmatrix} 237 \\ 38 \\ -113 \end{Bmatrix} = \begin{Bmatrix} 569 \\ 76 \\ -597 \end{Bmatrix} kN$$

THIRD MODE RESPONSE (T$_3$ = 0.237 sec)

Elastic Response

Viscous Damping Ratio: $\beta_v = 0.076$ (TABLE G-2)

Effective damping ratio: $\beta_{3D} = 0.05 + 0.076 = 0.126$ (A13.3.3-1)

Damping Coefficient: $B_{3D} = 1.278$ (Table A13.3.1)

Roof Displacement, D_{3D}:

$$D_{3D} = \left(\frac{9810}{4\pi^2}\right) \times 0.15 \times \frac{1.000}{1.278} \times 0.237^2 = 1.64mm \approx 2\,mm \qquad \text{(A13.5.4.3-2)}$$

Base Shear

Seismic Coefficient:

$$C_{s3} = \left(\frac{8}{5.5}\right) \times \frac{1.0}{3 \times 1.278} = 0.38 \qquad \text{(A13.5.3.6-2)}$$

Base Shear: $V_3 = 0.38 \times 398 = 151\,kN$ (A13.5.3.2-1)

Required Base Shear Strength:
$$V_3 = \left(\frac{3 \times 5.5}{8}\right) \times 151 = 311\,kN$$

Response at Stage of Maximum Displacement

Lateral Displacements, δ_{i3}, and Story Drifts, Δ_{i3}

$$\delta_{i3} = 2 \times \begin{Bmatrix} 1.000 \\ -1.2237 \\ 1.6536 \end{Bmatrix} = \begin{Bmatrix} 2 \\ -2 \\ 3 \end{Bmatrix} mm \qquad \text{(A13.5.4.2-1)}$$

$$\Delta_{i3} = \begin{Bmatrix} 4 \\ -5 \\ 3 \end{Bmatrix} mm$$

Lateral Inertia Forces, F_{i3}

$$F_{i3} = \begin{Bmatrix} 1567 \times 1.0 \times \dfrac{0.15}{398} \times 151 \\ 2900 \times (-1.2237) \times \dfrac{0.15}{398} \times 151 \\ 2900 \times 1.6536 \times \dfrac{0.15}{398} \times 151 \end{Bmatrix} = \begin{Bmatrix} 89 \\ -202 \\ 273 \end{Bmatrix} kN \qquad \text{(A13.5.3.7-1)}$$

Floor Acceleration, A_{i3}

$$A_{i3} = \begin{Bmatrix} \dfrac{87}{1567} \\ \dfrac{-206}{2900} \\ \dfrac{270}{2900} \end{Bmatrix} \times \left(\dfrac{3 \times 5.5}{8} \right) = \begin{Bmatrix} 0.115 \\ -0.147 \\ 0.192 \end{Bmatrix} g$$

Story shear, V_{i3}

$$V_{i3} = \begin{Bmatrix} 87 \\ -119 \\ 151 \end{Bmatrix} kN$$

Response at Stage of Maximum Velocity

Story Velocities, ∇_{i3D}

$$\nabla_{i3D} = \dfrac{2\pi}{0.237} \begin{Bmatrix} 4 \\ -5 \\ 3 \end{Bmatrix} = \begin{Bmatrix} 106 \\ -133 \\ 80 \end{Bmatrix} mm/sec \qquad \text{(A13.5.4.5.-1)}$$

Forces in Damping Devices, F_{di3D}

$$F_{d_{i3D}} = \begin{Bmatrix} 106 \\ -133 \\ 80 \end{Bmatrix} \cos 27.6° = \begin{Bmatrix} 43 \\ -54 \\ 32 \end{Bmatrix} kN \qquad \text{(7-23)}$$

Horizontal Component of the Viscous Damping Force

$$V_{d_{i3D}} = \left\{ \begin{array}{c} 43 \\ -54 \\ 32 \end{array} \right\} \cos 27.6° = \left\{ \begin{array}{c} 38 \\ -48 \\ 28 \end{array} \right\} kN$$

Damper Axial Restoring Force, F_{Ri3}

Storage stiffness:
$$K_3 = \frac{3.2 \times 10^{-3} \times 626330}{140} = 14.32 kN / mm \qquad (7\text{-}43)$$

Damper Axial Restoring Force: $F_{Ri3} = 14.32 \times \left\{ \begin{array}{c} 4 \\ -5 \\ 3 \end{array} \right\} \cos 27.6° = \left\{ \begin{array}{c} 51 \\ -63 \\ 38 \end{array} \right\} kN$

Maximum Axial Damping Force, F_{Di3}

Storage and Shear Moduli: $G'_{(\omega)} = 3.20$ MPa; $G''_{(\omega)} = 2.70$ MPa (Table G-2)

Loss Factor:
$$\eta = \frac{G''(w)}{G'(w)} = \frac{2.70}{3.20} = 0.844 \qquad (7\text{-}44)$$

Maximum Axial Damping Force

$tan^{-1} \eta = tan^{-1} (0.844) \qquad = 0.701$
$cos (tan^{-1} \eta) = cos (0.701) = 0.764$
$sin (tan^{-1} \eta) = sin (0.701) \quad = 0.645$

$$F_{D_{i3}} = 0.764 \times \left\{ \begin{array}{c} 51 \\ -63 \\ 38 \end{array} \right\} + 0.645 \times \left\{ \begin{array}{c} 43 \\ -54 \\ 32 \end{array} \right\} = \left\{ \begin{array}{c} 67 \\ -83 \\ 50 \end{array} \right\} kN$$

Response at Stage of Maximum Acceleration

Force Coefficients

Effective viscous damping ratio: $\beta_{veff} = 0.05 + 0.076 = 0.126$

Parameter δ: $\delta = tan^{-1} (2 \times 0.126) = 0.252$ (4-36)

358

Force coefficient CF_1: $CF_1 = cos\ (0.252) = 0.968$ (4-41)

Force Coefficient CF_2: $CF_2 = sin\ (0.252) = 0.249$ (4-39)

Maximum Acceleration, A_{i3}

$$A_{i3} = [0.968 + 2 \times 0.126 \times 0.249] \times \begin{Bmatrix} 0.115 \\ -0.147 \\ 0.192 \end{Bmatrix} = \begin{Bmatrix} 0.119 \\ -0.152 \\ 0.198 \end{Bmatrix} g \qquad (4\text{-}40)$$

Maximum Story Shear, $V_{i3,max}$

$$V_{i3,max} = CF_1 V_{i3}\big|_{Max\ Disp.} + CF_2 V_{i3}\big|_{Max\ Velocity}$$

$$V_{i3\,max} = 0.968 \begin{Bmatrix} 179 \\ -245 \\ 311 \end{Bmatrix} + 0.249 \times \begin{Bmatrix} 38 \\ -48 \\ 28 \end{Bmatrix} = \begin{Bmatrix} 179 \\ -249 \\ 308 \end{Bmatrix}\ kN$$

RESIDUAL MODE RESPONSE ($T_R = 0.589$ sec $< T_s$)

Elastic Response

Viscous Damping Ratio: $\beta_{vR} = 0.198$ (TABLE G-2)

Effective Damping Ratio: $B_R = 0.05 + 0.198 = 0.248$ (A13.3.3-1)

Damping Coefficient: $B_R = 1.644$ (Table A13.3.1)

Roof Displacement: $D_{RD} = \left(\dfrac{9810}{4\pi^2}\right) \times 0.38 \times \dfrac{1.000}{1.644} \times 0.589^2 = 20\,mm$ (A13.4.4.3-2)

Base Shear

Seismic Coefficient: $C_{sR} = \left(\dfrac{8}{5.5}\right) \times \dfrac{1.0}{3 \times 1.644} = 0.295$ (A13.4.3.8-1)

Base Shear: $V_R = 0.295 \times 1354 = 399\ kN$ (A13.4.3.6-1)

Required Base Shear Strength: $V_R = \left(\dfrac{3 \times 5.5}{8}\right) \times 399 = 823\ kN$

359

Response at Stage of Maximum Displacement

Lateral Displacements, δ_{iR}, and Story Drifts, Δ_{i3}

$$\delta_{iR} = 20 \times \left\{ \begin{array}{c} 1.000 \\ -0.1458 \\ -1.6343 \end{array} \right\} = \left\{ \begin{array}{c} 20 \\ -3 \\ -33 \end{array} \right\} mm \tag{A13.4.4.2-2}$$

$$\Delta_{iR} = \left\{ \begin{array}{c} 23 \\ 30 \\ -33 \end{array} \right\} mm$$

Lateral Inertia Forces, F_{iR}

$$F_{iR} = \left\{ \begin{array}{c} 1567 \times 1.000 \times \dfrac{0.38}{1354} \times 399 \\ 2900 \times (-0.146) \times \dfrac{0.38}{1354} \times 399 \\ 2900 \times (-1.634) \times \dfrac{0.38}{1354} \times 399 \end{array} \right\} = \left\{ \begin{array}{c} 176 \\ -47 \\ -531 \end{array} \right\} kN \tag{A13.4.3.9-2}$$

Floor Acceleration, A_{iR}

$$A_{iR} = \left\{ \begin{array}{c} \dfrac{177}{1567} \\ \dfrac{-47}{2900} \\ \dfrac{-529}{2900} \end{array} \right\} \times \left(\dfrac{3 \times 5.5}{8} \right) = \left\{ \begin{array}{c} 0.233 \\ -0.033 \\ -0.376 \end{array} \right\} g$$

Story Shears, V_{iR}

$$V_{iR} = \left\{ \begin{array}{c} 177 \\ 130 \\ -399 \end{array} \right\} kN$$

360

Response at Stage of Maximum Velocity

Story Velocities, ∇_{iRD}

$$\nabla_{iRD} = \frac{2\pi}{0.589} \times \begin{Bmatrix} 23 \\ 30 \\ -33 \end{Bmatrix} = \begin{Bmatrix} 245 \\ 320 \\ -352 \end{Bmatrix} mm/sec \qquad (A13.4.4.5.-3)$$

Forces in Damping Devices, F_{diRD}

$$F_{diRD} = 0.83 \times \begin{Bmatrix} 245 \\ 320 \\ -352 \end{Bmatrix} \cos 27.6° = \begin{Bmatrix} 180 \\ 235 \\ -259 \end{Bmatrix} kN \qquad (7-23)$$

Horizontal Component of the Viscous Damping Force

$$Vd_{iRD} = \begin{Bmatrix} 180 \\ 235 \\ -259 \end{Bmatrix} \cos 27.6° = \begin{Bmatrix} 160 \\ 208 \\ -230 \end{Bmatrix} kN$$

Damper Axial Restoring Force, F_{Ri3}

Storage Stiffness:
$$K_R = \frac{1.4 \times 10^{-3} \times 626330}{140} = 6.26 kN/mm \qquad (7-43)$$

Damper Axial Restoring Force:
$$F_{RiR} = 6.26 \times \begin{Bmatrix} 23 \\ 30 \\ -33 \end{Bmatrix} \cos 27.6° = \begin{Bmatrix} 128 \\ 166 \\ -183 \end{Bmatrix} kN$$

Maximum Axial Damping Force, F_{DiR}

Storage and Shear Moduli: $G'_{(\omega)} = 1.4$ MPa; $G''_{(\omega)} = 1.98$ MPa (Table G-2)

Loss Factor:
$$\eta = \frac{1.98}{1.40} = 1.414 \qquad (7-44)$$

Maximum Axial Damping Force:

$$tan^{-1}\eta = tan^{-1}(1.414) \qquad = 0.955$$
$$cos\,(tan^{-1}\eta) = cos\,(0.955) \qquad = 0.578$$
$$sin\,(tan^{-1}\eta) = sin\,(0.955) \qquad = 0.816$$

$$F_{DiR} = 0.578 \times \begin{Bmatrix} 128 \\ 166 \\ -183 \end{Bmatrix} + 0.816 \times \begin{Bmatrix} 180 \\ 235 \\ -259 \end{Bmatrix} = \begin{Bmatrix} 221 \\ 288 \\ -317 \end{Bmatrix} \ kN$$

Response at Stage of Maximum Acceleration

Force Coefficients

Effective viscous damping ratio: $\beta_{veff} = 0.05 + 0.198 = 0.248$

Parameter δ: $\qquad\qquad \delta = tan^{-1} (2 \times 0.248) = 0.460$ $\qquad\qquad$ (4-36)

Force coefficient CF_1: $\qquad CF_1 = cos\ (0.460) = 0.896$ $\qquad\qquad$ (4-41)

Force Coefficient CF_2: $\qquad CF_2 = sin\ (0.460) = 0.444$ $\qquad\qquad$ (4-39)

Maximum Acceleration, A_{iRmax}

$$A_{iR\,max} = [0.896 + 2 \times 0.248 \times 0.444] \times \begin{Bmatrix} 0.233 \\ -0.033 \\ -0.376 \end{Bmatrix} = \begin{Bmatrix} 0.260 \\ -0.037 \\ -0.420 \end{Bmatrix} g \qquad (4\text{-}40)$$

Maximum Story Shear, $V_{iR,max}$

$$V_{iR\,max} = CF_1 V_{iR}\big|_{Max\,Disp.} + CF_2 V_{iR}\big|_{Max\,Velocity}$$

$$V_{iR\,max} = 0.896 \times \begin{Bmatrix} 365 \\ 268 \\ -823 \end{Bmatrix} + 0.444 \times \begin{Bmatrix} 160 \\ 208 \\ -230 \end{Bmatrix} = \begin{Bmatrix} 398 \\ 332 \\ -840 \end{Bmatrix} kN$$

Total responses resulting from modal combinations were calculated by use of the SRSS combination rule. Table G-1 presents a summary of the modal properties of the frame (inclusive of the damping devices) and Table G-2 presents a summary of the calculations of the storage stiffness and loss stiffness and viscous damping ratio under elastic conditions of the system at each mode. Tables G-3 and G-4 present summaries of the results of the analysis for each mode and the total response obtained by both the ELF and RSA procedures for the DBE and MCE, respectively.

362

TABLE G-1 Modal Properties of Frame 3S-75 with Viscoelastic Devices

Quantity	Mode 1	Mode 2	Mode 3	Residual Mode
T_m, sec	1.473	0.446	0.237	0.589
$\{\phi_{im}\}$	1.000 0.684 0.275	1.000 -0.458 -0.680	1.000 -1.224 1.654	1.0000 -0.146 -1.634
$\overline{W}_m$, kN	6013	956	398	1354
Γ_m	1.38	-0.53	0.15	-0.38

TABLE G-2 Calculation of Storage Stiffness, Loss Stiffness of Viscoelastic Damping Devices and Viscous Damping Ratio under Elastic Conditions

Mode	Period (assumed) sec	Frequency f Hz	G' MPa	G'' MPa	K_j kN/mm (7-43)	C_j kN.s/mm (7-43)	Period (actual) sec	β_V (7-29)
1	1.44	0.70	0.83	0.83	3.70	0.876	1.473	0.086
2	0.475	2.11	1.82	2.23	8.14	0.857	0.446	0.176
3	0.253	3.95	3.20	2.70	14.3	0.456	0.237	0.076
Residual	0.589	1.70	1.40	1.98	6.26	0.830	0.589	0.198

Values of G' and G'' at given frequencies are obtained from Figure G-1.

TABLE G-3 Modal Response Calculations for Example No.8: 3-Story Frame (V_min=0.75 V_y) with Viscoelastic Damping System. Analysis for the DBE

Quantity	Units	Mode 1 (m=1)	Mode 2 (m=2)	Mode 3 (m=3)	Mode R (m=R)	ELF	SRSS RSA
1. Elastic Response							
Damping Ratio, β_{Ve}		0.086	0.176	0.076	0.198		
Total Damping Ratio, β_{V+I}		0.135	0.226	0.126	0.248		
Damping Coefficient, B_m		1.308	1.578	1.278	1.644		
Elastic Displacement, D_{em}	mm	232	17	2	20		
2. Roof Displacement and Base Shear							
Assumed Ductility, μ		1.21	1.0	1.0	1.0		
Effective Period, T_{1D}	sec	1.618	0.446	0.237	0.589		
Eff. Viscous Damping Ratio, β_V		0.095	0.176	0.076	0.198		
Hysteretic Damping, β_H		0.051	0.000	0.000	0.000		
Effective Damping, β_m		0.196	0.226	0.126	0.248		
Damping Coefficient, B_m		1.488	1.578	1.278	1.644		
Displacement, D_{mD}	mm	223					
Corrected Displacement, D_{mD}	mm	232	17	2	20		
Seismic Coefficient, C_s		0.121	0.307	0.379	0.295		
Seismic Base Shear, V_m	kN	792	294	151	399	887	858
Yield Displacement, D_y	mm	186	--------	--------	--------		
Computed Ductility, μ		1.25	--------	--------	--------		

364

TABLE G-3 continued

3. Response at Stage of Maximum Displacement

	Unit						
Lateral Floor Displacement, δ_{ij}	mm	232	17	2	20		
		159	-8	-2	-3		
		64	-11	3	-33		
Story Drift, Δ_{jm}	mm	73	24	4	23	76	77
		95	4	-5	30	100	95
		64	-11	3	-33	72	65
Design Lateral Forces, F_{im} (including restoring force)	kN	285	255	89	176		
		361	-216	-202	-47		
		145	-321	273	-531		
Floor Acceleration, A_{im}	g	0.375	0.163	0.057	0.112		
		0.257	-0.075	-0.070	-0.016		
		0.103	-0.111	0.094	-0.183		
Actual Story Shear Forces, V_{jm} (including restoring force)	kN	588	526	184	362	691	810
		1332	80	-233	264	1358	1355
		1631	-582	330	-831	1831	1763

365

4. Response at Stage of Maximum Velocity

	Units						
Drift Velocity, ∇_{im}	mm/se	284	341	96	243	374	454
		369	52	-125	316	486	393
		249	-159	72	-347	427	304
Force in Damping Devices, Fd_{jm} (viscous component)	kN	221	259	39	179	284	342
		287	39	-50	233	369	294
		193	-121	29	-255	320	229
Horizontal Damper Force, Vd_{jm} (viscous force)	kN	196	229	35	159		
		254	35	-45	206		
		171	-107	26	-226		
Lateral Force (viscous component)	kN	196	229	35	159		
		58	-194	-79	47		
		-83	-142	70	-432		
G''	MPa	0.8300	2.3000	2.7000	1.9800		
G'	MPa	0.8300	1.9000	3.2000	1.4000		
η		1.000	1.211	0.844	1.414		
$\tan^{-1}\eta$		0.785	0.880	0.701	0.955		
$\cos(\tan^{-1}\eta)$		0.707	0.637	0.764	0.577		
$\sin(\tan^{-1}\eta)$		0.707	0.771	0.645	0.817		
Force in Damping Devices, Fd_{jm} (combination of viscous and restoring forces)	kN	325	316	60	219	392	457
		423	48	-84	297	517	434
		285	-147	48	-326	433	324

TABLE G-3 continued

5. Response at Stage of Maximum Acceleration

Ducitility, μ		1.25	1.00	1.00	1.00	1.00	1.00
Eff. Viscous Damping Ratio, β_v		0.145	0.23	0.13	0.25		
Parameter δ		0.282	0.42	0.25	0.46		
Coefficient CF_1		0.961	0.91	0.97	0.90		
Product $CF_1 \cdot \mu$		1.202	0.91	0.97	0.90		
Force Coefficient, CF_1 or C_{mFD}		1.000	0.912	0.970	0.896		
Force Coefficient, CF_2 or C_{mFV}		0.278	0.411	0.245	0.444		
Lateral Force F_{im} (combination of restoring and viscous forces)	kN	642	574	187	395		
		761	-487	-423	-66		
		276	-662	563	-1174		
Max.Floor Acc., $A_{im,max}$	g	0.408	0.366	0.119	0.252	0.480	0.561
		0.262	-0.168	-0.146	-0.023	0.263	0.343
		0.095	-0.228	0.194	-0.405	0.416	0.314
Maximum Story Shear, $V_{jm,max}$ (actual)	kN	643	574	187	395	755	882
		1403	87	-236	329	1441	1425
		1679	-575	326	-845	1880	1804

TABLE G-4 Modal Response Calculations for Example No.8: 3-Story Frame (V_min=0.75 V_y) with Viscoelastic Damping System. Analysis for the MCE

Quantity	Units	Mode 1 (m=1)	Mode 2 (m=2)	Mode 3 (m=3)	Mode R (m=R)	SRSS ELF	RSA
1. Elastic Response							
Damping Ratio, β_{Ve}		0.086	0.176	0.076	0.198		
Total Damping Ratio, β_{V+I}		0.136	0.226	0.126	0.248		
Damping Coefficient, B_m		1.308	1.578	1.278	1.644		
Elastic Displacement, D_{em}	mm	347	25	2	30		
2. Roof Displacement and Base Shear							
Assumed Ductility, μ		1.86	1.0	1.0	1.0		
Effective Period, T_{1D}	sec	2.009	0.446	0.237	0.589		
Eff. Viscous Damping Ratio, β_V		0.118	0.176	0.076	0.198		
Hysteretic Damping, β_H		0.136	0.000	0.000	0.000		
Effective Damping, β_m		0.304	0.226	0.126	0.248		
Damping Coefficient, B_m		1.812	1.578	1.278	1.644		
Displacement, D_{mD}	mm	342	-------	-------	-------		
Corrected Displacement, D_{mD}	mm	347	25	2	30		
Seismic Coefficient, C_s		0.120	0.461	0.569	0.442		
Seismic Base Shear, V_m	kN	946	441	226	599	1120	1068
Yield Displacement, D_y	mm	185	-------	-------	-------		
Computed Ductility, μ		1.88	-------	-------	-------		

TABLE G-4 continued

3. Response at Stage of Maximum Displacement

Lateral Floor Displacement, δ_{ij}	mm	347	25	2	30		115	116
		238	-11	-3	-4		149	143
		95	-17	4	-49		107	97
Story Drift, Δ_{jm}	mm	110	36	5	34			
		142	6	-7	44			
		95	-17	4	-49			
Design Lateral Forces, F_{im} (including restoring force)	kN	340	383	134	263			
		431	-324	-303	-71			
		173	-482	409	-797			
Floor Acceleration, A_{im}	g	0.217	0.244	0.085	0.168			
		0.149	-0.112	-0.104	-0.025			
		0.060	-0.166	0.141	-0.275			
Actual Story Shear Forces, V_{jm} (including restoring force)		702	789	276	543		888	1092
		1591	120	-349	397		1640	1633
		1948	-873	495	-1247		2313	2191

TABLE G-4 continued

4. Response at Stage of Maximum Velocity

Drift Velocity, ∇_{jm}	mm/sec	343	511	145	365	501	632
		445	78	-187	474	650	489
		298	-238	108	-521	600	397
Force in Damping Devices, Fd_{jm}	kN	266	388	58	268	378	474
(viscous component)		346	59	-76	349	491	359
		231	-181	43	-383	447	297
Horizontal Damper Force, Vd_{jm}	kN	236	344	52	238		
(viscous force)		306	52	-67	309		
		205	-160	39	-339		
Lateral Force	kN	236	344	52	238		
(viscous component)		71	-292	-119	71		
		-101	-213	106	-648		
G"	MPa	0.8300	2.3000	2.7000	1.9800		
G'	MPa	0.8300	1.9000	3.2000	1.4000		
η		1.000	1.211	0.844	1.414		
$\tan^{-1}\eta$		0.785	0.880	0.701	0.955		
$\cos(\tan^{-1}\eta)$		0.707	0.637	0.764	0.577		
$\sin(\tan^{-1}\eta)$		0.707	0.771	0.645	0.817		
Force in Damping Devices, Fd_{jm}	kN	442	473	91	329	551	654
(combination of viscous		574	72	-126	445	727	592
and restoring forces)		385	-221	72	-489	622	449

370

TABLE G-4 continued

5. Response at Stage of Maximum Acceleration

	Units						
Ducitility, μ		1.88	1.00	1.00	1.00		
Eff. Viscous Damping Ratio, β_v		0.17	0.23	0.13	0.25		
Parameter δ		0.32	0.42	0.25	0.46		
Coefficient CF_1		0.95	0.91	0.97	0.90		
Product $CF_1 \cdot \mu$		1.78	0.91	0.97	0.90		
Force Coefficient, CF_1 or C_{mFD}		1.000	0.912	0.970	0.896		
Force Coefficient, CF_2 or C_{mFV}		0.318	0.411	0.245	0.444		
Lateral Force F_{im}	kN	777	861	280	592		
(combination of restoring		912	-730	-635	-100		
and viscous forces)		325	-993	844	-1760		
	g	0.496	0.549	0.179	0.378	0.623	0.761
Max.Floor Acc., $A_{im,max}$		0.314	-0.252	-0.219	-0.034	0.316	0.458
		0.112	-0.342	0.291	-0.607	0.617	0.463
Maximum Story Shear, $V_{jim,max}$	kN	777	861	280	592	977	1193
(actual)		1688	131	-355	493	1759	1730
		2013	-862	490	-1268	2379	2244

371
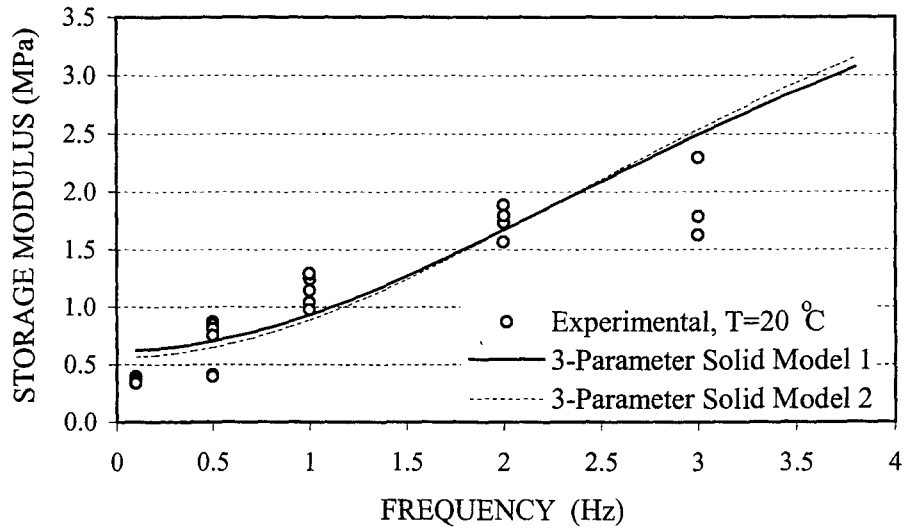
FIGURE G-1 Storage and Loss Modulus of Viscoelastic Damping Device
at Temperature T = 20 °C (Zimmer, 2000)

372

APPENDIX H
DETAILED CALCULATIONS FOR THE SIMPLIFIED ANALYSIS OF A 3-STORY FRAME WITH YIELDING DAMPING SYSTEM

H.1 Introduction

This appendix presents detailed calculations in the application of the equivalent lateral force procedure (ELF) and response-spectrum analysis (RSA) procedures of NEHRP (2000) for the analysis of buildings with yielding damping systems. These procedures are applied as described in Appendix A subject to the modifications described in Sections 7.5.4 and in Section 8.1. The presentation in the appendix consists of detailed calculations for the 3-story steel moment frame 3S-75 shown in Figure 8-9 and described as example No.9 in Section 8.

H.2 Detailed Calculations for 3-Story Frame 3S-75 with Metallic Yielding Damping Devices

Parameters

The seismic tributary weights of the third, second and first floors are 1567 kN, 2900 kN, and 2900 kN, respectively. The design coefficients per Table 5.2.2 1997 NEHRP Recommended Provisions for special steel moment frames are $R = 8.0$, $\Omega_o = 3.0$, $C_d = 5.5$, and $I = 1.0$. The devices are made of steel ($F_y = 248$ MPa) with dimensions base x height x thickness of 305 mm x 457 mm x 25.4 mm ($12''$x$18''$x$1''$).

Description of the System

The analyzed frame is the 3-story special steel moment frame with the yielding damping system shown in Figure 8-9. The damping system of the frame consists of triangular metallic yielding devices (Tsai et al., 1993) shown in Figure C-8(a). Section C.3.1 presents calculations for yield strength and yield displacement of these devices at the first story of this frame, $V_d = 320$ kN and $D_{yd} = 52.4$ mm, respectively. The base shear strength and yield displacement of the frame exclusive of the damping system, are $V_{yf} = 1220$ kN, and $D_{yf} = 182$ mm. The base shear strength of the frame inclusive of the damping system is $V = 1220 + 320 = 1540$ kN. Moreover, Section C.3.1 provides the yield displacement and effective initial (secant) period of the equivalent bilinear representation of the combined system (frame plus yielding devices) as $D_y =$

373

150.5 mm, and $T_1 = 1.327$ sec, respectively (see Fig. C-7). The required base shear strength was calculated by use of (7-72) to be $V_{min} \cdot \Omega_0 \cdot C_d/R$ in which V_{min} is the greater of V/B_{V+I} (equation A13.2.4-1) and 0.75V (equation A13.2.4.1-2). The seismic base shear V was calculated in Section B.3 to be 788.5 kN. Coefficient B_{V+I} was interpreted as the damping coefficient corresponding to the effective damping of the frame inclusive of the yielding damping system at displacement just below the effective yield displacement of the frame exclusive of the damping system. That is, at this level of displacements there is inelastic action in the yielding system. Therefore, the effective damping was calculated by use of (7-55) with $\mu_f = 1.0$, $A_d/A_y = 320/1220$ = 0.26, and $\mu_d = 182/52.4 = 3.47$. The result is

$$\beta_I = 0.05\left(\frac{1}{1+0.26}\right)^{1/2} + \frac{2 \times 0.26 \times \left(1 - \frac{1}{3.47}\right)}{\pi(1+0.26)} = 0.138$$

The corresponding damping coefficient is $B_{V+I} = 1.314$ (Table A13.3.1). Thus, $V_{min} = V/B_{V+I} = 788.5/1.314 = 600$ *kN* (which is greater than 0.75V=591 kN). The required base shear strength of the frame (7-72) is $V_y = 600 \times 3 \times 5.5/8 = 1237.5$ *kN*. The base shear strength of the frame (exclusive of the damping system) is $V_{yf} = 1220$ *kN* which is close to the required base shear strength.

The application of the ELF method of analysis of NEHRP (2000) requires that the period and mode shape of the first mode of vibration of the frame inclusive of the damping system is determined. Modal analysis of the frame inclusive of the metallic devices resulted in $T_1 = 1.133$ sec $\{\phi_{i1}\}^T = [1.0 \quad 0.708 \quad 0.296]$. However, direct use of the NEHRP (2000) analysis procedure requires that the effective initial (secant) period for the elastoplastic representation of the frame inclusive of the damping system is utilized. This period was calculated in Section C.3.1 using (C-13) to be $T_1 = 1.327$ sec. Since this period was calculated by simple procedures without the use of a computer model of the frame, the first mode shape was assumed to be that of the frame exclusive of the damping system: $\{\phi_{i1}\}^T = [1.0 \quad 0.657 \quad 0.250]$. Note that this mode shape is very close to the one of the frame inclusive of the damping system and that both mode shapes represent approximations to a more approximate mode shape that should have been calculated using effective member stiffnesses.

374

A similar complexity arises in the application of the RSA method of NEHRP (2000). Calculation of the modal properties of the frame inclusive of the damping system would require the use of effective stiffnesses for the yielding damping devices. To avoid such analysis and within the context of approximate analysis, the modal properties were calculated as follows:

(a)   The effective initial (secant) period $T_1 = 1.327$ sec was used for the first mode.

(b)   The periods $T_2 = 0.49$ sec and $T_3 = 0.24$ sec of the frame exclusive of the damping devices were used for the second and third modes, respectively. Note that the second- and third-mode periods of the frame inclusive of the damping devices (for elastic conditions of the metallic damping devices) are 0.40 sec and 0.23 sec, respectively. Use of effective stiffnesses for the metallic devices in the computer analysis would have resulted in values of periods T_2 and T_3 between 0.49 and 0.40 sec and between 0.24 and 0.23 sec, respectively. Such accuracy is, apparently, of little significance in an approximate analysis.

(c)   The mode shapes of the frame exclusive of the damping system were used. That is, $\{\phi_{i1}\}^T = [1.0 \quad 0.657 \quad 0.250]$, $\{\phi_{i2}\}^T = [1.0 \quad -0.560 \quad -0.690]$, and $\{\phi_{i3}\}^T = [1.0 \quad -1.618 \quad 2.096]$. By comparison, the mode shapes of the frame inclusive of the metallic yielding devices (for elastic conditions of these devices) are [1.0 0.708 0.296], [1.0 -0.472 -0.675] and [1.0 -1.548 1.840], respectively. Again, values of the modal displacements between these two bounding cases could have been used but it is apparent that this would have been of little significance in an approximate analysis.

The utilized modal properties of the frame are summarized in Table H-1. The yield displacement of the equivalent bilinear representation ($D_y = 150.5$ mm) was utilized for calculations of effective ductility demand.

CALCULATION OF RESPONSE IN DESIGN BASIS EARTHQUAKE

FIRST MODE RESPONSE (T_1=1.327 sec)

Equations (7-54) and (7-55) were used to calculate effective period and effective damping ratio in the first mode. The following two equations, defined in Figure 7-5, were needed:

$$A_d = \frac{V_d}{W_1} g = \frac{320}{5871} g = 0.054g$$

$$A_y = \frac{V_{yf}}{W_1} g = \frac{1220}{5871} g = 0.208g$$

Inelastic Roof Displacement

Assumed Effective Ductility: $\qquad \mu_D = 1.46$

Assumed Roof Displacement: $\qquad D_{ID} = \mu_D \cdot D_y = 1.46 \times 150.5 = 220 \ mm$ $\qquad$ (A13.3.4-1)

Spectral Roof Displacement: $D = \dfrac{D_{ID}}{\Gamma_1} = \dfrac{220}{1.399} = 157 \ mm$

Effective Period: $\qquad T_{ID} = 2 \times \pi \times \left(\dfrac{157}{0.264 \times 9810} \right)^{\frac{1}{2}} = 1.55 \ sec$ $\qquad$ (7-54)

Effective Damping Ratio:

Ductility Ratio for the Frame: $\qquad \mu_f = \dfrac{220}{182} = 1.209$ $\qquad$ (7-56)

Ductility Ratio for the Damping System: $\quad \mu_d = \dfrac{220}{52.4} = 4.20$ $\qquad$ (7-56)

Quality Factor: $\qquad q_H = 0.67 \times \dfrac{0.6}{1.327} = 0.30 < 0.50$ $\qquad$ (A13.3.3-1)

$$\text{use } q_H = 0.50$$

Hysteretic Damping (hysteretic component in (7-55)):

$$\beta_{HD} = \frac{2 \times 0.5 \times \left(1 - \dfrac{1}{1.209} \right) + 2 \times 0.26 \times \left(1 - \dfrac{1}{4.20} \right)}{\pi \times (1 + 0.26)} = 0.144$$

Effective Damping: $\quad \beta_{ID} = 0.05 \times \left(\dfrac{1}{1 + 0.26} \right)^{\frac{1}{2}} + 0.144 = 0.188$ $\qquad$ (7-55)

Damping Coefficient: $B_{ID} = 1.464$ $\qquad$ (Table A13.3.1)

376

Roof Displacement: $D_{ID} = \left(\dfrac{9810}{4\pi^2}\right) \times 1.399 \times \dfrac{0.6}{1.464} \times 1.55 = 221\,mm$ $\qquad$ (A13.4.4.3-1)

Corrected Roof Displacement

The roof displacement for elastic behavior of the frame is:

$$D = \left(\dfrac{9810}{4\pi^2}\right) \times 1.399 \times \dfrac{0.6}{1.0} \times 1.327 = 277\,mm$$

Since $D_{ID} < D$, use $D_{ID} = 277$ mm

Base Shear

Seismic Coefficient: $C_{s1} = \left(\dfrac{8}{5.5}\right) \times \dfrac{0.6}{1.55 \times (3 \times 1.464)} = 0.128$ $\qquad$ (A13.4.3.4-1)

Base Shear: $\qquad V_1 = 0.128 \times 5871 = 751\,kN$ $\qquad$ (A13.4.3.1-1)

The contribution of the first mode to the base shear strength of the frame is given by (7-72)

$$V_1 = 751 \times \dfrac{3 \times 5.5}{8} = 1549\,kN$$

The calculated contribution to the base shear strength of 1549 kN is nearly identical to the actual base shear strength of 1540 kN.

Displacement at Effective Yield (Yield Displacement) D$_y$

$$D_y = \left(\dfrac{9810}{4\pi^2}\right) \times \left(\dfrac{3 \times 5.5}{8}\right) \times 1.399 \times 0.128 \times 1.327^2 = 162\,mm \qquad \text{(A13.3.4-3)}$$

Effective Ductility Demand: $\qquad \mu_D = \dfrac{277}{162} = 1.71$ $\qquad$ (A13.3.4-1)

$$\mu_D < \mu_{MAX} = 2.67$$

The difference between the calculated and the assumed ductility demand is due to adjustment of the inelastic displacement to meet the condition that it is not less then the elastic displacement.

Response at stage of maximum displacement

Lateral Floor Displacements, δ_{iID}, and Story Drifts Δ_{iID}

$$\delta_{iID} = 277 \times \begin{Bmatrix} 1.000 \\ 0.657 \\ 0.250 \end{Bmatrix} = \begin{Bmatrix} 277 \\ 182 \\ 69 \end{Bmatrix} mm \qquad \text{(A13.4.4.2-1)}$$

$$\Delta_{iID} = \begin{Bmatrix} 95 \\ 113 \\ 69 \end{Bmatrix} (mm)$$

Design Lateral Forces, F_{iI}, Design Story Shear Forces, V_{iI}, and Floor Accelerations, A_{iI}

$$F_{iI} = \begin{Bmatrix} 1567 \times 1.000 \times \dfrac{1.399}{5871} \times 751 \\ 2900 \times 0.659 \times \dfrac{1.399}{5871} \times 751 \\ 2900 \times 0.250 \times \dfrac{1.399}{5871} \times 751 \end{Bmatrix} = \begin{Bmatrix} 280 \\ 342 \\ 130 \end{Bmatrix} kN \qquad \text{(A13.4.3.9-1)}$$

$$A_{iI} = \frac{F_{iI}}{w_i} \cdot \left(\frac{C_d \cdot \Omega_o}{R} \right) \begin{Bmatrix} \dfrac{280}{1567} \\ \dfrac{342}{2900} \\ \dfrac{130}{2900} \end{Bmatrix} \times \left(\frac{3 \times 5.5}{8} \right) = \begin{Bmatrix} 0.369 \\ 0.243 \\ 0.092 \end{Bmatrix} g$$

$$V_{iI} = \begin{Bmatrix} 280 \\ 622 \\ 752 \end{Bmatrix} kN$$

378

SECOND MODE RESPONSE ($T_2 = 0.49 < T_s$)

Effective Damping Ratio: $\beta_{2D} = 0.05$ $B_{2D} = 1.0$

Roof Displacement: $D_{2D} = \left(\dfrac{9810}{4\pi^2}\right) \times 0.533 \times \dfrac{1.0}{1.0} \times 0.49^2 = 32\,mm$ (A13.5.4.3-2)

Seismic Base Shear:

Seismic Coefficient: $C_{s2} = \left(\dfrac{8}{5.5}\right) \times \dfrac{1.0}{3 \times 1.0} = 0.485$ (A13.5.3.6-1)

Base Shear: $V_2 = 0.485 \times 1098 = 533\,kN$ (A13.5.3.2-1)

Response at Stage of Maximum Displacement

Lateral Floor Displacements, δ_{i2D}, and Story Drift, Δ_{i2D}

$$\delta_{i2D} = 32 \times \begin{Bmatrix} 1.000 \\ -0.560 \\ -0.690 \end{Bmatrix} = \begin{Bmatrix} 32 \\ -18 \\ -22 \end{Bmatrix} mm \qquad \text{(A13.5.4.2-1)}$$

$$\Delta_{i2D} = \begin{Bmatrix} 50 \\ 4 \\ -22 \end{Bmatrix} mm$$

Design Lateral Forces, F_{i2}, Design Story Shears, V_{i2}, and Floor Accelerations, A_{i2}

$$F_{i2} = \begin{Bmatrix} 1567 \times 1.0 \times \dfrac{0.533}{1098} \times 533 \\ 2900 \times (-0.560) \times \dfrac{0.533}{1098} \times 533 \\ 2900 \times (-0.690) \times \dfrac{0.533}{1098} \times 533 \end{Bmatrix} = \begin{Bmatrix} 405 \\ -420 \\ -518 \end{Bmatrix} kN \qquad \text{(A13.5.3.7-1)}$$

379

$$A_{i2} = \frac{F_{i2}}{w_i} \cdot \left(\frac{C_d \Omega_o}{R} \right) = \left\{ \begin{array}{c} \dfrac{405}{1567} \\ \dfrac{-420}{2900} \\ \dfrac{-518}{2900} \end{array} \right\} \times \left(\frac{3 \times 5.5}{8} \right) = \left\{ \begin{array}{c} 0.533 \\ -0.299 \\ -0.368 \end{array} \right\} g$$

$$V_{i2} = \left\{ \begin{array}{c} 405 \\ -15 \\ -533 \end{array} \right\} kN$$

THIRD MODE RESPONSE ($T_3 = 0.24$ sec $< T_s$)

Effective Damping Ratio: $\beta_{3D} = 0.05$ $B_{3D} = 1.0$

Roof Displacement: $D_{3D} = \left(\dfrac{9810}{4\pi^2} \right) \times 0.135 \times \dfrac{1.0}{1.0} \times 0.24^2 = 2\,mm$ (A13.5.4.3-2)

Seismic Base Shear:

Seismic Coefficient: $C_{s3} = \left(\dfrac{8}{5.5} \right) \times \dfrac{1.0}{3 \times 1.0} = 0.485$ (A13.5.3.6-1)

Base Shear: $V_3 = 0.485 \times 398 = 193\,kN$ (A13.5.3.2-1)

Response at Stage of Maximum Displacement

Lateral Floor Displacements, δ_{i3D}, and Story Drift, Δ_{i3D}

$$\delta_{i3D} = 2 \times \left\{ \begin{array}{c} 1.000 \\ -1.618 \\ 2.096 \end{array} \right\} = \left\{ \begin{array}{c} 2 \\ -3 \\ 4 \end{array} \right\} mm$$ (A13.5.4.2-1)

$$\Delta_{i3D} = \left\{ \begin{array}{c} 5 \\ -7 \\ 4 \end{array} \right\} mm$$

Design Lateral Forces, F_{i3}, Design Story Shears, V_{i3}, and Floor Accelerations, A_{i3}

$$F_{i3} = \left\{ \begin{array}{c} 1567 \times 1.0 \times \dfrac{0.135}{398} \times 193 \\ 2900 \times (-1.618) \times \dfrac{0.135}{398} \times 193 \\ 2900 \times (2.096) \times \dfrac{0.135}{398} \times 193 \end{array} \right\} = \left\{ \begin{array}{c} 103 \\ -307 \\ 398 \end{array} \right\} kN \qquad \text{(A13.5.3.7-1)}$$

$$A_{i3} = \dfrac{F_{i2}}{w_i} \cdot \left(\dfrac{C_d \Omega_o}{R} \right) = \left\{ \begin{array}{c} \dfrac{103}{1567} \\ \dfrac{-307}{2900} \\ \dfrac{398}{2900} \end{array} \right\} \times \left(\dfrac{3 \times 5.5}{8} \right) = \left\{ \begin{array}{c} 0.136 \\ -0.218 \\ 0.283 \end{array} \right\} g$$

$$V_{i3} = \left\{ \begin{array}{c} 103 \\ -204 \\ 194 \end{array} \right\} kN$$

RESIDUAL MODE RESPONSE (T_R = 0.4x1.327 = 0.531sec < T_s)

Effective Damping Ratio: $\quad \beta_{RD} = 0.05 \qquad\qquad B_{RD}=1.0$

Roof Displacement: $\quad D_{RD} = \left(\dfrac{9810}{4\pi^2} \right) \times 0.399 \times \dfrac{1.0}{1.0} \times 0.531^2 = 28\,mm \qquad \text{(A13.4.4.3-2)}$

Seismic Base Shear:

Seismic Coefficient: $\quad C_{sR} = \left(\dfrac{8}{5.5} \right) \times \dfrac{1.0}{3 \times 1.0} = 0.485 \qquad \text{(A13.4.3.8-1)}$

Base Shear: $\quad V_R = 0.485 \times 1496 = 725\,kN \qquad \text{(A13.4.3.6-1)}$

Response at Stage of Maximum Displacement

Lateral Floor Displacements, δ_{iRD}, and Story Drift, Δ_{iRD}

$$\delta_{iRD} = 28 \times \begin{Bmatrix} 1.000 \\ -0.2024 \\ -1.6292 \end{Bmatrix} = \begin{Bmatrix} 28 \\ -6 \\ -46 \end{Bmatrix} mm \qquad \text{(A13.4.4.2-2)}$$

$$\Delta_{iRD} = \begin{Bmatrix} 34 \\ 40 \\ -46 \end{Bmatrix} mm$$

Design Lateral Forces, F_{iR}, Design Story Shears, V_{iR}, and Floor Accelerations, A_{iR}

$$F_{iR} = \begin{Bmatrix} 1567 \times 1.0 \times \dfrac{0.399}{1496} \times 725 \\ 2900 \times (-0.2024) \times \dfrac{0.399}{1496} \times 725 \\ 2900 \times (-1.6292) \times \dfrac{0.399}{1496} \times 725 \end{Bmatrix} = \begin{Bmatrix} 303 \\ -113 \\ -913 \end{Bmatrix} kN \qquad \text{(A13.5.3.7-1)}$$

$$A_{iR} = \frac{F_{iR}}{w_i} \cdot \left(\frac{C_d \Omega_o}{R} \right) = \begin{Bmatrix} \dfrac{303}{1567} \\ \dfrac{-113}{2900} \\ \dfrac{-913}{2900} \end{Bmatrix} \times \left(\frac{3 \times 5.5}{8} \right) = \begin{Bmatrix} 0.399 \\ -0.080 \\ 0.649 \end{Bmatrix} g$$

$$V_{iR} = \begin{Bmatrix} 303 \\ 190 \\ -723 \end{Bmatrix} kN$$

Total responses resulting from modal combinations were calculated by use of the SRSS combination rule. Tables H-2 and H-3 present summaries of the results of the analysis for each mode and the total response calculated by both the ELF and RSA procedures for the DBE and MCE, respectively.

TABLE H-1 Modal Properties of Frame 3S-75

	Dynamic Properties			
Quantity	Mode 1 (m=1)	Mode 2 (m=2)	Mode 3 (m=3)	Residual Mode (m=R)
T_m, sec	1.327	0.49	0.24	0.531
$\{\phi_{im}\}$	1.000 0.657 0.250	1.000 -0.560 -0.690	1.000 -1.618 2.096	1.0000 -0.2024 -1.6292
$\overline{W}_m$, kN (7-12)	5871	1098	398	1496
Γ_m (7-16)	1.3991	-0.5334	0.1348	-0.3991

Note that period T_l is the effective initial (secant) period of the equivalent bilinear representation of the pushover curve of the frame (see Section C.3.1).

TABLE H-2 Modal Response of Example No.2: 3S-75 with Triangular Metallic Yielding Devices. Analyisis for the DBE

Quantity	Units	Mode 1 (m=1)	Mode 2 (m=2)	Mode 3 (m=3)	Mode R (m=R)	SRSS ELF	SRSS RSA
1. Elastic Response							
Damping Ratio, β_{Ve}		0.000	0.000	0.000	0.000		
Total Damping Ratio, β_{V+I}		0.050	0.050	0.050	0.050		
Damping Coefficient, B_m		1.000	1.000	1.000	1.000		
Elastic Displacement, D_{em}	mm	277	32	2	28		
2. Roof Displacement and Base Shear							
Assumed Ductility, μ		1.46	1	1	1		
Effective Period, T_{ID}	sec	1.55	0.49	0.24	0.531		
Eff. Viscous Damping Ratio, β_V		0.000	0.00	0.00	0.00		
Hysteretic Damping, β_H		0.144	0.00	0.00	0.00		
Effective Damping, βm		0.19	0.05	0.05	0.05		
Damping Coefficient, B_m		1.464	1	1	1		
Displacement, D_{mD}	mm	221	32	2	28		
Corrected Displacement, D_{mD}	mm	277	0.485	0.485	0.485		
Seismic Coefficient, C_s		0.128	0.485	0.485	0.485		
Seismic Base Shear, V_m	kN	751	533	193	725	1044	941
Yield Displacement, D_y	mm	162	---------	---------	---------		
Computed Ductility, μ		1.71	---------	---------	---------		
3. Response at Stage of Maximum Displacement							
Lateral Floor Displacement, δ_{ij}	mm	277 / 182 / 69	32 / -18 / -22	2 / -3 / 4	28 / -6 / -46		
Story Drift, Δ_{jm}	mm	95 / 113 / 69	50 / 4 / -22	5 / -7 / 4	34 / 40 / -46	100 / 119 / 83	107 / 113 / 72
Design Lateral Forces, F_{im}	kN	280 / 342 / 130	405 / -420 / -518	103 / -307 / 398	303 / -113 / -913		
Floor Acceleration, A_{im}	g	0.369 / 0.243 / 0.092	0.533 / -0.299 / -0.368	0.136 / -0.218 / 0.283	0.399 / -0.080 / 0.649	0.544 / 0.256 / 0.655	0.662 / 0.443 / 0.474
Actual Story Shear Forces, V_{jm}	kN	578 / 1282 / 1551	835 / -31 / -1099	212 / -421 / 400	625 / 392 / -1491	852 / 1340 / 2151	1037 / 1350 / 1942

TABLE H-3 Modal Response of Example No.2: 3S-75 with Triangular Metallic Yielding Devices, Analyisis for the MCE

Quantity	Units	Mode 1 (m=1)	Mode 2 (m=2)	Mode 3 (m=3)	Mode R (m=R)	SRSS ELF	SRSS RSA
1. Elastic Response							
Damping Ratio, β_{Ve}		0.000	0.000	0.000	0.000		
Total Damping Ratio, β_{V+I}		0.050	0.050	0.050	0.050		
Damping Coefficient, B_m		1.000	1.000	1.000	1.000		
Elastic Displacement, D_{em}	mm	413	48	3	42		
2. Roof Displacement and Base Shear							
Assumed Ductility, μ		2.35	1	1	1		
Effective Period, T_{ID}	sec	1.96	0.49	0.24	0.53		
Eff. Viscous Damping Ratio, β_V							
Hysteretic Damping, β_H		0.234	0	0	0		
Effective Damping, β_m		0.279	0.050	0.050	0.050		
Damping Coefficient, B_m	mm	1.737	1.000	1.000	1.000		
Displacement, D_{mD}	mm	353					
Corrected Displacement, D_{mD}		413	48	3	42		
Seismic Coefficient, C_s	kN	0.128	0.727	0.727	0.727	1323	1135
Seismic Base Shear, V_m	mm	752	798	290	1088		
Yield Displacement, D_y		162	----------	----------	----------		
Computed Ductility, μ		2.55	----------	----------	----------		
3. Response at Stage of Maximum Displacement							
Lateral Floor Displacement, δ_{ij}	mm	413 / 272 / 103	48 / -27 / -33	3 / -5 / 6	42 / -8 / -68		
Story Drift, Δ_{jm}	mm	142 / 168 / 103	75 / 6 / -33	8 / -11 / 6	50 / 59 / -68	150 / 178 / 124	160 / 169 / 109
Design Lateral Forces, F_{im}	kN	281 / 342 / 130	609 / -631 / -777	154 / -461 / 597	455 / -170 / -1371		
Floor Acceleration, A_{im}	g	0.369 / 0.243 / 0.092	0.801 / -0.449 / -0.553	0.203 / -0.328 / 0.424	0.599 / -0.121 / -0.975	0.703 / 0.271 / 0.980	0.905 / 0.606 / 0.703
Actual Story Shear Forces, V_{jm}	kN	579 / 1284 / 1552	1255 / -46 / -1648	317 / -633 / 598	938 / 587 / -2242	1103 / 1412 / 2727	1418 / 1432 / 2342

APPENDIX I

DETAILED CALCULATIONS FOR THE ANALYSIS OF A 3-STORY FRAME WITH LINEAR VISCOUS DAMPING SYSTEM USING THE FEMA 274 METHOD 2 NONLINEAR STATIC PROCEDURE

I.1 Introduction

This appendix presents detailed calculations of the application of Method 2 of FEMA, 1997 for the analysis of a building with a linear viscous damping system. This method is applied as described in Section 2 subject to the modifications described in Section 8.1. The application of this method is illustrated in Figure 2-1.

The presentation in the appendix consists of:

(a)   Detailed calculations for the 3-story special steel moment frame 3S-75 shown in Figure 8-2 and denoted as example No.2 in Section 8, using a distribution of lateral load based on the first mode pattern.

(b)   Summary calculations for the 3-story special steel moment frame 3S-75 shown in Figure · 8-2 and denoted as example No.2 in Section 8, using distributions of lateral load based on the modal, uniform, and adaptive patterns.

I.2 Detailed Calculations for 3-Story Frame 3S-75 with Linear Viscous Damping System

Design Parameters and Modal Properties

The design parameters for, and a description of the 3-story special steel moment frame 3S-75, example No.2are presented in Section E.2. The modal properties of the frame are presented in Table I.1.

Pushover Analysis

Pushover analysis is performed in IDARC2D-Version 4.0 (Valles et al., 1996) using a distribution of lateral load consistent with the first mode pattern. Table I.1 presents the lateral load distribution patterns utilized in the analysis. Elastoplastic behavior is assumed in the modeling of the plastic hinges. Parameters utilized for modeling of the plastic hinges are summarized in Table I-1. In addition it has been assumed that joints are stiffened within a length of half the depth of the beam ($d_b/2$) section in the vertical direction, and of half the depth of the column section ($d_c/2$) in the horizontal direction. In the first-story columns, the rigid offset above the base of the column is assumed to be equal to the column depth (d_c). Gravity load and P-Δ effects are disregarded in this analysis.

Table I-2 shows the values of base shear, V_1 at increments of roof displacement, D_{roof}, of 0.50 mm. It also shows the corresponding values of shear and drifts per story. Figure I-1(a) shows the pushover curve of the building and the sequence of yielding at several steps of the analysis. It also shows the approximate bilinear representation of the pushover curve, giving an approximate base shear strength, V_y, equal to 1232 kN and a displacement at yielding, D_y, of 182 mm. Figure I-1(b) shows the force displacement relationship of each story and its bilinear representation.

Modal Properties of the Frame at Various Stages of the Pushover Analysis

This section is included to illustrate the variation of the modal properties of the frame under inelastic action. Modal properties of the frame were obtained by eigenvalue analysis performed in program IDARC2D using the effective stiffness of each story at three different values of assumed roof displacement. At each assumed roof displacement, the story drift, Δ_j, and the story shear V_j were obtained from Table I-2. The effective stiffness at each story was obtained as $K_{effj} = V_j/\Delta_j$.

Eigenvalue analysis of the frame at the assumed displacement was performed using a shear building type of representation. Models were utilized in which the beams and columns sections were modified to approximately represent the reduction of stiffness due to yielding. Figure I-2 shows the shear type and the modified frame model of the structure that was used for eigenvalue analysis at different values of assumed roof displacement. In both models, the lateral stiffness at

each story was nearly equal with the corresponding effective stiffness at the assumed roof displacement as calculated in the pushover analysis. Table I-3 presents a summary of the modal properties of the frame at each value of assumed roof displacement. Substantial differences in the values of modal properties and effective viscous damping obtained by using both the shear building and the modified model representations of the frame are observed. It is evident that the modal properties of the frame at the various stages of pushover analysis examined depend strongly on the mathematical model, especially for the higher modes. This is an important issue when dealing with systems with rate-dependent damping devices. Magnitude and distribution of damping forces are significantly influenced by the modal properties of the building. Consequently, the model of the frame must represent the actual behavior of the building as close as possible. The "modified model" seems to be a more reasonable approach. Herein the results obtained by eigenvalue analysis of the modified frame are utilized for application of Method 2.

CALCULATION OF RESPONSE IN THE DESIGN BASIS EARTHQUAKE

FIRST MODE RESPONSE (T_1=1.58 sec)

Roof Displacement for Elastic Behavior

Viscous Damping Ratio (under elastic conditions): $\beta_{vl} = 0.10$

Effective Viscous Damping Ratio: $\beta_{V+I} = 0.10 + 0.05 = 0.15$

Damping Coefficient: $B_{V+I} = 1.35$ (Table A13.3.1)

Roof Displacement: $D = \left(\dfrac{9810}{4\pi^2}\right) \times 1.399 \times \dfrac{0.6}{1.35} \times 1.58 = 244 \ mm$

Assumed Roof Displacement: $D_{1D} = 244 \ mm$

For convenience the roof displacement is assumed to be equal to the elastic displacement.

Modal Properties at Assumed Roof Displacement

Table I-3 presents the results of the eigenvalue analysis for the assumed roof displacement.

Displacement Ductility Ratio: $\mu_D = \dfrac{244}{182} = 1.34$ (7-36)

Effective Period: from eigenvalue analysis, $T_{eff} = 1.808\ sec$ (Table I-3)

Note that (7-35) gives: $T_{eff} = T_1\sqrt{\mu} = 1.58\sqrt{1.34} = 1.829\ sec$

Effective Damping Ratio:

Effective Viscous Damping: $\beta_{v1} = 0.135$ (Table I-3)

(use of equation 7-29 with effective period and mode shape per Table I-3)

Quality Factor: $q_H = 0.67 \times \dfrac{0.6}{1.808} = 0.222 < 0.5$

use $q_H = 0.5$

(use q_H in NEHRP (2000) for consistency)

Hysteretic Damping Ratio: $\beta_{HD} = (0.64 - 0.05) \times 0.5 \times \left(1 - \dfrac{1}{1.34}\right) = 0.075$

(note use of term $2/\pi - \beta i$ rather than $2/\pi$ for consistency with NEHRP, 2000)

Effective Damping Ratio: $\beta_{eff} = 0.05 + 0.135 + 0.075 = 0.26$ (7-37)

Damping Coefficient: $B = 1.68$

(use of damping coefficient in NEHRP, 2000 for consistency)

Spectral Capacity Curve

To convert the bilinear representation of the pushover curve to a spectral capacity curve, it is necessary to determine the spectral coordinates at yielding of the frame, and at several other stages of pushover. Herein we utilize three points to define the spectral capacity curve by means

of (2-2) and (2-4) and the properties presented in Tables I-1 and I-3, and figure I-1 at different assumed roof displacements, as follows:

At yielding (D_y=182 mm): $S_{ay} = \dfrac{1232\,g}{5871} = 0.21\,g$, $S_{dy} = \dfrac{\delta_r}{\phi_{r1}\Gamma_1} = \dfrac{182}{1.0 \times 1.399} = 130\ mm$

At assumed D_{roof}= 244 mm: $S_a = \dfrac{1232\,g}{5599} = 0.22\,g$, $S_d = \dfrac{\delta_r}{\phi_{r1}\Gamma_1} = \dfrac{244}{1.0 \times 1.449} = 168\ mm$

At assumed D_{roof} = 419 mm): $S_a = \dfrac{1232\,g}{5852} = 0.21\,g$, $S_d = \dfrac{\delta_r}{\phi_{r1}\Gamma_1} = \dfrac{419}{1.0 \times 1.437} = 292\ mm$

Note that the spectral acceleration is not constant as it should have been in an elastoplastic model. The difference is a result of the approximate nature of the analysis. However, the difference is small and we proceed using $S_a = 0.22$ g.

Design Demand Curve

The design demand curve is established by using (2-5) and (3-1) and the damping coefficients from Table A13.3.1. Figure 2-2 shows the design demand curves for damping ratios from 5% to 100% for the design-basis earthquake.

Calculated Roof Displacement

Figure I-3 (a) shows the spectral capacity curve of the frame and the design demand curves for damping ratios of 0.15 and 0.26. The spectral displacement S_d is established at the intersection of the spectral capacity curve and the design demand curve for $\beta_{eff} = 0.26$. Note that the same point is also defined at the intersection of the straight line corresponding to the effective period at the assumed displacement, $T_{eff} = 1.808$ sec, and the design demand curve for $\beta_{eff} = 0.26$. The spectral displacement at the intersection is $S_d = 161$ mm. Accordingly, the calculated roof displacement is obtained from (2-4) as

$$D_{1D} = 161 \times 1.449 = 233\ mm$$

Corrected Roof Displacement

Since the calculated roof displacement D_{ID} = 233 *mm* is less than the elastic displacement D = *244* mm, then D_{ID} = *244 mm*. The spectral displacement for elastic behavior of the frame is shown in Figure I-3 (a) at the intersection of the straight line corresponding to the fundamental period of the frame (T_1 = *1.58 sec*) and the design demand curve for β_{V+I} = *0.15*. Also, the spectral acceleration corresponding to the spectral displacement for elastic behavior is S_a = *0.22*.

Base Shear

The base shear can be obtained from (2-2) as

$$V_1 = S_a \cdot \overline{W}_1 = 0.22 \times 5599 = 1232 \ kN$$

Response at Stage of Maximum Displacement

Lateral floor displacements, δ_{iID}, and story drifts, Δ_{iID}

$$\delta_{iID} = 244 \times \begin{Bmatrix} 1.000 \\ 0.574 \\ 0.210 \end{Bmatrix} = \begin{Bmatrix} 244 \\ 140 \\ 51 \end{Bmatrix} mm$$

Note that here use was made of the mode shape of the modified frame at a roof displacement equal to 244 mm (elastic displacement) and not the elastic mode shape (see Table I-1). One could have used the elastic mode shape.

$$\Delta_{iID} = \begin{Bmatrix} 104 \\ 89 \\ 51 \end{Bmatrix} mm$$

Lateral Inertia Forces, F_{il}, Story Shears, V_{il}, and Floor Accelerations, A_{il}

$$F_{il} = \begin{Bmatrix} 1567 \times 1.0 \times \dfrac{1.449}{5599} \times 1232 \\[2mm] 2900 \times 0.574 \times \dfrac{1.449}{5599} \times 1232 \\[2mm] 2900 \times 0.210 \times \dfrac{1.449}{5599} \times 1232 \end{Bmatrix} = \begin{Bmatrix} 500 \\ 531 \\ 194 \end{Bmatrix} kN$$

$$A_{il} = \frac{F_{il}}{w_i} = \begin{Bmatrix} \dfrac{500}{1567} \\[2mm] \dfrac{531}{2900} \\[2mm] \dfrac{194}{2900} \end{Bmatrix} = \begin{Bmatrix} 0.319 \\ 0.183 \\ 0.067 \end{Bmatrix} g$$

$$V_{il} = \begin{Bmatrix} 500 \\ 1031 \\ 1225 \end{Bmatrix} kN$$

Response at Stage of Maximum Velocity

Story velocity, ∇_{il}

Calculated as pseudovelocity

$$\nabla_{il} = \left(\frac{2\pi}{1.808} \right) \times \begin{Bmatrix} 104 \\ 89 \\ 51 \end{Bmatrix} = \begin{Bmatrix} 361 \\ 309 \\ 177 \end{Bmatrix} mm / sec$$

Force in Damping Devices, F_{dilD}

$$F_{dilD} = 0.90 \times \begin{Bmatrix} 361 \\ 309 \\ 177 \end{Bmatrix} \cos 27.6° = \begin{Bmatrix} 287 \\ 246 \\ 141 \end{Bmatrix} kN \tag{7-23}$$

Horizontal Component of Damping Force

$$V_{di1D} = \begin{Bmatrix} 287 \\ 246 \\ 141 \end{Bmatrix} \cos 27.6° = \begin{Bmatrix} 254 \\ 218 \\ 125 \end{Bmatrix} kN$$

Response at Stage of Maximum Acceleration

Force Coefficients

Effective Viscous Damping: $\beta_{v1} = 0.05 + 0.135 = 0.185$

Parameter δ: $\delta = tan^{-1}(2 \times 0.185) = 0.354$

Coefficient CF1:

$$CF_1 = cos\ (0.3543) = 0.938 \qquad\qquad (4\text{-}41)$$

$$CF_1\mu = 0.938 \times 1.34 = 1.26 > 1.00 \qquad use\ CF_1 = 1.0$$

Coefficient CF₂: $CF_2 = sin\ (0.354) = 0.347$ (4-39)

Maximum floor acceleration, $A_{i1,max}$

$$A_{i_{1,max}} = (CF_1 + 2\beta_{eff}CF_2)A_{i1} = (1.0 + 2 \times 0.185 \times 0.347) \times \begin{Bmatrix} 0.319 \\ 0.183 \\ 0.067 \end{Bmatrix} = \begin{Bmatrix} 0.360 \\ 0.206 \\ 0.076 \end{Bmatrix} g$$

Maximum story shears, $V_{i1,max}$

$$V_{i_1,max} = CF_1 \cdot V_{i_1}\big|_{Max\,Disp} + CF_2 \cdot V_{i_1}\big|_{Max\,Velocity}$$

$$V_{i_1,max} = 1.0 \times \begin{Bmatrix} 500 \\ 1031 \\ 1225 \end{Bmatrix} + 0.347 \times \begin{Bmatrix} 254 \\ 218 \\ 125 \end{Bmatrix} = \begin{Bmatrix} 588 \\ 1107 \\ 1268 \end{Bmatrix} kN$$

SECOND MODE RESPONSE (T_2=0.732 sec>T_s)

The higher mode responses are calculated without constructing the spectral-capacity and design-demand curves due to the assumption of elastic behavior. The graphical solution is also presented.

Roof Displacement

Viscous Damping Ratio: $\quad \beta_{v2} = 0.343$ (Table I-3)

Effective Damping Ratio: $\quad \beta_{2D} = 0.343 + 0.05 = 0.393$

Damping Coefficient: $\quad B_{2D} = 2.079$ (Table A13.3.1)

Roof Displacement: $\quad D_{2D} = \left(\dfrac{9810}{4\pi^2}\right) \times 0.528 \times \dfrac{0.6}{2.079} \times 0.732 = 28mm$

Seismic Base Shear

Figure I-3(b) shows the design demand curve for $\beta_{2D} = 0.393$ and the spectral capacity curve of the second mode denoted by the straight line corresponding to period $T_2 = 0.732$ sec. The corresponding spectral acceleration is obtained at the intersection point as $S_a = 0.394$ g. Accordingly, the base shear is obtained from (2-2) as

$$V_2 = 0.394 \times 1098 = 433\,kN$$

Response at Stage of Maximum Displacement

Lateral Floor Displacements, δ_{i2D}, and Story Drifts, Δ_{j2D}

$$\delta_{i2D} = 28 \times \begin{Bmatrix} 1.000 \\ -0.737 \\ -0.516 \end{Bmatrix} = \begin{Bmatrix} 28 \\ -21 \\ -14 \end{Bmatrix} mm$$

$$\Delta_{i2D} = \left\{ \begin{array}{c} 49 \\ -7 \\ -14 \end{array} \right\} mm$$

Lateral Inertia Forces, F_{i2}, Story Shears, V_{i2}, and Floor Accelerations, A_{i2}

$$F_{i2} = \left\{ \begin{array}{c} 1567 \times 1.0 \times \dfrac{0.528}{1098} \times 433 \\ 2900 \times (-0.737) \times \dfrac{0.528}{1098} \times 433 \\ 2900 \times (-0.516) \times \dfrac{0.528}{1098} \times 433 \end{array} \right\} = \left\{ \begin{array}{c} 326 \\ -445 \\ -312 \end{array} \right\} kN$$

$$A_{i2} = \dfrac{F_{i2}}{w_i} = \left\{ \begin{array}{c} \dfrac{326}{1567} \\ \dfrac{-445}{2900} \\ \dfrac{-312}{2900} \end{array} \right\} = \left\{ \begin{array}{c} 0.208 \\ -0.153 \\ -0.108 \end{array} \right\} g$$

$$V_{i2} = \left\{ \begin{array}{c} 326 \\ -119 \\ -431 \end{array} \right\} kN$$

Response at Stage of Maximum Velocity

Story Velocity
$$\nabla_{i2D} = \left(\dfrac{2\pi}{0.732} \right) \times \left\{ \begin{array}{c} 49 \\ -7 \\ -14 \end{array} \right\} = \left\{ \begin{array}{c} 421 \\ -60 \\ -120 \end{array} \right\} \dfrac{mm}{sec}$$

Forces in Damping Devices: $F_{di2} = 0.90 \times \left\{ \begin{array}{c} 421 \\ -60 \\ -120 \end{array} \right\} \times cos\,27.6 = \left\{ \begin{array}{c} 336 \\ -48 \\ -96 \end{array} \right\} kN$ (7-23)

396

Response at Stage of Maximum Acceleration

Force Coefficients

$$\beta_{V2} = 0.05 + 0.343 = 0.393$$

$$CF_1 = cos[tan^{-1} (2 \times 0.393)] = 0.786 \tag{4-41}$$

$$CF_2 = sin[tan^{-1} (2 \times 0.393)] = 0.618 \tag{4-39}$$

Maximum Floor Acceleration

$$A_{i2,max} = [0.786 + 2 \times 0.393 \times 0.618] \times \begin{Bmatrix} 0.208 \\ -0.154 \\ -0.107 \end{Bmatrix} = \begin{Bmatrix} 0.265 \\ -0.196 \\ -0.136 \end{Bmatrix} g \tag{4-40}$$

Maximum Story Shear

$$V_{i2,max} = CF_1 \cdot V_{i_2} \big|_{Max\,Disp} + CF_2 \cdot V_{i_2} \big|_{Max\,Velocity}$$

$$V_{i2\,max} = 0.786 \times \begin{Bmatrix} 326 \\ -119 \\ -431 \end{Bmatrix} + 0.618 \times \begin{Bmatrix} 298 \\ -43 \\ -85 \end{Bmatrix} = \begin{Bmatrix} 440 \\ -120 \\ -391 \end{Bmatrix} kN$$

THIRD MODE RESPONSE ($T_3 = 0.349$ sec $< T_s$)

Roof Displacement

Viscous Damping Ratio: $\beta_{v3} = 0.199$ (Table I-3)

Effective Damping Ratio: $\beta_{3D} = 0.199 + 0.05 = 0.249$

Damping Coefficient: $B_{3D} = 1.647$ (Table A13.3.1)

Roof Displacement: $D_{3D} = \left(\dfrac{9810}{4\pi^2} \right) \times 0.085 \times \dfrac{1.0}{1.647} \times 0.349^2 = 2mm$

Seismic Base Shear

Figure I-3(b) shows the design demand curve for $\beta_{3D} = 0.249$ and the spectral capacity curve of the second mode denoted by the straight line corresponding to period $T_3 = 0.349$ *sec*. The corresponding spectral acceleration is obtained at the intersection point as $S_a = 0.607$ *g*. Accordingly, the base shear is obtained from (2-2) as

$$V_3 = 0.607 \times 670 = 407\,kN$$

Response at Stage of Maximum Displacement

Lateral Floor Displacements, δ_{i3D}, and Story Drifts, Δ_{j3D}

$$\delta_{i3D} = 2 \times \begin{Bmatrix} 1.000 \\ -2.733 \\ 4.909 \end{Bmatrix} = \begin{Bmatrix} 2 \\ -5 \\ 10 \end{Bmatrix}\ mm$$

$$\Delta_{i3D} = \begin{Bmatrix} 7 \\ -15 \\ 10 \end{Bmatrix} mm$$

Lateral Inertia Forces, F_{i3}, Story Shears, V_{i3}, and Floor Accelerations, A_{i3}

$$F_{i3} = \begin{Bmatrix} 1567 \times 1.0 \times \dfrac{0.085}{670} \times 407 \\ 2900 \times (-2.733) \times \dfrac{0.085}{670} \times 407 \\ 2900 \times (4.909) \times \dfrac{0.085}{670} \times 407 \end{Bmatrix} = \begin{Bmatrix} 81 \\ -409 \\ 735 \end{Bmatrix} kN$$

$$A_{i3} = \dfrac{F_{i2}}{w_i} = \begin{Bmatrix} \dfrac{81}{1567} \\ \dfrac{-409}{2900} \\ \dfrac{735}{2900} \end{Bmatrix} = \begin{Bmatrix} 0.051 \\ -0.141 \\ 0.253 \end{Bmatrix} g$$

$$V_{i3} = \left\{ \begin{array}{c} 81 \\ -328 \\ 407 \end{array} \right\} kN$$

Response at Stage of Maximum Velocity

Story Velocity:
$$\nabla_{i3D} = \left(\frac{2\pi}{0.349}\right) \times \left\{ \begin{array}{c} 7 \\ -15 \\ 10 \end{array} \right\} = \left\{ \begin{array}{c} 126 \\ -270 \\ 180 \end{array} \right\} \frac{mm}{sec}$$

Forces in Damping Devices: $F_{di3} = 0.90 \times \left\{ \begin{array}{c} 126 \\ -270 \\ 180 \end{array} \right\} \times \cos 27.6 = \left\{ \begin{array}{c} 101 \\ -191 \\ 128 \end{array} \right\} kN$ (7-23)

Response at Stage of Maximum Acceleration

Force Coefficients

$$\beta_{V3} = 0.05 + 0.199 = 0.249$$

$$CF_1 = \cos[\tan^{-1}(2 \times 0.249)] = 0.895 \tag{4-41}$$

$$CF_2 = \sin[\tan^{-1}(2 \times 0.249)] = 0.446 \tag{4-39}$$

Maximum Floor Acceleration

$$A_{i3,max} = [0.895 + 2 \times 0.3249 \times 0.446] \times \left\{ \begin{array}{c} 0.051 \\ -0.141 \\ 0.253 \end{array} \right\} = \left\{ \begin{array}{c} 0.057 \\ -0.158 \\ 0.283 \end{array} \right\} g \tag{4-40}$$

Maximum Story Shear

$$V_{i3,max} = CF_1 \cdot V_{i_2}\big|_{Max\,Disp} + CF_2 \cdot V_{i_2}\big|_{Max\,Velocity}$$

$$V_{i3,max} = 0.895 \times \left\{ \begin{array}{c} 81 \\ -328 \\ -407 \end{array} \right\} + 0.446 \times \left\{ \begin{array}{c} 90 \\ -191 \\ 128 \end{array} \right\} = \left\{ \begin{array}{c} 112 \\ -379 \\ 421 \end{array} \right\} kN$$

TABLE I-1 Modal Properties and Modeling Information of Frame 3S-75 for Pushover Analysis in IDARC2D

Modal Properties (under elastic conditions)			
Quantity	Mode 1	Mode 2	Mode 3
T_m, sec	1.58	0.49	0.24
$\{\phi_{im}\}$	1.000 0.657 0.250	1.000 -0.560 -0.690	1.000 -1.618 2.096
$\overline{W_m}$, kN	5871	1098	398
Γ_m	1.399	-0.533	0.135

Lateral Force Distribution for Pushover			
Lateral Force Factor per Level	First Mode	Modal (C_{vx})	Uniform	Adaptive
λ_3 λ_2 λ_1	0.3733 0.4540 0.1727	0.4259 0.4250 0.1492	0.2127 0.3937 0.3937	Vary. Calculated by IDARC

Modeling Parameters for Time History Analysis				
Element	Section	M_p (kN-m)	ϕ_y	ϕ_u
Beam-3rd floor	W14x26	227	0.000310	0.015500
Beam-2^d floor	W16x45	411	0.000267	0.013400
Beam-1st floor	W16x50	465	0.000267	0.013400
Column	W14x109	1084	0.000294	0.014700

Table I-2 Base Shear-Roof Displacement and Story Shear-Story Drift Relationships of Frame of Example No.2 for First Mode Lateral Force Pattern

Pushover		Third Story		Second Story		First Story	
D_{roof} (mm)	Base Shear, V (kN)	Drift, Δ_3 (mm)	Shear, V_3 (kN)	Drift, Δ_2 (mm)	Shear, V_2 (kN)	Drift, Δ_1 (mm)	Shear, V_1 (kN)
0.0	0.0	0.0	0.0	0.0	0.0	0.0	0.0
0.7	4.4	0.2	1.7	0.3	3.7	0.2	4.4
1.3	8.8	0.5	3.3	0.5	7.4	0.3	8.8
2.0	13.3	0.7	5.0	0.8	11.0	0.5	13.3
2.6	17.7	0.9	6.6	1.1	14.7	0.7	17.7
3.3	22.1	1.1	8.3	1.3	18.4	0.8	22.1
3.9	26.5	1.4	10.0	1.6	22.1	1.0	26.5
4.6	30.9	1.6	11.6	1.9	25.7	1.1	30.9
5.3	35.4	1.8	13.3	2.1	29.4	1.3	35.4
5.9	39.8	2.0	14.9	2.4	33.1	1.5	39.8
6.6	44.2	2.3	16.6	2.7	36.8	1.6	44.2
7.2	48.6	2.5	18.3	2.9	40.5	1.8	48.6
7.9	53.0	2.7	19.9	3.2	44.1	2.0	53.0
8.5	57.5	2.9	21.6	3.5	47.8	2.1	57.5
9.2	62.6	3.2	23.2	3.7	51.5	2.3	62.6
9.9	67.0	3.4	24.9	4.0	55.2	2.5	67.0
10.5	71.5	3.6	26.6	4.3	58.9	2.6	71.5
11.2	75.9	3.8	28.2	4.5	62.5	2.8	75.9
11.8	80.3	4.1	29.9	4.8	66.2	3.0	80.3
12.5	84.7	4.3	31.5	5.1	69.9	3.1	84.7
13.1	89.1	4.5	33.2	5.3	73.6	3.3	89.1
13.8	93.6	4.7	34.9	5.6	77.2	3.4	93.6
14.5	98.0	5.0	36.5	5.9	80.9	3.6	98.0
15.1	102.4	5.2	38.2	6.1	84.6	3.8	102.4
.....		.....	.....	.....	.....	.....	.....
.....	200	.....	.....	.....	.....	.....	.....
200	1156	69	432	82	956	48	1156
.....		.....	.....	.....	.....	.....	.....
.....		.....	.....	.....	.....	.....	.....
244	1223	84	455	99	1008	57	1223
.....		.....	.....	.....	.....	.....	.....
.....		.....	.....	.....	.....	.....	.....
419	1241	146	463	160	1026	113	1241
.....		.....	.....	.....	.....	.....	.....
.....		.....	.....	.....	.....	.....	.....
474	1245	165	465	179	1030	130	1245
532	1249	185	466	199	1034	148	1249
593	1254	206	468	220	1037	168	1254
656	1258	227	470	241	1041	187	1258

TABLE I-3 Modal Properties of Example Frame at Various Stages of Pushover Analysis for First Mode Lateral Force Pattern.

| Assumed Roof Disp. mm	Effective Modal Quantities	Shear Building Model			Modified Model of Frame		
		Mode 1 $m=1$	Mode 2 $m=2$	Mode 3 $m=3$	Mode 1 $m=1$	Mode 2 $m=2$	Mode 3 $m=3$
200	T_m, sec	1.656	0.764	0.500	1.657	0.600	0.289
	$\{\phi_{im}\}$	1.000	1.000	1.000	1.000	1.000	1.000
		0.630	-0.738	-3.063	0.612	-0.677	-2.269
		0.195	-0.393	7.230	0.222	-0.538	3.827
	$\overline{W}_m, kN$	5524	813	1030	5707	1029	631
	Γ_m	1.400	-0.477	0.076	1.425	-0.524	0.103
	β_v	0.118	0.386	0.267	0.115	0.276	0.169
244	$T_m\ (sec)$	1.807	0.833	0.553	1.808	0.732	0.349
	$\{\phi_{im}\}$	1.000	1.000	1.000	1.000	1.000	1.000
		0.638	-0.704	-2.875	0.574	-0.737	-2.733
		0.216	-0.429	6.051	0.210	-0.516	4.909
	$\overline{W}_m, kN$	5655	832	879	5599	1098	670
	Γ_m	1.403	-0.486	0.082	1.449	-0.528	0.085
	β_v	0.123	0.411	0.304	0.135	0.343	0.199
419	T_m, sec	2.395	1.106	0.742	2.397	1.021	0.523
	$\{\phi_{im}\}$	1.000	1.000	1.000	1.000	1.000	1.000
		0.656	-0.612	-2.578	0.608	-0.668	-2.850
		0.274	-0.505	4.185	0.248	-0.503	4.829
	$\overline{W}_m, kN$	6000	825	542	5852	936	579
	Γ_m	1.406	-0.493	0.087	1.437	-0.509	0.079
	β_v	0.148	0.515	0.434	0.162	0.479	0.302

TABLE I-4 Modal Response Calculations for Example No.2: 3-Story Frame (V$_{min}$=0.75V) with Linear Viscous Damping System Using Method 2 (FEMA, 1997) for First Mode Lateral Force Pattern. Analysis for the DBE

Quantity	Units	Mode 1 (m=1)	Mode 2 (m=2)	Mode 3 (m=3)	SRSS
1. Elastic Response					
Damping Ratio, β_{Ve}		0.100	0.343	0.199	
Total Damping Ratio, β_{V+I}		0.150	0.393	0.249	
Damping Coefficient, B_m		1.350	2.079	1.647	
Elastic Displacement, D_{em}	mm	244	28	2	
2. Roof Displacement and Base Shear					
Assumed Displacement, D_{ID}	mm	244	28	2	
Effective Period, T_{eff}	sec	1.808	0.732	0.349	
Eff. Viscous Damping Ratio, β_V		0.135	0.393	0.249	
Hysteretic Damping, β_H		0.075	0	0	
Effective Damping, βm		0.260	0.393	0.249	
Damping Coefficient, B_m		1.680	2.079	1.647	
Displacement, D_{mD}	mm	233			
Corrected Displacement, D_{mD}	mm	244	28	2	
Spectral Acceleration	g	0.220	0.394	0.607	
Base Shear , V_m	kN	1232	433	407	1368

3. Response at Stage of Maximum Displacement					
Lateral Floor Displacement, δ_{ij}	mm	244 / 140 / 51	28 / -21 / -14	2 / -5 / 10	
Story Drift, Δ_{jm}	mm	104 / 89 / 51	49 / -7 / -14	7 / -15 / 10	115 / 91 / 54
Lateral Inertia Forces, F_{im}	kN	500 / 531 / 194	326 / -445 / -312	81 / -409 / 735	
Floor Acceleration, A_{im}	g	0.319 / 0.183 / 0.067	0.208 / -0.153 / -0.108	0.051 / -0.141 / 0.253	0.384 / 0.277 / 0.283
Story Shear Forces, V_{jm}	kN	500 / 1031 / 1225	326 / -119 / -431	81 / -328 / 407	602 / 1088 / 1361

TABLE I-4 continued

4. Response at Stage of Maximum Velocity					
Story Velocity, V_{im}	mm/sec	361	421	126	569
		309	-60	-270	415
		177	-120	180	280
Force in Damping Devices, Fd_{jm}	kN	287	336	101	453
		246	-48	-191	315
		141	-96	128	213
Horizontal Damper Force, Vd_{jm}	kN	254	298	90	
		218	-43	-169	
		125	-85	113	

5. Response at Stage of Maximum Acceleration					
Ductility, μ		1.33	1	1	
Eff. Viscous Damping Ratio, β_V		0.185	0.393	0.249	
Parameter δ		0.354	0.666	0.462	
Coefficient CF_1		0.938	0.786	0.895	
Product $CF_1 . \mu$		1.260	0.786	0.895	
Force Coefficient, CF_1 or C_{mFD}		1.000	0.786	0.895	
Force Coefficient, CF_2 or C_{mFV}		0.347	0.618	0.446	
Max.Floor Acc., $A_{im,max}$	(g)	0.360	0.265	0.057	0.451
		0.206	-0.196	-0.158	0.325
		0.076	-0.136	0.283	0.323
Maximum Story Shear, $V_{jm,max}$ (actual)	kN	588	440	112	743
		1107	-120	-379	1176
		1268	-391	421	1392
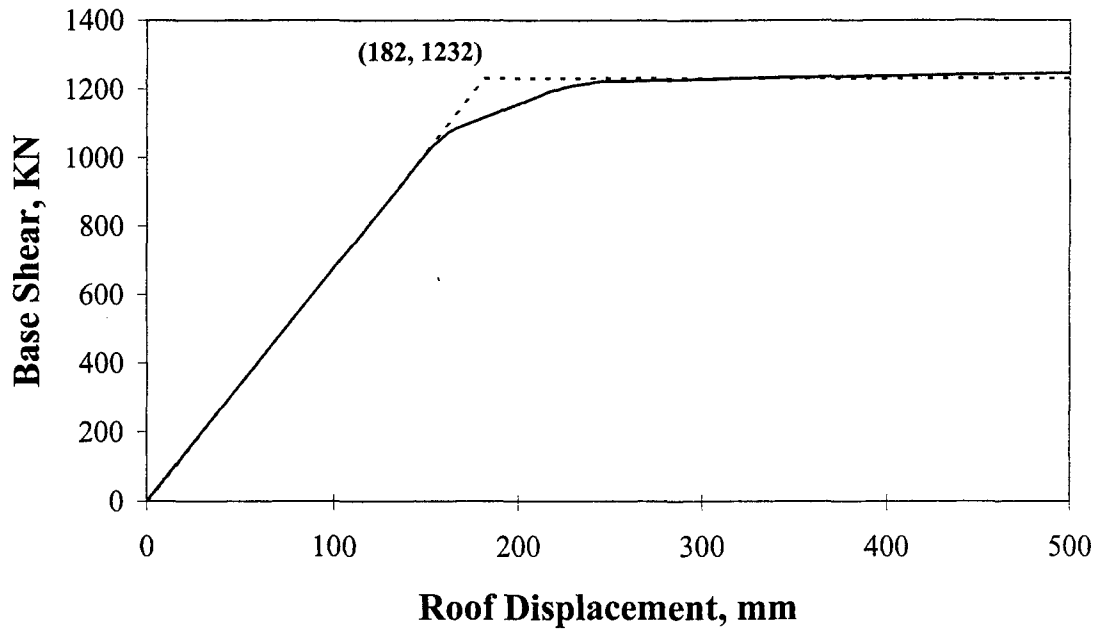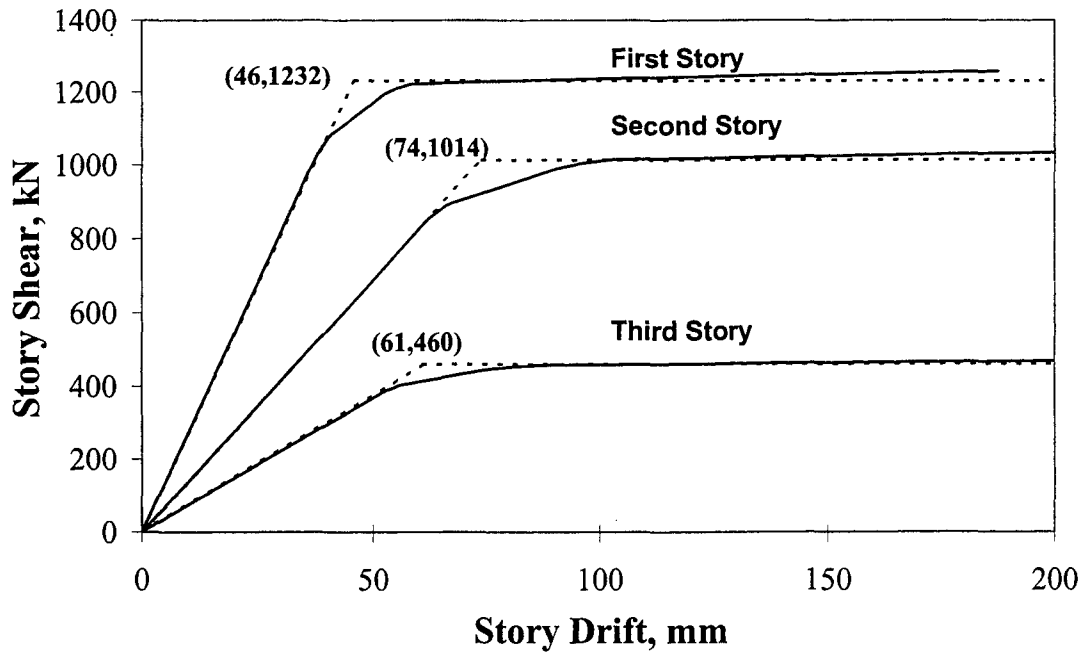
FIGURE I-1 Pushover Curve and Story Shear-Story Drift Relationships
of Frame 3S-75 for First Mode Lateral Force Pattern

405

[All Elements are Rectangular Steel Sections]
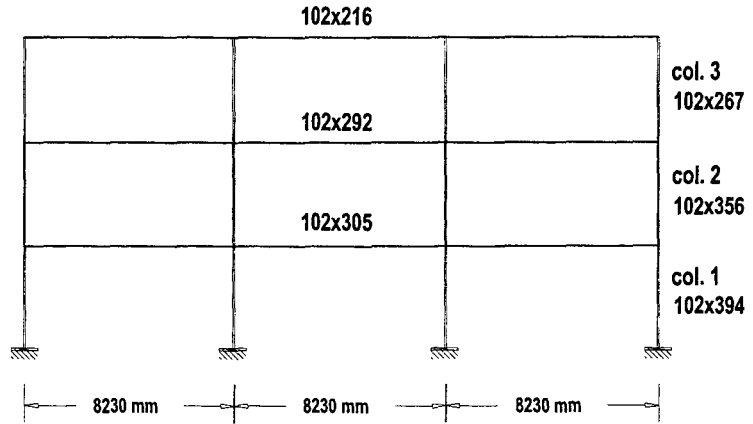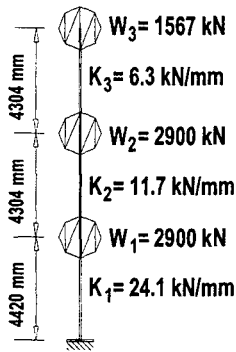
(a) at assumed roof displacement D_{roof}= 200 mm
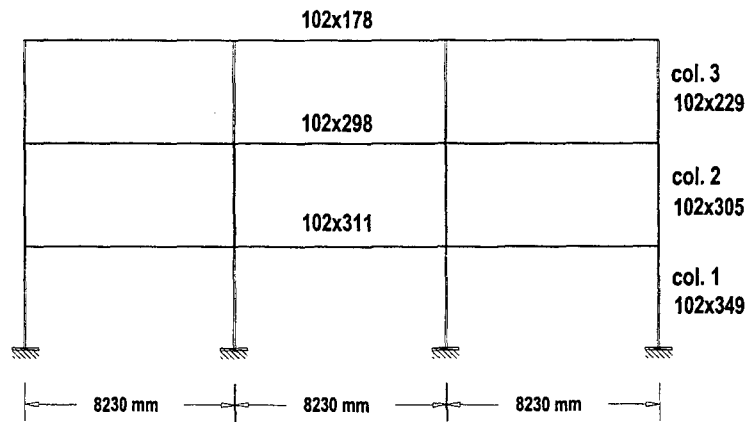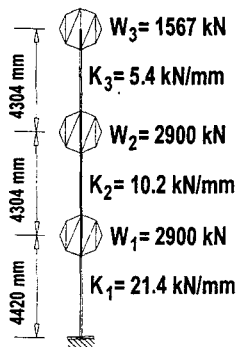
(b) at assumed roof displacement D_{roof}= 244 mm
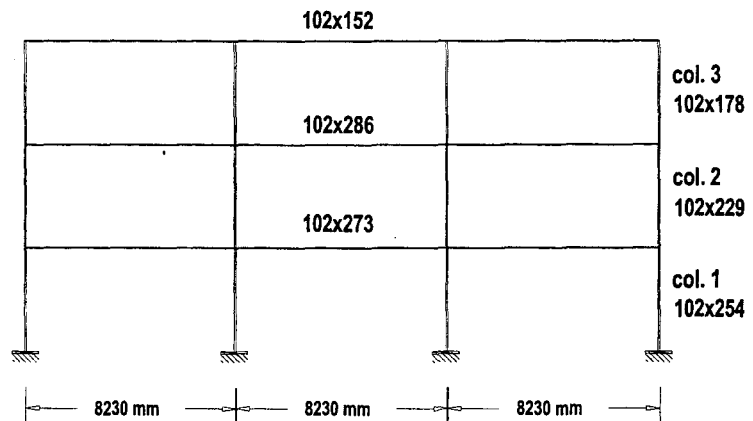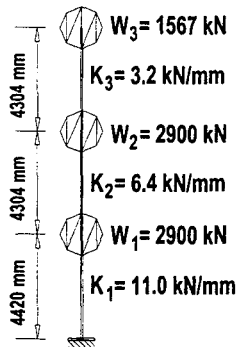
(c) at assumed roof displacement D_{roof}= 419 mm

**FIGURE I-2 Shear Building and Modified Model Representations of Frame 3S-75
for Eigenvalue Analysis at Different Values of Assumed Roof Displacement**

406
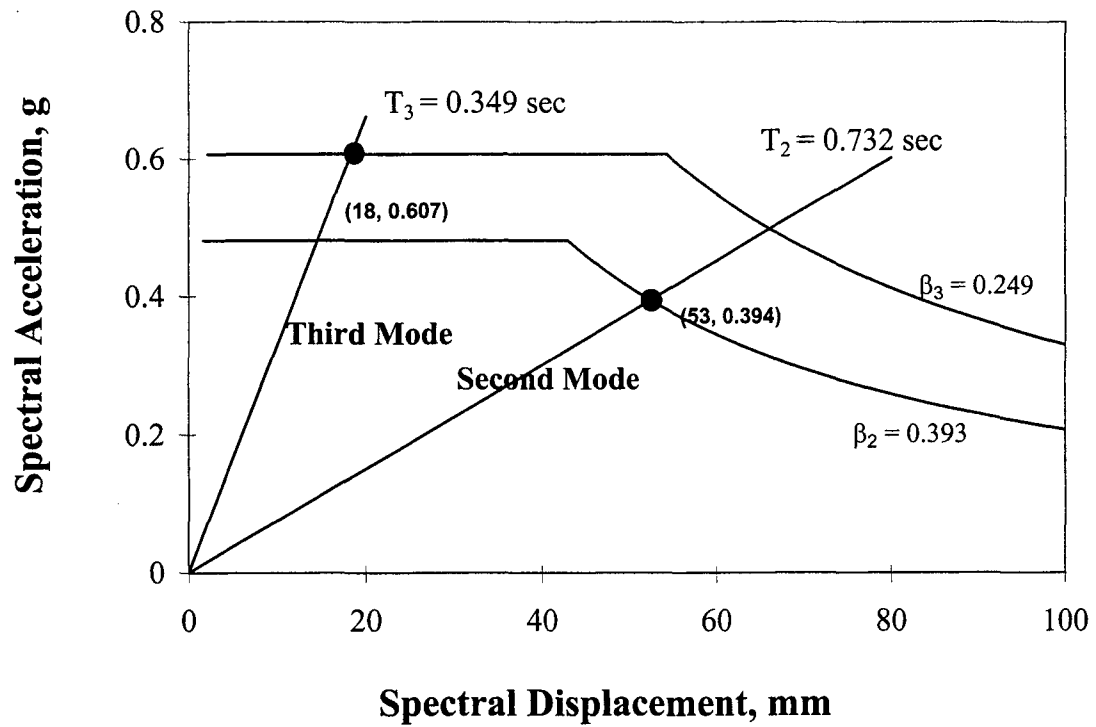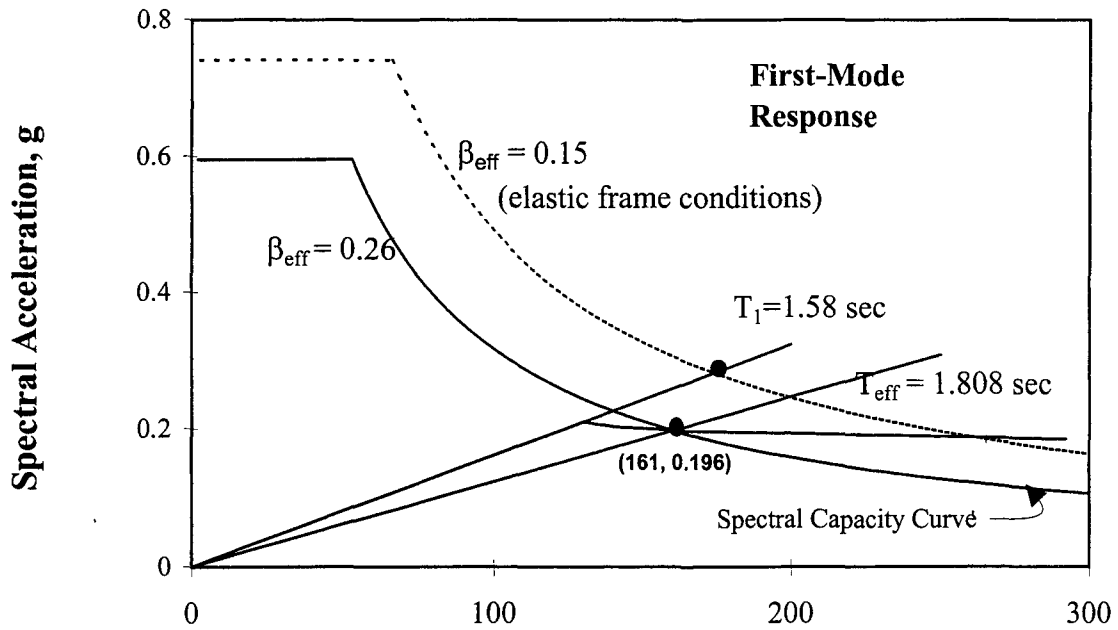
FIGURE I-3 Determination of Modal Spectral Response of
Frame 3S-75 Using Method 2 (FEMA.1997)

407

APPENDIX J

INPUT FILES FOR EIGENVALUE AND PUSHOVER ANALYSIS OF FRAMES WITH DAMPING SYSTEMS IN PROGRAM SAP2000-NL

J.1 Introduction

This appendix contains information on the input files for the eigenvalue and pushover analysis of selected examples of frames with damping systems in program SAP2000-NL Version 7.11. The input files of the following examples are presented:

(a)   3-story special steel moment frame designed to meet NEHRP (1997) criteria without a damping system.

(b)   Example No.2: frame 3S-75 with linear viscous damping system to provide 10% viscous damping ratio when assuming elastic frame behavior (Fig. 8-2).

(c)   Example No.5: frame 6S-75 with linear viscous damping system to provide 10% viscous damping ratio when assuming elastic frame behavior (Fig. 8-5).

(d)   Example No.8: frame 3S-75 with viscoelastic solid damping system to provide 8.5% viscous damping ratio when assuming elastic frame behavior (Fig. 8-8).

(e)   Example No.9: frame 3S-75 with metallic yielding damping system (Fig. 8-9).

Input files for the pushover analysis of the frames for three lateral force patterns are presented: (a) proportional to the first mode, (b) modal (Cvx) pattern, and (c) uniform pattern.

SAP2000-NL VERSION 7.11 INPUT FILE FOR EIGENVALUE AND PUSHOVER ANALYSIS OF 3-STORY SPECIAL STELL MOMENT FRAME DESIGNED TO MEET NEHRP (1997) CRITERIA WITHOUT A DAMPING SYSTEM

SYSTEM
 DOF=UX,UZ,RY LENGTH=IN FORCE=Kip PAGE=SECTIONS

JOINT
 17 X=-486 Y=0 Z=0
 18 X=-486 Y=0 Z=174
 19 X=-486 Y=0 Z=343.44
 20 X=-486 Y=0 Z=512.88
 21 X=-162 Y=0 Z=512.88
 22 X=162 Y=0 Z=512.88
 23 X=486 Y=0 Z=512.88
 24 X=486 Y=0 Z=343.44
 25 X=486 Y=0 Z=174
 26 X=486 Y=0 Z=0
 27 X=-162 Y=0 Z=343.44
 28 X=162 Y=0 Z=343.44
 29 X=-162 Y=0 Z=174
 30 X=162 Y=0 Z=174
 33 X=162 Y=0 Z=0
 34 X=-162 Y=0 Z=0

RESTRAINT
 ADD=17 DOF=U1,U2,U3,R1,R2,R3
 ADD=26 DOF=U1,U2,U3,R1,R2,R3
 ADD=33 DOF=U1,U2,U3,R1,R2,R3
 ADD=34 DOF=U1,U2,U3,R1,R2,R3

PATTERN
 NAME=DEFAULT

MASS
 ADD=20 U1=.222
 ADD=21 U1=.222
 ADD=22 U1=.222
 ADD=23 U1=.222
 ADD=18 U1=.41133
 ADD=19 U1=.4121
 ADD=24 U1=.4121
 ADD=25 U1=.41133
 ADD=27 U1=.4121
 ADD=28 U1=.4121
 ADD=29 U1=.41133
 ADD=30 U1=.41133

MATERIAL
 NAME=STEEL IDES=S M=7.324E-07 W=.000283
  T=0 E=29000 U=.3 A=.0000065 FY=50
 NAME=CONC IDES=C M=2.246377E-07 W=.0000868
  T=0 E=3600 U=.2 A=.0000055
 NAME=OTHER IDES=N M=2.246377E-07 W=.0000868
  T=0 E=3600 U=.2 A=.0000055

FRAME SECTION

NAME=W14X211 MAT=STEEL A=62 J=44.6 I=2660,1030 AS=15.406,41.08 S=338.4224,130.3797
Z=390,198 R=6.550056,4.075893 T=15.72,15.8,1.56,.98,15.8,1.56 SHN=W14X211 DSG=W

NAME=W18X46 MAT=STEEL A=13.5 J=1.22 I=712,22.5 AS=6.5016,6.1105 S=78.84829,7.425743
Z=90.7,11.7 R=7.262282,1.290994 T=18.06,6.06,.605,.36,6.06,.605 SHN=W18X46 DSG=W

NAME=W21X50 MAT=STEEL A=14.7 J=1.14 I=984,24.9 AS=7.9154,5.8226 S=94.47912,7.626339
Z=110,12.2 R=8.181612,1.301491 T=20.83,6.53,.535,.38,6.53,.535 SHN=W21X50 DSG=W

NAME=W24X62 MAT=STEEL A=18.2 J=1.71 I=1550,34.5 AS=10.208,6.9227 S=130.5813,9.801136
Z=153,15.7 R=9.228479,1.376809 T=23.74,7.04,.59,.43,7.04,.59 SHN=W24X62 DSG=W

FRAME
 22 J=17,18 SEC=W14X211 NSEG=2 ANG=0 IOFF=14 JOFF=12 RIGID=1
 23 J=18,19 SEC=W14X211 NSEG=2 ANG=0 IOFF=12 JOFF=10.5 RIGID=1
 24 J=19,20 SEC=W14X211 NSEG=2 ANG=0 IOFF=10.5 JOFF=9 RIGID=1
 25 J=20,21 SEC=W18X46 NSEG=4 ANG=0 IOFF=7 JOFF=7 RIGID=1
 26 J=21,22 SEC=W18X46 NSEG=4 ANG=0 IOFF=7 JOFF=7 RIGID=1
 27 J=22,23 SEC=W18X46 NSEG=4 ANG=0 IOFF=7 JOFF=7 RIGID=1
 28 J=23,24 SEC=W14X211 NSEG=2 ANG=0 IOFF=10.5 JOFF=9 RIGID=1
 29 J=24,25 SEC=W14X211 NSEG=2 ANG=0 IOFF=12 JOFF=10.5 RIGID=1
 30 J=25,26 SEC=W14X211 NSEG=2 ANG=0 IOFF=14 JOFF=12 RIGID=1
 31 J=19,27 SEC=W21X50 NSEG=4 ANG=0 IOFF=7 JOFF=7 RIGID=1
 32 J=27,28 SEC=W21X50 NSEG=4 ANG=0 IOFF=7 JOFF=7 RIGID=1
 33 J=28,24 SEC=W21X50 NSEG=4 ANG=0 IOFF=7 JOFF=7 RIGID=1
 34 J=18,29 SEC=W24X62 NSEG=4 ANG=0 IOFF=7 JOFF=7 RIGID=1
 35 J=29,30 SEC=W24X62 NSEG=4 ANG=0 IOFF=7 JOFF=7 RIGID=1
 36 J=30,25 SEC=W24X62 NSEG=4 ANG=0 IOFF=7 JOFF=7 RIGID=1
 38 J=33,30 SEC=W14X211 NSEG=2 ANG=0 IOFF=14 JOFF=12 RIGID=1
 39 J=30,28 SEC=W14X211 NSEG=2 ANG=0 IOFF=12 JOFF=10.5 RIGID=1
 40 J=28,22 SEC=W14X211 NSEG=2 ANG=0 IOFF=10.5 JOFF=9 RIGID=1
 41 J=34,29 SEC=W14X211 NSEG=2 ANG=0 IOFF=14 JOFF=12 RIGID=1
 42 J=29,27 SEC=W14X211 NSEG=2 ANG=0 IOFF=12 JOFF=10.5 RIGID=1
 43 J=27,21 SEC=W14X211 NSEG=2 ANG=0 IOFF=10.5 JOFF=9 RIGID=1

LOAD
 NAME=CVX
  TYPE=FORCE
   ADD=20 UX=.3942
   ADD=19 UX=.4301
   ADD=18 UX=.1757
 NAME=UNIFORM
  TYPE=FORCE
   ADD=20 UX=.2128
   ADD=19 UX=.3936
   ADD=18 UX=.3936
 NAME=NEHRPSTR
  TYPE=FORCE
   ADD=20 UX=49.4
   ADD=19 UX=55.8
   ADD=18 UX=24.2

411

```
NAME=GAVITY
 TYPE=DISTRIBUTED SPAN
   ADD=25 RD=0,1 UZ=-1,-1
   ADD=26 RD=0,1 UZ=-1,-1
   ADD=27 RD=0,1 UZ=-1,-1
   ADD=31 RD=0,1 UZ=-1,-1
   ADD=32 RD=0,1 UZ=-1,-1
   ADD=33 RD=0,1 UZ=-1,-1
   ADD=34 RD=0,1 UZ=-1,-1
   ADD=35 RD=0,1 UZ=-1,-1
   ADD=36 RD=0,1 UZ=-1,-1
NAME=NEHRPDRF
 TYPE=FORCE
   ADD=20 UX=45.2
   ADD=19 UX=50
   ADD=18 UX=20.9

MODE
 TYPE=EIGEN N=3 TOL=.00001

OUTPUT
; No Output Requested

END

; The following data is used for graphics, design and pushover analysis.
; If changes are made to the analysis data above, then the following data
; should be checked for consistency.
SAP2000 V7.11 SUPPLEMENTAL DATA
 GRID GLOBAL X "1" -486
 GRID GLOBAL X "2" -162
 GRID GLOBAL X "3" 162
 GRID GLOBAL X "4" 486
 GRID GLOBAL Y "5" 0
 GRID GLOBAL Z "6" 0
 GRID GLOBAL Z "7" 174
 GRID GLOBAL Z "8" 343.44
 GRID GLOBAL Z "9" 512.88
 MATERIAL STEEL FY 50
 MATERIAL CONC FYREBAR 60 FYSHEAR 40 FC 4 FCSHEAR 4
 FRAMESECTION FS1 NAME W21X62-A
 STATICLOAD CVX TYPE DEAD
 STATICLOAD UNIFORM TYPE DEAD
 STATICLOAD NEHRPSTR TYPE DEAD
 STATICLOAD GAVITY TYPE DEAD
 STATICLOAD NEHRPDRF TYPE DEAD
 PUSHCASE "PUSHM1" CONTROL DISP TARGET 20 JOINT 20 DOF U1
 PUSHCASE "PUSHM1" PDELTA NO
 PUSHCASE "PUSHM1" MINSTEPS 20 MAXNULLSTEPS 10 MAXTOTALSTEPS 220 MAXITER
10
 PUSHCASE "PUSHM1" ITERTOL .0001 EVENTTOL .01
 PUSHCASE "PUSHM1" LOADTYPE MODE NUMBER 1 SCALEFACTOR 1
 HINGE "USER" TYPE M3 SYMMETRIC
 HINGE "USER" TYPE M3 B 1 1 C 50 1 D 50 .2 E 80 .2
 HINGE "USER" TYPE M3 IO 2 LS 4 CP 6
 FRAMEHINGE 22 HINGE "USER" RDISTANCE .0805
```

```
FRAMEHINGE 22  HINGE "USER"  RDISTANCE .9224
FRAMEHINGE 23  HINGE "USER"  RDISTANCE .0797
FRAMEHINGE 23  HINGE "USER"  RDISTANCE .9292
FRAMEHINGE 24  HINGE "USER"  RDISTANCE .0708
FRAMEHINGE 24  HINGE "USER"  RDISTANCE .938
FRAMEHINGE 25  HINGE "USER"  RDISTANCE .03086
FRAMEHINGE 25  HINGE "USER"  RDISTANCE .969
FRAMEHINGE 26  HINGE "USER"  RDISTANCE .03086
FRAMEHINGE 26  HINGE "USER"  RDISTANCE .969
FRAMEHINGE 27  HINGE "USER"  RDISTANCE .03086
FRAMEHINGE 27  HINGE "USER"  RDISTANCE .969
FRAMEHINGE 28  HINGE "USER"  RDISTANCE .0708
FRAMEHINGE 28  HINGE "USER"  RDISTANCE .938
FRAMEHINGE 29  HINGE "USER"  RDISTANCE .0797
FRAMEHINGE 29  HINGE "USER"  RDISTANCE .9292
FRAMEHINGE 30  HINGE "USER"  RDISTANCE .0805
FRAMEHINGE 30  HINGE "USER"  RDISTANCE .9224
FRAMEHINGE 31  HINGE "USER"  RDISTANCE .03086
FRAMEHINGE 31  HINGE "USER"  RDISTANCE .969
FRAMEHINGE 32  HINGE "USER"  RDISTANCE .03086
FRAMEHINGE 32  HINGE "USER"  RDISTANCE .969
FRAMEHINGE 33  HINGE "USER"  RDISTANCE .03086
FRAMEHINGE 33  HINGE "USER"  RDISTANCE .969
FRAMEHINGE 34  HINGE "USER"  RDISTANCE .03086
FRAMEHINGE 34  HINGE "USER"  RDISTANCE .969
FRAMEHINGE 35  HINGE "USER"  RDISTANCE .03086
FRAMEHINGE 35  HINGE "USER"  RDISTANCE .969
FRAMEHINGE 36  HINGE "USER"  RDISTANCE .03086
FRAMEHINGE 36  HINGE "USER"  RDISTANCE .969
FRAMEHINGE 38  HINGE "USER"  RDISTANCE .0805
FRAMEHINGE 38  HINGE "USER"  RDISTANCE .9224
FRAMEHINGE 39  HINGE "USER"  RDISTANCE .0797
FRAMEHINGE 39  HINGE "USER"  RDISTANCE .9292
FRAMEHINGE 40  HINGE "USER"  RDISTANCE .0708
FRAMEHINGE 40  HINGE "USER"  RDISTANCE .938
FRAMEHINGE 41  HINGE "USER"  RDISTANCE .0805
FRAMEHINGE 41  HINGE "USER"  RDISTANCE .9224
FRAMEHINGE 42  HINGE "USER"  RDISTANCE .0797
FRAMEHINGE 42  HINGE "USER"  RDISTANCE .9292
FRAMEHINGE 43  HINGE "USER"  RDISTANCE .0708
FRAMEHINGE 43  HINGE "USER"  RDISTANCE .938
END SUPPLEMENTAL DATA
```

SYSTEM
 DOF=UX,UZ,RY LENGTH=IN FORCE=Kip PAGE=SECTIONS

JOINT
 17 X=-486 Y=0 Z=0
 18 X=-486 Y=0 Z=174
 19 X=-486 Y=0 Z=343.44
 20 X=-486 Y=0 Z=512.88
 21 X=-162 Y=0 Z=512.88
 22 X=162 Y=0 Z=512.88
 23 X=486 Y=0 Z=512.88
 24 X=486 Y=0 Z=343.44
 25 X=486 Y=0 Z=174
 26 X=486 Y=0 Z=0
 27 X=-162 Y=0 Z=343.44
 28 X=162 Y=0 Z=343.44
 29 X=-162 Y=0 Z=174
 30 X=162 Y=0 Z=174
 33 X=162 Y=0 Z=0
 34 X=-162 Y=0 Z=0

RESTRAINT
 ADD=17 DOF=U1,U2,U3,R1,R2,R3
 ADD=26 DOF=U1,U2,U3,R1,R2,R3
 ADD=33 DOF=U1,U2,U3,R1,R2,R3
 ADD=34 DOF=U1,U2,U3,R1,R2,R3

PATTERN
 NAME=DEFAULT

MASS
 ADD=20 U1=.228238
 ADD=21 U1=.228238
 ADD=22 U1=.228238
 ADD=23 U1=.228238
 ADD=18 U1=.4224093
 ADD=19 U1=.4224093
 ADD=24 U1=.4224093
 ADD=25 U1=.4224093
 ADD=27 U1=.4224093
 ADD=28 U1=.4224093
 ADD=29 U1=.4224093
 ADD=30 U1=.4224093

MATERIAL
 NAME=STEEL IDES=S M=7.324E-07 W=.000283
  T=0 E=29000 U=.3 A=.0000065 FY=50
 NAME=CONC IDES=C M=2.246377E-07 W=.0000868
  T=0 E=3600 U=.2 A=.0000055

NAME=OTHER IDES=N M=2.246377E-07 W=.0000868
 T=0 E=3600 U=.2 A=.0000055

FRAME SECTION
 NAME=W14X109 MAT=STEEL A=32 J=7.12 I=1240,447 AS=7.518,20.934 S=173.1844,61.21191
Z=192,92.7 R=6.22495,3.737479 T=14.32,14.605,.86,.525,14.605,.86 SHN=W14X109 DSG=W
 NAME=W16X40 MAT=STEEL A=11.8 J=.79 I=518,28.9 AS=4.8831,5.8875 S=64.70956,8.263045
Z=72.9,12.7 R=6.625579,1.564977 T=16.01,6.995,.505,.305,6.995,.505 SHN=W16X40 DSG=W
 NAME=W16X45 MAT=STEEL A=13.3 J=1.11 I=586,32.8 AS=5.5649,6.6246 S=72.65965,9.324804
Z=82.3,14.5 R=6.637782,1.570403 T=16.13,7.035,.565,.345,7.035,.565 SHN=W16X45 DSG=W
  NAME=W14X26 MAT=STEEL A=7.69 J=.36 I=245,8.91 AS=3.5471,3.5175 S=35.22646,3.546268
Z=40.2,5.54 R=5.644427,1.076405 T=13.91,5.025,.42,.255,5.025,.42 SHN=W14X26 DSG=W

FRAME
 1 J=18,29 SEC=W16X45 NSEG=4 ANG=0 IOFF=10 JOFF=10 RIGID=1
 2 J=29,30 SEC=W16X45 NSEG=4 ANG=0 IOFF=10 JOFF=10 RIGID=1
 3 J=30,25 SEC=W16X45 NSEG=4 ANG=0 IOFF=10 JOFF=10 RIGID=1
 4 J=19,27 SEC=W16X40 NSEG=4 ANG=0 IOFF=10 JOFF=10 RIGID=1
 5 J=27,28 SEC=W16X40 NSEG=4 ANG=0 IOFF=10 JOFF=10 RIGID=1
 6 J=28,24 SEC=W16X40 NSEG=4 ANG=0 IOFF=10 JOFF=10 RIGID=1
 7 J=20,21 SEC=W14X26 NSEG=4 ANG=0 IOFF=10 JOFF=10 RIGID=1
 8 J=21,22 SEC=W14X26 NSEG=4 ANG=0 IOFF=10 JOFF=10 RIGID=1
 9 J=22,23 SEC=W14X26 NSEG=4 ANG=0 IOFF=10 JOFF=10 RIGID=1
 22 J=17,18 SEC=W14X109 NSEG=2 ANG=0 IOFF=18 JOFF=10 RIGID=1
 23 J=18,19 SEC=W14X109 NSEG=2 ANG=0 IOFF=10 JOFF=10 RIGID=1
 24 J=19,20 SEC=W14X109 NSEG=2 ANG=0 IOFF=10 JOFF=9 RIGID=1
 28 J=23,24 SEC=W14X109 NSEG=2 ANG=0 IOFF=10 JOFF=9 RIGID=1
 29 J=24,25 SEC=W14X109 NSEG=2 ANG=0 IOFF=10 JOFF=10 RIGID=1
 30 J=25,26 SEC=W14X109 NSEG=2 ANG=0 IOFF=18 JOFF=10 RIGID=1
 38 J=33,30 SEC=W14X109 NSEG=2 ANG=0 IOFF=18 JOFF=10 RIGID=1
 39 J=30,28 SEC=W14X109 NSEG=2 ANG=0 IOFF=10 JOFF=10 RIGID=1
 40 J=28,22 SEC=W14X109 NSEG=2 ANG=0 IOFF=10 JOFF=9 RIGID=1
 41 J=34,29 SEC=W14X109 NSEG=2 ANG=0 IOFF=18 JOFF=10 RIGID=1
 42 J=29,27 SEC=W14X109 NSEG=2 ANG=0 IOFF=10 JOFF=10 RIGID=1
 43 J=27,21 SEC=W14X109 NSEG=2 ANG=0 IOFF=10 JOFF=9 RIGID=1

LOAD
 NAME=CVX
  TYPE=FORCE
   ADD=20 UX=.4576
   ADD=19 UX=.417
   ADD=18 UX=.1255
 NAME=NEHRP
  TYPE=FORCE
   ADD=20 UX=37.79
   ADD=19 UX=32.46
   ADD=18 UX=8.84
 NAME=GRAVITY
  TYPE=DISTRIBUTED SPAN
   ADD=7 RD=0,1 UZ=-.06,-.06
   ADD=8 RD=0,1 UZ=-.06,-.06
   ADD=9 RD=0,1 UZ=-.06,-.06
   ADD=1 RD=0,1 UZ=-.13,-.13
   ADD=2 RD=0,1 UZ=-.13,-.13
   ADD=3 RD=0,1 UZ=-.13,-.13
   ADD=4 RD=0,1 UZ=-.13,-.13

415

```
    ADD=5  RD=0,1  UZ=-.13,-.13
    ADD=6  RD=0,1  UZ=-.13,-.13
 NAME=1STMODE
  TYPE=FORCE
    ADD=20  UX=125.1
    ADD=19  UX=156.6
    ADD=18  UX=63.6
 NAME=RMODE
  TYPE=FORCE
    ADD=20  UX=93.9
    ADD=19  UX=-27
    ADD=18  UX=-275.7
 NAME=DEAD
 NAME=LIVE
 NAME=1MODDBE
  TYPE=FORCE
    ADD=20  UX=41.7
    ADD=19  UX=52.2
    ADD=18  UX=21.2
 NAME=RMODBE
  TYPE=FORCE
    ADD=20  UX=31.3
    ADD=19  UX=-9
    ADD=18  UX=-91.9
 NAME=DDLL
 NAME=UNIFORM
  TYPE=FORCE
    ADD=20  UX=.2127
    ADD=19  UX=.39365
    ADD=18  UX=.39365

MODE
 TYPE=EIGEN  N=3  TOL=.00001

COMBO
 NAME=DSTL1
  LOAD=CVX  SF=1
  LOAD=NEHRP  SF=1
  LOAD=GRAVITY  SF=1
  LOAD=1STMODE  SF=1
  LOAD=RMODE  SF=1
  LOAD=DEAD  SF=1
  LOAD=1MODDBE  SF=1
  LOAD=RMODBE  SF=1
  LOAD=DDLL  SF=1
  LOAD=UNIFORM  SF=1
 NAME=DSTL2
  LOAD=CVX  SF=1
  LOAD=NEHRP  SF=1
  LOAD=GRAVITY  SF=1
  LOAD=1STMODE  SF=1
  LOAD=RMODE  SF=1
  LOAD=DEAD  SF=1
  LOAD=LIVE  SF=1
  LOAD=1MODDBE  SF=1
  LOAD=RMODBE  SF=1
```

```
    LOAD=DDLL  SF=1
    LOAD=UNIFORM  SF=1

OUTPUT
; No Output Requested

END

; The following data is used for graphics, design and pushover analysis.
; If changes are made to the analysis data above, then the following data
; should be checked for consistency.
SAP2000 V7.11 SUPPLEMENTAL DATA
  GRID GLOBAL  X "1"  -486
  GRID GLOBAL  X "2"  -162
  GRID GLOBAL  X "3"  162
  GRID GLOBAL  X "4"  486
  GRID GLOBAL  Y "5"  0
  GRID GLOBAL  Z "6"  0
  GRID GLOBAL  Z "7"  174
  GRID GLOBAL  Z "8"  343.44
  GRID GLOBAL  Z "9"  512.88
  MATERIAL STEEL FY 50
  MATERIAL CONC FYREBAR 60 FYSHEAR 40 FC 4 FCSHEAR 4
  STATICLOAD CVX TYPE DEAD
  STATICLOAD NEHRP TYPE DEAD
  STATICLOAD GRAVITY TYPE DEAD
  STATICLOAD 1STMODE TYPE DEAD
  STATICLOAD RMODE TYPE DEAD
  STATICLOAD DEAD TYPE DEAD
  STATICLOAD LIVE TYPE LIVE
  STATICLOAD 1MODDBE TYPE DEAD
  STATICLOAD RMODBE TYPE DEAD
  STATICLOAD DDLL TYPE DEAD
  STATICLOAD UNIFORM TYPE DEAD
  COMBO DSTL1 DESIGN STEEL
  COMBO DSTL2 DESIGN STEEL
  STEELDESIGN "AISC-ASD89"
  PUSHCASE "PUSHUNO"  CONTROL DISP  TARGET 20  JOINT 20  DOF U1
  PUSHCASE "PUSHUNO"  PDELTA NO
  PUSHCASE "PUSHUNO"  MINSTEPS 50  MAXNULLSTEPS 50  MAXTOTALSTEPS 200
MAXITER 10
  PUSHCASE "PUSHUNO"  ITERTOL .0001 EVENTTOL .01
  PUSHCASE "PUSHUNO"  LOADTYPE MODE  NUMBER 1  SCALEFACTOR -1
  PUSHCASE "PUSHCVX"  CONTROL DISP  TARGET 20  JOINT 20  DOF U1
  PUSHCASE "PUSHCVX"  MINSTEPS 50  MAXNULLSTEPS 50  MAXTOTALSTEPS 200
MAXITER 10
  PUSHCASE "PUSHCVX"  ITERTOL .0001 EVENTTOL .01
  PUSHCASE "PUSHCVX"  LOADTYPE STATIC  LOAD CVX  SCALEFACTOR 1
  PUSHCASE "PUSHUNIF"  CONTROL DISP  TARGET 20  JOINT 20  DOF U1
  PUSHCASE "PUSHUNIF"  PDELTA NO
  PUSHCASE "PUSHUNIF"  MINSTEPS 50  MAXNULLSTEPS 50  MAXTOTALSTEPS 200
MAXITER 10
  PUSHCASE "PUSHUNIF"  ITERTOL .0001 EVENTTOL .01
  PUSHCASE "PUSHUNIF"  LOADTYPE STATIC  LOAD UNIFORM  SCALEFACTOR 1
  HINGE "USER"  TYPE M3 SYMMETRIC
  HINGE "USER"  TYPE M3  B 1 1  C 6 1  D 8 1  E 10 1
```

```
HINGE "USER"  TYPE M3  IO 2  LS 4  CP 6
FRAMEHINGE 22  HINGE "USER"  RDISTANCE 0
FRAMEHINGE 22  HINGE "USER"  RDISTANCE 1
FRAMEHINGE 23  HINGE "USER"  RDISTANCE 0
FRAMEHINGE 23  HINGE "USER"  RDISTANCE 1
FRAMEHINGE 24  HINGE "USER"  RDISTANCE 0
FRAMEHINGE 24  HINGE "USER"  RDISTANCE 1
FRAMEHINGE 28  HINGE "USER"  RDISTANCE 0
FRAMEHINGE 28  HINGE "USER"  RDISTANCE 1
FRAMEHINGE 29  HINGE "USER"  RDISTANCE 0
FRAMEHINGE 29  HINGE "USER"  RDISTANCE 1
FRAMEHINGE 30  HINGE "USER"  RDISTANCE 0
FRAMEHINGE 30  HINGE "USER"  RDISTANCE 1
FRAMEHINGE 38  HINGE "USER"  RDISTANCE 0
FRAMEHINGE 38  HINGE "USER"  RDISTANCE 1
FRAMEHINGE 39  HINGE "USER"  RDISTANCE 0
FRAMEHINGE 39  HINGE "USER"  RDISTANCE 1
FRAMEHINGE 40  HINGE "USER"  RDISTANCE 0
FRAMEHINGE 40  HINGE "USER"  RDISTANCE 1
FRAMEHINGE 41  HINGE "USER"  RDISTANCE 0
FRAMEHINGE 41  HINGE "USER"  RDISTANCE 1
FRAMEHINGE 42  HINGE "USER"  RDISTANCE 0
FRAMEHINGE 42  HINGE "USER"  RDISTANCE 1
FRAMEHINGE 43  HINGE "USER"  RDISTANCE 0
FRAMEHINGE 43  HINGE "USER"  RDISTANCE 1
FRAMEHINGE 1  HINGE "USER"  RDISTANCE 0
FRAMEHINGE 1  HINGE "USER"  RDISTANCE 1
FRAMEHINGE 2  HINGE "USER"  RDISTANCE 0
FRAMEHINGE 2  HINGE "USER"  RDISTANCE 1
FRAMEHINGE 3  HINGE "USER"  RDISTANCE 0
FRAMEHINGE 3  HINGE "USER"  RDISTANCE 1
FRAMEHINGE 4  HINGE "USER"  RDISTANCE 0
FRAMEHINGE 4  HINGE "USER"  RDISTANCE 1
FRAMEHINGE 5  HINGE "USER"  RDISTANCE 0
FRAMEHINGE 5  HINGE "USER"  RDISTANCE 1
FRAMEHINGE 6  HINGE "USER"  RDISTANCE 0
FRAMEHINGE 6  HINGE "USER"  RDISTANCE 1
FRAMEHINGE 7  HINGE "USER"  RDISTANCE 0
FRAMEHINGE 7  HINGE "USER"  RDISTANCE 1
FRAMEHINGE 8  HINGE "USER"  RDISTANCE 0
FRAMEHINGE 8  HINGE "USER"  RDISTANCE 1
FRAMEHINGE 9  HINGE "USER"  RDISTANCE 0
FRAMEHINGE 9  HINGE "USER"  RDISTANCE 1
END SUPPLEMENTAL DATA
```

SAP 2000-NL VERSION 7.11 INPUT FILE FOR THE EIGNEVALUE AND PUSHOVER ANALYSIS OF EXAMPLE No.5: FRAME 6S-75 WITH LINEAR VISCOUS DAMPING TO PROVIDE 10% VISCOUS DAMPING RATIO WHEN ASSUMING ELASTIC FRAME BEHAVIOR

SYSTEM
 DOF=UX,UZ,RY LENGTH=IN FORCE=Kip PAGE=SECTIONS

JOINT
  1 X=-486 Y=0 Z=0
  2 X=-486 Y=0 Z=174
  3 X=-486 Y=0 Z=343.44
  4 X=-486 Y=0 Z=512.88
  5 X=-486 Y=0 Z=682.32
 ‘6 X=-486 Y=0 Z=851.76
  7 X=-486 Y=0 Z=1021.2
  8 X=-162 Y=0 Z=0
  9 X=-162 Y=0 Z=174
 10 X=-162 Y=0 Z=343.44
 11 X=-162 Y=0 Z=512.88
 12 X=-162 Y=0 Z=682.32
 13 X=-162 Y=0 Z=851.76
 14 X=-162 Y=0 Z=1021.2
 15 X=162 Y=0 Z=0
 16 X=162 Y=0 Z=174
 17 X=162 Y=0 Z=343.44
 18 X=162 Y=0 Z=512.88
 19 X=162 Y=0 Z=682.32
 20 X=162 Y=0 Z=851.76
 21 X=162 Y=0 Z=1021.2
 22 X=486 Y=0 Z=0
 23 X=486 Y=0 Z=174
 24 X=486 Y=0 Z=343.44
 25 X=486 Y=0 Z=512.88
 26 X=486 Y=0 Z=682.32
 27 X=486 Y=0 Z=851.76
 28 X=486 Y=0 Z=1021.2

RESTRAINT
 ADD=1 DOF=U1,U2,U3,R1,R2,R3
 ADD=8 DOF=U1,U2,U3,R1,R2,R3
 ADD=15 DOF=U1,U2,U3,R1,R2,R3
 ADD=22 DOF=U1,U2,U3,R1,R2,R3

PATTERN
 NAME=DEFAULT

MASS
 ADD=7 U1=.22496
 ADD=14 U1=.22496
 ADD=21 U1=.22496
 ADD=28 U1=.22496
 ADD=2 U1=.412632
 ADD=3 U1=.41352
 ADD=4 U1=.414958

```
ADD=5   U1=.416
ADD=6   U1=.4278
ADD=9   U1=.412632
ADD=10  U1=.41352
ADD=11  U1=.414958
ADD=12  U1=.416
ADD=13  U1=.4278
ADD=16  U1=.412632
ADD=17  U1=.41352
ADD=18  U1=.414958
ADD=19  U1=.416
ADD=20  U1=.4278
ADD=23  U1=.412632
ADD=24  U1=.41352
ADD=25  U1=.414958
ADD=26  U1=.416
ADD=27  U1=.4278
```

MATERIAL
```
 NAME=STEEL  IDES=S  M=7.324E-07  W=.000283
  T=0  E=29000  U=.3  A=.0000065  FY=50
 NAME=CONC  IDES=C  M=2.246377E-07  W=.0000868
  T=0  E=3600  U=.2  A=.0000055
 NAME=OTHER  IDES=N  M=2.246377E-07  W=.0000868
  T=0  E=3600  U=.2  A=.0000055
```

FRAME SECTION

```
 NAME=W14X132 MAT=STEEL A=38.8 J=12.3 I=1530,548 AS=9.4557,25.278 S=208.7312,74.43124
Z=234,113 R=6.279569,3.758153 T=14.66,14.725,1.03,.645,14.725,1.03 SHN=W14X132 DSG=W
 NAME=W14X176 MAT=STEEL A=51.8 J=26.5 I=2140,838 AS=12.633,34.169 S=281.2089,107.0927
Z=320,163 R=6.427499,4.02214 T=15.22,15.65,1.31,.83,15.65,1.31 SHN=W14X176 DSG=W
 NAME=W16X31 MAT=STEEL A=9.12 J=.46 I=375,12.4 AS=4.367,4.0517 S=47.22922,4.488688
Z=54,7.03 R=6.412365,1.16604 T=15.88,5.525,.44,.275,5.525,.44 SHN=W16X31 DSG=W
 NAME=W16X40 MAT=STEEL A=11.8 J=.79 I=518,28.9 AS=4.8831,5.8875 S=64.70956,8.263045
Z=72.9,12.7 R=6.625579,1.564977 T=16.01,6.995,.505,.305,6.995,.505 SHN=W16X40 DSG=W
 NAME=W21X44 MAT=STEEL A=13 J=.77 I=843,20.7 AS=7.231,4.875 S=81.60697,6.369231
Z=95.4,10.2 R=8.052711,1.261867 T=20.66,6.5,.45,.35,6.5,.45 SHN=W21X44 DSG=W
 NAME=W21X50 MAT=STEEL A=14.7 J=1.14 I=984,24.9 AS=7.9154,5.8226 S=94.47912,7.626339
Z=110,12.2 R=8.181612,1.301491 T=20.83,6.53,.535,.38,6.53,.535 SHN=W21X50 DSG=W
 NAME=W21X62 MAT=STEEL A=18.3 J=1.83 I=1330,57.5 AS=8.396,8.446 S=126.727,13.95631
Z=144,21.7 R=8.525116,1.77259 T=20.99,8.24,.615,.4,8.24,.615 SHN=W21X62 DSG=W
 NAME=W24X62 MAT=STEEL A=18.2 J=1.71 I=1550,34.5 AS=10.208,6.9227 S=130.5813,9.801136
Z=153,15.7 R=9.228479,1.376809 T=23.74,7.04,.59,.43,7.04,.59 SHN=W24X62 DSG=W
 NAME=W14X90 MAT=STEEL A=26.5 J=4.06 I=999,362 AS=6.1688,17.182 S=142.5107,49.86226
Z=157,75.6 R=6.139879,3.695995 T=14.02,14.52,.71,.44,14.52,.71 SHN=W14X90 DSG=W
 NAME=W14X26 MAT=STEEL A=7.69 J=.36 I=245,8.91 AS=3.5471,3.5175 S=35.22646,3.546268
Z=40.2,5.54 R=5.644427,1.076405 T=13.91,5.025,.42,.255,5.025,.42 SHN=W14X26 DSG=W
```

FRAME
```
 1 J=1,2 SEC=W14X176 NSEG=2 ANG=0 IOFF=16 JOFF=13 RIGID=1
 2 J=2,3 SEC=W14X176 NSEG=2 ANG=0 IOFF=13 JOFF=11.5 RIGID=1
 3 J=3,4 SEC=W14X132 NSEG=2 ANG=0 IOFF=11.5 JOFF=11.5 RIGID=1
 4 J=4,5 SEC=W14X132 NSEG=2 ANG=0 IOFF=11.5 JOFF=11.5 RIGID=1
 5 J=5,6 SEC=W14X90 NSEG=2 ANG=0 IOFF=11.5 JOFF=9 RIGID=1
 6 J=6,7 SEC=W14X90 NSEG=2 ANG=0 IOFF=9 JOFF=9 RIGID=1
```

7 J=8,9 SEC=W14X176 NSEG=2 ANG=0 IOFF=16 JOFF=13 RIGID=1
8 J=9,10 SEC=W14X176 NSEG=2 ANG=0 IOFF=13 JOFF=11.5 RIGID=1
9 J=10,11 SEC=W14X132 NSEG=2 ANG=0 IOFF=11.5 JOFF=11.5 RIGID=1
10 J=11,12 SEC=W14X132 NSEG=2 ANG=0 IOFF=11.5 JOFF=11.5 RIGID=1
11 J=12,13 SEC=W14X90 NSEG=2 ANG=0 IOFF=11.5 JOFF=9 RIGID=1
12 J=13,14 SEC=W14X90 NSEG=2 ANG=0 IOFF=9 JOFF=9 RIGID=1
13 J=15,16 SEC=W14X176 NSEG=2 ANG=0 IOFF=16 JOFF=13 RIGID=1
14 J=16,17 SEC=W14X176 NSEG=2 ANG=0 IOFF=13 JOFF=11.5 RIGID=1
15 J=17,18 SEC=W14X132 NSEG=2 ANG=0 IOFF=11.5 JOFF=11.5 RIGID=1
16 J=18,19 SEC=W14X132 NSEG=2 ANG=0 IOFF=11.5 JOFF=11.5 RIGID=1
17 J=19,20 SEC=W14X90 NSEG=2 ANG=0 IOFF=11.5 JOFF=9 RIGID=1
18 J=20,21 SEC=W14X90 NSEG=2 ANG=0 IOFF=9 JOFF=9 RIGID=1
19 J=22,23 SEC=W14X176 NSEG=2 ANG=0 IOFF=16 JOFF=13 RIGID=1
20 J=23,24 SEC=W14X176 NSEG=2 ANG=0 IOFF=13 JOFF=11.5 RIGID=1
21 J=24,25 SEC=W14X132 NSEG=2 ANG=0 IOFF=11.5 JOFF=11.5 RIGID=1
22 J=25,26 SEC=W14X132 NSEG=2 ANG=0 IOFF=11.5 JOFF=11.5 RIGID=1
23 J=26,27 SEC=W14X90 NSEG=2 ANG=0 IOFF=11.5 JOFF=9 RIGID=1
24 J=27,28 SEC=W14X90 NSEG=2 ANG=0 IOFF=9 JOFF=9 RIGID=1
25 J=2,9 SEC=W24X62 NSEG=4 ANG=0 IOFF=11 JOFF=11 RIGID=1
26 J=3,10 SEC=W21X62 NSEG=4 ANG=0 IOFF=11 JOFF=11 RIGID=1
27 J=4,11 SEC=W21X50 NSEG=4 ANG=0 IOFF=11 JOFF=11 RIGID=1
28 J=5,12 SEC=W21X44 NSEG=4 ANG=0 IOFF=11 JOFF=11 RIGID=1
29 J=6,13 SEC=W16X40 NSEG=4 ANG=0 IOFF=11 JOFF=11 RIGID=1
30 J=7,14 SEC=W16X31 NSEG=4 ANG=0 IOFF=11 JOFF=11 RIGID=1
31 J=9,16 SEC=W24X62 NSEG=4 ANG=0 IOFF=11 JOFF=11 RIGID=1
32 J=10,17 SEC=W21X62 NSEG=4 ANG=0 IOFF=11 JOFF=11 RIGID=1
33 J=11,18 SEC=W21X50 NSEG=4 ANG=0 IOFF=11 JOFF=11 RIGID=1
34 J=12,19 SEC=W21X44 NSEG=4 ANG=0 IOFF=11 JOFF=11 RIGID=1
35 J=13,20 SEC=W16X40 NSEG=4 ANG=0 IOFF=11 JOFF=11 RIGID=1
36 J=14,21 SEC=W16X31 NSEG=4 ANG=0 IOFF=11 JOFF=11 RIGID=1
37 J=16,23 SEC=W24X62 NSEG=4 ANG=0 IOFF=11 JOFF=11 RIGID=1
38 J=17,24 SEC=W21X62 NSEG=4 ANG=0 IOFF=11 JOFF=11 RIGID=1
39 J=18,25 SEC=W21X50 NSEG=4 ANG=0 IOFF=11 JOFF=11 RIGID=1
40 J=19,26 SEC=W21X44 NSEG=4 ANG=0 IOFF=11 JOFF=11 RIGID=1
41 J=20,27 SEC=W16X40 NSEG=4 ANG=0 IOFF=11 JOFF=11 RIGID=1
42 J=21,28 SEC=W16X31 NSEG=4 ANG=0 IOFF=11 JOFF=11 RIGID=1

LOAD
 NAME=NEHRP
  TYPE=FORCE
   ADD=7 UX=27.2
   ADD=6 UX=34.6
   ADD=5 UX=21.8
   ADD=4 UX=12
   ADD=3 UX=5.2
   ADD=2 UX=1.3
 NAME=PITO
  TYPE=FORCE
   ADD=7 UX=.1815
   ADD=6 UX=.2939
   ADD=5 UX=.2317
   ADD=4 UX=.1639
   ADD=3 UX=.0937
   ADD=2 UX=.0353
 NAME=FIRSTM
  TYPE=FORCE

```
     ADD=7 UX=25.2
     ADD=6 UX=40.8
     ADD=5 UX=32.2
     ADD=4 UX=22.7
     ADD=3 UX=13
     ADD=2 UX=4.9
 NAME=RMODE
  TYPE=FORCE
   ADD=7 UX=9.84
   ADD=6 UX=10.4
   ADD=5 UX=-1.16
   ADD=4 UX=-13.76
   ADD=3 UX=-26.8
   ADD=2 UX=-37.6
 NAME=GRAVITY
  TYPE=DISTRIBUTED SPAN
   ADD=30 RD=0,1 UZ=-.085,-.085
   ADD=36 RD=0,1 UZ=-.085,-.085
   ADD=42 RD=0,1 UZ=-.085,-.085
   ADD=25 RD=0,1 UZ=-.167,-.167
   ADD=26 RD=0,1 UZ=-.167,-.167
   ADD=27 RD=0,1 UZ=-.167,-.167
   ADD=28 RD=0,1 UZ=-.167,-.167
   ADD=29 RD=0,1 UZ=-.167,-.167
   ADD=31 RD=0,1 UZ=-.167,-.167
   ADD=32 RD=0,1 UZ=-.167,-.167
   ADD=33 RD=0,1 UZ=-.167,-.167
   ADD=34 RD=0,1 UZ=-.167,-.167
   ADD=35 RD=0,1 UZ=-.167,-.167
   ADD=37 RD=0,1 UZ=-.167,-.167
   ADD=38 RD=0,1 UZ=-.167,-.167
   ADD=39 RD=0,1 UZ=-.167,-.167
   ADD=40 RD=0,1 UZ=-.167,-.167
   ADD=41 RD=0,1 UZ=-.167,-.167
 NAME=PUSHUNIF
  TYPE=FORCE
   ADD=7 UX=.0975
   ADD=6 UX=.1805
   ADD=2 UX=.1805
   ADD=3 UX=.1805
   ADD=4 UX=.1805
   ADD=5 UX=.1805
 NAME=UNIFORM
  TYPE=FORCE
   ADD=7 UX=9.752587E-02
   ADD=2 UX=.1804948
   ADD=3 UX=.1804948
   ADD=4 UX=.1804948
   ADD=5 UX=.1804948
   ADD=6 UX=.1804948

MODE
 TYPE=EIGEN N=6 TOL=.00001

OUTPUT
; No Output Requested
```

END

; The following data is used for graphics, design and pushover analysis.
; If changes are made to the analysis data above, then the following data
; should be checked for consistency.
SAP2000 V7.11 SUPPLEMENTAL DATA
  GRID GLOBAL X "1" -486
  GRID GLOBAL X "2" -162
  GRID GLOBAL X "3" 162
  GRID GLOBAL X "4" 486
  GRID GLOBAL Y "5" 0
  GRID GLOBAL Z "6" 0
  GRID GLOBAL Z "7" 174
  GRID GLOBAL Z "8" 343.44
  GRID GLOBAL Z "9" 512.88
  GRID GLOBAL Z "10" 682.32
  GRID GLOBAL Z "11" 851.76
  GRID GLOBAL Z "12" 1021.2
  MATERIAL STEEL FY 50
  MATERIAL CONC FYREBAR 60 FYSHEAR 40 FC 4 FCSHEAR 4
  STATICLOAD NEHRP TYPE QUAKE
  STATICLOAD PITO TYPE QUAKE
  STATICLOAD FIRSTM TYPE QUAKE
  STATICLOAD RMODE TYPE QUAKE
  STATICLOAD GRAVITY TYPE DEAD
  STATICLOAD PUSHUNIF TYPE QUAKE
  STATICLOAD UNIFORM TYPE QUAKE
  PUSHCASE "GRAVITY" CONTROL FORCE JOINT 7 DOF U3
  PUSHCASE "GRAVITY" MINSTEPS 1 MAXNULLSTEPS 50 MAXTOTALSTEPS 200 MAXITER
10
  PUSHCASE "GRAVITY" ITERTOL .0001 EVENTTOL .01
  PUSHCASE "GRAVITY" LOADTYPE STATIC LOAD GRAVITY SCALEFACTOR 1
  PUSHCASE "PUSHM1" CONTROL DISP TARGET 45 JOINT 7 DOF U1
  PUSHCASE "PUSHM1" STARTCASE "GRAVITY"
  PUSHCASE "PUSHM1" MINSTEPS 200 MAXNULLSTEPS 50 MAXTOTALSTEPS 200 MAXITER
10
  PUSHCASE "PUSHM1" ITERTOL .0001 EVENTTOL .01
  PUSHCASE "PUSHM1" LOADTYPE MODE NUMBER 1 SCALEFACTOR 1
  PUSHCASE "UNIFORM" CONTROL DISP TARGET 36 JOINT 7 DOF U1
  PUSHCASE "UNIFORM" MINSTEPS 50 MAXNULLSTEPS 50 MAXTOTALSTEPS 200
MAXITER 10
  PUSHCASE "UNIFORM" ITERTOL .0001 EVENTTOL .01
  PUSHCASE "UNIFORM" LOADTYPE STATIC LOAD UNIFORM SCALEFACTOR 1
  HINGE "USER" TYPE M3 SYMMETRIC
  HINGE "USER" TYPE M3 B 1 1 C 8 1 D 8 .2 E 10 .2
  HINGE "USER" TYPE M3 IO 2 LS 4 CP 6
  FRAMEHINGE 1 HINGE "Default-PMM" RDISTANCE 0
  FRAMEHINGE 1 HINGE "Default-PMM" RDISTANCE 1
  FRAMEHINGE 2 HINGE "Default-PMM" RDISTANCE 0
  FRAMEHINGE 2 HINGE "Default-PMM" RDISTANCE 1
  FRAMEHINGE 3 HINGE "Default-PMM" RDISTANCE 0
  FRAMEHINGE 3 HINGE "Default-PMM" RDISTANCE 1
  FRAMEHINGE 4 HINGE "Default-PMM" RDISTANCE 0
  FRAMEHINGE 4 HINGE "Default-PMM" RDISTANCE 1
  FRAMEHINGE 5 HINGE "Default-PMM" RDISTANCE 0

```
FRAMEHINGE 5  HINGE "Default-PMM"  RDISTANCE 1
FRAMEHINGE 6  HINGE "Default-PMM"  RDISTANCE 0
FRAMEHINGE 6  HINGE "Default-PMM"  RDISTANCE 1
FRAMEHINGE 7  HINGE "Default-PMM"  RDISTANCE 0
FRAMEHINGE 7  HINGE "Default-PMM"  RDISTANCE 1
FRAMEHINGE 8  HINGE "Default-PMM"  RDISTANCE 0
FRAMEHINGE 8  HINGE "Default-PMM"  RDISTANCE 1
FRAMEHINGE 9  HINGE "Default-PMM"  RDISTANCE 0
FRAMEHINGE 9  HINGE "Default-PMM"  RDISTANCE 1
FRAMEHINGE 10  HINGE "Default-PMM"  RDISTANCE 0
FRAMEHINGE 10  HINGE "Default-PMM"  RDISTANCE 1
FRAMEHINGE 11  HINGE "Default-PMM"  RDISTANCE 0
FRAMEHINGE 11  HINGE "Default-PMM"  RDISTANCE 1
FRAMEHINGE 12  HINGE "Default-PMM"  RDISTANCE 0
FRAMEHINGE 12  HINGE "Default-PMM"  RDISTANCE 1
FRAMEHINGE 13  HINGE "Default-PMM"  RDISTANCE 0
FRAMEHINGE 13  HINGE "Default-PMM"  RDISTANCE 1
FRAMEHINGE 14  HINGE "Default-PMM"  RDISTANCE 0
FRAMEHINGE 14  HINGE "Default-PMM"  RDISTANCE 1
FRAMEHINGE 15  HINGE "Default-PMM"  RDISTANCE 0
FRAMEHINGE 15  HINGE "Default-PMM"  RDISTANCE 1
FRAMEHINGE 16  HINGE "Default-PMM"  RDISTANCE 0
FRAMEHINGE 16  HINGE "Default-PMM"  RDISTANCE 1
FRAMEHINGE 17  HINGE "Default-PMM"  RDISTANCE 0
FRAMEHINGE 17  HINGE "Default-PMM"  RDISTANCE 1
FRAMEHINGE 18  HINGE "Default-PMM"  RDISTANCE 0
FRAMEHINGE 18  HINGE "Default-PMM"  RDISTANCE 1
FRAMEHINGE 19  HINGE "Default-PMM"  RDISTANCE 0
FRAMEHINGE 19  HINGE "Default-PMM"  RDISTANCE 1
FRAMEHINGE 20  HINGE "Default-PMM"  RDISTANCE 0
FRAMEHINGE 20  HINGE "Default-PMM"  RDISTANCE 1
FRAMEHINGE 21  HINGE "Default-PMM"  RDISTANCE 0
FRAMEHINGE 21  HINGE "Default-PMM"  RDISTANCE 1
FRAMEHINGE 22  HINGE "Default-PMM"  RDISTANCE 0
FRAMEHINGE 22  HINGE "Default-PMM"  RDISTANCE 1
FRAMEHINGE 23  HINGE "Default-PMM"  RDISTANCE 0
FRAMEHINGE 23  HINGE "Default-PMM"  RDISTANCE 1
FRAMEHINGE 24  HINGE "Default-PMM"  RDISTANCE 0
FRAMEHINGE 24  HINGE "Default-PMM"  RDISTANCE 1
FRAMEHINGE 25  HINGE "USER"  RDISTANCE 0
FRAMEHINGE 25  HINGE "USER"  RDISTANCE 1
FRAMEHINGE 26  HINGE "USER"  RDISTANCE 0
FRAMEHINGE 26  HINGE "USER"  RDISTANCE 1
FRAMEHINGE 27  HINGE "USER"  RDISTANCE 0
FRAMEHINGE 27  HINGE "USER"  RDISTANCE 1
FRAMEHINGE 28  HINGE "USER"  RDISTANCE 0
FRAMEHINGE 28  HINGE "USER"  RDISTANCE 1
FRAMEHINGE 29  HINGE "USER"  RDISTANCE 0
FRAMEHINGE 29  HINGE "USER"  RDISTANCE 1
FRAMEHINGE 30  HINGE "USER"  RDISTANCE 0
FRAMEHINGE 30  HINGE "USER"  RDISTANCE 1
FRAMEHINGE 31  HINGE "USER"  RDISTANCE 0
FRAMEHINGE 31  HINGE "USER"  RDISTANCE 1
FRAMEHINGE 32  HINGE "USER"  RDISTANCE 0
FRAMEHINGE 32  HINGE "USER"  RDISTANCE 1
FRAMEHINGE 33  HINGE "USER"  RDISTANCE 0
```

```
FRAMEHINGE 33  HINGE "USER"  RDISTANCE 1
FRAMEHINGE 34  HINGE "USER"  RDISTANCE 0
FRAMEHINGE 34  HINGE "USER"  RDISTANCE 1
FRAMEHINGE 35  HINGE "USER"  RDISTANCE 0
FRAMEHINGE 35  HINGE "USER"  RDISTANCE 1
FRAMEHINGE 36  HINGE "USER"  RDISTANCE 0
FRAMEHINGE 36  HINGE "USER"  RDISTANCE 1
FRAMEHINGE 37  HINGE "USER"  RDISTANCE 0
FRAMEHINGE 37  HINGE "USER"  RDISTANCE 1
FRAMEHINGE 38  HINGE "USER"  RDISTANCE 0
FRAMEHINGE 38  HINGE "USER"  RDISTANCE 1
FRAMEHINGE 39  HINGE "USER"  RDISTANCE 0
FRAMEHINGE 39  HINGE "USER"  RDISTANCE 1
FRAMEHINGE 40  HINGE "USER"  RDISTANCE 0
FRAMEHINGE 40  HINGE "USER"  RDISTANCE 1
FRAMEHINGE 41  HINGE "USER"  RDISTANCE 0
FRAMEHINGE 41  HINGE "USER"  RDISTANCE 1
FRAMEHINGE 42  HINGE "USER"  RDISTANCE 0
FRAMEHINGE 42  HINGE "USER"  RDISTANCE 1
END SUPPLEMENTAL DATA
```

SAP2000-NL VERSION 7.11 INPUT FILE FOR EIGENVALUE AND PUSHOVER ANALYSIS OF EXAMPLE No.8: FRAME 3S-75 WITH VISCOLEASTIC SOLID DAMPING SYSTEM TO PROVIDE 8.5% VISCOUS DAMPING RATIO WHEN ASSUMING ELASTIC FRAME BEHAVIOR

SYSTEM
 DOF=UX,UZ,RY LENGTH=IN FORCE=Kip PAGE=SECTIONS

JOINT
  17 X=-486 Y=0 Z=0
  18 X=-486 Y=0 Z=174
  19 X=-486 Y=0 Z=343.44
  20 X=-486 Y=0 Z=512.88
  21 X=-162 Y=0 Z=512.88
  22 X=162 Y=0 Z=512.88
  23 X=486 Y=0 Z=512.88
  24 X=486 Y=0 Z=343.44
  25 X=486 Y=0 Z=174
  26 X=486 Y=0 Z=0
  27 X=-162 Y=0 Z=343.44
  28 X=162 Y=0 Z=343.44
  29 X=-162 Y=0 Z=174
  30 X=162 Y=0 Z=174
  33 X=162 Y=0 Z=0
  34 X=-162 Y=0 Z=0

RESTRAINT
 ADD=17 DOF=U1,U2,U3,R1,R2,R3
 ADD=26 DOF=U1,U2,U3,R1,R2,R3
 ADD=33 DOF=U1,U2,U3,R1,R2,R3
 ADD=34 DOF=U1,U2,U3,R1,R2,R3

PATTERN
 NAME=DEFAULT

MASS
 ADD=20 U1=.22488
 ADD=21 U1=.22488
 ADD=22 U1=.22488
 ADD=23 U1=.22488
 ADD=18 U1=.41606
 ADD=19 U1=.41606
 ADD=24 U1=.41606
 ADD=25 U1=.41606
 ADD=27 U1=.41606
 ADD=28 U1=.41606
 ADD=29 U1=.41606
 ADD=30 U1=.41606

MATERIAL
 NAME=STEEL IDES=S M=7.324E-07 W=.000283
  T=0 E=29000 U=.3 A=.0000065 FY=50
 NAME=CONC IDES=C M=2.246377E-07 W=.0000868
  T=0 E=3600 U=.2 A=.0000055
 NAME=OTHER IDES=N M=2.246377E-07 W=.0000868

T=0 E=3600 U=.2 A=.0000055

FRAME SECTION
 NAME=W14X109 MAT=STEEL A=32 J=7.12 I=1240,447 AS=7.518,20.934 S=173.1844,61.21191
Z=192,92.7 R=6.22495,3.737479 T=14.32,14.605,.86,.525,14.605,.86 SHN=W14X109 DSG=W
NAME=W16X40 MAT=STEEL A=11.8 J=.79 I=518,28.9 AS=4.8831,5.8875 S=64.70956,8.263045
Z=72.9,12.7 R=6.625579,1.564977 T=16.01,6.995,.505,.305,6.995,.505 SHN=W16X40 DSG=W
  NAME=W16X45 MAT=STEEL A=13.3 J=1.11 I=586,32.8 AS=5.5649,6.6246 S=72.65965,9.324804
Z=82.3,14.5 R=6.637782,1.570403 T=16.13,7.035,.565,.345,7.035,.565 SHN=W16X45 DSG=W
NAME=W14X26 MAT=STEEL A=7.69 J=.36 I=245,8.91 AS=3.5471,3.5175 S=35.22646,3.546268
Z=40.2,5.54 R=5.644427,1.076405 T=13.91,5.025,.42,.255,5.025,.42 SHN=W14X26 DSG=W
  NAME=BRACE MAT=STEEL SH=R T=.426,.426 A=.181476 J=4.63814E-03 I=2.744462E-
03,2.744462E-03 AS=.15123,.15123

FRAME
  1 J=18,29 SEC=W16X45 NSEG=4 ANG=0 IOFF=7 JOFF=7 RIGID=1
  2 J=29,30 SEC=W16X45 NSEG=4 ANG=0 IOFF=7 JOFF=7 RIGID=1
  3 J=30,25 SEC=W16X45 NSEG=4 ANG=0 IOFF=7 JOFF=7 RIGID=1
  4 J=19,27 SEC=W16X40 NSEG=4 ANG=0 IOFF=7 JOFF=7 RIGID=1
  5 J=27,28 SEC=W16X40 NSEG=4 ANG=0 IOFF=7 JOFF=7 RIGID=1
  6 J=28,24 SEC=W16X40 NSEG=4 ANG=0 IOFF=7 JOFF=7 RIGID=1
  7 J=20,21 SEC=W14X26 NSEG=4 ANG=0 IOFF=7 JOFF=7 RIGID=1
  8 J=21,22 SEC=W14X26 NSEG=4 ANG=0 IOFF=7 JOFF=7 RIGID=1
  9 J=22,23 SEC=W14X26 NSEG=4 ANG=0 IOFF=7 JOFF=7 RIGID=1
 10 J=34,30 SEC=BRACE NSEG=2 ANG=0 IREL=R3 JREL=R3
 12 J=27,22 SEC=BRACE NSEG=2 ANG=0 IREL=R3 JREL=R3
 14 J=30,27 SEC=BRACE NSEG=2 ANG=0 IREL=R3 JREL=R3
 22 J=17,18 SEC=W14X109 NSEG=2 ANG=0 IOFF=14 JOFF=8 RIGID=1
 23 J=18,19 SEC=W14X109 NSEG=2 ANG=0 IOFF=8 JOFF=8 RIGID=1
 24 J=19,20 SEC=W14X109 NSEG=2 ANG=0 IOFF=8 JOFF=7 RIGID=1
 28 J=23,24 SEC=W14X109 NSEG=2 ANG=0 IOFF=8 JOFF=7 RIGID=1
 29 J=24,25 SEC=W14X109 NSEG=2 ANG=0 IOFF=8 JOFF=8 RIGID=1
 30 J=25,26 SEC=W14X109 NSEG=2 ANG=0 IOFF=14 JOFF=8 RIGID=1
 38 J=33,30 SEC=W14X109 NSEG=2 ANG=0 IOFF=14 JOFF=8 RIGID=1
 39 J=30,28 SEC=W14X109 NSEG=2 ANG=0 IOFF=8 JOFF=8 RIGID=1
 40 J=28,22 SEC=W14X109 NSEG=2 ANG=0 IOFF=8 JOFF=7 RIGID=1
 41 J=34,29 SEC=W14X109 NSEG=2 ANG=0 IOFF=14 JOFF=8 RIGID=1
 42 J=29,27 SEC=W14X109 NSEG=2 ANG=0 IOFF=8 JOFF=8 RIGID=1
 43 J=27,21 SEC=W14X109 NSEG=2 ANG=0 IOFF=8 JOFF=7 RIGID=1

LOAD
 NAME=CVX
  TYPE=FORCE
    ADD=20 UX=.4162
    ADD=19 UX=.4269
    ADD=18 UX=.1569
 NAME=NEHRP
  TYPE=FORCE
    ADD=20 UX=37.79
    ADD=19 UX=32.46
    ADD=18 UX=8.84
 NAME=GRAVITY
 NAME=1STMODE
  TYPE=FORCE
    ADD=20 UX=144
    ADD=19 UX=181.3

427

```
    ADD=18 UX=74.65
NAME=RMODE
 TYPE=FORCE
   ADD=20 UX=93.9
   ADD=19 UX=-27
   ADD=18 UX=-275.7
NAME=DEAD
NAME=LIVE
NAME=1MODDBE
 TYPE=FORCE
   ADD=20 UX=41.7
   ADD=19 UX=52.2
   ADD=18 UX=21.2
NAME=RMODBE
 TYPE=FORCE
   ADD=20 UX=31.3
   ADD=19 UX=-9
   ADD=18 UX=-91.9
NAME=DDLL
NAME=UNIFORM
 TYPE=FORCE
   ADD=20 UX=.2127
   ADD=19 UX=.39365
   ADD=18 UX=.39365

MODE
 TYPE=EIGEN N=3 TOL=.00001

COMBO
 NAME=DSTL1
  LOAD=CVX SF=1
  LOAD=NEHRP SF=1
  LOAD=GRAVITY SF=1
  LOAD=1STMODE SF=1
  LOAD=RMODE SF=1
  LOAD=DEAD SF=1
  LOAD=1MODDBE SF=1
  LOAD=RMODBE SF=1
  LOAD=DDLL SF=1
  LOAD=UNIFORM SF=1
 NAME=DSTL2
  LOAD=CVX SF=1
  LOAD=NEHRP SF=1
  LOAD=GRAVITY SF=1
  LOAD=1STMODE SF=1
  LOAD=RMODE SF=1
  LOAD=DEAD SF=1
  LOAD=LIVE SF=1
  LOAD=1MODDBE SF=1
  LOAD=RMODBE SF=1
  LOAD=DDLL SF=1
  LOAD=UNIFORM SF=1

OUTPUT
; No Output Requested
```

END

; The following data is used for graphics, design and pushover analysis.
; If changes are made to the analysis data above, then the following data
; should be checked for consistency.
SAP2000 V7.11 SUPPLEMENTAL DATA
  GRID GLOBAL X "1" -486
  GRID GLOBAL X "2" -162
  GRID GLOBAL X "3" 162
  GRID GLOBAL X "4" 486
  GRID GLOBAL Y "5" 0
  GRID GLOBAL Z "6" 0
  GRID GLOBAL Z "7" 174
  GRID GLOBAL Z "8" 343.44
  GRID GLOBAL Z "9" 512.88
  MATERIAL STEEL FY 50
  MATERIAL CONC FYREBAR 60 FYSHEAR 40 FC 4 FCSHEAR 4
  STATICLOAD CVX TYPE DEAD
  STATICLOAD NEHRP TYPE DEAD
  STATICLOAD GRAVITY TYPE DEAD
  STATICLOAD 1STMODE TYPE DEAD
  STATICLOAD RMODE TYPE DEAD
  STATICLOAD DEAD TYPE DEAD
  STATICLOAD LIVE TYPE LIVE
  STATICLOAD 1MODDBE TYPE DEAD
  STATICLOAD RMODBE TYPE DEAD
  STATICLOAD DDLL TYPE DEAD
  STATICLOAD UNIFORM TYPE DEAD
  COMBO DSTL1 DESIGN STEEL
  COMBO DSTL2 DESIGN STEEL
  STEELDESIGN "AISC-ASD89"
  PUSHCASE "PUSHUNO" CONTROL DISP TARGET 20 JOINT 20 DOF U1
  PUSHCASE "PUSHUNO" MINSTEPS 200 MAXNULLSTEPS 50 MAXTOTALSTEPS 200
MAXITER 10
  PUSHCASE "PUSHUNO" ITERTOL .0001 EVENTTOL .01
  PUSHCASE "PUSHUNO" LOADTYPE MODE NUMBER 1 SCALEFACTOR -1
  PUSHCASE "PUSHCVX" CONTROL DISP TARGET 20 JOINT 20 DOF U1
  PUSHCASE "PUSHCVX" MINSTEPS 10 MAXNULLSTEPS 50 MAXTOTALSTEPS 200
MAXITER 10
  PUSHCASE "PUSHCVX" ITERTOL .0001 EVENTTOL .01
  PUSHCASE "PUSHCVX" LOADTYPE STATIC LOAD CVX SCALEFACTOR 1
  PUSHCASE "PUSHUNIF" CONTROL DISP TARGET 20 JOINT 20 DOF U1
  PUSHCASE "PUSHUNIF" MINSTEPS 10 MAXNULLSTEPS 50 MAXTOTALSTEPS 200
MAXITER 10
  PUSHCASE "PUSHUNIF" ITERTOL .0001 EVENTTOL .01
  PUSHCASE "PUSHUNIF" LOADTYPE STATIC LOAD UNIFORM SCALEFACTOR 1
  HINGE "USER" TYPE M3 SYMMETRIC
  HINGE "USER" TYPE M3 B 1 1 C 6 1 D 8 1 E 10 1
  HINGE "USER" TYPE M3 IO 2 LS 4 CP 6
  FRAMEHINGE 22 HINGE "USER" RDISTANCE 0
  FRAMEHINGE 22 HINGE "USER" RDISTANCE 1
  FRAMEHINGE 23 HINGE "USER" RDISTANCE 0
  FRAMEHINGE 23 HINGE "USER" RDISTANCE 1
  FRAMEHINGE 24 HINGE "USER" RDISTANCE 0
  FRAMEHINGE 24 HINGE "USER" RDISTANCE 1
  FRAMEHINGE 28 HINGE "USER" RDISTANCE 0

429

```
FRAMEHINGE 28  HINGE "USER"  RDISTANCE 1
FRAMEHINGE 29  HINGE "USER"  RDISTANCE 0
FRAMEHINGE 29  HINGE "USER"  RDISTANCE 1
FRAMEHINGE 30  HINGE "USER"  RDISTANCE 0
FRAMEHINGE 30  HINGE "USER"  RDISTANCE 1
FRAMEHINGE 38  HINGE "USER"  RDISTANCE 0
FRAMEHINGE 38  HINGE "USER"  RDISTANCE 1
FRAMEHINGE 39  HINGE "USER"  RDISTANCE 0
FRAMEHINGE 39  HINGE "USER"  RDISTANCE 1
FRAMEHINGE 40  HINGE "USER"  RDISTANCE 0
FRAMEHINGE 40  HINGE "USER"  RDISTANCE 1
FRAMEHINGE 41  HINGE "USER"  RDISTANCE 0
FRAMEHINGE 41  HINGE "USER"  RDISTANCE 1
FRAMEHINGE 42  HINGE "USER"  RDISTANCE 0
FRAMEHINGE 42  HINGE "USER"  RDISTANCE 1
FRAMEHINGE 43  HINGE "USER"  RDISTANCE 0
FRAMEHINGE 43  HINGE "USER"  RDISTANCE 1
FRAMEHINGE 1  HINGE "USER"  RDISTANCE 0
FRAMEHINGE 1  HINGE "USER"  RDISTANCE 1
FRAMEHINGE 2  HINGE "USER"  RDISTANCE 0
FRAMEHINGE 2  HINGE "USER"  RDISTANCE 1
FRAMEHINGE 3  HINGE "USER"  RDISTANCE 0
FRAMEHINGE 3  HINGE "USER"  RDISTANCE 1
FRAMEHINGE 4  HINGE "USER"  RDISTANCE 0
FRAMEHINGE 4  HINGE "USER"  RDISTANCE 1
FRAMEHINGE 5  HINGE "USER"  RDISTANCE 0
FRAMEHINGE 5  HINGE "USER"  RDISTANCE 1
FRAMEHINGE 6  HINGE "USER"  RDISTANCE 0
FRAMEHINGE 6  HINGE "USER"  RDISTANCE 1
FRAMEHINGE 7  HINGE "USER"  RDISTANCE 0
FRAMEHINGE 7  HINGE "USER"  RDISTANCE 1
FRAMEHINGE 8  HINGE "USER"  RDISTANCE 0
FRAMEHINGE 8  HINGE "USER"  RDISTANCE 1
FRAMEHINGE 9  HINGE "USER"  RDISTANCE 0
FRAMEHINGE 9  HINGE "USER"  RDISTANCE 1
END SUPPLEMENTAL DATA
```

SAP2000-NL VERSION 7.11 INPUT FILE FOR EIGENVALUE AND PUSHOVER ANALYSIS OF EXAMPLE No.9: FRAME 3S-75 WITH METALLIC YIELDING DEVICES

SYSTEM
 DOF=UX,UZ,RY LENGTH=IN FORCE=Kip PAGE=SECTIONS

JOINT
  1 X=-5.333333 Y=0 Z=156
  2 X=-6 Y=0 Z=494.88
  3 X=6 Y=0 Z=494.88
  4 X=-6 Y=0 Z=325.44
  5 X=6 Y=0 Z=325.44
  6 X=-6 Y=0 Z=156
  7 X=6 Y=0 Z=156
  8 X=-6 Y=0 Z=512.88
  9 X=6 Y=0 Z=512.88
 10 X=-6 Y=0 Z=343.44
 11 X=6 Y=0 Z=343.44
 12 X=-6 Y=0 Z=174
 13 X=6 Y=0 Z=174
 14 X=-4.666667 Y=0 Z=494.88
 15 X=-3.333333 Y=0 Z=494.88
 16 X=-2 Y=0 Z=494.88
 17 X=-486 Y=0 Z=0
 18 X=-486 Y=0 Z=174
 19 X=-486 Y=0 Z=343.44
 20 X=-486 Y=0 Z=512.88
 21 X=-162 Y=0 Z=512.88
 22 X=162 Y=0 Z=512.88
 23 X=486 Y=0 Z=512.88
 24 X=486 Y=0 Z=343.44
 25 X=486 Y=0 Z=174 .
 26 X=-.6666667 Y=0 Z=494.88
 27 X=-162 Y=0 Z=343.44
 28 X=162 Y=0 Z=343.44
 29 X=-162 Y=0 Z=174
 30 X=162 Y=0 Z=174
 31 X=.6666667 Y=0 Z=494.88
 32 X=486 Y=0 Z=0
 33 X=162 Y=0 Z=0
 34 X=-162 Y=0 Z=0
 35 X=2 Y=0 Z=494.88
 36 X=3.333333 Y=0 Z=494.88
 37 X=4.666667 Y=0 Z=494.88
 38 X=-4.666667 Y=0 Z=325.44
 39 X=-3.333333 Y=0 Z=325.44
 40 X=-2 Y=0 Z=325.44
 41 X=-.6666667 Y=0 Z=325.44
 42 X=.6666667 Y=0 Z=325.44
 43 X=2 Y=0 Z=325.44
 44 X=3.333333 Y=0 Z=325.44
 45 X=4.666667 Y=0 Z=325.44
 46 X=-4.666667 Y=0 Z=156
 47 X=-3.333333 Y=0 Z=156

```
48  X=-2  Y=0  Z=156
49  X=-.6666667  Y=0  Z=156
50  X=.6666667  Y=0  Z=156
51  X=2  Y=0  Z=156
52  X=3.333333  Y=0  Z=156
53  X=4.666667  Y=0  Z=156
54  X=-4.666667  Y=0  Z=512.88
55  X=-3.333333  Y=0  Z=512.88
56  X=-2  Y=0  Z=512.88
57  X=-.6666667  Y=0  Z=512.88
58  X=.6666667  Y=0  Z=512.88
59  X=2  Y=0  Z=512.88
60  X=3.333333  Y=0  Z=512.88
61  X=4.666667  Y=0  Z=512.88
62  X=-4.666667  Y=0  Z=343.44
63  X=-3.333333  Y=0  Z=343.44
64  X=-2  Y=0  Z=343.44
65  X=-.6666667  Y=0  Z=343.44
66  X=.6666667  Y=0  Z=343.44
67  X=2  Y=0  Z=343.44
68  X=3.333333  Y=0  Z=343.44
69  X=4.666667  Y=0  Z=343.44
70  X=-4.666667  Y=0  Z=174
71  X=-3.333333  Y=0  Z=174
72  X=-2  Y=0  Z=174
73  X=-.6666667  Y=0  Z=174
74  X=.6666667  Y=0  Z=174
75  X=2  Y=0  Z=174
76  X=3.333333  Y=0  Z=174
77  X=4.666667  Y=0  Z=174
78  X=5.333333  Y=0  Z=156
79  X=-5.333333  Y=0  Z=174
80  X=5.333333  Y=0  Z=174

RESTRAINT
 ADD=17  DOF=U1,U2,U3,R1,R2,R3
 ADD=33  DOF=U1,U2,U3,R1,R2,R3
 ADD=34  DOF=U1,U2,U3,R1,R2,R3
 ADD=32  DOF=U1,U2,U3,R1,R2,R3

PATTERN
 NAME=DEFAULT

MASS
 ADD=20  U1=.228238
 ADD=21  U1=.228238
 ADD=22  U1=.228238
 ADD=23  U1=.228238
 ADD=18  U1=.4224093
 ADD=19  U1=.4224093
 ADD=24  U1=.4224093
 ADD=25  U1=.4224093
 ADD=27  U1=.4224093
 ADD=28  U1=.4224093
 ADD=29  U1=.4224093
 ADD=30  U1=.4224093
```

MATERIAL
 NAME=STEEL IDES=S M=7.324E-07 W=.000283
  T=0 E=29000 U=.3 A=.0000065 FY=50
 NAME=CONC IDES=C M=2.246377E-07 W=.0000868
  T=0 E=3600 U=.2 A=.0000055
 NAME=OTHER IDES=N M=2.246377E-07 W=.0000868
  T=0 E=3600 U=.2 A=.0000055
 NAME=A36 IDES=S M=7.324E-07 W=.000283
  T=0 E=29000 U=.3 A=.0000065 FY=36

FRAME SECTION
 NAME=W14X109 MAT=STEEL A=32 J=7.12 I=1240,447 AS=7.518,20.934 S=173.1844,61.21191
Z=192,92.7 R=6.22495,3.737479 T=14.32,14.605,.86,.525,14.605,.86 SHN=W14X109 DSG=W
   NAME=W16X40 MAT=STEEL A=11.8 J=.79 I=518,28.9 AS=4.8831,5.8875 S=64.70956,8.263045
Z=72.9,12.7 R=6.625579,1.564977 T=16.01,6.995,.505,.305,6.995,.505 SHN=W16X40 DSG=W
   NAME=W16X45 MAT=STEEL A=13.3 J=1.11 I=586,32.8 AS=5.5649,6.6246 S=72.65965,9.324804
Z=82.3,14.5 R=6.637782,1.570403 T=16.13,7.035,.565,.345,7.035,.565 SHN=W16X45 DSG=W
   NAME=W14X26 MAT=STEEL A=7.69 J=.36 I=245,8.91 AS=3.5471,3.5175 S=35.22646,3.546268
Z=40.2,5.54 R=5.644427,1.076405 T=13.91,5.025,.42,.255,5.025,.42 SHN=W14X26 DSG=W
   NAME=COREB MAT=A36 SH=R T=.3333,54 A=18 J=.6640741 I=.1666667,4374 AS=15,15
   NAME=FS6 MAT=STEEL A=14.4 J=217 I=131,131 AS=8,8 S=32.75,32.75 Z=39.7,39.7
R=3.01616,3.01616 T=8,8,.5,.5,0,0 SHN=TS8X8X1/2 DSG=B
NLPROP
 NAME=NLPR1   TYPE=Plastic1
  DOF=U1 KE=0 CE=0 K=320.32 YIELD=58.77 RATIO=0 EXP=1
 NAME=NLPR3   TYPE=Plastic1
  DOF=U1 KE=0 CE=0 K=223.73 YIELD=36.73 RATIO=0 EXP=1
 NAME=NLPR2   TYPE=Plastic1
  DOF=U1 KE=0 CE=0 K=258.36 YIELD=44 RATIO=0 EXP=1

FRAME
 1 J=18,29 SEC=W16X45 NSEG=4 ANG=0 IOFF=7 JOFF=7 RIGID=1
 2 J=26,57 SEC=COREB NSEG=2 ANG=0
 3 J=30,25 SEC=W16X45 NSEG=4 ANG=0 IOFF=7 JOFF=7 RIGID=1
 4 J=19,27 SEC=W16X40 NSEG=4 ANG=0 IOFF=7 JOFF=7 RIGID=1
 5 J=41,65 SEC=COREB NSEG=2 ANG=0
 6 J=28,24 SEC=W16X40 NSEG=4 ANG=0 IOFF=7 JOFF=7 RIGID=1
 7 J=20,21 SEC=W14X26 NSEG=4 ANG=0 IOFF=7 JOFF=7 RIGID=1
 9 J=22,23 SEC=W14X26 NSEG=4 ANG=0 IOFF=7 JOFF=7 RIGID=1
 10 J=49,73 SEC=COREB NSEG=2 ANG=0
 11 J=50,74 SEC=COREB NSEG=2 ANG=0
 12 J=6,1 SEC=FS1 NSEG=4 ANG=0
 13 J=1,46 SEC=FS1 NSEG=4 ANG=0
 14 J=53,78 SEC=FS1 NSEG=4 ANG=0
 15 J=78,7 SEC=FS1 NSEG=4 ANG=0
 16 J=12,79 SEC=W16X45 NSEG=4 ANG=0
 17 J=27,2 SEC=FS6 NSEG=2 ANG=0 IREL=R3 JREL=R3
 18 J=3,28 SEC=FS6 NSEG=2 ANG=0 IREL=R3 JREL=R3
 19 J=29,4 SEC=FS6 NSEG=2 ANG=0 IREL=R3 JREL=R3
 20 J=5,30 SEC=FS6 NSEG=2 ANG=0 IREL=R3 JREL=R3
 21 J=34,6 SEC=FS6 NSEG=2 ANG=0 IREL=R3 JREL=R3
 22 J=17,18 SEC=W14X109 NSEG=2 ANG=0 IOFF=14 JOFF=8 RIGID=1
 23 J=18,19 SEC=W14X109 NSEG=2 ANG=0 IOFF=8 JOFF=8 RIGID=1
 24 J=19,20 SEC=W14X109 NSEG=2 ANG=0 IOFF=8 JOFF=7 RIGID=1
 25 J=7,33 SEC=FS6 NSEG=2 ANG=0 IREL=R3 JREL=R3

433

```
26 J=21,8  SEC=W14X26  NSEG=4  ANG=0  IOFF=7  RIGID=1
27 J=79,70  SEC=W16X45  NSEG=4  ANG=0
28 J=23,24  SEC=W14X109  NSEG=2  ANG=0  IOFF=8  JOFF=7  RIGID=1
29 J=24,25  SEC=W14X109  NSEG=2  ANG=0  IOFF=8  JOFF=8  RIGID=1
30 J=9,22  SEC=W14X26  NSEG=4  ANG=0  JOFF=7  RIGID=1
31 J=27,10  SEC=W16X40  NSEG=4  ANG=0  IOFF=7  RIGID=1
32 J=77,80  SEC=W16X45  NSEG=4  ANG=0
33 J=11,28  SEC=W16X40  NSEG=4  ANG=0  JOFF=7  RIGID=1
34 J=29,12  SEC=W16X45  NSEG=4  ANG=0  IOFF=7  RIGID=1
35 J=80,13  SEC=W16X45  NSEG=4  ANG=0
36 J=13,30  SEC=W16X45  NSEG=4  ANG=0  JOFF=7  RIGID=1
37 J=2,14  SEC=FS1  NSEG=4  ANG=0
38 J=14,15  SEC=FS1  NSEG=4  ANG=0
39 J=30,28  SEC=W14X109  NSEG=2  ANG=0  IOFF=8  JOFF=8  RIGID=1
40 J=28,22  SEC=W14X109  NSEG=2  ANG=0  IOFF=8  JOFF=7  RIGID=1
41 J=15,16  SEC=FS1  NSEG=4  ANG=0
42 J=29,27  SEC=W14X109  NSEG=2  ANG=0  IOFF=8  JOFF=8  RIGID=1
43 J=27,21  SEC=W14X109  NSEG=2  ANG=0  IOFF=8  JOFF=7  RIGID=1
44 J=25,32  SEC=W14X109  NSEG=2  ANG=0  IOFF=14  JOFF=8  RIGID=1
45 J=16,26  SEC=FS1  NSEG=4  ANG=0
46 J=26,31  SEC=FS1  NSEG=4  ANG=0
47 J=31,35  SEC=FS1  NSEG=4  ANG=0
48 J=35,36  SEC=FS1  NSEG=4  ANG=0
49 J=36,37  SEC=FS1  NSEG=4  ANG=0
50 J=37,3  SEC=FS1  NSEG=4  ANG=0
51 J=4,38  SEC=FS1  NSEG=4  ANG=0
52 J=38,39  SEC=FS1  NSEG=4  ANG=0
53 J=39,40  SEC=FS1  NSEG=4  ANG=0
54 J=40,41  SEC=FS1  NSEG=4  ANG=0
55 J=41,42  SEC=FS1  NSEG=4  ANG=0
56 J=42,43  SEC=FS1  NSEG=4  ANG=0
57 J=43,44  SEC=FS1  NSEG=4  ANG=0
58 J=44,45  SEC=FS1  NSEG=4  ANG=0
59 J=45,5  SEC=FS1  NSEG=4  ANG=0
60 J=1,79  SEC=COREB  NSEG=2  ANG=0
61 J=46,47  SEC=FS1  NSEG=4  ANG=0
62 J=47,48  SEC=FS1  NSEG=4  ANG=0
63 J=48,49  SEC=FS1  NSEG=4  ANG=0
64 J=49,50  SEC=FS1  NSEG=4  ANG=0
65 J=50,51  SEC=FS1  NSEG=4  ANG=0
66 J=51,52  SEC=FS1  NSEG=4  ANG=0
67 J=52,53  SEC=FS1  NSEG=4  ANG=0
68 J=78,80  SEC=COREB  NSEG=2  ANG=0
69 J=8,54  SEC=W14X26  NSEG=4  ANG=0
70 J=54,55  SEC=W14X26  NSEG=4  ANG=0
71 J=55,56  SEC=W14X26  NSEG=4  ANG=0
72 J=56,57  SEC=W14X26  NSEG=4  ANG=0
73 J=57,58  SEC=W14X26  NSEG=4  ANG=0
74 J=58,59  SEC=W14X26  NSEG=4  ANG=0
75 J=59,60  SEC=W14X26  NSEG=4  ANG=0
76 J=60,61  SEC=W14X26  NSEG=4  ANG=0
77 J=61,9  SEC=W14X26  NSEG=4  ANG=0
78 J=10,62  SEC=W16X40  NSEG=4  ANG=0
79 J=62,63  SEC=W16X40  NSEG=4  ANG=0
80 J=63,64  SEC=W16X40  NSEG=4  ANG=0
81 J=64,65  SEC=W16X40  NSEG=4  ANG=0
```

```
 82 J=65,66 SEC=W16X40 NSEG=4 ANG=0
 83 J=66,67 SEC=W16X40 NSEG=4 ANG=0
 84 J=67,68 SEC=W16X40 NSEG=4 ANG=0
 85 J=68,69 SEC=W16X40 NSEG=4 ANG=0
 86 J=69,11 SEC=W16X40 NSEG=4 ANG=0
 87 J=39,63 SEC=COREB NSEG=2 ANG=0
 88 J=70,71 SEC=W16X45 NSEG=4 ANG=0
 89 J=71,72 SEC=W16X45 NSEG=4 ANG=0
 90 J=72,73 SEC=W16X45 NSEG=4 ANG=0
 91 J=73,74 SEC=W16X45 NSEG=4 ANG=0
 92 J=74,75 SEC=W16X45 NSEG=4 ANG=0
 93 J=75,76 SEC=W16X45 NSEG=4 ANG=0
 94 J=76,77 SEC=W16X45 NSEG=4 ANG=0
 95 J=44,68 SEC=COREB NSEG=2 ANG=0
 96 J=2,8 SEC=COREB NSEG=2 ANG=0
 97 J=3,9 SEC=COREB NSEG=2 ANG=0
 98 J=60,36 SEC=COREB NSEG=2 ANG=0
 99 J=15,55 SEC=COREB NSEG=2 ANG=0
100 J=31,58 SEC=COREB NSEG=2 ANG=0
101 J=4,10 SEC=COREB NSEG=2 ANG=0
102 J=5,11 SEC=COREB NSEG=2 ANG=0
103 J=38,62 SEC=COREB NSEG=2 ANG=0
104 J=45,69 SEC=COREB NSEG=2 ANG=0
105 J=40,64 SEC=COREB NSEG=2 ANG=0
106 J=43,67 SEC=COREB NSEG=2 ANG=0
107 J=12,6 SEC=COREB NSEG=2 ANG=0
108 J=13,7 SEC=COREB NSEG=2 ANG=0
109 J=70,46 SEC=COREB NSEG=2 ANG=0
110 J=77,53 SEC=COREB NSEG=2 ANG=0
111 J=71,47 SEC=COREB NSEG=2 ANG=0
112 J=76,52 SEC=COREB NSEG=2 ANG=0
113 J=72,48 SEC=COREB NSEG=2 ANG=0
114 J=75,51 SEC=COREB NSEG=2 ANG=0
115 J=35,59 SEC=COREB NSEG=2 ANG=0
127 J=34,29 SEC=W14X109 NSEG=2 ANG=0 IOFF=14 JOFF=8 RIGID=1
130 J=33,30 SEC=W14X109 NSEG=2 ANG=0 IOFF=14 JOFF=8 RIGID=1

LOAD
 NAME=CVX
  TYPE=FORCE
   ADD=20 UX=.3929
   ADD=19 UX=.4303
   ADD=18 UX=.1768
 NAME=NEHRP
  TYPE=FORCE
   ADD=20 UX=43.7
   ADD=19 UX=47.9
   ADD=18 UX=19.7
 NAME=GRAVITY
  TYPE=DISTRIBUTED SPAN
   ADD=7 RD=0,1 UZ=-.06,-.06
   ADD=9 RD=0,1 UZ=-.06,-.06
   ADD=26 RD=0,1 UZ=-.06,-.06
   ADD=30 RD=0,1 UZ=-.06,-.06
   ADD=1 RD=0,1 UZ=-.13,-.13
   ADD=3 RD=0,1 UZ=-.13,-.13
```

435

```
    ADD=4  RD=0,1  UZ=-.13,-.13
    ADD=6  RD=0,1  UZ=-.13,-.13
    ADD=31 RD=0,1  UZ=-.13,-.13
    ADD=33 RD=0,1  UZ=-.13,-.13
    ADD=34 RD=0,1  UZ=-.13,-.13
    ADD=36 RD=0,1  UZ=-.13,-.13
  NAME=1STMODE
   TYPE=FORCE
    ADD=20  UX=125.1
    ADD=19  UX=156.6
    ADD=18  UX=63.6
  NAME=RMODE
   TYPE=FORCE
    ADD=20  UX=93.9
    ADD=19  UX=-27
    ADD=18  UX=-275.7
  NAME=DEAD
  NAME=LIVE
  NAME=1MODDBE
   TYPE=FORCE
    ADD=20  UX=41.7
    ADD=19  UX=52.2
    ADD=18  UX=21.2
  NAME=RMODBE
   TYPE=FORCE
    ADD=20  UX=31.3
    ADD=19  UX=-9
    ADD=18  UX=-91.9
  NAME=DDLL
  NAME=UNIFORM
   TYPE=FORCE
    ADD=20  UX=.2127
    ADD=19  UX=.39365
    ADD=18  UX=.39365

MODE
 TYPE=EIGEN N=3 TOL=.00001

COMBO
 NAME=DSTL1
  LOAD=CVX  SF=1
  LOAD=NEHRP  SF=1
  LOAD=GRAVITY  SF=1
  LOAD=1STMODE  SF=1
  LOAD=RMODE  SF=1
  LOAD=DEAD  SF=1
  LOAD=1MODDBE  SF=1
  LOAD=RMODBE  SF=1
  LOAD=DDLL  SF=1
  LOAD=UNIFORM  SF=1
 NAME=DSTL2
  LOAD=CVX  SF=1
  LOAD=NEHRP  SF=1
  LOAD=GRAVITY  SF=1
  LOAD=1STMODE  SF=1
  LOAD=RMODE  SF=1
```

```
      LOAD=DEAD  SF=1
      LOAD=LIVE  SF=1
      LOAD=1MODDBE  SF=1
      LOAD=RMODBE  SF=1
      LOAD=DDLL  SF=1
      LOAD=UNIFORM  SF=1

OUTPUT
; No Output Requested

END

; The following data is used for graphics, design and pushover analysis.
; If changes are made to the analysis data above, then the following data
; should be checked for consistency.
SAP2000 V7.12 SUPPLEMENTAL DATA
  GRID GLOBAL  X "1"  -486
  GRID GLOBAL  X "2"  -162
  GRID GLOBAL  X "3"  -6
  GRID GLOBAL  X "4"  6
  GRID GLOBAL  X "5"  162
  GRID GLOBAL  X "6"  486
  GRID GLOBAL  Y "7"  0
  GRID GLOBAL  Z "8"  0
  GRID GLOBAL  Z "9"  156
  GRID GLOBAL  Z "10"  174
  GRID GLOBAL  Z "11"  325.44
  GRID GLOBAL  Z "12"  343.44
  GRID GLOBAL  Z "13"  494.88
  GRID GLOBAL  Z "14"  512.88
  MATERIAL STEEL FY 50
  MATERIAL A36 FY 36
  MATERIAL CONC FYREBAR 60 FYSHEAR 40 FC 4 FCSHEAR 4
  FRAMESECTION FS1 NAME BASEPLAT
  FRAMESECTION FS2 NAME TS10X10X5/8
  FRAMESECTION FS3 NAME TS8X8X1/4
  FRAMESECTION FS4 NAME TS6X6X1/4
  FRAMESECTION FS5 NAME TS6X6X3/8
  FRAMESECTION FS6 NAME TS8X8X1/2
  STATICLOAD CVX TYPE DEAD
  STATICLOAD NEHRP TYPE DEAD
  STATICLOAD GRAVITY TYPE DEAD
  STATICLOAD 1STMODE TYPE DEAD
  STATICLOAD RMODE TYPE DEAD
  STATICLOAD DEAD TYPE DEAD
  STATICLOAD LIVE TYPE LIVE
  STATICLOAD 1MODDBE TYPE DEAD
  STATICLOAD RMODBE TYPE DEAD
  STATICLOAD DDLL TYPE DEAD
  STATICLOAD UNIFORM TYPE DEAD
  COMBO DSTL1 DESIGN STEEL
  COMBO DSTL2 DESIGN STEEL
  STEELDESIGN "AISC-ASD89"
  PUSHCASE "GRAVITY"  CONTROL FORCE  JOINT 20  DOF U3
  PUSHCASE "GRAVITY"  PDELTA NO
```

437

PUSHCASE "GRAVITY" MINSTEPS 1 MAXNULLSTEPS 50 MAXTOTALSTEPS 200 MAXITER 10
PUSHCASE "GRAVITY" ITERTOL .0001 EVENTTOL .01
PUSHCASE "GRAVITY" LOADTYPE STATIC LOAD GRAVITY SCALEFACTOR 1
PUSHCASE "PUSHM1" CONTROL DISP TARGET 20.5152 JOINT 20 DOF U1
PUSHCASE "PUSHM1" STARTCASE "GRAVITY"
PUSHCASE "PUSHM1" MINSTEPS 10 MAXNULLSTEPS 50 MAXTOTALSTEPS 200 MAXITER 10
PUSHCASE "PUSHM1" ITERTOL .0001 EVENTTOL .01
PUSHCASE "PUSHM1" LOADTYPE MODE NUMBER 1 SCALEFACTOR 1
PUSHCASE "PUSHUNIF" CONTROL DISP TARGET 20.5152 JOINT 20 DOF U1
PUSHCASE "PUSHUNIF" STARTCASE "GRAVITY"
PUSHCASE "PUSHUNIF" MINSTEPS 10 MAXNULLSTEPS 50 MAXTOTALSTEPS 200 MAXITER 10
PUSHCASE "PUSHUNIF" ITERTOL .0001 EVENTTOL .01
PUSHCASE "PUSHUNIF" LOADTYPE STATIC LOAD UNIFORM SCALEFACTOR 1
PUSHCASE "PUSHCVX" CONTROL DISP TARGET 20.5152 JOINT 20 DOF U1
PUSHCASE "PUSHCVX" STARTCASE "GRAVITY"
PUSHCASE "PUSHCVX" MINSTEPS 10 MAXNULLSTEPS 50 MAXTOTALSTEPS 200 MAXITER 10
PUSHCASE "PUSHCVX" ITERTOL .0001 EVENTTOL .01
PUSHCASE "PUSHCVX" LOADTYPE STATIC LOAD CVX SCALEFACTOR 1
HINGE "USER" TYPE M3 SYMMETRIC
HINGE "USER" TYPE M3 B 1 1 C 6 1 D 8 1 E 10 1
HINGE "USER" TYPE M3 IO 2 LS 4 CP 6
HINGE "USERP" TYPE M3 SYMMETRIC
HINGE "USERP" TYPE M3 B 1 1 C 16 1 D 20 1 E 40 1
HINGE "USERP" TYPE M3 IO 2 LS 4 CP 6
FRAMEHINGE 22 HINGE "USER" RDISTANCE .08046
FRAMEHINGE 22 HINGE "USER" RDISTANCE .87356
FRAMEHINGE 23 HINGE "USER" RDISTANCE .12984
FRAMEHINGE 23 HINGE "USER" RDISTANCE .87016
FRAMEHINGE 24 HINGE "USER" RDISTANCE .12984
FRAMEHINGE 24 HINGE "USER" RDISTANCE .8760623
FRAMEHINGE 28 HINGE "USER" RDISTANCE .12984
FRAMEHINGE 28 HINGE "USER" RDISTANCE .8760623
FRAMEHINGE 29 HINGE "USER" RDISTANCE .12984
FRAMEHINGE 29 HINGE "USER" RDISTANCE .87016
FRAMEHINGE 39 HINGE "USER" RDISTANCE .12984
FRAMEHINGE 39 HINGE "USER" RDISTANCE .87016
FRAMEHINGE 40 HINGE "USER" RDISTANCE .12984
FRAMEHINGE 40 HINGE "USER" RDISTANCE .8760623
FRAMEHINGE 42 HINGE "USER" RDISTANCE .12984
FRAMEHINGE 42 HINGE "USER" RDISTANCE .87016
FRAMEHINGE 43 HINGE "USER" RDISTANCE .12984
FRAMEHINGE 43 HINGE "USER" RDISTANCE .8760623
FRAMEHINGE 1 HINGE "USER" RDISTANCE .0648
FRAMEHINGE 1 HINGE "USER" RDISTANCE .935185
FRAMEHINGE 3 HINGE "USER" RDISTANCE .070988
FRAMEHINGE 3 HINGE "USER" RDISTANCE .9290125
FRAMEHINGE 4 HINGE "USER" RDISTANCE .0648
FRAMEHINGE 4 HINGE "USER" RDISTANCE .935185
FRAMEHINGE 6 HINGE "USER" RDISTANCE .070988
FRAMEHINGE 6 HINGE "USER" RDISTANCE .9290125
FRAMEHINGE 7 HINGE "USER" RDISTANCE .0648
FRAMEHINGE 7 HINGE "USER" RDISTANCE .935185

```
FRAMEHINGE 9  HINGE "USER"  RDISTANCE .0648
FRAMEHINGE 9  HINGE "USER"  RDISTANCE .9352
FRAMEHINGE 44  HINGE "USER"  RDISTANCE .08046
FRAMEHINGE 44  HINGE "USER"  RDISTANCE .87356
FRAMEHINGE 127  HINGE "USER"  RDISTANCE .08046
FRAMEHINGE 127  HINGE "USER"  RDISTANCE .87356
FRAMEHINGE 130  HINGE "USER"  RDISTANCE .08046
FRAMEHINGE 130  HINGE "USER"  RDISTANCE .87356
FRAMEHINGE 26  HINGE "USER"  RDISTANCE .12963
FRAMEHINGE 26  HINGE "USER"  RDISTANCE 1
FRAMEHINGE 30  HINGE "USER"  RDISTANCE 0
FRAMEHINGE 30  HINGE "USER"  RDISTANCE .87037
FRAMEHINGE 31  HINGE "USER"  RDISTANCE .149753
FRAMEHINGE 31  HINGE "USER"  RDISTANCE 1
FRAMEHINGE 33  HINGE "USER"  RDISTANCE 0
FRAMEHINGE 33  HINGE "USER"  RDISTANCE .858025
FRAMEHINGE 34  HINGE "USER"  RDISTANCE .149753
FRAMEHINGE 34  HINGE "USER"  RDISTANCE 1
FRAMEHINGE 36  HINGE "USER"  RDISTANCE 0
FRAMEHINGE 36  HINGE "USER"  RDISTANCE .858025
FRAMEHINGE 96  HINGE "USERP"  RDISTANCE 0
FRAMEHINGE 96  HINGE "USERP"  RDISTANCE 1
FRAMEHINGE 97  HINGE "USERP"  RDISTANCE 0
FRAMEHINGE 97  HINGE "USERP"  RDISTANCE 1
FRAMEHINGE 98  HINGE "USERP"  RDISTANCE 0
FRAMEHINGE 98  HINGE "USERP"  RDISTANCE 1
FRAMEHINGE 99  HINGE "USERP"  RDISTANCE 0
FRAMEHINGE 99  HINGE "USERP"  RDISTANCE 1
FRAMEHINGE 100  HINGE "USERP"  RDISTANCE 0
FRAMEHINGE 100  HINGE "USERP"  RDISTANCE 1
FRAMEHINGE 101  HINGE "USERP"  RDISTANCE 0
FRAMEHINGE 101  HINGE "USERP"  RDISTANCE 1
FRAMEHINGE 102  HINGE "USERP"  RDISTANCE 0
FRAMEHINGE 102  HINGE "USERP"  RDISTANCE 1
FRAMEHINGE 103  HINGE "USERP"  RDISTANCE 0
FRAMEHINGE 103  HINGE "USERP"  RDISTANCE 1
FRAMEHINGE 104  HINGE "USERP"  RDISTANCE 0
FRAMEHINGE 104  HINGE "USERP"  RDISTANCE 1
FRAMEHINGE 105  HINGE "USERP"  RDISTANCE 0
FRAMEHINGE 105  HINGE "USERP"  RDISTANCE 1
FRAMEHINGE 106  HINGE "USERP"  RDISTANCE 0
FRAMEHINGE 106  HINGE "USERP"  RDISTANCE 1
FRAMEHINGE 107  HINGE "USERP"  RDISTANCE 0
FRAMEHINGE 107  HINGE "USERP"  RDISTANCE 1
FRAMEHINGE 108  HINGE "USERP"  RDISTANCE 0
FRAMEHINGE 108  HINGE "USERP"  RDISTANCE 1
FRAMEHINGE 109  HINGE "USERP"  RDISTANCE 0
FRAMEHINGE 109  HINGE "USERP"  RDISTANCE 1
FRAMEHINGE 110  HINGE "USERP"  RDISTANCE 0
FRAMEHINGE 110  HINGE "USERP"  RDISTANCE 1
FRAMEHINGE 111  HINGE "USERP"  RDISTANCE 0
FRAMEHINGE 111  HINGE "USERP"  RDISTANCE 1
FRAMEHINGE 112  HINGE "USERP"  RDISTANCE 0
FRAMEHINGE 112  HINGE "USERP"  RDISTANCE 1
FRAMEHINGE 113  HINGE "USERP"  RDISTANCE 0
FRAMEHINGE 113  HINGE "USERP"  RDISTANCE 1
```

FRAMEHINGE 114 HINGE "USERP" RDISTANCE 0
FRAMEHINGE 114 HINGE "USERP" RDISTANCE 1
FRAMEHINGE 2 HINGE "USERP" RDISTANCE 0
FRAMEHINGE 2 HINGE "USERP" RDISTANCE 1
FRAMEHINGE 5 HINGE "USERP" RDISTANCE 0
FRAMEHINGE 5 HINGE "USERP" RDISTANCE 1
FRAMEHINGE 10 HINGE "USERP" RDISTANCE 0
FRAMEHINGE 10 HINGE "USERP" RDISTANCE 1
FRAMEHINGE 11 HINGE "USERP" RDISTANCE 0
FRAMEHINGE 11 HINGE "USERP" RDISTANCE 1
FRAMEHINGE 60 HINGE "USERP" RDISTANCE 0
FRAMEHINGE 60 HINGE "USERP" RDISTANCE 1
FRAMEHINGE 68 HINGE "USERP" RDISTANCE 0
FRAMEHINGE 68 HINGE "USERP" RDISTANCE 1
FRAMEHINGE 87 HINGE "USERP" RDISTANCE 0
FRAMEHINGE 87 HINGE "USERP" RDISTANCE 1
FRAMEHINGE 95 HINGE "USERP" RDISTANCE 0
FRAMEHINGE 95 HINGE "USERP" RDISTANCE 1
FRAMEHINGE 115 HINGE "USERP" RDISTANCE 0
FRAMEHINGE 115 HINGE "USERP" RDISTANCE 1
END SUPPLEMENTAL DATA

APPENDIX K

INPUT FILES FOR NONLINEAR TIME-HISTORY AND PUSHOVER ANALYSIS OF FRAMES WITH DAMPING SYSTEMS IN PROGRAM IDARCD2D

K.1 Introduction

This appendix contains information on the input files for the nonlinear time-history and pushover analysis of selected examples of frames with damping systems in program IDARC2D-Version 5.0. Figure K-1 shows the connectivity and the numbers of beams, columns and energy dissipating braces as required in this program. The input files for nonlinear time history analysis of the following examples are presented:

(a)   Example No.2: frame 3S-75 with linear viscous damping system to provide 10% viscous damping ratio when assuming elastic frame behavior (Fig. 8-2).

(b)   Example No.5: frame 6S-75 with linear viscous damping system to provide 10% viscous damping ratio when assuming elastic frame behavior (Fig. 8-5).

(c)   Example No.6: frame 3S-80 with nonlinear viscous damping system to provide 10% viscous damping ratio when assuming elastic frame behavior in the design basis earthquake (DBE) (Fig. 8-6).

(d)   Example No.8: frame 3S-75 with viscoelastic solid damping system to provide 8.5% viscous damping ratio when assuming elastic frame behavior (Fig. 8-8).

(e)   Example No.9: frame 3S-75 with metallic yielding damping system (Fig. 8-9).

Moreover, input files for the pushover analysis of example No.1: frame 3S-60 with linear viscous damping system to provide 10% viscous damping ratio when assuming elastic frame behavior (Fig. 8-1) are presented. Files for four lateral force patterns are presented: (a) proportional to the first mode, (b) modal (Cvx) pattern, (c) uniform pattern, and (d) modal adaptive pattern.
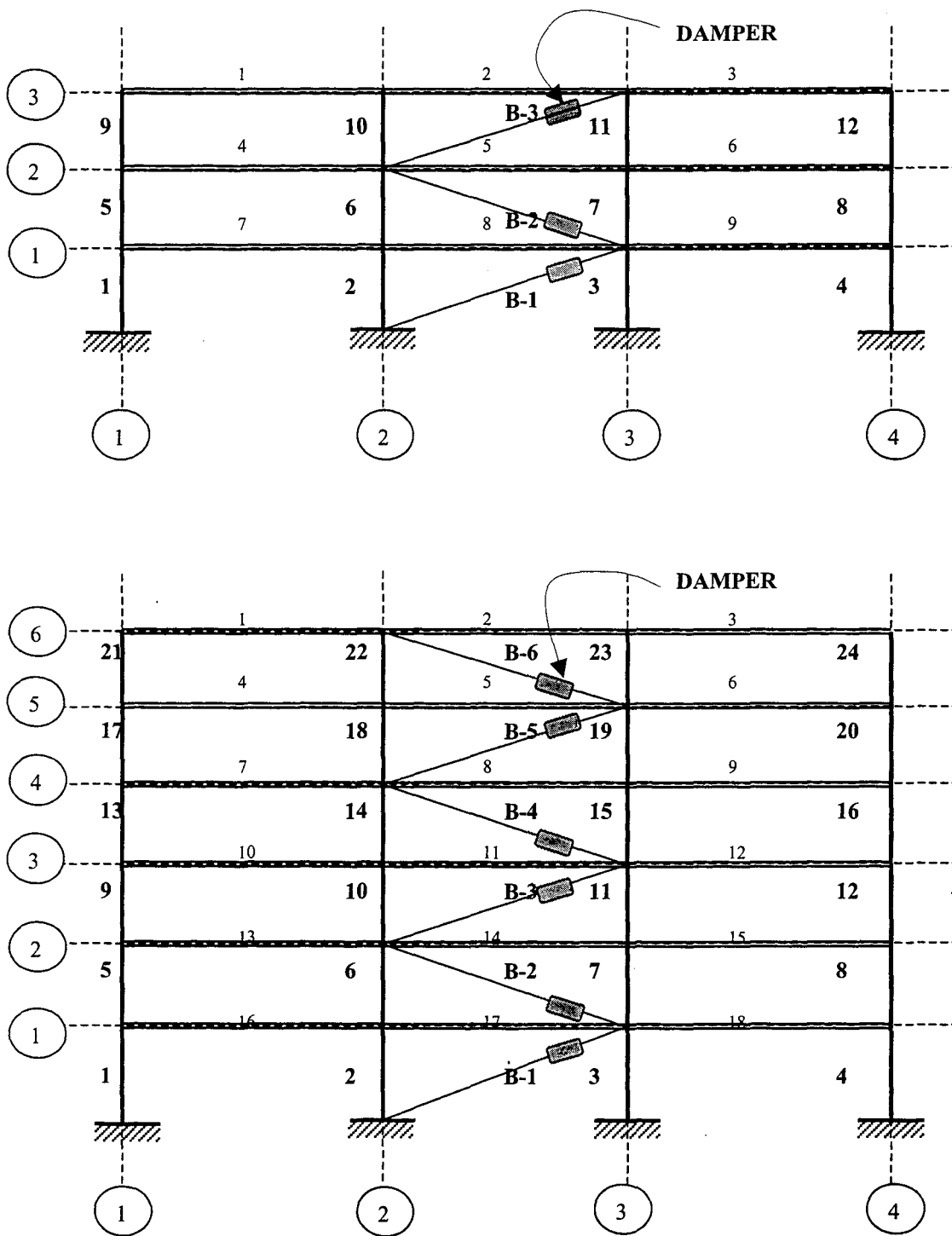
FIGURE K-1 Frame Connectivity and Member Numbers of 3- and 6-story Frame Models in Program IDARC2D

442

IDARC-2D INPUT FILE FOR NONLINEAR TIME HISTORY ANALYSIS OF EXAMPLE No.2: FRAME 3S-75 WITH LINEAR VISCOUS DAMPING SYSTEM TO PROVIDE 10% VISCOUS DAMPING RATIO WHEN ASSUMING ELASTIC FRAME BEHAVIOR

EXAMPLE No.2: FRAME 3S-75 + 10% LVD. ANALYSIS FOR THE DBE.
SET A - CONTROL DATA SET
3, 1, 0, 0, 0, 0, 1, 1
SET A1 - ELEMENTS TYPE
3, 3, 0, 0, 0, 0, 1, 0, 0, 0
SET A2 - ELEMENT DATA
12, 9, 0, 0, 0, 0, 0, 3, 0
SET A3 - SYSTEM OF UNITS
1

SET A4 - FLOOR ELEVATIONS
174.0, 343.44, 512.88
SET A5 - DESCRIPTION OF IDENTICAL FRAMES
1
SET A6 - PLAN CONFIGURATION
4
SET A7 - NODAL WEIGHTS
1, 1, 0, 652.2, 0, 0
2, 1, 0, 652.2, 0, 0
3, 1, 0, 352.4, 0, 0
SET B - MATERIAL PROPERTIES SET
1
SET C - HYSTERETIC MODELING RULES
1
1, 1, 200, 0.001, 0.001, 1.0, 0
SET D - COLUMN PROPERTIES
1
SET D3 COLUMN DATA
1, 174.00, 14.0, 8.0, 0
-1 36.0E6 5.33E3 8.72E4 9.12E3 9.60E3 2.94E-4 1.47E-2 1
                      9.12E3 9.60E3 2.94E-4 1.47E-2 1
2, 169.44, 8.0, 8.0, 0
-1 36.0E6 5.48E3 8.72E4 9.12E3 9.60E3 2.94E-4 1.47E-2 1
                      9.12E3 9.60E3 2.94E-4 1.47E-2 1
3, 169.44, 8.0, 7.0, 0
-1 36.0E6 5.48E3 8.72E4 9.12E3 9.60E3 2.94E-4 1.47E-2 1
                      9.12E3 9.60E3 2.94E-4 1.47E-2 1
SET E - BEAM PROPERTIES
1
SET E2 - BEAM DATA
1 324.0 7.0 7.0 0
-1 7.10E6 4.11E4 1.91E3 2.01E3 3.10E-4 1.55E-2 1

```
                    1.91E3   2.01E3   3.10E-4   1.55E-2   1
2 324.0 7.0 7.0 0
-1 15.02E6 5.66E4   3.46E3   3.64E3   2.67E-4   1.34E-2   1
                    3.46E3   3.64E3   2.67E-4   1.34E-2   1
3 324.0 7.0 7.0 0
-1 16.99E6 6.45E4   3.91E3   4.12E3   2.67E-4   1.34E-2   1
                    3.91E3   4.12E3   2.67E-4   1.34E-2   1
```
BRACE PROPERTIES - J1
```
0 0
1 5.15 875.28 1.0
```
COLUMN CONNECTIVITY - L1
```
1,1,1,1,0,1
2,1,1,2,0,1
3,1,1,3,0,1
4,1,1,4,0,1
5,2,1,1,1,2
6,2,1,2,1,2
7,2,1,3,1,2
8,2,1,4,1,2
9,3,1,1,2,3
10,3,1,2,2,3
11,3,1,3,2,3
12,3,1,4,2,3
```
BEAMS CONNECTIVITY - L2
```
1,1,3,1,1,2
2,1,3,1,2,3
3,1,3,1,3,4
4,2,2,1,1,2
5,2,2,1,2,3
6,2,2,1,3,4
7,3,1,1,1,2
8,3,1,1,2,3
9,3,1,1,3,4
```
BRACES CONNECTIVITY - L8
```
1,1,1,1,1,0,3,2,367.77
2,1,1,1,2,1,2,3,365.63
3,1,1,1,3,2,3,2,365.63
```
SET M - ANALYSIS OPTION
```
3
```
SET M1 - LONG-TERM STATIC LOADING
```
0, 0, 0, 0
```
SET M3 - DYNAMIC ANALYSIS
```
0.5021, 0.0, 0.005, 60.0, 5, 1
```
HORIZONTAL ACC
```
0, 3000, 0.02
```
GROUNDMOTION

```
EQ10.DAT
SET N1.2
0
0, 0, 0, 0, 0
SET N2 - STORY OUTPUT CONTROL
3, 0.02, 1, 2, 3
LEV1E10.OUT
LEV2E10.OUT
LEV3E10.OUT
SET N3 - ELEMENT HYSTERESIS OUTPUT
0, 1, 0, 0, 3, 0
BEAM OUTPUT
4
BRACES OUTPUT
1,2,3
```

IDARC-2D INPUT FILE FOR NONLINEAR TIME HISTORY ANALYSIS OF EXAMPLE No.5: FRAME 6S-75 WITH LINEAR VISCOUS DAMPING SYSTEM TO PROVIDE 10% VISCOUS DAMPING RATIO WHEN ASSUMING ELASTIC FRAME BEHAVIOR

EXAMPLE No.5: FRAME 6S-75 + 10% LINEAR VISCOUS DAMPING. ANALYSIS FOR THE DBE
SET A - CONTROL DATA SET
6, 1, 0, 0, 0, 1, 1, 1
SET A1 - ELEMENTS TYPE
6, 6, 0, 0, 0, 0, 3, 0, 0, 0
SET A2 - ELEMENT DATA
24, 18, 0, 0, 0, 0, 0, 6, 0
SET A3 - SYSTEM OF UNITS
1
SET A4 - FLOOR ELEVATIONS
174.0 343.44 512.88 682.32 851.76 1021.2
SET A5 - DESCRIPTION OF IDENTICAL FRAMES
1
SET A6 - PLAN CONFIGURATION
4
SET A7 - NODAL WEIGHTS
1, 1, 0, 652.2, 0, 0
2, 1, 0, 652.2, 0, 0
3, 1, 0, 652.2, 0, 0
4, 1, 0, 652.2, 0, 0
5, 1, 0, 652.2, 0, 0
6, 1, 0, 352.4, 0, 0
SET B - MATERIAL PROPERTIES SET
1
SET C - HYSTERETIC MODELING RULES
1
1, 1, 200, 0.001, 0.001, 1.0, 0
SET D - COLUMN PROPERTIES
1
SET D3 - COLUMN DATA
1, 174.00, 14.0, 12.0, 0
-1 62.1E6 8.63E3 14.7E4 1.30E4   1.37E4   2.42E-4   1.21E-2 1
                            1.30E4   1.37E4   2.42E-4   1.21E-2 1
2, 169.44, 12.0, 10.5, 0
-1 62.1E6 8.87E3 14.7E4 1.34E4   1.41E4   2.49E-4   1.25E-2 1
                            1.34E4   1.41E4   2.49E-4   1.25E-2 1
3, 169.44, 10.5, 10.5, 0
-1 44.4E6 6.64E3 11.0E4 9.72E3   10.2E3 2.54E-4 1.27E-2 1
                            9.72E3   10.2E3 2.54E-4 1.27E-2 1
4, 169.44, 10.5, 10.5, 0

446

```
-1 44.4E6  6.64E3  11.0E4   10.1E3   10.7E3   2.64E-4  1.32E-2  1
                            10.1E3   10.7E3   2.64E-4  1.32E-2  1
5, 169.44, 10.5,  8.0, 0
-1 29.0E6  4.54E3  7.15E4   6.87E3   7.23E3   2.75E-4  1.37E-2  1
                            6.87E3   7.23E3   2.75E-4  1.37E-2  1
6, 169.44,  8.0,  8.0, 0
-1 29.0E6  4.54E3  7.15E4   7.26E3   7.64E3   2.90E-4  1.45E-2  1
                            7.26E3   7.64E3   2.90E-4  1.45E-2  1
SET E  - BEAM PROPERTIES
1
SET E2 - BEAM DATA
1 324.0  7.0 7.0  0
-1 10.9E6  5.07E4  2.57E3  2.70E3  2.73E-4  1.37E-2  1
                   2.57E3  2.70E3  2.73E-4  1.37E-2  1
2 324.0  7.0 7.0  0
-1 15.0E6  5.66E4  3.46E3  3.65E3  2.67E-4  1.33E-2  1
                   3.46E3  3.65E3  2.67E-4  1.33E-2  1
3 324.0  7.0 7.0  0
-1 24.4E6  8.39E4  4.53E3  4.77E3  2.15E-4  1.07E-2  1
                   4.53E3  4.77E3  2.15E-4  1.07E-2  1
4 324.0  7.0 7.0  0
-1 28.5E6  9.19E4  5.23E3  5.50E3  2.12E-4  1.06E-2  1
                   5.23E3  5.50E3  2.12E-4  1.06E-2  1
5 324.0  7.0 7.0  0
-1 38.6E6  9.74E4  6.84E3  7.20E3  2.05E-4  1.03E-2  1
                   6.84E3  7.20E3  2.05E-4  1.03E-2  1
6 324.0  7.0 7.0  0
-1 45.0E6  11.8E4  7.27E3  7.65E3  1.87E-4  9.36E-3  1
                   7.27E3  7.65E3  1.87E-4  9.36E-3  1
BRACE PROPERTIES - J1
1 0
1  12.96    1142.0   1.0
2  9.620    1142.0   1.0
3  7.854    1142.0   1.0
COLUMN CONNECTIVITY - L1
1,1,1,1,0,1
2,1,1,2,0,1
3,1,1,3,0,1
4,1,1,4,0,1
5,2,1,1,1,2
6,2,1,2,1,2
7,2,1,3,1,2
8,2,1,4,1,2
9,3,1,1,2,3
10,3,1,2,2,3
11,3,1,3,2,3
```

12,3,1,4,2,3
13,4,1,1,3,4
14,4,1,2,3,4
15,4,1,3,3,4
16,4,1,4,3,4
17,5,1,1,4,5
18,5,1,2,4,5
19,5,1,3,4,5
20,5,1,4,4,5
21,6,1,1,5,6
22,6,1,2,5,6
23,6,1,3,5,6
24,6,1,4,5,6
BEAMS CONNECTIVITY - L2
1,1,6,1,1,2
2,1,6,1,2,3
3,1,6,1,3,4
4,2,5,1,1,2
5,2,5,1,2,3
6,2,5,1,3,4
7,3,4,1,1,2
8,3,4,1,2,3
9,3,4,1,3,4
10,4,3,1,1,2
11,4,3,1,2,3
12,4,3,1,3,4
13,5,2,1,1,2
14,5,2,1,2,3
15,5,2,1,3,4
16,6,1,1,1,2
17,6,1,1,2,3
18,6,1,1,3,4
BRACES CONNECTIVITY - L8
1,1,1,1,1,0,3,2,367.77
2,1,1,1,2,1,2,3,365.63
3,1,1,2,3,2,3,2,365.63
4,1,1,2,4,3,2,3,355.63
5,1,1,3,5,4,3,2,365.63
6,1,1,3,6,5,2,3,365.63
SET M - ANALYSIS OPTION
3
SET M1 - LONG-TERM STATIC LOADING
18, 0, 0, 0
1 0
UNIFORMLY LOADED BEAMS
1 1 0.08

448

```
1  2  0.08
1  3  0.08
2  4  0.16
2  5  0.16
2  6  0.16
2  7  0.16
2  8  0.16
2  9  0.16
2  10  0.16
2  11  0.16
2  12  0.16
2  13  0.16
2  14  0.16
2  15  0.16
2  16  0.16
2  17  0.16
2  18  0.16
SET M3 - DYNAMIC ANALYSIS
0.2331, 0.0, 0.005, 98.0, 5, 1
HORIZONTAL ACC
0, 4932, 0.02
GROUNDMOTION
EQ20.DAT
SET N1.2
0
0, 0, 0, 0, 0
SET N2 - STORY OUTPUT CONTROL
6, 0.02, 1, 2, 3, 4, 5, 6
LEV1E20.OUT
LEV2E20.OUT
LEV3E20.OUT
LEV4E20.OUT
LEV5E20.OUT
LEV6E20.OUT
SET N3 - ELEMENT HYSTERESIS OUTPUT
0, 0, 0, 0, 0, 0
```

IDARC-2D INPUT FILE FOR NONLINEAR TIME HISTORY ANALYSIS OF EXAMPLE No.6: FRAME 3S-80 WITH NONLINEAR VISCOUS DAMPING SYSTEM TO PROVIDE 10% VISCOUS DAMPING RATIO WHEN ASSUMING ELASTIC FRAME BEHAVIOR IN THE DESIGN BASIS EARTHQUAKE

FRAME 3S80 + 10% NONLINEAR DAMPING IN DBE - ANALYSIS FOR THE DBE
SET A - CONTROL DATA SET
3, 1, 0, 0, 0, 0, 1, 1
SET A1 - ELEMENTS TYPE
3, 3, 0, 0, 0, 0, 1, 0, 0, 0
SET A2 - ELEMENT DATA
12, 9, 0, 0, 0, 0, 0, 3, 0
SET A3 - SYSTEM OF UNITS
1
SET A4 - FLOOR ELEVATIONS
174.0, 343.44, 512.88
SET A5 - DESCRIPTION OF IDENTICAL FRAMES
1
SET A6 - PLAN CONFIGURATION
4
SET A7 - NODAL WEIGHTS
1, 1, 0, 652.2, 0, 0
2, 1, 0, 652.2, 0, 0
3, 1, 0, 352.4, 0, 0
SET B - MATERIAL PROPERTIES SET
1
SET C - HYSTERETIC MODELING RULES
1
1, 1, 200, 0.001, 0.001, 1.0, 0
SET D - COLUMN PROPERTIES
1
SET D3 - COLUMN DATA
1, 174.00, 14.0, 9.0, 0
-1 36.0E6 5.33E3 8.72E4 9.12E3 9.60E3 2.94E-4 1.47E-2 1
                         9.12E3 9.60E3 2.94E-4 1.47E-2 1
2, 169.44, 9.0, 9.0, 0
-1 36.0E6 5.48E3 8.72E4 9.12E3 9.60E3 2.94E-4 1.47E-2 1
                         9.12E3 9.60E3 2.94E-4 1.47E-2 1
3, 169.44, 9.0, 7.0, 0
-1 36.0E6 5.48E3 8.72E4 9.12E3 9.60E3 2.94E-4 1.47E-2 1
                         9.12E3 9.60E3 2.94E-4 1.47E-2 1
SET E - BEAM PROPERTIES
1
SET E2 - BEAM DATA

1 324.0 7.0 7.0 0
-1 8.44E6 4.33E4 2.13E3 2.37E3 3.08E-4 9.25E-3 1
                2.13E3 2.37E3 3.08E-4 9.25E-3 1
2 324.0 7.0 7.0 0
-1 14.8E6 6.16E4 3.16E3 3.33E3 2.47E-4 7.41E-3 1
                3.16E3 3.33E3 2.47E-4 7.41E-3 1
3 324.0 7.0 7.0 0
-1 20.65E6 7.52E4 4.31E3 4.54E3 2.42E-4 7.25E-3 1
                4.31E3 4.54E3 2.42E-4 7.25E-3 1
BRACE PROPERTIES - J1
0 0
1 16.35 875.28 0.5
COLUMN CONNECTIVITY - L1
1,1,1,1,0,1
2,1,1,2,0,1
3,1,1,3,0,1
4,1,1,4,0,1
5,2,1,1,1,2
6,2,1,2,1,2
7,2,1,3,1,2
8,2,1,4,1,2
9,3,1,1,2,3
10,3,1,2,2,3
11,3,1,3,2,3
12,3,1,4,2,3
BEAMS CONNECTIVITY - L2
1,1,3,1,1,2
2,1,3,1,2,3
3,1,3,1,3,4
4,2,2,1,1,2
5,2,2,1,2,3
6,2,2,1,3,4
7,3,1,1,1,2
8,3,1,1,2,3
9,3,1,1,3,4
BRACES CONNECTIVITY - L8
1,1,1,1,1,0,3,2,365.63
2,1,1,1,2,1,2,3,365.63
3,1,1,1,3,2,3,2,365.63
SET M - ANALYSIS OPTION
3
SET M1 - LONG-TERM STATIC LOADING
0, 0, 0, 0
SET M3 - DYNAMIC ANALYSIS
0.258, 0.0, 0.005, 98, 5, 1
HORIZONTAL ACC

0, 4932, 0.02
GROUNDMOTION
EQ19.DAT
SET N1.2
0
0, 0, 0, 0, 0
SET N2 - STORY OUTPUT CONTROL
3, 0.02, 1, 2, 3
LEV1E19.OUT
LEV2E19.OUT
LEV3E19.OUT
SET N3 - ELEMENT HYSTERESIS OUTPUT
0, 0, 0, 0, 3, 0
braces output
1,2,3

IDARC-2D INPUT FILE FOR NONLINEAR TIME HISTORY ANALYSIS OF EXAMPLE No.8: FRAME 3S-75 WITH VISCOELASTIC SOLID DAMPING SYSTEM TO PROVIDE 8.5% VISCOUS DAMPING RATIO WHEN ASSUMING ELASTIC FRAME BEHAVIOR

FRAME 3S-75 WITH SOLID VE DEVICES + 8.5% LINEAR VISCOUS DAMPING.
SET A - CONTROL DATA SET
3, 1, 0, 0, 0, 0, 1, 1
SET A1 - ELEMENTS TYPE
3, 3, 0, 0, 0, 0, 2, 0, 0, 0
SET A2 - ELEMENT DATA
12, 9, 0, 0, 0, 0, 0, 6, 0
SET A3 - SYSTEM OF UNITS
1
SET A4 - FLOOR ELEVATIONS
174.0, 343.44, 512.88
SET A5 - DESCRIPTION OF IDENTICAL FRAMES
1
SET A6 - PLAN CONFIGURATION
4
SET A7 - NODAL WEIGHTS
1, 1, 0, 652.2, 0, 0
2, 1, 0, 652.2, 0, 0
3, 1, 0, 352.4, 0, 0
SET B - MATERIAL PROPERTIES SET
1
SET C - HYSTERETIC MODELING RULES
1
1, 1, 200, 0.001, 0.001, 1.0, 0
SET D - COLUMN PROPERTIES
1
SET D3 - COLUMN DATA
1, 174.00, 14.0, 8.0, 0
-1 36.0E6 5.33E3 8.72E4 9.12E3 9.60E3 2.94E-4 1.47E-2 1
                            9.12E3 9.60E3 2.94E-4 1.47E-2 1
2, 169.44, 8.0, 8.0, 0
-1 36.0E6 5.48E3 8.72E4 9.12E3 9.60E3 2.94E-4 1.47E-2 1
                            9.12E3 9.60E3 2.94E-4 1.47E-2 1
3, 169.44, 8.0, 7.0, 0
-1 36.0E6 5.48E3 8.72E4 9.12E3 9.60E3 2.94E-4 1.47E-2 1
                            9.12E3 9.60E3 2.94E-4 1.47E-2 1
SET E - BEAM PROPERTIES
1
SET E2 - BEAM DATA
1 324.0 7.0 7.0 0
-1 7.10E6 4.11E4 1.91E3 2.01E3 3.10E-4 1.55E-2 1

```
                     1.91E3   2.01E3   3.10E-4  1.55E-2  1
2 324.0  7.0  7.0  0
-1 15.02E6  5.66E4   3.46E3   3.64E3   2.67E-4  1.34E-2  1
                     3.46E3   3.64E3   2.67E-4  1.34E-2  1
3 324.0  7.0  7.0  0
-1 16.99E6  6.45E4   3.91E3   4.12E3   2.67E-4  1.34E-2  1
                     3.91E3   4.12E3   2.67E-4  1.34E-2  1
```
VISCOELASTIC BRACE PROPERTIES - J3
```
0  0
1    5.6  139.8  1.00
2  500.0  14.4  1.00
```
COLUMN CONNECTIVITY - L1
```
1,1,1,1,0,1
2,1,1,2,0,1
3,1,1,3,0,1
4,1,1,4,0,1
5,2,1,1,1,2
6,2,1,2,1,2
7,2,1,3,1,2
8,2,1,4,1,2
9,3,1,1,2,3
10,3,1,2,2,3
11,3,1,3,2,3
12,3,1,4,2,3
```
BEAMS CONNECTIVITY - L2
```
1,1,3,1,1,2
2,1,3,1,2,3
3,1,3,1,3,4
4,2,2,1,1,2
5,2,2,1,2,3
6,2,2,1,3,4
7,3,1,1,1,2
8,3,1,1,2,3
9,3,1,1,3,4
```
BRACES CONNECTIVITY - L8
```
1,1,1,1,1,0,3,2,367.77
2,1,1,1,2,1,2,3,365.63
3,1,1,1,3,2,3,2,365.63
4,1,1,2,1,0,2,1,367.77
5,1,1,2,2,1,1,2,365.63
6,1,1,2,3,2,2,1,365.63
```
SET M - ANALYSIS OPTION
```
3
```
SET M1 - LONG-TERM STATIC LOADING
```
0, 0, 0, 0
```
SET M3 - DYNAMIC ANALYSIS

0.2331, 0.0, 0.005, 98.0, 5, 1
HORIZONTAL ACC
0, 4932, 0.02
GROUNDMOTION
EQ20.DAT
SET N1.2
0
0, 0, 0, 0, 0
SET N2 - STORY OUTPUT CONTROL
3, 0.02, 1, 2, 3
LEV1E20.OUT
LEV2E20.OUT
LEV3E20.OUT
SET N3 - ELEMENT HYSTERESIS OUTPUT
12, 0, 0, 0, 6, 0
COLUMNS OUTPUT
1,2,3,4,5,6,7,8,9,10,11,12
BRACES OUTPUT
1,2,3,4,5,6

FRAME 3S-75V METALLIC YIELDING DEVICES. ANALYSIS FOR DBE.
SET A - CONTROL DATA SET
3, 1, 0, 0, 0, 0, 1, 1
SET A1 - ELEMENTS TYPE
3, 3, 0, 0, 0, 0, 0, 3, 0, 0
SET A2 - ELEMENT DATA
12, 9, 0, 0, 0, 0, 0, 3, 0
SET A3 - SYSTEM OF UNITS
1
SET A4 - FLOOR ELEVATIONS
174.0, 343.44, 512.88
SET A5 - DESCRIPTION OF IDENTICAL FRAMES
1
SET A6 - PLAN CONFIGURATION
4
SET A7 - NODAL WEIGHTS
1, 1, 0, 652.2, 0, 0
2, 1, 0, 652.2, 0, 0
3, 1, 0, 352.4, 0, 0
SET B - MATERIAL PROPERTIES SET
1
SET C - HYSTERETIC MODELING RULES
1
1, 1, 200, 0.001, 0.001, 1.0, 0
SET D - COLUMN PROPERTIES
1
SET D3 - COLUMN DATA
1, 174.00, 14.0, 8.0, 0
-1 36.0E6 5.33E3 8.72E4 9.12E3 9.60E3 2.94E-4 1.47E-2 1
                        9.12E3 9.60E3 2.94E-4 1.47E-2 1
2, 169.44, 8.0, 8.0, 0
-1 36.0E6 5.48E3 8.72E4 9.12E3 9.60E3 2.94E-4 1.47E-2 1
                        9.12E3 9.60E3 2.94E-4 1.47E-2 1
3, 169.44, 8.0, 7.0, 0
-1 36.0E6 5.48E3 8.72E4 9.12E3 9.60E3 2.94E-4 1.47E-2 1
                        9.12E3 9.60E3 2.94E-4 1.47E-2 1
SET E - BEAM PROPERTIES
1
SET E2 - BEAM DATA
1 324.0 7.0 7.0 0
-1 7.10E6 4.11E4 1.91E3 2.01E3 3.10E-4 1.55E-2 1
                1.91E3 2.01E3 3.10E-4 1.55E-2 1

2 324.0 7.0 7.0 0
-1 15.02E6 5.66E4 3.46E3 3.64E3 2.67E-4 1.34E-2 1
                3.46E3 3.64E3 2.67E-4 1.34E-2 1
3 324.0 7.0 7.0 0
-1 16.99E6 6.45E4 3.91E3 4.12E3 2.67E-4 1.34E-2 1
                3.91E3 4.12E3 2.67E-4 1.34E-2 1
BRACE PROPERTIES - J3
0
1 152 81.25 0.0005
2 114 60.93 0.0005
3 88.6 47.39 0.0005
COLUMN CONNECTIVITY - L1
1,1,1,1,0,1
2,1,1,2,0,1
3,1,1,3,0,1
4,1,1,4,0,1
5,2,1,1,1,2
6,2,1,2,1,2
7,2,1,3,1,2
8,2,1,4,1,2
9,3,1,1,2,3
10,3,1,2,2,3
11,3,1,3,2,3
12,3,1,4,2,3
BEAMS CONNECTIVITY - L2
1,1,3,1,1,2
2,1,3,1,2,3
3,1,3,1,3,4
4,2,2,1,1,2
5,2,2,1,2,3
6,2,2,1,3,4
7,3,1,1,1,2
8,3,1,1,2,3
9,3,1,1,3,4
BRACES CONNECTIVITY - L8
1,1,2,1,1,0,3,2,367.77
2,1,2,2,2,1,2,3,365.63
3,1,2,3,3,2,3,2,365.63
SET M - ANALYSIS OPTION
3
SET M1 - LONG-TERM STATIC LOADING
0, 0, 0, 0
SET M3 - DYNAMIC ANALYSIS
0.2331, 0.0, 0.005, 98, 5, 1
HORIZONTAL ACC
0, 4932, 0.02

```
GROUNDMOTION
EQ20.DAT
SET N1.2
0
0, 0, 0, 0, 0
SET N2 - STORY OUTPUT CONTROL
3, 0.02, 1, 2, 3
LEV1E20.OUT
LEV2E20.OUT
LEV3E20.OUT
SET N3 - ELEMENT HYSTERESIS OUTPUT
0, 0, 0, 0, 3, 0
BRACES OUTPUT
1,2,3
```

IDARC-2D INPUT FILE FOR PUSHOVER ANALYSIS OF EXAMPLE No.1: FRAME 3S-60 WITH LINEAR VISCOUS DAMPING SYSTEM TO PROVIDE 10% VISCOUS DAMPING RATIO WHEN ASSUMING ELASTIC FRAME BEHAVIOR. FIRST MODE LATERAL FORCE PATTERN.

FRAME 3S-60 - PUSHOVER ANALYSIS- FIRST MODE PATTERN
SET A - CONTROL DATA SET
3, 1, 0, 0, 0, 0, 1, 1
SET A1 - ELEMENTS TYPE
3, 3, 0, 0, 0, 0, 0, 0, 0, 0
SET A2 - ELEMENT DATA
12, 9, 0, 0, 0, 0, 0, 0, 0
SET A3 - SYSTEM OF UNITS
1
SET A4 - FLOOR ELEVATIONS
174., 343.44, 512.88
SET A5 - DESCRIPTION OF IDENTICAL FRAMES
1
SET A6 - PLAN CONFIGURATION
4
SET A7 - NODAL WEIGHTS
1, 1, 0, 652.2, 0, 0
2, 1, 0, 652.2, 0, 0
3, 1, 0, 352.4, 0, 0
SET B - MATERIAL PROPERTIES SET
1
SET C - HYSTERETIC MODELING RULES
1
1, 1, 200, 0.001, 0.001, 1.0, 0
SET D - COLUMN PROPERTIES
1
SET D3 - COLUMN DATA
1, 174.00, 14.0, 8.0, 0
-1 29.0E6 4.42E3 7.16E4 7.46E3 7.85E3 2.98E-4 1.49E-2 0.10
                       7.46E3 7.85E3 2.98E-4 1.49E-2 0.10
2, 169.44, 8.0, 8.0, 0
-1 29.0E6 4.54E3 7.16E4 7.46E3 7.85E3 2.98E-4 1.49E-2 0.10
                       7.46E3 7.85E3 2.98E-4 1.49E-2 0.10
3, 169.44, 8.0, 7.0, 0
-1 29.0E6 4.54E3 7.16E4 7.46E3 7.85E3 2.98E-4 1.49E-2 0.10
                       7.46E3 7.85E3 2.98E-4 1.49E-2 0.10
SET E - BEAM PROPERTIES
1
SET E2 - BEAM DATA
1 324.0 7.0 7.0 0
-1 7.10E6 4.11E4 1.91E3 2.01E3 3.10E-4 1.55E-2 0.10

```
                    1.91E3   2.01E3   3.10E-4  1.55E-2  0.10
2 324.0 7.0 7.0 0
-1 10.88E6 4.60E4  2.57E3   2.70E3   2.93E-4  1.47E-2  0.10
                    2.57E3   2.70E3   2.93E-4  1.47E-2  0.10
3 324.0 7.0 7.0 0
-1 12.99E6 5.43E4  3.04E3   3.20E3   2.70E-4  1.35E-2  0.10
                    3.04E3   3.20E3   2.70E-4  1.35E-2  0.10
```
COLUMN CONNECTIVITY - L1
1,1,1,1,0,1
2,1,1,2,0,1
3,1,1,3,0,1
4,1,1,4,0,1
5,2,1,1,1,2
6,2,1,2,1,2
7,2,1,3,1,2
8,2,1,4,1,2
9,3,1,1,2,3
10,3,1,2,2,3
11,3,1,3,2,3
12,3,1,4,2,3
BEAMS CONNECTIVITY - L2
1,1,3,1,1,2
2,1,3,1,2,3
3,1,3,1,3,4
4,2,2,1,1,2
5,2,2,1,2,3
6,2,2,1,3,4
7,3,1,1,1,2
8,3,1,1,2,3
9,3,1,1,3,4
SET M - ANALYSIS OPTION
2
SET M1 - LONG-TERM STATIC LOADING
0, 0, 0, 0
SET M2 - TYPE OF PUSHOVER
1
SET M2.1 - FORCE CONTROLLED INPUT
4
SET M2.2 - USER INPUT
3
1,2,3
86.9 229.95 185.15
500 5.0
SET N1.1 - PUSHOVER SNAPSHOT CONTROL DATA
0
0 0 0 0 0

SET N2 - STORY OUTPUT CONTROL
3 1 1 2 3
PUSHM1LEV1.OUT
PUSHM1LEV2.OUT
PUSHM1LEV3.OUT
SET N3 - ELEMENT OUTPUT CONTROL
0 0 0 0 0 0

FRAME 3S-60 - PUSHOVER ANALYSIS- MODAL (Cvx) PATTERN
SET A - CONTROL DATA SET
3, 1, 0, 0, 0, 0, 1, 1
SET A1 - ELEMENTS TYPE
3, 3, 0, 0, 0, 0, 0, 0, 0, 0
SET A2 - ELEMENT DATA
12, 9, 0, 0, 0, 0, 0, 0, 0
SET A3 - SYSTEM OF UNITS
1
SET A4 - FLOOR ELEVATIONS
174., 343.44, 512.88
SET A5 - DESCRIPTION OF IDENTICAL FRAMES
1
SET A6 - PLAN CONFIGURATION
4
SET A7 - NODAL WEIGHTS
1, 1, 0, 652.2, 0, 0
2, 1, 0, 652.2, 0, 0
3, 1, 0, 352.4, 0, 0
SET B - MATERIAL PROPERTIES SET
1
SET C - HYSTERETIC MODELING RULES
1
1, 1, 200, 0.001, 0.001, 1.0, 0
SET D - COLUMN PROPERTIES
1
SET D3 - COLUMN DATA
1, 174.00, 14.0, 8.0, 0
-1 29.0E6 4.42E3 7.16E4 7.46E3 7.85E3 2.98E-4 1.49E-2 0.10
                        7.46E3 7.85E3 2.98E-4 1.49E-2 0.10
2, 169.44, 8.0, 8.0, 0
-1 29.0E6 4.54E3 7.16E4 7.46E3 7.85E3 2.98E-4 1.49E-2 0.10
                        7.46E3 7.85E3 2.98E-4 1.49E-2 0.10
3, 169.44, 8.0, 7.0, 0
-1 29.0E6 4.54E3 7.16E4 7.46E3 7.85E3 2.98E-4 1.49E-2 0.10
                        7.46E3 7.85E3 2.98E-4 1.49E-2 0.10
SET E - BEAM PROPERTIES
1
SET E2 - BEAM DATA
1 324.0 7.0 7.0 0

```
-1  7.10E6  4.11E4  1.91E3  2.01E3  3.10E-4  1.55E-2  0.10
                    1.91E3  2.01E3  3.10E-4  1.55E-2  0.10
2 324.0 7.0 7.0 0
-1 10.88E6  4.60E4  2.57E3  2.70E3  2.93E-4  1.47E-2  0.10
                    2.57E3  2.70E3  2.93E-4  1.47E-2  0.10
3 324.0 7.0 7.0 0
-1 12.99E6  5.43E4  3.04E3  3.20E3  2.70E-4  1.35E-2  0.10
                    3.04E3  3.20E3  2.70E-4  1.35E-2  0.10
COLUMN CONNECTIVITY - L1
1,1,1,1,0,1
2,1,1,2,0,1
3,1,1,3,0,1
4,1,1,4,0,1
5,2,1,1,1,2
6,2,1,2,1,2
7,2,1,3,1,2
8,2,1,4,1,2
9,3,1,1,2,3
10,3,1,2,2,3
11,3,1,3,2,3
12,3,1,4,2,3
BEAMS CONNECTIVITY - L2
1,1,3,1,1,2
2,1,3,1,2,3
3,1,3,1,3,4
4,2,2,1,1,2
5,2,2,1,2,3
6,2,2,1,3,4
7,3,1,1,1,2
8,3,1,1,2,3
9,3,1,1,3,4
SET M - ANALYSIS OPTION
2
SET M1 - LONG-TERM STATIC LOADING
0, 0, 0, 0
SET M2 - TYPE OF PUSHOVER
1
SET M2.1 - FORCE CONTROLLED INPUT
4
SET M2.2 - USER INPUT
3
1,2,3
70.0 210.0 220.0
500 5.0
SET N1.1 - PUSHOVER SNAPSHOT CONTROL DATA
0
```

0 0 0 0 0
SET N2 - STORY OUTPUT CONTROL
3 1 1 2 3
CVXLEV1.OUT
CVXLEV2.OUT
CVXLEV3.OUT
SET N3 - ELEMENT OUTPUT CONTROL
0 0 0 0 0 0

FRAME 3S-60 - PUSHOVER ANALYSIS. UNIFOR PATTERN
SET A - CONTROL DATA SET
3, 1, 0, 0, 0, 0, 1, 1
SET A1 - ELEMENTS TYPE
3, 3, 0, 0, 0, 0, 0, 0, 0, 0
SET A2 - ELEMENT DATA
12, 9, 0, 0, 0, 0, 0, 0, 0
SET A3 - SYSTEM OF UNITS
1
SET A4 - FLOOR ELEVATIONS
174., 343.44, 512.88
SET A5 - DESCRIPTION OF IDENTICAL FRAMES
1
SET A6 - PLAN CONFIGURATION
4
SET A7 - NODAL WEIGHTS
1, 1, 0, 652.2, 0, 0
2, 1, 0, 652.2, 0, 0
3, 1, 0, 352.4, 0, 0
SET B - MATERIAL PROPERTIES SET
1
SET C - HYSTERETIC MODELING RULES
1
1, 1, 200, 0.001, 0.001, 1.0, 0
SET D - COLUMN PROPERTIES
1
SET D3 - COLUMN DATA
1, 174.00, 14.0, 8.0, 0
-1 29.0E6 4.42E3 7.16E4 7.46E3 7.85E3 2.98E-4 1.49E-2 0.10
                        7.46E3 7.85E3 2.98E-4 1.49E-2 0.10
2, 169.44, 8.0, 8.0, 0
-1 29.0E6 4.54E3 7.16E4 7.46E3 7.85E3 2.98E-4 1.49E-2 0.10
                        7.46E3 7.85E3 2.98E-4 1.49E-2 0.10
3, 169.44, 8.0, 7.0, 0
-1 29.0E6 4.54E3 7.16E4 7.46E3 7.85E3 2.98E-4 1.49E-2 0.10
                        7.46E3 7.85E3 2.98E-4 1.49E-2 0.10
SET E - BEAM PROPERTIES
1
SET E2 - BEAM DATA
1 324.0 7.0 7.0 0

-1 7.10E6 4.11E4 1.91E3 2.01E3 3.10E-4 1.55E-2 0.10
                  1.91E3 2.01E3 3.10E-4 1.55E-2 0.10
2 324.0 7.0 7.0 0
-1 10.88E6 4.60E4 2.57E3 2.70E3 2.93E-4 1.47E-2 0.10
                   2.57E3 2.70E3 2.93E-4 1.47E-2 0.10
3 324.0 7.0 7.0 0
-1 12.99E6 5.43E4 3.04E3 3.20E3 2.70E-4 1.35E-2 0.10
                   3.04E3 3.20E3 2.70E-4 1.35E-2 0.10
COLUMN CONNECTIVITY - L1
1,1,1,1,0,1
2,1,1,2,0,1
3,1,1,3,0,1
4,1,1,4,0,1
5,2,1,1,1,2
6,2,1,2,1,2
7,2,1,3,1,2
8,2,1,4,1,2
9,3,1,1,2,3
10,3,1,2,2,3
11,3,1,3,2,3
12,3,1,4,2,3
BEAMS CONNECTIVITY - L2
1,1,3,1,1,2
2,1,3,1,2,3
3,1,3,1,3,4
4,2,2,1,1,2
5,2,2,1,2,3
6,2,2,1,3,4
7,3,1,1,1,2
8,3,1,1,2,3
9,3,1,1,3,4
SET M - ANALYSIS OPTION
2
SET M1 - LONG-TERM STATIC LOADING
0, 0, 0, 0
SET M2 - TYPE OF PUSHOVER
1
SET M2.1 - FORCE CONTROLLED INPUT
4
SET M2.2 - USER INPUT
3
1,2,3
196.8 196.8 106.4
500 5.0
SET N1.1 - PUSHOVER SNAPSHOT CONTROL DATA
0

```
0 0 0 0 0
SET N2 - STORY OUTPUT CONTROL
3  1  1  2  3
UNIFLEV1.OUT
UNIFLEV2.OUT
UNIFLEV3.OUT
SET N3 - ELEMENT OUTPUT CONTROL
0 0 0 0 0 0
```

FRAME 3S-60 – PUSHOVER ANALYSIS. MODAL ADAPTIVE PATTERN
SET A - CONTROL DATA SET
3, 1, 0, 0, 0, 0, 1, 1
SET A1 - ELEMENTS TYPE
3, 3, 0, 0, 0, 0, 0, 0, 0, 0
SET A2 - ELEMENT DATA
12, 9, 0, 0, 0, 0, 0, 0, 0
SET A3 - SYSTEM OF UNITS
1
SET A4 - FLOOR ELEVATIONS
174.0, 343.44, 512.88
SET A5 - DESCRIPTION OF IDENTICAL FRAMES
1
SET A6 - PLAN CONFIGURATION
4
SET A7 - NODAL WEIGHTS
1, 1, 0, 652.2, 0, 0
2, 1, 0, 652.2, 0, 0
3, 1, 0, 352.4, 0, 0
SET B - MATERIAL PROPERTIES SET
1
SET C - HYSTERETIC MODELING RULES
1
1, 1, 200, 0.001, 0.001, 1.0, 0
SET D - COLUMN PROPERTIES
1
SET D3 - COLUMN DATA
1, 174.00, 14.0, 8.0, 0
-1 29.0E6 4.42E3 7.16E4 7.46E3 7.85E3 2.98E-4 1.49E-2 0.10
                            7.46E3 7.85E3 2.98E-4 1.49E-2 0.10
2, 169.44, 8.0, 8.0, 0
-1 29.0E6 4.54E3 7.16E4 7.46E3 7.85E3 2.98E-4 1.49E-2 0.10
                            7.46E3 7.85E3 2.98E-4 1.49E-2 0.10
3, 169.44, 8.0, 7.0, 0
-1 29.0E6 4.54E3 7.16E4 7.46E3 7.85E3 2.98E-4 1.49E-2 0.10
                            7.46E3 7.85E3 2.98E-4 1.49E-2 0.10
SET E - BEAM PROPERTIES
1
SET E2 - BEAM DATA
1 324.0 7.0 7.0 0

468

```
-1 7.10E6  4.11E4  1.91E3  2.01E3  3.10E-4  1.55E-2  0.10
                   1.91E3  2.01E3  3.10E-4  1.55E-2  0.10
2 324.0 7.0 7.0 0
-1 10.88E6 4.60E4  2.57E3  2.70E3  2.93E-4  1.47E-2  0.10
                   2.57E3  2.70E3  2.93E-4  1.47E-2  0.10
3 324.0 7.0 7.0 0
-1 12.99E6 5.43E4  3.04E3  3.20E3  2.70E-4  1.35E-2  0.10
                   3.04E3  3.20E3  2.70E-4  1.35E-2  0.10
COLUMN CONNECTIVITY - L1
1,1,1,1,0,1
2,1,1,2,0,1
3,1,1,3,0,1
4,1,1,4,0,1
5,2,1,1,1,2
6,2,1,2,1,2
7,2,1,3,1,2
8,2,1,4,1,2
9,3,1,1,2,3
10,3,1,2,2,3
11,3,1,3,2,3
12,3,1,4,2,3
BEAMS CONNECTIVITY - L2
1,1,3,1,1,2
2,1,3,1,2,3
3,1,3,1,3,4
4,2,2,1,1,2
5,2,2,1,2,3
6,2,2,1,3,4
7,3,1,1,1,2
8,3,1,1,2,3
9,3,1,1,3,4
SET M - ANALYSIS OPTION
2
SET M1 - LONG-TERM STATIC LOADING
0, 0, 0, 0
SET M2 - TYPE OF PUSHOVER
1
SET M2.1 - FORCE CONTROLLED INPUT
3
0.40  500  5.0
3 2 1
SET N1.1 - PUSHOVER SNAPSHOT CONTROL DATA
0
0 0 0 0 0
SET N2 - STORY OUTPUT CONTROL
3  1  1  2  3
```

ADAPTLEV1.OUT
ADAPTLEV2.OUT
ADAPTLEV3.OUT
SET N3 - ELEMENT OUTPUT CONTROL
0 0 0 0 0 0

Multidisciplinary Center for Earthquake Engineering Research
List of Technical Reports

The Multidisciplinary Center for Earthquake Engineering Research (MCEER) publishes technical reports on a variety of subjects related to earthquake engineering written by authors funded through MCEER. These reports are available from both MCEER Publications and the National Technical Information Service (NTIS). Requests for reports should be directed to MCEER Publications, Multidisciplinary Center for Earthquake Engineering Research, State University of New York at Buffalo, Red Jacket Quadrangle, Buffalo, New York 14261. Reports can also be requested through NTIS, 5285 Port Royal Road, Springfield, Virginia 22161. NTIS accession numbers are shown in parenthesis, if available.

NCEER-87-0001   "First-Year Program in Research, Education and Technology Transfer," 3/5/87, (PB88-134275, A04, MF-A01).

NCEER-87-0002   "Experimental Evaluation of Instantaneous Optimal Algorithms for Structural Control," by R.C. Lin, T.T. Soong and A.M. Reinhorn, 4/20/87, (PB88-134341, A04, MF-A01).

NCEER-87-0003   "Experimentation Using the Earthquake Simulation Facilities at University at Buffalo," by A.M. Reinhorn and R.L. Ketter, to be published.

NCEER-87-0004   "The System Characteristics and Performance of a Shaking Table," by J.S. Hwang, K.C. Chang and G.C. Lee, 6/1/87, (PB88-134259, A03, MF-A01). This report is available only through NTIS (see address given above).

NCEER-87-0005   "A Finite Element Formulation for Nonlinear Viscoplastic Material Using a Q Model," by O. Gyebi and G. Dasgupta, 11/2/87, (PB88-213764, A08, MF-A01).

NCEER-87-0006   "Symbolic Manipulation Program (SMP) - Algebraic Codes for Two and Three Dimensional Finite Element Formulations," by X. Lee and G. Dasgupta, 11/9/87, (PB88-218522, A05, MF-A01).

NCEER-87-0007   "Instantaneous Optimal Control Laws for Tall Buildings Under Seismic Excitations," by J.N. Yang, A. Akbarpour and P. Ghaemmaghami, 6/10/87, (PB88-134333, A06, MF-A01). This report is only available through NTIS (see address given above).

NCEER-87-0008   "IDARC: Inelastic Damage Analysis of Reinforced Concrete Frame - Shear-Wall Structures," by Y.J. Park, A.M. Reinhorn and S.K. Kunnath, 7/20/87, (PB88-134325, A09, MF-A01). This report is only available through NTIS (see address given above).

NCEER-87-0009   "Liquefaction Potential for New York State: A Preliminary Report on Sites in Manhattan and Buffalo," by M. Budhu, V. Vijayakumar, R.F. Giese and L. Baumgras, 8/31/87, (PB88-163704, A03, MF-A01). This report is available only through NTIS (see address given above).

NCEER-87-0010   "Vertical and Torsional Vibration of Foundations in Inhomogeneous Media," by A.S. Veletsos and K.W. Dotson, 6/1/87, (PB88-134291, A03, MF-A01). This report is only available through NTIS (see address given above).

NCEER-87-0011   "Seismic Probabilistic Risk Assessment and Seismic Margins Studies for Nuclear Power Plants," by Howard H.M. Hwang, 6/15/87, (PB88-134267, A03, MF-A01). This report is only available through NTIS (see address given above).

NCEER-87-0012   "Parametric Studies of Frequency Response of Secondary Systems Under Ground-Acceleration Excitations," by Y. Yong and Y.K. Lin, 6/10/87, (PB88-134309, A03, MF-A01). This report is only available through NTIS (see address given above).

NCEER-87-0013   "Frequency Response of Secondary Systems Under Seismic Excitation," by J.A. HoLung, J. Cai and Y.K. Lin, 7/31/87, (PB88-134317, A05, MF-A01). This report is only available through NTIS (see address given above).

NCEER-87-0014 "Modelling Earthquake Ground Motions in Seismically Active Regions Using Parametric Time Series Methods," by G.W. Ellis and A.S. Cakmak, 8/25/87, (PB88-134283, A08, MF-A01). This report is only available through NTIS (see address given above).

NCEER-87-0015 "Detection and Assessment of Seismic Structural Damage," by E. DiPasquale and A.S. Cakmak, 8/25/87, (PB88-163712, A05, MF-A01). This report is only available through NTIS (see address given above).

NCEER-87-0016 "Pipeline Experiment at Parkfield, California," by J. Isenberg and E. Richardson, 9/15/87, (PB88-163720, A03, MF-A01). This report is available only through NTIS (see address given above).

NCEER-87-0017 "Digital Simulation of Seismic Ground Motion," by M. Shinozuka, G. Deodatis and T. Harada, 8/31/87, (PB88-155197, A04, MF-A01). This report is available only through NTIS (see address given above).

NCEER-87-0018 "Practical Considerations for Structural Control: System Uncertainty, System Time Delay and Truncation of Small Control Forces," J.N. Yang and A. Akbarpour, 8/10/87, (PB88-163738, A08, MF-A01). This report is only available through NTIS (see address given above).

NCEER-87-0019 "Modal Analysis of Nonclassically Damped Structural Systems Using Canonical Transformation," by J.N. Yang, S. Sarkani and F.X. Long, 9/27/87, (PB88-187851, A04, MF-A01).

NCEER-87-0020 "A Nonstationary Solution in Random Vibration Theory," by J.R. Red-Horse and P.D. Spanos, 11/3/87, (PB88-163746, A03, MF-A01).

NCEER-87-0021 "Horizontal Impedances for Radially Inhomogeneous Viscoelastic Soil Layers," by A.S. Veletsos and K.W. Dotson, 10/15/87, (PB88-150859, A04, MF-A01).

NCEER-87-0022 "Seismic Damage Assessment of Reinforced Concrete Members," by Y.S. Chung, C. Meyer and M. Shinozuka, 10/9/87, (PB88-150867, A05, MF-A01). This report is available only through NTIS (see address given above).

NCEER-87-0023 "Active Structural Control in Civil Engineering," by T.T. Soong, 11/11/87, (PB88-187778, A03, MF-A01).

NCEER-87-0024 "Vertical and Torsional Impedances for Radially Inhomogeneous Viscoelastic Soil Layers," by K.W. Dotson and A.S. Veletsos, 12/87, (PB88-187786, A03, MF-A01).

NCEER-87-0025 "Proceedings from the Symposium on Seismic Hazards, Ground Motions, Soil-Liquefaction and Engineering Practice in Eastern North America," October 20-22, 1987, edited by K.H. Jacob, 12/87, (PB88-188115, A23, MF-A01). This report is available only through NTIS (see address given above).

NCEER-87-0026 "Report on the Whittier-Narrows, California, Earthquake of October 1, 1987," by J. Pantelic and A. Reinhorn, 11/87, (PB88-187752, A03, MF-A01). This report is available only through NTIS (see address given above).

NCEER-87-0027 "Design of a Modular Program for Transient Nonlinear Analysis of Large 3-D Building Structures," by S. Srivastav and J.F. Abel, 12/30/87, (PB88-187950, A05, MF-A01). This report is only available through NTIS (see address given above).

NCEER-87-0028 "Second-Year Program in Research, Education and Technology Transfer," 3/8/88, (PB88-219480, A04, MF-A01).

NCEER-88-0001 "Workshop on Seismic Computer Analysis and Design of Buildings With Interactive Graphics," by W. McGuire, J.F. Abel and C.H. Conley, 1/18/88, (PB88-187760, A03, MF-A01). This report is only available through NTIS (see address given above).

NCEER-88-0002 "Optimal Control of Nonlinear Flexible Structures," by J.N. Yang, F.X. Long and D. Wong, 1/22/88, (PB88-213772, A06, MF-A01).

NCEER-88-0003 "Substructuring Techniques in the Time Domain for Primary-Secondary Structural Systems," by G.D. Manolis and G. Juhn, 2/10/88, (PB88-213780, A04, MF-A01).

NCEER-88-0004 "Iterative Seismic Analysis of Primary-Secondary Systems," by A. Singhal, L.D. Lutes and P.D. Spanos, 2/23/88, (PB88-213798, A04, MF-A01).

NCEER-88-0005 "Stochastic Finite Element Expansion for Random Media," by P.D. Spanos and R. Ghanem, 3/14/88, (PB88-213806, A03, MF-A01).

NCEER-88-0006 "Combining Structural Optimization and Structural Control," by F.Y. Cheng and C.P. Pantelides, 1/10/88, (PB88-213814, A05, MF-A01).

NCEER-88-0007 "Seismic Performance Assessment of Code-Designed Structures," by H.H-M. Hwang, J-W. Jaw and H-J. Shau, 3/20/88, (PB88-219423, A04, MF-A01). This report is only available through NTIS (see address given above).

NCEER-88-0008 "Reliability Analysis of Code-Designed Structures Under Natural Hazards," by H.H-M. Hwang, H. Ushiba and M. Shinozuka, 2/29/88, (PB88-229471, A07, MF-A01). This report is only available through NTIS (see address given above).

NCEER-88-0009 "Seismic Fragility Analysis of Shear Wall Structures," by J-W Jaw and H.H-M. Hwang, 4/30/88, (PB89-102867, A04, MF-A01).

NCEER-88-0010 "Base Isolation of a Multi-Story Building Under a Harmonic Ground Motion - A Comparison of Performances of Various Systems," by F-G Fan, G. Ahmadi and I.G. Tadjbakhsh, 5/18/88, (PB89-122238, A06, MF-A01). This report is only available through NTIS (see address given above).

NCEER-88-0011 "Seismic Floor Response Spectra for a Combined System by Green's Functions," by F.M. Lavelle, L.A. Bergman and P.D. Spanos, 5/1/88, (PB89-102875, A03, MF-A01).

NCEER-88-0012 "A New Solution Technique for Randomly Excited Hysteretic Structures," by G.Q. Cai and Y.K. Lin, 5/16/88, (PB89-102883, A03, MF-A01).

NCEER-88-0013 "A Study of Radiation Damping and Soil-Structure Interaction Effects in the Centrifuge," by K. Weissman, supervised by J.H. Prevost, 5/24/88, (PB89-144703, A06, MF-A01).

NCEER-88-0014 "Parameter Identification and Implementation of a Kinematic Plasticity Model for Frictional Soils," by J.H. Prevost and D.V. Griffiths, to be published.

NCEER-88-0015 "Two- and Three- Dimensional Dynamic Finite Element Analyses of the Long Valley Dam," by D.V. Griffiths and J.H. Prevost, 6/17/88, (PB89-144711, A04, MF-A01).

NCEER-88-0016 "Damage Assessment of Reinforced Concrete Structures in Eastern United States," by A.M. Reinhorn, M.J. Seidel, S.K. Kunnath and Y.J. Park, 6/15/88, (PB89-122220, A04, MF-A01). This report is only available through NTIS (see address given above).

NCEER-88-0017 "Dynamic Compliance of Vertically Loaded Strip Foundations in Multilayered Viscoelastic Soils," by S. Ahmad and A.S.M. Israil, 6/17/88, (PB89-102891, A04, MF-A01).

NCEER-88-0018 "An Experimental Study of Seismic Structural Response With Added Viscoelastic Dampers," by R.C. Lin, Z. Liang, T.T. Soong and R.H. Zhang, 6/30/88, (PB89-122212, A05, MF-A01). This report is available only through NTIS (see address given above).

NCEER-88-0019 "Experimental Investigation of Primary - Secondary System Interaction," by G.D. Manolis, G. Juhn and A.M. Reinhorn, 5/27/88, (PB89-122204, A04, MF-A01).

NCEER-88-0020 "A Response Spectrum Approach For Analysis of Nonclassically Damped Structures," by J.N. Yang, S. Sarkani and F.X. Long, 4/22/88, (PB89-102909, A04, MF-A01).

NCEER-88-0021 "Seismic Interaction of Structures and Soils: Stochastic Approach," by A.S. Veletsos and A.M. Prasad, 7/21/88, (PB89-122196, A04, MF-A01). This report is only available through NTIS (see address given above).

NCEER-88-0022 "Identification of the Serviceability Limit State and Detection of Seismic Structural Damage," by E. DiPasquale and A.S. Cakmak, 6/15/88, (PB89-122188, A05, MF-A01). This report is available only through NTIS (see address given above).

NCEER-88-0023 "Multi-Hazard Risk Analysis: Case of a Simple Offshore Structure," by B.K. Bhartia and E.H. Vanmarcke, 7/21/88, (PB89-145213, A05, MF-A01).

NCEER-88-0024 "Automated Seismic Design of Reinforced Concrete Buildings," by Y.S. Chung, C. Meyer and M. Shinozuka, 7/5/88, (PB89-122170, A06, MF-A01). This report is available only through NTIS (see address given above).

NCEER-88-0025 "Experimental Study of Active Control of MDOF Structures Under Seismic Excitations," by L.L. Chung, R.C. Lin, T.T. Soong and A.M. Reinhorn, 7/10/88, (PB89-122600, A04, MF-A01).

NCEER-88-0026 "Earthquake Simulation Tests of a Low-Rise Metal Structure," by J.S. Hwang, K.C. Chang, G.C. Lee and R.L. Ketter, 8/1/88, (PB89-102917, A04, MF-A01).

NCEER-88-0027 "Systems Study of Urban Response and Reconstruction Due to Catastrophic Earthquakes," by F. Kozin and H.K. Zhou, 9/22/88, (PB90-162348, A04, MF-A01).

NCEER-88-0028 "Seismic Fragility Analysis of Plane Frame Structures," by H.H-M. Hwang and Y.K. Low, 7/31/88, (PB89-131445, A06, MF-A01).

NCEER-88-0029 "Response Analysis of Stochastic Structures," by A. Kardara, C. Bucher and M. Shinozuka, 9/22/88, (PB89-174429, A04, MF-A01).

NCEER-88-0030 "Nonnormal Accelerations Due to Yielding in a Primary Structure," by D.C.K. Chen and L.D. Lutes, 9/19/88, (PB89-131437, A04, MF-A01).

NCEER-88-0031 "Design Approaches for Soil-Structure Interaction," by A.S. Veletsos, A.M. Prasad and Y. Tang, 12/30/88, (PB89-174437, A03, MF-A01). This report is available only through NTIS (see address given above).

NCEER-88-0032 "A Re-evaluation of Design Spectra for Seismic Damage Control," by C.J. Turkstra and A.G. Tallin, 11/7/88, (PB89-145221, A05, MF-A01).

NCEER-88-0033 "The Behavior and Design of Noncontact Lap Splices Subjected to Repeated Inelastic Tensile Loading," by V.E. Sagan, P. Gergely and R.N. White, 12/8/88, (PB89-163737, A08, MF-A01).

NCEER-88-0034 "Seismic Response of Pile Foundations," by S.M. Mamoon, P.K. Banerjee and S. Ahmad, 11/1/88, (PB89-145239, A04, MF-A01).

NCEER-88-0035 "Modeling of R/C Building Structures With Flexible Floor Diaphragms (IDARC2)," by A.M. Reinhorn, S.K. Kunnath and N. Panahshahi, 9/7/88, (PB89-207153, A07, MF-A01).

NCEER-88-0036 "Solution of the Dam-Reservoir Interaction Problem Using a Combination of FEM, BEM with Particular Integrals, Modal Analysis, and Substructuring," by C-S. Tsai, G.C. Lee and R.L. Ketter, 12/31/88, (PB89-207146, A04, MF-A01).

NCEER-88-0037 "Optimal Placement of Actuators for Structural Control," by F.Y. Cheng and C.P. Pantelides, 8/15/88, (PB89-162846, A05, MF-A01).

NCEER-88-0038 "Teflon Bearings in Aseismic Base Isolation: Experimental Studies and Mathematical Modeling," by A. Mokha, M.C. Constantinou and A.M. Reinhorn, 12/5/88, (PB89-218457, A10, MF-A01). This report is available only through NTIS (see address given above).

NCEER-88-0039 "Seismic Behavior of Flat Slab High-Rise Buildings in the New York City Area," by P. Weidlinger and M. Ettouney, 10/15/88, (PB90-145681, A04, MF-A01).

NCEER-88-0040 "Evaluation of the Earthquake Resistance of Existing Buildings in New York City," by P. Weidlinger and M. Ettouney, 10/15/88, to be published.

NCEER-88-0041 "Small-Scale Modeling Techniques for Reinforced Concrete Structures Subjected to Seismic Loads," by W. Kim, A. El-Attar and R.N. White, 11/22/88, (PB89-189625, A05, MF-A01).

NCEER-88-0042 "Modeling Strong Ground Motion from Multiple Event Earthquakes," by G.W. Ellis and A.S. Cakmak, 10/15/88, (PB89-174445, A03, MF-A01).

NCEER-88-0043 "Nonstationary Models of Seismic Ground Acceleration," by M. Grigoriu, S.E. Ruiz and E. Rosenblueth, 7/15/88, (PB89-189617, A04, MF-A01).

NCEER-88-0044 "SARCF User's Guide: Seismic Analysis of Reinforced Concrete Frames," by Y.S. Chung, C. Meyer and M. Shinozuka, 11/9/88, (PB89-174452, A08, MF-A01).

NCEER-88-0045 "First Expert Panel Meeting on Disaster Research and Planning," edited by J. Pantelic and J. Stoyle, 9/15/88, (PB89-174460, A05, MF-A01).

NCEER-88-0046 "Preliminary Studies of the Effect of Degrading Infill Walls on the Nonlinear Seismic Response of Steel Frames," by C.Z. Chrysostomou, P. Gergely and J.F. Abel, 12/19/88, (PB89-208383, A05, MF-A01).

NCEER-88-0047 "Reinforced Concrete Frame Component Testing Facility - Design, Construction, Instrumentation and Operation," by S.P. Pessiki, C. Conley, T. Bond, P. Gergely and R.N. White, 12/16/88, (PB89-174478, A04, MF-A01).

NCEER-89-0001 "Effects of Protective Cushion and Soil Compliancy on the Response of Equipment Within a Seismically Excited Building," by J.A. HoLung, 2/16/89, (PB89-207179, A04, MF-A01).

NCEER-89-0002 "Statistical Evaluation of Response Modification Factors for Reinforced Concrete Structures," by H.H-M. Hwang and J-W. Jaw, 2/17/89, (PB89-207187, A05, MF-A01).

NCEER-89-0003 "Hysteretic Columns Under Random Excitation," by G-Q. Cai and Y.K. Lin, 1/9/89, (PB89-196513, A03, MF-A01).

NCEER-89-0004 "Experimental Study of 'Elephant Foot Bulge' Instability of Thin-Walled Metal Tanks," by Z-H. Jia and R.L. Ketter, 2/22/89, (PB89-207195, A03, MF-A01).

NCEER-89-0005 "Experiment on Performance of Buried Pipelines Across San Andreas Fault," by J. Isenberg, E. Richardson and T.D. O'Rourke, 3/10/89, (PB89-218440, A04, MF-A01). This report is available only through NTIS (see address given above).

NCEER-89-0006 "A Knowledge-Based Approach to Structural Design of Earthquake-Resistant Buildings," by M. Subramani, P. Gergely, C.H. Conley, J.F. Abel and A.H. Zaghw, 1/15/89, (PB89-218465, A06, MF-A01).

NCEER-89-0007 "Liquefaction Hazards and Their Effects on Buried Pipelines," by T.D. O'Rourke and P.A. Lane, 2/1/89, (PB89-218481, A09, MF-A01).

NCEER-89-0008 "Fundamentals of System Identification in Structural Dynamics," by H. Imai, C-B. Yun, O. Maruyama and M. Shinozuka, 1/26/89, (PB89-207211, A04, MF-A01).

NCEER-89-0009 "Effects of the 1985 Michoacan Earthquake on Water Systems and Other Buried Lifelines in Mexico," by A.G. Ayala and M.J. O'Rourke, 3/8/89, (PB89-207229, A06, MF-A01).

NCEER-89-R010 "NCEER Bibliography of Earthquake Education Materials," by K.E.K. Ross, Second Revision, 9/1/89, (PB90-125352, A05, MF-A01). This report is replaced by NCEER-92-0018.

NCEER-89-0011 "Inelastic Three-Dimensional Response Analysis of Reinforced Concrete Building Structures (IDARC-3D), Part I - Modeling," by S.K. Kunnath and A.M. Reinhorn, 4/17/89, (PB90-114612, A07, MF-A01). This report is available only through NTIS (see address given above).

NCEER-89-0012 "Recommended Modifications to ATC-14," by C.D. Poland and J.O. Malley, 4/12/89, (PB90-108648, A15, MF-A01).

NCEER-89-0013 "Repair and Strengthening of Beam-to-Column Connections Subjected to Earthquake Loading," by M. Corazao and A.J. Durrani, 2/28/89, (PB90-109885, A06, MF-A01).

NCEER-89-0014 "Program EXKAL2 for Identification of Structural Dynamic Systems," by O. Maruyama, C-B. Yun, M. Hoshiya and M. Shinozuka, 5/19/89, (PB90-109877, A09, MF-A01).

NCEER-89-0015 "Response of Frames With Bolted Semi-Rigid Connections, Part I - Experimental Study and Analytical Predictions," by P.J. DiCorso, A.M. Reinhorn, J.R. Dickerson, J.B. Radziminski and W.L. Harper, 6/1/89, to be published.

NCEER-89-0016 "ARMA Monte Carlo Simulation in Probabilistic Structural Analysis," by P.D. Spanos and M.P. Mignolet, 7/10/89, (PB90-109893, A03, MF-A01).

NCEER-89-P017 "Preliminary Proceedings from the Conference on Disaster Preparedness - The Place of Earthquake Education in Our Schools," Edited by K.E.K. Ross, 6/23/89, (PB90-108606, A03, MF-A01).

NCEER-89-0017 "Proceedings from the Conference on Disaster Preparedness - The Place of Earthquake Education in Our Schools," Edited by K.E.K. Ross, 12/31/89, (PB90-207895, A012, MF-A02). This report is available only through NTIS (see address given above).

NCEER-89-0018 "Multidimensional Models of Hysteretic Material Behavior for Vibration Analysis of Shape Memory Energy Absorbing Devices, by E.J. Graesser and F.A. Cozzarelli, 6/7/89, (PB90-164146, A04, MF-A01).

NCEER-89-0019 "Nonlinear Dynamic Analysis of Three-Dimensional Base Isolated Structures (3D-BASIS)," by S. Nagarajaiah, A.M. Reinhorn and M.C. Constantinou, 8/3/89, (PB90-161936, A06, MF-A01). This report has been replaced by NCEER-93-0011.

NCEER-89-0020 "Structural Control Considering Time-Rate of Control Forces and Control Rate Constraints," by F.Y. Cheng and C.P. Pantelides, 8/3/89, (PB90-120445, A04, MF-A01).

NCEER-89-0021 "Subsurface Conditions of Memphis and Shelby County," by K.W. Ng, T-S. Chang and H-H.M. Hwang, 7/26/89, (PB90-120437, A03, MF-A01).

NCEER-89-0022 "Seismic Wave Propagation Effects on Straight Jointed Buried Pipelines," by K. Elhmadi and M.J. O'Rourke, 8/24/89, (PB90-162322, A10, MF-A02).

NCEER-89-0023 "Workshop on Serviceability Analysis of Water Delivery Systems," edited by M. Grigoriu, 3/6/89, (PB90-127424, A03, MF-A01).

NCEER-89-0024 "Shaking Table Study of a 1/5 Scale Steel Frame Composed of Tapered Members," by K.C. Chang, J.S. Hwang and G.C. Lee, 9/18/89, (PB90-160169, A04, MF-A01).

NCEER-89-0025 "DYNA1D: A Computer Program for Nonlinear Seismic Site Response Analysis - Technical Documentation," by Jean H. Prevost, 9/14/89, (PB90-161944, A07, MF-A01). This report is available only through NTIS (see address given above).

NCEER-89-0026 "1:4 Scale Model Studies of Active Tendon Systems and Active Mass Dampers for Aseismic Protection," by A.M. Reinhorn, T.T. Soong, R.C. Lin, Y.P. Yang, Y. Fukao, H. Abe and M. Nakai, 9/15/89, (PB90-173246, A10, MF-A02). This report is available only through NTIS (see address given above).

NCEER-89-0027 "Scattering of Waves by Inclusions in a Nonhomogeneous Elastic Half Space Solved by Boundary Element Methods," by P.K. Hadley, A. Askar and A.S. Cakmak, 6/15/89, (PB90-145699, A07, MF-A01).

NCEER-89-0028 "Statistical Evaluation of Deflection Amplification Factors for Reinforced Concrete Structures," by H.H.M. Hwang, J-W. Jaw and A.L. Ch'ng, 8/31/89, (PB90-164633, A05, MF-A01).

NCEER-89-0029 "Bedrock Accelerations in Memphis Area Due to Large New Madrid Earthquakes," by H.H.M. Hwang, C.H.S. Chen and G. Yu, 11/7/89, (PB90-162330, A04, MF-A01).

NCEER-89-0030   "Seismic Behavior and Response Sensitivity of Secondary Structural Systems," by Y.Q. Chen and T.T. Soong, 10/23/89, (PB90-164658, A08, MF-A01).

NCEER-89-0031   "Random Vibration and Reliability Analysis of Primary-Secondary Structural Systems," by Y. Ibrahim, M. Grigoriu and T.T. Soong, 11/10/89, (PB90-161951, A04, MF-A01).

NCEER-89-0032   "Proceedings from the Second U.S. - Japan Workshop on Liquefaction, Large Ground Deformation and Their Effects on Lifelines, September 26-29, 1989," Edited by T.D. O'Rourke and M. Hamada, 12/1/89, (PB90-209388, A22, MF-A03).

NCEER-89-0033   "Deterministic Model for Seismic Damage Evaluation of Reinforced Concrete Structures," by J.M. Bracci, A.M. Reinhorn, J.B. Mander and S.K. Kunnath, 9/27/89, (PB91-108803, A06, MF-A01).

NCEER-89-0034   "On the Relation Between Local and Global Damage Indices," by E. DiPasquale and A.S. Cakmak, 8/15/89, (PB90-173865, A05, MF-A01).

NCEER-89-0035   "Cyclic Undrained Behavior of Nonplastic and Low Plasticity Silts," by A.J. Walker and H.E. Stewart, 7/26/89, (PB90-183518, A10, MF-A01).

NCEER-89-0036   "Liquefaction Potential of Surficial Deposits in the City of Buffalo, New York," by M. Budhu, R. Giese and L. Baumgrass, 1/17/89, (PB90-208455, A04, MF-A01).

NCEER-89-0037   "A Deterministic Assessment of Effects of Ground Motion Incoherence," by A.S. Veletsos and Y. Tang, 7/15/89, (PB90-164294, A03, MF-A01).

NCEER-89-0038   "Workshop on Ground Motion Parameters for Seismic Hazard Mapping," July 17-18, 1989, edited by R.V. Whitman, 12/1/89, (PB90-173923, A04, MF-A01).

NCEER-89-0039   "Seismic Effects on Elevated Transit Lines of the New York City Transit Authority," by C.J. Costantino, C.A. Miller and E. Heymsfield, 12/26/89, (PB90-207887, A06, MF-A01).

NCEER-89-0040   "Centrifugal Modeling of Dynamic Soil-Structure Interaction," by K. Weissman, Supervised by J.H. Prevost, 5/10/89, (PB90-207879, A07, MF-A01).

NCEER-89-0041   "Linearized Identification of Buildings With Cores for Seismic Vulnerability Assessment," by I-K. Ho and A.E. Aktan, 11/1/89, (PB90-251943, A07, MF-A01).

NCEER-90-0001   "Geotechnical and Lifeline Aspects of the October 17, 1989 Loma Prieta Earthquake in San Francisco," by T.D. O'Rourke, H.E. Stewart, F.T. Blackburn and T.S. Dickerman, 1/90, (PB90-208596, A05, MF-A01).

NCEER-90-0002   "Nonnormal Secondary Response Due to Yielding in a Primary Structure," by D.C.K. Chen and L.D. Lutes, 2/28/90, (PB90-251976, A07, MF-A01).

NCEER-90-0003   "Earthquake Education Materials for Grades K-12," by K.E.K. Ross, 4/16/90, (PB91-251984, A05, MF-A05). This report has been replaced by NCEER-92-0018.

NCEER-90-0004   "Catalog of Strong Motion Stations in Eastern North America," by R.W. Busby, 4/3/90, (PB90-251984, A05, MF-A01).

NCEER-90-0005   "NCEER Strong-Motion Data Base: A User Manual for the GeoBase Release (Version 1.0 for the Sun3)," by P. Friberg and K. Jacob, 3/31/90 (PB90-258062, A04, MF-A01).

NCEER-90-0006   "Seismic Hazard Along a Crude Oil Pipeline in the Event of an 1811-1812 Type New Madrid Earthquake," by H.H.M. Hwang and C-H.S. Chen, 4/16/90, (PB90-258054, A04, MF-A01).

NCEER-90-0007   "Site-Specific Response Spectra for Memphis Sheahan Pumping Station," by H.H.M. Hwang and C.S. Lee, 5/15/90, (PB91-108811, A05, MF-A01).

NCEER-90-0008   "Pilot Study on Seismic Vulnerability of Crude Oil Transmission Systems," by T. Ariman, R. Dobry, M. Grigoriu, F. Kozin, M. O'Rourke, T. O'Rourke and M. Shinozuka, 5/25/90, (PB91-108837, A06, MF-A01).

NCEER-90-0009 "A Program to Generate Site Dependent Time Histories: EQGEN," by G.W. Ellis, M. Srinivasan and A.S. Cakmak, 1/30/90, (PB91-108829, A04, MF-A01).

NCEER-90-0010 "Active Isolation for Seismic Protection of Operating Rooms," by M.E. Talbott, Supervised by M. Shinozuka, 6/8/9, (PB91-110205, A05, MF-A01).

NCEER-90-0011 "Program LINEARID for Identification of Linear Structural Dynamic Systems," by C-B. Yun and M. Shinozuka, 6/25/90, (PB91-110312, A08, MF-A01).

NCEER-90-0012 "Two-Dimensional Two-Phase Elasto-Plastic Seismic Response of Earth Dams," by A.N. Yiagos, Supervised by J.H. Prevost, 6/20/90, (PB91-110197, A13, MF-A02).

NCEER-90-0013 "Secondary Systems in Base-Isolated Structures: Experimental Investigation, Stochastic Response and Stochastic Sensitivity," by G.D. Manolis, G. Juhn, M.C. Constantinou and A.M. Reinhorn, 7/1/90, (PB91-110320, A08, MF-A01).

NCEER-90-0014 "Seismic Behavior of Lightly-Reinforced Concrete Column and Beam-Column Joint Details," by S.P. Pessiki, C.H. Conley, P. Gergely and R.N. White, 8/22/90, (PB91-108795, A11, MF-A02).

NCEER-90-0015 "Two Hybrid Control Systems for Building Structures Under Strong Earthquakes," by J.N. Yang and A. Danielians, 6/29/90, (PB91-125393, A04, MF-A01).

NCEER-90-0016 "Instantaneous Optimal Control with Acceleration and Velocity Feedback," by J.N. Yang and Z. Li, 6/29/90, (PB91-125401, A03, MF-A01).

NCEER-90-0017 "Reconnaissance Report on the Northern Iran Earthquake of June 21, 1990," by M. Mehrain, 10/4/90, (PB91-125377, A03, MF-A01).

NCEER-90-0018 "Evaluation of Liquefaction Potential in Memphis and Shelby County," by T.S. Chang, P.S. Tang, C.S. Lee and H. Hwang, 8/10/90, (PB91-125427, A09, MF-A01).

NCEER-90-0019 "Experimental and Analytical Study of a Combined Sliding Disc Bearing and Helical Steel Spring Isolation System," by M.C. Constantinou, A.S. Mokha and A.M. Reinhorn, 10/4/90, (PB91-125385, A06, MF-A01). This report is available only through NTIS (see address given above).

NCEER-90-0020 "Experimental Study and Analytical Prediction of Earthquake Response of a Sliding Isolation System with a Spherical Surface," by A.S. Mokha, M.C. Constantinou and A.M. Reinhorn, 10/11/90, (PB91-125419, A05, MF-A01).

NCEER-90-0021 "Dynamic Interaction Factors for Floating Pile Groups," by G. Gazetas, K. Fan, A. Kaynia and E. Kausel, 9/10/90, (PB91-170381, A05, MF-A01).

NCEER-90-0022 "Evaluation of Seismic Damage Indices for Reinforced Concrete Structures," by S. Rodriguez-Gomez and A.S. Cakmak, 9/30/90, PB91-171322, A06, MF-A01).

NCEER-90-0023 "Study of Site Response at a Selected Memphis Site," by H. Desai, S. Ahmad, E.S. Gazetas and M.R. Oh, 10/11/90, (PB91-196857, A03, MF-A01).

NCEER-90-0024 "A User's Guide to Strongmo: Version 1.0 of NCEER's Strong-Motion Data Access Tool for PCs and Terminals," by P.A. Friberg and C.A.T. Susch, 11/15/90, (PB91-171272, A03, MF-A01).

NCEER-90-0025 "A Three-Dimensional Analytical Study of Spatial Variability of Seismic Ground Motions," by L-L. Hong and A.H.-S. Ang, 10/30/90, (PB91-170399, A09, MF-A01).

NCEER-90-0026 "MUMOID User's Guide - A Program for the Identification of Modal Parameters," by S. Rodriguez-Gomez and E. DiPasquale, 9/30/90, (PB91-171298, A04, MF-A01).

NCEER-90-0027 "SARCF-II User's Guide - Seismic Analysis of Reinforced Concrete Frames," by S. Rodriguez-Gomez, Y.S. Chung and C. Meyer, 9/30/90, (PB91-171280, A05, MF-A01).

NCEER-90-0028   "Viscous Dampers: Testing, Modeling and Application in Vibration and Seismic Isolation," by N. Makris and M.C. Constantinou, 12/20/90 (PB91-190561, A06, MF-A01).

NCEER-90-0029   "Soil Effects on Earthquake Ground Motions in the Memphis Area," by H. Hwang, C.S. Lee, K.W. Ng and T.S. Chang, 8/2/90, (PB91-190751, A05, MF-A01).

NCEER-91-0001   "Proceedings from the Third Japan-U.S. Workshop on Earthquake Resistant Design of Lifeline Facilities and Countermeasures for Soil Liquefaction, December 17-19, 1990," edited by T.D. O'Rourke and M. Hamada, 2/1/91, (PB91-179259, A99, MF-A04).

NCEER-91-0002   "Physical Space Solutions of Non-Proportionally Damped Systems," by M. Tong, Z. Liang and G.C. Lee, 1/15/91, (PB91-179242, A04, MF-A01).

NCEER-91-0003   "Seismic Response of Single Piles and Pile Groups," by K. Fan and G. Gazetas, 1/10/91, (PB92-174994, A04, MF-A01).

NCEER-91-0004   "Damping of Structures: Part 1 - Theory of Complex Damping," by Z. Liang and G. Lee, 10/10/91, (PB92-197235, A12, MF-A03).

NCEER-91-0005   "3D-BASIS - Nonlinear Dynamic Analysis of Three Dimensional Base Isolated Structures: Part II," by S. Nagarajaiah, A.M. Reinhorn and M.C. Constantinou, 2/28/91, (PB91-190553, A07, MF-A01). This report has been replaced by NCEER-93-0011.

NCEER-91-0006   "A Multidimensional Hysteretic Model for Plasticity Deforming Metals in Energy Absorbing Devices," by E.J. Graesser and F.A. Cozzarelli, 4/9/91, (PB92-108364, A04, MF-A01).

NCEER-91-0007   "A Framework for Customizable Knowledge-Based Expert Systems with an Application to a KBES for Evaluating the Seismic Resistance of Existing Buildings," by E.G. Ibarra-Anaya and S.J. Fenves, 4/9/91, (PB91-210930, A08, MF-A01).

NCEER-91-0008   "Nonlinear Analysis of Steel Frames with Semi-Rigid Connections Using the Capacity Spectrum Method," by G.G. Deierlein, S-H. Hsieh, Y-J. Shen and J.F. Abel, 7/2/91, (PB92-113828, A05, MF-A01).

NCEER-91-0009   "Earthquake Education Materials for Grades K-12," by K.E.K. Ross, 4/30/91, (PB91-212142, A06, MF-A01). This report has been replaced by NCEER-92-0018.

NCEER-91-0010   "Phase Wave Velocities and Displacement Phase Differences in a Harmonically Oscillating Pile," by N. Makris and G. Gazetas, 7/8/91, (PB92-108356, A04, MF-A01).

NCEER-91-0011   "Dynamic Characteristics of a Full-Size Five-Story Steel Structure and a 2/5 Scale Model," by K.C. Chang, G.C. Yao, G.C. Lee, D.S. Hao and Y.C. Yeh," 7/2/91, (PB93-116648, A06, MF-A02).

NCEER-91-0012   "Seismic Response of a 2/5 Scale Steel Structure with Added Viscoelastic Dampers," by K.C. Chang, T.T. Soong, S-T. Oh and M.L. Lai, 5/17/91, (PB92-110816, A05, MF-A01).

NCEER-91-0013   "Earthquake Response of Retaining Walls; Full-Scale Testing and Computational Modeling," by S. Alampalli and A-W.M. Elgamal, 6/20/91, to be published.

NCEER-91-0014   "3D-BASIS-M: Nonlinear Dynamic Analysis of Multiple Building Base Isolated Structures," by P.C. Tsopelas, S. Nagarajaiah, M.C. Constantinou and A.M. Reinhorn, 5/28/91, (PB92-113885, A09, MF-A02).

NCEER-91-0015   "Evaluation of SEAOC Design Requirements for Sliding Isolated Structures," by D. Theodossiou and M.C. Constantinou, 6/10/91, (PB92-114602, A11, MF-A03).

NCEER-91-0016   "Closed-Loop Modal Testing of a 27-Story Reinforced Concrete Flat Plate-Core Building," by H.R. Somaprasad, T. Toksoy, H. Yoshiyuki and A.E. Aktan, 7/15/91, (PB92-129980, A07, MF-A02).

NCEER-91-0017   "Shake Table Test of a 1/6 Scale Two-Story Lightly Reinforced Concrete Building," by A.G. El-Attar, R.N. White and P. Gergely, 2/28/91, (PB92-222447, A06, MF-A02).

NCEER-91-0018   "Shake Table Test of a 1/8 Scale Three-Story Lightly Reinforced Concrete Building," by A.G. El-Attar, R.N. White and P. Gergely, 2/28/91, (PB93-116630, A08, MF-A02).

NCEER-91-0019   "Transfer Functions for Rigid Rectangular Foundations," by A.S. Veletsos, A.M. Prasad and W.H. Wu, 7/31/91, to be published.

NCEER-91-0020   "Hybrid Control of Seismic-Excited Nonlinear and Inelastic Structural Systems," by J.N. Yang, Z. Li and A. Danielians, 8/1/91, (PB92-143171, A06, MF-A02).

NCEER-91-0021   "The NCEER-91 Earthquake Catalog: Improved Intensity-Based Magnitudes and Recurrence Relations for U.S. Earthquakes East of New Madrid," by L. Seeber and J.G. Armbruster, 8/28/91, (PB92-176742, A06, MF-A02).

NCEER-91-0022   "Proceedings from the Implementation of Earthquake Planning and Education in Schools: The Need for Change - The Roles of the Changemakers," by K.E.K. Ross and F. Winslow, 7/23/91, (PB92-129998, A12, MF-A03).

NCEER-91-0023   "A Study of Reliability-Based Criteria for Seismic Design of Reinforced Concrete Frame Buildings," by H.H.M. Hwang and H-M. Hsu, 8/10/91, (PB92-140235, A09, MF-A02).

NCEER-91-0024   "Experimental Verification of a Number of Structural System Identification Algorithms," by R.G. Ghanem, H. Gavin and M. Shinozuka, 9/18/91, (PB92-176577, A18, MF-A04).

NCEER-91-0025   "Probabilistic Evaluation of Liquefaction Potential," by H.H.M. Hwang and C.S. Lee," 11/25/91, (PB92-143429, A05, MF-A01).

NCEER-91-0026   "Instantaneous Optimal Control for Linear, Nonlinear and Hysteretic Structures - Stable Controllers," by J.N. Yang and Z. Li, 11/15/91, (PB92-163807, A04, MF-A01).

NCEER-91-0027   "Experimental and Theoretical Study of a Sliding Isolation System for Bridges," by M.C. Constantinou, A. Kartoum, A.M. Reinhorn and P. Bradford, 11/15/91, (PB92-176973, A10, MF-A03).

NCEER-92-0001   "Case Studies of Liquefaction and Lifeline Performance During Past Earthquakes, Volume 1: Japanese Case Studies," Edited by M. Hamada and T. O'Rourke, 2/17/92, (PB92-197243, A18, MF-A04).

NCEER-92-0002   "Case Studies of Liquefaction and Lifeline Performance During Past Earthquakes, Volume 2: United States Case Studies," Edited by T. O'Rourke and M. Hamada, 2/17/92, (PB92-197250, A20, MF-A04).

NCEER-92-0003   "Issues in Earthquake Education," Edited by K. Ross, 2/3/92, (PB92-222389, A07, MF-A02).

NCEER-92-0004   "Proceedings from the First U.S. - Japan Workshop on Earthquake Protective Systems for Bridges," Edited by I.G. Buckle, 2/4/92, (PB94-142239, A99, MF-A06).

NCEER-92-0005   "Seismic Ground Motion from a Haskell-Type Source in a Multiple-Layered Half-Space," A.P. Theoharis, G. Deodatis and M. Shinozuka, 1/2/92, to be published.

NCEER-92-0006   "Proceedings from the Site Effects Workshop," Edited by R. Whitman, 2/29/92, (PB92-197201, A04, MF-A01).

NCEER-92-0007   "Engineering Evaluation of Permanent Ground Deformations Due to Seismically-Induced Liquefaction," by M.H. Baziar, R. Dobry and A-W.M. Elgamal, 3/24/92, (PB92-222421, A13, MF-A03).

NCEER-92-0008   "A Procedure for the Seismic Evaluation of Buildings in the Central and Eastern United States," by C.D. Poland and J.O. Malley, 4/2/92, (PB92-222439, A20, MF-A04).

NCEER-92-0009   "Experimental and Analytical Study of a Hybrid Isolation System Using Friction Controllable Sliding Bearings," by M.Q. Feng, S. Fujii and M. Shinozuka, 5/15/92, (PB93-150282, A06, MF-A02).

NCEER-92-0010   "Seismic Resistance of Slab-Column Connections in Existing Non-Ductile Flat-Plate Buildings," by A.J. Durrani and Y. Du, 5/18/92, (PB93-116812, A06, MF-A02).

NCEER-92-0011   "The Hysteretic and Dynamic Behavior of Brick Masonry Walls Upgraded by Ferrocement Coatings Under Cyclic Loading and Strong Simulated Ground Motion," by H. Lee and S.P. Prawel, 5/11/92, to be published.

NCEER-92-0012   "Study of Wire Rope Systems for Seismic Protection of Equipment in Buildings," by G.F. Demetriades, M.C. Constantinou and A.M. Reinhorn, 5/20/92, (PB93-116655, A08, MF-A02).

NCEER-92-0013   "Shape Memory Structural Dampers: Material Properties, Design and Seismic Testing," by P.R. Witting and F.A. Cozzarelli, 5/26/92, (PB93-116663, A05, MF-A01).

NCEER-92-0014   "Longitudinal Permanent Ground Deformation Effects on Buried Continuous Pipelines," by M.J. O'Rourke, and C. Nordberg, 6/15/92, (PB93-116671, A08, MF-A02).

NCEER-92-0015   "A Simulation Method for Stationary Gaussian Random Functions Based on the Sampling Theorem," by M. Grigoriu and S. Balopoulou, 6/11/92, (PB93-127496, A05, MF-A01).

NCEER-92-0016   "Gravity-Load-Designed Reinforced Concrete Buildings: Seismic Evaluation of Existing Construction and Detailing Strategies for Improved Seismic Resistance," by G.W. Hoffmann, S.K. Kunnath, A.M. Reinhorn and J.B. Mander, 7/15/92, (PB94-142007, A08, MF-A02).

NCEER-92-0017   "Observations on Water System and Pipeline Performance in the Limón Area of Costa Rica Due to the April 22, 1991 Earthquake," by M. O'Rourke and D. Ballantyne, 6/30/92, (PB93-126811, A06, MF-A02).

NCEER-92-0018   "Fourth Edition of Earthquake Education Materials for Grades K-12," Edited by K.E.K. Ross, 8/10/92, (PB93-114023, A07, MF-A02).

NCEER-92-0019   "Proceedings from the Fourth Japan-U.S. Workshop on Earthquake Resistant Design of Lifeline Facilities and Countermeasures for Soil Liquefaction," Edited by M. Hamada and T.D. O'Rourke, 8/12/92, (PB93-163939, A99, MF-E11).

NCEER-92-0020   "Active Bracing System: A Full Scale Implementation of Active Control," by A.M. Reinhorn, T.T. Soong, R.C. Lin, M.A. Riley, Y.P. Wang, S. Aizawa and M. Higashino, 8/14/92, (PB93-127512, A06, MF-A02).

NCEER-92-0021   "Empirical Analysis of Horizontal Ground Displacement Generated by Liquefaction-Induced Lateral Spreads," by S.F. Bartlett and T.L. Youd, 8/17/92, (PB93-188241, A06, MF-A02).

NCEER-92-0022   "IDARC Version 3.0: Inelastic Damage Analysis of Reinforced Concrete Structures," by S.K. Kunnath, A.M. Reinhorn and R.F. Lobo, 8/31/92, (PB93-227502, A07, MF-A02).

NCEER-92-0023   "A Semi-Empirical Analysis of Strong-Motion Peaks in Terms of Seismic Source, Propagation Path and Local Site Conditions, by M. Kamiyama, M.J. O'Rourke and R. Flores-Berrones, 9/9/92, (PB93-150266, A08, MF-A02).

NCEER-92-0024   "Seismic Behavior of Reinforced Concrete Frame Structures with Nonductile Details, Part I: Summary of Experimental Findings of Full Scale Beam-Column Joint Tests," by A. Beres, R.N. White and P. Gergely, 9/30/92, (PB93-227783, A05, MF-A01).

NCEER-92-0025   "Experimental Results of Repaired and Retrofitted Beam-Column Joint Tests in Lightly Reinforced Concrete Frame Buildings," by A. Beres, S. El-Borgi, R.N. White and P. Gergely, 10/29/92, (PB93-227791, A05, MF-A01).

NCEER-92-0026   "A Generalization of Optimal Control Theory: Linear and Nonlinear Structures," by J.N. Yang, Z. Li and S. Vongchavalitkul, 11/2/92, (PB93-188621, A05, MF-A01).

NCEER-92-0027   "Seismic Resistance of Reinforced Concrete Frame Structures Designed Only for Gravity Loads: Part I - Design and Properties of a One-Third Scale Model Structure," by J.M. Bracci, A.M. Reinhorn and J.B. Mander, 12/1/92, (PB94-104502, A08, MF-A02).

NCEER-92-0028   "Seismic Resistance of Reinforced Concrete Frame Structures Designed Only for Gravity Loads: Part II - Experimental Performance of Subassemblages," by L.E. Aycardi, J.B. Mander and A.M. Reinhorn, 12/1/92, (PB94-104510, A08, MF-A02).

NCEER-92-0029   "Seismic Resistance of Reinforced Concrete Frame Structures Designed Only for Gravity Loads: Part III - Experimental Performance and Analytical Study of a Structural Model," by J.M. Bracci, A.M. Reinhorn and J.B. Mander, 12/1/92, (PB93-227528, A09, MF-A01).

NCEER-92-0030   "Evaluation of Seismic Retrofit of Reinforced Concrete Frame Structures: Part I - Experimental Performance of Retrofitted Subassemblages," by D. Choudhuri, J.B. Mander and A.M. Reinhorn, 12/8/92, (PB93-198307, A07, MF-A02).

NCEER-92-0031   "Evaluation of Seismic Retrofit of Reinforced Concrete Frame Structures: Part II - Experimental Performance and Analytical Study of a Retrofitted Structural Model," by J.M. Bracci, A.M. Reinhorn and J.B. Mander, 12/8/92, (PB93-198315, A09, MF-A03).

NCEER-92-0032   "Experimental and Analytical Investigation of Seismic Response of Structures with Supplemental Fluid Viscous Dampers," by M.C. Constantinou and M.D. Symans, 12/21/92, (PB93-191435, A10, MF-A03). This report is available only through NTIS (see address given above).

NCEER-92-0033   "Reconnaissance Report on the Cairo, Egypt Earthquake of October 12, 1992," by M. Khater, 12/23/92, (PB93-188621, A03, MF-A01).

NCEER-92-0034   "Low-Level Dynamic Characteristics of Four Tall Flat-Plate Buildings in New York City," by H. Gavin, S. Yuan, J. Grossman, E. Pekelis and K. Jacob, 12/28/92, (PB93-188217, A07, MF-A02).

NCEER-93-0001   "An Experimental Study on the Seismic Performance of Brick-Infilled Steel Frames With and Without Retrofit," by J.B. Mander, B. Nair, K. Wojtkowski and J. Ma, 1/29/93, (PB93-227510, A07, MF-A02).

NCEER-93-0002   "Social Accounting for Disaster Preparedness and Recovery Planning," by S. Cole, E. Pantoja and V. Razak, 2/22/93, (PB94-142114, A12, MF-A03).

NCEER-93-0003   "Assessment of 1991 NEHRP Provisions for Nonstructural Components and Recommended Revisions," by T.T. Soong, G. Chen, Z. Wu, R-H. Zhang and M. Grigoriu, 3/1/93, (PB93-188639, A06, MF-A02).

NCEER-93-0004   "Evaluation of Static and Response Spectrum Analysis Procedures of SEAOC/UBC for Seismic Isolated Structures," by C.W. Winters and M.C. Constantinou, 3/23/93, (PB93-198299, A10, MF-A03).

NCEER-93-0005   "Earthquakes in the Northeast - Are We Ignoring the Hazard? A Workshop on Earthquake Science and Safety for Educators," edited by K.E.K. Ross, 4/2/93, (PB94-103066, A09, MF-A02).

NCEER-93-0006   "Inelastic Response of Reinforced Concrete Structures with Viscoelastic Braces," by R.F. Lobo, J.M. Bracci, K.L. Shen, A.M. Reinhorn and T.T. Soong, 4/5/93, (PB93-227486, A05, MF-A02).

NCEER-93-0007   "Seismic Testing of Installation Methods for Computers and Data Processing Equipment," by K. Kosar, T.T. Soong, K.L. Shen, J.A. HoLung and Y.K. Lin, 4/12/93, (PB93-198299, A07, MF-A02).

NCEER-93-0008   "Retrofit of Reinforced Concrete Frames Using Added Dampers," by A. Reinhorn, M. Constantinou and C. Li, to be published.

NCEER-93-0009   "Seismic Behavior and Design Guidelines for Steel Frame Structures with Added Viscoelastic Dampers," by K.C. Chang, M.L. Lai, T.T. Soong, D.S. Hao and Y.C. Yeh, 5/1/93, (PB94-141959, A07, MF-A02).

NCEER-93-0010   "Seismic Performance of Shear-Critical Reinforced Concrete Bridge Piers," by J.B. Mander, S.M. Waheed, M.T.A. Chaudhary and S.S. Chen, 5/12/93, (PB93-227494, A08, MF-A02).

NCEER-93-0011   "3D-BASIS-TABS: Computer Program for Nonlinear Dynamic Analysis of Three Dimensional Base Isolated Structures," by S. Nagarajaiah, C. Li, A.M. Reinhorn and M.C. Constantinou, 8/2/93, (PB94-141819, A09, MF-A02).

NCEER-93-0012   "Effects of Hydrocarbon Spills from an Oil Pipeline Break on Ground Water," by O.J. Helweg and H.H.M. Hwang, 8/3/93, (PB94-141942, A06, MF-A02).

NCEER-93-0013   "Simplified Procedures for Seismic Design of Nonstructural Components and Assessment of Current Code Provisions," by M.P. Singh, L.E. Suarez, E.E. Matheu and G.O. Maldonado, 8/4/93, (PB94-141827, A09, MF-A02).

NCEER-93-0014   "An Energy Approach to Seismic Analysis and Design of Secondary Systems," by G. Chen and T.T. Soong, 8/6/93, (PB94-142767, A11, MF-A03).

NCEER-93-0015   "Proceedings from School Sites: Becoming Prepared for Earthquakes - Commemorating the Third Anniversary of the Loma Prieta Earthquake," Edited by F.E. Winslow and K.E.K. Ross, 8/16/93, (PB94-154275, A16, MF-A02).

NCEER-93-0016   "Reconnaissance Report of Damage to Historic Monuments in Cairo, Egypt Following the October 12, 1992 Dahshur Earthquake," by D. Sykora, D. Look, G. Croci, E. Karaesmen and E. Karaesmen, 8/19/93, (PB94-142221, A08, MF-A02).

NCEER-93-0017   "The Island of Guam Earthquake of August 8, 1993," by S.W. Swan and S.K. Harris, 9/30/93, (PB94-141843, A04, MF-A01).

NCEER-93-0018   "Engineering Aspects of the October 12, 1992 Egyptian Earthquake," by A.W. Elgamal, M. Amer, K. Adalier and A. Abul-Fadl, 10/7/93, (PB94-141983, A05, MF-A01).

NCEER-93-0019   "Development of an Earthquake Motion Simulator and its Application in Dynamic Centrifuge Testing," by I. Krstelj, Supervised by J.H. Prevost, 10/23/93, (PB94-181773, A-10, MF-A03).

NCEER-93-0020   "NCEER-Taisei Corporation Research Program on Sliding Seismic Isolation Systems for Bridges: Experimental and Analytical Study of a Friction Pendulum System (FPS)," by M.C. Constantinou, P. Tsopelas, Y-S. Kim and S. Okamoto, 11/1/93, (PB94-142775, A08, MF-A02).

NCEER-93-0021   "Finite Element Modeling of Elastomeric Seismic Isolation Bearings," by L.J. Billings, Supervised by R. Shepherd, 11/8/93, to be published.

NCEER-93-0022   "Seismic Vulnerability of Equipment in Critical Facilities: Life-Safety and Operational Consequences," by K. Porter, G.S. Johnson, M.M. Zadeh, C. Scawthorn and S. Eder, 11/24/93, (PB94-181765, A16, MF-A03).

NCEER-93-0023   "Hokkaido Nansei-oki, Japan Earthquake of July 12, 1993, by P.I. Yanev and C.R. Scawthorn, 12/23/93, (PB94-181500, A07, MF-A01).

NCEER-94-0001   "An Evaluation of Seismic Serviceability of Water Supply Networks with Application to the San Francisco Auxiliary Water Supply System," by I. Markov, Supervised by M. Grigoriu and T. O'Rourke, 1/21/94, (PB94-204013, A07, MF-A02).

NCEER-94-0002   "NCEER-Taisei Corporation Research Program on Sliding Seismic Isolation Systems for Bridges: Experimental and Analytical Study of Systems Consisting of Sliding Bearings, Rubber Restoring Force Devices and Fluid Dampers," Volumes I and II, by P. Tsopelas, S. Okamoto, M.C. Constantinou, D. Ozaki and S. Fujii, 2/4/94, (PB94-181740, A09, MF-A02 and PB94-181757, A12, MF-A03).

NCEER-94-0003   "A Markov Model for Local and Global Damage Indices in Seismic Analysis," by S. Rahman and M. Grigoriu, 2/18/94, (PB94-206000, A12, MF-A03).

NCEER-94-0004   "Proceedings from the NCEER Workshop on Seismic Response of Masonry Infills," edited by D.P. Abrams, 3/1/94, (PB94-180783, A07, MF-A02).

NCEER-94-0005   "The Northridge, California Earthquake of January 17, 1994: General Reconnaissance Report," edited by J.D. Goltz, 3/11/94, (PB193943, A10, MF-A03).

NCEER-94-0006   "Seismic Energy Based Fatigue Damage Analysis of Bridge Columns: Part I - Evaluation of Seismic Capacity," by G.A. Chang and J.B. Mander, 3/14/94, (PB94-219185, A11, MF-A03).

NCEER-94-0007   "Seismic Isolation of Multi-Story Frame Structures Using Spherical Sliding Isolation Systems," by T.M. Al-Hussaini, V.A. Zayas and M.C. Constantinou, 3/17/94, (PB193745, A09, MF-A02).

NCEER-94-0008   "The Northridge, California Earthquake of January 17, 1994: Performance of Highway Bridges," edited by I.G. Buckle, 3/24/94, (PB94-193851, A06, MF-A02).

NCEER-94-0009   "Proceedings of the Third U.S.-Japan Workshop on Earthquake Protective Systems for Bridges," edited by I.G. Buckle and I. Friedland, 3/31/94, (PB94-195815, A99, MF-A06).

NCEER-94-0010   "3D-BASIS-ME: Computer Program for Nonlinear Dynamic Analysis of Seismically Isolated Single and Multiple Structures and Liquid Storage Tanks," by P.C. Tsopelas, M.C. Constantinou and A.M. Reinhorn, 4/12/94, (PB94-204922, A09, MF-A02).

NCEER-94-0011   "The Northridge, California Earthquake of January 17, 1994: Performance of Gas Transmission Pipelines," by T.D. O'Rourke and M.C. Palmer, 5/16/94, (PB94-204989, A05, MF-A01).

NCEER-94-0012   "Feasibility Study of Replacement Procedures and Earthquake Performance Related to Gas Transmission Pipelines," by T.D. O'Rourke and M.C. Palmer, 5/25/94, (PB94-206638, A09, MF-A02).

NCEER-94-0013   "Seismic Energy Based Fatigue Damage Analysis of Bridge Columns: Part II - Evaluation of Seismic Demand," by G.A. Chang and J.B. Mander, 6/1/94, (PB95-18106, A08, MF-A02).

NCEER-94-0014   "NCEER-Taisei Corporation Research Program on Sliding Seismic Isolation Systems for Bridges: Experimental and Analytical Study of a System Consisting of Sliding Bearings and Fluid Restoring Force/Damping Devices," by P. Tsopelas and M.C. Constantinou, 6/13/94, (PB94-219144, A10, MF-A03).

NCEER-94-0015   "Generation of Hazard-Consistent Fragility Curves for Seismic Loss Estimation Studies," by H. Hwang and J-R. Huo, 6/14/94, (PB95-181996, A09, MF-A02).

NCEER-94-0016   "Seismic Study of Building Frames with Added Energy-Absorbing Devices," by W.S. Pong, C.S. Tsai and G.C. Lee, 6/20/94, (PB94-219136, A10, A03).

NCEER-94-0017   "Sliding Mode Control for Seismic-Excited Linear and Nonlinear Civil Engineering Structures," by J. Yang, J. Wu, A. Agrawal and Z. Li, 6/21/94, (PB95-138483, A06, MF-A02).

NCEER-94-0018   "3D-BASIS-TABS Version 2.0: Computer Program for Nonlinear Dynamic Analysis of Three Dimensional Base Isolated Structures," by A.M. Reinhorn, S. Nagarajaiah, M.C. Constantinou, P. Tsopelas and R. Li, 6/22/94, (PB95-182176, A08, MF-A02).

NCEER-94-0019   "Proceedings of the International Workshop on Civil Infrastructure Systems: Application of Intelligent Systems and Advanced Materials on Bridge Systems," Edited by G.C. Lee and K.C. Chang, 7/18/94, (PB95-252474, A20, MF-A04).

NCEER-94-0020   "Study of Seismic Isolation Systems for Computer Floors," by V. Lambrou and M.C. Constantinou, 7/19/94, (PB95-138533, A10, MF-A03).

NCEER-94-0021   "Proceedings of the U.S.-Italian Workshop on Guidelines for Seismic Evaluation and Rehabilitation of Unreinforced Masonry Buildings," Edited by D.P. Abrams and G.M. Calvi, 7/20/94, (PB95-138749, A13, MF-A03).

NCEER-94-0022   "NCEER-Taisei Corporation Research Program on Sliding Seismic Isolation Systems for Bridges: Experimental and Analytical Study of a System Consisting of Lubricated PTFE Sliding Bearings and Mild Steel Dampers," by P. Tsopelas and M.C. Constantinou, 7/22/94, (PB95-182184, A08, MF-A02).

NCEER-94-0023   "Development of Reliability-Based Design Criteria for Buildings Under Seismic Load," by Y.K. Wen, H. Hwang and M. Shinozuka, 8/1/94, (PB95-211934, A08, MF-A02).

NCEER-94-0024 "Experimental Verification of Acceleration Feedback Control Strategies for an Active Tendon System," by S.J. Dyke, B.F. Spencer, Jr., P. Quast, M.K. Sain, D.C. Kaspari, Jr. and T.T. Soong, 8/29/94, (PB95-212320, A05, MF-A01).

NCEER-94-0025 "Seismic Retrofitting Manual for Highway Bridges," Edited by I.G. Buckle and I.F. Friedland, published by the Federal Highway Administration (PB95-212676, A15, MF-A03).

NCEER-94-0026 "Proceedings from the Fifth U.S.-Japan Workshop on Earthquake Resistant Design of Lifeline Facilities and Countermeasures Against Soil Liquefaction," Edited by T.D. O'Rourke and M. Hamada, 11/7/94, (PB95-220802, A99, MF-E08).

NCEER-95-0001 "Experimental and Analytical Investigation of Seismic Retrofit of Structures with Supplemental Damping: Part 1 - Fluid Viscous Damping Devices," by A.M. Reinhorn, C. Li and M.C. Constantinou, 1/3/95, (PB95-266599, A09, MF-A02).

NCEER-95-0002 "Experimental and Analytical Study of Low-Cycle Fatigue Behavior of Semi-Rigid Top-And-Seat Angle Connections," by G. Pekcan, J.B. Mander and S.S. Chen, 1/5/95, (PB95-220042, A07, MF-A02).

NCEER-95-0003 "NCEER-ATC Joint Study on Fragility of Buildings," by T. Anagnos, C. Rojahn and A.S. Kiremidjian, 1/20/95, (PB95-220026, A06, MF-A02).

NCEER-95-0004 "Nonlinear Control Algorithms for Peak Response Reduction," by Z. Wu, T.T. Soong, V. Gattulli and R.C. Lin, 2/16/95, (PB95-220349, A05, MF-A01).

NCEER-95-0005 "Pipeline Replacement Feasibility Study: A Methodology for Minimizing Seismic and Corrosion Risks to Underground Natural Gas Pipelines," by R.T. Eguchi, H.A. Seligson and D.G. Honegger, 3/2/95, (PB95-252326, A06, MF-A02).

NCEER-95-0006 "Evaluation of Seismic Performance of an 11-Story Frame Building During the 1994 Northridge Earthquake," by F. Naeim, R. DiSulio, K. Benuska, A. Reinhorn and C. Li, to be published.

NCEER-95-0007 "Prioritization of Bridges for Seismic Retrofitting," by N. Basöz and A.S. Kiremidjian, 4/24/95, (PB95-252300, A08, MF-A02).

NCEER-95-0008 "Method for Developing Motion Damage Relationships for Reinforced Concrete Frames," by A. Singhal and A.S. Kiremidjian, 5/11/95, (PB95-266607, A06, MF-A02).

NCEER-95-0009 "Experimental and Analytical Investigation of Seismic Retrofit of Structures with Supplemental Damping: Part II - Friction Devices," by C. Li and A.M. Reinhorn, 7/6/95, (PB96-128087, A11, MF-A03).

NCEER-95-0010 "Experimental Performance and Analytical Study of a Non-Ductile Reinforced Concrete Frame Structure Retrofitted with Elastomeric Spring Dampers," by G. Pekcan, J.B. Mander and S.S. Chen, 7/14/95, (PB96-137161, A08, MF-A02).

NCEER-95-0011 "Development and Experimental Study of Semi-Active Fluid Damping Devices for Seismic Protection of Structures," by M.D. Symans and M.C. Constantinou, 8/3/95, (PB96-136940, A23, MF-A04).

NCEER-95-0012 "Real-Time Structural Parameter Modification (RSPM): Development of Innervated Structures," by Z. Liang, M. Tong and G.C. Lee, 4/11/95, (PB96-137153, A06, MF-A01).

NCEER-95-0013 "Experimental and Analytical Investigation of Seismic Retrofit of Structures with Supplemental Damping: Part III - Viscous Damping Walls," by A.M. Reinhorn and C. Li, 10/1/95, (PB96-176409, A11, MF-A03).

NCEER-95-0014 "Seismic Fragility Analysis of Equipment and Structures in a Memphis Electric Substation," by J-R. Huo and H.H.M. Hwang, (PB96-128087, A09, MF-A02), 8/10/95.

NCEER-95-0015 "The Hanshin-Awaji Earthquake of January 17, 1995: Performance of Lifelines," Edited by M. Shinozuka, 11/3/95, (PB96-176383, A15, MF-A03).

NCEER-95-0016   "Highway Culvert Performance During Earthquakes," by T.L. Youd and C.J. Beckman, available as NCEER-96-0015.

NCEER-95-0017   "The Hanshin-Awaji Earthquake of January 17, 1995: Performance of Highway Bridges," Edited by I.G. Buckle, 12/1/95, to be published.

NCEER-95-0018   "Modeling of Masonry Infill Panels for Structural Analysis," by A.M. Reinhorn, A. Madan, R.E. Valles, Y. Reichmann and J.B. Mander, 12/8/95, (PB97-110886, MF-A01, A06).

NCEER-95-0019   "Optimal Polynomial Control for Linear and Nonlinear Structures," by A.K. Agrawal and J.N. Yang, 12/11/95, (PB96-168737, A07, MF-A02).

NCEER-95-0020   "Retrofit of Non-Ductile Reinforced Concrete Frames Using Friction Dampers," by R.S. Rao, P. Gergely and R.N. White, 12/22/95, (PB97-133508, A10, MF-A02).

NCEER-95-0021   "Parametric Results for Seismic Response of Pile-Supported Bridge Bents," by G. Mylonakis, A. Nikolaou and G. Gazetas, 12/22/95, (PB97-100242, A12, MF-A03).

NCEER-95-0022   "Kinematic Bending Moments in Seismically Stressed Piles," by A. Nikolaou, G. Mylonakis and G. Gazetas, 12/23/95, (PB97-113914, MF-A03, A13).

NCEER-96-0001   "Dynamic Response of Unreinforced Masonry Buildings with Flexible Diaphragms," by A.C. Costley and D.P. Abrams," 10/10/96, (PB97-133573, MF-A03, A15).

NCEER-96-0002   "State of the Art Review: Foundations and Retaining Structures," by I. Po Lam, to be published.

NCEER-96-0003   "Ductility of Rectangular Reinforced Concrete Bridge Columns with Moderate Confinement," by N. Wehbe, M. Saiidi, D. Sanders and B. Douglas, 11/7/96, (PB97-133557, A06, MF-A02).

NCEER-96-0004   "Proceedings of the Long-Span Bridge Seismic Research Workshop," edited by I.G. Buckle and I.M. Friedland, to be published.

NCEER-96-0005   "Establish Representative Pier Types for Comprehensive Study: Eastern United States," by J. Kulicki and Z. Prucz, 5/28/96, (PB98-119217, A07, MF-A02).

NCEER-96-0006   "Establish Representative Pier Types for Comprehensive Study: Western United States," by R. Imbsen, R.A. Schamber and T.A. Osterkamp, 5/28/96, (PB98-118607, A07, MF-A02).

NCEER-96-0007   "Nonlinear Control Techniques for Dynamical Systems with Uncertain Parameters," by R.G. Ghanem and M.I. Bujakov, 5/27/96, (PB97-100259, A17, MF-A03).

NCEER-96-0008   "Seismic Evaluation of a 30-Year Old Non-Ductile Highway Bridge Pier and Its Retrofit," by J.B. Mander, B. Mahmoodzadegan, S. Bhadra and S.S. Chen, 5/31/96, (PB97-110902, MF-A03, A10).

NCEER-96-0009   "Seismic Performance of a Model Reinforced Concrete Bridge Pier Before and After Retrofit," by J.B. Mander, J.H. Kim and C.A. Ligozio, 5/31/96, (PB97-110910, MF-A02, A10).

NCEER-96-0010   "IDARC2D Version 4.0: A Computer Program for the Inelastic Damage Analysis of Buildings," by R.E. Valles, A.M. Reinhorn, S.K. Kunnath, C. Li and A. Madan, 6/3/96, (PB97-100234, A17, MF-A03).

NCEER-96-0011   "Estimation of the Economic Impact of Multiple Lifeline Disruption: Memphis Light, Gas and Water Division Case Study," by S.E. Chang, H.A. Seligson and R.T. Eguchi, 8/16/96, (PB97-133490, A11, MF-A03).

NCEER-96-0012   "Proceedings from the Sixth Japan-U.S. Workshop on Earthquake Resistant Design of Lifeline Facilities and Countermeasures Against Soil Liquefaction, Edited by M. Hamada and T. O'Rourke, 9/11/96, (PB97-133581, A99, MF-A06).

NCEER-96-0013   "Chemical Hazards, Mitigation and Preparedness in Areas of High Seismic Risk: A Methodology for Estimating the Risk of Post-Earthquake Hazardous Materials Release," by H.A. Seligson, R.T. Eguchi, K.J. Tierney and K. Richmond, 11/7/96, (PB97-133565, MF-A02, A08).

NCEER-96-0014   "Response of Steel Bridge Bearings to Reversed Cyclic Loading," by J.B. Mander, D-K. Kim, S.S. Chen and G.J. Premus, 11/13/96, (PB97-140735, A12, MF-A03).

NCEER-96-0015   "Highway Culvert Performance During Past Earthquakes," by T.L. Youd and C.J. Beckman, 11/25/96, (PB97-133532, A06, MF-A01).

NCEER-97-0001   "Evaluation, Prevention and Mitigation of Pounding Effects in Building Structures," by R.E. Valles and A.M. Reinhorn, 2/20/97, (PB97-159552, A14, MF-A03).

NCEER-97-0002   "Seismic Design Criteria for Bridges and Other Highway Structures," by C. Rojahn, R. Mayes, D.G. Anderson, J. Clark, J.H. Hom, R.V. Nutt and M.J. O'Rourke, 4/30/97, (PB97-194658, A06, MF-A03).

NCEER-97-0003   "Proceedings of the U.S.-Italian Workshop on Seismic Evaluation and Retrofit," Edited by D.P. Abrams and G.M. Calvi, 3/19/97, (PB97-194666, A13, MF-A03).

NCEER-97-0004   "Investigation of Seismic Response of Buildings with Linear and Nonlinear Fluid Viscous Dampers," by A.A. Seleemah and M.C. Constantinou, 5/21/97, (PB98-109002, A15, MF-A03).

NCEER-97-0005   "Proceedings of the Workshop on Earthquake Engineering Frontiers in Transportation Facilities," edited by G.C. Lee and I.M. Friedland, 8/29/97, (PB98-128911, A25, MR-A04).

NCEER-97-0006   "Cumulative Seismic Damage of Reinforced Concrete Bridge Piers," by S.K. Kunnath, A. El-Bahy, A. Taylor and W. Stone, 9/2/97, (PB98-108814, A11, MF-A03).

NCEER-97-0007   "Structural Details to Accommodate Seismic Movements of Highway Bridges and Retaining Walls," by R.A. Imbsen, R.A. Schamber, E. Thorkildsen, A. Kartoum, B.T. Martin, T.N. Rosser and J.M. Kulicki, 9/3/97, (PB98-108996, A09, MF-A02).

NCEER-97-0008   "A Method for Earthquake Motion-Damage Relationships with Application to Reinforced Concrete Frames," by A. Singhal and A.S. Kiremidjian, 9/10/97, (PB98-108988, A13, MF-A03).

NCEER-97-0009   "Seismic Analysis and Design of Bridge Abutments Considering Sliding and Rotation," by K. Fishman and R. Richards, Jr., 9/15/97, (PB98-108897, A06, MF-A02).

NCEER-97-0010   "Proceedings of the FHWA/NCEER Workshop on the National Representation of Seismic Ground Motion for New and Existing Highway Facilities," edited by I.M. Friedland, M.S. Power and R.L. Mayes, 9/22/97, (PB98-128903, A21, MF-A04).

NCEER-97-0011   "Seismic Analysis for Design or Retrofit of Gravity Bridge Abutments," by K.L. Fishman, R. Richards, Jr. and R.C. Divito, 10/2/97, (PB98-128937, A08, MF-A02).

NCEER-97-0012   "Evaluation of Simplified Methods of Analysis for Yielding Structures," by P. Tsopelas, M.C. Constantinou, C.A. Kircher and A.S. Whittaker, 10/31/97, (PB98-128929, A10, MF-A03).

NCEER-97-0013   "Seismic Design of Bridge Columns Based on Control and Repairability of Damage," by C-T. Cheng and J.B. Mander, 12/8/97, (PB98-144249, A11, MF-A03).

NCEER-97-0014   "Seismic Resistance of Bridge Piers Based on Damage Avoidance Design," by J.B. Mander and C-T. Cheng, 12/10/97, (PB98-144223, A09, MF-A02).

NCEER-97-0015   "Seismic Response of Nominally Symmetric Systems with Strength Uncertainty," by S. Balopoulou and M. Grigoriu, 12/23/97, (PB98-153422, A11, MF-A03).

NCEER-97-0016   "Evaluation of Seismic Retrofit Methods for Reinforced Concrete Bridge Columns," by T.J. Wipf, F.W. Klaiber and F.M. Russo, 12/28/97, (PB98-144215, A12, MF-A03).

NCEER-97-0017 "Seismic Fragility of Existing Conventional Reinforced Concrete Highway Bridges," by C.L. Mullen and A.S. Cakmak, 12/30/97, (PB98-153406, A08, MF-A02).

NCEER-97-0018 "Loss Asssessment of Memphis Buildings," edited by D.P. Abrams and M. Shinozuka, 12/31/97, (PB98-144231, A13, MF-A03).

NCEER-97-0019 "Seismic Evaluation of Frames with Infill Walls Using Quasi-static Experiments," by K.M. Mosalam, R.N. White and P. Gergely, 12/31/97, (PB98-153455, A07, MF-A02).

NCEER-97-0020 "Seismic Evaluation of Frames with Infill Walls Using Pseudo-dynamic Experiments," by K.M. Mosalam, R.N. White and P. Gergely, 12/31/97, (PB98-153430, A07, MF-A02).

NCEER-97-0021 "Computational Strategies for Frames with Infill Walls: Discrete and Smeared Crack Analyses and Seismic Fragility," by K.M. Mosalam, R.N. White and P. Gergely, 12/31/97, (PB98-153414, A10, MF-A02).

NCEER-97-0022 "Proceedings of the NCEER Workshop on Evaluation of Liquefaction Resistance of Soils," edited by T.L. Youd and I.M. Idriss, 12/31/97, (PB98-155617, A15, MF-A03).

MCEER-98-0001 "Extraction of Nonlinear Hysteretic Properties of Seismically Isolated Bridges from Quick-Release Field Tests," by Q. Chen, B.M. Douglas, E.M. Maragakis and I.G. Buckle, 5/26/98, (PB99-118838, A06, MF-A01).

MCEER-98-0002 "Methodologies for Evaluating the Importance of Highway Bridges," by A. Thomas, S. Eshenaur and J. Kulicki, 5/29/98, (PB99-118846, A10, MF-A02).

MCEER-98-0003 "Capacity Design of Bridge Piers and the Analysis of Overstrength," by J.B. Mander, A. Dutta and P. Goel, 6/1/98, (PB99-118853, A09, MF-A02).

MCEER-98-0004 "Evaluation of Bridge Damage Data from the Loma Prieta and Northridge, California Earthquakes," by N. Basoz and A. Kiremidjian, 6/2/98, (PB99-118861, A15, MF-A03).

MCEER-98-0005 "Screening Guide for Rapid Assessment of Liquefaction Hazard at Highway Bridge Sites," by T. L. Youd, 6/16/98, (PB99-118879, A06, not available on microfiche).

MCEER-98-0006 "Structural Steel and Steel/Concrete Interface Details for Bridges," by P. Ritchie, N. Kauhl and J. Kulicki, 7/13/98, (PB99-118945, A06, MF-A01).

MCEER-98-0007 "Capacity Design and Fatigue Analysis of Confined Concrete Columns," by A. Dutta and J.B. Mander, 7/14/98, (PB99-118960, A14, MF-A03).

MCEER-98-0008 "Proceedings of the Workshop on Performance Criteria for Telecommunication Services Under Earthquake Conditions," edited by A.J. Schiff, 7/15/98, (PB99-118952, A08, MF-A02).

MCEER-98-0009 "Fatigue Analysis of Unconfined Concrete Columns," by J.B. Mander, A. Dutta and J.H. Kim, 9/12/98, (PB99-123655, A10, MF-A02).

MCEER-98-0010 "Centrifuge Modeling of Cyclic Lateral Response of Pile-Cap Systems and Seat-Type Abutments in Dry Sands," by A.D. Gadre and R. Dobry, 10/2/98, (PB99-123606, A13, MF-A03).

MCEER-98-0011 "IDARC-BRIDGE: A Computational Platform for Seismic Damage Assessment of Bridge Structures," by A.M. Reinhorn, V. Simeonov, G. Mylonakis and Y. Reichman, 10/2/98, (PB99-162919, A15, MF-A03).

MCEER-98-0012 "Experimental Investigation of the Dynamic Response of Two Bridges Before and After Retrofitting with Elastomeric Bearings," by D.A. Wendichansky, S.S. Chen and J.B. Mander, 10/2/98, (PB99-162927, A15, MF-A03).

MCEER-98-0013 "Design Procedures for Hinge Restrainers and Hinge Sear Width for Multiple-Frame Bridges," by R. Des Roches and G.L. Fenves, 11/3/98, (PB99-140477, A13, MF-A03).

MCEER-98-0014   "Response Modification Factors for Seismically Isolated Bridges," by M.C. Constantinou and J.K. Quarshie, 11/3/98, (PB99-140485, A14, MF-A03).

MCEER-98-0015   "Proceedings of the U.S.-Italy Workshop on Seismic Protective Systems for Bridges," edited by I.M. Friedland and M.C. Constantinou, 11/3/98, (PB2000-101711, A22, MF-A04).

MCEER-98-0016   "Appropriate Seismic Reliability for Critical Equipment Systems: Recommendations Based on Regional Analysis of Financial and Life Loss," by K. Porter, C. Scawthorn, C. Taylor and N. Blais, 11/10/98, (PB99-157265, A08, MF-A02).

MCEER-98-0017   "Proceedings of the U.S. Japan Joint Seminar on Civil Infrastructure Systems Research," edited by M. Shinozuka and A. Rose, 11/12/98, (PB99-156713, A16, MF-A03).

MCEER-98-0018   "Modeling of Pile Footings and Drilled Shafts for Seismic Design," by I. PoLam, M. Kapuskar and D. Chaudhuri, 12/21/98, (PB99-157257, A09, MF-A02).

MCEER-99-0001   "Seismic Evaluation of a Masonry Infilled Reinforced Concrete Frame by Pseudodynamic Testing," by S.G. Buonopane and R.N. White, 2/16/99, (PB99-162851, A09, MF-A02).

MCEER-99-0002   "Response History Analysis of Structures with Seismic Isolation and Energy Dissipation Systems: Verification Examples for Program SAP2000," by J. Scheller and M.C. Constantinou, 2/22/99, (PB99-162869, A08, MF-A02).

MCEER-99-0003   "Experimental Study on the Seismic Design and Retrofit of Bridge Columns Including Axial Load Effects," by A. Dutta, T. Kokorina and J.B. Mander, 2/22/99, (PB99-162877, A09, MF-A02).

MCEER-99-0004   "Experimental Study of Bridge Elastomeric and Other Isolation and Energy Dissipation Systems with Emphasis on Uplift Prevention and High Velocity Near-source Seismic Excitation," by A. Kasalanati and M. C. Constantinou, 2/26/99, (PB99-162885, A12, MF-A03).

MCEER-99-0005   "Truss Modeling of Reinforced Concrete Shear-flexure Behavior," by J.H. Kim and J.B. Mander, 3/8/99, (PB99-163693, A12, MF-A03).

MCEER-99-0006   "Experimental Investigation and Computational Modeling of Seismic Response of a 1:4 Scale Model Steel Structure with a Load Balancing Supplemental Damping System," by G. Pekcan, J.B. Mander and S.S. Chen, 4/2/99, (PB99-162893, A11, MF-A03).

MCEER-99-0007   "Effect of Vertical Ground Motions on the Structural Response of Highway Bridges," by M.R. Button, C.J. Cronin and R.L. Mayes, 4/10/99, (PB2000-101411, A10, MF-A03).

MCEER-99-0008   "Seismic Reliability Assessment of Critical Facilities: A Handbook, Supporting Documentation, and Model Code Provisions," by G.S. Johnson, R.E. Sheppard, M.D. Quilici, S.J. Eder and C.R. Scawthorn, 4/12/9, (PB2000-101701, A18, MF-A04).

MCEER-99-0009   "Impact Assessment of Selected MCEER Highway Project Research on the Seismic Design of Highway Structures," by C. Rojahn, R. Mayes, D.G. Anderson, J.H. Clark, D'Appolonia Engineering, S. Gloyd and R.V. Nutt, 4/14/99, (PB99-162901, A10, MF-A02).

MCEER-99-0010   "Site Factors and Site Categories in Seismic Codes," by R. Dobry, R. Ramos and M.S. Power, 7/19/99, (PB2000-101705, A08, MF-A02).

MCEER-99-0011   "Restrainer Design Procedures for Multi-Span Simply-Supported Bridges," by M.J. Randall, M. Saiidi, E. Maragakis and T. Isakovic, 7/20/99, (PB2000-101702, A10, MF-A02).

MCEER-99-0012   "Property Modification Factors for Seismic Isolation Bearings," by M.C. Constantinou, P. Tsopelas, A. Kasalanati and E. Wolff, 7/20/99, (PB2000-103387, A11, MF-A03).

MCEER-99-0013   "Critical Seismic Issues for Existing Steel Bridges," by P. Ritchie, N. Kauhl and J. Kulicki, 7/20/99, (PB2000-101697, A09, MF-A02).

MCEER-99-0014   "Nonstructural Damage Database," by A. Kao, T.T. Soong and A. Vender, 7/24/99, (PB2000-101407, A06, MF-A01).

MCEER-99-0015   "Guide to Remedial Measures for Liquefaction Mitigation at Existing Highway Bridge Sites," by H.G. Cooke and J. K. Mitchell, 7/26/99, (PB2000-101703, A11, MF-A03).

MCEER-99-0016   "Proceedings of the MCEER Workshop on Ground Motion Methodologies for the Eastern United States," edited by N. Abrahamson and A. Becker, 8/11/99, (PB2000-103385, A07, MF-A02).

MCEER-99-0017   "Quindío, Colombia Earthquake of January 25, 1999: Reconnaissance Report," by A.P. Asfura and P.J. Flores, 10/4/99, (PB2000-106893, A06, MF-A01).

MCEER-99-0018   "Hysteretic Models for Cyclic Behavior of Deteriorating Inelastic Structures," by M.V. Sivaselvan and A.M. Reinhorn, 11/5/99, (PB2000-103386, A08, MF-A02).

MCEER-99-0019   "Proceedings of the 7th U.S.- Japan Workshop on Earthquake Resistant Design of Lifeline Facilities and Countermeasures Against Soil Liquefaction," edited by T.D. O'Rourke, J.P. Bardet and M. Hamada, 11/19/99, (PB2000-103354, A99, MF-A06).

MCEER-99-0020   "Development of Measurement Capability for Micro-Vibration Evaluations with Application to Chip Fabrication Facilities," by G.C. Lee, Z. Liang, J.W. Song, J.D. Shen and W.C. Liu, 12/1/99, (PB2000-105993, A08, MF-A02).

MCEER-99-0021   "Design and Retrofit Methodology for Building Structures with Supplemental Energy Dissipating Systems," by G. Pekcan, J.B. Mander and S.S. Chen, 12/31/99, (PB2000-105994, A11, MF-A03).

MCEER-00-0001   "The Marmara, Turkey Earthquake of August 17, 1999: Reconnaissance Report," edited by C. Scawthorn; with major contributions by M. Bruneau, R. Eguchi, T. Holzer, G. Johnson, J. Mander, J. Mitchell, W. Mitchell, A. Papageorgiou, C. Scaethorn, and G. Webb, 3/23/00, (PB2000-106200, A11, MF-A03).

MCEER-00-0002   "Proceedings of the MCEER Workshop for Seismic Hazard Mitigation of Health Care Facilities," edited by G.C. Lee, M. Ettouney, M. Grigoriu, J. Hauer and J. Nigg, 3/29/00, (PB2000-106892, A08, MF-A02).

MCEER-00-0003   "The Chi-Chi, Taiwan Earthquake of September 21, 1999: Reconnaissance Report," edited by G.C. Lee and C.H. Loh, with major contributions by G.C. Lee, M. Bruneau, I.G. Buckle, S.E. Chang, P.J. Flores, T.D. O'Rourke, M. Shinozuka, T.T. Soong, C-H. Loh, K-C. Chang, Z-J. Chen, J-S. Hwang, M-L. Lin, G-Y. Liu, K-C. Tsai, G.C. Yao and C-L. Yen, 4/30/00.

MCEER-00-0004   "Seismic Retrofit of End-Sway Frames of Steel Deck-Truss Bridges with a Supplemental Tendon System: Experimental and Analytical Investigation," by G. Pekcan, J.B. Mander and S.S. Chen, 7/1/00.

MCEER-00-0005   "Sliding Fragility of Unrestrained Equipment in Critical Facilities," by W.H. Chong and T.T. Soong, 7/5/00.

MCEER-00-0006   "Seismic Response of Reinforced Concrete Bridge Pier Walls in the Weak Direction," by N. Abo-Shadi, M. Saiidi and D. Sanders, 7/17/00.

MCEER-00-0007   "Low-Cycle Fatigue Behavior of Longitudinal Reinforcement in Reinforced Concrete Bridge Columns," by J. Brown and S.K. Kunnath, 7/23/00.

MCEER-00-0008   "Soil Structure Interaction of Bridges for Seismic Analysis," I. PoLam and H. Law, 9/25/00.

MCEER-00-0009   "Proceedings of the MCEER Workshop on Mitigation of Earthquake Disaster by Advanced Technologies (MEDAT-1), edited by M. Shinozuka, D.J. Inman and T.D. O'Rourke, 11/10/00.

MCEER-00-0010   "Development and Evaluation of Simplified Procedures for Analysis and Design of Buildings with Passive Energy Dissipation Systems," by O.M. Ramirez, M.C. Constantinou, C.A. Kircher, A.S. Whittaker, M.W. Johnson, and J.D. Gomez, 12/8/00.